CASE FILE
COPY

NASA TECHNICAL
TRANSLATION

NASA TT F-338

NASA TT F-338

PHYSICAL METALLURGY OF TITANIUM

I. I. Kornilov, Editor in Chief

Science Publishing House, Moscow, 1964.

NATIONAL AERONAUTICS AND SPACE ADMINISTRATION • WASHINGTON, D. C. • NOVEMBER 1965

NASA TT F-338

PHYSICAL METALLURGY OF TITANIUM

I. I. Kornilov, Editor in Chief

Works of the Fifth Conference on Metallurgy, Physical Metallurgy, and Application of Titanium and Its Alloys

March 1963

A. A. Baykov Institute of Metallurgy

Izdatel'stvo Nauka
Moscow, 1964

NATIONAL AERONAUTICS AND SPACE ADMINISTRATION

For sale by the Clearinghouse for Federal Scientific and Technical Information
Springfield, Virginia 22151 – Price $7.00

TABLE OF CONTENTS

		Page
PREFACE		vi
PART I.	METAL CHEMISTRY OF TITANIUM ALLOYS	1
	Prospects for the Development of Investigations of the Heat Resistance of Titanium Alloys	1
	Phase Diagram of the System Ti-O_2 and Some Properties of the Alloys of This System	12
	Equilibrium Diagram of the Quarternary System Ti-Al-Mo-V	29
	Phase Structure of Alloys of the System Ti-Al-Fe-Cr-Si with a Constant Content of Aluminum and Silicon	35
	Study of the Alloys of the Ternary System Ti-Al-Zr	46
	Phase Equilibrium of Alloys of the Section Ti_3Al-Zr of the Ternary System Ti-Al-Zr	53
	Study of the Phase Structure of the Alloys of the System Ti-Al-Zr Along the Section Ti_3Al-Zr	58
	Relationship of Structures Formed on Quenching Titanium Alloys to Equilibrium Phase Diagrams	67
	Stability of β Alloys of the System Ti-Mo-Cr-Fe-Al	72
	Metastable Polymorphism of Alloys Based on Elements of Group IV of the Periodic System	90
	Dilatometric Study of Transformations in Titanium Alloys	99
	Dislocation Theory of the Hydrogen Brittleness of Titanium Alloys	110
	Effect of Alloying on the Physicochemical Properties of Titanium	120
	Determination of the Characteristics of the Interdiffusion of Titanium and Molybdenum From the Attenuation of γ Radiation	137

Page

PART II. INTERACTION OF TITANIUM WITH GASES AND THE CORROSION PROPERTIES OF ALLOYS 146

On the Redistribution of Impurities in Titanium and Its Alloys During Oxidation 146

Effect of Oxygen on the Mechanical Properties of Heat-Treated Alloys AT3 and AT8 155

Characteristics of the Oxidation of Certain Titanium Alloys During Heating Prior to Plastic Deformation 161

Nitriding of Titanium Alloys at High Pressures 166

Corrosion of Titanium Alloys of Series VT and AT in Solutions of Sulfuric Acid Containing Nickel Sulfate 175

Chemical Stability of Titanium in Certain Aggressive Media and Scope of Its Use in Chemical Industrial Equipment 181

Chemical Stability of Titanium in Hydrohalic Acids and Halogens 188

Effect of Sodium Nitrite on the Corrosion of Titanium by Hydrochloric and Sulfuric Acid 202

Study of the Use of Titanium Alloys in the Construction of Food Machines 211

PART III. MECHANICAL AND TECHNOLOGICAL PROPERTIES OF TITANIUM ALLOYS 222

Basic Prerequisites for Developing High-Strength Titanium Alloys With an $\alpha + \beta$-Structure by Means of Alloying and Heat Treating 222

Strength of Interatomic Bonding of Single-Phase Alloys in the System Ti-Nb-Cr 223

Study of the Creep of Alloys in the System Ti-V-Nb-Mo 231

Characteristics of the Cold Brittleness of Titanium 239

Creep of Alloy AT3 at 350° 249

Study of the Creep and Thermal Stability of Alloy AT4 at 500° 255

Determination of the Relaxation Resistance of Alloy AT3 261

Creep of Alloys of the Quaternary System Ti-Zr-Al-Sn at 750° 269

Page

Study of the Mechanical Properties of Titanium Alloys AT3, AT4, AT6 and AT8 in Relation to the Testing Temperature 276

Study of the Comparative Heat Resistance of Titanium Alloys Sheet and Its Weld Joints at 450, 550, 650 and 700° 282

High-Temperature Strength of Alloys of the Quaternary System Ti-Al-Mo-V 283

Heat Resistance of Titanium Alloy AT8 in Short-Time Tests 289

Thermal Stability of Alloys AT3 at Temperatures of 350 and 400° 290

Effect of Conditions of Plastic Deformation and Subsequent Treatment on the Properties of Certain Titanium Alloys 297

Study of the Basic Parameters of Hot and Medium Temperature Rolling of Some Titanium Alloys Under Special Conditions of Stress 304

Some Studies of the Structure and Properties of Alloy VT5-1 During Heating for Stamping 305

Some Characteristics of the Heat Treatment of Alloy AT3 With a Low Content of Alloying Elements 311

Some Problems of Fusion Welding of Titanium and Its Alloys 318

Submerged Double-Arc Welding of Medium and Large Thickness Semifinished Products of Titanium Alloys 319

Study of the Mutual Diffusion of Titanium With Copper and Other Metals Suitable for Brazing 320

Use of Optical Emission Microanalysis in the Study of Titanium Alloys 321

Defect Inclusions in Titanium Ingots 332

Metastable Phases of Titanium Alloys and Conditions of Their Formation 340

PREFACE

The holding of annual scientific and technical conferences on the problem of titanium has become an established tradition. At such conferences, the results of research done by many scientific institutions and enterprises on various aspects of this problem during the preceding year are presented, and plans are drawn up for the further development of research and experimental industrial work on titanium and its alloys.

The present collection includes the works of the Fifth Scientific Conference, held in Moscow in March, 1963.

The section "Metal Chemistry of Titanium Alloys" offers the results of a further development in research on the chemical interaction between titanium and the major elements of the periodic system in simple and multicomponent systems, and presents phase diagrams with titanium as the main component that are of great scientific and practical interest.

Of particular importance are the results of research on the interaction of titanium and its alloys with gaseous admixtures, particularly oxygen, nitrogen, and hydrogen, and on the influence of these admixtures on the physical and mechanical properties of the alloys described in the second section of the collection. This section also provides data on the chemical stability and corrosion resistance of titanium and some of its alloys in various corrosive media.

The physical and mechanical properties of the alloys, the results of studies of the creep and relaxation resistance and comparative high-temperature strength of experimental industrial and mass produced alloys are comprehensively discussed in the third section of the collection.

The present collection constitutes evidence of the further progress made in the research on processes and phenomena taking place in titanium alloys under various conditions of industrial production and application, and directs the scientific and engineering thought toward the establishment of new goals in the problem of titanium and its alloys.

It is hoped that the publication of the present collection will be met with interest by the scientists, engineers, and technicians of the country and will foster further progress in the scientific investigation, production and extensive introduction of titanium and its alloys into various branches of modern technology.

I. I. Kornilov

PART I. METAL CHEMISTRY OF TITANIUM ALLOYS

PROSPECTS FOR THE DEVELOPMENT OF INVESTIGATIONS OF THE HEAT RESISTANCE OF TITANIUM ALLOYS

I. I. Kornilov

The problem of development of investigations into the heat resistance of titanium alloys has not been extensively treated in the literature. The statements of certain authors to the effect that on the basis of calculations of the diffusional mobility of titanium atoms it is difficult to expect a rise in the temperature limit of the high-temperature strength of titanium alloys above 400-450° are incorrect and have not been confirmed in practice. In its pure form, titanium displays creep even at room temperature, and this creep increases with rising temperature.

There are some real possibilities of substantially increasing the high resistance of titanium. They pertain to the physicochemical factors of the hardening of metals. By increasing the strength of the chemical bond obtained by forming solid solutions and compounds of titanium, one can raise the temperature level of the strength of titanium. These basic factors involved in raising the high-temperature strength of metals are discussed in references 1-4.

From the standpoint of the physicochemical theory of heat resistance of metal alloys which we formulated and developed (ref. 3), high-temperature hardening is determined by the nature of the chemical interaction of the components, the nature of the phases formed in the system, their state, which depends on equilibrium factors, and transformations in the solid state. An increase in high-temperature strength is achieved primarily as a result of the action of the solution and dispersion mechanisms of hardening of metal alloys (ref. 3). For this reason, an important aspect of the high-temperature strength of titanium alloys is the interaction of titanium with other elements.

On the basis of the chemical properties of titanium (refs. 4 and 5), we divided all the elements of the periodic system into three main groups in relation to titanium; these elements form with the latter:

(1) continuous solid solutions;
(2) limited solid solutions with metal compounds, and
(3) ionic compounds.

Of all the elements of the periodic system, those which are the most important for alloying titanium and hardening its alloys at high temperatures are those which we classified in the first and second group. There are over 50 such elements.

According to the classification which we adopted (ref. 4), the elements of these two groups are characterized by the following types of equilibrium diagrams:

1. Continuous solid solutions with α- and β-modifications of titanium, with $\beta \rightleftarrows \alpha$-transformations; these include systems of titanium with its close analogues Zr and Hf.

2. Continuous solid solutions with β-Ti, very limited solid solutions with α-Ti, and the two-phase $\beta + \alpha$ region; these include systems of titanium with metals of transition groups located close to titanium: V, Nb, Ta, Mo and U.

3. Limited solid solutions of α- and β-Ti with a peritectoid reaction and formation of compounds; these include systems with Al, Ge, Sn, Pb, La, Ce, B, C, O, N, etc.

4. Limited solid solutions of α- and β-Ti with a eutectoid reaction and the formation of compounds; these include systems with Cr, Mn, Fe, Co, Ni, Cu, Si, and many others.

All these types of interaction are reflected in the phase diagrams of these systems (ref. 6). We represented them in reference 5 in the form of generalized equilibrium diagrams according to the types of interaction.

In addition to these equilibrium diagrams of binary systems, one can also distinguish, in the corresponding ternary and more complex systems, quasi-binary and quasi-ternary systems which include systems made up of two, three or more metallic compounds of titanium. Among them, one can distinguish systems composed of isomorphous compounds such as Ti_3Al-Ti_3Sn, Ti_3Al-Ti_3In, Ti_3Sn-Ti_3In, $TiCr_2$-$TiFe_2$, $TiCr_2$-$ZrCr_2$, Ti_3Al-Ti_3Sn-Ti_3In, and many others. When certain conditions are maintained, all these systems of metallic compounds are capable of producing solid metallic solutions or ternary compounds.

The physicochemical theory of high-temperature strength (ref. 3) and the equilibrium diagrams of the systems make it possible to determine the dependence of the high-temperature strength on the composition and structure of the alloys, and to use the derived relationships for the establishment of the scientific principles to be used in the development of new heat-resistant titanium alloys.

Let us examine some experimental data on the high-temperature strength of titanium systems. As was shown in references 7 and 8 in the Ti-Zr system at relatively low temperatures (300-400°), the high-temperature strength in the

region of continuous solid solutions based on α-Ti changes with the composition by passing through a smooth maximum; as the temperature of the $\alpha \rightleftarrows \beta$ transformation (860°) is approached, the high-temperature strength is affected by the activated state of the atoms in the solid solution, which causes an increase in the rate of creep of the alloys. The same type of change in high-temperature strength should be expected in the Ti-Hf system.

In systems with continuous β solid solutions limited by α solid solutions of titanium and an intermediate two-phase $\alpha + \beta$ region, the high-temperature strength not only increases in the region of α solid solutions, reaching a small maximum near the boundary of the two-phase $\alpha + \beta$ region; in the two-phase region, the high-temperature strength decreases considerably, and as one moves into the region of β solid solutions and of increasing concentration of elements, the high-temperature strength increases again. We illustrated this with examples of the high-temperature strength of Ti-V and Ti-Nb systems (ref. 9). "Composition-high-temperature strength" diagrams of the systems Ti-Mo and Ti-Ta, which have not been studied experimentally, should be similar in character. Thus, in systems with continuous β solid solutions and limited α solid solutions, the "composition-high-temperature strength" diagrams show only one maximum near the boundary of the $\alpha \rightleftarrows \beta$ transformation, a minimum in the region of $\alpha + \beta$ phases, and an increase in high-temperature strength in the region of β solid solutions. Elements forming limited solid solutions with a peritectoid reaction have an appreciable effect on the increase in the high-temperature strength of titanium. Most effective in this respect were found to be alloys of the Ti-Al system in the region of α limited solid solutions. Here a major part is apparently played by Kurnakov-type compounds, which form in this system owing to the ordering of the structure of α solid solutions. Without considering the results of studies (refs. 5, 6, 10 and 11) on the refinement of the equilibrium diagram of the system to be definitive, one can tell that from the α solid solutions of this system are formed the compounds Ti_6Al and Ti_3Al (ref. 11) and, according to literature data (ref. 6), the compound TiAl, which crystallizes from the peritectic reaction. The presence of these compounds is particularly manifested in the variation of the mechanical properties (ref. 12) and high-temperature strength (ref. 13) of alloys of this system. The Ti-Sn is interesting in this respect. It also has a region of limited α solid solutions with a peritectoid reaction, and the compound Ti_3Sn, having a hexagonal lattice, is formed therein (ref. 14). The high-temperature strength of the alloys of this system with limited α solid solutions is characterized by a maximum near the limit of maximum solubility, a maximum value of the high-temperature strength of the δ phase based on the compound Ti_3Sn, and a minimum of high-temperature strength in the two-phase $\alpha + \delta$ region. "Composition-high-temperature strength" diagrams of this type should apply to the following analogous systems with limited solid solutions: Ti-Ag, Ti-Ge, Ti-In, Ti-Ga, Ti-Pb, Ti-Ce, etc.

The above-enumerated systems of limited α solid solutions of titanium and peritectoid reactions are the most promising for the development of heat-resistant titanium alloys. The high-temperature strength of systems with a low solubility of the components in α-Ti and a eutectoid reaction has been studied to a lesser extent. These systems (fig. 1) are characterized by low temperatures of the eutectoid transformation. The lowest temperature of the eutectoid

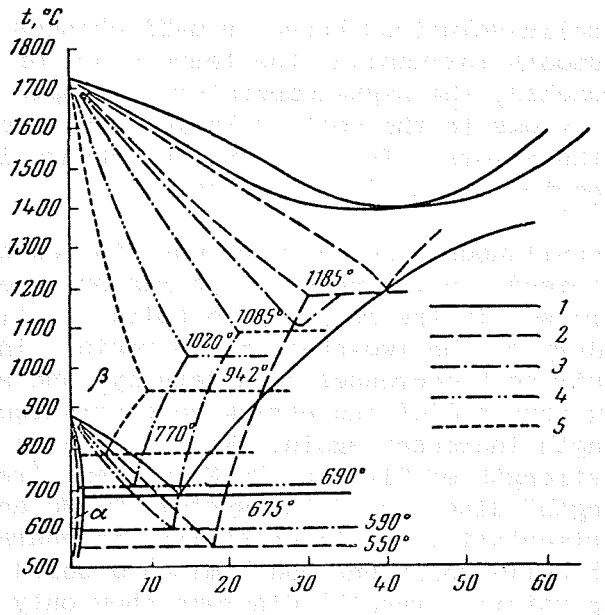

Figure 1. Phase diagrams of titanium systems with a eutectoid transformation. 1, Ti-Cr; 2, Ti-Mn; 3, Ti-Fe; 4, Ti-Co; 5, Ti-Ni.

transformation is found in the system Ti-Mn; the temperature of the eutectoid transformation rises as the elements of the 4th period become farther removed from Ti. On this basis, elements of the 4th period can be arranged in a series characterized by a gradual rise in the temperature of the eutectoid transformation, as follows: Mn → Fe → Cr → Co → Ni → Cu. A certain deviation of Mn and Fe from the sequence of this series has thus far remained unexplained. The solubility of these metals in α-Ti (fig. 1) amounts to tenths of one percent, with the exception of copper, in which it attains 2 atomic (at.) percent. The very limited solubility of these metals in α-Ti and the eutectoid transformation determine the high-temperature strength of the alloys of similar binary systems. A low strength can be expected in the systems Ti-Mn and Ti-Fe with low temperatures of the eutectoid transformation and a gradual rise in this strength can be expected as one passes to the systems Ti-Cr, Ti-Co and Ti-Ni, since in the latter a gradual rise in the temperatures of the eutectoid transformation is observed. The highest values of the high-temperature strength can be assumed to prevail in alloys of the system Ti-Cu, both because of the high concentration of solid solutions of copper in α-Ti, and because of the maximum value of the temperature of the eutectoid transformation of this system. An additional hardening in these systems also can be caused by dispersed precipitates of the excess phase from supersaturated α solid solutions of titanium. However, no experimental data are available on the high-temperature strength of such binary systems, and the latter must be investigated independently.

Systems composed of titanium compounds with other metals are promising for increasing the high-temperature strength of titanium. One of such interesting

systems is a quasi-binary section of the ternary system Ti-Al-Sn (refs. 15 and 16) passing through the compositions of two compounds: Ti_3Al and Ti_3Sn. An experimental study of this system showed that on the polythermal section of the alloys of these two compounds at high temperatures (fig. 2, upper part), the system is not quasi-binary and the alloys crystallize in the eutectic type. At low temperatures, below the temperature of formation of the compound Ti_3Al from the α solid solution, the system becomes a quasi-binary one composed of two intermetallic compounds, Ti_3Al-Ti_3Sn, Ti_3Al being formed from the α solid solution, and Ti_3Sn being formed during crystallization. These two compounds with an isomorphous hexagonal lattice form continuous solid solutions, as was shown in reference 16.

A study of the high-temperature strength of the alloys of this section as a function of Ti_3Sn content (by the flexural method) has shown that the strength changes in accordance with the "composition-high-temperature strength" diagram of the first type. As is evident from the series of curves in the lower part of

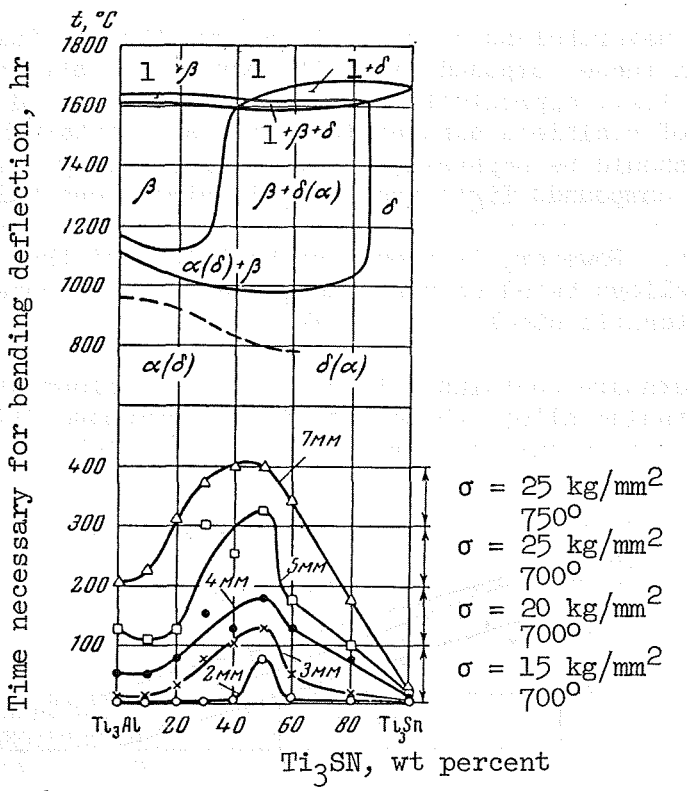

Figure 2. Phase diagrams and composition versus high-temperature strength of alloys of the ternary system Ti-Al-Sn along the section Ti_3Al-Ti_3Sn.

figure 2, the time necessary for the bending deflection to reach 2, 3, 4, 5 and 7 mm passes through a smooth maximum in the region of alloys containing 40-60 percent Ti_3Sn. The selected temperatures were 700-750°, and the stresses, 15-25 kg/mm^2. We obtained similar results on the section corresponding to compositions of the compounds Ti_6Al-Ti_3Sn.

Taking as the basis the compositions of the compounds Ti_6Al and Ti_3Al, by additional alloying with hardening elements, the author in collaboration with T. T. Nartova developed new heat-resistant titanium alloys based on Ti_6Al compounds with a working temperature up to 700°, and alloys based on Ti_3Al with a working temperature up to 800° (refs. 17 and 18).

In a study of the stress-rupture strength of alloys based on the compound Ti_6Al at 700° (fig. 3) by the standard extension method, we established the dependence of the time of failure of the specimens on the given stress (ref. 18).

Although data on the high-temperature strength and many other properties of alloys based on the compounds Ti_6Al and Ti_3Al have thus far been insufficient, it is nevertheless possible to assume that certain compositions of alloys based on these compounds make it possible to attain working temperatures of 600-800°, i.e., approximately those which correspond to the temperatures of application of stainless austenitic steels and certain heat-resistant nickel alloys. It should be emphasized that the specific gravity of titanium alloys based on the compounds Ti_6Al and Ti_3Al is almost one-half of that of steel and nickel alloys. However, it should be kept in mind that the plastic properties of titanium alloys based on these compounds will be considerably lower than those of austenitic steels and nickel alloys.

The literature contains evidence on the development of highly heat-resistant titanium alloys whose base is the compound TiAl (ref. 19), as we had also pointed out in our work (ref. 20). Of special significance is the group

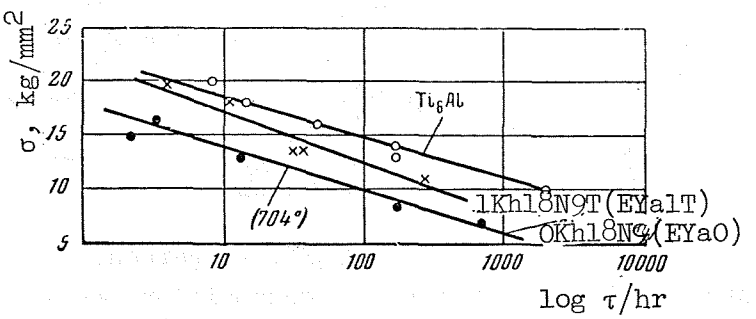

Figure 3. Stress-rupture strength of titanium alloy based on the compounds Ti_6Al and of austenitic steels at 700°.

of alloys based on intermetallic compounds that are heat-resistant casting titanium alloys. Real prospects for the development of new heat-resistant titanium alloys are opening up thanks to studies of multicomponent systems. This was pointed out in connection with the development of heat-resistant titanium alloys based on α solid solutions of the system Ti-Al-Cr-Fe-Si-B (ref. 21). Of great interest in this respect are ternary, quaternary and more complex systems based on titanium. In these systems, one can distinguish alloy compositions corresponding to the region of solid solutions of α- and β-Ti, and to quasi-binary and quasi-ternary sections of intermetallic systems.

Among promising heat-resistant alloys based on the α-structure one should also distinguish such important ternary systems as Ti-Al-Sn, Ti-Al-Zr, Ti-Al-Cu, Ti-Al-Mo and many others. Among quaternary systems of this series, the following may be considered important: Ti-Al-Sn-Zr, Ti-Al-Zr-Cu, Ti-Al-Zr-Cr, Ti-Al-V-Mo, etc.[1]

Let us examine the three-dimensional diagram of a part of the quaternary system Ti-Al-V-Mo (fig. 4). A wide region of α solid solutions which is adjacent to the edge of the tetrahedron is visible in this figure. In addition, in the portion of the system under study, there is a region of quaternary β solid solutions which is of interest in a study of heat-resistant alloys based on the stable β-structure.

An example of titanium alloys with a wide region of the stable β-structure is the ternary system Ti-Cr-Mo, studied in reference 22. One of the isotherms (at 600°) of the system (fig. 5) shows the principal phase regions in this

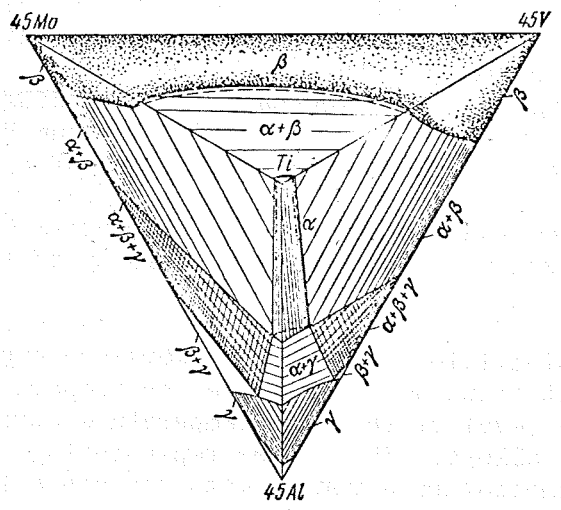

Figure 4. Three-dimensional diagram of a part of the quaternary system Ti-Al-Mo-V.

[1]The system Ti-Al-V-Mo was studied in detail by Ye. N. Pylayeva and Ko Chih-ming (see this collection, pp. 26-29).

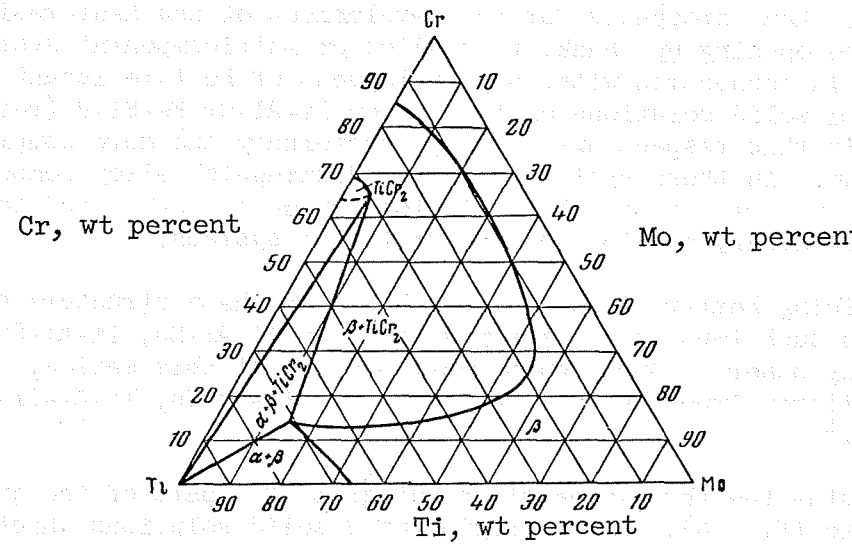

Figure 5. Isothermal section of the ternary system Ti-Cr-Mo at 600°.

system, including the wide region of β-ternary solid solutions. This system and other similar ones make it possible to develop new heat-resistant titanium alloys based on the stable β-structure.

Using the data of Ye. N. Pylayeva and Ko Chih-ming, we present a "composition-high-temperature strength" diagram of the alloys of the quaternary system Ti-Al-Mo-V (fig. 6). The alloys correspond to a radial section with 20 percent Al and a variable content of the sum V + Mo = 1:1. The same figure shows curves characterizing the time necessary for a bending deflection of 2, 5 and 10 mm as a function of the variable content of the sum V + Mo (from 0 to 5 percent). The tests were carried out at 700-800° and at a constant stress of 15 kg/mm^2. The curves show that the alloys of this system have maximum values of high-temperature strength at 700-800 in the vicinity of the saturation limit of the α solid solution.

Considering the possibilities of obtaining working temperatures of 600-800° for certain heat-resistant titanium alloys, one can compare the rates of increase in the temperature level of the high-temperature strength of titanium alloys with those of nickel alloys. The curves representing the rise in the temperature level of high-temperature strength with the years for titanium alloys (fig. 7, lower curve) and nickel alloys (fig. 7, upper curve) show that in approximately ten years (1952-1962) the temperature level of the strength of titanium alloys rose from 200 to 800°, i.e., by 600°, while the temperature level of nickel alloys increased in ten years (1949-1959) from 700 to 950°, i.e., by 250°.

This is explained by the fact that in titanium alloys there are unexploited possibilities of hardening and raising the temperature level of the high-temperature strength. Studies in this direction were begun only 5-6 years

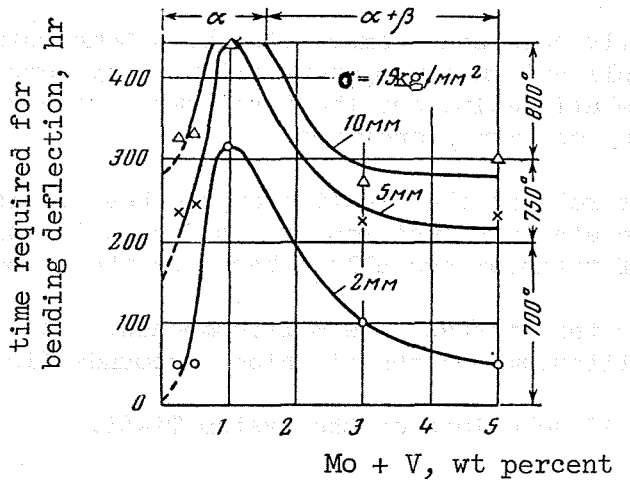

Figure 6. "Composition-high-temperature strength" diagram at 700-800° of alloys of the system Ti-Al-Mo-V; section with 20 percent Al at a variable content V:Mo = 1:1.

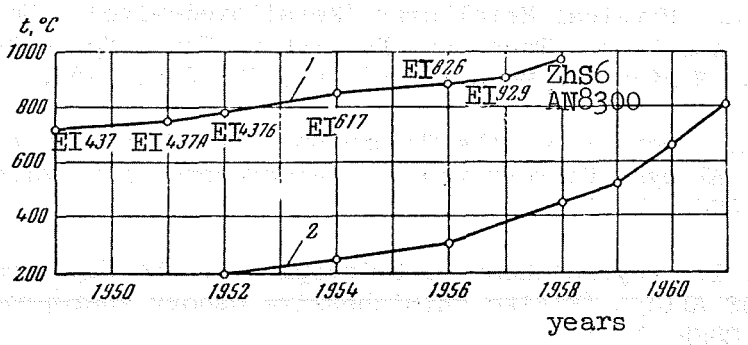

Figure 7. Rise in the temperature level of the strength of nickel (1) and titanium (2) alloys in 10 years.

ago, whereas the high-temperature strength of nickel alloys has now been studied for over 15 years, and the basic factors affecting their hardening have now been almost exhausted. The prospects for a further increase in the temperature level of the high-temperature strength of titanium alloys have not yet been exhausted, and further systematic investigations will make it possible to raise it still further.

Summary

1. The article has established certain relationships governing the dependence of the high-temperature strength of titanium alloys on the nature of the interaction of the components with titanium, types of equilibrium diagrams of the systems, and structure of the alloys.

2. Experimentally obtained "composition-high-temperature strength" diagrams of certain simple and multicomponent titanium systems will make it possible to use these relationships for the development of new heat-resistant titanium alloys having optimum properties.

3. An important role in the creation of new heat-resistant titanium alloys is played by the stable structures of α and β solid solutions and also by metallic compounds of titanium and alloys based on these compounds.

4. Promising in this respect are multicomponent α and β solid solutions of systems based on titanium and the titanium compounds Ti_6Al and Ti_3Al, which are formed from α solid solutions of the system Ti-Al.

5. Alloys made from the phases enumerated above can have working temperatures up to 600-800°.

REFERENCES

1. Bochvar, A. A. Physical Metallurgy (Metallovedeniye). Metallurgizdat, (State Scientific and Technical Publishing House for Literature on Ferrous and Nonferrous Metallurgy), pp. 287-297, 1956.

2. Osipov, K. A. Problems of the Theory and High-Temperature Strength of Metals and Alloys (Voprosy teorii zharoprochnosti metallov i splavov). Izd-vo AN SSSR, 1960.

3. Kornilov, I. I. Physicochemical Principles of the High-Temperature Strength of Alloys (Fiziko-khimicheskiye osnovy zharoprochnosti splavov). Izd-vo AN SSSR, 1961.

4. --- Izv. AN SSSR, OKhN, No. 4, p. 395, 1957.

5. --- Coll. "Titanium and Its Alloys" (Sb. "Titan i yego splavy"), No. 7, p. 5, 1962; No. 10, p. 10, 1963.

6. Hansen, M. and Anderko, K. Structures of Binary Alloys (Struktury dvoynykh splavov). Metallurgizdat, 1962.

7. Glazova, V. V. and Kurnakov, N. N. Izv. AN SSSR, OTN, Metallurgiya i Toplivo, No. 3, p. 67, 1961.

8. Grigorovich, V. K. and Safonov, Yu. S. Izv. AN SSSR, OTN, Metallurgiya i Toplivo, No. 5, p. 38, 1960.

9. Kornilov, I. I. and Vlasov, V. S. Izv. AN SSSR, OTN, Metallurgiya i Toplivo, No. 4, p. 31, 1958.

10. Ence, E. and Anderko, K. Trans. AIME, Vol. 221, No. 1, p. 151, 1961.

11. Grum-Grzhimaylo, N. V., Kornilov, I. I., Pylayeva, Ye. N. and Volkova, M.A. Dokl. AN SSSR, Vol. 137, No. 3, p. 599, 1961.

12. Moiseyev, V. N. Metallovedeniye i termicheskaya obrabotka metallov, No. 6, p. 30, 1960.

13. Kornilov, I. I., Pylayeva, Ye. N. and Volkova, M. A. Izv. AN SSSR, OKhN, No. 7, p. 771, 1956.

14. Kornilov, I. I. and Nartova, T. T. Zhurnal neorganicheskoy khimii, Vol. 5, No. 3, p. 662, 1960.

15. --- Dokl. AN SSSR, Vol. 131, No. 4, p. 837, 1960.

16. --- Dokl. AN SSSR, Vol. 140, No. 4, p. 829, 1961.

17. --- Izv. AN SSSR, OTN, Metallurgiya i Toplivo, No. 6, p. 142, 1962.

18. --- Dokl. AN SSSR, Vol. 148, No. 3, p. 644, 1963.

19. Andrew, J. and Kessler, H. J. Metals, Vol. 8, No. 10, 1956.

20. Kornilov, I. I. Izv. AN SSSR, OTN, Metallurgiya i Toplivo, No. 6, p. 130, 1960.

21. Kornilov, I. I., Mikheyev, V. S., Chernova, T. S. and Markovich, K. P. Sb. "Titan i yego splavy," Izd-vo AN SSSR, No. 7, p. 141, 1962.

22. Grum-Grzhimaylo, N. V. and Gromova, V. G. Coll. "Titanium and Its Alloys" (Sb. "Titan i yego splavy"). Izd-vo AN SSSR, No. 7, p. 36, 1962.

PHASE DIAGRAM OF THE SYSTEM Ti-O_2 AND SOME PROPERTIES OF THE ALLOYS OF THIS SYSTEM

I. I. Kornilov and V. V. Glazova

The character of the interaction between titanium and oxygen and the equilibrium diagram of this system heretofore have been based on the concept of the existence of a wide region of α solid solutions of titanium with oxygen and on the existence of the compounds TiO, Ti_2O_3 and TiO_2 in this system (fig. 1).

The variation in the physicochemical, mechanical and other properties of the alloys of the system Ti-O_2 has been also represented until now on the basis of a wide region of interstitial-type α solid solutions, up to 32 at.percent O_2 (refs. 1-7). The literature contains only limited data on detailed studies of the behavior of oxygen in the region of α solid solutions and on the influence of certain possible reactions in the alloys in the solid state on the properties of titanium alloys.

In the last few years, evidence has accumulated in some studies on the possibility of the formation of an ordered structure in the region of the α solid solution of titanium with oxygen. Investigations of alloys of titanium with oxygen by methods of x-ray structural analysis (refs. 8 and 9) and by the electrical resistance method (ref. 10) revealed an anomalous variation in properties when the alloy contained about 25 at percent O_2.

It was noted that the ordered state of alloys of this system is stable at temperatures up to 400° (ref. 8). Ye. S. Makarov (ref. 11) used the x-ray method to reaffirm the continuous nature of the variation in the crystal structure of the chemical compound of variable composition of α-phase-type in the system Ti-O_2; in the view of the authors of this article, this is associated with the continuous reaction of addition $Ti + xO = TiO_x + Q$, where x can change continuously from zero to a value corresponding to the boundary of phase inhomogeneity. This purely physical interpretation of the behavior of oxygen in α solid solutions based on titanium has not accounted for the chemical role of this metalloid in the formation of various types of compounds in a medium of metallic solid solutions.

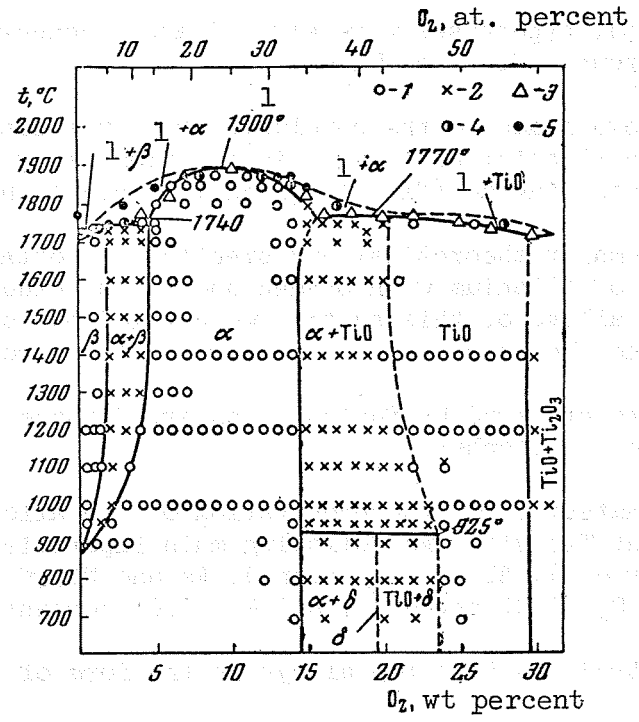

Figure 1. Equilibrium phase diagram of alloys of the system Ti-O_2 (according to the data of reference 5).

1, one phase; 2, mixture of phases; 3, start of fusion; 4, partial fusion; 5, complete fusion.

An analysis of the data on the interaction of metals of group IV of the periodic system with oxygen has enabled one of the authors (ref. 12) to postulate a possible formation of the compound Ti_3O in this system. This is confirmed in particular by a smooth maximum on the constitution diagram of the system Ti-O_2 corresponding to the region of 25 at.percent O_2 (fig. 1). The expressed arguments concerning possible suboxide compounds of titanium with a metallic bond character follow from an analysis of the chemical properties of titanium and its tendency to form intermetallic compounds with electronegative elements (refs. 12 and 13).

Considering the pronounced activity of oxygen atoms in interstitial solid solutions, one could assume the formation of similar compounds from the α solid solution in the system Ti-O_2 on slow cooling or prolonged exposure to low temperature conditions.

Later, on the basis of the very incomplete investigations of Hurlin (ref. 14) into the structure of the scale and investigations into the dependence of the electrical resistance of cast alloys on the composition carried out by

Wasilewsky (ref. 15), hypotheses were also advanced concerning the possible existence of the compounds Ti_6O and Ti_3O.

All of the above leads to the conclusion that the nature of the chemical interaction between titanium and oxygen is far from being as simple as would follow from the phase diagram (fig. 1) given in Hansen's handbook (ref. 5).

Attributing a major theoretical and practical importance to the problem of the interaction of titanium with oxygen and to the elucidation of the chemical nature of the alloys of this system, we carried out a detailed study of the system Ti-O_2 and the range of concentrations from zero to 35 at. percent O_2.

The alloys were prepared by fusion in an arc furnace with a nonconsumable electrode in an argon atmosphere.

The starting material for the preparation of the alloys was iodide titanium (99.9 percent Ti) with the following main impurities: Mg (0.01 percent), Si (0.01 percent), Al (0.01 percent), Fe and Ni (< 0.01 percent), Cr (0.01 percent), O_2 (0.01 percent), and N_2 (0.01 percent).

Oxygen was introduced into the alloys in the form of a Ti-O_2 master alloy containing 15.8 wt percent. The master alloy was prepared by melting bars pressed from titanium and titanium dioxide of 99.93 percent purity in an arc furnace.

The above method was used to prepare alloys containing 0, 1, 3, 5, 7, etc. at. percent oxygen up to 35 at. percent.

Alloys of 10 compositions were subjected to chemical analysis by using the vacuum fusion method. Results of the analysis showed that the oxygen content of the initial mixture was in good agreement with the data of the chemical analysis.

The cast alloys were subjected to homogenizing annealing in vacuum at 800° for 1000 hours.

After the homogenizing annealing at 800°, the alloys were annealed at 400, 600, 800, 850, 1000 and 1400° for 600, 400, 1000, 100, 100 and 2 hrs, respectively, and quenched in ice water.

In the study of the alloys, use was made of methods of physicochemical analysis developed by N. S. Kurnakov, which involved the plotting of "composition-property" phase diagrams (refs. 16 and 17).

Such methods included microscopic and x-ray structural analyses, measurement of microhardness, electrical resistance, and temf.

The microhardness was measured with a PMT-3 instrument under a load of 200 g using the method described in reference 18.

The etchant used to develop the microstructure of the alloys was a mixture made up of 20 pts. HF, 20 pts. HNO_3, and 60 pts. glycerin (by volume).

The electrical resistance of the alloys was measured by the probe method, since alloys containing more than 10 at. percent O_2 were brittle and could not be subjected to any kind of machining.

Specimens for the measurement of the electrical resistance were made by casting the alloys in ingots 6 mm in diameter. The electrical resistance was measured on specimens 25-30 mm high.

The temf was measured on specimens on which the electrical resistance had been studied earlier, in contact with copper.

The x-ray structural analysis was performed on powders prepared from samples for microscopic investigation and heat-treated at 400, 600, 800 and 1000°. The x-ray patterns were recorded with copper radiation and a nickel filter, using two films. Studies of alloys of the Ti-O_2 system by the above methods gave the following results.

Microstructural analysis of alloys quenched after prolonged annealing at 400° showed that alloys containing less than 10 and more than 22 at. percent O_2 consisted of a single phase. A second phase appeared in the structure of alloys with 10, 11, 12 and 13 at. percent O_2 and also in that of alloys with 16-21 at. percent O_2. Alloys with 14 and 15 at. percent had a single phase.

The structure of alloys quenched from 600° was approximately the same as that of alloys quenched from 400°.

The alloy with 5 at. percent O_2 has a polyhedral structure (fig. 2a), and the alloys with 10 and 16 at. percent O_2, a two-phase structure (fig. 2b and c). The alloy with 25 at. percent O_2 is characterized by the presence of slip lines in the structure (fig. 2d). The same structure was observed in alloys with a higher oxygen content, up to 30 at. percent (fig. 2e). The microstructure of the alloy with 35 percent oxygen is shown in figure 2f.

Microscopic analysis of alloys quenched from 800° showed that those with 13, 14 and 16 at percent O_2 were two-phase alloys, and that the structure of the remaining ones was polyhedral. It should be noted that all specimens of alloys containing more than 10 at. percent O_2 were covered with cracks and pores whose quantity increased with rising oxygen content.

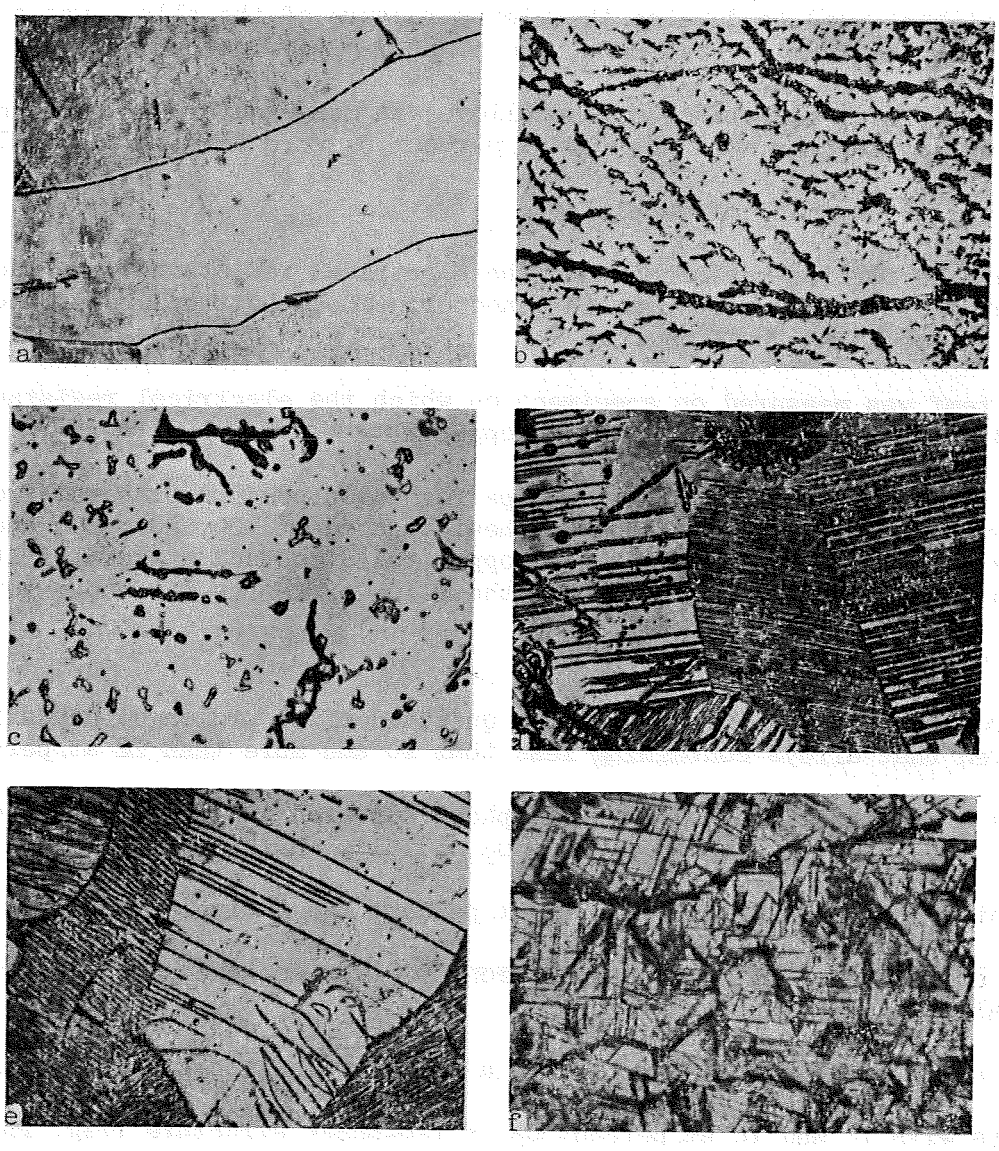

Figure 2. Microstructures of alloys of the system Ti-O_2 with the following content: a, 5 percent O_2, quenching after annealing at 600°, x 500; b, 10 percent O_2, quenching after annealing at 600°, x 500; c, 16 percent O_2, quenching after annealing at 600°, x 500; d, 25 percent O_2, quenching after annealing at 600°, x 200; e, 30 percent O_2, quenching after annealing at 800°, x 200; f, 35 percent O_2, cast state, x 200.

Alloys quenched from 850° had a polyhedral structure, with the exception of the alloy with 25 at. percent O_2, which retained the slip lines at all quenching temperatures.

In the analysis of the microhardness of alloys of the Ti-O_2 system quenched from 400 and 600°, the "microhardness-composition" curves displayed two singular minima corresponding to compositions with 14.5 and 25 at. percent O_2 (fig. 3a).

The isotherm at 800° has a noticeable inflection on the curve at 14.5 at. percent O_2, and a marked minimum at 25 at. percent O_2.

Isotherms at 1000 and 1400° of the "microhardness-composition" curves display singular minima for the composition with 25 percent O_2.

It should be emphasized that one group of alloys in the cast state exhibited a microhardness maximum in the alloy with 25 at. percent O_2, which following heat treatment at 800° changed into a minimum.

Figure 3b shows the dependence of the electrical resistance on the composition of alloys quenched after holding at 800, 1000 and 1400°.

On quenching from 800°, the electrical resistance rises abruptly from 45.8 mohm/cm for pure titanium to 158 mohm/cm for the alloy with 10 at. percent O_2. In the alloy with 15 at. percent O_2, the electrical resistance rises sharply, reaching 466 mohm/cm; this is followed by a rise to 500 mohm/cm for the alloy with 22 at. percent O_2, then by a sharp decline in electrical resistance.

The alloy with 25 at. percent O_2 has a resistance of 150 mohm/cm. As the oxygen content increases, the electrical resistance rises to 639 mohm/cm.

An analysis of the curve representing the electrical resistance of alloys quenched from 1000 and 1400° versus composition shows the presence of a singular minimum at 25 at. percent O_2. It should be noted that in many cases at 25 at. percent O_2, the cast specimens display a maximum which after a prolonged annealing of the specimens changes into a minimum.

Let us examine the dependence of the temf of alloys of the Ti-O_2 system on the oxygen content, in a couple with copper after quenching from 800, 1000 and 1400° (fig. 3c)

On quenching from 800°, the temf decreases sharply from pure titanium (30 mV/deg) to a composition with 14 at. percent O_2 (-78 mV/deg). It should be

noted that at a content of 5 at. percent O_2, the temf changes sign, indicating a change in the type of conduction from hole to electron conduction. In the alloy with 25 percent O_2, the value of temf is at a minimum.

On the isotherms at 1000 and 1400°, a singular minimum is preserved only in the composition with 25 at. percent O_2.

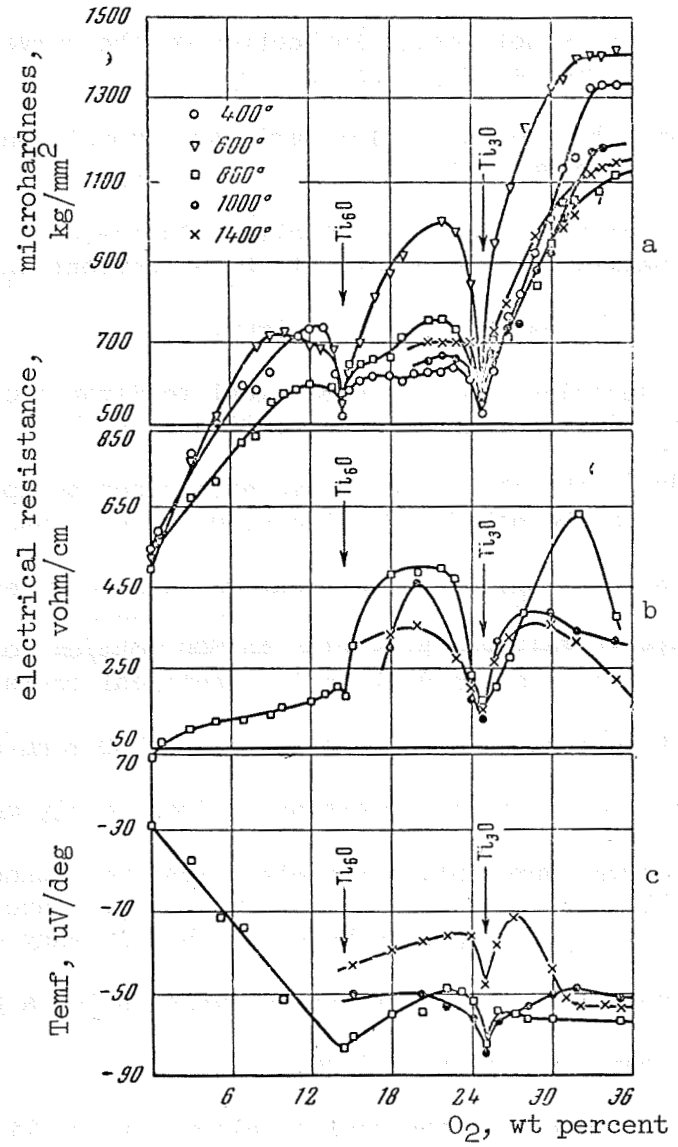

Figure 3. Dependence of the microhardness (a), electrical resistance (b) and temf (c) on the composition of alloys of the system Ti-O_2 after quenching from various temperatures.

Preliminary data of x-ray structural analysis show that the alloy with 25 at. percent O_2 at temperatures up to 1400° has one superstructure line, while no superstructure lines have thus far been observed in the alloy with 14.5 at. percent O_2 under these conditions of heat treatment.

Thus, based on the results of microstructural analysis and on the "composition-property" diagrams in the concentration range studied, one can assume that in the Ti-O_2 system there are two new compounds: Ti_6O and Ti_3O.

The nature of the "composition-property" chemical diagrams at 800° and also data of the microscopic analysis lead to the conclusion that the compound Ti_6O is stable up to 820-830°.

The compound Ti_3O with an ordered structure is apparently stable above 1400°, since the singular character of the "composition-property" diagrams at this temperature remains unchanged.

A study of the state of this compound at higher temperatures up to the melting point (1900°) requires a special investigation.

The results of the present study have produced a new equilibrium phase diagram of the alloys of the Ti-O_2 system for compositions containing less than 35 at. percent O_2. It follows from this diagram that the compounds Ti_6O and and Ti_3O are formed in the Ti-O_2 system.

The similarity between titanium and zirconium and the nature of their interaction with oxygen leads to the assumption that the compound Zr_6O and Zr_3O may exist in the system Zr-O_2.

The new compounds Ti_6O and Ti_3O established in the present work, and the regions of their existence on the phase diagram of the Ti-O_2 system are of major importance in the metal chemistry and physical metallurgy of titanium alloys. These new compounds should serve as a basis for the study of equilibria in complex titanium systems with oxygen, and for the elucidation of the influence of oxygen on the physicochemical and mechanical properties of titanium and its alloys (ref. 19).

In the light of what was stated above, it appears very interesting to study the influence of oxygen on the characteristics of the stability of the chemical bond, since it is these characteristics which, in the final analysis, determine the degree of stability of the alloys in applications at high temperatures.

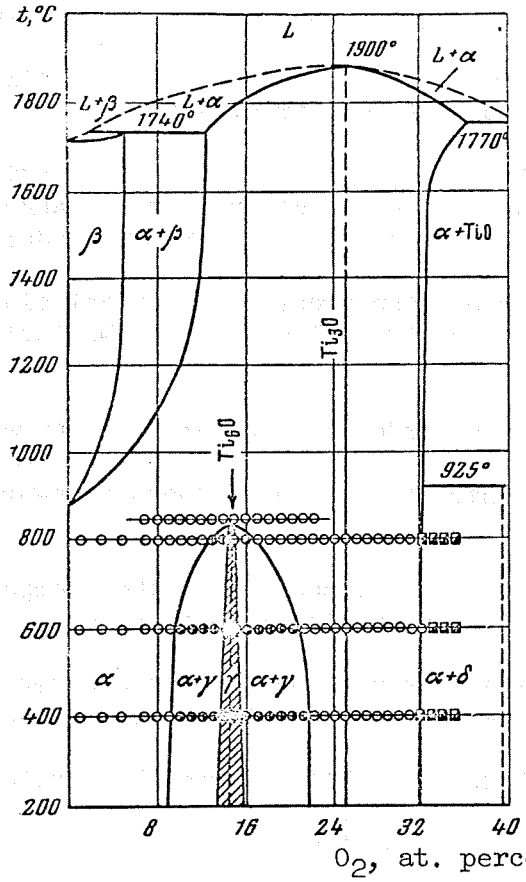

Figure 4. Phase diagram of alloys of the system Ti-O_2 (based on the data of the present work).

o, structure of the α solid solution; ●, α + γ phase; ■, α + δ phase.

The pertinent data for the Ti-O_2 system which are available in the literature are scarce and pertain to a concentration range of not more than 20 at. percent O_2.

To solve this problem, we undertook detailed investigations of the thermal expansion of the alloys of the Ti-O_2 system in the concentration range from zero to 32 at. percent O_2 at temperatures up to 800°. This study was made with an indicator dilatometer (ref. 20), using specimens quenched from 800° after soaking for 1000 hrs.

The heating was carried out at the rate of 4 deg/min.

In order to compare the Ti-O_2 system with the equilibrium phase diagram (fig. 5a), we show the dependence of the ratio $\Delta l/l$ on the composition of the alloy at 100, 200, 300, 400, 500, 600, 700 and 800° (fig. 5b).

It follows from this figure that all the isotherms are qualitatively similar in character. At first, when titanium is alloyed with oxygen, the thermal expansion at every given temperature shows a certain decrease. A relatively slight minimum corresponds to the composition Ti_6O. A further rise in oxygen content causes an increase in thermal expansion up to 23 at. percent O_2, and this is followed by a precipitous decline. A marked singular minimum corresponds to the composition Ti_3O.

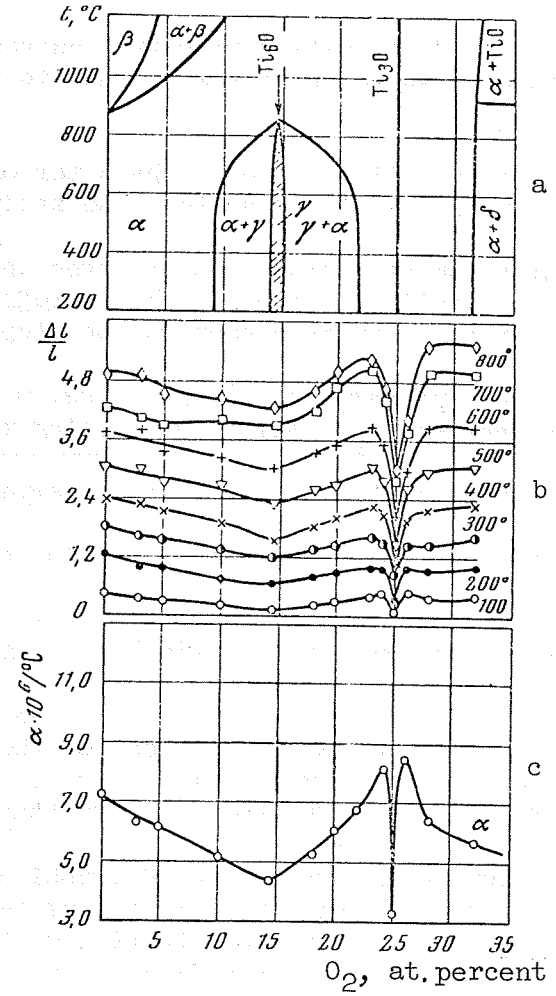

Figure 5. Comparison with the equilibrium phase diagram (a) of the dependence of the thermal expansion (b) and its coefficient (c) on the composition of alloys of the system Ti-O_2.

From these data, values of the coefficient of thermal expansion α as a function of the composition for the temperature range of 20-100° were calculated (fig. 5c). It follows from this figure that the concentration dependence α is qualitatively similar in character to the dependence of Δ 1/1 on the composition (fig. 5b).

The data obtained on the thermal expansion of alloys of the Ti-O_2 system over a wide concentration range lead to the conclusion that when titanium is alloyed with oxygen, the stability of the chemical bond in the alloys increases up to 14.5 at. percent O_2. The character of the concentration dependence of this characteristic is distinguished by the presence of specific points corresponding to the compounds Ti_6O and Ti_3O.

It should be noted that the compound Ti_3O is particularly characterized by sharp singular extrema of the "composition-property" curves; this feature sets it apart as a chemical species whose interatomic bonds in the crystal lattice are very strong.

In connection with the investigated novel character of the chemical interaction and phase equilibrium in the Ti-O_2 system, the study of the influence of oxygen on the creep of titanium at various temperatures appeared of great interest. In contrast to the studies of other authors (refs. 1-4), this property was studied over a wide range of oxygen concentrations (up to 18 at. percent).

To this end, alloys were prepared containing 0.02, 0.39, 0.75, 1.25, 1.66, 3, 4, 8, 10, 15 and 18 at. percent O_2. Alloys containing more than 4 at. percent O_2 were prepared by the powder method at a sintering temperature of 1500°. Alloys of all compositions were annealed at 800° for 200 hr and were slowly cooled from this temperature.

Tests for hot hardness were made with a VIM-1 unit at pressures of 10^{-3}-10^{-4} mm Hg. The hardness was determined by indenting the specimen with a diamond pyramid having a leap angle of 136°. The load on the indenter was 1 kg. The duration of deformation at each temperature was 0.5, 5 and 50 min. The measurements were made at 300, 400, 500, 600 and 700° (table 1).

The results of the measurements were treated graphically by plotting the diagonal of the indentation versus log time for various temperatures. It was thus established that the time dependence of the size of the diagonal of the indentation at each temperature is described fairly rigorously by the equation

$$d = a\tau^b, \qquad (1)$$

where a and b are parameters dependent on the nature of the alloy, the testing temperature and the load on the indenter; τ is the testing time.

Parameters a and b were determined (table 2) from the working graphs for the dependence of the logarithm of the holding time under load.

On the basis of these data and from the equation

$$\lg V_d^* = \lg b + \frac{\lg a - \lg d}{b}, \qquad (2)$$

proposed in references 22 and 23, a calculation was made of the rate of creep at the instant when a given value of the indentation diameter was reached.

In references 21 and 22 it was shown that the concentration dependence of the log of the rate of creep for a series of alloys was in qualitative agreement with the concentration dependence of the rate of creep obtained during extension.

Values of log V_d of alloys of the Ti-O_2 system for d = 0.12 mm (at 300, 400 and 500°) and d = 0.18 mm (at 600 and 700°), calculated from equation (2) are shown in Table 2.

We shall compare the concentration dependence of the log of the rate of creep, log V_d (figs. 6b and c), with the equilibrium phase diagram of the system Ti-O_2 (fig. 6a).

The concentration dependences of log V_d shown on the graph give a clear representation of the behavior of the alloys of the Ti-O_2 system at high temperatures under load. It should be noted that in an analysis of these results, the highest stability of the alloys under load corresponds to the lowest negative values of log V_d.

At 300°, the isotherm of log V_d is characterized by an appreciable drop in the concentration range from zero to 2 at. percent, where oxygen has practically no influence on the change in log V_d, and hence, on the stability of the alloys under load.

A further increase in oxygen content causes a sharp drop on the curve representing the concentration dependence of log V_d; this corresponds to an increase in the stability of the alloys under load, and log V_d becomes 4 times smaller than in pure titanium. A comparison of this curve with the equilibrium

TABLE 1. VALUES OF THE DIAGONAL OF THE INDENTATION (IN mm) OF THE DIAMOND PYRAMID FOR ALLOYS OF THE SYSTEM Ti-O_2 AT VARIOUS TEMPERATURES AND TESTING TIMES OF 0.5, 5 AND 50 MIN.

O_2 content at. percent	300°			400°			500°			600°			700°		
	0.5 min	5 min	50 min	0.5 min	5 min	50 min	0.5 min	5 min	50 min	0.5 min	5 min	50 min	0.5 min	5 min	50 min
0,02	0,164	0,173	0,183	0,190	0,194	0,198	0,192	0,198	0,283	0,236	0,238	0,242	0,229	0,298	0,395
0,39	0,111	0,128	0,134	0,145	0,151	0,154	0,156	0,166	0,175	0,177	0,182	0,190	0,194	0,217	0,254
0,75	0,101	0,107	0,112	0,111	0,121	0,132	0,132	0,144	0,158	0,159	0,166	0,199	0,174	0,209	0,243
1,21	0,097	0,099	0,109	0,111	0,120	0,128	0,135	0,142	0,149	0,13	0,153	0,170	0,186	0,228	0,284
1,66	0,099	0,102	0,106	0,105	0,112	0,126	0,116	0,125	0,132	0,130	0,145	0,157	0,162	0,190	0,221
3	0,08	0,087	0,095	0,092	0,099	0,107	0,112	0,121	0,132	0,128	0,142	0,159	0,169	0,209	0,260
4	0,0815	0,0915	0,099	0,098	0,109	0,113	0,113	0,113	0,114	0,114	0,130	0,160	0,153	0,179	0,206
8	0,063	0,064	0,071	0,070	0,072	0,077	0,077	0,080	0,0845	0,084	0,088	0,112	0,112	0,125	0,197
10	0,0605	0,063	0,064	0,0675	0,071	0,072	0,0735	0,076	0,079	0,079	0,082	0,105	0,120	0,162	0,201
15	0,057	0,059	0,061	0,0615	0,0625	0,063	0,062	0,0705	0,0795	0,084	0,086	0,094	0,099	0,121	0,150
18	—	—	—	0,060	0,0645	0,0715	0,0715	0,078	0,0905	0,084	0,093	0,107	0,100	0,104	0,138

TABLE 2. VALUES OF THE PARAMETERS a, b AND LOG V_d AT VARIOUS TEMPERATURES.

O_2 content at. percent	300°			400°			500°			600°			700°		
	a	b	lg V_d	a	b	lg V_d	a	b	lg V_d	a	b	lg V_d	a	b	lg V_d
0,02	0,1677	0,025	+4,21	0,1788	0,03	+4,25	0,1979	0,04	+ 4,024	0,205	0,045	—0,106	0,2483	0,12	+0,24
0,39	0,1219	0,025	—1,323	0,1461	0,025	+1,88	0,1607	0,025	+ 3,4	0,1712	0,025	—0,80	0,2016	0,055	—0,21
0,75	0,1031	0,025	—4,41	0,1141	0,04	—1,96	0,1349	0,045	— 0,25	0,1648	0,05	—2,16	0,1830	0,07	—0,72
1,21	0,0902	0,03	—5,86	0,1135	0,035	—2,26	0,1247	0,045	— 1,13	0,1371	0,055	—3,62	0,1977	0,09	—1,22
1,66	0,0975	0,02	—10,7	0,1072	0,03	—3,19	0,1172	0,035	— 2,03	0,1340	0,045	—4,45	0,1698	0,065	—1,65
3,0	0,0824	0,035	—6,31	0,0933	0,04	—4,15	0,1154	0,04	— 1,9	0,1321	0,055	—4,11	0,1803	0,09	—1,60
4,0	0,0851	0,03	—6,53	0,1005	0,035	—3,46	0,098	0,04	— 2,0	0,0645	0,07	—4,73	0,1607	0,075	—1,93
8,0	0,0631	0,035	—6,2	0,071	0,035	—3,30	0,078	0,04	— 1,1	0,085	0,075	—4,5	0,113	0,075	—2,05
10,0	0,0614	0,015	—21,1	0,068	0,02	—14,2	0,0738	0,025	—10,41	0,0785	0,065	—6,89	0,1306	0,12	—2,18
15,0	0,0577	0,015	—21,3	0,061	0,02	—16,7	0,065	0,05	— 6,71	0,0785	0,055	—8,0	0,1002	0,095	—3,66
18,0	—	—	—	0,0614	0,04	—8,9	0,0735	0,05	— 5,71	0,0857	0,06	—6,73	0,1059	0,07	—4,59

Note: Commas represent decimal points in tables.

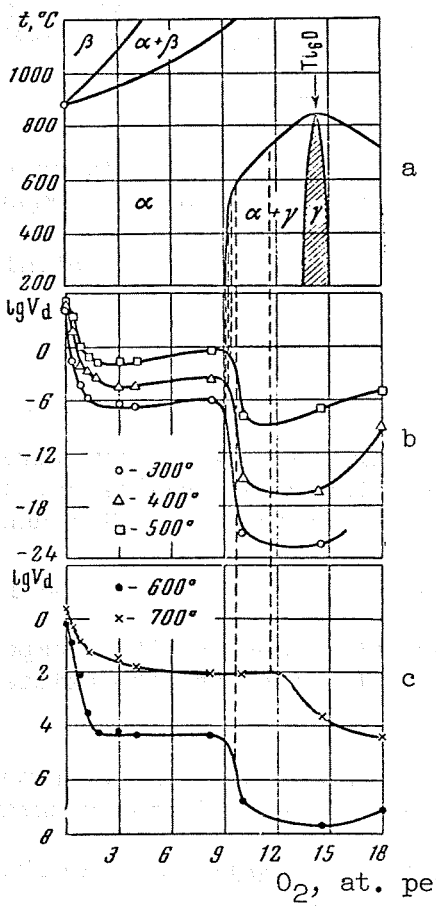

Figure 6. Comparison of the equilibrium phase diagram with the dependence of the creep rate on the composition of the alloys of the system Ti-O_2.

phase diagram of the Ti-O_2 system shows that a sharp increase in the resistance to plastic deformation, according to the physicochemical theory of high-temperature strength (ref. 23), is associated with a shift to the two-phase region ($\alpha + \gamma$), in which the second (γ) phase is a solid solution based on the compound Ti_6O and belonging to the class of Kurnakov's compounds.

The isotherms of log V_d at 400, 500 and 600° are completely similar in character, and in the concentration range of 2-8 at. percent O_2 there is even observed a tendency toward an increase in log V_d or a decrease in the resistance to the plastic deformation of the alloys at these temperatures.

The isotherm of log V_d at 700° for the alloy with 10 at. percent (3.58 wt percent) O_2 does not show any increase in the resistance to plastic deformation,

as in the case of other temperatures, and this again corresponds to the established phase diagram of the Ti-O_2 system, since at 700° the alloy with 10 at. percent O_2 remains a single-phase alloy.

Thus, a complete correlation is observed between the nature of the chemical interaction in the Ti-O_2 system, the type of "composition-creep" diagram at various temperatures, and the character of the atomic interaction in this system.

Summary

1. Methods of microstructural and x-ray structural analysis as well as measurements of microhardness, electrical resistance, and temf were used to study the alloys of the Ti-O_2 system quenched after annealing at various temperatures in the concentration range of zero to 35 at. percent O_2.

2. Results of these investigations and the "composition-property" diagrams obtained made it possible to establish the existence of the new compounds Ti_6O and Ti_3O.

3. The concentration and temperature limits of the existence of these compounds were determined, and a new equilibrium diagram of the Ti-O_2 system was proposed. The compound Ti_6O is stable up to 820-830°, while the compound Ti_3O is thought to be stable above 1400°. The compositions of the compounds should be characterized by a maximum degree of ordering of oxygen atoms in the lattice of the α solid solution.

4. The thermal expansion of the alloys of the Ti-O_2 system was studied over a wide temperature and concentration range. On the basis of the data obtained, the dependence of the coefficient of thermal expansion on the composition of the alloys of the Ti-O_2 system was established. Analysis of the concentration dependence of this property led to the conclusion that the stability of the chemical bond between the atoms of titanium and oxygen increases in the crystal lattice of alloys and compounds Ti_6O and Ti_3O.

5. The hot hardness of the alloys of the Ti-O_2 system were studied in the concentration range of zero to 18 at. percent and in the temperature range of 300-700° for various holding times under load at each temperature. From the data obtained, the rates of plastic flow of the alloys of this system at the instant when a given value of the indentation size was reached were calculated.

6. The general nature of the influence of oxygen on the behavior of titanium under load at various temperatures was established, and a correlation between this dependence and the new equilibrium phase diagram of the Ti-O_2 system was noted.

Finally, the authors express their thanks to T. F. Zhuchkova, who was of great assistance in the execution of this work.

REFERENCES

1. Borisova, A. A. Coll. "Titanium and Its Alloys," Izd-vo AN SSSR, No. 3, p. 23, 1960.

2. Jehknis, A. and Worher, H. J. Inst. Metals, Vol. 80, No. 4, p. 157, 1951.

3. Yakimova, A. Ya. Influence of Hydrogen and Oxygen on the Properties and Structure of Titanium Alloys. Author's abstract of candidate's dissertation (Vliyaniye vodoroda i kisloroda na svoystva i strukturu titanovykh splavov. Avtoref. kand. diss.). Institut metallurgii imeni A. A. Baykova (A. A. Baykov Institute of Metallurgy), Moscow, 1959.

4. Suiter, J. J. Inst. Metals, Vol. 83, part 10, p. 460, June 1955.

5. Hansen, M. and Anderko, K. Structure of Binary Alloys (Struktura dvoynykh splavov). Metallurgizdat, Vol. 2, 1962.

6. Ehrlich, P. P. z. Anorg. Chem., Vol. 247, p. 53, 1941.

7. Bamps, E., Kessler, H. and Hansen, M. TASM, Vol. 45, p. 1008, 1953.

8. Anderson, S., Collen, B., Kuylenstierna, U. and Magnelli, A. Acta Chem. Scand., Vol. 7, No. 10, p. 1641, 1957.

9. Nowotny, H. and Dimakopoulu, E. Monatshf. f. Chem., Vol. 90, No. 5, p. 620, 1959.

10. Wasilewsky, R. Trans. AJME, p. 3, November 1957.

11. Makarov, Ye. S. and Kuznetsov, L. M. Zhurnal Strukturnoy Khimii, Vol. 1, No. 2, p. 170, 1960.

12. Kornilov, I. I. Trudy Komissii po analiticheskoy khimii AN SSSR (Transactions of the Commission on Analytical Chemistry of the Academy of Sciences of the USSR), Izd-vo AN SSSR, Vol. 10, p. 18, 1960.

13. --- Izv. AN SSSR, OTN, Metallurgiya i Gornoye Delo, No. 1, p. 152, 1963.

14. Hurlen, T. J. Inst. Metals, Vol. 89, No. 4, 1960.

15. Wasilewsky, R. J. Trans. AJME, No. 4, p. 8, 1962.

16. Kurnakov, N. S. Introduction to Physicochemical Analysis (Vvedeniye v fiziko-khimicheskiy analiz). Izd-vo AN SSSR, 1938.

17. Pogodin, S. A. and Anosov, V. A. Fundamentals of Physicochemical Analysis. Izd-vo AN SSSR, 1947.

18. Glazov, V. M. and Vigdorovich, V. N. Microhardness of Metals (Mikrotverdost' metallov). Metallurgizdat, 1960.

19. Kornilov, I. I. and Glazova, V. V. Doklady AN SSSR, Vol. 150, No. 2, p. 313, 1963.

20. Mints, R. S. Zav. lab., No. 12, p. 1526, 1958.

21. Osipov, K. A. and T'ien Te-ch'eng. Izv. AN SSSR, Metallurgiya i Toplivo, No. 4, p. 77, 1959.

22. Osipov, K. A. Problems of the Theory and High-Temperature Strength of Metals and Alloys (Voprosy teorii zharoprochnosti metallov i splavov). Izd-vo AN SSSR, 1960.

23. Kornilov, I. I. Physiochemical Principles of High-Temperature Strength (Fiziko-khimicheskiye osnovy zharoprochnosti). Izd-vo AN SSSR, 1961.

EQUILIBRIUM DIAGRAM OF THE QUATERNARY SYSTEM Ti-Al-Mo-V

E. N. Pylayeva and Ko Chih-ming

The study of the phase equilibrium of alloys of the quaternary system Ti-Al-Mo-V adjacent to the titanium vertex of the tetrahedron (fig. 1) is of theoretical and practical importance, since this system can be used as the basic multicomponent system for the development of new high-strength and heat-resistant alloys of low density.

In its chemical properties, aluminum differs substantially from titanium and forms limited solid solutions and a series of metallic compounds with its α and β modifications (refs. 1-3).

Vanadium and molybdenum are located in the fifth and sixth groups of the periodic system, close the titanium group, and are close to the latter in atomic radii, electronegativity and other properties. They are capable of forming continuous binary and ternary solid solutions with β-Ti and limited solid solutions with α-Ti (refs. 1 and 4). Vanadium and molybdenum are important alloying elements for high-strength titanium alloys having a β structure.

The position of vanadium and molybdenum in the periodic system in relation to titanium and their similar chemical properties also account for their similar behavior in titanium alloys. Thus, for example, the binary systems Ti-Mo and Ti-V have the same type of phase diagram (ref. 1).

In the ternary system Ti-Mo-V, there is observed a continuous shift of the α and β solid solutions and of the two-phase $\alpha + \beta$ region from the system Ti-Mo to the system Ti-V. This is clearly indicated by the isothermal section of the ternary system Ti-Mo-V at 600° (fig. 2).

The phase regions α, $\alpha + \beta$ and β shift from the side of Ti-Mo toward that of Ti-V, the region of the α solid solution expanding continuously from the side of Ti-Mo (up to 0.8 percent Mo) to the side of Ti-V (2 percent V). The boundary between the $\alpha + \beta$ and β region passes through the points of 28 percent Mo in the Ti-Mo system, 31 percent (Mo + V) in the Ti- (Mo:V = 1:1) system, and 22 percent V in the Ti-V system.

The similarity in the chemical properties of molybdenum and vanadium in relation to titanium explains the possibility of formation of similar phase

diagrams not only in the binary systems Ti-Mo and Ti-V but also in ternary systems in the portion rich in titanium, for example, in the systems Ti-Al-Mo and Ti-Al-V (refs. 5 and 6).

In order to study the phase equilibrium in the quaternary system Ti-Al-Mo-V, we investigated the ternary system Ti-Al-Mo and the system Ti-Al- (Mo:V = 1:1), which is the section of the concentration tetrahedron of the quaternary system originating at the edge of the binary system Ti-Al with a constant ratio of the weight concentration Mo:V = 1:1. The position of these two systems in the tetrahedron is shown in figure 1 and their investigated portions are shaded.

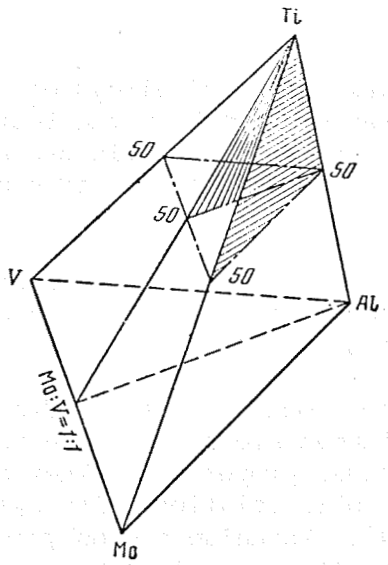

Figure 1. Concentration tetrahedron of the quaternary system Ti-Al-Mo-V.

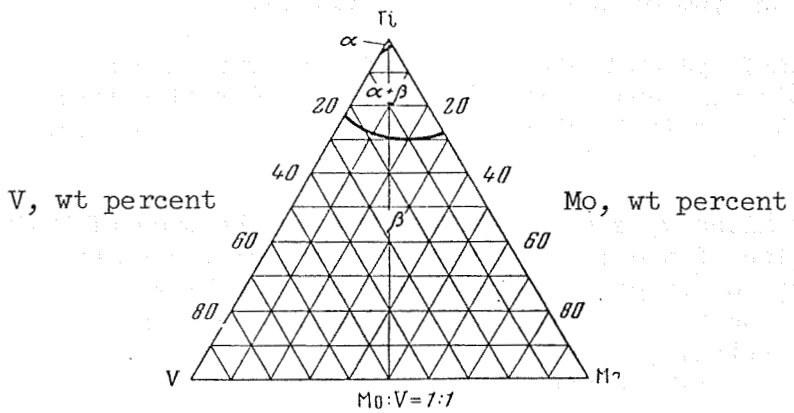

Figure 2. Isothermal section of the ternary system Ti-Mo-V at 600°.

Let us examine (figs. 3 and 4) the isothermal sections at 600° of the systems Ti-Al-Mo and Ti-Al-(Mo:V = 1:1). A comparison of the isothermal sections of these systems at 600° with the system Ti-Al-V (ref. 6) leads to the conclusion that in these three systems in the portion rich in titanium, the same phase regions are in equilibrium, namely:

a. Solid solutions based on α-Ti with a hexagonal close-packed structure;

b. Solid solutions based on β-Ti with a cubic body-centered structure;

c. Limited γ solid solutions based on the compound TiAl with an ordered face-centered tetragonal structure;

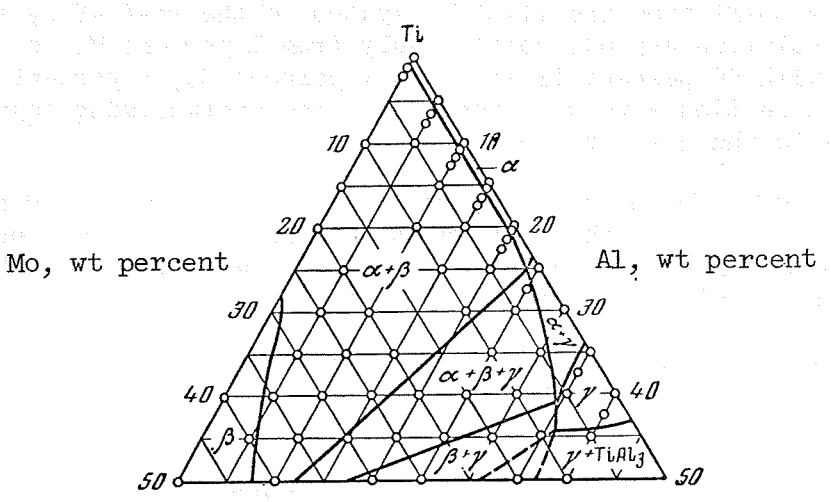

Figure 3. Isothermal section of a part of the ternary system Ti-Al-Mo at 600°.

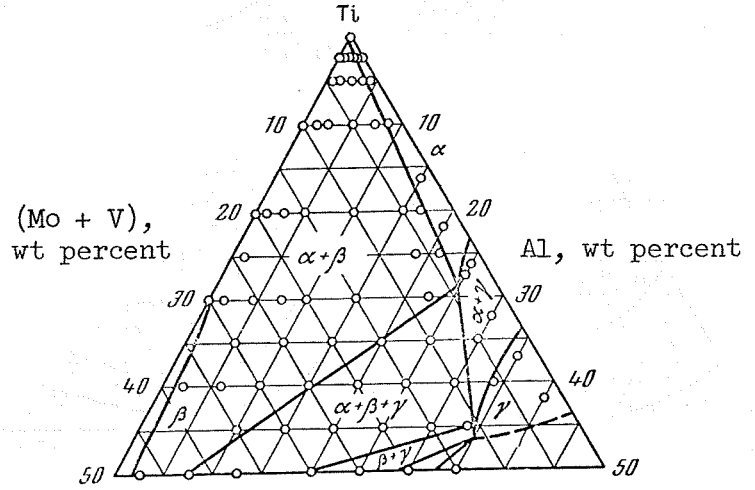

Figure 4. Isothermal section of a part of the system Ti-Al-(Mo:V = 1:1) at 600°.

d. Two-phase $\alpha + \beta$, $\alpha + \gamma$, and $\beta + \gamma$ regions;

e. Three-phase $\alpha + \beta + \gamma$ region.

The performed investigation shows that in the phase-equilibrium tetrahedron of the quaternary system Ti-Al-Mo-V, the above-indicated phase regions shift steadily from the system Ti-Al-Mo via the intermediate system Ti-Al-(Mo:V = 1:1) toward the system Ti-Al-V. For the sake of a clear treatment of the process of this shift, we shall consider five sections of the phase-equilibrium tetrahedron of the quaternary system Ti-Al-Mo-V at 600° with a constant titanium concentration of 90, 80, 70, 60 and 50 wt percent (fig. 5).

The sections with 90 and 80 percent Ti cut through the α and $\alpha + \beta$ phase regions. In the shift from the Ti-Al-Mo system to the Ti-Al-V system, the field of the α solid solution expands continuously from 1 percent Mo to 2.5 percent V on the section with 90 percent Ti and from 1 percent Mo, 3 percent (Mo-V) to 4 percent V on the section with 80 percent Ti. The overwhelming majority of these sections belong to the $\alpha + \beta$ region.

The section with 70 percent Ti shows $\alpha + \gamma$, $\alpha + \beta + \gamma$, $\alpha + \beta$ and β phase regions. In the shift from the Ti-Al-Mo to the Ti-Al-V system, the $\alpha + \gamma$ region expands, and the $\alpha + \beta + \gamma$ region narrows down. A wide field of the $\alpha + \beta$ region is found in the middle portion of this section.

The regions of β solid solutions, which extend from the systems Ti-Al-Mo and Ti-Al-V, become joined together on this section.

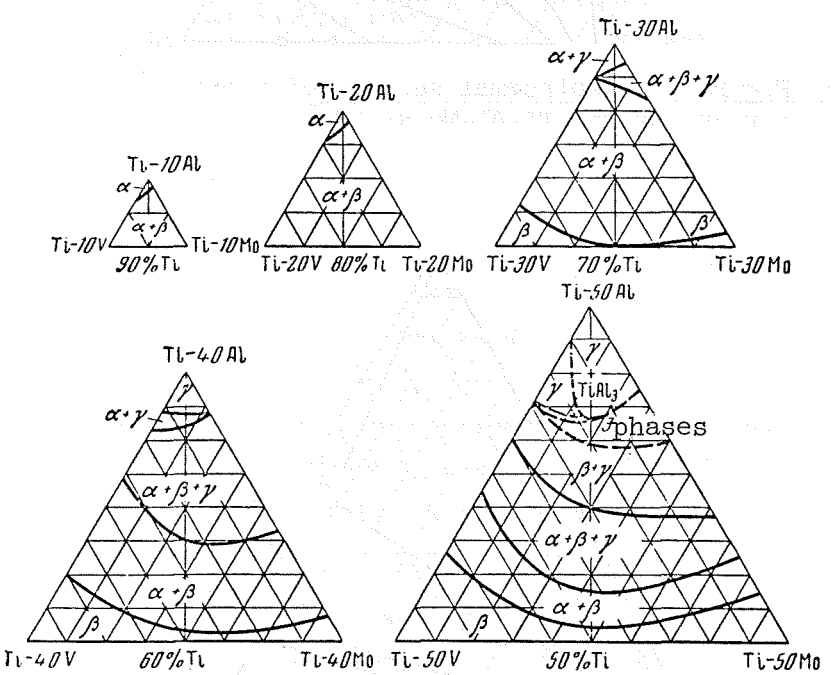

Figure 5. Parallel sections of the tetrahedron of the phase equilibrium of the quaternary system Ti-Al-Mo-V at 600° at a constant titanium concentration of 90, 80, 70, 60 and 50 wt percent.

The section with 60 percent Ti is distinguished by the fact that it displays simultaneously the processes of gradual shift of γ, $\alpha + \gamma$, $\alpha + \beta + \gamma$, $\alpha + \beta$, and β regions in the tetrahedron. In the course of the shift from the Ti-Al-Mo system to the Ti-Al-V system, the region of the β phase narrows down smoothly at first, then expands, passing through the system Ti-Al-(Mo:V = 1:1).

A new phase region ($\beta + \gamma$ region) which shifts steadily from the Ti-Al-Mo system to the Ti-Al-V system appears on the section with 50 percent Ti. On this section, in the portion adjacent to the side of the Ti-Al system of the tetrahedron, the complete shift of the individual phase regions is impaired under the influence of a complex interaction of the phases at the aluminum vertex of the tetrahedron.

On the basis of the above investigation, we plotted a diagram of the phase equilibrium of the quaternary system Ti-Al-V-Mo in the region of alloys rich in titanium at 600° (fig. 6).

In the phase-equilibrium tetrahedron, the volume of the α solid solution is adjacent to the side of the binary system Ti-Al from zero to 25 percent Al. The quaternary β solid solution is adjacent to the face of the ternary system Ti-Mo-V when the total content of aluminum, molybdenum and vanadium is over 22 percent. The quaternary γ solid solution based on TiAl extends from the binary system Ti-Al toward the interior of the tetrahedron. The central portion of the tetrahedron is occupied by a two-phase $\alpha + \beta$ volume. The three-phase $\alpha + \beta + \gamma$ volume borders on the two-phase $\alpha + \beta$, $\alpha + \gamma$, and $\beta + \gamma$ volumes and traverses the tetrahedron from the face of the ternary system Ti-Al-Mo to the face of the ternary system Ti-Al-V.

Thus, a geometrical representation of the studied portion of the phase equilibrium tetrahedron at 600° reveals the character of the interaction between the components and clearly shows the expansion of the phase regions in the quaternary system Ti-Al-Mo-V.

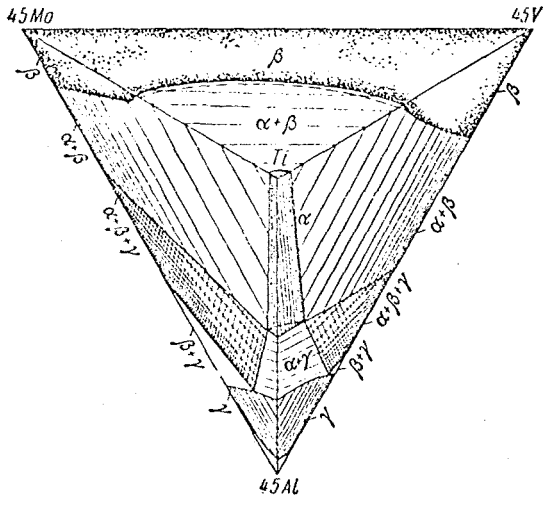

Figure 6. Phase equilibrium diagram of the quaternary system Ti-Al-Mo-V in the region of alloys rich in titanium at 600°.

REFERENCES

1. Kornilov, I. I. and Budberg, P. B. Phase Diagrams of Binary and Ternary Titanium Systems (Diagrammy sostoyaniya dvoynykh i troynykh sistem titana). Publ. Acad. Sci. USSR, p. 22, 1961.

2. Grum-Grzhimaylo, N. V., Kornilov, I. I., Pylayeva, Ye. N. and Volkova, M. A. Dokl. AN SSSR, Vol. 137, No. 3, p. 599, 1961.

3. Kornilov, I. I. Metallovedeniye i termicheskaya obrabotka metallov, No. 2, p. 7, 1963.

4. Kornilov, I. I. and Polyakova, R. S. Izv. AN SSSR, OTN, Metallurgiya i Toplivo, No. 1, p. 85, 1960.

5. Kornilov, I. I., Pylayeva, Ye. N. and Ko Chih-ming. Zh. Neorg. Khim., Vol. 8, No. 2, p. 366, 1963.

6. Kornilov, I. I., Pylayeva, Ye. N. and Volkova, M. A. Sb. "Titan i yego splavy," Publ. Acad. Sci. USSR, No. 7, p. 89, 1962.

PHASE STRUCTURE OF ALLOYS OF THE SYSTEM Ti-Al-Fe-Cr-Si WITH A CONSTANT CONTENT OF ALUMINUM AND SILICON

V. S. Mikheyev and K. P. Myasnikova

Industrial alloys of the AT series (ref. 1) are high-strength alloys based on α-Ti alloyed with aluminum, chromium, iron, silicon and boron. This multicomponent system has been studied in several works (refs. 2 and 3). In reference 2, a study was made of the system Ti-Al-Cr-Fe-Si-B with a variable content of aluminum (from zero to 7.5 wt percent) and a constant content of chromium, iron and silicon (0.5 wt percent of each alloying element). In reference 3, phase transformations in the system Ti-Al-Cr-Fe-Si with a constant content of aluminum (6.0 wt percent) and silicon (0.3 wt percent) and a variable content of iron and chromium were studied.

The object of the present investigation was a study of the phase equilibrium in alloys of the section of the tetrahedron Ti(+0.3 percent Si)-Al-Fe-Cr at a constant aluminum content (7.5 wt percent). Iron and chromium were introduced in the proportion of 3:1, 1:1 and 1:3, the total being up to 30 percent. Henceforth, the corresponding radial sections will be termed sections I, II and III.

The basis for the plotting of the equilibrium diagram of the alloys of the selected section of the five-component system was a method of spatial representation of partial multicomponent systems for any given number of components entering into the composition of the solid solution of the solvent (ref. 4).

One of the vertices of the concentration triangle which we studied was made up of the α solid solution with 7.5 wt percent Al and 0.3 wt percent Si, and the other two were iron and chromium.

The chemical interaction of titanium with aluminum, chromium, iron and silicon in binary systems and also the structure of ternary titanium alloys are described in monographs (refs. 5-7).

With the above-indicated elements, titanium forms a wide region of β solid solution and a narrow region of α solid solution. As the temperature is lowered, the solid solution based on β-Ti undergoes a eutectoid transformation with the precipitation of the α solid solution and of the corresponding intermetallic compounds: Ti_5Si_3 in the system Ti-Si, TiFe in the system Ti-Fe, and $TiCr_2$ in the system Ti-Cr.

The solubility of each of the enumerated elements in α-Ti is 0.3-0.5 percent at the temperature of the eutectoid transformation (refs. 8-10).

Aluminum raises the temperature of the polymorphic transformation of titanium and forms a wide region of solid solutions based on α-Ti.

An investigation of the properties of α solid solutions in the Ti-Al system revealed the presence of chemical compounds corresponding to the compositions Ti_6Al, Ti_3Al and Ti_2Al (ref. 11).

In the three-component system Ti-Fe-Cr, the β solid solution is stable over a wide temperature range. Iron and chromium lower the temperature of the polymorphic transformation of titanium. The eutectoid decomposition of the β phase is associated with the formation of the α phase, TiFe and $TiCr_2$ (ref. 12).

In the other ternary systems Ti-Al-Fe and Ti-Al-Cr, on the polythermal sections at a constant aluminum content of 7.5 percent, phases based on α- and β-Ti are in equilibrium with intermetallic compounds corresponding to the composition TiFe in the first system and $TiCr_2$ in the second (refs. 13 and 14).

Starting Materials and Method of Preparation of the Alloys

The compositions of the investigated alloys are shown in the table. The starting materials for the preparation of the samples were: TG00 titanium sponge, electrolytic chromium, KR1 silicon, A00 aluminum, and iron (0.03 percent C; 0.01 percent Mn; 0.008 percent P; traces of S).

CHEMICAL COMPOSITION OF THE ALLOYS STUDIED (IN wt PERCENT)

Ti	Fe			Cr		
	Section					
	I	II	III	I	II	III
92,0	0,15	0,10	0,05	0,05	0,10	0,15
91,7	0,375	0,25	0,125	0,125	0,25	0,375
91,2	0,75	0,50	0,25	0,25	0,50	0,75
88,7	1,875	1,25	0,625	0,625	1,25	1,875
87,2	3,75	2,50	1,25	1,25	2,50	3,75
84,7	5,625	3,75	1,875	1,875	3,75	5,625
82,2	7,50	5,0	2,50	2,50	5,0	7,50
77,2	11,25	7,50	3,75	3,75	7,50	11,25
72,2	15,0	10,0	5,0	5,0	10,0	15,0
62,2	22,5	15,0	7,5	7,5	15,0	22,5

Note: All alloys contain 0.3 wt percent Si and 7.5 wt percent Al.
Note: All commas represesent decimal points.

Samples of the alloys weighing 20 g were prepared by arc fusion in argon. The weight loss was no more than 0.5 percent. The cast samples were forged in air into rods 7 mm in diameter after being heated at 1200°.

The heat treatment was carried out in sealed and evacuated quartz ampules. To prevent the titanium alloys from reacting with quartz, the samples were placed in a tube made of thin molybdenum sheet.

The heat treatment consisted in annealing the samples at 1100, 1000 and 800 and 500° with a holding time of 10, 15, 300 and 750 hr, respectively.

After annealing at 1100, 1000 and 800°, one group of the samples was quenched in water, and the other was furnace-cooled after annealing at 500°.

The study of the partial system was carried out by means of microstructural and x-ray analysis. After each type of heat treatment, the electrical resistivity and hardness of the alloys were measured.

The hardness was measured with a Vickers instrument by indenting the sample with a diamond pyramid having a leap angle of 136° at a load of 10 kg. The electrical resistivity of the alloys was studied potentiometrically. The x-ray structural analysis was performed by using unfiltered vanadium radiation in a RKD camera.

Results

The microstructure of the alloys was studied in the cast, quenched and annealed state.

The samples were etched with a mixture of hydrofluoric and nitric acid with glycerin (in the proportion of 1:1:1).

Microstructural analysis of the cast samples showed that the phase which crystallizes first in the alloys of all three sections is a solid solution based on β-Ti. The structure of the cast alloys of sections I, II and III had a single phase, with the exception of the alloy containing 30 wt percent (Fe + Cr) of section I, where the precipitation of a second phase was observed (fig. 1a).

At 1100° in the range of concentrations of Fe + Cr from zero to 20 wt percent of sections I and III and up to 30 wt percent of section II, the alloys have the structure of the β solid solution. Quenching from this temperature causes a $\beta \rightarrow \alpha'$ martensite transformation (fig. 1b) in alloys containing up to 5 wt percent (Fe + Cr). In higher alloys, the β phase becomes fixed (fig. 1c).

In alloys with 30 wt percent (Fe + Cr) of sections I and III, the precipitation of a second phase is observed along the boundaries and the field of β grains (fig. 1d and e). X-ray diffraction analysis established that the secondary phase precipitating from the β solid solution is the intermetallic compound TiFe (δ phase) in alloys of section I, and in alloys of section III, the intermetallic compound $TiCr_2$ of hexagonal modification (γ phase).

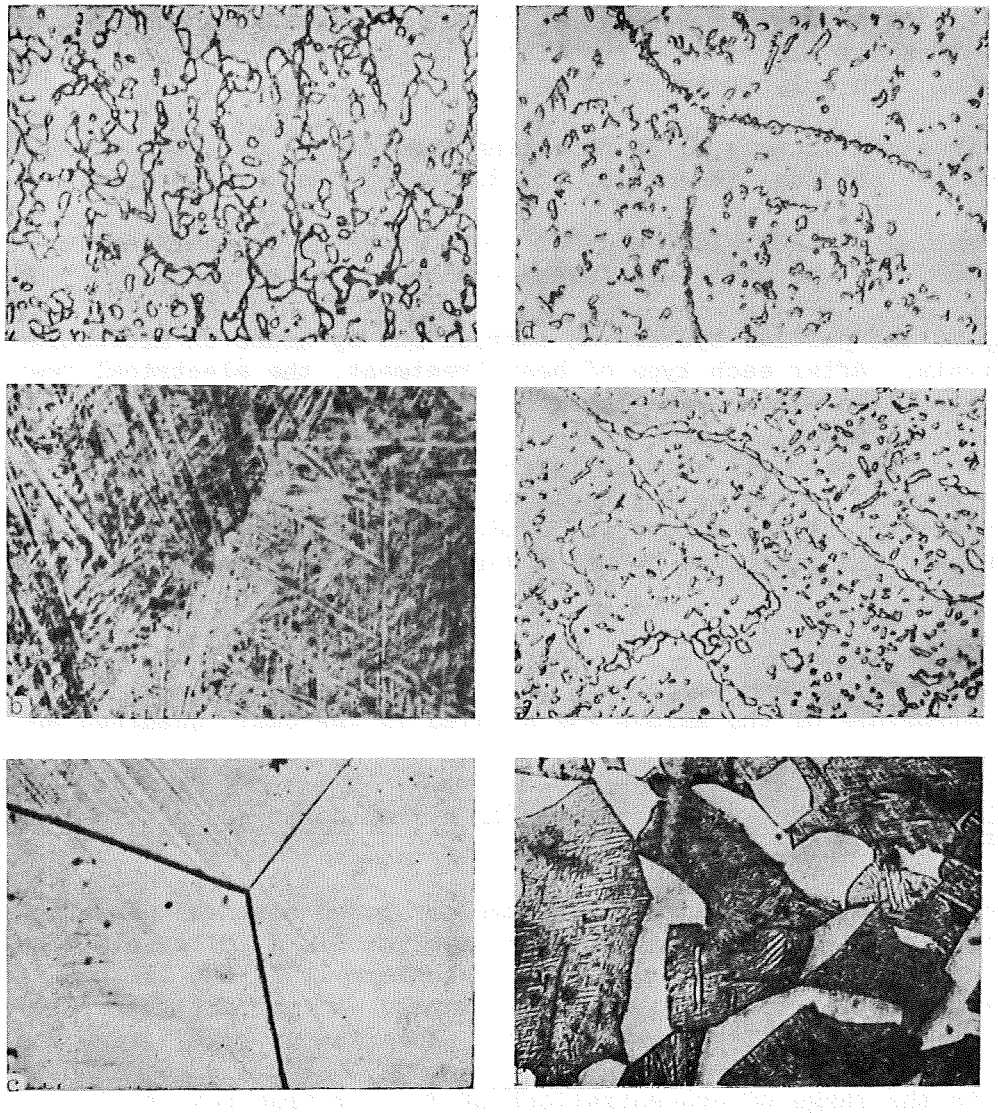

Figure 1. Microstructure of the alloys after various heat treatments, x 340. a, alloy of section I with 30 percent (Fe + Cr), cast; b, alloy of section II with 5 percent (Fe + Cr), quenching from 1100°; c, alloy of section I with 7.5 percent (Fe + Cr) at 1100°; d, alloy of section I with 30 percent (Fe + Cr), quenching from 1100°; e, alloy of section III with 30 percent (Fe + Cr), quenching from 1100°; f, alloy of section I with 2.5 percent (Fe + Cr), quenching from 1000°; g, alloy of section I with 0.2 percent (Fe + Cr), quenching from 800°; h, alloy of section II with 7.5 percent (Fe + Cr), quenching from 800°; i, alloy of section II with 20 percent (Fe + Cr), quenching from 800°; j, alloy of section III with 7.5 percent (Fe + Cr), annealing at 600°.

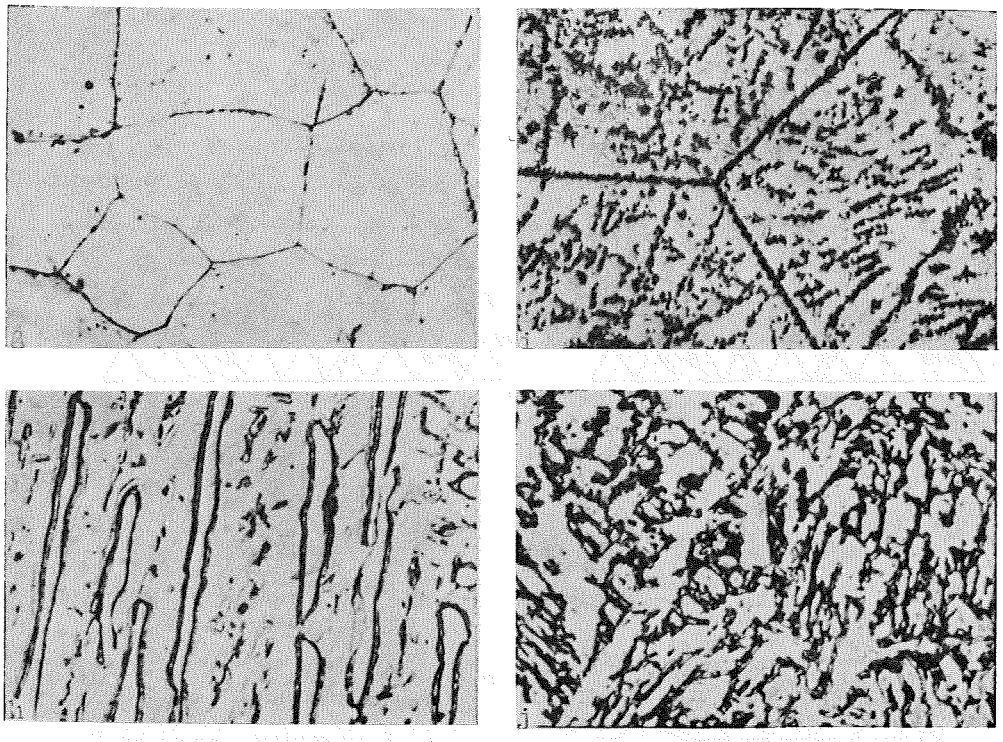

Figure 1. (Concluded)

Figure 2a shows an isothermal section of the tetrahedron Ti (+0.3 percent Si)-Al-Fe-Cr with a constant aluminum content (7.5 wt percent) at 1100°. The main portion of the concentration triangle is occupied by the five-component β solid solution. The boundaries of the two-phase regions β + δ and β + γ were not accurately determined, and they are therefore represented by broken lines.

The compositions of the alloys on the isothermal section at 1100° which undergo a martensite transformation are marked with crosses.

On quenching from 1000°, the alloys containing iron and chromium (up to 2.5 wt percent) together with the β and α' phases contain the equilibrium α phase formed as a result of the polymorphic β → α transformation (fig. 1f). The amount of the α solid solution in the alloys decreases as the sum of iron and chromium increases.

The pure β solid solution becomes fixed in alloys containing 5-20 wt percent (Fe + Cr) of section I. In the microstructure of alloys with 5 wt percent of the alloying components in sections II and III, martensite needles are observed; their highest quantity is found in the alloy of section II, at the ratio Fe:Cr = 1:1. An increase in the content of iron and chromium in the alloys of these sections causes a stabilization of the β phase. At 1000°, the region of existence of the β solid solution narrows down considerably owing to the appearance of the two-phase α + β region and the expansion of both the β + δ and β + γ regions as a result of a decrease in the solubility of the intermetallic compounds in β-Ti with increasing temperature (fig. 2b).

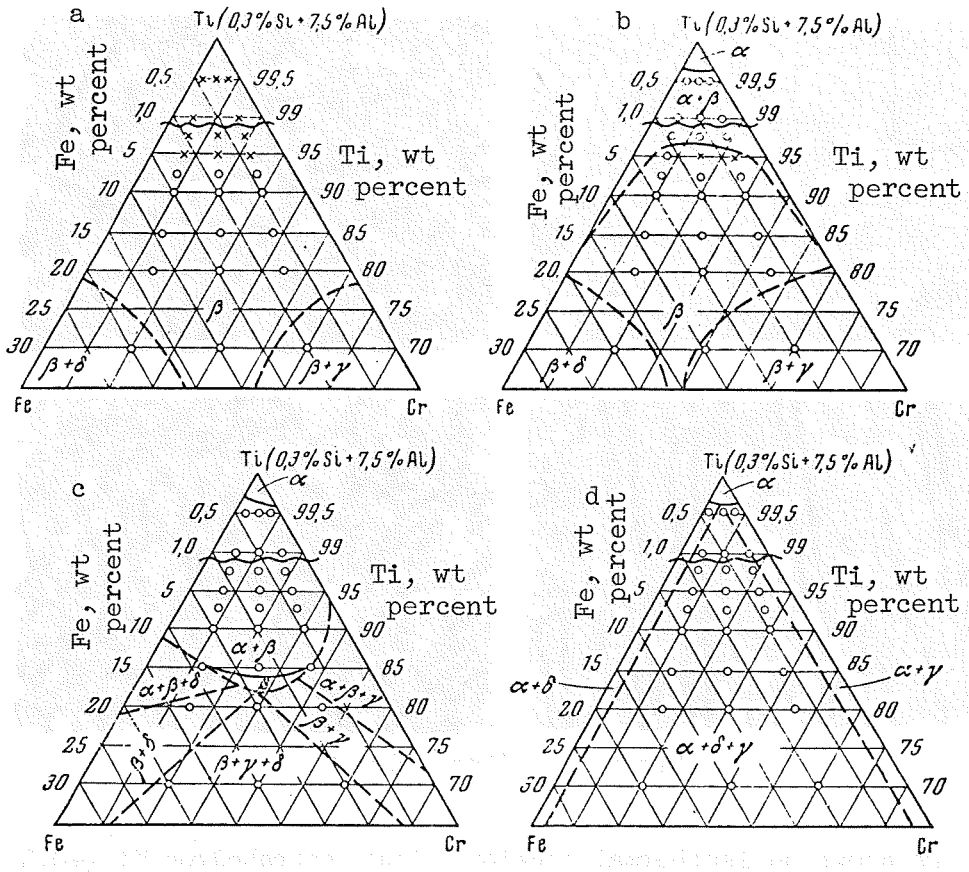

Figure 2. Isothermal sections of the tetrahedron: a, at 1100°; b, at 1000°; c, at 800°; d, at 500°.

After annealing at 800° and quenching from this temperature, the alloys rich in titanium and containing up to 0.2 wt percent (Fe + Cr) have the polyhedral structure of the α solid solution (fig. 1g). In the concentration range of iron and chromium of 0.5-15 wt percent, all the alloys consist of two phases ($\alpha + \beta$).

It should be noted that the microstructure of alloys with 7.5 wt percent (Fe + Cr) reflects the peritectoid character of the interaction of the phase components (fig. 1h). This may be a confirmation of the phase diagram of Ti-Al proposed by Zwicker et al. (ref. 15), with a peritectoid nature of the formation of the α phase by the reaction $\beta + \alpha_2 \rightarrow \alpha$.

However, the available data pertaining to this problem are insufficient to allow any definitive conclusions. A further study of the phase transformations in the α solid solution of titanium in binary, ternary and multicomponent systems with aluminum is necessary.

Alloys with a high total content of iron and chromium (20-30 wt percent) have a two-phase structure $\beta + \delta$ (alloys of section I) or $\beta + \gamma$ (alloys of

section III) or a three-phase structure $\beta + \delta + \gamma$ (alloys of section II). A characteristic structure of the three-phase state is shown in figure 1i.

In the study of the microstructure of alloys quenched from 800°, no single-phase structure of the β solid solution was observed, probably because we did not investigate the compositions of alloys with 15-20 wt percent (Fe + Cr).

On the basis of the studies made in reference 3 and data of microstructural and x-ray structural analysis on the phase equilibrium in alloys with higher or lower content of iron or chromium, it is possible to postulate the existence of a narrow region of a single-phase β solid solution on the isothermal section at 800°.

Figure 2c shows a phase diagram of the section of the tetrahedron Ti(+0.3 percent Si)-Al-Cr-Fe at 800°.

The five-component β solid solution at this temperature is in a two-phase and three-phase equilibrium with the $\alpha + \gamma$ and δ phases. The maximum solubility of the sum of iron and chromium at 800° in the five-component α solid solution amounts to no more than 0.4 wt percent.

Long annealing for 750 hr at 500° leads to a complete eutectoid decomposition of the β solid solution (fig. 1j). According to the x-ray structural analysis, all the alloys at 500° have a three-phase structure $\alpha + \delta + \gamma$.

A phase diagram at 500° is shown in figure 2d.

Thus, the investigation of the five-component system Ti-Al-Fe-Cr-Si containing up to 30 percent (Fe + Cr) at 1100, 1000, 800 and 500° has shown that α and β solid solutions and intermetallic phases TiFe and $TiCr_2$ are formed in this system. However, a more complex character of interaction can be postulated in this system. In particular, as was indicated above, the formation of the chemical compound Ti_3Al (α_2 phase) is possible. Because the nature of the interaction in the binary system Ti-Al in the region of the α solid solution has not been definitely established, and the influence of iron or chromium in the three-component systems Ti-Al-Fe and Ti-Al-Cr has not been elucidated, in plotting the isothermal sections we did not take into account the regions of phase equilibria with the α_2 phase.

The investigation which was carried out makes it possible to draw some conclusions with regard to the influence of aluminum on the chemical interaction of titanium with chromium and iron. Aluminum raises the temperature of the polymorphic transformation, as indicated by the phase equilibria on the isothermal sections at 1000 and 800°. Furthermore, aluminum decreases the solubility of the intermetallic phases in β-Ti, and as a result, the boundaries of the two-phase $\beta + \delta$ and $\beta + \gamma$ regions with the single-phase region of the β phase shift toward a lower total content of iron and chromium as the content of aluminum in the alloys increases (refs. 3 and 12).

Hardness of the Alloys

The hardness of the alloys was measured on samples quenched from 1000 and 800° and annealed at 500°.

The hardness of the alloys versus their composition is shown graphically in figure 3.

The maximum hardness is exhibited by alloys containing 2.5 wt percent (Fe + Cr) of sections I and III and 5 wt percent (Fe + Cr) of section II.

The most pronounced martensite decomposition of β grains is observed in these alloys, and this is what causes such an increase in hardness.

The hardest alloy was found to be the one containing 5 wt percent (Fe + Cr) of section II. It is interesting to note that in the ternary system Ti-Fe-Cr, the maximum hardness in the quenched state is also displayed by alloys with the ratio Fe:Cr = 1:1 at a content of about 5 wt percent (Fe + Cr) (ref. 12).

The minimum on the curves representing the dependence of the hardness on the composition corresponds to a content of 7.5 wt percent (Fe + Cr) in the alloys. These alloys have the structure of a fixed β solid solution. A further increase in the content of alloying components in the β phase promotes an increase in hardness.

At 800°, the change in the hardness of the alloys as a function of composition follows the phase transformations in the system.

In the region of the α solid solution, the hardness rises with the sum of iron and chromium, reaching maximum values at the limit of maximum solubility of the alloying elements in α-Ti.

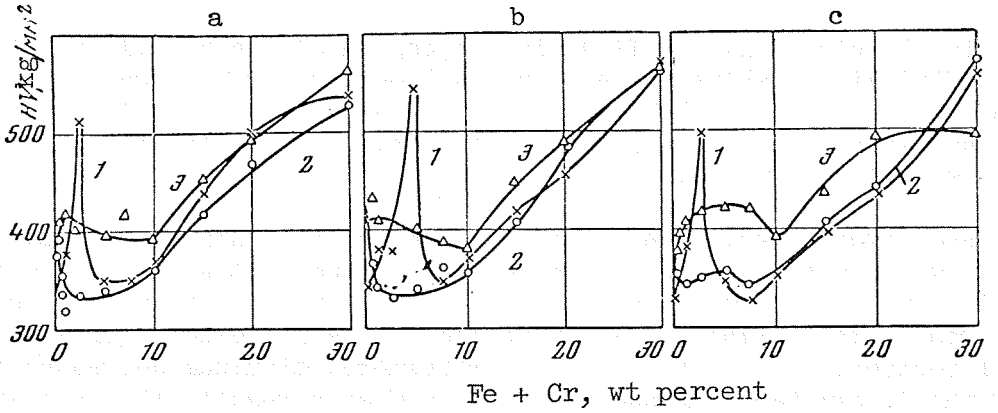

Figure 3. Hardness of the alloys versus composition and temperature: a, section I, Fe:Cr = 3:1; b, section II, Fe:Cr = 1:1; c, section III, Fe:Cr = 1:3; 1, alloys quenched from 1000°; 2, alloys quenched from 800°; 3, alloys annealed at 500°.

The appearance of the β phase and increase in its quantity cause a decrease in the hardness of the alloys. However, in alloys containing from 7.5 wt percent (Fe + Cr) (as well as on the "composition-hardness" curve at 1000°), the hardness increases, since the β phase is hardened by the alloying.

The curve representing the dependence of the hardness of the alloy on its composition at 500° lies above an analogous curve for alloys quenched from 800°. This is explained by the presence in the alloys of intermetallic phases resulting from the eutectoid decomposition of the β phase. The hardness of the alloys at 500° in the region of α solid solution varies as does the hardness at 800°.

In the three-phase region, because of the increase in the content of the intermetallic compounds TiFe and $TiCr_2$ in the alloys, the hardness should increase. No such regular change in hardness is observed on curve 3 (fig. 3). The alloys of all the sections containing about 10 wt percent (Fe + Cr) have minimum values of the hardness. This anomalous character of the dependence of the hardness on the composition can be attributed either to an incomplete eutectoid decomposition of the β phase or to the formation of the phase Ti_3Al.

Electrical Resistivity

The electrical resistivity was studied on samples 5 mm in diameter quenched from 1000 and 800° and annealed for a long time at 500°.

Results of the measurements are shown graphically in figure 4.

The phase transformations in the alloys at 1000° are reflected by the curve representing the electrical resistivity versus the composition.

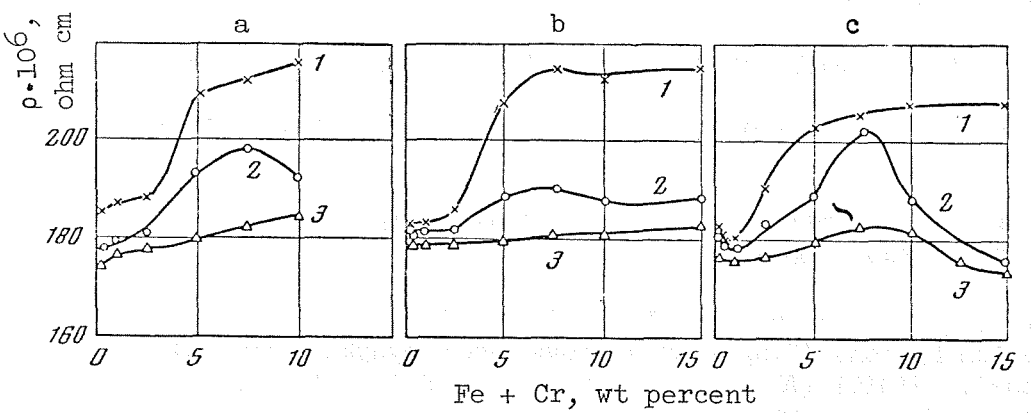

Figure 4. Electrical resistivity of the alloys versus composition and temperature: a, section I, Fe:Cr = 3:1; b, section II, Fe:Cr = 1:1; c, section III, Fe:Cr = 1:3; 1, alloys quenched from 1000°; 2, alloys quenched from 800°; 3 alloys annealed at 500°.

In the two-phase $\alpha + \beta$ region, the electrical resistivity of the alloys changes insignificantly when they are alloyed with iron or chromium (up to 2.5 wt percent). The shift to the single-phase β region is associated with an abrupt increase in the electrical resistivity of the alloys, probably due to a maximum stress condition of the β grains during the formation of the α' phase. A further increase in the content of iron and chromium has little effect on the change in the electrical resistivity of the alloys.

At 800°, the curve of composition versus electrical resistivity rises monotonically up to a content of 7.5 wt percent (Fe + Cr), then descends. This pattern of change in the electrical resistivity of the alloys at 800° may be due to the transformations discussed above.

The eutectoid decomposition of the β phase at 500° has a negligible influence on the dependence of the electrical resistivity of the alloys on the composition.

Thus, the greatest influence on the dependence of the electrical resistivity of the alloys on the composition is exerted by the structural stress condition of the grains of the β solid solution during quenching as a result of the formation of metastable phases.

REFERENCES

1. Kornilov, I. I., Mikheyev, V. S., Chernova, T. S. and Markovich, K. P. Coll. "Titanium and Its Alloys," Izd-vo AN SSSR, No. 7, p. 140, 1962.

2. Kornilov, I. I., Mikheyev, V. S. and Chernova, T. S. Izv. AN SSSR, OTN, Metallurgiya i Toplivo, No. 3, p. 70, 1960.

3. Kornilov, I. I. and Boriskina, N. G. Coll. "Titanium and Its Alloys," Izd-vo AN SSSR, No. 10, p. 86, 1963.

4. Kornilov, I. I. Dokl. AN SSSR, Vol. 81, No. 2, p. 191, 1951.

5. McQuillen, A. D. and McQuillen, M. K. Titanium (Titan), Metallurgizdat, 1958.

6. Yeremenko, V. N. Titanium and Its Alloys (Titan i yego splavy). Izd-vo AN UkSSR, Kiev, 1960.

7. Kornilov, I. I. and Budberg, P. B. Phase Diagrams of Binary and Ternary Titanium Systems (Diagrammy sostoyaniya dvoynykh i troynykh sistem titana). VINITI (All-Union Institute of Scientific and Technical Information), Moscow, 1960.

8. Boriskina, N. G. and Myasnikova, K. P. Coll. "Titan i yego splavy," Izd-vo AN SSSR, No. 7, p. 61, 1962.

9. Mikheyev, V. S. and Chernova, T. S. Coll. "Titan i yego splavy," Izd-vo AN SSSR, No. 7, p. 68, 1962.

10. Pylayeva, Ye. N. and Volkova, M. A. Coll. "Titan i yego splavy," Izd-vo AN SSSR, No. 7, p. 74, 1962.

11. Grum-Grzhimaylo, N. V., Kornilov, I. I., Pylayeva, Ye. N. and Volkova, M. A. Dokl. AN SSSR, Vol. 137, No. 3, p. 599, 1961.

12. Van Thyne, Kessler, H. and Hansen, M. J. Metals, Vol. 5, p. 1209, 1953.

13. Kornilov, I. I., Pylayeva, Ye. N. and Volkova, M. A. Zhurnal Neorganicheskoy Khimii, Vol. 2, No. 6, p. 1391, 1958.

14. Kornilov, I. I., Mikheyev, V. S. and Chernova, T. S. Zh. neorg. khim., Vol. 3, No. 3, p. 786, 1958.

15. Sagel, K., Schulz, E. and Zwicker, U. Zs. Metallkunde, Vol. 47, p. 529, 1956.

STUDY OF THE ALLOYS OF THE TERNARY SYSTEM Ti-Al-Zr

Ye. N. Pylayeva and M. A. Volkova

The study of the phase diagram of the ternary system Ti-Al-Zr is of great practical interest because this system should contain a wide region of solid solutions which may serve as the basis for the development of alloys operating at high temperatures. Literature data pertaining to phase diagrams of this system are lacking. In reference 1, a study was made of the mechanical properties of ternary alloys of titanium with aluminum and zirconium, and it was found that alloying of α-Ti with aluminum and zirconium (up to 8-18 percent Al + Zr) raises the high-temperature strength of the alloys of the system at temperatures of 20-650°. We have studied the alloys of the ternary system Ti-Al-Zr along the section originating from the vertex of pure zirconium and extending to the composition of the alloy of the binary system Ti-Al, containing 9 percent Al and 91 percent Ti (the alloy has the hexagonal structure of α-Ti). In composition, this alloy corresponds approximately to the proposed compound Ti_6Al (8.7 percent Al; 91.3 percent Ti). The possibility of the existence of the compound Ti_6Al was demonstrated by results of measurements of the Hall constant for alloys of the system Ti-Al (ref. 2). The problem of the existence of this compound has not been definitively solved.

The system Ti-Al is characterized by a complex chemical interaction of the components, which form a series of metallic compounds, and the literature contains contradictory views concerning the stoichiometric composition of these compounds (Ti_6Al (ref. 2), Ti_3Al (refs. 2-4), Ti_3Al_2 (ref. 5), Ti_2AL (refs. 4 and 5)).

Titanium and zirconium (α and β modifications) form a continuous series of solid solutions with a minimum (fig. 1).

Zirconium and aluminum form a phase diagram with a limited solubility and several metallic compounds: Zr_5Al_3, Zr_2Al, Zr_3Al, etc. (ref. 6).

In this work, use was made of methods of thermal and microstructural analysis, and the electrical resistivity and hardness of the alloys were determined.

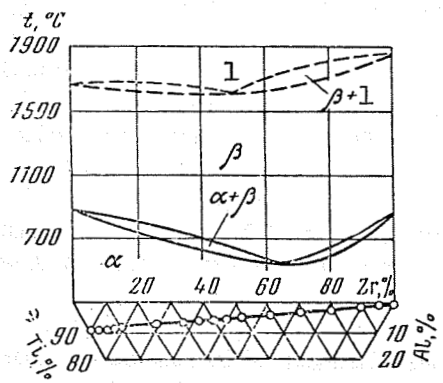

Figure 1. Concentration triangle of a part of the ternary system Ti-Al-Zr.

The starting materials were: iodide zirconium, TG00 titanium sponge, and AV000 aluminum.

The compositions of the alloys studied were as follows:

COMPOSITION OF ALLOYS (IN THE INITIAL MIXTURE) (IN wt PERCENT).

Zr	Al	Ti	Ti_3Al	Zr	Al	Ti	Ti_3Al
0	9,0	91,0	100	40	5,22	54,8	60
1	8,62	90,4	99	50	4,36	45,7	50
3	8,44	88,6	97	60	3,48	36,5	40
5	8,26	86,8	95	70	2,61	27,39	30
7	8,1	84,9	93	75	2,18	22,82	25
10	7,8	82,2	90	80	1,74	18,26	20
15	7,4	77,6	85	90	0,87	9,13	10
25	7,53	68,5	75	95	0,44	4,56	5
30	6,1	63,9	70	100	0	0	0
35	5,66	59,4	65				

In order to study the microstructure and hardness, the alloys were melted in an arc furnace in argon; to study the electrical resistivity, the alloys were prepared by floating zone-melting in helium. The difference in the weight of the samples before and after the fusion did not exceed 0.5 percent, and for this reason the alloys were not analyzed chemically.

The heat treatment of the alloys was as follows: 1200°, 6 hr; 1100°, 50 hr; 1000°, 100 hr; 850°, 200 hr; 800°, 300 hr; 700°, 300 hr; 600°, 400 hr; 500°, 750 hr. The alloys were quenched from 1100, 850, 700 and 500°.

In order to determine the critical point of the alloys in the solid state, a differential recording of the heating and cooling curves was carried out with a Kurnakov pyrometer using samples annealed as indicated above. The recording was carried out in air (for alloys of all compositions) and simultaneously in a vacuum, in evacuated and sealed Stepanov quartz vessels (for certain alloy compositions).

For alloys with 70-90 percent Zr, the difference in the temperatures obtained in both cases was ~30°, and for alloys with a lower zirconium content, no more than 20°.

The thermograms displayed thermal effects corresponding to the following phase transformations: on heating, $\alpha \rightarrow \alpha + \beta$ and on cooling, $\beta \rightarrow \alpha + \beta$. The critical points in the solid state are shown on the graph of figure 2.

As can be seen from figure 2, the temperature of the $\alpha \rightarrow \alpha + \beta$ transformation decreases as the content of zirconium in the alloys rises from zero to ~65 percent, and passes through a minimum at ~660°.

The microstructure of the alloys was studied on cast samples and after quenching from 1100, 800 and 500°, and in certain alloys also after quenching from 850 and 700°. The cast alloys and the majority of the alloys quenched from 1200° have the structure of the transformed β phase. A characteristic appearance of such a microstructure is shown in figure 3a. After quenching from 1100°, the alloys containing from zero to 3 percent Zr had an $\alpha + \alpha$ acicular structure (fig. 3b), where the acicular structure of the decomposed α phase is visible between the light grains of the β phase, i.e., at 1100° these alloys are in the $\alpha + \beta$ region.

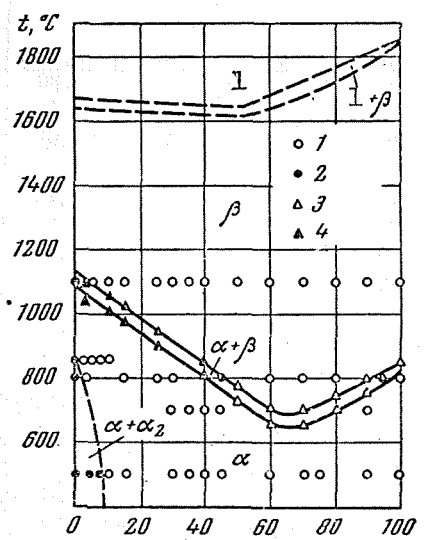

Figure 2. Polythermal section of the ternary system Ti-Al-Zr: 1, single-phase alloys; 2, two-phase alloys; 3, data of thermal analysis conducted in a vacuum; 4, data of thermal analysis conducted in air.

After quenching from 800°, depending on their content of zirconium, the alloys display the polyhedral structure of the α solid solution (fig. 3c), the structure of the acicular α phase (similar to the structure shown in figure 3a), and also a mixed structure of the polyhedra of the α solid solution and of the acicular β phase (analogous to the structure shown in figure 3b). The phase composition of the alloys studied by the microscopic method is shown in figure 2.

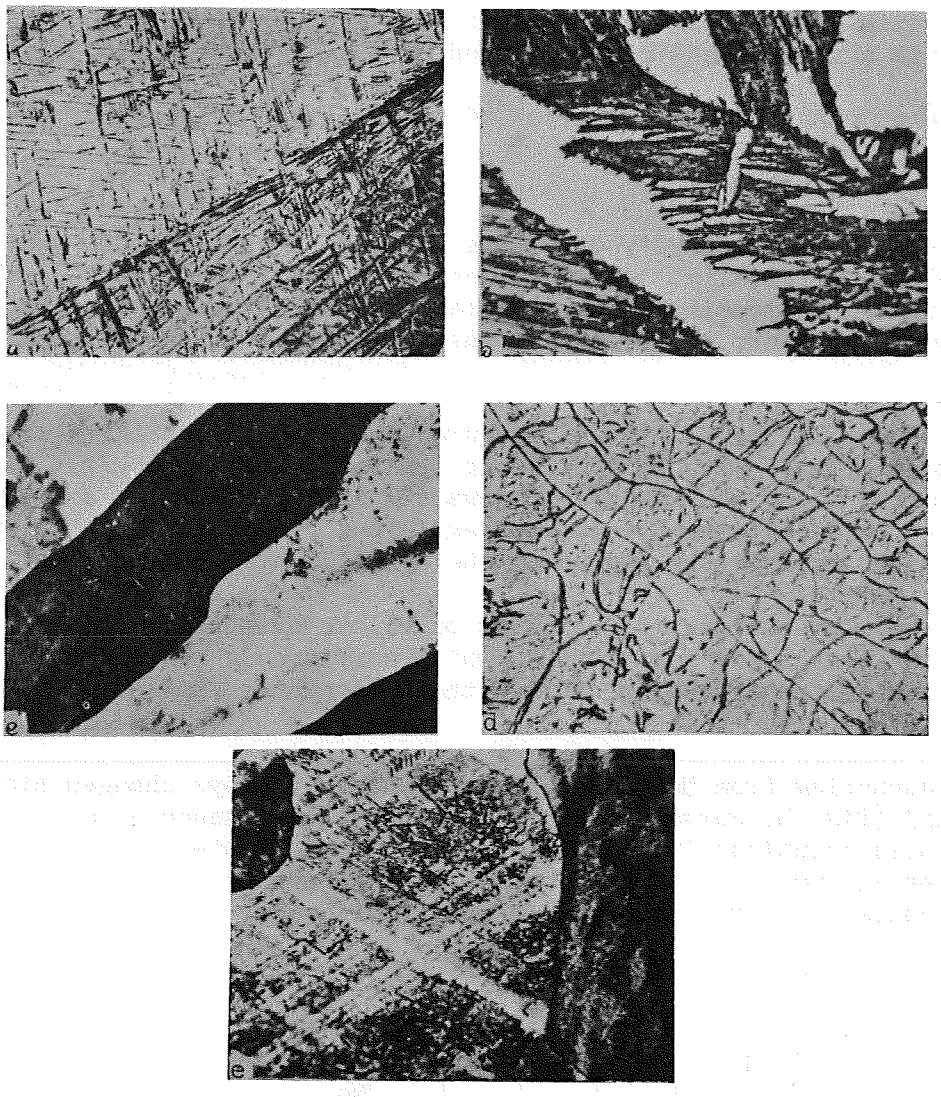

Figure 3. Microstructure of alloys of the ternary system Ti-Al-Zr, x 200: a, alloy of 82.2 percent Ti + 10 percent Zr + 7.8 percent Al; quenching from 1100°; transformed β phase; b, alloy of 91 percent Ti + 9 percent Al; quenching from 1100°, α + transform β phase: c, alloy of 82.2 percent Ti + 10 percent Zr + 7.8 percent Al; quenching from 800°, α phase; d, alloy of 86.8 percent Ti + 5 percent Zr + 8.2 percent Al; quenching from 500°, $\alpha + \alpha_2$; e, alloy of 91 percent Ti + 9 percent Al; quenching from 800°, $\alpha + \alpha_2$.

The majority of the alloys quenched from 500° have the structure of the α solid solution. However, in alloys with 3, 5 and 7 percent Zr, a second phase precipitates. The structure of the alloy in this region is shown in figure 3d. This phase is marked α_2 phase on the polythermal section and is probably based on the metallic compound Ti_3Al (refs. 2 and 3).

Alloys with 0 and 1 percent Zr after quenching from 800 and 500° have a structure with a very slight precipitation of the α_2 phase (fig. 3e). These data associated with the precipitation of the α_2 phase require further refinement.

The electrical resistivity of alloys quenched from 1100, 800 and 500° was measured potentiometrically. As is evident from the graph (fig. 4), the resistivity of the alloys remains nearly constant as the zirconium content increases from zero to 50 percent, and as it increases further, the resistivity declines smoothly.

The hardness of the alloys was measured by means of a Vickers instrument with a diamond pyramid at a load of 10 kg. In alloys quenched from 1100°, the hardness changes along a curve arched upward (fig. 5, curve 1), and the maximum values of the hardness can obviously be explained by the formation of metastable phases on quenching from the region of the β solid solution.

The curve representing the hardness of alloys quenched from 800° (fig. 5, curve 2) also shows a hardness maximum which corresponds to alloys that underwent a martensite transformation during their quenching from the region of the β solid solution.

After quenching from 500°, the hardness of the alloys changes along a curve arched upward (fig. 5, curve 3), which confirms the presence of a continuous series of solid solutions in the alloys of the investigated section. The trend of the curves did not show any evidence of the appearance of a second phase in the alloys containing from zero to 7 percent zirconium.

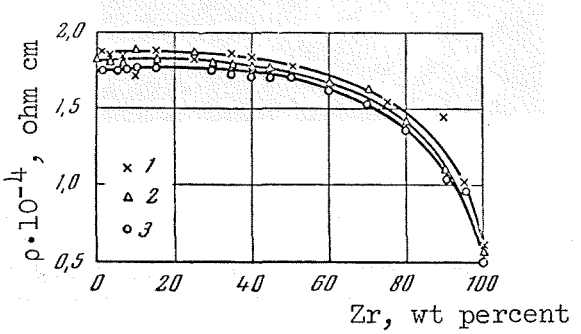

Figure 4. Electrical resistivity of alloys of the ternary system Ti-Al-Zr versus zirconium content: 1, quenching from 1100°; 2, quenching from 800°; 3, quenching from 500°.

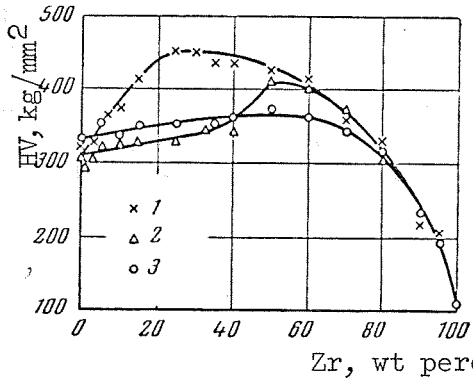

Figure 5. Dependence of the hardness of alloys of the ternary system: 1, quenching from 1100°; 2, quenching from 800°; 3, quenching from 500°.

Summary

1. A study of the alloys of the ternary system Ti-Al-Zr along a radial section at a ratio Al:Ti = 9:91 by methods of microstructural and thermal analysis and determination of the electrical resistivity and hardness shows the existence of a continuous series of solid solutions, with the exception of the $\alpha + \alpha_2$ region adjacent to the alloy with 9 percent Al and 91 percent Ti (500°, zirconium content ranging from zero to 10 percent; see figure 2).

2. All the alloys of this section undergo a polymorphic transformation analogous to the transformation in pure titanium and zirconium and in the system Ti-Zr, the change in the temperatures of the polymorphic transformation occurring along curves with a minimum (660°, ~65 percent Zr).

3. The electrical resistivity and hardness of the alloys after quenching from 1100, 800 and 500° changes along curves protruding upward; the maximum values of the hardness correspond to alloys quenched from the region of the β solid solution.

REFERENCES

1. Mikheyev, V. S. and Markovich, K. P. Coll. "Titanium and Its Alloys," Izd-vo AN SSSR, No. 7, p. 114, 1962.

2. Grum-Grzhimaylo, N. V., Kornilov, I. I., Pylayeva, Ye. N. and Volkova, M. A. Dokl. AN SSSR, Vol. 137, No. 3, p. 339, 1961.

3. Anderko, K., Sagel, K. and Zwicker, U. Zs. Metallkunde, Vol. 48, p. 57, 1957.

4. Ence, E. and Margolin, H. Trans. AIME, Vol. 221, p. 151, 1961.

5. Sato, T., Huong, Y. C. and Kondo, Y. Sumitomo Light Metal Technical Reports. Japan, No. 1, 30-35, 1960.

6. McPherson, D. and Hansen, M. Metallography and Binary Systems of Zirconium (Metallografiya i dvoynyye sistemy tsirkoniya). Part II, Collection of translated articles, Foreign Literature Publishing House (IL), p. 84, 1955.

PHASE EQUILIBRIUM OF ALLOYS OF THE SECTION Ti_3Al-Zr OF THE TERNARY SYSTEM Ti-Al-Zr

I. I. Kornilov, T. T. Nartova and M. M. Savel'yeva

The study of the phase diagram of Ti-Al-Zr is of great practical interest because it can serve as a basis for the development of highly heat-resistant titanium alloys.

Data on the phase diagram of this system are lacking in the literature. The binary phase diagrams Ti-Al, Ti-Zr and Zr-Al have been studied by many authors (ref. 1).

The Ti-Zr phase diagram is characterized by unlimited solubility between the α and β modifications of titanium and zirconium (ref. 2).

According to the data of recent investigations, a series of metallic compounds are formed in the system Ti-Al in the region of the α solid solution, the presence of the compound Ti_3Al being the most probable (refs. 3 and 4).

The purpose of the present work was to study the phase equilibrium and certain properties of the alloys of the system Ti-Zr-Al along a radial section extending from the zirconium vertex to the side of Ti-Al to an alloy composition corresponding to the compound Ti_3Al (16 wt percent Al).

The indicated section and the compositions of the investigated alloys are shown on the concentration triangle of a portion of the Ti-Zr-Al system (fig. 1).

The samples were prepared by induction melting in the floating state (ref. 5). The starting materials were iodide titanium (99.87 percent purity), iodide zirconium (99.9 percent purity), and AV000 aluminum. The chemical composition of the alloys was checked by weighing the samples before and after fusion. The loss did not exceed 1 percent.

The samples were subjected to homogenizing annealing in vacuum for 6 hrs at 1200° and 50 hrs at 1100°.

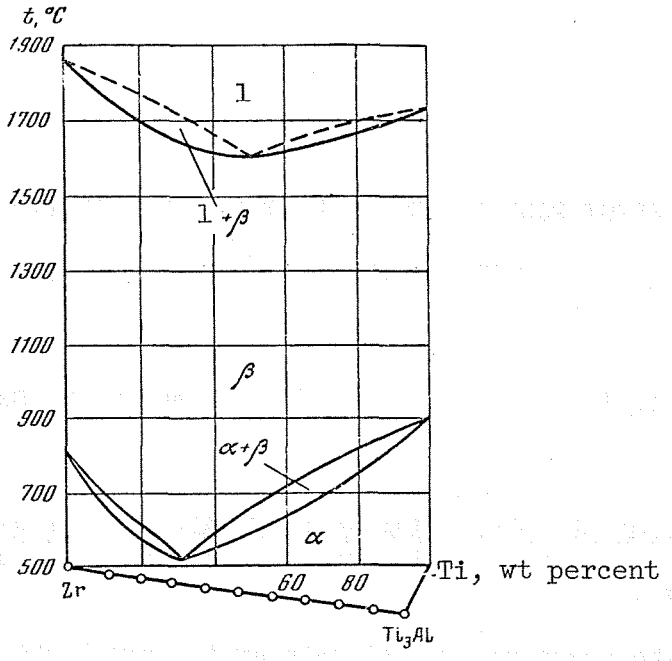

Figure 1. Concentration triangle of a part of the ternary system Ti-Zr-Al.

The quenching of the homogenized samples in water was carried out under the following conditions:

Quenching temperature, °C . .	1200	1100	1000	900	850	750	700	500
Holding time, hours	6	50	100	150	250	400	500	750

At the same time, samples of alloys of the same compositions were forged and subjected to prolonged annealing for 2500 hrs at 800° and for 3000 hrs at 500°.

In order to study the alloys of the Ti_3Al-Zr section, thermal, microstructural, and x-ray analyses were performed, the temperature of the start of the fusion was determined, and the dependence of the density, hardness, microhardness and electrical resistance at room temperature on the composition of the alloys was studied by commonly used techniques. In order to develop the microstructure of the alloys, an etchant of the following composition was employed: 8 pts. glycerin, 1 pt. hydrofluoric acid, 1/2 pt. nitric acid, and 3-4 pts. water.

We shall examine the characteristic microstructures of the alloys of this section from various phase regions (fig. 2) and the phase equilibrium diagram of the section Ti_3Al-Zr (fig. 3).

In plotting the line of the solids of the Ti_3Al-Zr section, we used data obtained from the determination of the temperatures of the start of fusion of

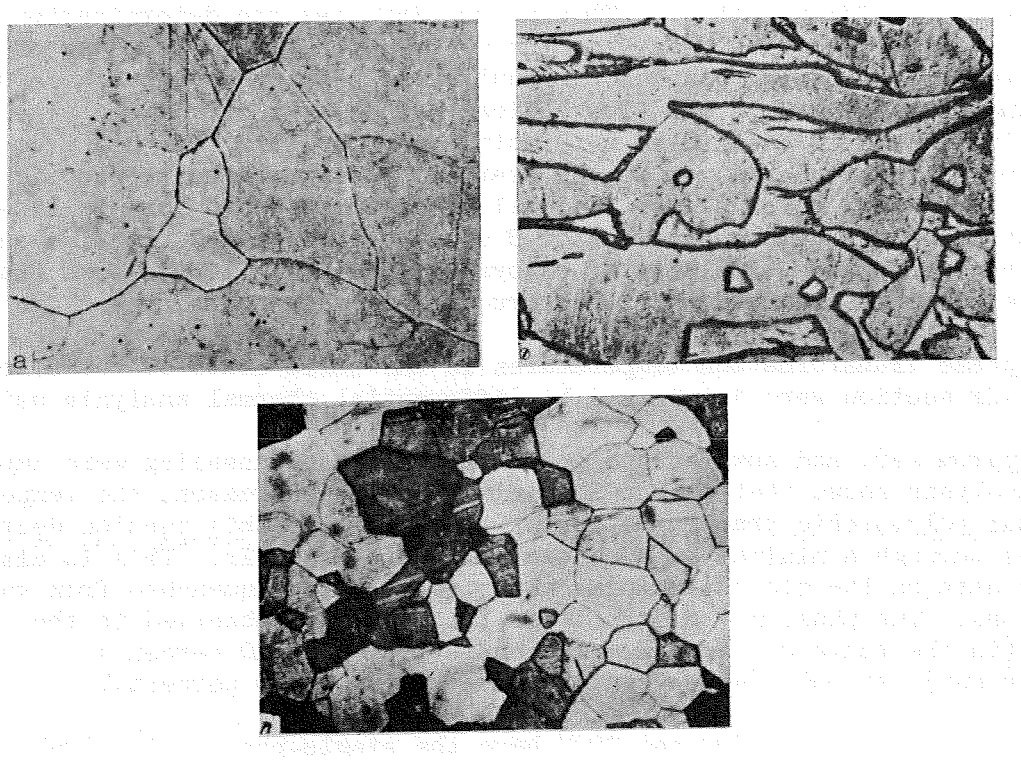

Figure 2. Microstructure of alloy containing 20 percent Zr, x 200: a, alloy quenched from 1200°; b, alloy quenched from 1100°; c, alloy quenched from 500°.

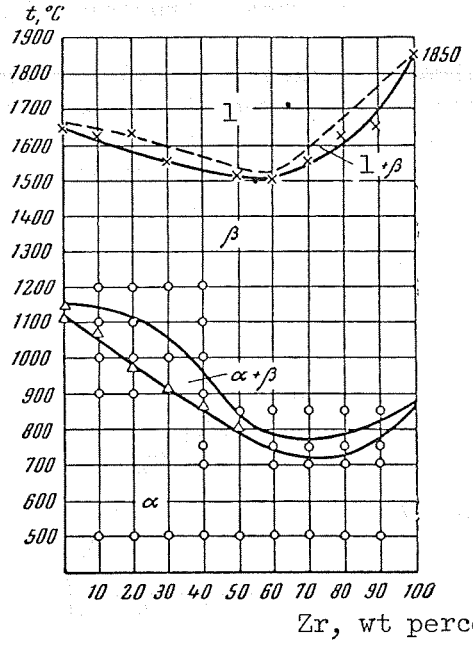

Figure 3. Phase diagram of the section Ti_3Al-Zr: ●, alloy compositions; Δ, data of thermal analysis (method due to N.S. Kurnakov); ×, data of thermal analysis (optical method).

the alloys by the "drop method." This method involves the determination of the temperature of the start of fusion of the alloys in a vacuum by means of an OP-48 optical pyrometer on samples of round cross section having a hole 0.8-1 mm in diameter and 3-4 mm deep. The optical pyrometer recorded the time when the hole in the sample was filled with molten metal. Data obtained from the determination of the temperatures at the start of fusion and a microscopic analysis of the cast structures showed that alloys of this section crystallized with the formation of a continuous series of β solid solutions and titanium and zirconium. Microstructural analysis of alloys quenched from 1200° shows that they retain the single-phase β-transformed structure of martensite type (fig. 2a).

The phase transformation temperatures in the solid state of the alloys of the Ti_3Al-Zr section were determined by differential thermal analysis using a Kurnakov pyrometer, and samples subjected to prolonged annealing were employed. Thermal analysis shows that as the zirconium content increases, the temperature of the polymorphic transformation of the alloys of this section decreases and passes through a minimum at a content of ~70 percent Zr. This is also confirmed by data on the microstructural analysis of alloys quenched from various temperatures. Two-phase α + β structures (fig. 2b) are observed in the alloys at 1100° (in the range of zirconium concentration of 10-20 percent), at 1000° (20-30 percent), at 900° (40 percent), and at 750° (60-80 percent).

Alloys quenched from 500 and 700° have the single-phase polyhedral structure of the α solid solution over the entire section (fig. 2c).

X-ray analysis confirms that at low temperatures, the alloys of the Ti_3Al-Zr section have the single-phase hexagonal structure of α-Ti or α-Zr.

The presence of a continuous series of solid solutions at low temperatures is also confirmed by the "composition-property" diagrams (fig. 4). The hardness of the alloys changes along a curve with a smooth maximum in the region corresponding to 60-70 percent Zr. The electrical resistance of the same alloys

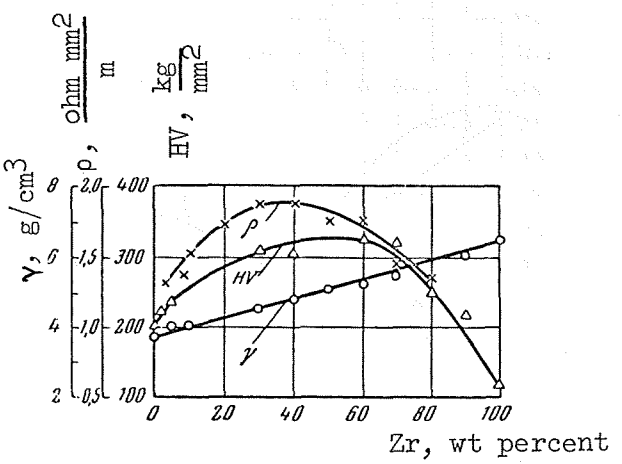

Figure 4. Properties of alloys of the section Ti_3Al-Zr versus zirconium content.

changes in similar fashion as a function of the composition and is characterized by a smooth change in this property. The density of the alloys of the investigated section changes linearly, rising with increasing zirconium content.

As was shown by the investigations, the chemical interaction of the alloys of the Ti_3Al-Zr section is similar to the interaction of titanium and zirconium in the binary system Ti-Zr and is characterized by the presence of a continuous series of solid solutions based on α- and β-Ti(Zr).

REFERENCES

1. Mikheyev, V. S. and Markovich, K. P. Coll. "Titanium and Its Alloys," Izd-vo AN SSSR, No. 7, p. 114, 1962.

2. Hansen, M. Structure of Binary Alloys (Struktura binarnykh splavov). Metallurgizdat, Part 1, p. 160, 1941.

3. Hayes, E. T., Roberson, A. H. and Paasche, O. S. Rep. Inv. US Bur. Min., No. 826, 1951.

4. Duwes, P. J. Inst. Metals., No. 80, p. 525, 1951-1952.

5. Grum-Grzhimaylo, N. V., Kornilov, I. I., Pylayeva, Ye. N. and Volkova, M. A. Dokl. AN SSSR, Vol. 137, No. 3, p. 599, 1961.

6. Ense, E. and Margolin, H. Trans. AIME, Vol. 221, No. 1, p. 151, 1961.

7. Clark, D and Terry, J. C. Bull. Inst. Metals, Vol. 3, p. 116, 1956.

8. Anderko, K., Sagel, K. and Zwicker, U. Zs. Metallkunde, Vol. 48, p. 57, 1957.

9. Fogel', A. A. Izv. AN SSSR, OTN, Metallurgiya i Toplivo, No. 2, p. 24, 1959.

10. Kurnakov, N. S. Introduction to Physicochemical Analysis (Vvedeniye v fiziko-khimicheskiy analiz). Izd-vo AN SSSR, 1941.

STUDY OF THE PHASE STRUCTURE OF THE ALLOYS OF THE SYSTEM Ti-Al-Zr ALONG THE SECTION Ti_3Al-Zr

I. I. Kornilov and N. G. Boriskina

Aluminum and zirconium have a desirable influence on certain mechanical properties of ternary alloys based on α-Ti at room temperature and high temperatures (ref. 1). However, the literature lacks data on the phase structure of the alloys of the system Ti-Al-Zr, as a result of which a more extensive development of alloys of optimum compositions based on this system is hindered. Binary phase diagrams Ti-Zr, Zr-Al and Ti-Al have now been studied in detail. The Ti-Zr system is characterized by the formation of a continuous series of solid solutions based on β-Ti and β-Zr at high temperatures and on α-Ti and α-Zr at low temperatures (ref. 2).

Zirconium and aluminum form a complex phase diagram with a limited solubility of aluminum in β- and α-Zr and of zirconium and aluminum. These elements form eight metallic compounds (ref. 3) of which those richest in zirconium correspond to the composition Zr_3Al, Zr_2Al and Zr_5Al_3.

The Ti-Al system is characterized by the formation of a series of metallic compounds: $TiAl_3$, TiAl and Ti_3Al (refs. 4 and 5). The authors of references 6 and 7 have established the formation of the compound Ti_2Al in the system Ti-Al. Certain anomalies in the change of the Hall effect of the alloys of this system have enabled the authors of reference 8 to propose the existence of the compound Ti_6Al.

To contribute to the study of the alloys of the system Ti-Al-Zr (see pp. 46-57) we investigated the alloys of the section Ti_2Al-Zr. According to the data of reference 7, the compound Ti_2Al forms by the peritectoid reaction $\beta\text{-Ti} + Ti_3Al_2 \rightarrow Ti_2Al$ occurring at a temperature of approximately 1300-1400°.

The compositions of the investigated alloys of the section Ti_2Al-Zr are shown in the table. The starting materials used were iodide zirconium and titanium sponge TG00, in which the total impurities amounted respectively to 0.3 and 0.18 percent, and AV000 aluminum.

ELECTRICAL RESISTIVITY AND DENSITY VERSUS COMPOSITION OF TITANIUM ALLOYS.

Content, wt percent			Electrical resistivity, ohm.m/mm^2			Density, g/cm^3
Ti	Al	Zr	1100°	800°	500°	
78,0	22,0	—	2,1323	2,1223	2,1033	4,0815
77,20	21,80	1,00	2,0745	2,0754	2,0634	4,0998
75,70	21,30	3,00	2,0735	2,0705	2,0654	4,1288
74,10	20,90	5,00	2,0957	2,0938	2,0897	4,1831
72,60	20,40	7,00	2,0522	2,0537	2,0456	4,2154
70,20	19,80	10,00	2,0142	1,9983	1,9918	4,2924
66,30	18,70	15,00	1,5446	1,4265	1,3520	4,3458
62,40	17,60	20,00	1,8691	—	—	4,4585
58,50	16,50	25,00	1,8124	1,6834	1,6603	4,5547
54,60	15,40	30,00	1,5260	1,5285	1,5285	4,5782
46,80	13,20	40,00	1,6138	1,5733	1,5079	4,7660
42,90	12,10	45,00	1,2756	1,6952	1,6533	4,7789
39,40	11,60	50,00	1,4534	1,4641	1,3947	4,9823
31,20	8,80	60,00	1,7514	1,7787	1,6813	5,2389
23,40	6,60	70,00	1,2256	1,2603	1,2232	5,3706
15,60	4,40	80,00	1,6063	1,3026	1,2643	5,6961
11,70	3,30	85,00	1,9805	1,4424	1,4375	5,7739
7,80	2,20	90,00	1,5139	1,4547	1,3734	5,9588
3,90	1,10	95,00	1,2165	1,1660	1,1369	6,0835
1,95	0,55	97,5	—	—	—	—

The alloys were prepared by arc fusion with a nonconsumable electrode in argon.

Samples of the alloys, sealed in double quartz ampules under vacuum, were subjected to the following heat treatment: homogenizing annealing at 1100° for 10 hrs, furnace cooling, and holding under the following conditions: 1000°, 25 hrs; 800°, 300 hrs; 600°, 400 hrs; 500°, 750 hrs. A certain change in the conditions of the heat treatment of the alloys of the Ti_2Al-Zr section as compared to the conditions of the heat treatment of alloys of the sections Ti_6Al-Zr and Ti_3Al-Zr is due to the higher volatility in vacuum of the components of the alloys of the investigated section at 1200-1100°.

The alloys were studied by microstructural and partly by x-ray and thermal analyses. In addition, the electrical resistivity and macro- and microhardness of the alloys were measured. Alloys in the cast state and after quenching (in water with ice) from 1100, 800 and 500° were subjected to the microstructural analysis.

Microstructural analysis of alloys of the section Ti_2Al-Zr in the cast state showed that as in the case of alloys of the sections Ti_6Al-Zr and Ti_3Al-Zr, solid solutions based on β-Ti and β-Zr crystallize from the liquid over the entire concentration range of the components at high temperatures. In cast alloys of the composition Ti_2Al and in alloys with 1 and 3 percent Zr, a coarse-grained polyhedral structure (of α-Ti type, fig. 1a) is observed. The β solid solution of alloys containing 5-30 and 80-97 percent Zr undergoes a martensite transformation in the course of the cooling, whereas cast alloys with 40-70 percent Zr retain the structure of the β solid solution.

After quenching from 1100°, the polyhedral structure of the alloy of the composition Ti_2Al is retained in alloys containing up to 7 percent Zr. In the range of concentrations of 10-30 percent Zr, the alloys have the structure of α + β solid solutions (fig. 1b). The amount of the β solid solution increases with increasing zirconium content of the alloys. The alloy with 40 percent Zr is a pure β solid solution. At 1100°, the solid solution of the alloy with 45.0 percent Zr undergoes a decomposition with the formation of finely dispersed precipitates of a second phase. The microhardness of this phase is considerably higher that that of the β solid solution, and it can therefore be assumed that this phase is a chemical compound.

The microstructure of alloys with 50-70 percent Zr is similar to the microstructure shown in figure 1c, although the precipitates of the second phase are still more finely dispersed. In alloys containing over 70 percent Zr, a martensite decomposition of the β solid solution is observed. It should be noted that the etchant used in this work (1 pt. HF, 1 pt. HNO_3 and 1 pt. glycerin) satisfactorily reveals the phase components of the alloys of the investigated section, which contain up to 50-60 percent Zr. At a higher zirconium content, even on high dilution with glycerin and water, this etchant causes a marked etching of the surface of the polished sections, and this hinders the analysis of the alloys.

At 800°, the structure of the solid solution of the alloy of the composition Ti_2Al is preserved in alloys containing up to 5-6 percent Zr. In the alloy with 7 percent Zr, there is observed a thickening of the grain boundaries; this is obviously due to the precipitation of the second phase. In the concentration range of 10-70 percent Zr, the β solid solution of the alloys undergoes a transformation which ends in a eutectoid decomposition. In the course of cooling from 1100 to 800°, the β solid solution of alloys containing respectively 20 and 50 percent Zr decomposes with the formation of an additional quantity of the α phase. Grains of the β solid solution which did not decompose during the polymorphic transformation subsequently undergo a decomposition according to the reaction $\beta \rightarrow \alpha$ + metallic compound (fig. 1d and e). At a higher zirconium content, there is observed a separation of coarse grains of a phase (fig. 1f) whose microhardness HB = 500 (whereas the microhardness of the α phase HB = 312).

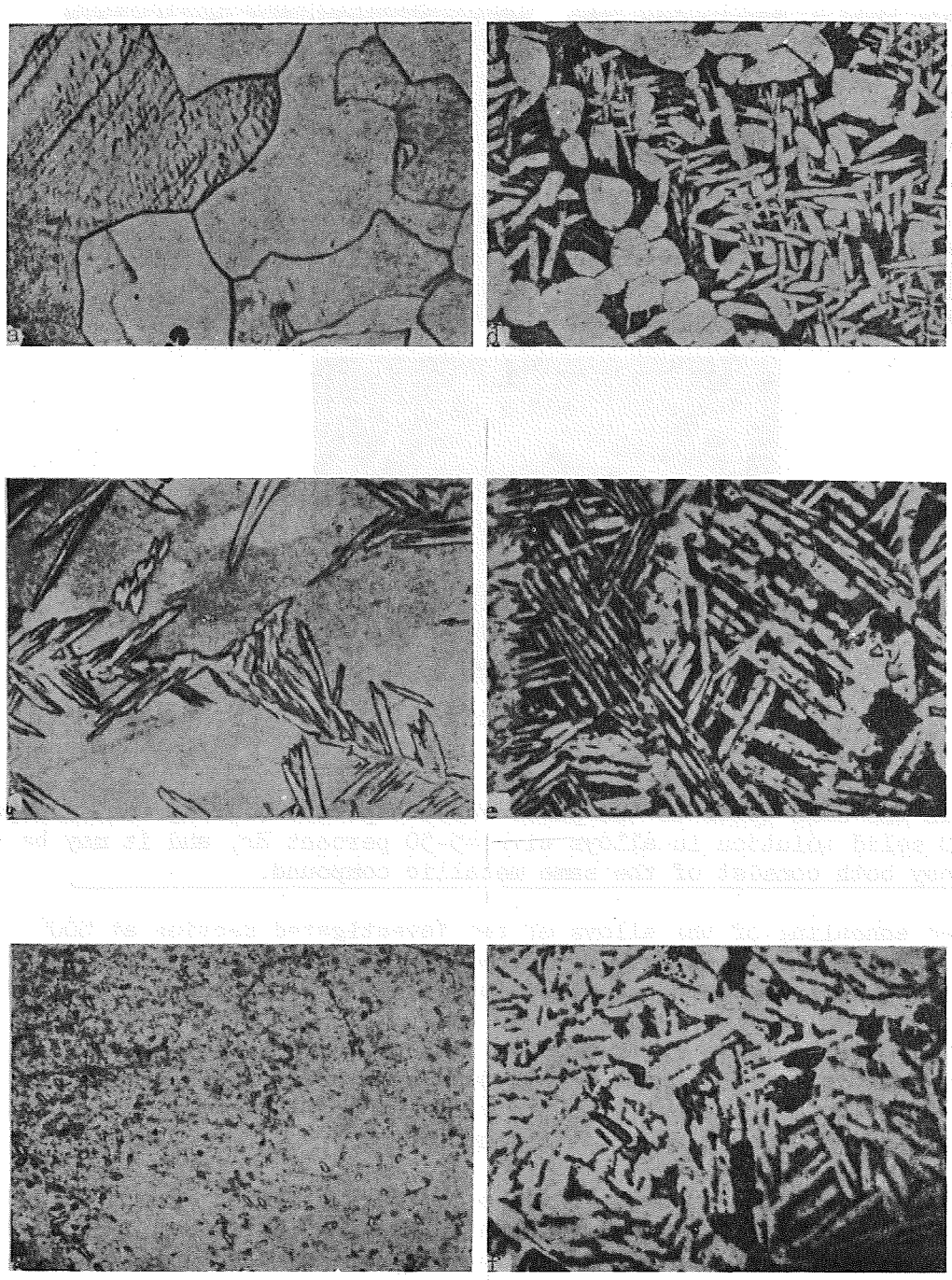

Figure 1. Microstructure of alloys after various heat treatments, x 315: a, cast Ti_2Al alloy; b, alloy with 30 percent Zr, quenching from 1100°; c, alloy with 45 percent Zr, quenching from 1100°; d, alloy with 20 percent Zr, quenching from 800°; e, alloy with 50 percent Zr, quenching from 800°; f, alloy with 70 percent Zr, quenching from 800°; g, alloy with 30 percent Zr, quenching from 500°; h, alloy with 50 percent Zr, quenching from 500°; i, alloy with 60 percent Zr, quenching from 500°.

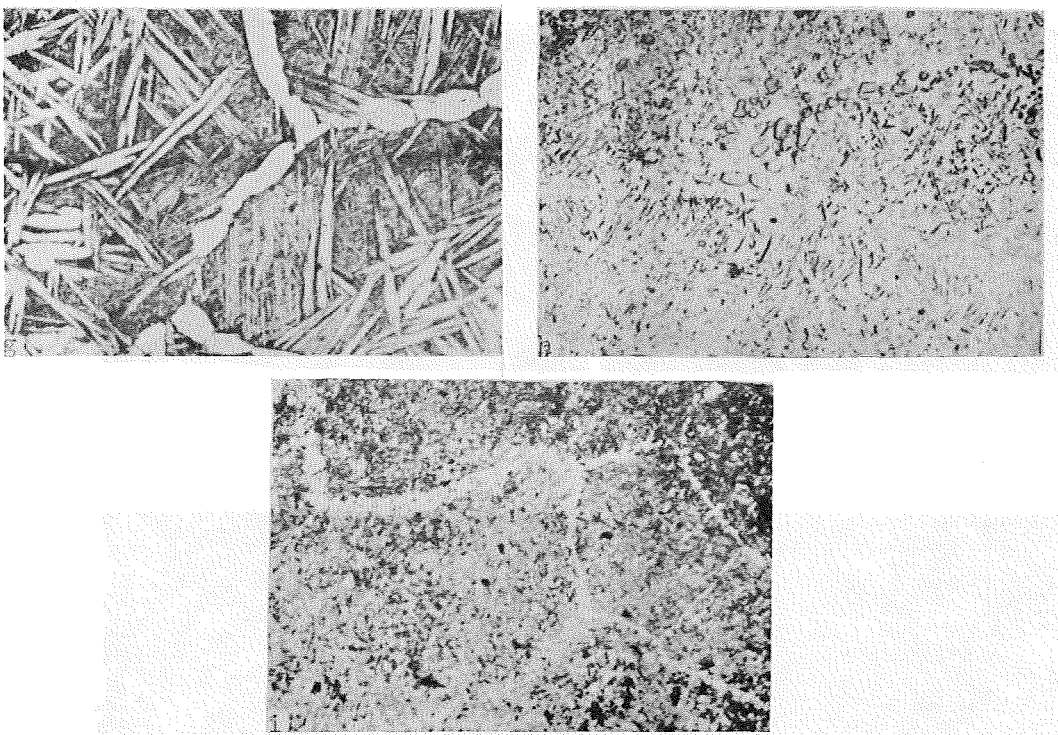

Figure 1. (Concluded)

This phase has the same color as the phase which separated during the decomposition of the β solid solution in alloys with 45-50 percent Zr, and it may be assumed that they both consist of the same metallic compound.

Prolonged annealing of the alloys of the investigated section at 500° caused a decrease in the solubility of zirconium in the solid solution based on the alloy corresponding to the composition Ti_2Al to 3-4 percent. As shown by the photomicrographs (fig. 1g, h and i), at 500° there is observed an increase in the quantity of the metallic compound as a result of decomposition of the α phase; this is in agreement with the very low solubility of aluminum in the solid solution based on α-Zr at this temperature.

Some alloys with a characteristic microstructure quenched from 800° and annealed at 500° were subjected to x-ray analysis. The latter was done in an RKU-86 camera by the powder method, with copper K_α emission and the use of a metal filter.

The alloy powders were additionally annealed in quartz ampules at 800° for 50 hrs and at 500° for 100 hrs.

The x-ray powder patterns of the investigated alloys quenched from 800° (fig. 2) show that the main phase constituting the alloys containing up to 50 percent Zr is a solid solution based on α-Ti and α-Zr.

According to the data of the x-ray analysis, the alloys with 60 percent Zr have a three-phase structure consisting of $\alpha + \beta + Zr_3Al$. The presence of very faint individual reflection lines which may be attributed to the compound Zr_5Al_3 (δ phase) indicates the formation of the compound Zr_3Al (γ phase); this presence is just as evident as in the binary system Zr-Al.

In alloys with 20, 50 and 85 percent Zr, the metallic compound formed also corresponds to the composition Zr_3Al. In the alloy with 85 percent Zr, the main phase component is a solid solution based on the β modification of titanium and zirconium.

X-ray analysis of alloys with 45, 50 and 90 percent Zr annealed at 500° showed that the β solid solution of these alloys decomposed with the formation of the α phase and of the compound Zr_3Al.

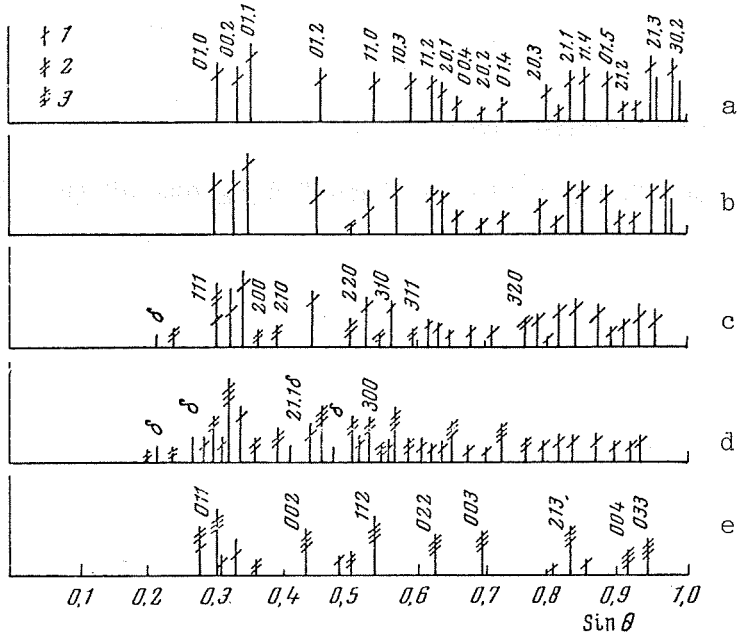

Figure 2. X-ray powder patterns of alloys of the section Ti_2Al-Zr after quenching from 800°: a, alloy Ti_2Al; b, alloy with 20 percent Zr; c, alloy with 50 percent Zr; d, alloy with 60 percent Zr; e, alloy with 85 percent Zr; 1, α phase; 2, γ phase; 3, β phase.

The diffuseness of the reflection lines on the x-ray patterns of these alloys indicates a certain lack of equilibrium in this state, although the x-ray patterns do not show the reflection lines of the β solid solution. X-ray analysis of alloys with 45-60 percent Zr quenched from 1100° heretofore has not permitted any definite conclusion to be drawn concerning the composition of the compound formed by the decomposition of the β phase in the temperature range of 1000-1100°. For this reason, and also because of the insufficiently complete data of the thermal analysis, the polythermal cross section of the Ti_2Al-Zr section plotted on the basis of the data of microstructural and x-ray analyses (fig. 3) is only tentative. The transformations observed in the alloys of this section indicate the presence of a region of a three-phase equilibrium of α + β + Zr_3Al; the existence of this region is confirmed by the results of the thermal analysis performed on alloys containing 10-70 percent Zr. The thermal analysis was carried out by differential recording of heating curves with the Kurnakov pyrometer. The alloys were heated in air up to 1100-1150°. As is evident from figure 3, the temperature of the eutectoid transformation of the β phase decreases from 975 to 780° as the zirconium content of the alloys increases from 10-70 percent.

It was impossible to obtain data on the temperatures of the phase transformations of the component alloys containing over 70 percent Zr because of the high rate of their oxidation.

Thermograms of the investigated alloys show that in the range of 15-45 percent Zr, the highest oxidation rate begins at temperatures of 950-920°. In the alloy containing 50 percent Zr, it begins at 755°, and in the alloy with 90 percent Zr, this temperature drops to 600°.

Let us examine the "composition-hardness" diagrams of the alloys of the Ti_2Al-Zr section at the three temperatures of the heat treatment (fig. 4). The

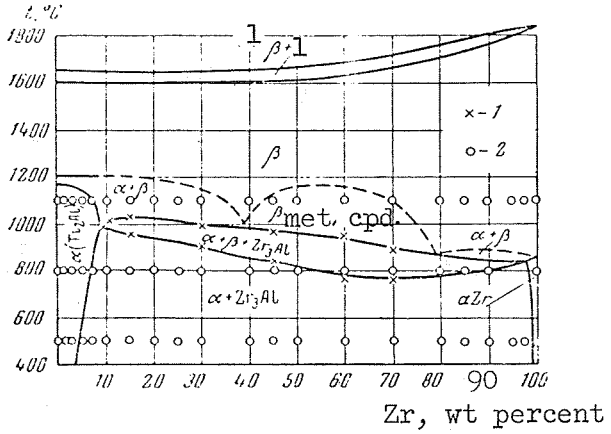

Figure 3. Polythermal cross section of the section Ti_2Al-Zr: 1, data of thermal analysis; 2, compositions of alloys studied.

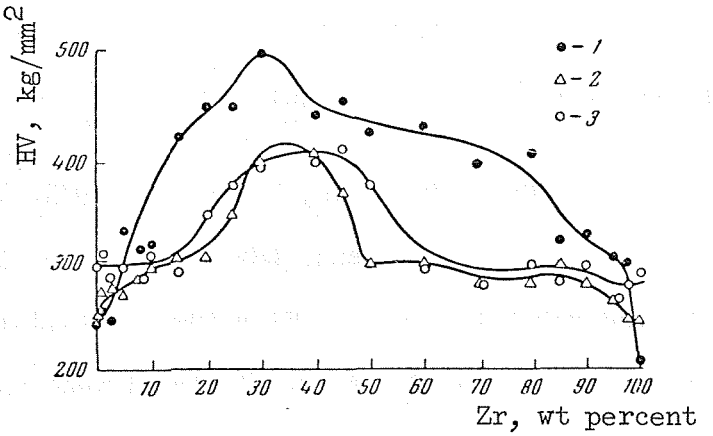

Figure 4. Hardness versus composition of alloys after quenching: 1, at 1100°; 2, at 800°; 3, at 500°.

hardness of these alloys changes along curves having a maximum corresponding to 30 percent Zr at a hardening temperature of 1100° and 30-40 percent Zr at 800 and 500°. In the concentration range of 15-90 percent Zr, the alloys quenched from 1100° have hardness values that are 50-100 units higher than those of the alloys quenched from 800 and 500°; this is explained by the formation of martensitelike structures of the metallic compound in the course of quenching from 1100°. The appearance of a substantial quantity of equilibrium grains of the α phase at 800 and 500° is associated with a decrease in the hardness of these alloys. The hardness values of alloys of this section at temperatures of 800 and 500° lie approximately within the same limits, and the hardness increases slightly in the region of certain alloys owing to the formation of an additional quantity of the metallic compound. Measurements made on the electrical resistivity of the alloys of the Ti_2Al-Zr section, the results of which

are shown in the table, do not permit one to relate this property to the microstructure. However, the data indicate that the maximum values of the electrical resistivity are displayed by the alloy of the composition Ti_2Al,

which is richest in aluminum. The introduction of up to 10 percent Zr slightly decreases the electrical resistivity of the alloys. A further increase in the zirconium content of the alloys causes a drop in resistivity, which reaches minimum values in the alloy with 90 percent Zr. Values of the specific gravity of the alloys of the Ti_2Al-Zr section are also given in the table.

The above investigation has shown that the chemical interaction of titanium, aluminum and zirconium in the alloys of the Ti_2Al-Zr section has a more complex course than in the alloys of the sections Ti_6Al-Zr and Ti_3Al-Zr, in

which it remains analogous to the interaction of titanium with zirconium.

An increase in the aluminum content of the alloys of the Ti_2Al-Zr system

leads to the appearance of phase components characteristic of the binary system Zr-Al.

REFERENCES

1. Mikheyev, V. S. and Markovich, K. P. Coll. Titanium and Its Alloys (Titan i yego splavy). Izd-vo AN SSSR, No. 7, p. 111, 1962.

2. Fast, I. D. Rec. Trav. Chim. Pays-Bas, Vol. 58, p. 973, 1939.

3. McPherson, D. J. and Hansen, M. Trans. ASM, Vol. 46, p. 354, 1954.

4. McQuillen, A. D. and McQuillen, M. A. Titanium. Metallurgizdat, 1956.

5. Yeremenko, V. N. Titanium and Its Alloys (Titan i yego splavy). Izd-vo AN UkSSR, Kiev, 1960.

6. Ence, E. and Margolin, H. Trans. AIME, Vol. 209, p. 484, 1957.

7. Sato, T., Huang, Y. C. and Kondo, Y. J. Japan Inst. Metals, Vol. 23, No. 81, p. 456, 1959.

8. Grum-Grzhimaylo, N. V., Kornilov, I. I., Pylayeva, Ye. N. and Volkova, M. A. Dokl. AN SSSR, Vol. 137, No. 3, p. 599, 1961.

RELATIONSHIP OF STRUCTURES FORMED ON QUENCHING TITANIUM ALLOYS TO EQUILIBRIUM PHASE DIAGRAMS

B. A. Kolachev and V. A. Livano

Recently, a number of published studies (refs. 1-4) have shown metastable phase diagrams of titanium alloys illustrating structures arising in the alloys after quenching. These diagrams are plotted in the coordinates temperature of heating for quenching versus concentration of alloying elements. In principle, metastable phase composition diagrams of titanium alloys can be easily related to their equilibrium phase diagrams if the metastable properties of the β phase are already known.

As an example, we shall examine the phase diagram of titanium with a β stabilizer represented by a transition element (fig. 1). In the problem under consideration, to a first approximation, it is not important whether or not there is a eutectoid transformation in the system under study, since in titanium systems with transition elements, eutectoid transformations occur extremely slowly and do not have any appreciable effect on the structures obtained on quenching.

We shall assume further that in alloys having a concentration of alloying elements in the β phase lower than the critical concentration (C_2), there takes place during quenching a martensite transformation starting at some temperature

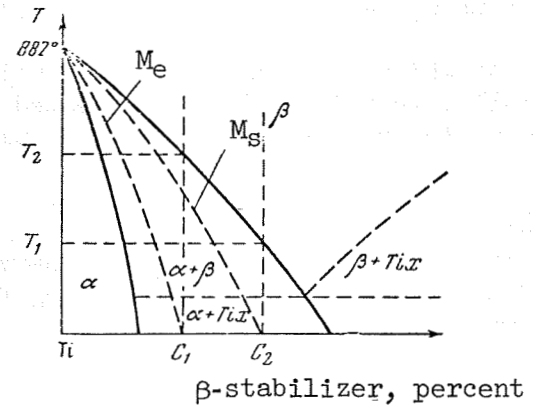

Figure 1. Schematic phase diagram of alloys of titanium with a transition element.

M_s which decreases with increasing content of the alloying element (fig. 1). In keeping with the general principles of such transformations, one can assume that the martensite transformations in titanium alloys end at a certain temperature M_e which also decreases with increasing content of the β stabilizer, and which at a certain concentration C_1 reaches the room temperature value (ref. 5).

In this case, on quenching from the β region in alloys with a concentration of the alloying element less than C_1, the martensite transformation will go to completion, and the structure of such alloys in the quenched state should be represented only by the martensitic α' phase. At a concentration of the alloying elements from C_1 to C_2, the martensite transformation does not go to completion, and the structure of alloys with such a concentration of the β stabilizer after quenching from the β region will be represented by two phases: α' and β. Finally, if the concentration of the β stabilizer exceeds the critical value C_2, only the β phase will be fixed on quenching from the β region.

In the two-phase α + β region at temperatures below T_1, the concentration of the β stabilizer in the β phase is greater than the critical value, and for this reason it will not undergo a martensite transformation on quenching. The structure of alloys after cooling from temperatures corresponding to this region of the phase diagram will be represented by α and β phases. In the temperature range from T_1 to T_2, the concentration of the β stabilizer in the β phase in the two-phase α + β region is below critical, and therefore the β phase changes into a phase of martensite type during quenching. Since the martensite transformation in the β phase with a concentration of the β stabilizer from C_1 to C_2 does not go to completion, the final structure of the quenched alloys will be represented by α, α' and β phases. During heating for quenching up to the two-phase α + β region above temperature T_2, the concentration of the β stabilizer in the β phase is less than C_1, and therefore the $\beta \rightarrow \alpha'$ transformation goes to completion, as a result of which the final structure will be represented by the α and α' phases. Naturally, when low alloys are heated for quenching up to temperatures corresponding to the α region, the structure of these alloys after quenching will be represented only by the α phase.

As was shown by the work of N. V. Ageyev (ref. 1-4), it may be considered a firmly established fact that in the majority of binary alloys of titanium with transition elements, if the temperature of the heating for quenching is high enough, the ω phase separates on quenching from the β phase. The metastable diagram of the phase composition of the titanium alloys after quenching can then be represented by the diagram shown in figure 2.

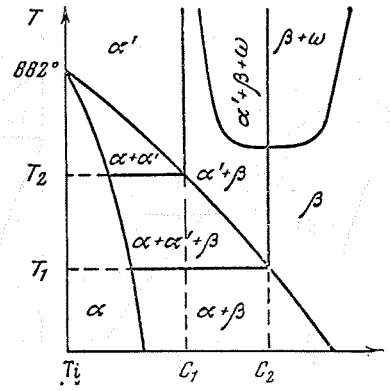

Figure 2. Schematic metastable diagram of the phase composition of high-purity titanium alloys.

In alloys of technical-grade purity, owing to the presence of impurities, the lines of the phase diagram which bound the two-phase region do not converge at one point, and the metastable diagrams of the phase composition of titanium alloys can then be described by the diagram shown in figure 3a. The region of decomposition of the β phase with the precipitation of the ω phase can be wedged into the $\alpha + \alpha' + \beta$ region or even into the $\alpha + \beta$ region of the metastable diagram, and the latter then assumes the form illustrated in figures 3b and c, respectively.

It is interesting to note that in the illustrated metastable diagram of titanium alloys, regions which differ in phase composition by only one phase border on one another directly. The only exception is the boundary between the α and $\alpha' + \alpha + \beta$ regions, which separates regions differing by two phases. This exception is obviously due to the fact that the α region of figure 2 and 3 is essentially a region of an equilibrium phase diagram and not a metastable region.

Apparently, the law of adjacent state spaces operating in equilibrium systems, by which "only state spaces which differ by one phase" (ref. 6, p. 39) border directly on one another in the system, can be extended to metastable diagrams as well. However, this law should not be applied to metastable diagrams without certain qualifications. Thus, for example, the law of adjacent state spaces will not be obeyed if any high-temperature phase changes into two metastable phases on quenching.

In order to compare the diagrams proposed above with the published metastable phase-composition diagrams plotted experimentally, metastable diagrams for alloys of the system Ti-Fe (fig. 4) and Ti-Ni (fig. 5), plotted from the data of references 2 and 3, are illustrated. These experimentally plotted metastable diagrams unquestionably confirm the proposed diagrams. At the same time, the theoretical diagrams permit a more accurate interpretation of the experimental data. Thus, for example, the line separating the $\alpha + \alpha'$ and $\alpha' + \alpha + \beta$ regions from the α' and $\alpha' + \beta$ regions (fig. 4) should be somewhat inclined toward the

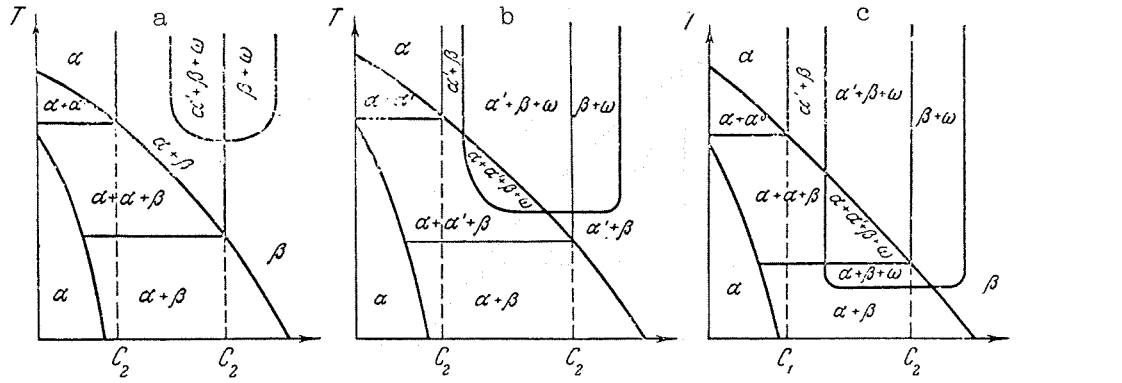

Figure 3. Schematic metastable diagram of the phase composition of titanium alloys of technical-grade purity.

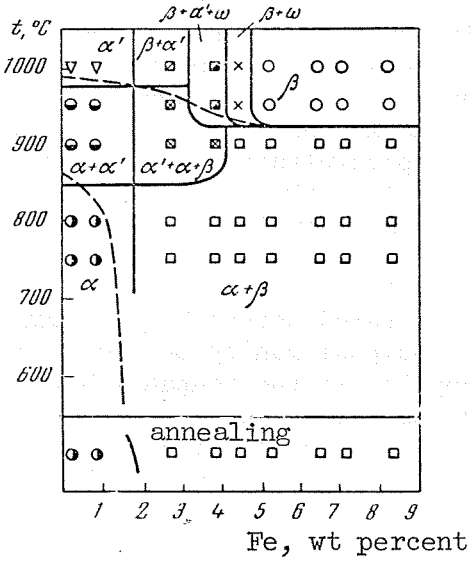

Figure 4. Metastable diagram of the phase composition of alloys of the system Ti-Fe.

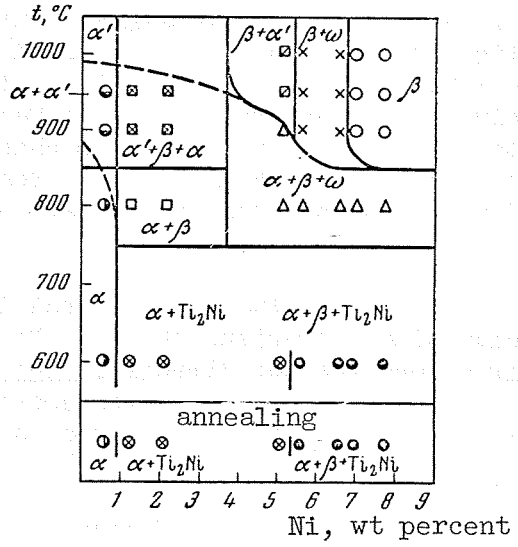

Figure 5. Metastable diagram of the phase composition of alloys of the system Ti-Ni.

axis of abscissas, while the line separating the $\alpha' + \beta$ region from the $\alpha' + \beta + \alpha$ region (fig. 5) should be drawn as shown by the broken line.

Not all of the published metastable diagrams of titanium alloys agree so well with the proposed diagrams as those shown in figures 4 and 5. These discrepancies may be caused by the following:

1. Some phase region of the metastable diagram may be so small that at the chosen concentrations of the alloying elements and temperatures it could not be detected.

2. The holding time during heating for quenching was insufficient for the establishment of the phase equilibrium corresponding to the selected temperature of the heating for quenching.

3. In any specific system, the behavior of the β phase on quenching may differ from the behavior taken as the basis for the proposed diagrams, and the latter should then be revised in accordance with the altered basic assumptions.

Summary

1. On the basis of the equilibrium phase diagrams of alloys of titanium with transition elements and transformations occurring in these alloys on quenching, schematic metastable phase composition diagrams have been plotted.

2. The proposed sketches of metastable diagrams are in satisfactory agreement with the published experimentally plotted diagrams.

3. The theoretical metastable diagrams permit a more accurate interpretation of the experimental data.

REFERENCES

1. Ageyev, N. V. and Petrova, L. A. Coll. Titanium and Its Alloys (Titan i yego splavy). Metallurgy and Metallography, Izd-vo AN SSSR, pp. 3-16, 1958.

2. Ageyev, N. V. and Smirnova, Z. M. Coll. Titanium and Its Alloys (Titan i yego splavy). Metallurgy and Metallography, Izd-vo AN SSSR, pp. 17-24, 1958.

3. Ageyev, N. V. and Petrova, L. A. Zh. neorg. khim., Vol. 4, No. 8, 1959.

4. --- Zh. neorg. khim., Vol. 4, No. 5, 1959.

5. Jaffy, R. I. Advances in Metal Physics (Uspekhi fiziki metallov). Metallurgizdat, Vol. 4, pp. 77-192, 1961.

6. Volovik, B. Ye. and Zakharov, M. V. Ternary and Quaternary Systems (Troynyye i chetvernyye sistemy). Metallurgizdat, p. 39, 1948.

STABILITY OF β ALLOYS OF THE SYSTEM Ti-Mo-Cr-Fe-Al

N. V. Ageyev, S. G. Glazunov, L. A. Petrova,
G. N. Tarasenko and L. P. Grankova

A study of the stability of heating of the metastable β solid solution of titanium alloys with a relatively constant critical content of the alloying agent (6-9 percent) has shown that the most stable binary β alloys are alloys of titanium with rhenium, nickel, molybdenum and tungsten (ref. 1). If an alloy is taken containing 6 at. percent Fe, i.e., with an iron content exceeding the critical value necessary for the stability of the β phase in the Ti-Fe alloy, the stability of the β solid solution of this alloy will be equivalent to that of the β solid solution of the alloy of titanium with the critical content of nickel (6.3 at. percent Ni).

These data as well as data on other titanium alloys (ref. 1) have led to the conclusion that an increase in the concentration of the alloying agent causes an increase in stability which is greater the higher the content of the alloying agent. It should be borne in mind, however, that an increase in the content of the alloying agent affects the increase in stability up to a certain limit above which the stability remains the same as in alloys with a lower content of the alloying agent.

If the increase in the concentration of the alloying agents promoted not only an increase in stability but also an improvement in mechanical characteristics, it would be possible to develop alloys with a high content of alloying elements despite the rise in the density of the alloy. It is known, however, that over the entire range of possible concentrations of the alloying elements, binary titanium alloys do not exhibit high mechanical characteristics, with the exception of the system Ti-Mo, in which it is possible to obtain σ_b = 91.7 kg/mm^2 at δ = 16 percent, but whose density is 20 percent higher than that of pure titanium (ref. 2).

At the present time, major attention is concentrated in the development of new titanium alloys on multicomponent alloys with a metastable β structure which combine a high technological plasticity in the hardened state, necessary for the manufacture of intricate-shape parts, with a high strength after aging (ref. 3).

On the basis of what was stated above concerning the effect of alloying elements on the stability of titanium alloys, and also on the basis of

literature data on the influence of these elements on the various properties of the alloys, which will be discussed below, we selected the system Ti-Mo-Fe-Cr-Al for our investigation.

The purpose of the work, on the one hand, was a study of the stability on heating of the metastable β phase and, on the other hand, a study of the decomposition and the selection of alloys for a more detailed investigation.

It is known that molybdenum not only improves the mechanical properties of titanium alloys, but has a desirable effect on the stability of the β phase, and hence on the thermal stability. Iron increases the strength of titanium alloys, but decreases the thermal stability somewhat. Chromium increases the strength and heat resistance of titanium alloys (ref. 4), increases the calcinability (ref. 3), and owing to the high rate of decomposition of the β phase (the alloy of titanium with the critical content of 8.48 at. percent chromium decomposes at room temperature in 50 days (ref. 1)), makes it possible to obtain the desired properties with a shorter holding time during aging, a feature important in practice. Although aluminum is an α stabilizer, when present in small amounts (1.5-4 wt. percent) in titanium alloys, it acts like β stabilizers and decreases the critical concentration of elements which is required for the stabilization of the β solid solution. By depressing the formation of metastable phases during the heat treatment, aluminum increases the thermal stability and decreases the brittleness of the alloy. The combined presence of aluminum and chromium has a desirable effect on the heat resistance of titanium alloys and on the increase in thermal stability.

Since the β phase can be obtained in the metastable state in titanium alloys at an electron concentration of 4.20 el/atom (ref. 5), the compositions of the alloys of the system Ti-Mo-Cr-Fe-Al were chosen (table 1) so that they would be quenched into a β solid solution.

The alloys were prepared from sponge TG00 (0.05 percent Fe; 0.03 percent Si; 0.05 percent C; 0.028 percent N; HV = 121 kg/mm^2; σ_b = 37.9 kg/mm^2; δ = 47.8 percent, ψ = 80.5 percent) from the master alloy Al-Mo (29.8 percent Al; 70.6 percent Mo; 0.05 percent Si; 0.08 percent Fe); AV000 aluminum, Kh0 chromium, and armco iron in an arc furnace by the double remelting method. After the remelting, ingots weighing 400 g were turned on a lathe and forged into rods 15 mm in diameter and squares 15 x 15 mm. The ingots were heated for forging in an electric furnace at 1000-1100° for 15 min with subsequent intermediate heating for 2-3 min.

After forging, the ingots were turned on a milling machine and cut into specimens for studying the microstructure, x-ray photographing of the polished sections, and hardness measurements, and into microspecimens for tensile testing (length l = 25 mm; diameter of the working part d = 1.5 mm; size of head 5 x 5 mm^2), and impact (l = 40 mm; a = 5 mm).

TABLE 1. COMPOSITION OF ALLOYS OF THE SYSTEM Ti-Mo-Cr-Fe-Al (IN wt PERCENT).

Alloy number	Charge					Chemical analysis							
	Mo	Cr	Fe	Al	Ti	Mo	Cr	Fe	Al	N	O	H	C
First series													
1	2	9	3	3	83	2,13	9,07	2,8	2,7	0,025			0,086
2	2	8	4	3	83	2,16	6,2	4,0	3,1			0,0061	
3	2	5	7	3	83	2,2	5,2	6,68	2,81	0,036	0,05		0,024
4	2	4	8	3	83	2,2	3,76	7,35	3,15	0,025			0,076
Second series													
6	3	8	3	3	83	3,0	8,80	2,80	2,90		0,082	0,01	
	3	7	4	3	83	3,15	7,23	4,20	3,14				
7	3	6	5	3	83	2,83	5,22	5,10	2,95				
8	5	4,5	5	3	82,5	3,17	3,10	5,20	3,00	0,042		0,0045	0,047
9	3	5	6	3	83	3,0	5,0	6,0	3,0				
10	5	3,5	6	3	82,5	3,24	3,5	8,5	2,89	0,025		0,0070	0,057
Third series													
11	4	7,5	3	3	82,5	4,20	5,90	3,05	3,13	0,036			0,039
12	4	5,5	5	3	82,5	4,20	6,90	5,15	2,95	0,036			0,033
13	4	4,5	6	3	82,5	4,20	4,65	5,90	3,01	0,042			0,026
14	4	3,5	7	3	82,5	4,06	5,22	7,01	2,95	0,236			0,076
Fourth series													
15	5	6,5	3	3	82,5	4,80	9,40	3,04	2,96	0,025			
16	5	5,5	4	3	82,5	4,88	5,65	5,02	3,00				
17	6	4,0	5	3	82	5,10	4,08	4,90	3,13	0,042	0,093		0,027
18	7	5,5	3	3	81,5	5,80	5,35	3,29	2,6		0,127	0,0054	
19	6	5	4	3	82	6,10	3,69	4,05	3,01	0,025	0,097		0.038
Fifth series													
20	7	4,5	4	3	81,5	7,15	4,6	4,0	3,01	0,034			0,031
21	7	3,5	5	3	81,5	7,20	3,55	4,83	3,20		0,109	0,0087	
22	8	4	4	3	81,0	7,80	4,10	3,94	3,18				

The alloys were studied by metallographic and x-ray analyses. The hardness was measured with a Vickers instrument with a 10 kg load. The mechanical properties (σ_b, δ and a_H) were determined at room temperature. The x-ray patterns were taken from a polished section in CuK α radiation with a nickel filter in an RKU evacuated camera, and the heat treatment of the alloys was carried out in sealed quartz and molybdenum ampules preevacuated to 10^{-4} mm Hg. To quench the alloys, the ampules were crushed directly in water.

In order to determine the quenching temperature from which the metastable β phase is frozen, the alloy specimens (d = 10 mm, h = 5 mm and abh = 10·10·5 mm)

were quenched from 750, 800 and 850° in water. Alloys with a high content of alloying agents were quenched from 800°, but for the most part the alloys were quenched from 850°. To compare the behavior of the alloys during aging, they were quenched from the same temperature at 850°.

The hypothesis that the selected alloys with an electron concentration of 4.20 el/atom should have a metastable β phase on cooling in water was confirmed by metallographical and x-ray phase analysis which showed that the alloys of the compositions indicated in table 1 had a metastable β structure after quenching from 850°. Their structure differed in grain size only (fig. 1a and b).

All the alloys with the metastable β structure were tempered at 100, 200, 300, 350, 400, 450 and 500° for 1-100 hrs, and in some cases for up to 169 hrs. The dependence of the hardness of the alloys on the aging temperature and on the holding time is illustrated graphically (figs. 2-6).

For convenience, these alloys were divided into five series depending upon the molybdenum content. The aluminum content in all the alloys was 3 percent.

In the alloys of the first series (with 2 percent Mo), the amount of iron increased from 2.8 to 7.35 percent and the amount of chromium decreased from 9.07 to 3.76 percent from alloy 1 to alloy 4.

The hardness of alloys 2, 3 and 4 does not change during heating to 200° in the course of 100 hr, whereas in alloy 1 it increases after 9 hrs. The constant hardness of alloys 2, 3 and 4 indicates the stability of the β solid solution at this temperature. A proof of the stability of the β solid solution in this case is the presence of only the lines of the β solid solution on the x-ray patterns of these alloys. The x-ray pattern of alloy 1, tempered for

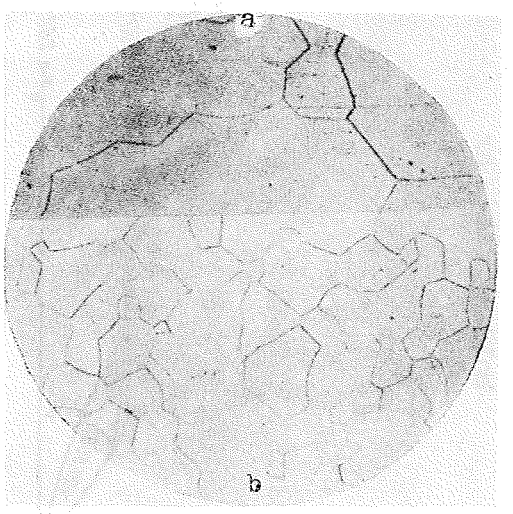

Figure 1. Microstructure of alloys of the system Ti-Mo-Cr-Fe-Al quenched in water from 850°, x 120: a, alloy 15; b, alloy 18.

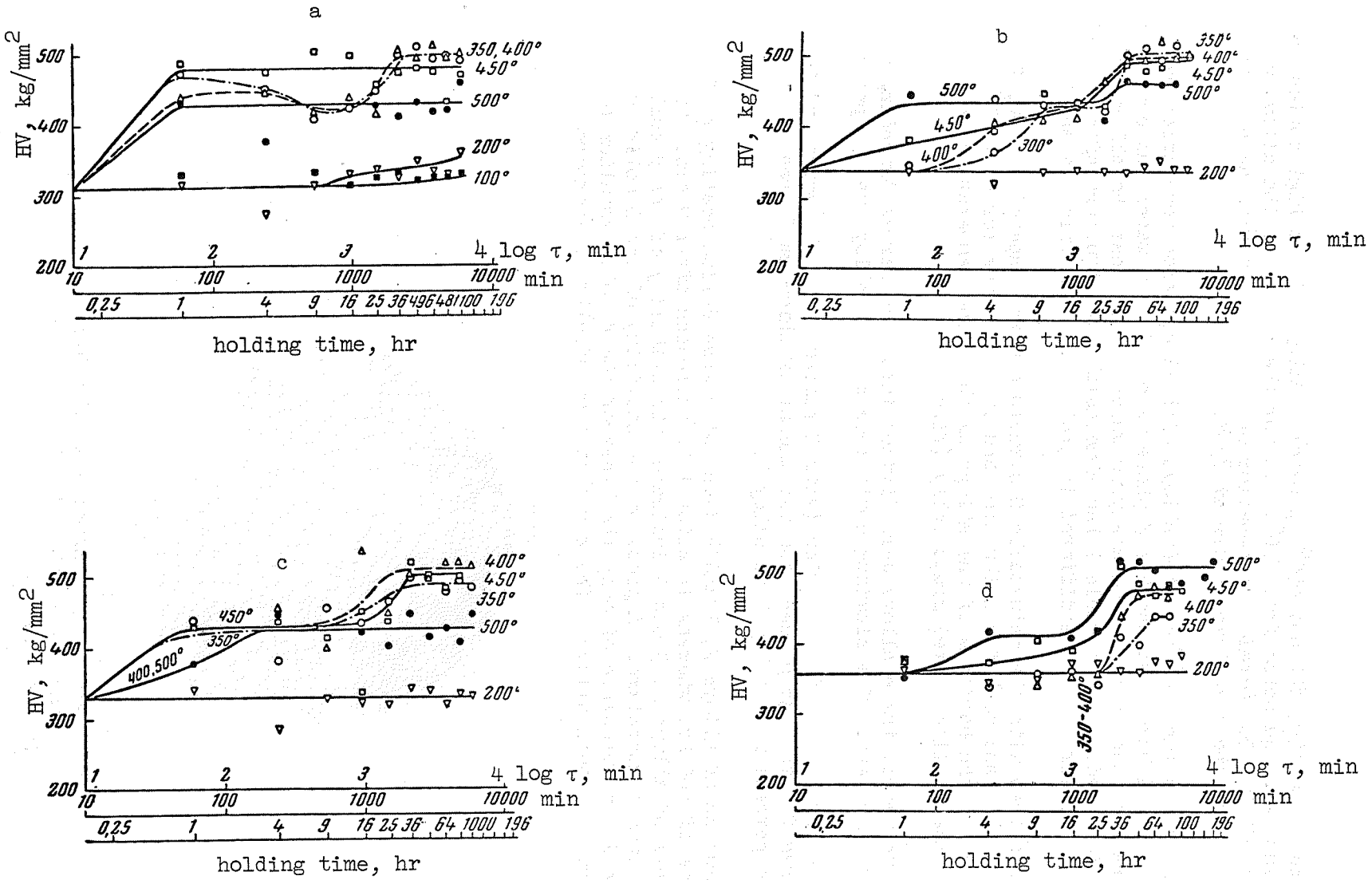

Figure 2. Hardness of alloys of the first series versus aging temperature and holding time: a, alloy 1; b, alloy 2; c, alloy 3; d, alloy 4.

9-100 hrs at 200°, shows the ω phase, which is responsible for the increase in the hardness of alloy 1 under the same aging conditions.

An inspection of the curves of the hardness of the alloys subjected to aging at higher temperatures leads to the conclusion that the higher the chromium content and the lower the iron content of the alloy, the faster is the decomposition of the β solid solution and the increase in hardness (see fig. 2a, b, c and d). In the case of aging at 350-500°, the β solid solution of alloys 1 and 2, containing up to 4 percent Fe, decomposes at once, and that of alloys 3 and 4 (~7 percent Fe), after some time, so that the hardness curves of these alloys are also shifted to the right. In all alloys except alloy 1 aged at 350-400°, and in all alloys aged at 400-500°, a gradual decomposition of the β solid solution and hence a gradual increase in hardness are observed. The hardness of alloy 1 decreases during aging for 1-9 hrs, and increases again as the aging time is raised to 49 hrs. This shape of the hardness curves is explained by the fact that on aging in the temperature range of 350-400° for 1 hr, alloy 1 decomposes not with the separation of the α phase, as in the case of all the alloys, but ω phase, which, as the duration of the aging increases, changes into the α phase, as a result of which the hardness of the alloy increases again after 16 hrs.

The high iron content of alloy 4 as compared to alloys 1, 2 and 3 promotes an increase in the stability of this alloy on aging. Alloy 4, which contains twice as much iron (7.35 percent) as chromium (3.76 percent), decomposes at an aging temperature of 350-400° after 25 hrs, and at an aging temperature of 450-500° after 1 hr.

The decreased hardness of this alloy at an aging temperature of 350-400° and even 450° in the course of 100 hrs as compared to its hardness at an aging temperature of 500° for the same period of time is probably a result of the slower decomposition of the β solid solution of the alloy at an aging temperature of 350-450° than at 500°. In order to reach the hardness obtained at an aging temperature of 500° or even a higher value, a longer holding time than 100 hrs is necessary during aging at 350-450°.

From an analysis of the hardness curves of the alloys of the first series (containing 2 percent Mo) it follows that all alloys with the exception of alloy 4 practically reached a stable value of the hardness after 36 hrs of holding time. Of the alloys in this series, the one deserving most attention is alloy 3, which has the lowest scatter of stable hardness.

Let us examine the change in the hardness of alloys of the second series, containing 3 percent Mo and various quantities of iron and chromium. The amount of iron increases from 2.8 to 8.5 percent from alloy 5 to alloy 10, and the amount of chromium decreases from 8.8 to 3.5 percent. The hardness of all the investigated alloys during aging at 200° for 100 hrs remains practically unchanged (see fig. 3a, b, c, d and e), indicating the stability of the alloys under these conditions. The data on the hardness are supported by microstructural and x-ray analyses, which indicate the presence of the β solid solution alone. On heating to higher temperatures (300° and higher), the β solid solution of the alloys decomposes, and hence the hardness increases.

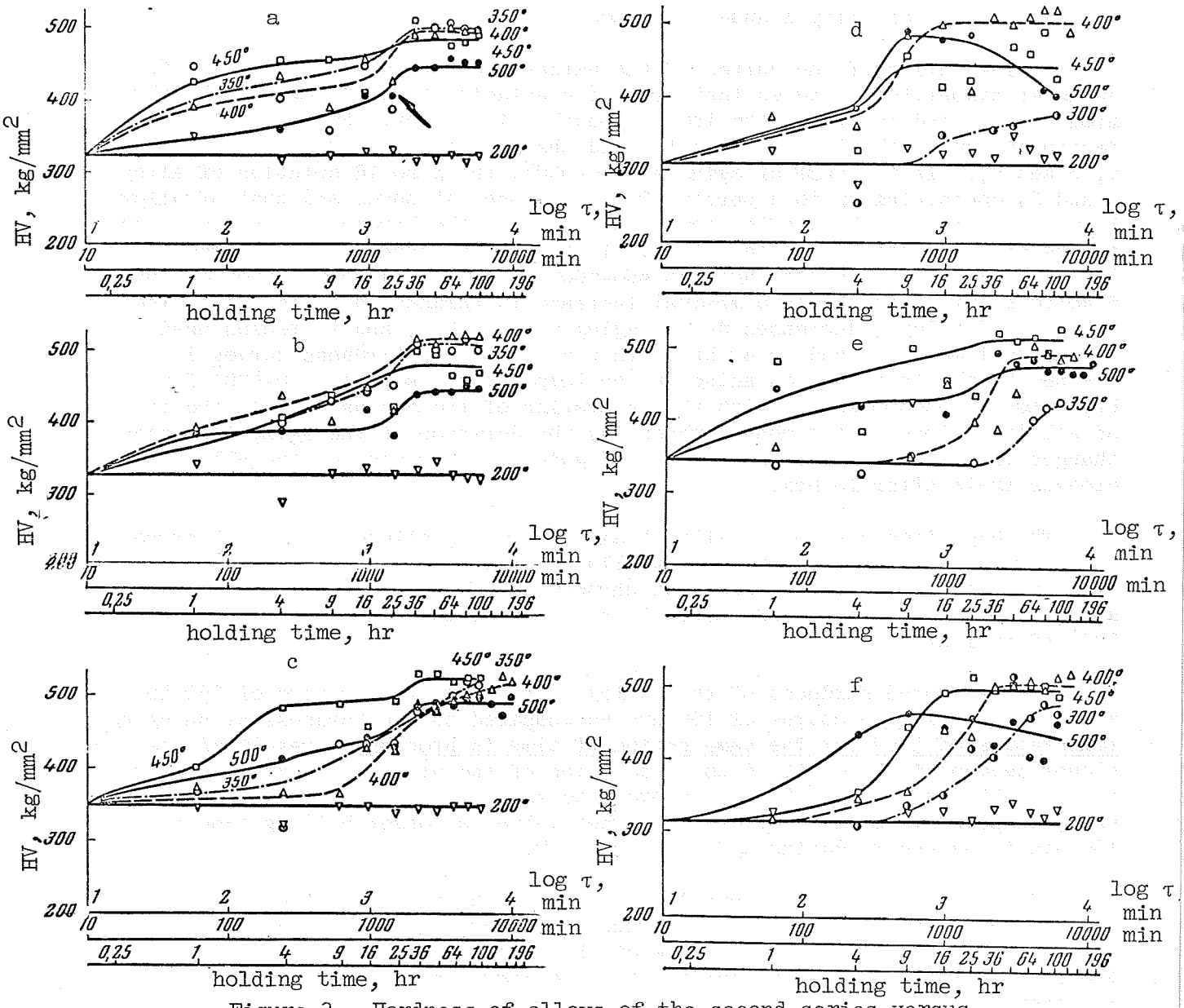

Figure 3. Hardness of alloys of the second series versus aging temperature and holding time: a, alloy 5; b, alloy 6; c, alloy 7; d, alloy 8; e, alloy 9; f, alloy 10.

An increase in the content of iron and a decrease in the content of chromium in the alloys of this series as well as in the alloys of the preceding series raises the stability of the β solid solution somewhat. In alloys 10, 8 and 9, the hardness at an aging temperature of 300-350° remains practically unchanged at holding times of 4, 9 and 16 hrs, respectively, in contrast to alloys 5, 6 and 7, in which the change in hardness becomes insignificant 1 hr after heating. An increase in the iron content and decrease in the chromium content of the alloys also promote a great maximum hardness on aging. Thus, in

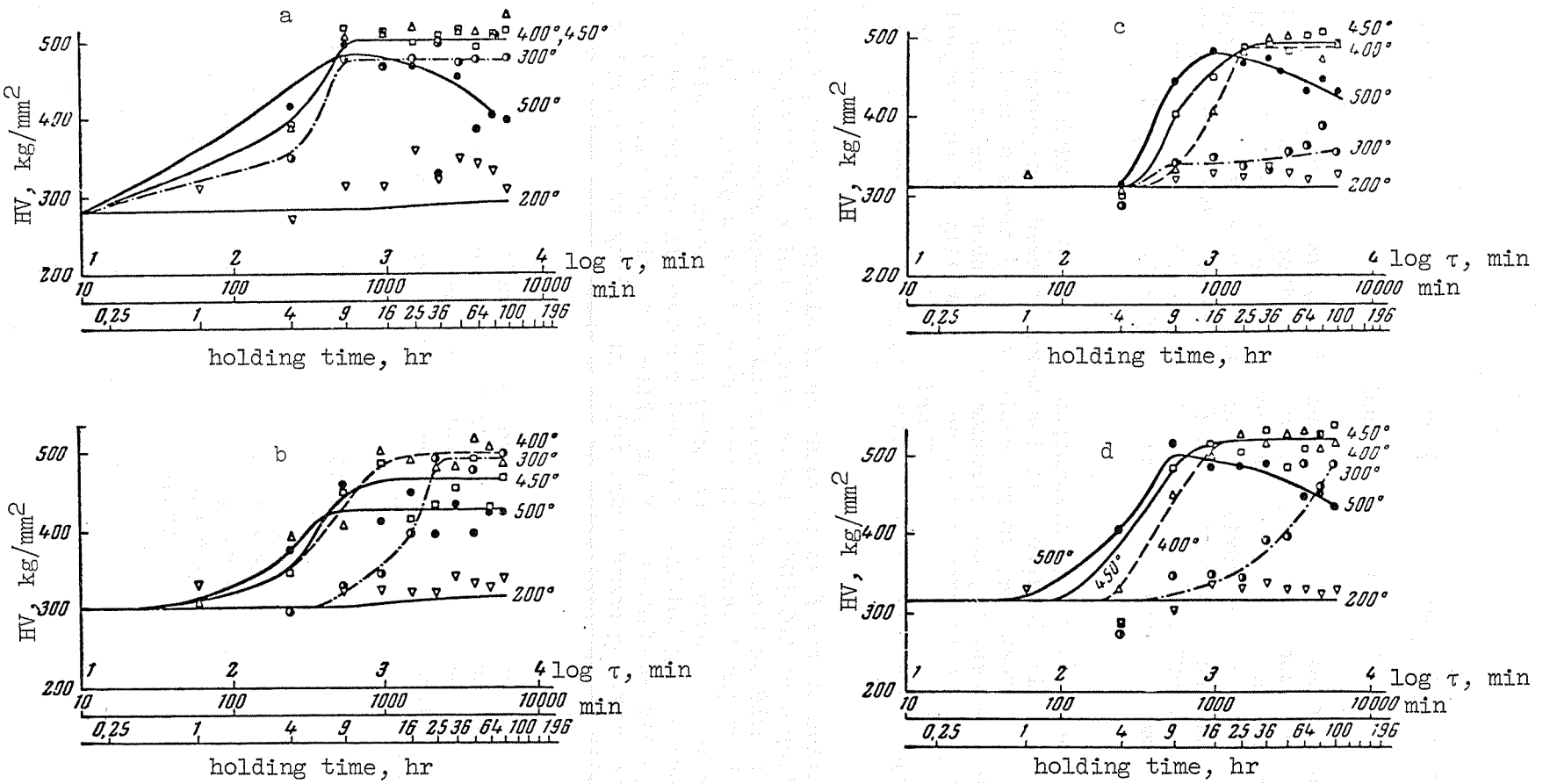

Figure 4. Hardness of alloys of the third series versus aging temperature and holding time: a, alloy 11; b, alloy 12; c, alloy 13; d, alloy 14.

the range of 500-350°, the hardness of alloy 5 is equal to 450-500 kg/mm^2, and that of alloy 7, 490 and 530 kg/mm^2 at 500 and 450°, respectively. At 350 and 400°, the hardness of alloy 7, having reached ~520 kg/mm^2, continues to increase. However, alloy 8, which contains the same amount of iron as alloy 7 but 2.12 percent less chromium, and alloy 10, which contains the largest amount of iron of all the alloys in the second series, do not differ in maximum hardness from alloy 5, which has the lowest iron content (2.8 percent). Furthermore, in alloys 8 and 10, on heating to 500°, the hardness, having reached a maximum value up to 9 hours, does not remain constant as in the case of alloys 5, 6, 7 and 9, and decreases.

The data obtained lead to the assumption that in alloys with 3 percent Mo, iron does not have a desirable effect if its amount exceeds ~5 percent. In alloys containing 3-4 percent Fe, there should be 1.5-2 times as much chromium, and in alloys with 5 percent Fe, the chromium content should be no less than 5 percent, since this has an adverse effect on the stability of the properties (fig. 3d and f). The hardness of alloys 7 and 9, which contain approximately 5 percent Fe and Cr each and are aged at 500°, is stable, whereas it decreases in alloy 8.

The decomposition of the β solid solution of alloys 5, 6 and 7 during aging at 350-500°, of alloy 8 at 400-500°, and of alloys 9 and 10 at 450-500° begins immediately after a holding time of one hour and proceeds with the precipitation of the α phase without the formation of the intermediate ω phase. The α phase which precipitates in the course of the aging process, even at a relatively high temperature and a long holding time, was observed in the form of very finely dispersed particles (fig. 7). X-ray phase analysis of these alloys confirmed the presence of the α phase (fig. 8a). On heating to 300°, alloys 8, 9 and 10 decompose with the precipitation of the ω phase, which exists for another 100 hours (fig. 8b).

Analyzing the data on alloys 5-10, one can assume that alloy 5 with an equal content of molybdenum, iron and aluminum (~3 percent) and with the highest content of chromium (~9 percent) is of greatest interest for a detailed investigation, owing to the highest rate of decomposition of the β solid solution, and to the establishment of a stable hardness at all aging temperatures in 36 hours.

Let us examine the curves representing the variation in the hardness of the alloys of the third series, containing 4 percent Mo and various quantities of iron and chromium (see fig. 4a, b, c, d and e). Alloy 11 (5.9 percent Cr and 3.05 percent Fe) decomposes practically at once at all aging temperatures except 200°, at which it is stable for 16 hours. Alloy 13 (4.65 percent Cr and 5.9 percent Fe) is stable at temperatures of 200 and 300° for 100 hours and at temperatures of 400 and 500° for 4 hours.

An increase in the hardness of alloy 13 at an aging temperature of 300° in 9 hours is probably due to a certain enrichment of the β solid solution with the alloying elements during the period preceding the separation of the decomposition products.

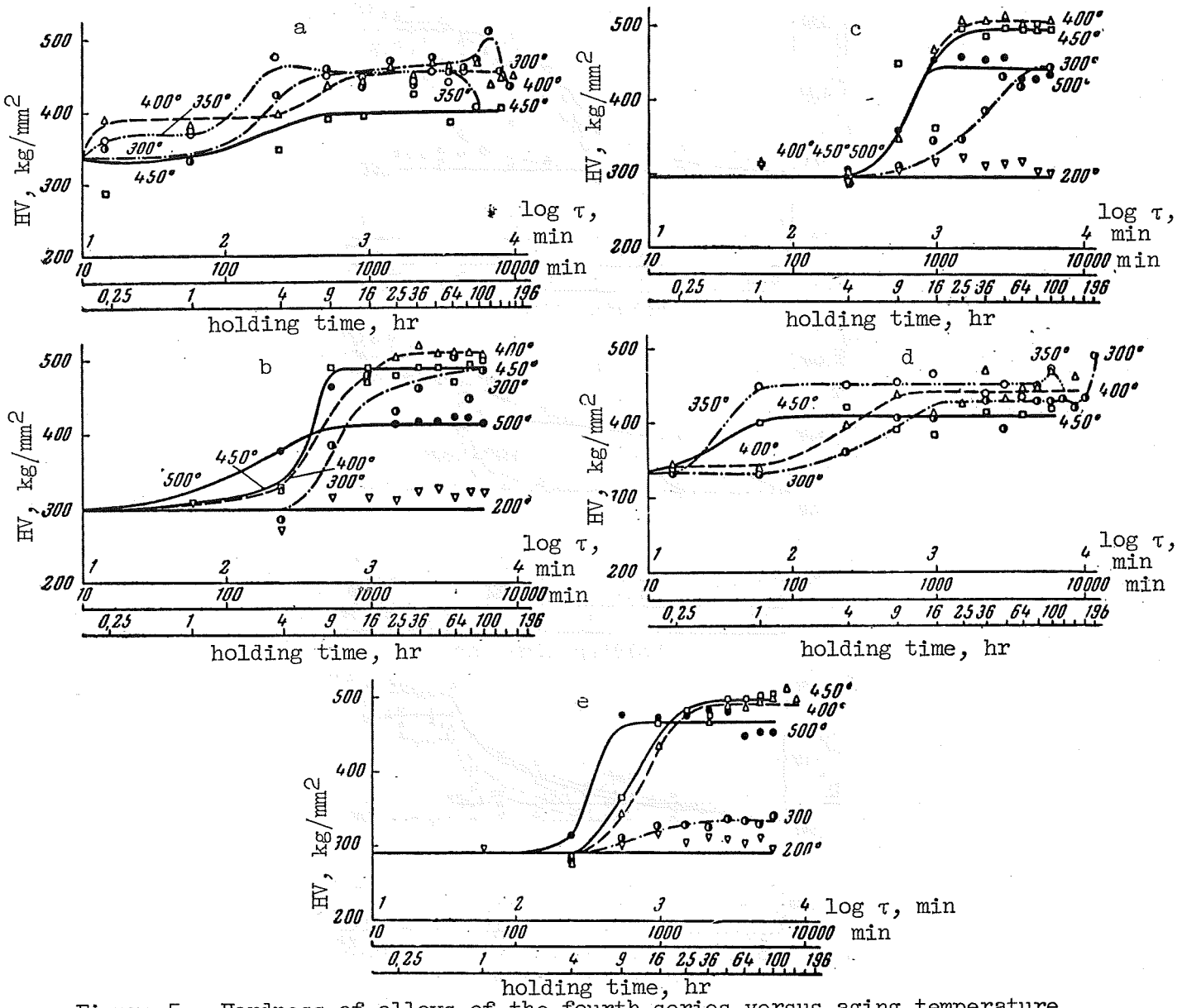

Figure 5. Hardness of alloys of the fourth series versus aging temperature and holding time: a, alloy 15; b, alloy 16; c, alloy 17; d, alloy 18; e, alloy 19.

When alloys 11, 13 and 14 are aged from 500° after the hardness maximum has been reached, a decline in hardness is observed; in alloy 11 (with the smallest iron content), the hardness decreases in 9 hours, and in alloy 13, containing 2.85 percent more iron, in 16 hours. The decline in hardness in alloys 11 and 13 at 500° is apparently related to an insufficient quantity of chromium. Like alloys 5 and 7, alloys 11 and 13, which contain approximately the same amount of iron, have a stable hardness on heating at 500° if no less than 7 and 5 percent chromium is present in the alloys.

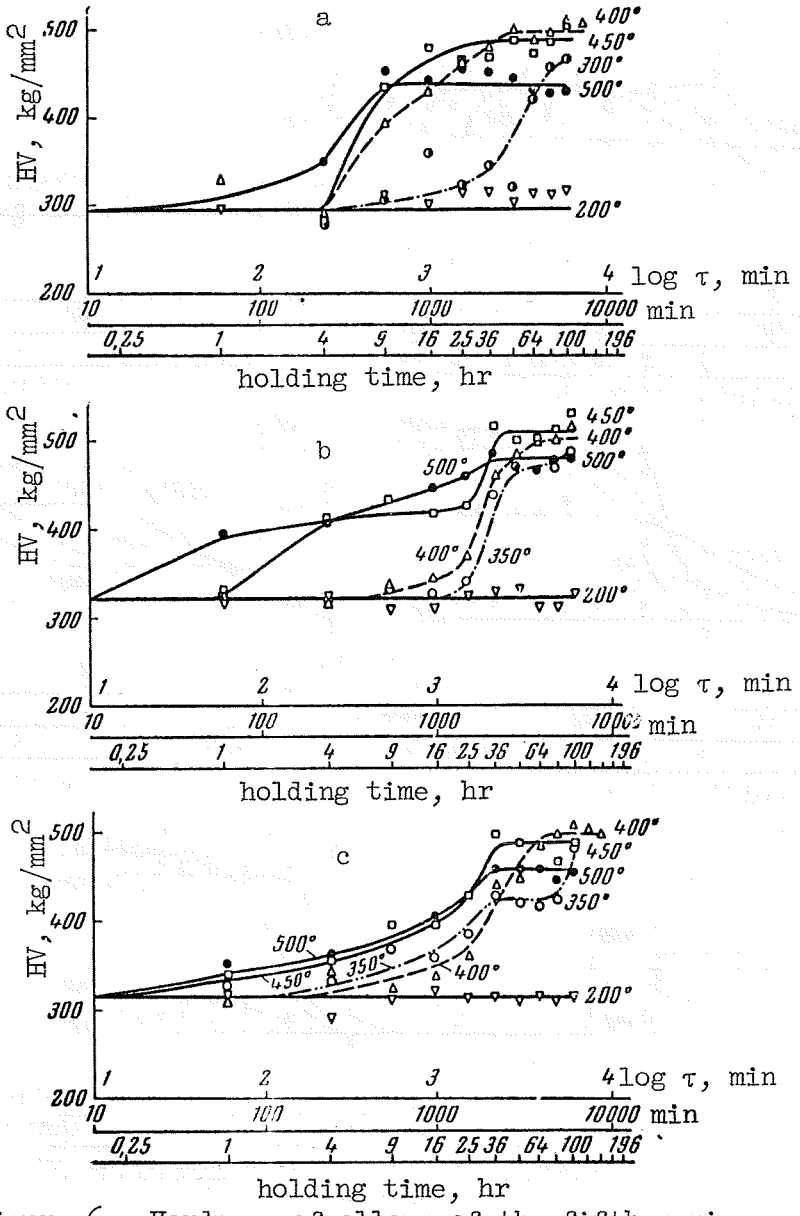

Figure 6. Hardness of alloys of the fifth series versus aging temperature and holding time: a, alloy 20; b, alloy 21; c, alloy 22.

Alloy 12 (6.9 percent Cr and 1.15 percent Fe) is stable at 200° for 100 hrs, but decomposes in 1 hr when heated at 450 and 500°, in 4 hrs at 400°, and in 9 hrs at 300°, in contrast to alloy 13, which contains a larger amount of iron but is less stable.

Alloy 14 (5.22 percent Cr and 7.01 percent Fe) is somewhat more stable than alloy 11, but less stable than alloy 13. On heating at 300-450°, alloy 12 decomposes essentially like alloy 14, but the latter on heating at 300° decomposes with the precipitation of the intermediate α phase, which is stable for

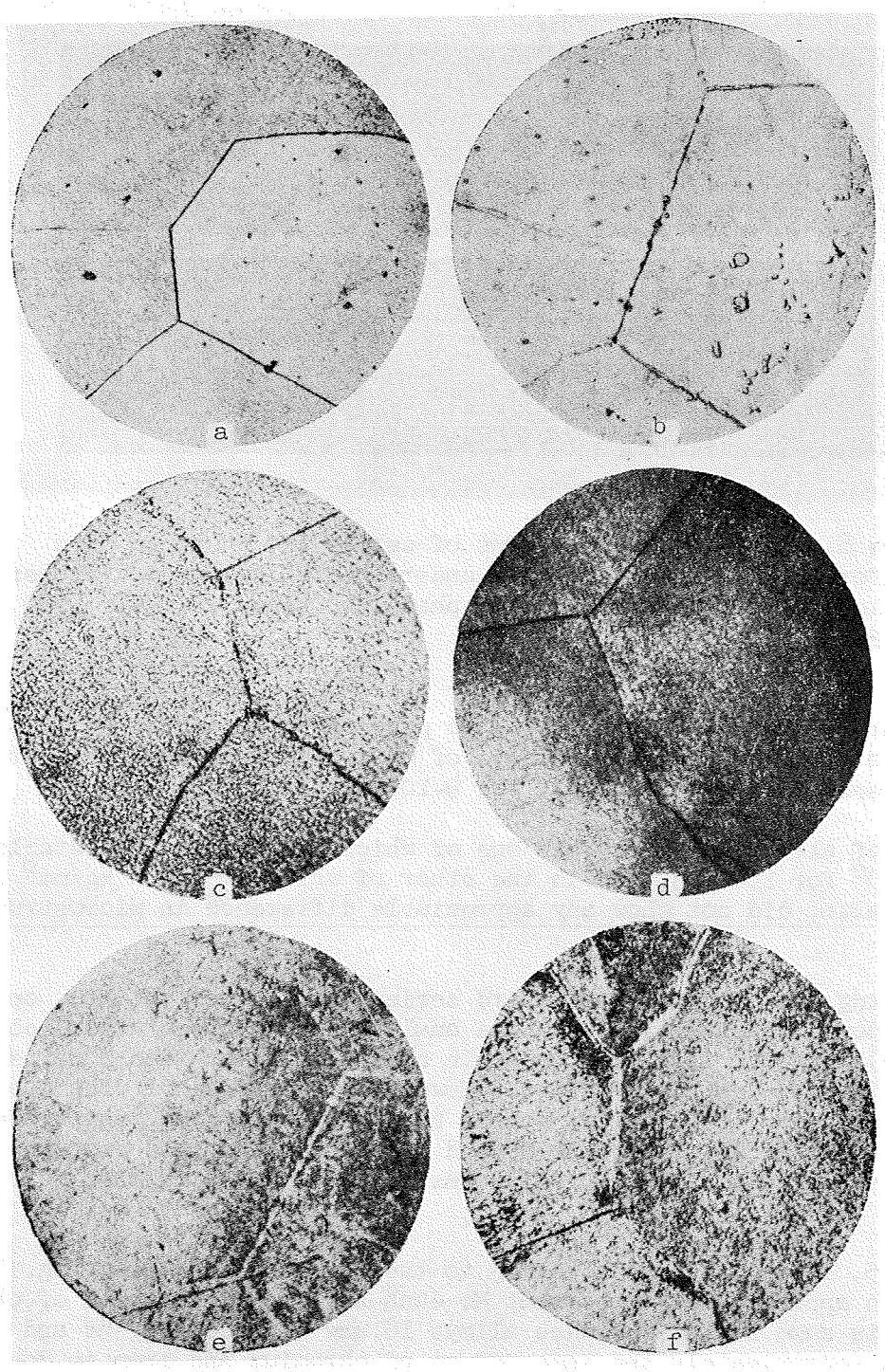

Figure 7. Microstructure of alloys of the second series quenched from 850° 1 hour in water and aged under the following conditions: a, alloy 5, 350°, 1 hr, x 340; b, alloy 5, 450°, 1 hr, x 1350; c, alloy 5, 400°, 100 hrs, x 1350; d, alloy 7, 400°, 100 hrs, x 1350; e, alloy 10, 400°, 100 hrs, x 1350; f, alloy 10, 450°, 100 hrs, x 1350.

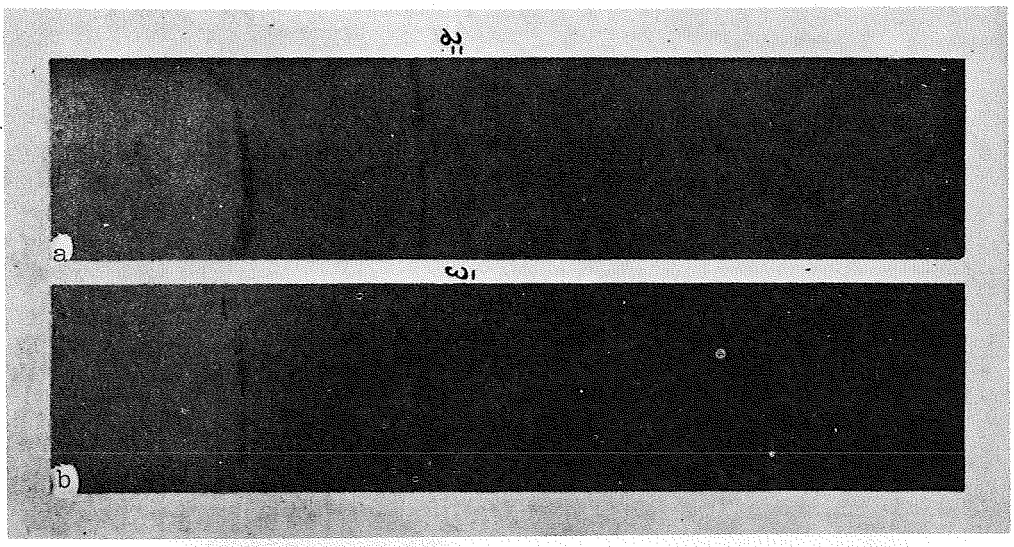

Figure 8. X-ray powder patterns of series II, quenched from 850° for 1 hr in water and aged under the following conditions: a, alloy 7, 350°, 100 hrs, β + α phase; b, alloy 10, 300°, 100 hrs, β + ω phase.

another 100 hrs (fig. 9), but not with the precipitation of the ω phase. In contrast to alloy 14 and other alloys of this series, alloy 12 retains the maximum hardness when heated at 500° for 9-100 hrs.

A study of alloys 12 and 13, in one of which the hardness is stable on heating at 500° for 100 hrs, and in the other of which it is 50 kg/mm^2 below the maximum value, did not show any appreciable difference in microstructure (fig. 10).

Considering the alloys of the third series (with 4 percent Mo), one can state as was done in connection with the analysis of alloys of the second series (3 percent Mo), that if iron is present in amounts greater than 5 percent, it does not display any desirable effect. However, as before, it should be borne in mind that in order to acquire a stable hardness at an aging temperature of 500°, an alloy containing 4 percent Mo and 5 percent Fe should contain 5 percent Cr. An example is alloy 12, which was selected for a further investigation.

Alloys 15, 16 and 17, which belong to the fourth series (see fig. 5a, b and c) contain approximately 5 percent Mo each and various amounts of chromium and iron. This same series includes alloys 18 and 19 (see fig. 5d and e), which contain approximately the same amount of chromium and iron as does alloy 17, but which differ from the latter in that they contain approximately 1 percent more molybdenum.

As was already noted in the case of alloy 5 (8.8 percent Cr and 2.8 percent Fe), alloy 15 (9.4 percent Cr and 3.04 percent Fe), which contains the greatest amount of chromium and the smallest amount of iron in the series of

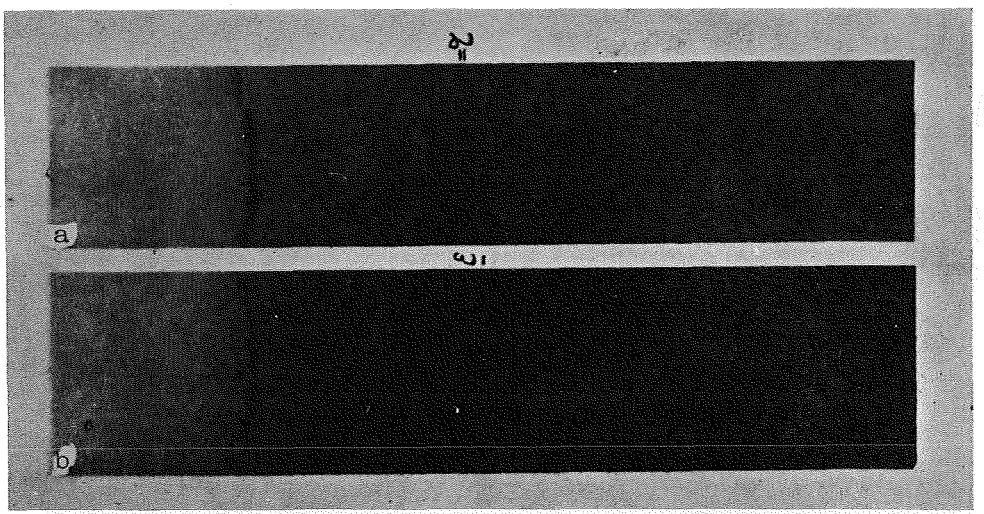

Figure 9. X-ray powder patterns of alloys of series III quenched from 850° for 1 hr in water and aged at 300° for 100 hrs: a, alloy 12, β + α phase; b, alloy 14, β + ω phase.

alloys under consideration, decomposes at once at all aging temperatures except 300°, at which the β solid solution is stable for 15 min. An increase in the iron content and decrease in chromium content in alloy 16 as compared to alloy 15 increases the stability of the β solid solution at the start of the aging; this effect is more significant the lower the temperature. Alloy 16 is stable for 4 hrs at 300°, and the hardness curves for aging at temperatures above 300° are displaced to the right.

Despite the different content of iron and chromium, alloys 15 and 16 have the same decomposition mechanism. On heating at 300°, alloys 15 and 16 decompose with the precipitation of the ω phase in 1 and 4 hrs, respectively. On heating at 350°, the precipitation of the ω phase in alloy 15 takes place in 15 min. This phase, which exists in alloy 15 at 300° for 121 hrs and at 350° for 81 hrs, changes into the α phase in 144 and 100 hrs, respectively. During aging at 400 and 450°, alloys 15 and 16 decompose at once with the precipitation of the α phase.

Alloy 17, which contains approximately the same amount of molybdenum and iron as alloy 16 but 1.5 percent less chromium, has a still greater stability during aging than alloy 16, i.e., alloy 17 practically does not decompose for 4 hrs.

A comparison of alloy 16 (4.88 percent Mo + 5.65 percent Cr + 5.02 percent Fe) and 7 (2.83 percent Mo + 5.22 percent Cr + 5.10 percent Fe) shows that molybdenum increases the stability of the alloy somewhat at the start of the aging. A 1 percent increase in the molybdenum content of alloy 19 as compared to alloy 17, the content of the other alloying elements being the same, also increases the stability of the β alloys. During heating at 400, 450 and 500°, alloy 19 is as stable as alloy 17 for approximately 4 hrs, but on heating at 300°, alloy 17 in contrast to alloy 19, which is stable at this temperature for

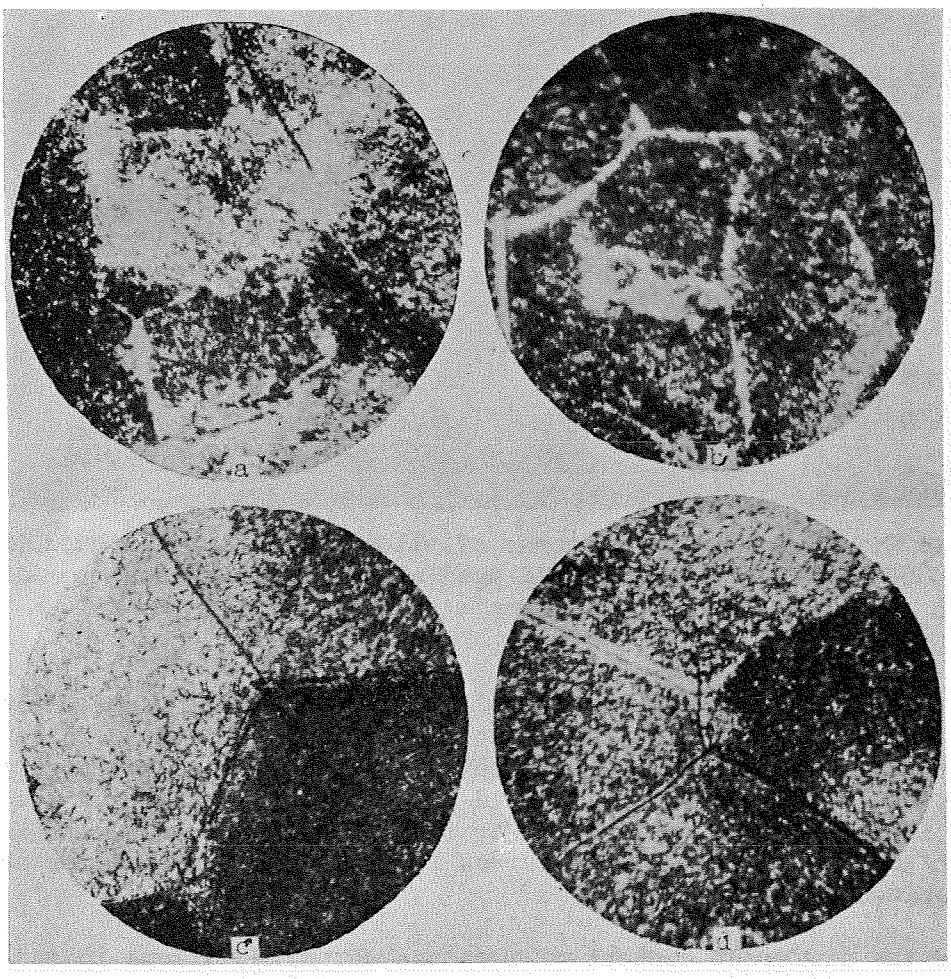

Figure 10. Microstructure of alloys of the third series quenched from 850° for 1 hr in water and aged at 500° for 100 hrs: a, alloy 12, in polarized light, x 340; b, alloy 13, in polarized light, x 340; c, alloy 12, x 1350; d, alloy 13, x 1350.

100 hrs, decomposes after the same period of time with the precipitation of the ω phase. The positive influence of molybdenum is manifested not only in an increase of the stability of the alloys on heating, but also in the preservation of the maximum value of the hardness obtained in the course of decomposition of the alloy at an aging temperature of 500°, independently of the iron and chromium content of the alloy.

Alloy 18, which contains the same amount of molybdenum as alloy 19, but less iron and more chromium, decomposes at once when heated at 350, 400 and 450°, and in 4 hrs when heated at 300°. At aging temperatures of 300 and 350°, alloy 18 decomposes with the precipitation of the ω phase, the existence of which is observed up to 144 and 121 hrs, respectively. On aging at 400 and 450°, alloy 18 decomposes immediately with the separation of the α phase.

From an analysis of the hardness curves of the alloys of the fourth series, it follows that the most interesting alloys are 18 and 19, which reach a stable hardness most rapidly and the lowest difference in the value of the maximum hardness during aging in the range of 500-400°. Since the composition of alloys 18 and 19 is almost the same, an alloy with an average composition in iron and chromium and with 6 percent Mo was selected for a further investigation.

Let us examine alloys 20 and 21 (see fig. 6a and b) containing 7 percent Mo each and different amounts of iron and chromium (alloy 21 contains approximately 1 percent less chromium and 0.8 percent more iron than alloy 20). The presence of large amounts of iron in alloy 21 causes a more sluggish decomposition of this alloy on heating, as a result of which the hardness reaches its maximum value and becomes stable after longer holding times. By comparing alloys 20 and 21 with alloy 22 (fig. 6c), which differ from the first two in their molybdenum content, it can be seen that a further increase in the molybdenum content of the alloy slows down the decomposition process even more.

Despite the different decomposition rates at the start of the aging at 300-500°, alloys 20-22 decompose according to the same pattern, i.e., with the precipitation of a finely dispersed α phase whose size and character of distribution are analogous to those observed in the alloys considered earlier (see fig. 7).

Analyzing alloys 15-22 (with 5-8 percent Mo), one can conclude that a 1-2 percent increase in the molybdenum content of alloys 18-22 as compared to its content of alloys 15-17 slightly increases the stability of the β alloy, and that a slow decomposition process is even undesirable in these alloys. Among alloys containing over 7 percent Mo, alloy 21, whose hardness scatter was lowest, was chosen for a further investigation.

The curves representing the dependence of the hardness of all the investigated alloys on the temperature and duration of aging show that in alloys with 2 percent Mo (3.76 percent Cr + 7.35 percent Fe + 3.15 percent Al and 5.2 percent Cr + 6.68 percent Fe + 2.81 percent Al), at an aging temperature of 500°, the hardness, having reached its maximum value, does not change as the holding time increases to 100 hrs, and that in alloys with 3 and 4 percent Mo and approximately the same content of chromium, iron and aluminum (respectively 3.5 percent Cr + 8.5 percent Fe + 2.89 percent Al and 5.22 percent Cr + 7.01 percent Fe + 2.9 percent Al), the hardness declines. In our view, at an aging temperature of 500°, the hardness should drop more rapidly in alloys with 2 percent Mo, and not in alloys with a higher content of molybdenum (3-4 percent), which promotes an increase in stability. The stable hardness in alloys with 2 percent Mo is apparently explained by the fact that in alloys with a small amount of molybdenum, the latter manifests itself more effectively than in alloys with 3-4 percent Mo, and acts as in alloys with 5 percent Mo.

Since the mechanical properties of the alloys of the system Ti-Mo-Cr-Fe-Al quenched from 850° for 1 hr in water (table 2) were obtained by testing microspecimens sensitive to all types of notches and microcracks, the data of this table should be regarded with some reservations. However, these data

TABLE 2. MECHANICAL PROPERTIES OF ALLOYS OF THE SYSTEM Ti-Mo-Cr-Fe-Al.

Alloy number	σ_b, kg/mm^2	$\sigma_s(\sigma_{0.2})$, kg/mm^2	δ, percent	a_n kgm/mm^2
1	105	104	8	2.3
2	103	102	9	2.4
3	115	111	10	3
4	112	108	head unchanged	1
5	98	97	13	2.4
6	102	101	8	not tested
7	102	85	14	not tested
8	86	77	14	not tested
9	106	94	9	not tested
10	97	94	7	not tested
11	93	92	3	1.4
12	113	111	10	3.33
13	102	101	14	1.81
14	95	91	5	2.05
15	98	96	8	2.28
16	107	103	4	1.47
17	91	91	7	3.36 bent
18	98	97	8	5.15 bent
19	100	98	7	2.12
20	103	101	14	2.60
21	100	99	12	2.9
22	73	70	11	1.63

confirm the correctness of the selection of alloys 3, 5, 12, 17, 18, 19 and 21 for a more detailed investigation, since these alloys have shown the highest mechanical characteristics.

Summary

1. All the investigated alloys of the system Ti-Mo-Cr-Fe-Al with the exception of alloy 1 are stable for 100 hrs at 200°. Alloy 1 is stable for 9 hrs at 200°. Only alloys 13 and 19 are stable for 100 hrs at 300°. All the remaining alloys decompose; alloys 10, 14, 16 and 17 decompose with the precipitation with the ω phase, which exists for another 100 hrs, and all the other alloys decompose with the precipitation of the α phase.

2. In alloys containing 2 and 5 percent Mo, the stability of the properties is independent of the ratio of chromium to iron within the investigated limits. The chromium content in alloys with 2 percent Mo decreased from 9.07 to 3.76 percent, and the iron content increased from 2.8 to 7.3 percent; the chromium content in alloys with 5 percent Mo decreased from 9.40 to 4.08 percent, while the iron content increased from 3.04 to 5 percent.

3. For alloys containing 3-5 percent Mo, not more than 5 percent Fe should be used, since a higher iron content has an adverse effect on the stability of the properties. In alloys with 3-4 percent Fe, the amount of chromium should be 1.5-2 times greater, and in alloys with 5 percent Fe, the chromium content should not be less than 5 percent.

4. In alloys containing up to 5 percent Cr and up to 5 percent Fe, not more than 5 percent Mo should be taken. A 1-2 percent increase in the amount of molybdenum slightly increases the stability of the β alloys, and a slow decomposition process is undesirable because of the presence of this amount of molybdenum.

REFERENCES

1. Ageyev, N. V. and Petrova, L. A. Coll. Titanium and Its Alloys (Titan i yego splavy), Izd-vo AN SSSR, No. 7, p. 26, 1962.

2. McQuillen, A. D. and McQuillen, M. K. Titanium. Metallurgizdat, p. 372, 1958.

3. Tarasenko, G. N. and Glazunov, S. G. Metallovedeniye i Termicheskaya Obrabotka Metallov, No. 2, p. 41, 1963.

4. Pul'tsin, N. M. Titanium Alloys and Their Use in Machine Building (Titanovyye splavy i ikh primeneniye v mashinostroyenii). Mashgiz (State Scientific and Technical Publishing House of Literature on Machinery), p. 73, 1962.

5. Ageyev, N. V. and Petrova, L. A. Dokl. AN SSSR, Vol. 138, No. 2, p. 359, 1961.

METASTABLE POLYMORPHISM OF ALLOYS BASED ON ELEMENTS OF GROUP IV OF THE PERIODIC SYSTEM

N. F. Lashko

I

It is a well-known fact that in titanium-base alloys, four types of metastable polymorphic transformations have been established during quenching from temperatures of the β region: 1, $\beta \rightarrow \alpha'$; 2, $\beta \rightarrow \alpha''$; 3, $\beta \rightarrow \beta + \omega$; 4, $\beta_{stab} \rightarrow \beta_{metastab}$. In zirconium-base alloys, three types of transformations have been established: 1, $\beta \rightarrow \alpha'$; 2, $\beta \rightarrow \beta + \omega$; 3, $\beta_{stab} \rightarrow \beta_{metastab}$. In hafnium alloys, none of these reactions has been reliably established thus far.

A number of studies have defended the thesis that the transformations $\beta \rightarrow \alpha''$, $\beta \rightarrow \beta + \omega$, $\beta_{stab} \rightarrow \beta_{metastab}$ are determined by the concentration of the outer electrons of transition metals in these alloys (refs. 1-4). The conditions of the metastable polymorphic transformations may be written as follows:

$$\frac{(100-x)\cdot 4 + x(4+y)}{100} = 4 + \frac{xy}{100} = a_i \, (i = 2, 3, 4),$$

where a_i is the constant of the i-th transformation; x is the concentration of the alloying element in at. percent; y is the number of its outer electrons minus four.

Two conclusions result:

1. The metastable polymorphic transformations should occur with a decreasing concentration of the alloying element, increasing number of the group of the periodic system, and increasing number of outer electrons;

2. The transformation in alloys containing alloying elements of one group of the periodic system should occur at the same electron concentration, i.e., when the number of outer electrons per atom is the same.

Neither conclusion has been confirmed experimentally. This is particularly apparent from the most complete data on the conditions of the fixation of the metastable phase during quenching, when $\beta_{stab} \rightarrow \beta_{metastab}$ (table 1). The concentration of the alloying elements, which fix the β phase during the quenching of binary titanium alloys and in the state of equilibrium form a eutectoid reaction, decreases at first as the number of the group of the periodic system increases (up to group VIII), and then the concentration increases. Nor is this concentration constant in alloys with alloying elements of the same group (for example, in alloys with elements of group VI).

The fixing of the metastable β phase on quenching should be determined by the relative stability of this phase on cooling. This phase is naturally less stable in alloys with a peritectoid transformation and more stable in binary alloys with a eutectoid transformation or in alloys forming continuous β and limited α solid solutions. The degree of stability of the ω phase in alloys of the latter type should be determined by the change in the temperature of the equilibrium $\beta \rightarrow \alpha + \beta$ and $\alpha + \beta \rightarrow \alpha$ relative to the concentration of the alloying elements. To a first approximation, in alloys with a eutectoid transformation, this quantity should be characterized by the temperature of the eutectoid transformation. Indeed, as the number of the group of the alloying element increases within the confines of the same period, the change in its concentration, which causes the fixing of the metastable ω phase in the alloy, is symbatic with the change in the eutectoid temperature.

This also applies to alloys with alloying elements of the same group (for example, to the alloys Ti-Cr and Ti-W).

The fixing of the metastable β phase in binary titanium alloys, which form a continuous series of β solid solutions and a limited series of α solid solutions, takes place at a lower concentration of the alloying elements the more pronounced is the decrease in the temperature of the stable transformation $\beta \rightarrow \alpha + \beta$ and $\alpha + \beta \rightarrow \alpha$. In order of decreasing stability of the β phase, such alloys can be arranged in the following sequence: Ti-Mo, Ti-V, Ti-Ta, Ti-Nb. As an arbitrary characteristic of the degree of stability of the β phase during the cooling of these alloys, one can take the concentration of the alloying elements which give rise to the equilibrium $\beta \rightarrow \beta + \alpha$ transformation at 600° (table 2).

This criterion of the relative metastability of the β phase in zirconium alloys cannot be verified because of insufficient data. It is justified in judging the conditions of formation of the ω phase during the quenching of certain alloys (table 3).

TABLE 1. CONDITIONS OF FIXATION OF THE METASTABLE β PHASE DURING QUENCHING OF TITANIUM ALLOYS (REFS. 1 AND 2).

Group of the periodic system	Element	Number of outer electrons	Minimum concentration of element at which the metastable phase is fixed, at. percent	Electron concentration el/atom	Eutectoid temperature °C
V	V	5	18.4	4.184	
VI	Cr	6	8.4	4.17	650-717
VI	Mo	6	5.8	4.12	
VI	W	6	8.7	4.17	715
VII	Mn	7	5.0	4.15	550
VIII	Fe	8	4.5-4.9	4.18-4.20	590
VIII	Co	9	4.9	4.20	685
VIII	Ni	10	5.8-6.3	4.35-4.38	770

TABLE 2. CONDITIONS OF FIXATION OF THE METASTABLE β PHASE DURING QUENCHING OF TITANIUM ALLOYS FORMING A CONTINUOUS SERIES OF β SOLID SOLUTIONS AND A LIMITED SERIES OF α SOLID SOLUTIONS (REFS. 1 AND 2).

Alloy system	Concentration of alloying elements (in at. percent) providing for	
	equilibrium transformation $\beta \rightarrow \alpha + \beta$	fixing of the metastable β phase during quenching
Ti-Mo	17	5.8
Ti-V	25	18.4
Ti-Ta	33	21
Ti-Nb	35	23

TABLE 3. CONDITIONS OF FORMATION OF THE METASTABLE ω PHASE IN ZIRCONIUM ALLOYS WITH A EUTECTOID TRANSFORMATION (REFS. 3 AND 4).

Alloy system	Content of alloying element at which the ω phase is formed, at. percent	Electron concentration el/atom	Eutectoid temperature, °C
Zr-Cr	4.5	4.09	835
Zr-Mo	4.0	4.08	780
Zr-W	7-13	4.13	860

II

When the temperature of the eutectoid transformation approaches the temperature of the polymorphic transformation $\beta \rightarrow \alpha$ in pure metals, conditions are created which depress the metastable polymorphic transformations. On cooling in air, the eutectoid reaction close to the equilibrium reaction occurs only in alloys with high eutectoid transformation temperature, when all main metastable polymorphic transformations ($\beta \rightarrow \alpha'$, $\beta \rightarrow \alpha''$, $\beta \rightarrow \beta + \omega$, $\beta_{stab} \rightarrow \beta_{metastab}$) are depressed. We observed the equilibrium product of the eutectoid transformation, for example, on cooling in air (from temperatures of the β region) alloys of the system Ti-Cu with a eutectoid temperature of 798° (the eutectoid $\alpha + Ti_2Cu$). A residual β phase was not observed in this case. It can be reliably stated that polymorphic metastable transformations should not take place in alloys of the system Ti-Ag and Ti-Au, the eutectoid temperatures of which are higher than in the alloys of the system Ti-Cu, and equal respectively to 855 and 832°.

We can also state that in the alloys of the system Hf-Fe, the eutectoid temperature of which is high and, according to reference 5, equal to 1235°, there should be no metastable polymorphic transformations on quenching from 1260°. As indicated by an analysis of their data (recording and calculation of x-ray diffraction patterns of an alloy of hafnium with 3.5 percent Fe after quenching from 1260°), the conclusions of the authors of reference 5 concerning the presence of $\beta \rightarrow \beta + \omega$ transformations in these alloys are incorrect. According to their data, the product of the eutectoid reaction--the phase Hf_2Fe-- is observed in the quenched alloy. The x-ray pattern which they cite and its calculation indicate beyond any doubt the presence of the α-Hf phase on quenching, not the presence of the $\beta + \omega$ phase, as indicated by the authors of reference 5, who proceeded from the assumption that the ω phase should be formed in this alloy with an outer-electron concentration of 4.14 el/atom. Hence, when this alloy is quenched in water from 1260°, the transformation taking place is $\beta \rightarrow \alpha + Hf_2Fe$. This example clearly shows the advantage of the above-indicated criterion for the degree of instability of the β phase over the quantitative criterion related to the electron concentration.

III

Metastable polymorphism in alloys based on titanium and zirconium with a eutectoid transformation is also manifested by the formation of a residual β phase during quenching. Its amount and resistance to decomposition on aging also depend on the eutectoid temperature. In titanium alloys with a high temperature of the eutectoid transformation, no residual β phase is formed. As was indicated above, in alloys of the system Ti-Cu, the β phase is converted into the products of the eutectoid reaction during quenching. It is usually stated that no residual β phase is formed in the system Ti-Si with a eutectoid temperature of 860°. In our earlier work (ref. 6), it was shown that in

technical alloys of the system Ti-Si, two phases were observed, $\alpha + Ti_5Si_3$, after a relatively short heating for quenching followed by quenching. However, an investigation of this system of alloys, which were first homogenized at 920° for 145 hrs, then furnace-cooled to 100-200° and aged at 600-840°, revealed the presence of a residual β phase (table 4). In ternary alloys of the system Ti-6 percent Al-Si, which were subjected to the same homogenizing treatment, no residual β phase was observed, but the phase Ti_5Si_3 was detected. The phases β and Ti_5Si_3 were found in the course of an x-ray structural analysis of anodic deposits isolated from the alloys in electrolytes of the following compositions:

1. Three g of potassium thiocyanate, 10 g of citric acid, 1000 ml of methanol;

2. Three g of lithium chloride, 10 g of citric acid, 25 ml of glycerin, 1000 ml of methanol.[1]

TABLE 4. RESULTS OF X-RAY STRUCTURAL ANALYSIS OF MONOLITHIC ALLOYS AND ANODIC DEPOSITS ISOLATED FROM ALLOYS OF THE SYSTEMS Ti-Si AND Ti-6 PERCENT Al-Si.

Alloy of the system Ti-Si				Alloy of the system Ti-6% Al-Si			
Si content, percent	Annealing conditions: Temperature, °C	Annealing conditions: Duration, hours	Phase composition	Si content, percent	Annealing conditions: Temperature, °C	Annealing conditions: Duration, hours	Phase composition
0,2	600	100	α	0,2	500	125	α
0,4	600	100	α + β	0,4	500	125	α + Ti_5Si_3
0,6	600	100	α + β	1,1	500	125	α + Ti_5Si_3
0,8	600	100	α + β	1,5	500	125	α + Ti_5Si_3
1,1	600	100	α + β	0,2	600	125	α + Ti_5Si_3
1,5	600	100	α + β	0,6	600	125	α + Ti_5Si_3
0,2	700	75	α	0,2	700	100	α + Ti_5Si_3
0,4	700	75	α	0,6	700	100	α + Ti_5Si_3
1,1	700	75	α + β	1,5	700	100	α + Ti_5Si_3
1,5	700	75	α + β	0,2	850	50	α + Ti_5Si_3
0,2	840	50	α	0,4	850	50	α + Ti_5Si_3
0,4	840	50	α	1,1	850	50	α + Ti_5Si_3
0,6	840	50	α + β	1,5	850	50	α + Ti_5Si_3
1,1	840	50	α + β				
1,5	840	50	α + β				

[1]The work was carried out in cooperation with Ye. A. Vinogradova and A. I. Glazova.

It is possible that the decomposition of the β phase and of the alloys of the system Ti-Si investigated earlier is promoted by impurities and a segregational structure. It is known that the maximum concentration of alloying elements in titanium alloys which causes the fixation of the β phase on quenching depends on the purity of the alloys. The homogenizing of the alloys of the system Ti-Si promotes an increase in the stability of the β phase. Alloying of these alloys with aluminum accelerates the decomposition of the β phase.

IV

The metastable polymorphic transformation $\beta \rightarrow \beta + \omega$ taking place in titanium and zirconium alloys during quenching or aging is attributed to martensite transformations of a special type (ref. 7). A characteristic feature of this martensite transformation is the mandatory existence of the ω phase, which is coherently bound to the β phase. Apparently, in contrast to the other martensite phases, the ω phase does not exist independently. When it is formed, the volume of the alloy decreases. The self-coherent bond of the two phases $\beta + \omega$ is a single phase. The likelihood of such an assumption is reinforced if three known facts are recalled:

1. There is no relief on the surface of the quenched alloy during the formation of the ω phase;

2. The main planes of reflection of x-rays from the β and ω phases coincide;

3. The ω phase cannot be distinguished metallographically as a separate component different from the matrix.

The statement made in reference 8 that some very small particles observed by means of the electron microscope constitute the ω phase is debatable. These authors observed the same kind of particles in the alloy Hf-3.5 percent Fe, where, as was shown above, there is no ω phase.

It is known that the ω phase is formed in medium titanium and zirconium alloys directly on quenching, whereas in higher alloys, it is formed with the participation of diffusion processes as a result of the heating of the metastable β phase fixed on quenching. In addition to the indicated characteristics of the β phase, one should note the independence of the temperature of the martensite transformation from the cooling rate, and also identical or similar parameters of the crystal structure of the ω phase in titanium alloys of different compositions (ref. 9). Hence, we conclude that diffusionless martensite transformations have a common feature. They occur when, as a result of some processes, the specific volume of a high-temperature phase is prepared for a diffusionless transformation into a low-temperature metastable phase. This may take place as a result of a volume change on cooling of the high-temperature phase or as a result of its diffusional change during aging.

The first condition of the preparation of a phase for a metastable polymorphic transformation was pointed out by the authors (ref. 10) and also by M. V. Yakutovich and V. D. Sadovskiy (ref. 11).

The diffusional preparation of a high-temperature phase for a subsequent diffusionless transformation may occur in two ways: $\beta \rightarrow \beta_1 + x$ or $\beta \rightarrow \beta_1 + \beta_2$, where β is the initial phase of the changed composition (depleted of alloying elements); x is the equilibrium phase; β_2 is the phase enriched with alloying elements. The first case is realized in the bainite transformation, when during the isothermal treatment austenite partially decomposes with the precipitation of cementite, and the austenite depleted of carbon changes into martensite.

The realization of the second type of transformation in titanium alloys was described in a report of R. M. Lerinman and T. V. Shchegoleva (ref. 12). They showed that when the metastable β phase of titanium alloys containing chromium and manganese ages, a demixing of the β phase and the formation of the ω phase take place.

We have observed various cases of formation of the ω phase in alloys of the system Zr-Nb. As we know, in the region of the existence of the β phase, zirconium and niobium form a continuous series of solid solutions and a limited region of solubility of niobium in α-Zr. The high-temperature β phase decomposes under equilibrium conditions in accordance with the eutectoid reaction $\beta \rightarrow \alpha$-Zr + Nb at 610°. Four alloys were taken which differed in the type of decomposition of the β phase on cooling in water and subsequent aging.

The results of the investigation are shown in table 5.

TABLE 5. RESULTS OF X-RAY STRUCTURAL ANALYSIS OF ALLOYS OF THE SYSTEM Zr-Nb AFTER QUENCHING IN WATER AND AGING.

Nb content, percent	Quenching temperature	Aging conditions			
		Temperature, °C	Duration, hrs	Phase compositions	Parameter of β phase, A
6	880	—	—	$\alpha + \beta$	
6	880	400	2	$\alpha + \beta$	3,56
6	880	550	50	α	—
8	880	—	—	$\beta + \omega$	$3,55_3$
8	880	400	2	$\beta + \omega$	$3,54_5$
8	880	430	0,5	$\beta + \omega$	$3,54_5$
		550	50	α	
15	800	—	—	β	$3,51_9$
15	800	400	2	$\beta_1 + \beta_2 + \omega$	$\beta_1 = 3,54_5$ $\beta_2 = 3,49_7$
15	800	550	50	α	
20	750	—	—	β	$3,51_2$
20	750	400	2	β	$3,51_2$
20	750	550	50	α-Zr + Nb	

After quenching, in the alloy containing 6 percent Nb there is formed a residual β phase which is relatively stable on heating for 2 hrs at 400° and which decomposes at 550°. It is possible that a small amount of a stable β phase which has not been detected by x-ray structural analysis is formed at the same time.

On quenching of the alloy containing 8 percent Nb, there is formed a relatively stable ω phase which does not decompose for 2 hrs at 400° and for 0.5 hr at 430°, but decomposes at 550°.

On quenching of the alloy containing 15 percent Nb, there is formed a metastable β phase decomposing in 2 hrs at 400° into a β_1 phase enriched with niobium and into a $\omega(\beta_2 + \omega)$ phase depleted of niobium. Aging at 550° leads to the decomposition of the metastable phases and to the formation of the α phase.

In the alloy containing 20 percent Nb, there is formed a relatively stable β phase which does not decompose for 2 hrs at 400° but does decompose at 550°.

REFERENCES

1. Bagaryatskiy, Yu. A., Nosova, G. I. and Tagunova, T. V. Dokl. AN SSSR, Vol. 122, No. 4, p. 593, 1958.

2. Ageyev, N. V. and Petrova, L. A. Dokl. AN SSSR, Vol. 138, No. 2, p. 359, 1961.

3. Bychkov, Yu. F., Maskalets, V. I. and Rozanov, A. N. Inzhenerno-fizicheskiy zhurnal, Vol. 3, No. 4, p. 95, 1960.

4. Gridnev, V. N. and Trefilov, V. I. Voprosy fiziki metallov i metallovedeniya, Izd-vo AN SSSR, No. 14, p. 5, 1962.

5. Gridnev, V. N., Rafalovskiy, V. A. and Trefilov, V. I. Voprosy fiziki metallov i metallovedeniya, Izd-vo AN SSSR, No. 14, p. 188, 1962.

6. Yelagina, L. A. and Lashko, N. F. Titanium in Industry (Titan v promyshlennosti). Oborongiz, p. 79, 1962.

7. Bagaryatskiy, Yu. A., Nosova, G. I. and Tagunova, T. V. Problemy metallovedeniya i fiziki metallov, Metallurgizdat, No. 7, p. 307, 1962.

8. Gridnev, V. N., Petrov, Yu. N., Rafalovskiy, V. A. and Trefilov, V. I. Voprosy fiziki metallov i metallovedeniya, Izd-vo AN SSSR, No. 11, p. 82, 1960.

9. Bagaryatskiy, Yu. A., Tagunova, T. V. and Nosova, G. I. Voprosy fiziki metallov i metallovedeniya, Izd-vo AN SSSR, No. 5, p. 210, 1958.

10. Lashko, N. F. Zh. tekhn. fiz., No. 7, p. 986, 1948.

11. Sadovskiy, V. D. and Yakutovich, M. V. Dokl. AN SSSR, Vol. 57, No. 4, p. 369, 1947.

12. Lerinman, R. M. and Shchegoleva, T. G. Abstracts of reports given at the 7th Scientific and Technical Conference on the Application of X-Rays to the Study of Materials (Tezisy dokladov VII nauchno-tekhnicheskogo soveshchaniya po primeneniyu rentgenovskikh luchey k issledovaniyu materialov), Izd-vo AN SSSR, Leningrad, p. 87, 1961.

DILATOMETRIC STUDY OF TRANSFORMATIONS IN TITANIUM ALLOYS

L. P. Luzhnikov, V. M. Novikova and A. P. Mareyev

The present study is a part of a more extensive investigation dealing with transformations during the heat treatment of titanium alloys. In addition to the dilatometric method, we also use the determination of mechanical properties, the end-quench method, microstructural analysis, and other methods.

The dilatometric method was used to study the transformations in the industrial alloys VT3-1, VT6, VT8, VT9 and VT14 (table 1), and was also applied to alloys of the following binary and ternary systems: Ti-Cr (2, 4, 6, 10 percent Cr), Ti-Mo (3, 6, 10 percent Mo), Ti-Al-Cr, Ti-Al-Mo.

The ternary alloys contained 4 percent Al and the same amount of β stabilizer as the corresponding binary alloys. The alloys were prepared by double fusion in vacuum arc furnaces followed by hot forging of ingots, and were studied in the forged state. Technical titanium (σ_b = 41 kg/mm^2; 0.08 percent O_2) was used for the preparation of the alloys. The alloys contained an average of 0.12-0.13 percent O_2.

The change in length was recorded with a Bollenrath dilatometer (made by the Leitz Company) with a programmed temperature regulator and a vacuum furnace.[1] The dilatometer provided a 194-fold magnification.

In the indicated series of experiments, the change in the length of the specimens (l = 50 mm) was recorded with the change in temperature. The heating was carried out at the rate of 4.5-5 deg/min. In many cases, the dilatometric curves were recorded for the same alloy on two or more specimens. The curves indicated a complete reproducibility of the data obtained. In one of the alloys (Ti + 10 percent Cr), the influence of the heating rate (3 and 6 deg/min) on the nature of the dilatometric curves was studied. It was found that within these limits, the change in the rate was not reflected in the magnitude and position of the dilatometric effects on the temperature scale.

---

[1] Vacuum (6×10^{-2} mm Hg) was used in certain cases; a neutral atmosphere was employed (pure argon). In all cases, no sign of oxidation of the specimens was observed after their removal.

TABLE 1. CHEMICAL COMPOSITION OF INDUSTRIAL ALLOYS (IN PERCENT).

Brand of Alloy	Al	Cr	Mo	V	Si	Sn
BT3-1	5	1,7	2	—	—	—
BT6	6	—	—	4	—	—
BT8	6,2	—	3	—	0,25	—
BT9	6,3	—	3,3	—	0,30	2,3
BT14	4	—	3	1	—	—

Note: Residual Ti

For reference purposes, dilatometric curves were recorded for iodide and technical titanium (fig. 1). These curves are illustrated together with the curves for the industrial alloys.

The temperature of the $\alpha \rightarrow \beta$ transformation for iodide titanium was found to be 880°, and for technical titanium, 862°. For iodide titanium, this is in good agreement with McQuillen's data (882.5°) (ref. 1). The decrease in the temperature of the polymorphic transformation in technical titanium is probably due to the predominant action of β stabilizing impurities (chiefly iron and silicon).

Before the dilatometric testing, the specimens of industrial alloys were quenched in water from the temperature chosen for each alloy. Blanks (rods 12-13 mm in diameter) from which the specimens were made were subjected to heating for quenching, and other heat treatments of the alloys were carried out in ordinary laboratory electric furnaces in an atmosphere of air. Specimens with diameters of 4 mm (dilatometry) and 5 mm (mechanical tests) were turned from these blanks. The gas-saturated layer was thus satisfactorily removed.

The dilatometric curves of most of the industrial alloys (VT6, VT8, VT9, VT14) did not show any noticeable effects (fig. 1); this is apparently due to the slight development of transformations in these alloys, and also to the small difference in the dilatometric characteristics of the phases participating in these transformations. This is confirmed by a relatively slight tendency of the alloys under consideration to harden on aging (aging effect, 10-15 percent). It is also possible that the slight effects were not detected by the dilatometer because the increase was too small.

Alloy VT3-1 (fig. 1) displays a distinct negative effect in the temperature range of 286-400° (contraction), followed by a positive effect (expansion),[1] which takes place at 450-470°.

[1]Here and subsequently the magnitude and position of the effects on the curves are measured by using a photographic plate 18 x 24 cm on which the dilatometric curves were recorded.

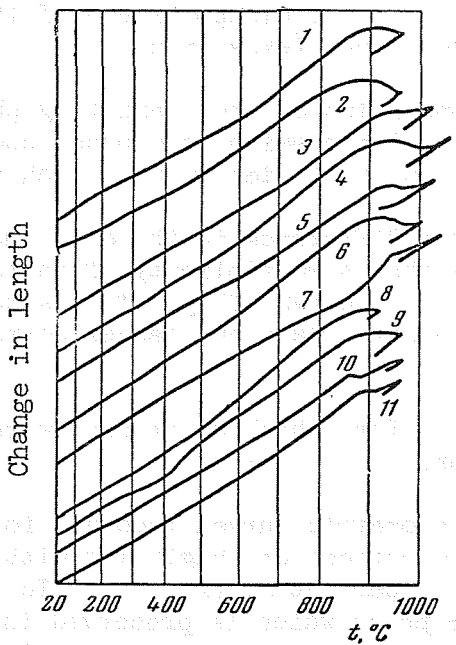

Figure 1. Dilatometric curves of industrial alloys: 1, alloy VT14 (temperature of heating for quenching 880°); 2, alloy VT14 (820°); 3, alloy VT9 (950°); 4, alloy VT9 (900°); 5, alloy VT8 (950°); 6, alloy VT8 (900°); 7, alloy VT6 (950°); 8, alloy VT6 (845°); 9, alloy VT3-1 (845°); 10, technical titanium (910°); 11, iodide titanium.

This dilatometric effect indicates the formation of the ω phase during the decomposition of the β solid solution, fixed by quenching of the alloy VT3-1. This is a new and important fact in the case of VT3-1.

Until now, almost all the investigators of this alloy have completely discounted the possibility that the ω phase could form in this alloy (ref. 2).

Certain investigators groundlessly attribute the positive effect on the dilatometric curves to the presence of the ω phase (ref. 3).

We shall discuss this question below in more detail.

At the same time, the dilatometric curves of the other alloys show that the formation of the ω phase in the latter is impossible. In any event, this fact is indisputable for the investigated temperatures of heating for quenching of these alloys. For the sake of a more correct and deeper understanding of the dilatometric effects observed in complex multicomponent alloys, a study was made of the dilatometric characteristics of a series of binary and ternary alloys.

It should be noted that all the data published up to the present time (refs. 4, 5, 6, etc.) indicate that the formation of the ω phase during the decomposition of the β solid solution is associated with a negative effect of

change in length (contraction). The disappearance of the ω phase on further heating is due to a positive effect (expansion).

The quantities and composition of the coexisting phases in multicomponent alloys depend, in addition to the chemical and phase composition of the alloy, on the temperature and the length of time during which they are exposed to it.

All of the above and the difference in the dilatometric characteristics of the various phases indicate that a multiplicity of factors determine the total (resultant) characteristics of a given alloy. This sometimes complicates the interpretation of the dilatometric data and causes certain discrepancies in the literature data.

The binary and ternary alloys which we studied were quenched in water after being heated in the β region.

Let us examine the dilatometric curves recorded for quenched specimens of alloys Ti-Cr (2, 4, 6 and 10 percent Cr) beginning with the upper curve corresponding to the alloy Ti + 10 percent Cr (fig. 2). In the quenched state, this alloy consists of a fixed β phase which is preserved in the metastable state approximately up to 180°; at this temperature, a negative effect (contraction) due to the formation of the ω phase appears. At a temperature of approximately 280-300°, the formation of the ω phase ceases, and this phase begins to dissolve in the β solid solution, while at the same time the dispersed α phase precipitates from the solution (up to 400°). Above 400° and up to 530°, the amount of the α phase continues to increase, and the latter coagulates. The subsequent course of the dilatometric curve (above 530°) corresponds to a change in the composition and relative amounts of the α and β phase in the two-phase system. No eutectoid temperature is observed on this and the other curves. The next curve pertains to the alloy Ti + 6 percent Cr. Since this alloy in the quenched state had a β + ω structure, its curve begins with a negative effect. The two-phase β + ω structure is preserved on heating up to about 350-400°. Between 400 and 500°, the amount of the ω phase decreases, owing to its dissolution, and

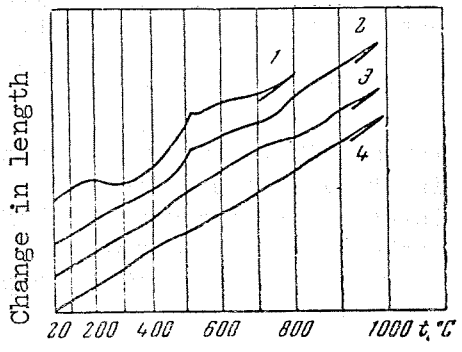

Figure 2. Dilatometric curves of alloys of the system Ti-Cr: 1, alloy Ti + 10 percent Cr; 2, alloy Ti + 6 percent Cr; 3, alloy Ti + 4 percent Cr; 4, alloy Ti + 2 percent Cr.

the amount of the α phase which precipitates from the solid solution increases. Above 500-530°, the α and β phases apparently exist, but their composition and relative amounts change.

The above explanation of the effects shown by the dilatometric curves is based on data for the dependence of the hardness on the aging temperature and also on studies (by the x-ray structural method) of transformations in analogous alloys described in references 4 and 7.

The curve for the alloy Ti + 4 percent Cr is generally similar to the preceding one, but as should be expected, the dilatometric effects are very weakly expressed in this case.

Finally, the last curve (for the alloy Ti + 2 percent Cr) is characteristic of quenched alloys with a martensite structure. It is a nearly straight line, indicating very slight transformations in these alloys during heating. This explanation of the course of the curves is also supported by the data on the end-quenching of the same alloys (fig. 3).

This mechanism makes it possible to superimpose the dilatometric curves (on the right) onto the curves of the end-quenching (on the left).[1] The alloy quenched to the β phase (curve 1) has a hardenability curve with a minimum hardness at the cooled end (point on the ordinate).

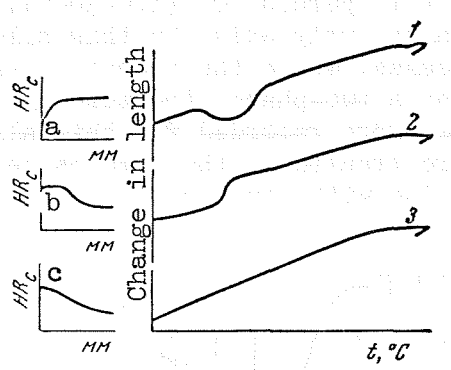

Figure 3. Curves of end-quenching (left) and dilatometric curves (right): 1, alloys quenched to the β solid solution; 2, alloys quenched to the β + ω structure; 3, alloys quenched to martensite; a, b and c--hardness values corresponding to the ordinate (maximum cooling rate on quenching).

[1]The curves of the end-quenching (GOST 5657-51) show the dependence of the hardness (axis of ordinates) on the distance to the end of the specimen cooled with water (axis of abscissas). As the distance from the end increases, the cooling rate decreases.

The alloy hardened to the two-phase $\beta + \omega$ structure (curve 2) has a maximum hardness at the cooled end and at an appreciable distance from the latter.

Finally, the alloy quenched to martensite (curve 3) has a maximum hardness at the cooled end; as the distance from the latter increases, the hardness decreases. The maximum hardness of the most abruptly quenched alloy (ordinate on the curves on the left) corresponds to the $\beta + \omega$ structure, which is followed by a martensite structure, and the minimum hardness corresponds to the fixed β phase ($a < c < b$).

The dilatometric curves corresponding to each of the alloys considered are shown in the same figure on the right.

A definite confirmation of these data is provided by results of mechanical tests of the alloys following various modes of aging. Let us examine the dilatometric curves of the ternary alloys Ti-Al-Cr containing 4 percent Al (fig. 4). It is known from the literature that the decomposition of the β solid solution with the formation of the ω phase is accelerated if the alloys contain interstitial elements (oxygen, nitrogen, carbon); this applies particularly to the action of oxygen. Aluminum retards this transformation. It apparently shifts the transformation $\beta \rightarrow \omega$ into a region of higher temperatures. This is particularly apparent in the alloy Ti + 4 percent Al + 10 percent Cr.

The negative effect associated with the formation of the ω phase (fig. 4) decreased markedly and shifted into the region of higher temperatures (250-350°) as compared to the alloy Ti + 10 percent Cr (180-300°). In the region of 350-480°, the $\beta + \omega + \alpha$ phases apparently exist in this alloy; the amount of the ω phase between 350-480° decreases, while the amount of the α phase increases. Above 480-500°, the alloy has a two-phase structure ($\alpha + \beta$). It should be noted that four dilatometric curves were recorded for this alloy on specimens which were different but which were treated in the same manner. All the curves were completely identical. Alloying with aluminum introduced a substantial change

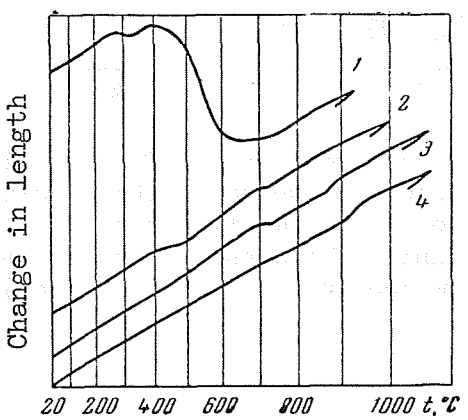

Figure 4. Dilatometric curves of alloys of the system Ti-Al-Cr: 1, alloy Ti + 4 percent Al + 10 percent Cr; 2, alloy Ti + 4 percent Al + 6 percent Cr; 3, alloy Ti + 4 percent Al + 4 percent Cr; 4, alloy Ti + 4 percent Al + 2 percent Cr.

into the course of the curve of the alloy Ti + 6 percent Cr; in this alloy, aluminum substantially depressed the tendency to form the ω phase during quenching. The influence of aluminum on the alloys Ti + 4 percent Cr and Ti + 2 percent Cr is slight.

The curves of Ti-Cr alloys with aluminum (fig. 4) show the eutectoid temperature (about 700°) fairly distinctly.

Let us examine the dilatometric curves for the alloys of the systems Ti-Mo (fig. 5) and Ti-Al-Mo (fig. 6).

The alloy Ti + 10 percent Mo is apparently quenched to the β solid solution with a small amount of the ω phase, since its curve begins with a negative effect; in the temperature range of 500-590°, a positive effect is observed.

Both of these effects shift into the range of 650-870° in the alloy Ti + 4 percent Al + 10 percent Mo (fig. 6).

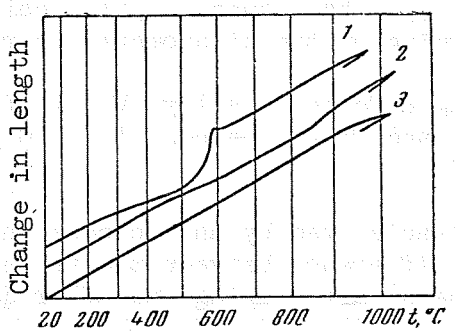

Figure 5. Dilatometric curves of alloys of the system Ti-Mo: 1, alloy Ti + 10 percent Mo; 2, alloy Ti + 6 percent Mo; 3, alloy Ti + 3 percent Mo.

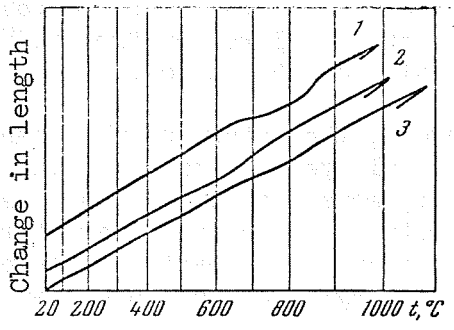

Figure 6. Dilatometric curves of alloys of the system Ti-Al-Mo: 1, alloy Ti + 4 percent Al + 10 percent Mo; 2, alloy Ti + 4 percent Al + 6 percent Mo; 3, alloy Ti + 4 percent Al + 3 percent Mo.

The curves of the alloys Ti + 6 percent Mo and Ti + 3 percent Mo do not display any appreciable effects. The addition of aluminum does not cause any substantial change in the character of the curves.

A series of additional experiments was carried out with the alloy VT3-1 for the purpose of confirming the possibility of the formation of the ω phase in this alloy.

First, a dilatometric curve was recorded for the alloy VT3-1 quenched from the β region (1050°). It shows the absence of any effects (fig. 7, curve 1). This is in agreement with the fact that in this case the alloy was quenched to the α' phase (martensite).

A curve was recorded for the alloy VT3-1 quenched from 800°. It is not illustrated here because its shape is the same as that of the curve which we have illustrated for the alloy quenched from 845° (see fig. 1).

Figure 7 also shows curve 2 for alloy VT3-1, recorded with a specimen after quenching from 845° and aging at 350° for 10 hrs. The curve does not show a negative effect, since aging at 350° had caused a practically complete $\beta \rightarrow \omega$ transformation prior to the recording of the dilatometric curve.

Let us examine the aging effects in alloys VT3-1 (fig. 8, curve 2), Ti + 10 percent Zr (fig. 8, curve 3) and Ti + 4 percent Al + 10 percent Cr (fig. 8, curve 1).

The aging effect is characterized by an increase in a given property as a result of aging, i.e., by a difference between the values of the property (in this case the Rockwell hardness) after aging and after quenching.

This increase of hardness (aging effect) in each alloy is expressed in percent relative to the hardness in the quenched state. The duration of aging at all temperatures was 10 hrs.

Quenching (in water) of the alloys Ti + 10 percent Cr and Ti + 10 percent Cr + 4 percent Al was carried out after they were heated in the β region. The alloy VT3-1 was quenched from the $\alpha + \beta$ region from 845°, the standard temperature of the heating for quenching of this alloy.

As is evident from figure 8, the nature of the change in the hardening effect during aging of the two β alloys is similar to the nature of the change in this effect in alloy VT3-1, or, more exactly, in the β solid solution of this two-phase alloy. The similarity of the curves characterizing the aging effect in alloys VT3-1 and Ti + 10 percent Cr is particularly pronounced. In the region of the maximum ($300-400^{\circ}$), their aging effects are even closer in magnitude.

This similarity in the character of the change and in the magnitude of the aging effects makes it possible to assume a similarity in the nature of the $\beta \rightarrow \omega$ transformation as well.

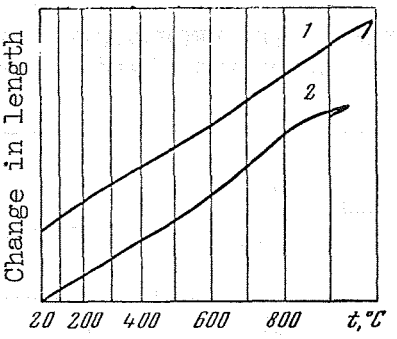

Figure 7. Dilatometric curves of the alloy VT3-1: 1, quenching in water from 1050°, 30 min; 2, quenching in water from 845° for 1 hr and aging at 350° for 10 hrs.

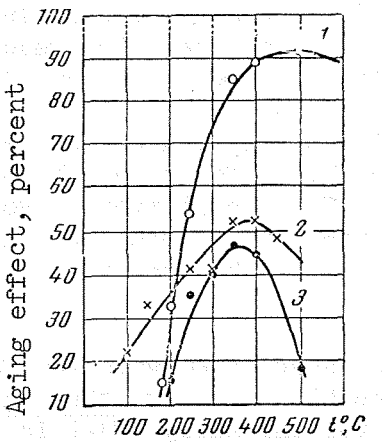

Figure 8. Aging effect of titanium alloys for an aging time of 10 hrs: 1, alloy Ti + 10 percent Cr + 4 percent Al (quenched in the β region); 2, alloy VT3-1 (quenched in water from 845°); 3, alloy Ti + 10 percent Cr (quenched in the β region).

Finally, we shall cite the dependence of certain mechanical characteristics of the alloy VT3-1 on the duration of aging after quenching from 845° (table 2).

After aging at 350° (the temperature of rapid formation of the ω phase for this alloy) for various periods of time, the plasticity, particularly as characterized by elongation, decreased at first, reaching a minimum in 3 hrs, then increased again substantially after aging for 24 hrs. Apparently, the plasticity minimum corresponds to the fullest $\beta \rightarrow \omega$ transformation, and the increase in the duration of aging to 24 hrs, upon further decomposition of the β solid solution, leads to the appearance of the α phase, a decrease in the amount of the ω phase, and an increase in plasticity. Aging for 6 hrs at 550° leads to

TABLE 2. DEPENDENCE OF THE MECHANICAL CHARACTERISTICS ON THE AGING TIME OF ALLOY VT3-1 AFTER QUENCHING FROM 845°.

Aging mode		σ_b	δ	ψ
t, °C	τ, hours	kg/mm^2	percent	percent
--	--	115	15	41
350	0.5	141	8	25
350	1	144	5.5	20
350	3	147	4.5	16
350	24	154	7	9
550	6	128	12	39

an appreciable increase in ductility and a decrease in strength. This corresponds to a change in the properties of the alloy resulting from the decomposition of the β solid solution with the precipitation of the α phase.

Thus, the above material definitely indicates the possibility of the formation of the ω phase in the alloy VT3-1 following the heat treatment of this alloy under certain conditions. These conditions involve its quenching from the two-phase $\alpha + \beta$ region (845°), when the β phase containing chromium and molybdenum above the critical concentration becomes fixed, and to aging at temperatures in the range of 286-460°.

The pronounced aging effect associated with the formation of the ω phase (up to 50 percent) makes it possible to assert that the maximum amount of the β phase (5-8 percent) determined for the alloy VT3-1 in reference 2 is quite erroneous. In our view, the amount of the β phase in this alloy can reach 30-40 percent.

Summary

1. A study was made of the transformations associated with the heat treatment of industrial titanium alloys VT3-1, VT6, VT8, VT9 and VT14, and also alloys of the systems Ti-Cr, Ti-Mo, Ti-Al-Cr and Ti-Al-Mo by the dilatometric and other methods.

2. These industrial alloys in the quenched state do not show any appreciable dilatometric effects during heating. An exception is the alloy VT3-1, which has a negative effect in the temperature range of 286-400° after quenching from the two-phase region (845°).

3. The dilatometric characteristics of a series of binary and ternary (with aluminum) alloys were studied; this facilitated the interpretation of the experimental data for the alloy VT3-1.

4. The dilatometric investigation, the study of aging, and the use of the end-quench method make it possible to assert that after quenching of the alloy VT3-1 from 845°, a β solid solution of supercritical concentration is fixed together with the α phase. The ω phase is formed as a result of the aging (particularly in the range of 350-500°). The amount of the fixed β phase can apparently reach 30-40 percent. This explains the relatively pronounced aging effect of the alloy VT3-1 (up to 50 percent).

REFERENCES

1. McQuillen, A. D. and McQuillen, M. K. Titanium (Titan). Metallurgizdat, Moscow, 1958.

2. Vinogradova, Ye. A., Kohkhova, G. M. and Lashko, N. F. Titan v promyshlennosti, Oborongiz (State Publishing House of the Defense Industry), p. 121, 1961.

3. Verigina, Z. S. Study of Phase Transformations in Industrial Titanium Alloys VT3 and VT3-1 (Issledovaniye fazovykh prevrashcheniy v promyshlennykh titanovykh splavakh VT3 i VT3-1). Author's abstract of Candidate's Dissertation, Moscow, 1962.

4. Bagaryatskiy, Yu. A., Tagunova, T. V. and Nosova, G. I. Problemy metallovedeniya i fiziki metallov, Metallurgizdat, Moscow, No. 5, 1958.

5. Brotzen, F. R., Harmon, E. L. and Troiano, A. R. Trans. AIME, Vol. 203, p. 413, 1955.

6. Gridnev, V. N., Rafalovskiy, V. A., Trefilov, V. I. and Chernenko, N. F. Voprosy fiziki metallov i metallovedeniya, Izd-vo AN SSSR, No. 10, p. 77, 1959.

7. Nosova, G. I. X-Ray Diffraction Study of Phase Transformations in Titanium-Base Alloys (Rentgenograficheskoye issledovaniye fazovykh prevrashcheniy v splavakh na osnove titana). Author's abstract of Candidate's Dissertation, TsNIIChM (Central Scientific Research Institute of Ferrous Metallurgy), 1961.

DISLOCATION THEORY OF THE HYDROGEN BRITTLENESS OF TITANIUM ALLOYS

B. A. Kolachev, V. A. Livanov and A. A. Bukhanova

Numerous studies made by both Soviet and foreign investigators have shown that there are two kinds of hydrogen brittleness of titanium and its alloys.

Brittleness of the first kind manifests itself at high deformation rates and is associated with the appearance, in the structure of titanium and its alloys, of hydride-phase precipitates which essentially act as internal cuts in the metal. The explanation of the nature of this kind of brittleness presents no difficulties.

Hydrogen brittleness of the second kind is manifested at low deformation rates. It develops primarily in quenched alloys in which the hydrogen content exceeds the solubility limit at the temperature of the tests. In this case, solid solutions supersaturated with hydrogen are fixed on quenching which decompose on prolonged exposure to applied stresses with the formation of finely dispersed hydride precipitates, causing a certain hardening of the alloys and a sharp decrease in plasticity.

Hydrogen brittleness caused by decomposition which develops in the course of deformation is the term applied to irreversible brittleness of the second kind in the sense that if after a prolonged exposure to stresses the load is removed, the plasticity of the alloys is not restored, and brittle failure is observed in subsequent tests conducted at a high rate after any period of time following the removal of the load. The explanation of brittleness of this type does not present any particular difficulties either.

The most complex nature of hydrogen brittleness is that which develops in titanium alloys at low deformation rates when the hydrogen content is below the solubility limit at the temperature of the tests, and the development of brittleness is not accompanied by the appearance of hydride-phase precipitates. In its most characteristic form, this brittleness develops in typical $\alpha + \beta$ alloys. It may be termed reversible brittleness of the second kind. If an $\alpha + \beta$ titanium alloy saturated with hydrogen is subjected to the prolonged action of stresses, sources of hydrogen brittleness will arise in it, and if mechanical tests are performed at a high rate immediately after the stresses are relieved, the alloys will display a low plasticity. However, after the $\alpha + \beta$ alloy is aged following the relief of previously applied stresses, its plasticity will be almost completely restored. Thus, after the relieving of preliminary stresses, the sources of hydrogen brittleness are partially destroyed and their embrittling effect is eliminated.

The following rules govern reversible hydrogen brittleness of the second kind (ref. 1).

1. Brittleness of the second kind is manifested over a definite temperature range which depends on the deformation rate, nature of the alloys (α, $\alpha + \beta$ or β alloy) and their chemical composition.

2. As the deformation rate increases, the temperature range over which the plasticity decreases is reduced, the plastic characteristics increase, and if the deformation rate exceeds a certain limit, brittleness is no longer observed.

3. The temperature of the transition from viscous failure to brittle failure rises with a decreasing deformation rate and increasing hydrogen content.

4. Failure at a low deformation rate takes place along the grain boundaries.

Several theories of the hydrogen brittleness of $\alpha + \beta$ alloys have been proposed. However, as was shown in reference 2, these theories cannot account for all the details of this phenomenon. In the present work, an attempt is made to explain the basic regularities of reversible hydrogen brittleness of the second kind from the standpoint of the dislocation theory.

It is postulated that at a temperature below some critical temperature T_0, hydrogen is formed on the dislocations of the Cottrell atmosphere. If the deformation rate is low and the temperature is not too high, so that the mobility of the hydrogen atoms is comparable to the rate of displacement of the dislocations, the atmospheres will accompany the dislocations, lagging a certain distance behind them. Since the dislocation is then acted upon by a force which repels it back to the initial position at the center of the atmosphere, the resistance to plastic deformation is somewhat increased. Plastic deformation is created not only by the movement of the dislocations present in the crystal, but also by the generation of new dislocations by any source under the influence of applied stresses and their displacement along the glide plane. Under the indicated conditions, newly formed dislocations will become surrounded by hydrogen atmospheres, and their behavior should not be substantially different from that of "old" dislocations. The dislocations together with the hydrogen atmospheres, moving under the influence of the applied stresses, reach the grain boundary and may either vanish at the latter, producing a shear step (in this case the hydrogen atmospheres are freed), or form a pileup at this boundary. In either of these cases, hydrogen accumulates at the grain boundary. Since up to 100 and more dislocations can move along a single acting glide plane, and the pileup may consist of the same number of dislocations, a considerable segregation of hydrogen at the grain boundaries should be expected. If the actual stresses are high enough, a crack is generated at the grain boundary on the step or at the top of the pileup, and hydrogen apparently facilitates not only the generation of the crack but also its further propagation.

The reversible nature of this brittleness may be explained by the fact that if the load is removed prior to the appearance of cracks, thermal diffusion will gradually equalize the hydrogen concentration over the volume of the metal and will at least partially eliminate the segregation of hydrogen at the grain boundary.

It should be noted that in principle, dislocation pileups may arise not only at the boundary of the grain but also within the latter. However, these pileups apparently do not play a decisive part in the development of hydrogen brittleness. Before the conditions of the pileup inside the grain become conducive to the formation of a crack, the crack is generated and begins to propagate at the grain boundary because of the higher degree of segregation of hydrogen and a lesser regularity in the arrangement of the atoms. Thus, a vital concept in the postulated theory of hydrogen brittleness is the hypothesis that under certain conditions, the dislocations move toward the grain boundaries together with the hydrogen atmospheres surrounding them, and the progressing segregation of hydrogen causes a premature failure.

The nature of the interaction of hydrogen atoms with moving dislocations depends substantially on the deformation temperature. If this temperature is too low, the mobility of the hydrogen atoms will be so slight that even at a relatively low deformation rate v_1 (fig. 1), the dislocations will not entrain the hydrogen atmospheres, but escape out of them and move freely through the metal. In this case, the extension curve shows a yield dent, so that the yield point rises, but the plasticity remains high for two reasons:

a. The motion of the dislocations is not retarded by hydrogen clouds;

b. The dislocations do not supply hydrogen atoms to the grain boundaries.

As the temperature rises, the mobility of the hydrogen atoms increases, and at a certain temperature T_n becomes comparable to the velocity of the dislocations at the same deformation rate v_1. Starting at this temperature, the

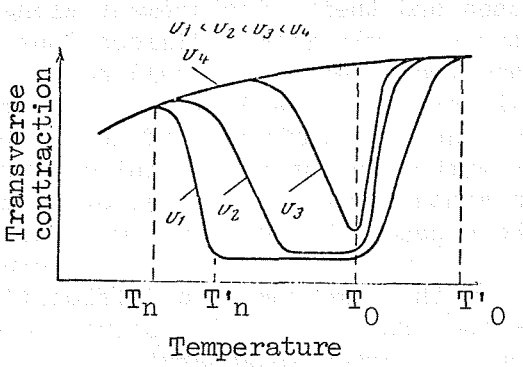

Figure 1. Diagram of the influence of testing temperature and deformation rate on the transverse contraction of titanium alloys saturated with hydrogen.

dislocations begin to partially entrain the hydrogen atmospheres, and this causes a decrease in plasticity. At some temperature T'_n, the hydrogen atmospheres are completely entrained by the dislocations.

If the deformation rate remains unchanged at v_1, any further rise in temperature should not affect the plasticity appreciably.

Actually, from the equation relating the deformation rate v to the velocity of the dislocations v_d, the dislocation density ρ, and the minimum interatomic distance b (ref. 3),

$$v = v_d \rho b \tag{1}$$

it follows that under the indicated conditions (v = const) the quantity of dislocations reaching the boundary per unit time remains unchanged to a first approximation. Although the resistance of the accompanying atmosphere to the motion of dislocations should decrease to some extent as the temperature rises, the amount of hydrogen supplied by the dislocations to the grain boundary will be the same as at temperature T'_n. Consequently, the specimens at temperatures above T'_n will exhibit failure almost as brittle as at temperature T_n.

Finally, temperature T_0 becomes so high that the Cottrell atmospheres start being broken down by the thermal motion. The density of the hydrogen atmospheres decreases, and their resistance to the motion of the dislocations decreases. In addition, each dislocation brings fewer hydrogen atoms to the grain boundary than in the case of lower temperatures.

In summary, beginning at temperature T_0, the plasticity rises sharply, and when the Cottrell atmospheres are completely broken down, hydrogen brittleness disappears.

If the deformation rate is greater than v_1, such as, v_2, the decrease in plasticity begins at a higher temperature, since the mobility of the hydrogen atoms should be greater at a greater velocity of the dislocations, so that these atoms can interact with a moving dislocation and accompany it. Finally, at a certain deformation rate v_3, the temperature T'_n, at which the Cottrell atmospheres begin to be completely entrained by the moving dislocations, coincides with temperature T_0, above which the Cottrell atmospheres are unstable, and a sharp minimum then appears on the "plasticity-temperature" curve.

The temperature of the complete restoration of plasticity, T'_0, apparently depends on the deformation rate. As was indicated earlier, above temperature T_0, the Cottrell atmospheres become unstable and are gradually broken down by the thermal motion. If it is considered that the moving dislocation scatters its energy along the path of its motion and that for this reason, in addition to the thermal energy, the adjacent atoms acquire energy of scattering which increases with rising velocity of the dislocation, then one should expect the temperature of the complete restoration of plasticity to decrease with an increasing deformation rate.

At sufficiently high deformation rates of the order of v_4, the dislocations escape from the surrounding hydrogen atmospheres over the entire temperature interval of existence of these atmospheres.

Let us now turn to a mathematical analysis of the picture drawn above. The critical velocity v_c at which the atmospheres begin to be entrained by the moving dislocations is given according to Cottrell (ref. 3) by the equation

$$v_c = \frac{4D}{l}$$

where D is the diffusion coefficient of the impurity; l is the characteristic length.

The characteristic length l may be found from the equation

$$l = \frac{A}{kT} = \frac{4\mu b \varepsilon r^2}{kT}, \qquad (2)$$

where μ is the shear modulus; ε are the stresses caused by the dissolved atoms; r is the radius of the impurity atom; k is Boltzmann's constant; T is the absolute temperature.

On the basis of equation (1), the critical deformation rate may then be expressed by the equation

$$v_{cr} = v_c \rho b = \frac{4D\rho b k T}{A}.$$

Assuming that $D = D_0 e^{-\frac{Q}{kT}}$, where Q is the activation energy of the diffusion of hydrogen in titanium, we find that

$$v_{cr} = \frac{4D_0\rho b}{A} kTe^{-\frac{Q}{kT}}. \qquad (3)$$

Thus, in keeping with the general assumptions made above, the critical deformation rate at which the dislocations begin to entrain the hydrogen atmospheres increases with rising temperature. It is important to note, however, that this rate is independent of the hydrogen content of the alloy.

On the contrary, the temperature at which the plasticity begins to be restored, T_0, and the related temperature T'_0 depend strongly on the average hydrogen concentration C_0 (ref. 3), so that

$$T_0 = \frac{u_{max}}{k \ln \frac{1}{C_0}}, \qquad (4)$$

where u_{max} is the maximum bond energy of the hydrogen atom, equal to $\frac{A}{r_0 + d}$, r_0 being the minimum distance of the impurity atom from the dislocation center and d being the effective dislocation width.

The dependence of T'_0 on the hydrogen content is shown graphically (fig. 2). The same figure shows the temperatures T_1, T_2, T_3 and T_4 given by equation (3), below which the hydrogen brittleness does not develop when the tests are carried out at the rates v_1, v_2, v_3 and v_4, since the velocity of the dislocations considerably exceeds the mobility of the atoms. Thus, the temperature range in

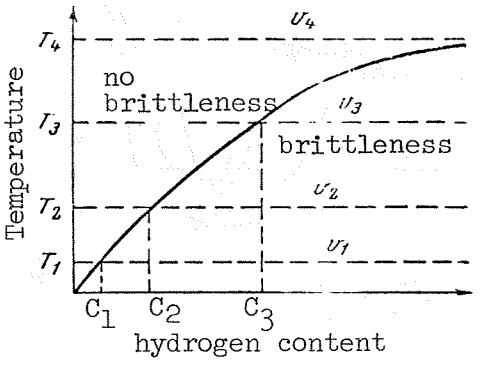

Figure 2. Dependence of the temperature range of hydrogen brittleness of titanium alloys on the hydrogen content.

which the hydrogen brittleness can develop is limited at the top by the temperature of the breakdown of the Cottrell atmospheres T_0, and at the bottom by the temperature T_n below which the dislocations escape from the Cottrell atmospheres. The point of intersection characterizing these temperatures determines the maximum permissible hydrogen concentration up to which the hydrogen brittleness is not manifested at a given deformation rate. Thus, for example, at a deformation rate v_1, hydrogen brittleness is not displayed over the entire temperature interval if the hydrogen content is less than C_1.

If the hydrogen concentration is greater than C_1, the temperature range of hydrogen brittleness increases with rising hydrogen content. As the deformation rate increases, the hydrogen concentration at which hydrogen brittleness begins to be observed rises, and the brittleness temperature range becomes smaller.

Such are the basic assumptions of the dislocation theory of hydrogen brittleness. The following question arises: How closely do they agree with the experimental data? We illustrate (fig. 3) the dependence of the transverse contraction of the alloy Ti 140A (2 percent Fe; 2 percent Cr; 2 percent Mo) on the temperature of the tests for various displacement rates of the cross-bars of the rupture-test machine (ref. 4). The qualitative agreement of the behavior of hydrogen-saturated titanium alloys predicted by the theory with the experimental data is unquestionable.

The same data make it possible to carry out an approximate but quantitative verification of the proposed theory. If it is assumed in accordance with Haynes (ref. 5) that $\mu = 4 \cdot 10^{11}$ dynes/cm^2, $r = 1.5 \cdot 10^{-8}$ cm, $b = 3 \cdot 10^{-8}$ cm, and $\epsilon = 0.04$,

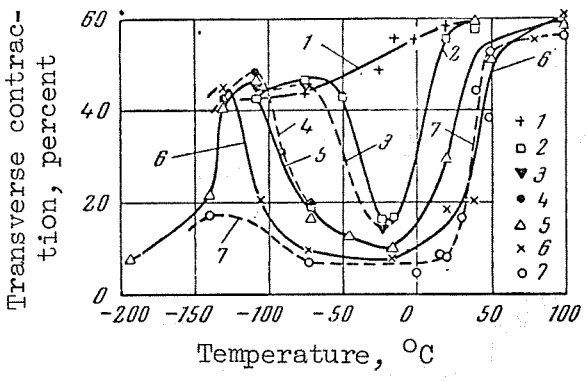

Figure 3. Dependence of the transverse contraction of Ti 140A on the testing temperature at various deformation rates: 1, 25.4 mm/min; 2, 12.7 mm/min; 3, 6.35 mm/min; 4, 2.54 mm/min; 5, 1.27 mm/min; 6, 0.64 mm;min; 7, 0.13 mm/min.

then $A = 6.5 \cdot 10^{-21}$ erg cm. The dislocation density ρ in annealed metals is of the order of 10^8 cm^{-2}. Thus, the only remaining unknown quantities in equation (3) are D_0 and Q. From reference 5 it follows that the activation energy of hydrogen diffusion in the β phase of the alloy Ti 140A in the temperature range of -120 to +50° is approximately 3000 cal/mole. Assuming the diffusion coefficient of hydrogen in the β phase of the alloy Ti 140A at room temperature to be the same as in the alloy Ti-4 percent Al-4 percent Mn, namely $1.9 \cdot 10^{-9}$ cm^2/sec, we find D_0, and for the critical rate of relative deformation we obtain the formula

$$v = 4.8 \cdot 10^{-8} \rho T e^{-\frac{1500}{T}} \text{ 1/min.}$$

For dislocation densities of $0.5 \cdot 10^8$, $0.75 \cdot 10^8$ and 10^8 cm^{-2}, this equation is represented graphically (fig. 4). The same graph shows the temperatures at which the plasticity of the alloy Ti 140A begins to decrease at various deformation rates.

Further, if it is assumed that $r_0 = 1.5 \cdot 10^{-8}$ cm and $b = 3 \cdot 10^{-8}$ cm, the maximum bond energy u_{max} turns out to be 0.093 eV. In this case, equation (4) assumes the form shown graphically in figure 5. The same graph shows the

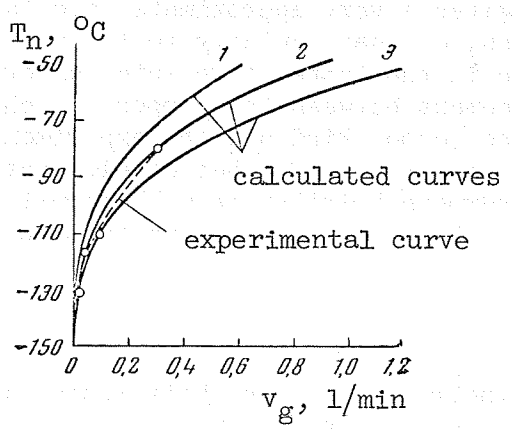

Figure 4. Temperature of the start of decrease in plasticity T_n versus deformation rate v_d for alloy Ti 140A: 1, $p = 0.5 \cdot 10^8$ cm^{-2}; 2, $p = 0.75 \cdot 10^8$ cm^{-2}; 3, $p = 10^8$ cm^{-2}; ●, experimental points.

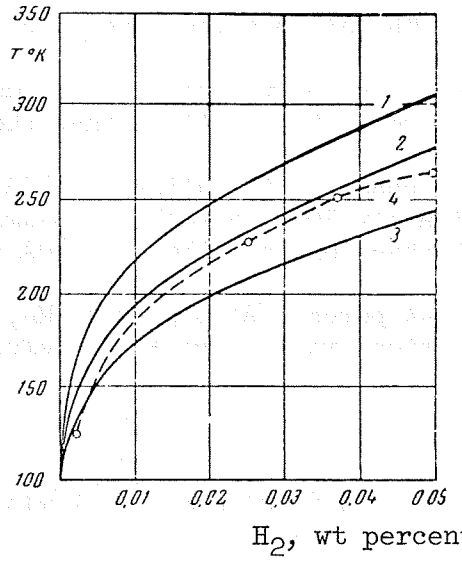

Figure 5. Temperature of the start of restoration of plasticity T_0 versus hydrogen content for the alloy Ti 140A: 1, u_{max} = 0.1 eV; 2, u_{max} = 0.09 eV; 3, u_{max} = 0.08 eV; 4, experimental curve.

expected curves for bond energies from 0.08 to 0.1 eV, and gives temperatures corresponding to the sharp minimum on the "cross section-testing temperature" curves for the alloy Ti 140A with various hydrogen contents.

Since the article gives a very approximate calculation which includes a number of simplifications, due particularly to the fact that not all the physical quantities are known in the temperature interval of interest, it should be recognized that the agreement between the proposed mechanism of reversible hydrogen brittleness of the second kind and the experimental data is fully satisfactory. It may be assumed that a further development and refinement of the dislocation theory of hydrogen brittleness will permit a more rigorous quantitative interpretation of the observed experimental facts.

Summary

1. A dislocation theory of hydrogen brittleness developing at low deformation rates is proposed, based on the assumption that on the dislocations, hydrogen forms Cottrell atmospheres which are entrained by the dislocations over a certain temperature range. The dislocations transport the hydrogen toward the grain boundaries, causing the appearance of hydrogen segregations which facilitate the generation and propagation of cracks.

2. This theory makes it possible to account for the basic regularities involved in the hydrogen brittleness of $\alpha + \beta$ alloys:

a. Increase in their tendency toward hydrogen brittleness with an increase in hydrogen content, decrease in temperature, and decrease in the deformation rate;

b. Intercrystalline character of the failure;

c. Increase in the temperature of the transition from viscous failure to brittle failure with increasing hydrogen content.

3. The relationships predicted by the dislocation theory of hydrogen brittleness are in satisfactory agreement with the experimental data for the alloy Ti 140A.

REFERENCES

1. Livanov, V. A., Bukhanova, A. A. and Kolachev, B. A. Hydrogen in Titanium (Vodorod v titane). Metallurgizdat, 1962.

2. Livanov, V. A., Bukhanova, A. A., Kolachev, B. A. and Gusel'nikov, N. N. Titanium and Its Alloys (Titan i yego splavy). Izd-vo AN SSSR, No. 10, p. 207, 1963.

3. Cottrell, A. H. Dislocations and Plastic Flow in Crystals, Metallurgizdat, 1958.

4. Williams, D. N., Schwarzberg, F. K. and Jaffee, R. I. Trans. ASM, Vol. 60, p. 802-804, 1959.

5. Haynes, R. J. Inst. Metals, Vol. 88, No. 12, p. 509-512, 1960.

EFFECT OF ALLOYING ON THE PHYSICOCHEMICAL PROPERTIES OF TITANIUM

S. F. Kovtun and R. A. Ul'yanov

Because of their high strength, low density, and high corrosion resistance, titanium and its alloys are finding increasingly wider applications in technology.

In addition to the study of the mechanical properties of titanium-base alloys, the investigation of the physical properties of these alloys, particularly the electrical resistivity and coefficient of linear expansion, are of scientific and practical interest.

In the present work, a study was made of the influence of a series of additions on the variation in the electrical resistivity and coefficient of linear expansion of titanium and also its oxidizability. The additions used were elements contained in mass-produced Soviet alloys (aluminum, chromium, molybdenum) as well as elements which thus far have not been used for alloying but which can be employed to raise the high-temperature strength (rhenium, tantalum, iridium), the chemical stability (palladium, beryllium) and to improve the technological properties (lanthanum). The alloys were prepared by melting in an arc furnace with a nonconsumable electrode in an atmosphere of argon which was first purified by being passed through molten lithium (ref. 1).

The starting materials used were titanium sponge TGO, aluminum AOO, electrolytic chromium, 99.9 percent pure rhenium, and other elements of high purity.

In order to achieve a uniform distribution of the alloying elements in the ingots, the alloys were remelted at least 5 times. To avoid the evaporation of volatile components during melting (chromium, lanthanum, etc.), the argon pressure in the arc furnace was raised to the atmospheric value and higher. After the melting, the alloys were rolled into rods on a vacuum rolling mill; this caused an additional degassing of the metals and prevented their oxidation (ref. 2). Prior to the investigation, the specimens prepared from the rods were vacuum-annealed for 40 hours at 1200°.

Electrical Resistivity of the Alloys

The electrical resistivity of the alloys was studied in the temperature range of -195 to 1250°. The resistivity was measured by the compensation method in a vacuum unit with a residual pressure in the working chamber no higher than $1 \cdot 10^{-5}$ mm Hg. The measurements established that as the temperature rises from -195° to about 350-400°, the change in the resistivity of both iodide and technical titanium (fig. 1) was linear.

As the heating increased further, the temperature coefficient of the electrical resistivity, while remaining positive, decreased in magnitude as the temperature rose. This may be explained by the fact that in transition metals, which include titanium, the number of s electrons passing into the d orbital decreases with rising temperature, and the relation $\rho = f(t)$ deviates from linearity (ref. 3).

In both technical and iodide titanium, the electrical resistivity decreases sharply at 882° due to a polymorphic transformation. In iodide titanium, the temperature range of the transformation is no greater than 6 to 10°, and in technical titanium it widens to 20° owing to the presence of impurities.

As the temperature is raised further, the resistivity of both iodide and technical titanium increases, but the temperature coefficient of the resistivity of β-Ti is considerably smaller than that of α-Ti.

The value of the resistivity of iodide and technical titanium and the character of their temperature dependence are in agreement with the data of reference 4.

The investigations showed that the effectiveness of the influence of alloying elements on the hardness and electrical resistivity of titanium (fig. 2) follow the same pattern as in the case of metals of the cubic system. At the same atomic concentration, a greater increase in hardness and resistivity is produced by alloying elements whose atomic diameters differ more strongly from the atomic diameter of titanium, independently of the type of the crystal lattice. The only exception is lanthanum, which causes a less pronounced increase in hardness and resistivity; this may be due to its deoxidizing effect. Lanthanum, which has a great affinity for oxygen, rids titanium of a certain amount of its impurities.

It follows from the graphs of figures 3 and 4 that the alloying of titanium causes an increase in the electrical resistivity and changes the temperature and range of the $\alpha \rightarrow \beta$ transformation. Among the investigated metals at equal concentrations, the greatest increase in resistivity is produced by aluminum, rhenium, and chromium. The lesser increase in resistivity upon alloying with molybdenum may be due to the presence of the β phase. The graphs also show that both in the alloys and in pure titanium, the temperature coefficient of electrical resistivity decreases with the temperature, and this decrease is more pronounced the higher the content of the alloying element.

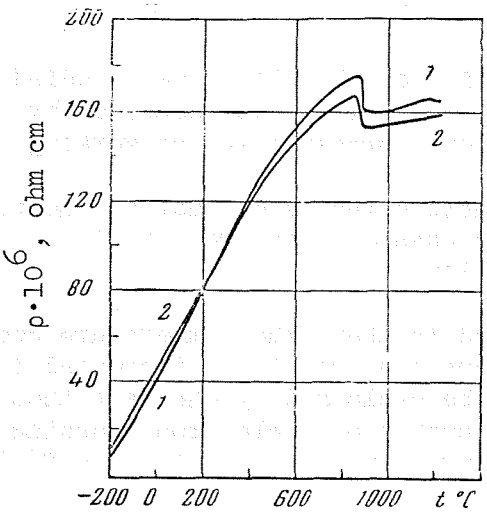

Figure 1. Temperature dependence of electrical resistivity: 1, iodide titanium; 2, technical titanium.

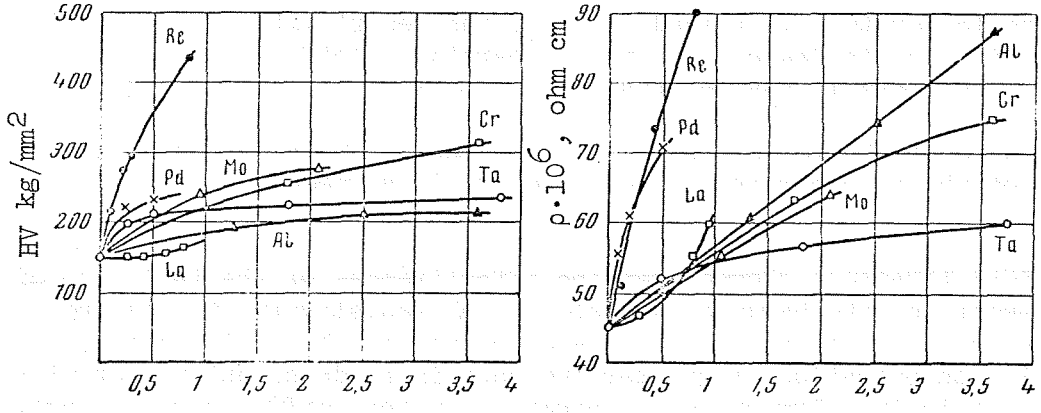

Content of alloying element, at. percent

a

Content of alloying element, at. percent

b

Figure 2. Effect of alloying elements on the hardness (a) and electrical resistivity (b) of titanium at 20°.

At temperatures from -196 to 200°, the higher the content of chromium in the alloy, the more it raises the electrical resistivity of titanium. At higher temperatures, the resistivity of the alloy with 4 wt percent Cr (3.6 at. percent) is found to be smaller than in the alloy with 2 wt percent Cr, which may be due to the presence of a eutectoid in the alloy, or more probably of the chemical compound $TiCr_2$, which enters into the eutectoid.

In the region of the β phase, the increase of resistivity in alloys with 2 percent Cr, and particularly in the alloy with 4 percent Cr, is considerably

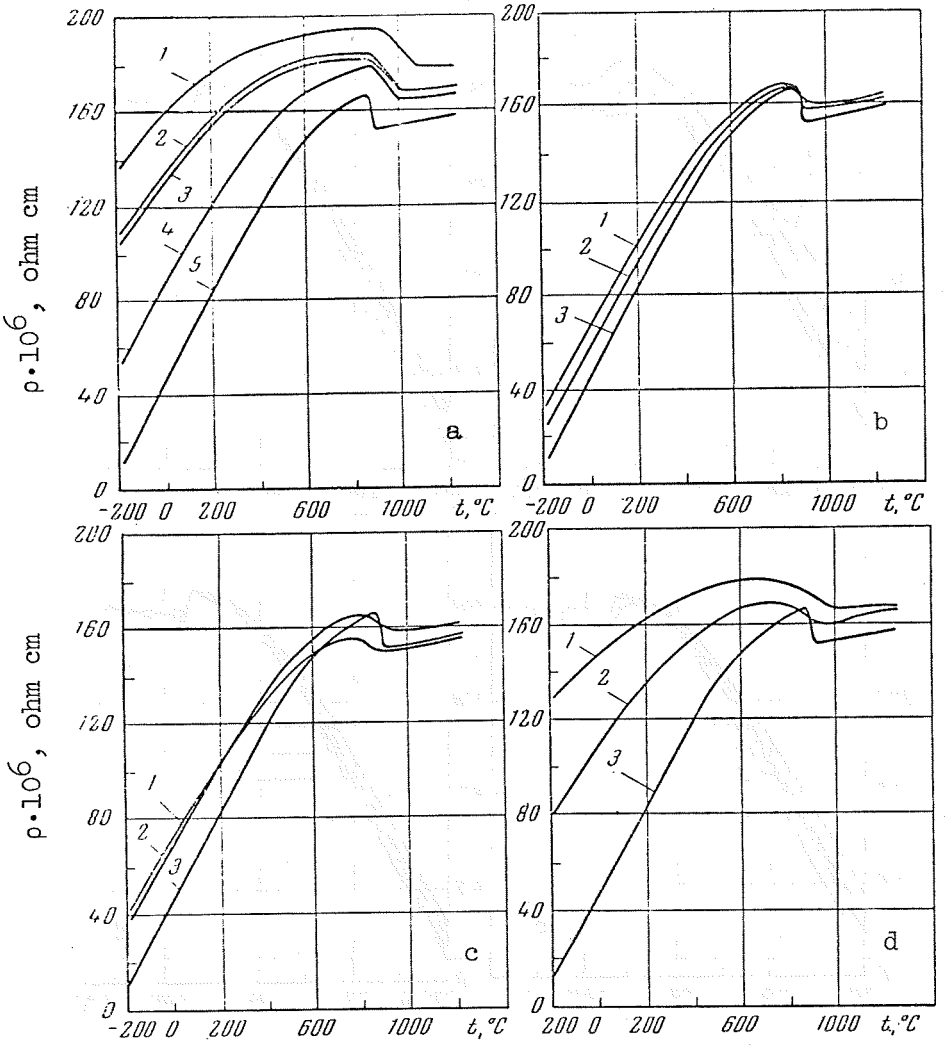

Figure 3. Temperature dependence of the electrical resistivity of alloys of titanium with aluminum, molybdenum, and chromium: a, alloy Ti-Al (1, 6 percent Al; 2, VT5; 3, 4 percent Al; 4, 2 percent Al; 5, TGO); b, alloy Ti-Mo (1, 4 percent Mo; 2, 2 percent Mo; 3, TGO); c, alloy Ti-Cr (1, 4 percent Cr; 2, 2 percent Cr; 3, TGO); d, alloy of the system Ti-Al-Mo-Cr (1, 5 percent Al + 2 percent Mo + 2 percent Cr; 2, 2 percent Al + 2 percent Mo + 2 percent Cr; 3, TGO).

less than in the region of the α phase. Molybdenum and chromium lower the temperature of the $\alpha \rightarrow \beta$ transformation, while aluminum raises it. Apparently, the widening of the $\alpha \rightarrow \beta$ region upon alloying with aluminum which we observed is due to the influence of oxygen and nitrogen, which are present in technical titanium in larger quantities than in the iodide titanium used to plot the Ti-Al phase diagram in reference 5.

Complex alloying leads to an increase in resistivity over the entire range of -196 to 1250°. The resistivity of the alloys of the system Ti-Al-Mo-Cr is

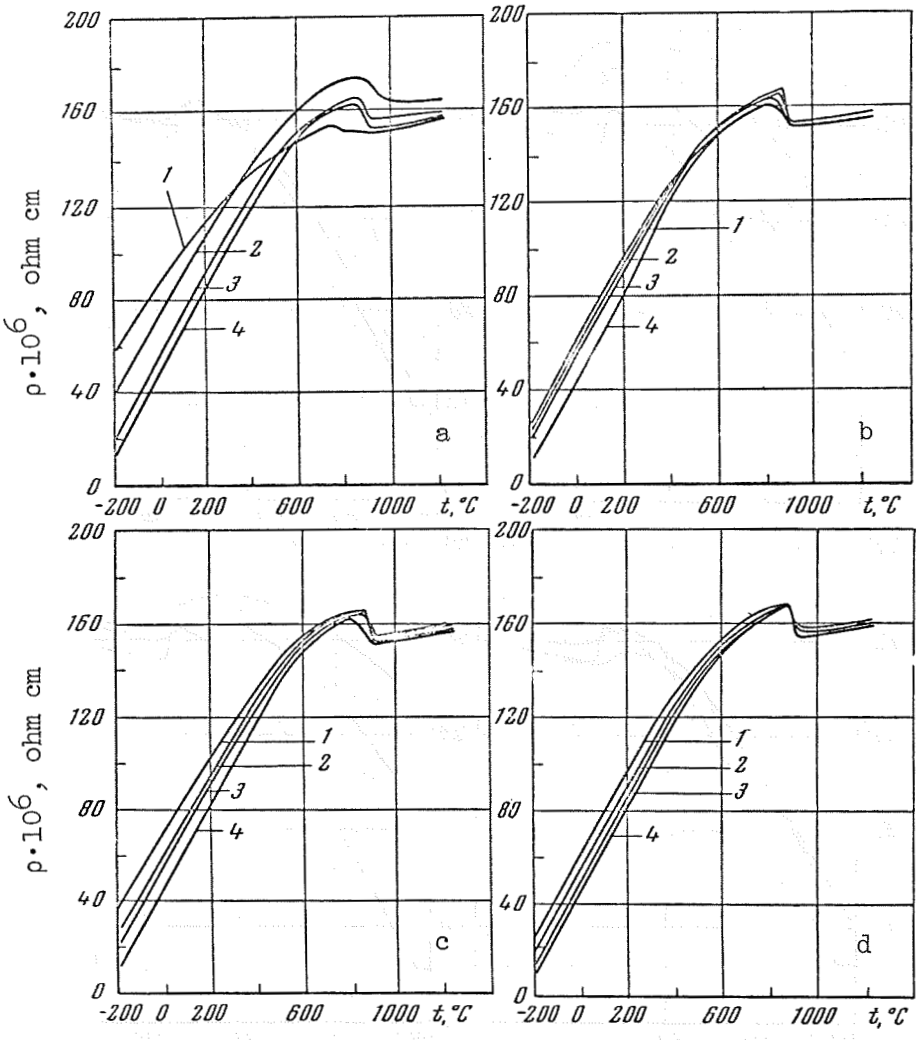

Figure 4. Temperature dependence of the electrical resistivity of electrolytic alloys of titanium with rhenium, tantalum, palladium and lanthanum: a, alloy Ti-Re (1, 3 percent Re; 2, 1 percent Re; 3, 0.7 percent Re; 4, 0.4 percent Re); b, alloy Ti-Ta (1, 13 percent Ta; 2, 6.5 percent Ta; 3, 1.7 percent Ta; 4, TGO); c, alloy Ti-Pd (1, 2 percent Pd; 2, 0.8 percent Pd; 3, 0.2 percent Pd; 4, TGO); d, alloy Ti-La (1, 2.2 percent La; 2, 1.8 percent La; 3, 1 percent La; 4, 0.4 percent La).

higher than in binary alloys, particularly at room temperatures and negative temperatures. The temperature of the start of the $\alpha \rightarrow \beta$ transformation in complex alloys decreases, and the transformation range expands to 200-300° instead of the 20° for technical titanium. When up to 1 wt percent rhenium is added, it raises the resistivity over the entire temperature range. It stabilizes the β phase by decreasing the temperature of the $\alpha \rightarrow \beta$ transformation and extending the $\alpha + \beta$ region, as was found earlier by other methods of investigation (ref. 6). At 3 wt percent Re, the resistivity of the alloy also increases with the

temperature, but less than in pure titanium and in alloys with a low rhenium content. For this reason, at temperatures above 350°, owing to the presence of the β phase, the resistivity is less than in alloys with a rhenium concentration up to 1 wt percent and even less than in pure titanium.

When titanium is alloyed with tantalum (up to 10 wt percent), the resistivity changes insignificantly over the entire temperature range. At temperatures above 600°, the alloys of the system Ti-Ta have a lower resistivity than technical titanium. Tantalum lowers the temperature of the $\alpha \rightarrow \beta$ transformation appreciably.

In alloys of titanium with palladium, the resistivity increases over the entire temperature range as the palladium content rises. Palladium lowers the temperature of the $\alpha \rightarrow \beta$ transformation by stabilizing the β phase.[1] Lanthanum slightly increases the resistivity of the alloys over the entire temperature range. Lanthanum also slightly increases the temperature of the polymorphic transformation of titanium, as was established earlier by other methods of investigation.

Thermal Expansion

The coefficient of linear expansion of the alloys was measured by means of a vacuum dilatometer having a reading scale with a precision of 0.002 mm. The vacuum was maintained at $1 \cdot 10^{-5}$ mm Hg at all temperatures. Graphs of the elongation per unit length were plotted by taking into account the expansion of the quartz of the dilatometer.

Results of the measurements showed that the dilatometric curves of iodide and technical titanium (fig. 5) coincide up to 800°.

At the temperature of the phase transformation there is observed a distinct inflection indicating a change in the coefficient of linear expansion associated with the transformation to the β phase.

In accordance with the graph, the temperature dependence of the linear expansion in the range from zero to 700° is expressed by the formula

$$l_t = l_0(1 + \alpha' t + \beta t^2),$$

where $\alpha' = 8.0 \cdot 10^{-6}$, $\beta = 2.7 \cdot 10^{-9}$, and t is the temperature in °C.

In the indicated temperature range, the coefficient of linear expansion

$\alpha = 8.0 \cdot 10^{-6} + 5.4 \cdot 10^{-9}$ t.

---

[1] At a content of 0.4 wt percent Pd, the resistivity of the alloy increases irregularly over the entire temperature range.

According to Grüneisen's equation, the breakdown of the crystal lattice (fusion) of pure metals occurs at temperatures at which the volume increases by 6 percent over the volume at absolute zero. Hence, the lower the melting point of the metal, the higher the coefficient of linear expansion, since in this case a 6 percent increase in volume takes place over a narrower temperature range, from absolute zero to the melting point.

When titanium is alloyed, the change in the average coefficient of linear expansion depends primarily on the content of the alloying elements (fig. 6). The higher the concentration of the alloying element, the greater is the change in the coefficient of linear expansion.

On alloying with chromium, aluminum, lanthanum and palladium, the coefficient of linear expansion of the alloys increases, while tantalum, molybdenum, and particularly rhenium decrease this coefficient. Rhenium, tantalum, chromium

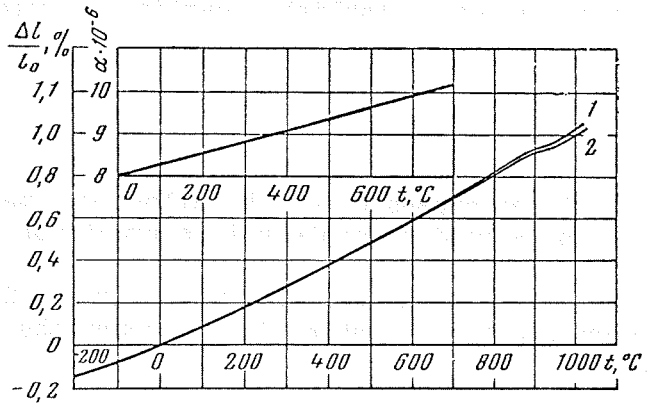

Figure 5. Dilatometric curves of iodide (1) and technical (2) titanium and temperature dependence of the medium (0-400°) coefficient of linear expansion of titanium.

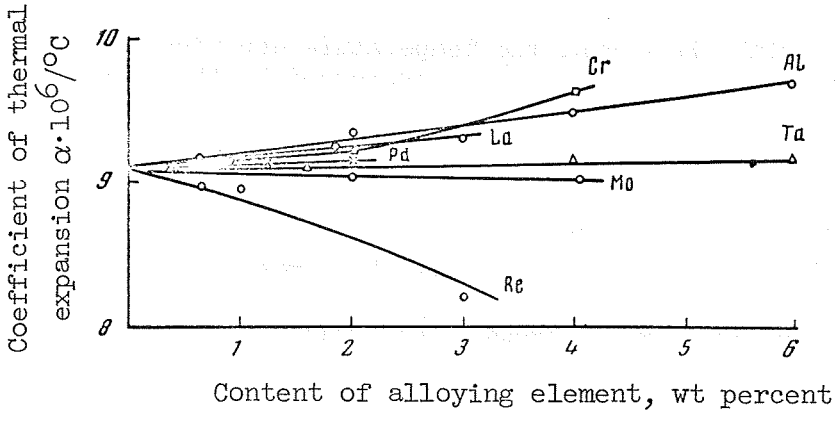

Figure 6. Effect of alloying elements on the medium coefficient of thermal expansion of titanium in the range of 0-400°.

and molybdenum have a lower coefficient of linear expansion than titanium, while in palladium and aluminum, this coefficient is higher than in titanium.

The change in the coefficient of linear expansion upon alloying is chiefly determined by the relation of the coefficients of linear expansion of the base of the alloy to that of the alloying elements. This is probably what causes the increase in the coefficient of linear expansion of titanium on alloying with chromium, whose coefficient is smaller than that of titanium. In addition, the average coefficient of linear expansion is affected by the phase composition of the alloys (at the concentrations studied, the alloys with chromium may contain the chemical compound $TiCr_2$).

In a study of the effect of alloying on the coefficient of linear expansion, it was noted that when the alloys were heated to temperatures above those of the phase transformations and subsequently cooled, a residual change in the length of the specimens took place (at thermal cycles below the temperature of phase transformations practically no change in the length of the specimens was observed. Since no data on titanium are given in works devoted to the influence of thermal cycles on metals and alloys (refs. 8 and 9), it appeared interesting to carry out these investigations.

The measurements showed that the most effective change in length was displayed by specimens of alloys of titanium with molybdenum, although small changes were noted in specimens of pure titanium and its alloys with chromium, aluminum, palladium, tantalum and other metals. The specimens were heated and cooled in a vacuum. The heating rate was 1 deg/min, and the cooling rate, 18 deg/min.

The heating curves of all the cycles at the phase transformation temperature (about 880°) clearly show an inflection indicating a decrease in the coefficient of linear expansion of the β phase (fig. 7). When the alloy is cooled from 1000° to the phase transformation temperature, the cooling curve coincides with the heating curve. At the temperature of the phase $\beta \rightarrow \alpha$ transformation, the cooling curve shows an abrupt contraction in the length of the specimen (0.02-0.03 percent), due to a decrease in volume as a result of the shift into the region of the α phase. The heating and cooling rates employed give rise to a certain temperature gradient along the cross section of the samples, and the $\alpha \rightarrow \beta$ and $\beta \rightarrow \alpha$ transformations encompass successive layers of the material, moving from the edge to the center.

The difference in the atomic volume of the α and β phases in the specimen gives rise to stresses which relax following plastic flow, and this accounts for the deformation.

Since the atomic volume of the α phase is less than that of the β phase, then during heating, the upper layers by changing into the β phase have a greater volume and tend to expand the part of the specimen in the α phase.

On cooling, the upper layers, which assume the structure of the α phase, contract the inner portion of the specimen in the β phase. Since the temperature gradient along the cross section of the specimen is greater during cooling than during heating (the cooling rate is higher than the heating rate), then

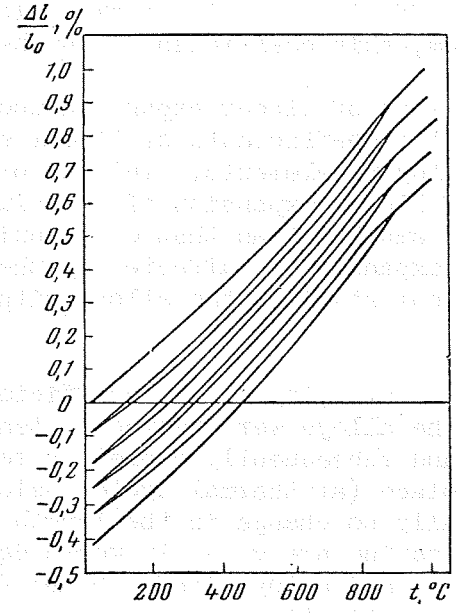

Figure 7. Series of dilatometric curves of the alloy Ti-Mo (2 wt percent Mo).

even if one assumes the same yield point of the α and β phases at the transformation temperature, the contracting stresses on cooling will be greater than the expanding stresses on heating. For this reason, the length of the titanium alloy decreases irreversibly on slow heating and fast cooling (fig. 7). Another cause of the deformation of titanium and its alloys may be the phase transformations which take place in the metastable β solid solutions in the investigated alloys during cooling (from the formation of α' and ω phases to equilibrium structures). The increase in the stability of the β phase during cooling is obviously the reason for the greater (five-fold) deformation of specimens of alloys of the system Ti-Mo as compared to the deformation of specimens of technical titanium (fig. 8). A magnitude of the same order as in the alloy of the system Ti-Mo is observed in specimens of pure zirconium and iron.

Oxidizability of Alloys at High Temperatures

In addition to studying the physical properties of the alloys, it appeared interesting to investigate the influence of the alloying elements on the oxidizability of titanium and depth of diffusional saturation of the metal by gases in the course of the oxidation. The oxidizability of the alloys was studied primarily by determining the increase in weight following intermittent exposures to the testing temperature.

When titanium is alloyed with aluminum, the oxidizability of the alloys at 800° increases with rising aluminum concentration (fig. 9). At 900°, the oxidation rate of the alloys decreases with rising aluminum content, but remains above the oxidation rate of titanium. Obviously, the decrease in the oxidation rate is caused in this case by a change in the composition of the oxide

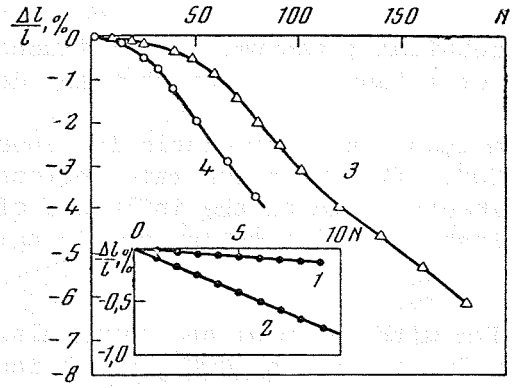

Figure 8. Dependence of the dimensions of metal specimens on the number of cycles (for titanium and the alloy Ti-Mo, a temperature range of 1000-20°, and for zirconium and iron, 1000-250°): 1, titanium TG0; 2, alloy Ti-Mo; 3, iodide zirconium; 4, "armco" iron.

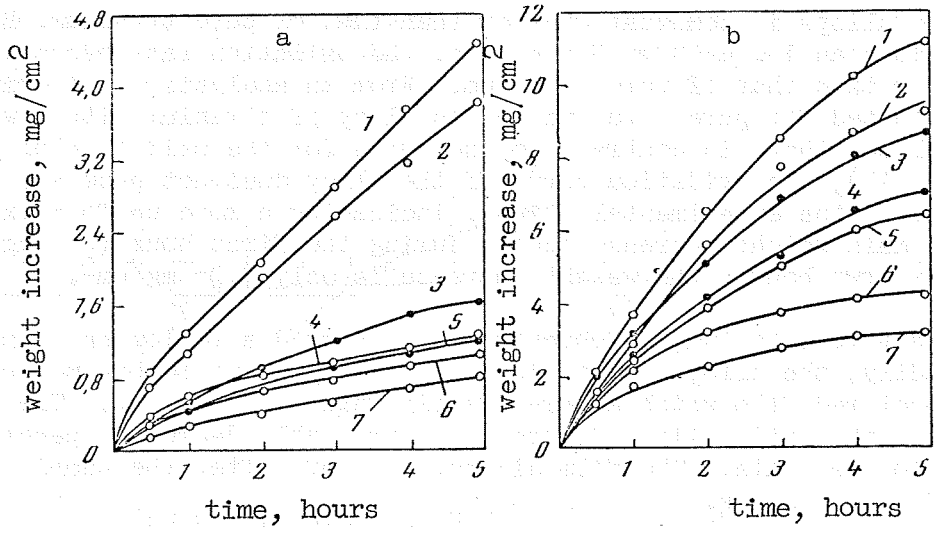

Figure 9. Oxidizability of alloys of titanium with aluminum, chromium, and molybdenum at 800 and 900°: a, t = 800° (1, 4 percent Cr; 2, 2 percent Cr; 3, 6 percent Al; 4, 2 percent Mo; 5, 4 percent Al; 6, Ti; 7, 2 percent Mo); b, t = 900° (1, 4 percent Cr; 2, 2 percent Cr; 3, 6 percent Al; 4, 4 percent Al; 5, 4 percent Mo; 6, Ti; 7, 2 percent Mo).

film and its sintering. The change in the chemical composition of the oxide film is indicated by data of the chemical analysis of the scale on a titanium-aluminum alloy (ref. 10) and also by an appreciable increase in the stability to oxidation of an alloy with 15 percent Al at 700° (ref. 11).

The oxidation rate of alloys of the system Ti-Mo at 800 and 900° is close to the oxidation rate of technical titanium. The influence of molybdenum additions on the oxidizability of titanium did not show any definite regularity.

Alloying with chromium causes an appreciable increase in the oxidation rate of the alloys at 800 and 900°. The oxidation rate increases with rising chromium concentration. Experimental data on the influence of chromium, aluminum and molybdenum on the oxidizability of titanium are in agreement with the data of references 10 and 11.

The alloying of titanium with tantalum and particularly lanthanum (fig. 10) causes a rise in the oxidation rate at 800°, which increases with rising concentration of these elements.

Alloying of titanium with palladium and rhenium has a favorable influence on the protective properties of the oxide film. The oxidation rate of alloys of titanium with palladium during the initial stage of oxidation is somewhat greater than that of pure titanium, but later, owing to the better protective properties of the oxide film, it decreases. The oxidation rate of alloys containing 0.4 wt percent Pd remains less than that of titanium over the course of the entire period of oxidation. At low rhenium concentrations, the oxidizability of the alloys is somewhat greater than that of pure titanium. However, at concentrations as low as 3 wt percent Re, the oxidation rate becomes appreciably lower than that of pure titanium. From an analysis of kinetic oxidation curves plotted for pure titanium and an alloy of titanium with 3 wt percent Re it follows that, in contrast to the curve for the oxidation of pure titanium (fig. 11), the oxidation curve of the alloy does not show any appreciable scatter of the experimental points, indicating a more uniform oxidation process. The main weight increase occurs during the first hour (0.2 mg/cm^2). During the next two hours, the weight increase is only 0.05 mg/cm^2.

In contrast to titanium, on which there is formed a yellowish film which peels off readily, the alloy of titanium with 3 wt percent Re becomes coated with a steel-colored film which adheres fairly well to the metal. The change in the color of the oxide film indicates an appreciable degree of penetration of rhenium into the scale. The film did not peel off after the samples were exposed to 800° for 72 hrs.

According to Wagner's theory, the oxidation rate during alloying may be reduced by decreasing the number of defects in the lattice of the scale. Titanium dioxide is an anion-deficient oxide, and titanium is oxidized owing to the diffusion of oxygen through the oxide layer; the front of the reaction is located at the oxide-metal phase boundary (ref. 12). In this case, the introduction of ions with a higher valence (above four) should decrease the concentration of the oxygen vacancies and the oxidation rate, while on the contrary, the addition of ions of lower valence should increase the concentration of oxygen vacancies and the oxidation rate. The increase in the oxidation rate upon alloying with chromium, aluminum, and lanthanum, and decrease in the oxidation rate on alloying with rhenium are in accord with Wagner's theory, but the latter is contradicted in the case of alloying with tantalum and

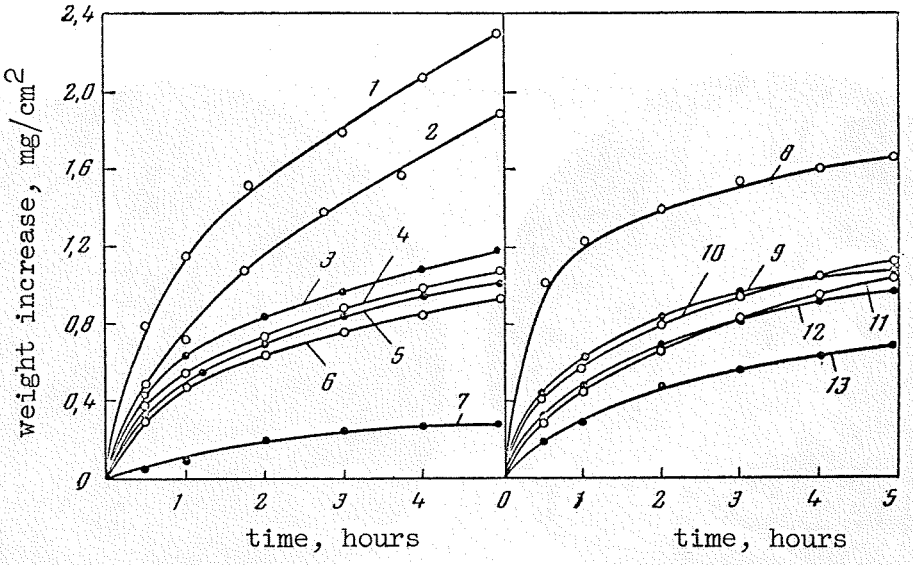

Figure 10. Effect of alloying with tantalum, lanthanum, palladium and rhenium on the oxidizability of titanium at 800°: 1, 3 percent La; 2, 1.8 percent La; 3, 0.5 percent Re; 4, 0.5 percent La; 5, 1 percent Re; 6, Ti; 7, 3 percent Re; 8, 13 percent Ta; 9, 5 percent Ta; 10, 3 percent Pd; 11, 0.6 percent Ta; 12, 1 percent Pd; 13, 0.4 percent Pd.

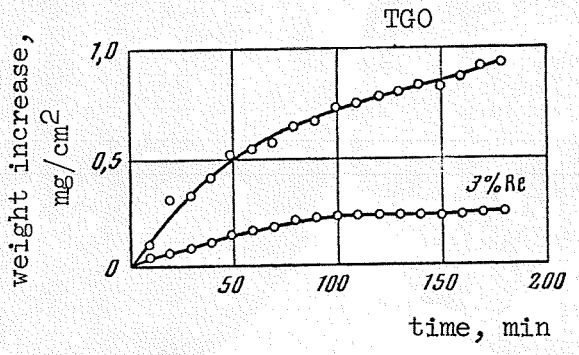

Figure 11. Kinetic curves of oxidation of titanium and the alloy Ti + 3 percent Re.

molybdenum. The disagreement with Wagner's theory in the case of alloying with tantalum and molybdenum is apparently due to a slight penetration of these elements into the scale.

Alloys of titanium and rhenium deserve particular attention. Rhenium is a stabilizer of the β phase (ref. 13), raises the hardness and strength of the alloys considerably, as well as the recrystallization temperature (ref. 14).

We have established that rhenium is very effective in preventing the growth of grains when the metal is heated (fig. 12) and slows down the diffusion

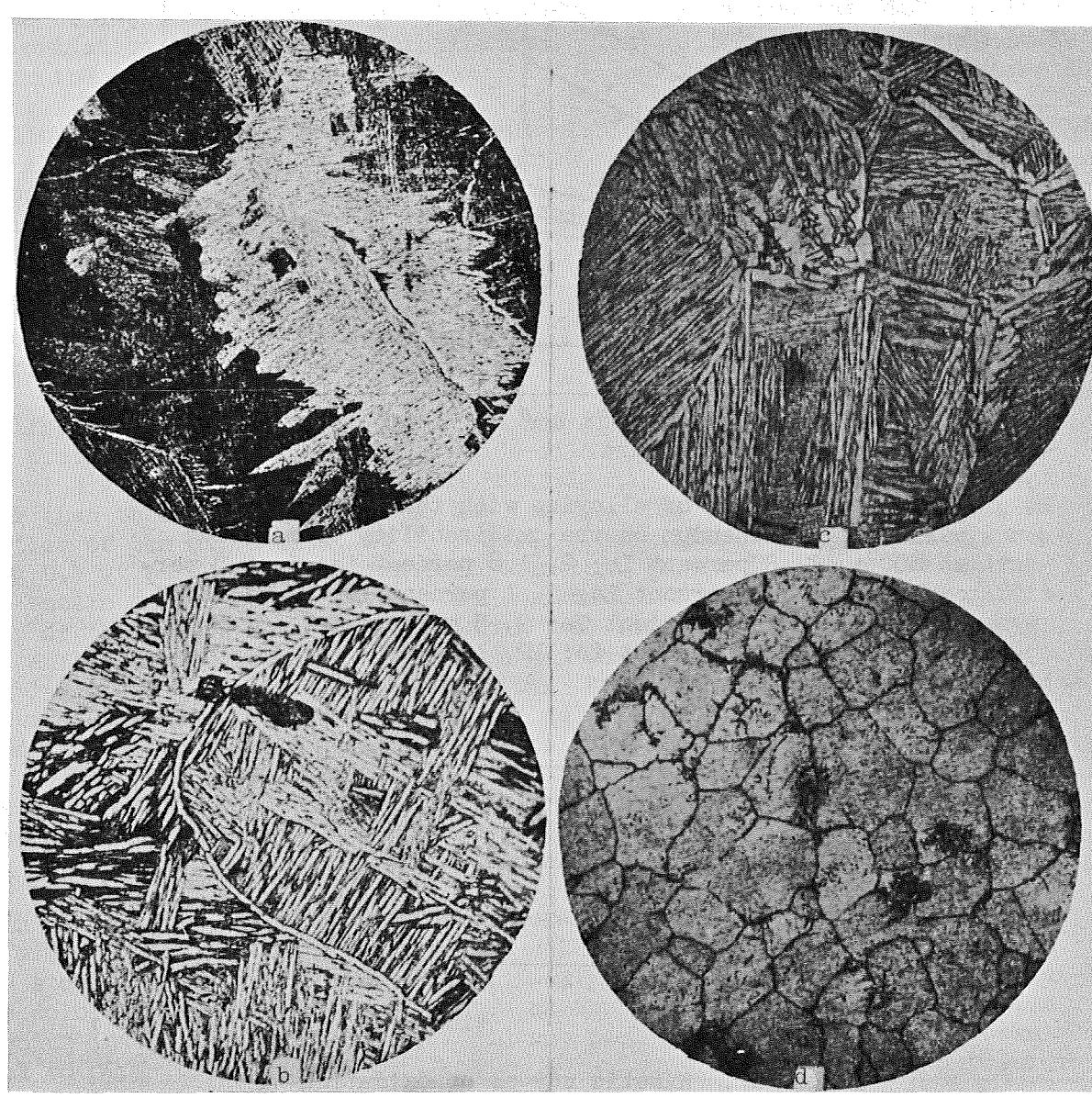

Figure 12. Microstructure of alloys of titanium with rhenium, x 70: a, 0.1 percent Re; b, 0.5 percent Re; c, 1.0 percent Re; d, 3 percent Re.

of oxygen and nitrogen into the metal during heating. In addition, the investigated alloys containing up to 5 wt percent Re are easily rolled into bars and strips and are satisfactorily machined by cutting. All this leads to the assumption that alloying with rhenium, particularly in alloys of complex composition, may turn out to be very effective in raising the high-temperature strength of the alloys.

When titanium is oxidized, in addition to the formation of the oxide film, the surface layer of the metal becomes saturated with oxygen and nitrogen, and this causes an appreciable increase in the hardness of the metal and a decrease in its plasticity.

For this reason, it was interesting to study the influence of alloying elements on the diffusion of atmospheric gases into the metal.

The study was carried out by measuring the microhardness (at a load of 50 g) along the direction from the surface to the center of the samples following oxidation at 800° for 72 hrs.

It was found that in alloying with tantalum and lanthanum, the depth of oxygen diffusion into the metal increases as the concentration of the alloying element rises (fig. 13). Palladium has little effect on the depth of oxygen diffusion. It is characteristic that the alloy with 0.4 wt percent Pd is distinguished by a great hardness. Earlier, an abnormally high electrical resistivity and a high oxidation resistance were observed in an alloy of this composition. The microstructure of the alloy has a characteristic "basketlike" structure.

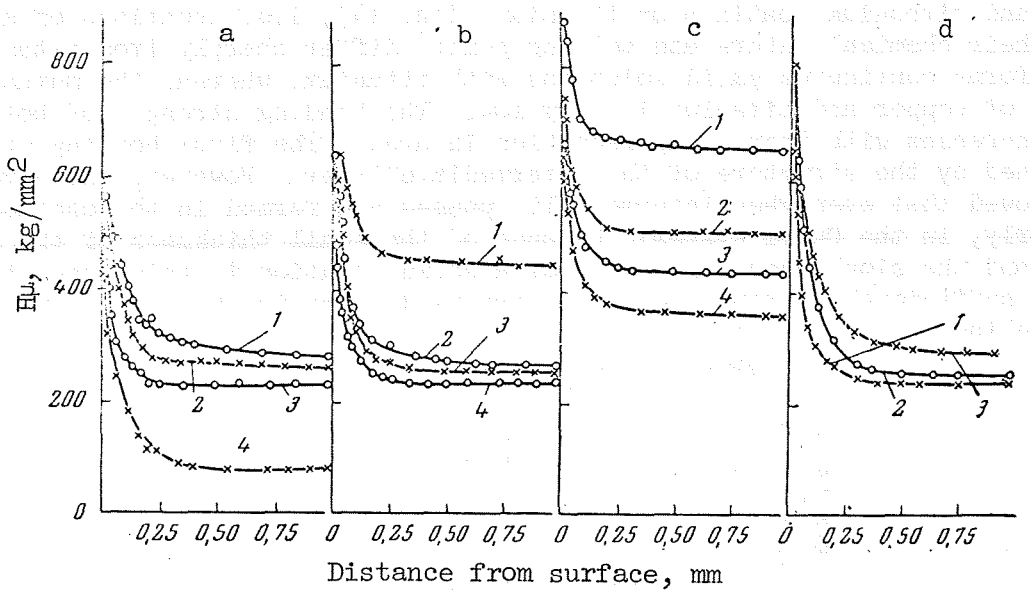

Figure 13. Variation in microhardness (measured with a PMT-3 instrument at a load of 50 g) in the alloys: a, Ti-Ta (1, 10 percent Ta; 2, 5 percent Ta; 3, 1 percent Ta; 4, 0 percent Ta); b, Ti-Pd (1, 0.4 percent Pd; 2, 3 percent Pd; 3, 1 percent Pd; 4, 0.1 percent Pd); c, Ti-Re (1, 3 percent Re; 2, 1 percent Re; 3, 0.5 percent Re; 4, 0.2 percent Re); d, Ti-La (1, 3 percent La; 2, 0.5 percent La; 3, 0.1 percent La).

A more pronounced decrease in the depth of diffusion of gases into the metal is observed when titanium is alloyed with rhenium. It is apparent from the graph that the depth of the diffusion layer decreases with rising concentration, and is less than 0.1 mm at a content of 3 wt percent Re (for iodide titanium, ~0.4 mm). Since it is somewhat difficult to insure a sufficient high-temperature oxidation resistance of the alloys during the alloying, we investigated the possibilities of obtaining protective coatings on titanium and its alloys by cladding, particularly since electrolytic coatings and coatings obtained by diffusional saturation have not produced satisfactory results thus far (refs. 15-18). Such coatings could give protection not only against oxidation but also against the action of oxygen-containing media (refs. 19, 20).

The cladding process was carried out in a vacuum; this not only excluded the formation of oxides and nitrides on the contact surfaces, but also promoted the removal of gases "trapped" by the cladding metal and desorbed at a high temperature. Thus, when the joint deformation of the metal and coating is sufficiently high, forces of atomic interaction arise between the metal and the coating, and high temperatures promote diffusion processes with the formation of a zone of interdiffusion. The investigations showed that in the joining of metals with the same or a different base but a sufficient solubility in the solid state, diffusion welding takes place when the total reduction of area is only 15 percent (ref. 22). This is illustrated by the dependence of the strength of copper and zirconium coatings on titanium (fig. 14), i.e., coatings of metals which in their chemical nature and melting points differ sharply from titanium. Zirconium forms continuous solid solutions with titanium, whereas the mutual solubility of copper and titanium is very low. The bonding strength of both coatings increases with increasing reduction in area. The final bonding strength is determined by the structure of the intermediate layer. However, the investigations showed that even when intermetallic phases are formed in the contact zone (particularly, in the Cu-Ti system), because of the small thickness of the contact zone and the simultaneous presence of a solid solution in this zone, the bonding is sufficiently strong, since it permits deformation and multiple bends without peeling.

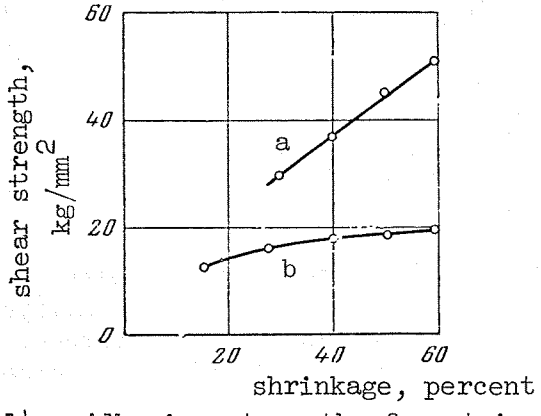

Figure 14. Adhesive strength of certain coatings on titanium versus shrinkage: a, Ti-Zr, rolling temperature, 880°; b, Ti-Cu, rolling temperature, 780°.

Summary

1. When titanium is alloyed in the region of solid solutions, the change in hardness and electrical resistivity at temperatures from -196° to the temperatures of phase transformations is determined by the relative atomic diameters and chemical nature of the alloying elements. Elements with a greater difference in atomic diameters and chemical properties at the same concentrations cause a greater increase in hardness and electrical resistivity.

2. As the temperature is raised, the temperature coefficient of the electrical resistivity of titanium and its alloys increases in magnitude while remaining positive. The decrease in the coefficient of linear expansion of the alloys is more pronounced the higher the concentration of the alloying elements.

3. Alloying elements in concentrations soluble in the α phase with a coefficient of thermal expansion smaller than that of titanium decrease the coefficient of thermal expansion of the alloys, while alloying elements with a coefficient greater than that of titanium increase this coefficient.

4. At thermal cycles encompassing the region of phase transformations, an irreversible change in shape takes place in titanium and its alloys as a result of the relaxation of the stresses arising during the phase transformation.

5. Chromium, tantalum and lanthanum markedly increase the oxidation rate of titanium at 800°. Palladium in small concentrations and rhenium have a favorable effect on the protective properties of the oxide film at this temperature. Rhenium substantially decreases the oxidation and depth of diffusion of the gases into the metal.

REFERENCES

1. Ul'yanov, R. A., Nechiporenko, Ye. P. and Tarsov, N. D. Fizika metallov i metallovedeniye, Vol. 11, No. 3, pp. 461-465, 1961.

2. Ivanov, V. Ye., Kovtun, S. F., Tarasov, N. D. and Ul'yanov, R. A. Tsvetnyye metally, No. 11, pp. 85-89, 1962.

3. Potter, H. H. Proc. Phys. Soc., Vol. 53, No. 300, p. 695, 1941.

4. Wyatt, J. L. J. Metals, Vol. 5, No. 7, p. 903, 1953.

5. Ogden, H. R., Maykuth, D. I., Finlay, W. Z. and Jaffee, R. I. J. Metals, Vol. 3, No. 12, p. 1150, 1951.

6. Savitskiy, Ye. M., Tylkina, M. A. and Zot'yev, Yu. A. Zh. neorg. khim., Vol. 4, No. 3, pp. 702-704, 1959.

7. Savitskiy, Ye. M. and Burkhanov, G. S. Zh. neorg. khim., Vol. 3, No. 11, p. 1609, 1957.

8. Davidenkov, N. N. and Likhachev, V. V. Irreversible Deformation of Metals Subjected to Cyclic Thermal Effects (Neobratimoye formoizmeneniye metallov pri tsiklicheskom teplovom vozdeystvii). Mashgiz (State Scientific and Technical Publishing House of Literature on Machinery), 1962.

9. Akimov, L. M. and Sklyarov, N. M. Heat Resistance of Alloys (Termostoykost' splavov). Coll. of Papers edited by N. M. Sklyarov, GNTI (State Publishing House of Science and Technology), 1962.

10. Revyakin, A. V. Titanium and Its Alloys (Titan i yego splavy). Izd-vo AN SSSR, No. 8, pp. 175-189, 191-205, 1962.

11. Kornilov, I. I. Khimicheskaya nauka i promyshlennost', Vol. 3, No. 8, p. 6, 1958.

12. Jenkis, A. E. J. Inst. Metals, Vol. 82, No. 5, p. 213-221, 1954.

13. Savitskiy, Ye. M. and Tylkina, M. A. Zh. neorg. khim., Vol. 3, No. 3, p. 820, 1958.

14. Savitskiy, Ye. M., Tylkina, M. A. and Tsiganova, I. A. Izv. AN SSSR, OTN, No. 3, p. 96, 1958.

15. Leyner, V. I. Electroplating of Light Alloys (Gal'vanicheskiye pokrytiya legkikh splavov). Metallurgizdat, 1959.

16. Smolenskaya, G. N., Kudryavtsev, N. T. and Karantayev, V. M. Metallovedeniye i termicheskaya obrabotka metallov, No. 11, p. 42, 1960.

17. Anitov, I. S. and Maksimova, A. G. Zh. prikl. khim., No. 12, p. 2724, 1960.

18. Stroyev, A. S. and Novikova, Ye. N. Titanium and Its Alloys (Titan i yego splavy). Izd-vo AN SSSR, pp. 107-113, 1958.

19. Borisova, Ye. A. and Bogdanov, K. V. Metallovedeniye i termicheskaya obrabotka metallov, No. 2, pp. 37-40, 1963.

20. I. B. Rittenhouse. Trans. ASM, Vol. 51, No. 871-895, 1959.

21. Kovtun, S. F. and Tarasov, N. D. Avt. svid. SSSR, No. 111925, 5 August 1957.

22. Ul'yanov, R. A., Tarasov, N. D. and Kovtun, S. F. Tsvetnyye metally, No. 3, pp. 74-76, 1953.

DETERMINATION OF THE CHARACTERISTICS OF THE INTERDIFFUSION OF TITANIUM AND MOLYBDENUM FROM THE ATTENUATION OF γ RADIATION

A. Ya. Shinyayev, V. O. Akopyan, L. F. Sokiryanskiy
and I. V. Bogolyubova

The study of the interdiffusion of titanium and molybdenum is of great theoretical interest, since these metals differ strongly in physical properties, and this may substantially affect the diffusion process. Furthermore, the study of this problem is of great practical interest. In reference 1 it was shown that in order to obtain a good adhesion between a molybdenum coating and titanium and its alloys, the formation of diffusion layers is necessary between the base metal and the coating, and the bonding strength is directly related to the thickness and structure of these layers. For this reason, a rational selection of the temperature conditions for applying the coating (this insures the creation of a diffusion zone of definite thickness) and the knowledge of the characteristics of the structure of the diffusion zone made it necessary to study the rate of interdiffusion between titanium and molybdenum. The material used to prepare the samples was titanium obtained from titanium sponge TG00 by double fusion in a vacuum electric arc furnace with the use of a consumable electrode and cast molybdenum. After preliminary stripping, titanium rods 18 mm in diameter were subjected to homogenizing annealing for 6 hrs at 1250°. The annealed rods were used to prepare samples in the shape of beakers; a molybdenum plug 8 mm in diameter and 12 mm long was pressed into the opening of these samples. Prior to the pressing, the samples were degreased in benzene or carbon tetrachloride. The homogenizing of the samples was carried out in a vacuum at temperatures of 905, 1005, 1100, 1111 and 1210° with a holding time of 7-240 hrs.

At the first stage of the experiments, in order to study the interdiffusion between titanium and molybdenum, the microhardness was measured and the microstructure of the diffusion layers was examined. However, these methods did not permit the determination of the extent of the diffusion zone. The values of the microhardness associated with a change in the concentration of the titanium and molybdenum components differ only slightly, so that practically no diffusion zone is observed. The diffusion zone of Ti-Mo does not show up in the microstructural analysis either.

In the present work, in order to determine the concentration of titanium and molybdenum in the diffusion zone, use was made of a new method based on the principle of attenuation of the intensity of a narrow beam (10-15 μ wide) of γ

radiation passing through various microsections of the zone. Details of this method and certain features of the apparatus used to perform the analysis of the diffusion zone are described in reference 2.

In order to study the diffusion layers by this method, plates 1.5-2.0 mm thick were cut from the annealed specimens and reduced to a thickness of 75-150 μ by plane-parallel grinding. The specimen was mounted on a special base connected to a series of micrometer screws parallel to the working slit emitting a beam of radioactive radiation. The device was used to determine the curves of the attenuation of γ ray intensity in passing from molybdenum to titanium over the entire diffusion zone every 5 μ. Let us examine a typical curve for a specimen annealed at 1100° for 40 hrs (fig. 1). It is apparent from the figure that in passing from titanium to molybdenum, the radiation intensity changes by a factor of no less than 15. This makes it possible to carry out the analysis for the content of titanium and molybdenum in each segment of the zone with great precision.

The relation between the degree of absorption of γ radiation, given by the ratio of the intensity of γ radiation which has traversed the section of the specimen under consideration to the original intensity of the incident radiation, and the concentrations of the components of the binary system may be derived from the following system of equations:

$$\left.\begin{aligned} \frac{\mu(x)}{\rho(x)} &= p_1(x)\frac{\mu_1}{\rho_1} + p_2(x)\frac{\mu_2}{\rho_2}, \\ \rho(x) &= p_1(x)\rho_1 + p_2(x)\rho_2, \\ p_1(x) + p_2(x) &= 1, \\ \mu(x) &= \mu_1 - \frac{1}{b}\ln\frac{I(x)}{I_1}, \\ c_1(x) &= 200\frac{p_1(x)}{1 + p_1(x)}, \end{aligned}\right\} \qquad (1)$$

where μ is the linear absorption coefficient, cm^{-1}; ρ is the density, g/cm^3; p is the weight fraction of the component; c is the concentration of the component, at. percent; I is the counting rate, cpm; b is the thickness of the specimen, cm; x is the position of the microsection being analyzed relative to the diffusion zone.

Subscripts 1 and 2 pertain to pure titanium and molybdenum, respectively.

By solving system (1) with respect to the concentration $c_1(x)$ after substituting the values of the absorption coefficients μ and density of the components ρ (μ_{Ti} = 94 cm^{-1}; μ_{Mo} = 355 cm^{-1}; ρ_{Ti} = 4.505 g/cm^3; ρ_{Mo} = 10.22 g/cm^3) we obtain the following equation for determining the titanium concentration as

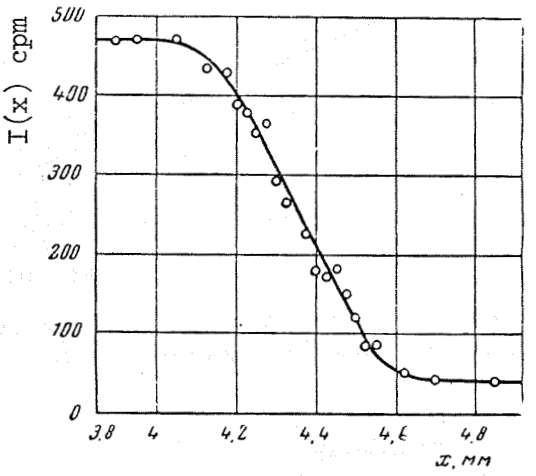

Figure 1. Change in the intensity of γ radiation passing through the diffusion zone from titanium to molybdenum.

a function of the intensity of the radiation passing through each segment of the specimen whose position is given by the coordinate x:

$$c_{\mathrm{Ti}}(x) = 200\,\frac{19.11 - \sqrt{104.2 - \frac{1}{b}\ln\frac{I(x)}{I_{\mathrm{Ti}}}}}{28.01 - \sqrt{104.2 - \frac{1}{b}\ln\frac{I(x)}{I_{\mathrm{Ti}}}}}. \qquad (2)$$

A nomogram (fig. 2) for use in the calculations was constructed on the basis of this equation.

The results of the measurement of the titanium concentration (the molybdenum concentration was the balance adding up to 100 percent) in all the investigated specimens were expressed as the graphical dependence of this concentration on the distance in the diffusion zone. As an example, a curve of this type is illustrated for a specimen annealed for 40 hrs at 1100° (fig. 3).

From the data obtained for the distribution of the diffusing elements, one can calculate the coefficients of interdiffusion from the familiar Boltzmann formula

$$D_{\mathrm{inter}} = \frac{1}{2\tau}\frac{dx}{dc}\int_0^c x\,dc. \qquad (3)$$

The Matano graphical method usually employed in such calculations is very cumbersome and has some important disadvantages. This method is applicable only

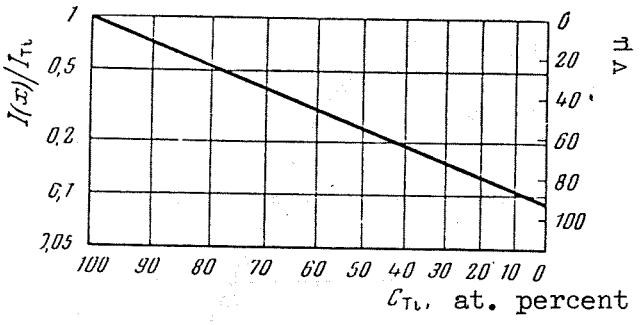

Figure 2. Nomograph for determining the concentration of the components from the absorption of γ radiation.

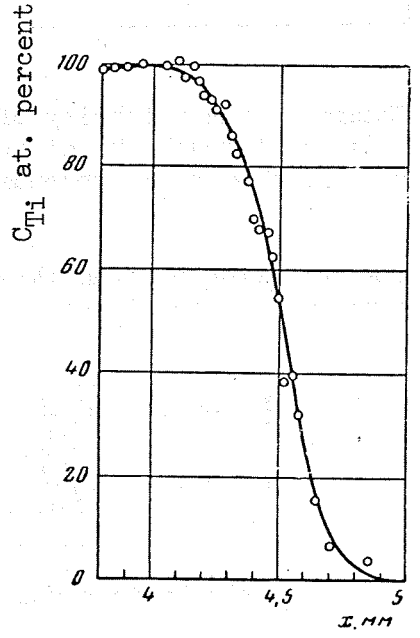

Figure 3. Distribution of the concentration of the component and the diffusion zone.

to the complete curve of concentration versus depth of penetration of the components. The plotting of such a curve involves considerable experimental difficulties. Thus, at a specimen thickness of over 100 μ, the γ radiation is attenuated very strongly in the molybdenum portion of the specimen, resulting in a sharp decrease in the sensitivity of the method, while at a specimen thickness of approximately 140 μ, the γ radiation is almost completely absorbed by the specimens. At the same time, specimens 100-150 μ thick are fully adequate for the establishment of a distribution of the components in the titanium portion of the diffusion zone. However, it does not seem possible to calculate graphically the values of the diffusion constants in the titanium region alone in this case. Furthermore, the graphical method has another serious drawback: its precision at the end segments of the diffusion zone on both sides decreases sharply owing to a large error in the graphical differentiation.

In order to avoid these drawbacks in the calculation of the diffusion constants, use is made in the present work of an analytical method of calculation based on a linearization of the experimental concentration curve in a probability grid (ref. 4). The concentration curve taken from figure 3 is shown in this grid (fig. 4).

The concentration scale corresponds to the equation

$$c_{\mathrm{Ti}}(x) = \frac{100}{\sqrt{\pi}} \int_{-\infty}^{u} \exp(-z^2)\, dz. \tag{4}$$

Along the vertical on the right side of figure 4 is given the scale of arguments of the probability integral u. The distance from the cross section under consideration to the initial boundary of Ti-Mo is plotted along the abscissa. The initial position of the phase boundary was determined from experiments with inert marks and controlled by observing the changes in the thickness of the molybdenum coating in the course of the homogenizing. For all the experiments considered, the concentration dependences in the probability grid consisted of segments of straight lines having a common initial ordinate k and slopes h_1 and h_2 respectively for the titanium [$c_1(x) > 50$ percent] and molybdenum [$c_2(x) < 50$ percent] sections of the diffusion zone. Using equation (4) and the linearization condition of the segments of the component distribution curve, which can be written in the form of the equation

$$u = hx + k, \tag{5}$$

one can readily obtain, from expression (3), a formula for the calculation of the interdiffusion coefficients:

$$D_{\mathrm{inter}} = \frac{1}{4h^2\tau}\left[1 + k\sqrt{\pi}\,\varphi(c)\right], \tag{6}$$

where

$$\varphi(c) = \frac{2}{\sqrt{\pi}} \exp(u^2) \int_{-\infty}^{u} \exp(-u^2)\, du.$$

The function $\varphi(c)$ takes into account the dependence of the interdiffusion coefficient on the concentration of the components (fig. 5).

Results of calculations of interdiffusion coefficients[1] (fig. 6) showed that at concentrations of 50-90 at. percent Ti, the interdiffusion coefficient

---

[1] L. G. Maksimova took part in the calculations.

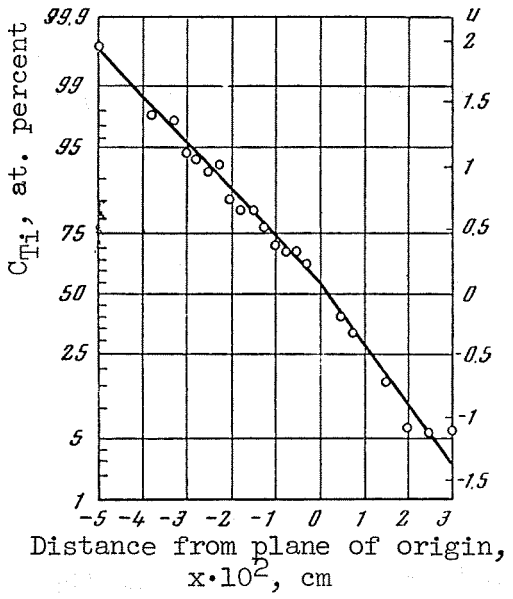

Figure 4. Distribution of the concentration of the components in the probability grid.

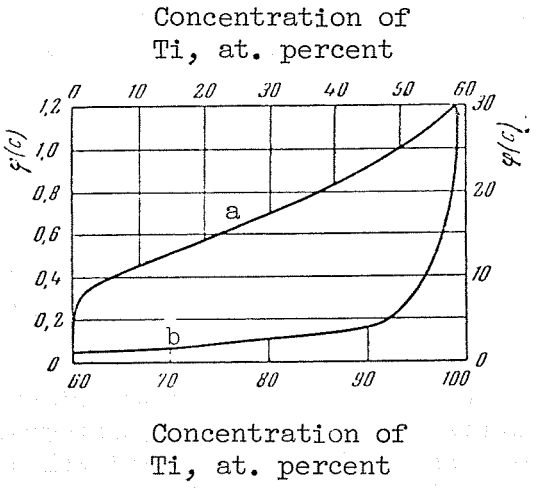

Figure 5. Function φ (c) versus concentration: a, molybdenum region; b, titanium region.

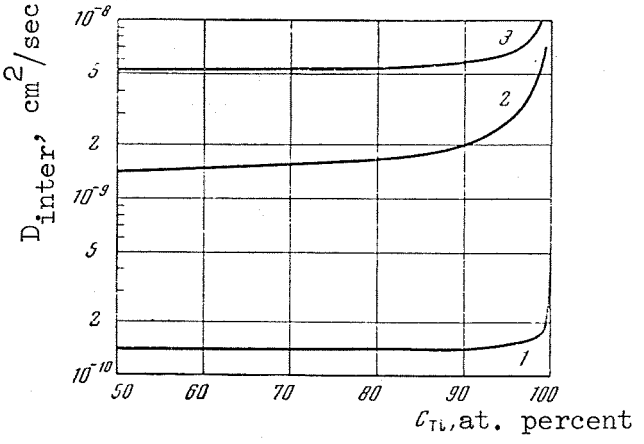

Figure 6. Coefficient of interdiffusion versus concentration of components for the titanium region: 1, at 905°; 2, at 1100°; 3, at 1210°.

D_{inter} remains practically constant for the given temperature. Only at concentrations of 90-98 at. percent Ti is an appreciable increase observed in D_{inter}.

In the molybdenum region (100-150 percent Mo), the value of D_{inter} is independent of the molybdenum concentration. Results of a determination of D_{inter}

values and of the width of the diffusion zone for the annealing modes investigated are shown in the table.

In calculating the values of D_{inter} by the analytical method one should keep in mind that in the vicinity of 50 percent the value of D_{inter} shows a discontinuity because the curve representing the distribution of elements in the diffusion zone is approximated by two segments of straight lines in the probability grid. That is why the analytical method in the vicinity of 50 percent gives a less accurate result than the Matano method. However, the analytical method gives accurate values of D_{inter} at the ends of the diffusion zone, where the Matano method is practically impossible to apply. Therefore, in a more detailed study of interdiffusion, the use of both methods is recommended, since they supplement each other.

As was indicated above, the energy of the γ radiation which we used made it possible to determine fairly accurately the values of D_{inter} in the titanium region. Here the accuracy of the measurement of D_{inter} was 20-30 percent. The parameters of the diffusion process in the Arrhenius equation--activation energy E_{inter} and value of the preexponential factor--were determined from the slope of the straight line in the coordinates $\ln D_{inter}$--1/T (fig. 7).

The value of E_{inter} obtained was found to be 41 kcal/mole, $D_0 \approx 5.6 \cdot 10^{-3}$ cm^2/sec.

DIFFUSION CHARACTERISTICS UNDER VARIOUS ANNEALING CONDITIONS FOR THE SYSTEM Ti-Mo.

Temperature, °C	Time, hr	Total depth of diffusion zone, mm	Coefficient of interdiffusion, cm^2/sec	
			Titanium region	Molybdenum region
905	239.5	0.47	$1.5 \cdot 10^{-10}$	--
1100	40	0.91	$1.58 \cdot 10^{-9}$	$7.5 \cdot 10^{-10}$
1111	21	0.52	$1.6 \cdot 10^{-9}$	$1.9 \cdot 10^{-9}$
1210	7.3	1.60	$5.5 \cdot 10^{-9}$	$2.8 \cdot 10^{-8}$

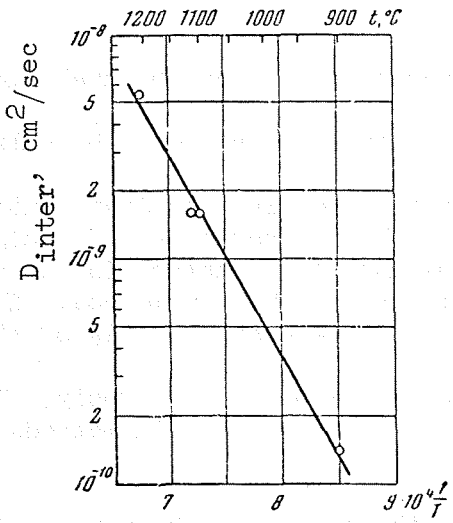

Figure 7. Coefficients of interdiffusion versus temperature for the titanium region.

From these characteristics, using the equation of the temperature dependence of the diffusion coefficient $D_{inter} = D_0 e^{-\frac{E}{RT}}$, one can determine the value of D_{inter} for any temperature in the β region.

In the molybdenum region, the density of the radiation passing through the specimen decreased sharply, making it difficult to obtain the necessary light statistics. For this reason, the accuracy of the measurement of D_{inter} in this region was considerably lower. It was found that in the molybdenum region, the activation energy was considerably greater than in the titanium region. A more accurate analysis of this part of the diffusion zone requires γ radiation of 0.1-0.3 MeV energy. However, in this case the sensitivity of the analysis of the titanium region decreases.

The interdiffusion between titanium and molybdenum at molybdenum concentrations up to 8 at. percent was studied earlier in reference 5. The results which we obtained at low molybdenum concentrations are in good agreement with the data of this work.

In conclusion, the authors express their appreciation to Prof. S. S. Mozhayev for his cooperation in the execution of the computational part of this work.

REFERENCES

1. Tour, S., Styka, A. and Fischer, G. J. Metals, Vol. 7, No. 2, p. 291, 1955.

2. Shinyayen, A. Ya., Bondarev, V. V. and Sergeyeva, Ye. V. This Collection, p. 320. J.P.R.S. Translation No. 28,176; TT:65-30080, pp. 63-69.

3. Matano, C. Japan J. Phys., Vol. 8, p. 109, 1933.

4. Holl, L. D. J. Chem. Phys., Vol. 21, p. 87, 1953.

5. Goold, B. J. Inst. Metals, Vol. 88, p.444, 1960.

PART II. INTERACTION OF TITANIUM WITH GASES AND THE CORROSION PROPERTIES OF ALLOYS

ON THE REDISTRIBUTION OF IMPURITIES IN TITANIUM AND ITS ALLOYS DURING OXIDATION

N. V. Korolev, S. A. Gorbunov, A. S. Bogdanov and G. P. Nadutenko

In addition to alloying elements, titanium alloys contain impurity elements whose quantity depends on the method of preparation and grade of the titanium sponge. The purest semifinished product used for melting titanium alloys - sponge TG00 obtained by the magnesiothermic method - contains about 0.50% of impurity elements.

Harmful elements which markedly reduce the mechanical characteristics of alloys are oxygen, nitrogen, and carbon. These elements form interstitial solid solutions with titanium and, even when present in extremely small amounts (hundredths and thousandths of one percent) have a harmful effect on a plastic metal, changing it into a brittle substance. In addition to the indicated elements, undesirable impurities also include silicon, iron and hydrogen.

The alloys are strongly oxidized in various metallurgical processes (rolling, forging, heat treatment, etc.).

The oxidized surface of the specimen is covered with a scale under which there is formed a so-called gas-saturated layer which is basically a solid solution of oxygen in titanium.

On the basis of thermodynamic calculations made in order to establish the possibility of formation of oxides of impurity elements and titanium, one could expect carbon, nitrogen and iron to accumulate in the surface layer of the metal as the oxidation time increased.

The present work was devoted to verifying the possibility of redistributing the impurity elements between the surface layers of the bulk of the titanium specimen in the course of oxidation in air.

Materials and Method

The study was carried out on specimens (20 x 20 x 20 mm) of technically pure titanium VT1 and some titanium alloys melted with TG0 sponge.

According to TsMTU (Tekhnicheskiye usloviya tsvetnoy metallurgii - Specifications for nonferrous metallurgy) 4732-56, the chemical composition of the VT1

alloy should be as follows: base, Ti; 0.3% Fe; 0.15% Si; 0.1% C; 0.15% O_2; 0.015% H_2; 0.05% N_2; 0.06% Cl.

In addition to these elements, a certain amount of calcium and magnesium (of the order of 0.01-0.02%) and up to 0.30-0.40% Al were observed in the alloy VT1.

The samples to be tested were oxidized in undried laboratory air in a periodic weighing unit at temperatures of 800-1200°. The temperature was controlled within ±5°. After oxidation followed by cooling in air, the scale was removed from the specimens, and the latter were used to prepare transverse polished sections for the purpose of studying the distribution of microhardness over the depth of the gas-saturated layer. The microhardness was measured with a PMT-3 instrument (at a load of 50 g).

The emission spectral analysis and in some cases local analysis of the specimens were carried out with an instrument described in ref. 1. The analysis was performed in a straight pulsed spark with the following parameters of the unit: capacity of the working condenser 0.01 μF; charge current of the working condenser 8.0 mA; auxiliary gap 1.50 mm; analytical gap 0.75 mm. In the determination of nitrogen, use was made of a spark burning in a stream of pure argon No. 1 (0.02% O_2; 0.17% N_2; 0.01% CO_2). To this end, a chamber was prepared which was mounted on the rim of the objective of the microscope and which made it possible to blow a uniform stream of argon onto the section under analysis. Microelectrodes 0.20 mm thick were made out of electrolytic copper M0. The duration of the exposure for the determination of iron, silicon, carbon and magnesium was 1 min, and for the determination of aluminum, calcium and nitrogen, 5 sec. The following lines were selected for the analytical tests: iron 2755.737 II Å, silicon 2881.578 I Å, aluminum 3961.527 I Å, calcium 3968.468 II Å, carbon 2296.89 III Å, magnesium 2795.53 II Å, nitrogen 3994.995 II Å.

The standards used for the quantitative comparison were specimens of the original alloys subjected to oxidation, titanium nitride and carbide, alloy with 0.2% C, and alloys of titanium with 1.5% Fe, Si and Al. The content of the elements in the standards was checked by chemical analysis.

After a photometric analysis of the plates, the relative intensity of the spectral lines of the impurity element was determined with respect to the lines of titanium by means of the formulas

$$I_x = 10^{\frac{\Delta S_{x-\Phi}}{\gamma}} - 1,$$

$$I_{Ti} = 10^{\frac{\Delta S_{Ti-\Phi}}{\gamma}} - 1,$$

where I_X and I_{Ti} are the line intensities of the element being analyzed and of titanium; $\Delta S_{X-\Phi}$ and $\Delta S_{Ti-\Phi}$ is the difference in blackening between the lines of the impurity element or titanium and the background.

The quantitative content of the elements was calculated from the formula

$$\frac{c_x}{c_{Ti}} = \left(\frac{c_x}{c_{Ti}}\right)_{st} \cdot \frac{I_x/I_{Ti}}{(I_x/I_{Ti})_{st}},$$

where c_x/c_{Ti} and $(c_x/c_{Ti})_{st}$ is the ratio of the amount of the impurity element to the amount of titanium in the alloy and standard, respectively; I_x/I_{Ti} and $(I_x/I_{Ti})_{st}$ is the ratio of the intensities of the element being determined to the line of titanium in the alloy and in the standard, respectively.

In the calculations of the amount of nitrogen, account was also taken of the nitrogen present in technical argon. When no standards were available for certain elements, the change in the amount of the impurity on the surface of the specimen as compared to the readings for the unoxidized surface at the center of the transverse polished section was estimated from the difference in the ratio of the intensities of the element being determined to the titanium on the oxidized surface and at the center of the section.

Results

The results of spectral analysis for impurity elements on the outside surface of gas-saturated layers in specimens oxidized at 800-1200° are shown in the table below. The depth of the investigated layer was 10-15 μ. According to the data of the table, the surface gas-saturated layer on specimens oxidized at

Testing temperature °C	Duration of tests, hr	Chemical composition, %				
		N	C	Al	Fe	Si
1200	0.05	0.0	0.04	--	--	--
1200	0.10	0.5	0.02	--	--	--
1200	0.20	0.7	0.04	--	--	--
1200	0.50	3.6	0.12	--	--	--
1200	1	3.3	0.65	0.50	0.20	1.64
1200	4	1.7	1.16	0.71	0.65	0.66
1100	4	3.5	--	0.50	0.20	0.12
1100	8	1.7	0.3	0.50	0.12	--
1100	16	3.5	0.35	0.40	0.12	0.12
1000	8	0.0	0.04	0.30	0.04	0.16
1000	16	0.0	0.06	0.52	0.02	0.18
900	8	0.0	0.05	0.36	0.06	0.16
900	16	0.0	0.06	0.26	0.10	0.02
800	8	0.0	0.1	0.50	0.30	0.16
800	96	0.0	0.14	0.30	0.04	0.02

Note. Sensitivity of determination: nitrogen, 0.3%; carbon and iron, 0.03%; aluminum, 0.1%; silicon, 0.05%.

1100-1200° has a high nitrogen content (up to 3%) and carbon content (up to 1%). It is characteristic that the highest quantity of nitrogen was observed during the initial period of the oxidation.

Fig. 1 shows the temperature dependence of the free energy of formation of oxides of the impurity elements and of titanium, titanium nitride, and titanium carbide, calculated from literature data (refs. 2, 3). The values of the thermodynamic characteristics lead one to expect an accumulation of nitrogen and carbon in the surface layer because the change ΔF° for titanium oxides has a much

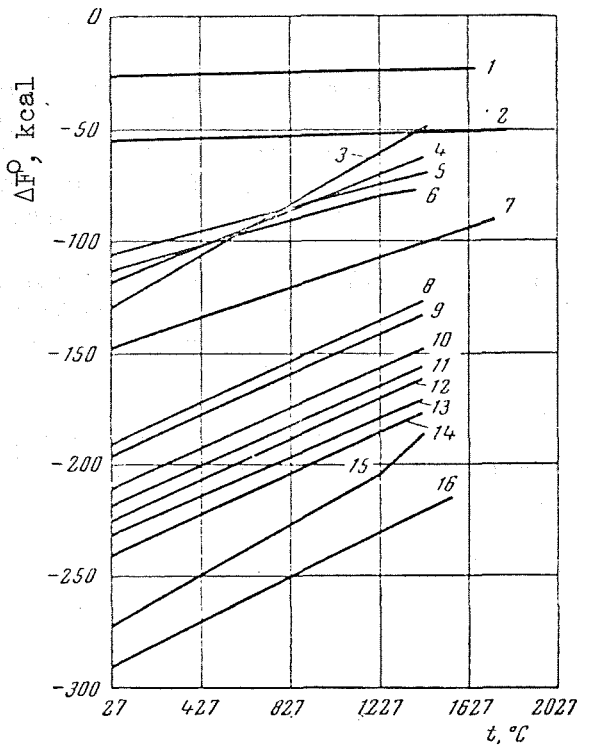

Figure 1. Free energy of formation of some compounds of titanium and impurity elements versus temperature (based on 1 g/mole O_2).

1--SiC; 2--TiC; 3--$1/2Fe_3O_4$; 4--$2/3Fe_2O_3$; 5--2FeO; 6--2SnO; 7--2TiN; 8--2SiO; 9--SiO_2; 10--TiO_2; 11--$2/5Ti_3O_5$; 12--$2/3Ti_2O_3$; 13--2TiO; 14--$2/3Al_2O_3$; 15--2MgO; 16--2CaO.

more negative value than for titanium nitride and carbide. The thicker the oxide film, the more of these elements should be present in the external layer of the metal, since they should not penetrate into the scale. However, the calculated amount of nitrogen was much less than the experimental value. To elucidate

this question, special experiments were set up for the simultaneous oxidation of a titanium specimen at temperatures of 1000-1200°. During the initial period of oxidation (from 3 min to 1 hr) it was found that during the same testing time, the oxide layer at the spot where the temperature was 1200° had a smaller thickness than at 1000°.

The corresponding calculations of the possibility of accumulation of nitrogen during this testing time and the obtained experimental data lead to the conclusion that the principal cause of enrichment with nitrogen is the reaction of titanium with the nitrogen of air, which takes place largely during the initial period of the oxidation.

The high carbon content in the surface layer of the metal is due not only to the thermodynamically possible accumulation, but probably also to the reaction of titanium with the carbon dioxide present in air.

Measurement of microhardness on transverse and oblique polished sections prepared from specimens oxidized at 1100-1200° gave very high values (1700-2350 kg/mm^2) in the metal layer adjacent to the scale. A comparison of these values with the microhardness of α-Ti having the maximum oxygen content of 12.8 wt % O_2 (1250-2350 kg/mm^2) and with the microhardness of titanium carbide (2850 kg/mm^2) and titanium nitride (1782 kg/mm^2) confirms the presence of nitrogen and carbon in the solid solution of α-Ti. The depth of the layer with the high microhardness did not exceed 10-15 μ in specimens oxidized for 4 hours at 1100-1200°.

Let us examine the pattern of distribution of the microhardness in specimens of technically pure titanium oxidized at 1100-1200° (fig. 2).

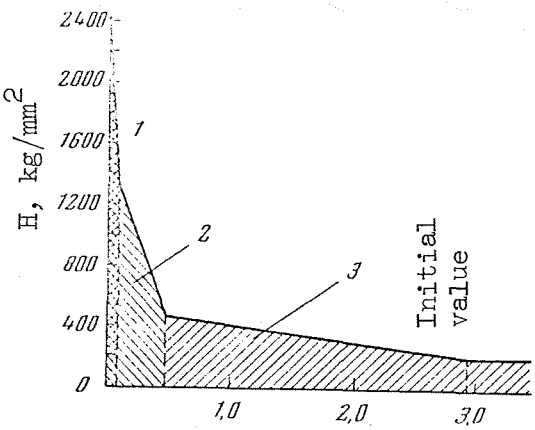

Figure 2. Diagram of the distribution of microhardness in samples of alloy VT1 oxidized at 1100-1200°.

1--Carbonitride layer saturated with oxygen; 2--α-Ti; 3--transformed β-Ti.

The gas-saturated layer formed is made up of three parts. The first part consists of an oxygen-saturated carbonitride layer with a hardness of 1350-2350 kg/mm^2, the second part of α-Ti with a microhardness up to 400-500 kg/mm^2, and in the third part, the structure is that of transformed β-Ti with a maximum hardness of 400-500 kg/mm^2, which corresponds to the maximum solubility of oxygen in β-Ti (4.0-5.0 wt % O^2)[1].

In 1952, on the basis of precise x-ray diffraction analyses of titanium scale obtained in air, V. I. Arkhanov and G. P. Luchkin postulated that the defect structure of titanium dioxide arises because trivalent nitrogen ions participate in the process of its formation. A consequence of the defect structure of the scale was a greater oxidizability of titanium at temperatures above 1100° in air than in oxygen. The investigation performed is the first experimental confirmation of this hypothesis concerning the participation of nitrogen in the process of oxidation of titanium in air, since the high quantity of nitrogen in the metal proves the penetration of nitrogen through the scale and the possibility of the creation of an anomaly in the structure of rutile.

After the oxidation, aluminum and iron accumulate in the surface layer at 1100-1200°, whereas an increase in the silicon content was noted only at 1200°. The amount of aluminum and silicon at temperatures of 800-1000° is approximately the same as in the initial alloy; the content of iron at 900-1000° changes somewhat. The accumulation of iron and silicon at high temperatures may be explained by the drastic conditions of formation of the corresponding oxides, and an important part is probably played by kinetic factors in the process of enrichment of the metal surface with aluminum. Calcium and magnesium can reduce all the titanium oxides (see fig. 1) and hence, should be the first to penetrate into the scale. This is confirmed by spectral analysis. At 900-1200°, no increase in the content of calcium and magnesium was observed on the surface of the metal. After testing at 800°, the content of these elements on the titanium surface was 2-3 times their amount in the alloy prior to the oxidation. Apparently, at 800° there takes place an appreciable diffusion of magnesium and calcium ions toward the metal-scale boundary, and their penetration into the scale is difficult. At higher temperatures, this barrier is removed as a result of the greater mobility of the atoms.

Thus, the surface layer on specimens oxidized at 1100-1200° is a interstitial solid solution of oxygen, nitrogen, and carbon, also enriched with aluminum and iron, and at 1200° with silicon. In addition to oxygen, the presence in the surface layer of other elements, primarily nitrogen and carbon, does not permit us to estimate the amount of oxygen from the change in the parameter c of the hexagonal lattice, since these elements also change the lattice parameters. Thus, data on the change in parameter c with the quantity of oxygen present in titanium, obtained in ref. 5, cannot be used under equilibrium annealing conditions to determine the amount of oxygen absorbed by the titanium from parameter

---

[1]The problem of gas-saturated layers is discussed in more detail in an article by S. A. Gorbunov and I. S. Anitov in the collection "Titanium and Its Alloys," No. 10, Izd-vo AN SSSR, 1963, p. 100.

c, not only for the oxidation of the specimens in air, but also for the oxidation in oxygen because of the redistribution of the impurity elements. In the various operations of thermal treatment and welding of titanium and its alloys, it is necessary to take into account the possibility of redistribution of the elements both on heating in air and in vacuum, where the vaporization of different elements takes place at different rates.

The results obtained for the redistribution of the impurity elements were also confirmed by studying certain titanium alloys.

An interesting feature encountered in the work was the nonuniformity of the distribution of the impurity elements not only in different melts but also in a single melt from one specimen to another. Thus, for example, the amount of calcium and magnesium in certain specimens was 5-6 times the average content. In some melts of technically pure titanium VT1, aluminum was detected in amounts of 0.3-0.4%, although according to the GOST (Gosudarstvennyy obshchesoyuznyy standart - All-Union State Standard) no aluminum whatever should be present in this alloy. The nonuniformity in the content of the impurity elements in titanium and its alloys may be the cause of the great scatter in the mechanical properties.

In the course of the investigation, the contamination of certain alloys with alloying elements not listed in the certificate of the alloy was established. For example, a small amount of tin or chromium was detected in certain

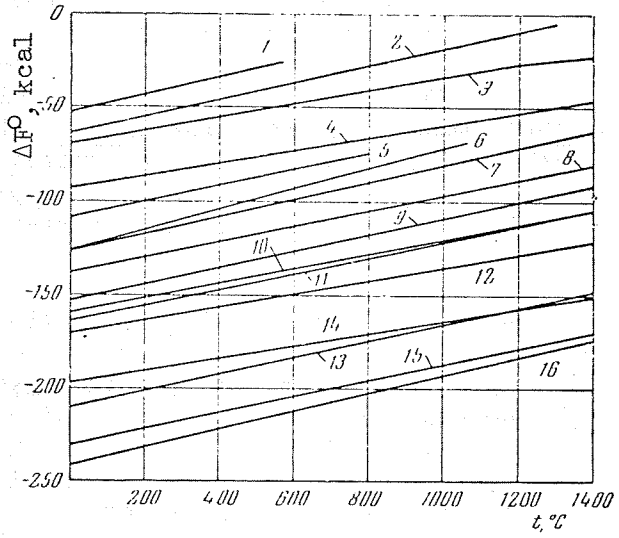

Figure 3. Temperature dependence of free energy of formation for oxides of alloying elements and titanium (based on 1 g/mole O_2).

1--$2V_2O_5$; 2--2CuO; 3--$2Cu_2O$; 4--VO_2; 5--2/3 MoO_3; 6--2SnO; 7--SnO_2; 8--2/3 Mn_2O_3; 9--1/2 Mn_3O_4; 10--2/3 Cr_2O_3; 11--2/3 V_2O_3; 12--2MnO; 13--TiO_2; 14--2VO; 15--2TiO; 16--2/3 Al_2O_3.

specimens of alloy VT1. When alloying elements are present in an alloy, their redistribution is possible, just as in the case of the impurity elements.

Let us examine the temperature dependence of the free energy of formation of oxides of a series of alloying elements and titanium (fig. 3). Molybdenum, vanadium, chromium, iron, manganese, tin, silicon, nickel, and copper, which have more positive values of the change in free energy of formation of the corresponding oxides than titanium oxides, can accumulate in the surface layer at the metal-scale boundary. However, an important part in the oxidation process should be played by kinetic factors as well (for example, the vaporization of volatile oxides, etc.). Results of spectral analysis following oxidation in air of the binary alloys Ti - Mo, Ti - V, Ti - Cr, Ti - Mn, Ti - Sn, Ti - Cu, containing up to 10% of alloying elements have shown that the surface layer of the metal becomes enriched with these elements. For example, at certain temperatures, the amount of molybdenum, vanadium, and chromium on the surface of the metal exceeds the initial content by a factor of 2-3, and nearly pure tin and copper are formed on the surface of the alloys with tin and copper.

Summary

1. The article examined the problems of redistribution of carbon, nitrogen, iron, aluminum, silicon, calcium, and magnesium between the surface layers and bulk of titanium specimens after heating in air at 800-1200°.

2. Spectral analysis and microhardness measurements established that the gas-saturated layer on specimens of titanium oxidized in air at 1100-1200° consists of an interstitial solid solution of not only oxygen but also carbon (up to 1.0%) and nitrogen (up to 3.0%); in addition, the surface layer becomes saturated to some extent with iron, chromium, and aluminum.

3. The study showed that at 1100-1200° the increase in the content of nitrogen in the surface layers is due mainly to a reaction of titanium with the nitrogen of air.

4. Thermodynamic calculations of the temperature dependence of the free energy of formation of oxides of impurity and alloying elements confirmed the possibility of redistribution of these elements in the course of the oxidation.

5. It was established that the gas-saturated layer becomes enriched with the alloying elements following oxidation in air of the following binary alloys: Ti - Mo, Ti - V, Ti - Cr, Ti - Mn, Ti - Sn, Ti - Cu.

REFERENCES

1. Genkin, A. D. and Korolev, N. V. Geologiya Rudnykh Mestorozhdeniy, No. 5, p. 64, 1961.

2. Yesin, O. A. and Gel d, P. V., Physical Chemistry of Pyrometallurgical Processes (Fizicheskaya khimiya pirometallurgicheskikh protsessov), Pt. 1, Metallurgizdat, 1962.

3. Kubaschewski, O. and Evans, E. Thermochemistry in Metallurgy. IL, 1955.

4. Arkharov, V. I. and Luchkin, G. P. Dokl. AN SSSR, Vol. 83, No. 6, p. 837, 1952.

5. Bumps, E. S., Kessler, H. A., and Hausen, M. Trans. ASM, Vol. 45, p. 1008, 1953.

6. Yeremenko, V. N. In: "Titanium and Its Alloys" (Titan i yego splavy), Izd-vo AN USSR, Kiev, 1960.

7. Gerasimov, Ya. I., Kystovnikov, A. N., and Shakhov, A. S. Chemical Thermodynamics in Nonferrous Metallurgy (Khimicheskaya termodinamika v tsvetnoy metallurgii). Metallurgizdat, Vol. 1, 1960; Vol. 2, 1961; Vol. 3, 1963.

EFFECT OF OXYGEN ON THE MECHANICAL PROPERTIES OF HEAT-TREATED ALLOYS AT3 AND AT8

B. K. Vul'f and S. A. Yudina

(Preliminary Report)

According to the diagram of Ti-O (ref. 1), oxygen raises the temperatures of the $\alpha \rightarrow \beta$ phase transformation, particularly the critical points of the transition into the β region (fig. 1) and hence, is an α stabilizer. By forming interstitial solid solutions with titanium, oxygen increases the lattice constant c of the α solution, having practically no effect on constant a. As a result of the resulting complication of the lattice structure, the stresses causing plastic deformation of the α solution are increased, and this may explain the observed hardening effect.

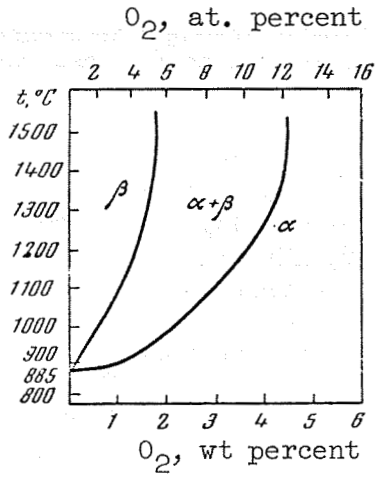

Figure 1. Effect of oxygen on the polymorphic transformation of titanium (ref. 1).

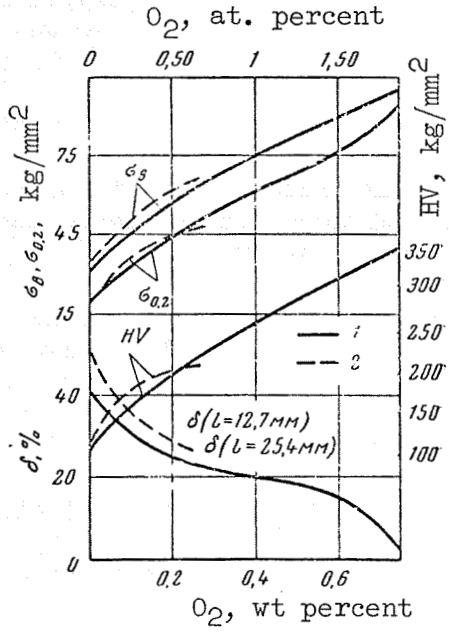

Figure 2. Effect of oxygen on the mechanical characteristics of titanium.

1--data of ref. 2;
2--data of ref. 3.

The effect of oxygen on the mechanical properties of titanium and its alloys has been studied by several authors. Thus, it was shown in ref. 1 that a rise in oxygen content from 0.2 to 13 wt % increases the hardness of titanium from HV = 170 kg/mm^2 to HV = 950-1100 kg/mm^2.

A diagram showing the effect of oxygen on the mechanical properties of titanium, plotted on the basis of the data given in refs. 2 and 3, shows that as the oxygen content rises, the strength of the specimens increases, while the elongation decreases somewhat (fig. 2).

It has been pointed out in many papers that oxygen increases the sensitivity of titanium to notching and appreciably decreases its impact strength.

Oxygen has a similar effect on titanium alloys.

Thus, in the case of alloy VT8 belonging to the system Ti-Al-Mo, it was shown (ref. 4) that as the oxygen content rises from 0.1 to 0.3%, "hydrogen embrittlement" is strongly manifested, i.e., there is a decrease in the impact strength under the influence of hydrogen. According to the view of the authors of ref. 4, this is due to a decrease in the solubility of hydrogen and oxygen in titanium when both are present.

In ref. 5, the effect of oxygen on the mechanical characteristics of certain alloys of the system Ti-Al-O was studied; in an alloy with 7.2 wt % Al, corresponding in aluminum content to the alloy AT8, a rise in oxygen content from 0.18 to 0.46 wt % causes an increase in the ultimate strength from 80 to 120 kg/mm^2, and a decrease in elongation from 23 to 4%.

As the temperature rises to 600°, the ultimate strength decreases, and the elongation undergoes little change approximately up to 500°, after which it increases sharply at 600°.

The dependence of the properties of alloy AT4 on the content of oxygen and hydrogen was studied by A. M. Yakimova (refs. 6-8) and other investigators. It should be noted that alloy AT4 was studied after cooling in air from 800°. In these studies it was shown that oxygen substantially strengthens alloy AT4 (an average of 10 kg/mm^2 for every 0.1 wt % O_2). The values of the elongation and transverse contraction underwent little change, but the impact strength a_n decreased more abruptly than under the influence of hydrogen. The effect of oxygen on the mechanical properties of alloy AT4 (at a content of 0.005 wt % H_2) is shown in fig. 3.

Certain data indicate a positive influence of oxygen on the high-temperature strength of titanium alloys.

It has been noted that oxygen increases the creep resistance (ref. 6). The author explains this phenomenon by the stabilization of the α phase as a result of the retardation of the diffusion processes in the presence of oxygen.

The data cited indicate that under the influence of oxygen which they contain, pure titanium and some of its alloys change their mechanical characteris-

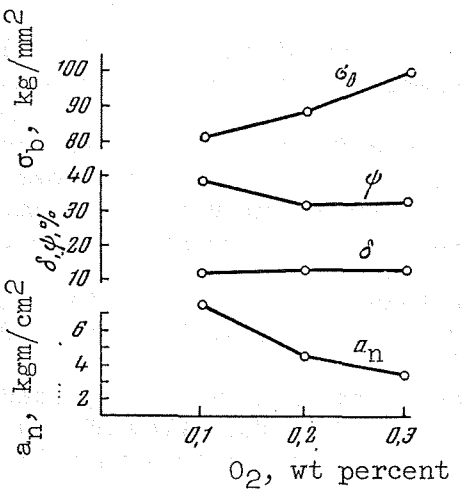

Figure 3. Effect of oxygen on the mechanical characteristics of alloy AT4 (data of ref. 7).

tics substantially; in many cases, the tensile strength values increase without any substantial decrease in plasticity. Consequently, some authors did not include oxygen in the category of absolutely harmful impurities, and in some cases, its introduction as an alloying element for increasing the strength and high-temperature strength of titanium alloys has even been recommended.

In this connection, it seems interesting to examine in more detail the effect of oxygen on the structure, properties and thermal stability of titanium alloys now being widely used in industrial applications.

In the present study, the effect of oxygen content on the mechanical properties of alloys of type AT has been investigated; alloys with the lowest (AT_3) and highest (AT8) aluminum content were selected.

Alloys AT_3 and AT8 were melted in arc furnaces with a consumable electrode by the method of double fusion. Electrodes weighing 5 kg were pressed out of prepared mixtures; aluminum, chromium, iron, and silicon were introduced in pure form during the preparation of the charge, while boron was introduced in the form of a 10% Cr-B master alloy. Oxygen was introduced in the form of powdered TiO_2.

In order to obtain alloys with a minimum oxygen content, use was made of titanium TG1113 with σ_b = 32.8 kg/mm^2, and titanium TG00 with σ_b = 37.3 kg/mm^2 was used to prepare the remaining alloys.

The alloys obtained contained an average of 0.7% Cr, 0.4% Fe, 0.4% Si and 0.01% B; the amount of aluminum was 3.0% in alloy AT_3 and 7.0% in alloy AT8.

The content of the oxygen introduced, based on the charge, was: 0.10, 0.13, 0.23, 0.28, 0.33 and 0.43 wt %.

Check analyses for the content of oxygen performed on some of the specimens showed a satisfactory agreement with the calculated data.

After casting, turning, and facing in order to remove the cavities, the ingots were forged into rods of round and square cross sections 12 mm thick. The forging was open and was carried out with a pneumatic hammer. Prior to forging, the ingots were heated in an electric furnace.

For the AT3 alloy, the temperatures of the start and end of the forging were 1000 and 800°, and for the AT8 alloy, 1150 and 900°, respectively.

After the forging, some of the rods were subjected to a heat treatment consisting in quenching in air from 850° for alloy AT3 and from 950° for alloy AT8 (holding at the quenching temperature for less than 45 min).

Gagarin-type specimens were cut from the rods for tensile tests, and specimens with a Menager-type notch were prepared to determine the impact strength.

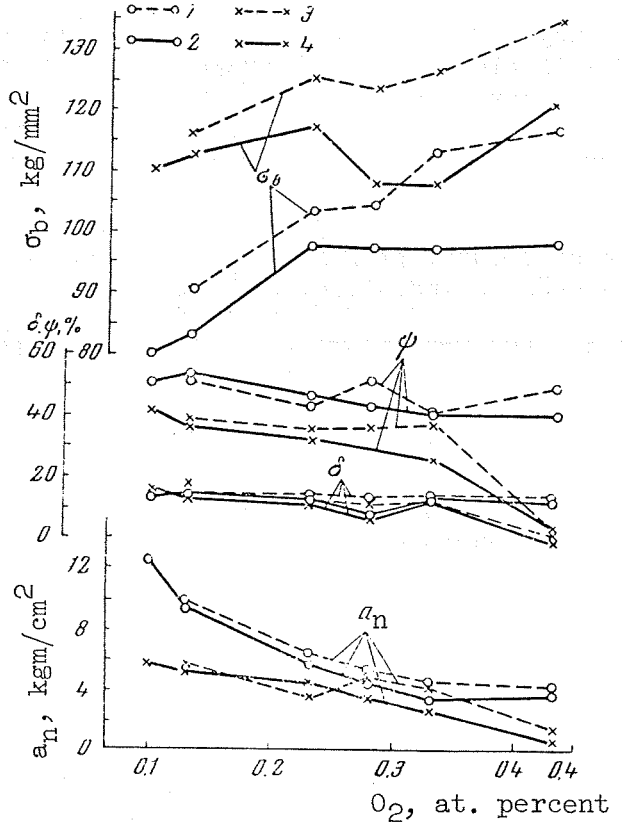

Figure 4. Effect of oxygen on the mechanical properties of alloys AT3 and AT8.

1--alloy AT3 in initial state; 2--alloy AT3 after quenching from 850° and cooling in air; 3--alloy AT8 in initial state; 4--alloy AT8 after quenching from 950° and cooling in air.

The mechanical tests showed (fig. 4 and table) that in alloys AT3 and AT8 tested in the original state, a rise in oxygen content from 0.10 to 0.43% leads to an increase in strength, but decreases the plasticity and impact strength.

MECHANICAL PROPERTIES OF ALLOYS AT3 AND AT8.

O_2 content wt %	σ_b, kg/mm²	δ, %	ψ, %	a_n, kg·m/cm²	O_2 content wt %	σ_b, kg/mm²	δ, %	ψ, %	a_n, kg·m/cm²
Alloy AT3 in initial states					Alloy AT8 in initial states				
0.10	—	—	—	—	0.10	—	—	—	—
0.13	90.3	13.2	50.6	9.0	0.13	116.5	15.0	38.3	5.7
0.23	104.0	14.7	43.4	6.15	0.23	126.1	12.5	36.4	3.3
0.28	105.3	13.4	51.4	5.2	0.28	124.6	10.9	37.0	4.6
0.33	114.6	13.5	42.3	4.45	0.33	127.2	12.3	38.3	4.0
0.43	118.0	14.4	50.1	4.4	0.43	136.3	1.45	4.8	1.1
Alloy AT3 after quenching in air from 850°					Alloy AT8 after quenching in air from 950°				
0.10	80	13.9	51	12.6	0.10	110.4	16.0	42.4	5.8
0.13	83.6	14.7	53.3	8.7	0.13	113.9	14.6	36.2	5.1
0.23	98.3	13.5	47.2	5.85	0.23	117.9	11.1	32.8	4.2
0.28	98.0	8.6	44.9	4.3	0.28	108.7	6.2	—	3.35
0.33	98.1	14.3	42.0	3.45	0.33	109.6	12.0	26.9	2.6
0.43	99.5	14.3	42.0	3.7	0.43	122.2	0.0	5.5	0.6

In alloys AT3 and AT8 subjected to the heat treatment, a rise in oxygen content leads to a similar change in properties, but this effect is manifested to a lesser extent.

In alloy AT8 containing an relatively large amount of aluminum, the plasticity characteristics (δ and ψ) decrease more abruptly than in alloy AT3; on the contrary, in alloy AT3, a rise in the oxygen content up to 0.3% causes a more appreciable decrease in impact strength a_n, but practically does not affect the change in δ and ψ.

Summary

1. A rise in oxygen content in alloys AT3 and AT8 from 0.10 to 0.43% increases their strength but decreases their plasticity.

2. Alloy AT3 is less sensitive to a change in the mechanical properties than alloy AT8 when the oxygen content rises.

3. In the case of alloy AT3, as the oxygen content rises, there is observed an abrupt decrease in impact strength, whereas in the case of alloy AT8, the most sensitive characteristic in this respect is the transverse contraction.

REFERENCES

1. Bumps, E., Kessler, H., and Hansen, M. Trans. ASM, Vol. 45, p. 1008, 1953.

2. Jaffe, R. et al. J. Metals, Vol. 2, p. 1261, 1950.

3. Finlay, W. and Snyder, J. J. Metals, Vol. 2, p. 277, 1950.

4. Kornilov, I. I., Glazunov, S. G., and Yakimova, A. M. Fizika Metallov i Metallovedeniye, Vol. 8, No. 3, p. 370, 1959.

5. Suiter, J. J. Inst. Metals, Vol. 84, No. 4, p. 81, 1955.

6. Yakimova, A. M. Author's abstract of Candidate's Dissertation, A. A. Baykov Institute of Metallurgy (IMET), 1960.

7. --- Fizika Metallov i Metallovedeniye, Vol. 12, No. 6, p. 891, 1961.

8. --- Coll. Titanium and Its Alloys (Titan i yego splavy). Izd-vo AN SSSR, No. 7, p. 166, 1962.

CHARACTERISTICS OF THE OXIDATION OF CERTAIN TITANIUM ALLOYS DURING HEATING PRIOR TO PLASTIC DEFORMATION

I. M. Pavlov, A. Ye. Shelest, and Ye. G. Konstantinov

In the primary treatment, ingots and large blanks of titanium and its alloys are heated to high temperatures at which the processes of scaling oxidation and gas saturation develop simultaneously on the surface of the metal. These physicochemical processes are determined by the composition of the gaseous medium and of the alloys being heated, the temperature, and the duration of the heating. The magnitude of scaling oxidation and gas saturation depends on the rate of the chemical reactions at the boundary between the solid and gaseous phase and on the rate of diffusion of the interstitial elements into the solid phase.

The problem of scaling oxidation must be studied in order to determine the fundamental regularities of the distribution of gases between the scale and the metal, to establish the high-temperature oxidation resistance of titanium alloys in existence and under development, to select correctly the temperature and time conditions of heating of these alloys, and to account for the influence of the oxides on the boundary conditions (metal-instrument) under plastic deformation of titanium alloys. Many studies of foreign and Soviet authors have been devoted to these problems. It is sufficient to mention the work of V. I. Arkharov, A. V. Revyakin and others (refs. 1-5).

A comprehensive study of the conditions of plastic deformation of titanium alloys is being conducted at the laboratory of plastic deformation of metals and alloys at the A. A. Baykov Institute of Metallurgy. The present work offers the results of a study of the oxidation kinetics of certain titanium alloys.

There are several methods of studying the oxidation kinetics of metals, the most accurate being the method of continuous weighing of the specimens. However, when this method is used, it is impossible to draw intermediate samples in order to determine the thickness of the gas-saturated layer. Therefore, for each testing temperature we prepared a set of specimens which were then removed from the furnace in batches after a certain heating time had elapsed. The specimens were in the shape of cubes 10-16 mm on one side, all the faces of which were planed. They were placed in porcelain crucibles which had been ignited to constant weight, and air had free access to all the faces of the specimens. The specimens were heated in an electric furnace to 800-1200° (every 100°), and the heating lasted 15, 30, 60, 120 and 240 min. Before and after the heating, specimens with and without the crucibles and specimens with the scale removed were

weighed on ADV-200 analytical balances, and the change in weight was divided by the surface area of the specimen prior to the oxidation. This technique was used to study the oxidation of alloys VT1, OT4-1, OT4, VT6, VT14 and VT15. In such experiments, particular care should be taken to make sure that the preparation of the surface of all the specimens is identical, since it strongly affects the oxidation at short holding times and, in particular, the strength of adhesion of the scale to the base metal. For example, the rougher the treatment of the surface of the plane, the more effective is the surface of oxidation, and the stronger is the adhesion between the scale and the metal. Thus, the scale is not completely removed.

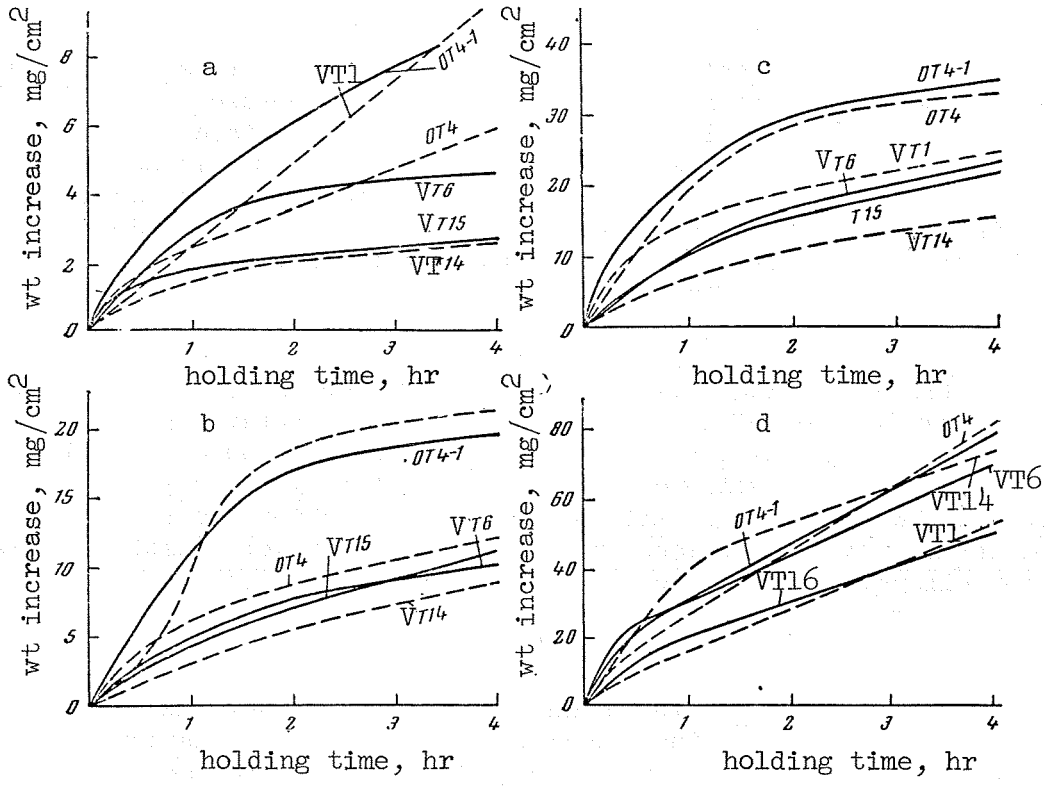

Figure 1. Oxidation of titanium alloys versus temperature and heating time.

a--at 900°; b--at 1000°; c--at 1100°; d--at 1200°.

After the heating, every specimen was inspected, and the color, macrostructure, thickness and strength of the scale were thoroughly described. All the quantities characterizing the oxidation kinetics were found directly by weighing or by simple calculations. The weighing was used to determine: Δg_0--the increase in the weight of the specimen as a result of oxidation and gas saturation per unit surface, mg/cm^2; Δg_4--the change in the weight of the specimen after removal of the scale per unit surface, mg/cm^2.

The unknown quantities were: weight of gases in the scale g_{gs}; weight of gases dissolved in the metal, g_{gm}; weight of metal which had passed into the scale, g_{ms}.

These quantities are related by the equations

$$g_{gm} + g_{gs} = \Delta g_s,$$

$$g_{gm} - g_{ms} = -\Delta g_4.$$

It should be kept in mind that in most titanium alloys the scale consists of rutile TiO_2, since titanium has a great affinity for oxygen, whose chemical activity is considerably lower than that of the other metals entering into the composition of the alloys.

Let us examine the kinetic oxidation curves of the investigated titanium alloys (fig. 1). They all show that during the first stage, the oxidation follows a parabolic law, which, as the duration of the oxidation increases, changes into a linear law.

Our experiments confirmed the hypothesis that the oxidation rate is governed by the concentration gradient of oxygen in the surface layers of the metal. The reaction of formation of titanium oxides takes place at first at the metal-scale phase boundary, and then shifts to the boundary between the solid and gaseous phase. This was demonstrated by means of inert graphite marks made on the surface of the gas-saturated specimens prior to their heating.

We shall agree to refer to the linear oxidation rate as the characteristic rate. Its value can be readily determined by graphical differentiation of the kinetic curves for longer oxidation periods. In general, however, the oxidation rate changes with time, decreasing and approaching some constant value which we shall call the characteristic rate. The determination of the characteristic rate of each alloy makes it possible to evaluate the degree of its oxidation at a given temperature. The data obtained in the present work on the characteristic oxidation rate of the investigated alloys are compiled in the table below.

CHARACTERISTIC OXIDATION RATE OF TITANIUM ALLOY DURING HEATING FOR 4 HR IN AIR IN AN ELECTRIC FURNACE
(in mg/cm^2 hr)

Temp., °C	VT1	OT4-1	OT4	VT6	VT14	VT15
800	0.17	0.30	0.33	0.10	0.10	0.27
900	2.30	1.30	1.15	0.25	0.30	0.30
1000	1.00	0.88	1.63	1.12	1.63	2.00
1100	2.75	2.25	1.60	3.25	2.50	2.75
1200	12.00	16.00	18.00	13.00	10.25	10.00

It is notable that in the $\alpha + \beta$ and β alloys VT6, VT14 and VT15, the oxidation rate increases monotonically with rising temperature, whereas in VT1 and OT4-1, which have an allotropic transition range, a sharp increase in the oxidation rate is observed in this range. This is explained by a weakening of the interatomic bonding forces in the metal lattice and by an increase in the mobility of the atoms in the temperature range of the allotropic transition.

The change in the weight of the specimens following the removal of the scale, Δg_t, should be considered separately. The sign of this quantity indicates the relative quantities of the metal which penetrated into the scale and of the gases which dissolved in the metal. The corresponding curves for each of the temperatures are shown in figure 2. Thus, the kinetic oxidation curve and curves representing the change in Δg_t clearly describe the condition of the processes of scaling oxidation of titanium alloys and gas saturation in the surface layers of the metal.

In practice, the conditions of the heating may differ from those under which the present work was carried out. Other quantitative characteristics of the oxidation can also be obtained, but the qualitative picture remains the same. The magnitude of scaling oxidation and gas saturation is strongly affected by the atmosphere of the furnace and the total thermal flux. A characteristic feature of oxidation under plastic deformation is the breakdown of the

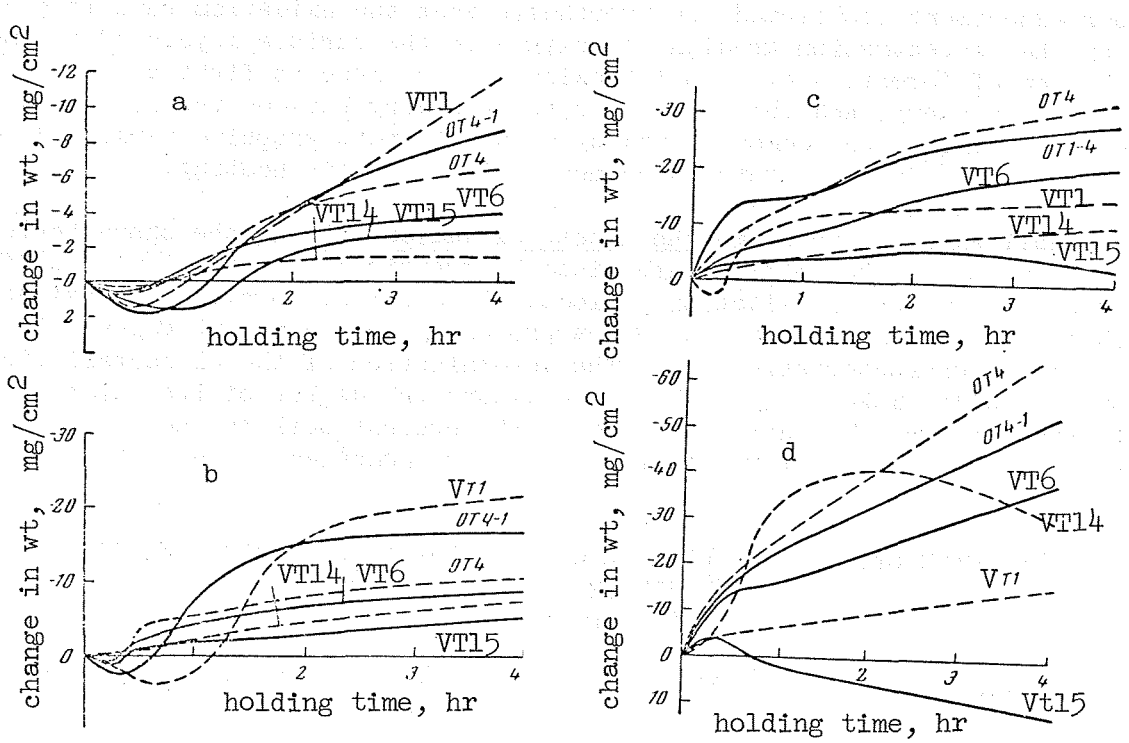

Figure 2. Change in weight of specimens of titanium alloys after removal of scale versus temperature and heating time.

a--at 900°; b--at 1000°; c--at 1100°; d--at 1200°.

primary scale, the renovation of the metal surface as a result of the emergence of deeper layers, and secondary oxidation which develops in the course of the treatment.

The data obtained in the present work can be used for a comparative characterization of the high-temperature oxidation resistance of titanium alloys and for estimating the effect of alloying elements on this important technological property of metals.

REFERENCES

1. Arkharov, V. I. and Blankova, Ye. B. Fizika Metallov i Metallovedeniye, Vol. 10, No. 1, 1960.

2. Revyakin, A. V. Izv. AN SSSR, OTN, Metallurgiya i Toplivo, No. 5, pp. 113-116, 1961.

3. Layner, D. I. and Tsypin, M. I. Metallovedeniye i Obrabotka Tsvetnykh Metallov, State Scientific Design and Planning Research Institute for Working of Nonferrous Metals (Giprotsmo), Metallurgizdat, No. 20, pp. 42-64, 1961.

4. Mozhayev, S. S., Sokiryanskiy, L. F., and Anitov, I. S. Fizika Metallov i Metallovedeniye, Vol. 14, No. 4, pp. 637-638, 1962.

5. Slesareva, Ye. N. Metallovedeniye i Obrabotka Tsvetnykh Metallov, Giprotsmo, Metallurgizdat, No. 20, pp. 65-80, 1961.

NITRIDING OF TITANIUM ALLOYS AT HIGH PRESSURES

Ye. N. Novikova

In studies conducted earlier on the nitriding of titanium alloys in pure nitrogen (refs. 1, 2) it was found that the diffusion layer on titanium is formed at temperatures above 800° in the course of chemical and thermal treatment of the latter in an atmosphere of pure nitrogen at normal pressure. The diffusion layer is made up of two zones. The upper zone consists of a thin nitride layer, and the lower, thicker zone consists of a layer of a solid solution of nitrogen in α-Ti.

As the saturated temperature rises, the depth of both layers and their nitrogen concentration increase, causing an increase in hardness. At temperatures above 950°, the diffusion layer becomes very brittle, and the strength and plasticity characteristics of the core of the specimen decrease substantially; for this reason, the temperature of 950° was taken as the maximum permissible temperature for the nitriding of articles made of titanium alloys.

It was also found that the absorption of nitrogen by titanium at 800-1200° follows the parabolic law, i.e., the rate of diffusion of nitrogen decreases with time. Thus, for each temperature it was possible to determine the time at which the thickness of the layer practically ceased to increase. Thus, at 950°, this period of time is equal to 25-30 hr.

The decrease in the rate of the growth of the diffusion layer with time is due to the formation and growth on the titanium surface of a nitride phase in which the diffusion coefficient of nitrogen is considerably smaller (by more than one order of magnitude) than in α- and β-Ti, and decreases with rising nitrogen concentration (ref. 3). As the depth of the nitride zone in the layer increases, the amount of nitrogen diffusing through it gradually decreases, and fresh amounts of nitrogen are chiefly consumed in the enrichment of the nitride zone alone, which hinders the penetration of nitrogen into the metal still more. Thus, the most saturated and hence most brittle part of the layer is the nitride zone.

The alloying of titanium has a marked influence on the depth and hardness of the diffusion layer. Table 1 gives the depth of the layer and the hardness at the surface of specimens of various alloys nitrided for 30 hr at 950° at a nitrogen supply rate of 0.2-0.3 l/min.

The first technological samplings of nitrided articles made of titanium alloys showed that in many cases the layer depth attained was insufficient.

TABLE 1

Alloy	Total depth of layer, mm	Hardness (p = 5 kg) on surface HV, kg/mm^2
Technical titanium VT1	0.06-0.08	750-850
VT3-1	0.04-0.05	700-750
VT5	0.08-0.10	750-800
VT4	0.10-0.12	800-900
VT8	0.12-0.14	700-750
VT10	0.10-0.12	700-750
VT14	0.14-0.16	750-850

Warpage of the parts is unavoidable in a high-temperature process. When the parts are reduced to the required dimensions, it is necessary to remove most of the diffusion layer and sometimes the entire layer. Furthermore, the brittleness of the nitride zone, whose depth in certain alloys reaches 15-20 μ, causes the chipping of sharp edges, which is completely unacceptable for many parts.

Thus, a more successful introduction of the nitriding processes into the industry requires the finding of methods of increasing the depth of the layer and eliminating the brittle nitride zone which hinders the penetration of nitrogen into titanium.

The achievement of a less brittle and deeper layer will in turn make it possible to lower the temperature of the process, this being very desirable for preserving the mechanical properties of the core of the part and decreasing their warpage.

It is clear from the above that in order to obtain a deeper diffusion layer on titanium, one must change the nitriding conditions in such a way that the saturation will proceed only with the formation of a solid solution of nitrogen in α-Ti and that no conditions will be created for the formation of the nitride zone. It was postulated that the formation of the nitride zone could be retarded by nitriding in a mixture of nitrogen and an inert gas (at a low partial pressure of nitrogen) or in rarefied nitrogen.

Further studies in this direction have confirmed our hypothesis.

The nitriding of titanium in a mixture of nitrogen and argon (refs. 4, 5) at a partial nitrogen pressure of 0.005-0.04 atm (the amount of nitrogen was 0.4-4 percent of that of argon) produced an increase in the depth of penetration of nitrogen into titanium, and the nitride zone was absent from the nitrided layer.

The positive effect of rarefying the gas during the saturation of titanium with argon is also indicated by the results of references 6 and 7; these studies were conducted for the purpose of determining the degree of contamination of

titanium with gases. It was shown in these studies that a decrease in pressure from 76 to 0.076 cm Hg at 850° increased the weight gain of the specimen per unit surface. After 2 hr of heating, the weight gain increased by a factor of almost 2. The depth and structure of the layer were not determined.

The effect of decreasing the pressure during nitriding on the depth of penetration of nitrogen and on the structure of the layer was studied in the present work.

The investigation was carried out on specimens of technical titanium VT1, industrial alloys VT3-1, VT4, VT5, and experimental alloys Ti-Al-Mo, Ti-Al-Sn, and Ti-Al-Cu. The content of alloying elements in these alloys was as follows: alloy VT5, 5.05 percent Al; alloy VT4, 4.8 percent Al and 0.9 percent Mn; alloy VT3-1, 5.2 percent, 1.9 percent Cr, 1.5 percent Mo and 0.4 percent Fe; alloy Ti-Al-Mo, 4.1 percent Al and 1.25 percent Mo; alloy Ti-Al-Sn, 4.98 percent Al and 0.70 percent Sn; alloy Ti-Al-Cu, 4.93 percent Al and 1.15 percent Cu.

Cylindrical specimens 10 mm in diameter and 10 mm high were cut from forged rods 14 mm in diameter.

The process of nitriding at low pressures is basically similar to nitriding at normal pressure: nitrogen from a cylinder is successively passed through vessels with substances absorbing moisture, a retort with heated titanium sponge (getter for removing oxygen) and the chamber of the nitriding furnace. However, in order to create a rarefied atmosphere of nitrogen in the heating zone as well, all the vessels and furnaces with the getter and specimens were placed in a vacuum chamber.

All the parts of the system were connected by means of vacuum tubing. A vessel with silica gel was connected to the aircock of the chamber through which nitrogen from the cylinder was introduced. The gases were evacuated from the chamber by means of a VN-1 preliminary vacuum pump and an M-20 diffusion pump (fig. 1).

The nitriding process consisted of the following operations:

(1) Charging of the specimens and titanium sponge into the furnace;

(2) Evacuation of air from the chamber;

(3) Filling of the chamber with nitrogen;

(4) Evacuation of nitrogen from the chamber (Operations 3 and 4 were repeated twice);

(5) Heating of the furnaces;

(6) Introduction of nitrogen and establishment of the selected pressure in the chamber;

(7) Soaking at a continuous flow of nitrogen and at the selected temperature and pressure;

(8) Cooling of the specimens in the stream of nitrogen;

(9) Emptying of the chamber.

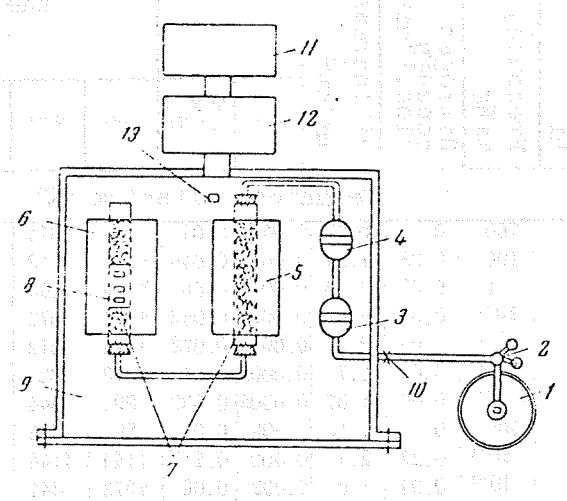

Figure 1. Diagram of the process of nitriding at low pressures: 1, nitrogen flask; 2, gas reducing valve; 3, container with silica gel; 4, container with P_2O_5; 5, furnace for getter; 6, furnace for nitriding; 7, titanium turnings; 8, specimens; 9, cylindrical vacuum furnace; 10, stopcock for evacuating and introducing the gas; 11, preliminary vacuum pump; 12, diffusion pump; 13, place for measuring the pressure.

The specimens were nitrided at 950° and partly at 870° at pressures of 760, 100, 1, 10^{-1} and 3×10^{-2} mm Hg.

The consumption of nitrogen was set at ~ 0.3 l/min. At a pressure of 10^{-1} mm Hg, two more processes were carried out with a lower consumption of nitrogen: 0.09 and 0.03 l/min (the nitrogen consumption was measured by the change of the gas pressure in the cylinder). Basically, the process lasted 8 hr. A 20-hr process was conducted at 950° and at the optimum pressure.

The pressure in the chamber (100 and 1 mm Hg) was measured with a V-shaped manometer, and smaller pressures were measured with a thermal manometer.

Let us examine the conditions and results of nitriding of certain alloys (table 2).

As is apparent from the tables, at a nitriding temperature of 950° and a nitrogen consumption of 0.3 l/min, the decrease in pressure from atmospheric to 1 mm Hg leads to a significant increase in the depth of the entire layer and to a very appreciable (severalfold) increase in the depth of the nitride zone. Thus, for example, in specimens of alloys VT5, Ti-Al-Sn and Ti-Al-Cu, the depth

TABLE 2. CONDITIONS AND RESULTS OF NITRIDING OF CERTAIN ALLOYS

Nitriding conditions					Depth of layer, mm		Hardness at a load of 50 g, kg/mm^2, at a distance from the surface, mm					
Temperature, °C	Duration, hr	Pressure, mmHg	Nitrogen consumption, l/min	wt increase, mg/cm^2	TiN	TiN + α-Ti	0,02	0,04	0,06	0,08	0,10	0,15
Technical titanium VT1												
950	8	760	0.3	0,97	0,005	0.04	1144	644	447	381	367	—
950	8	100	0,38	1.29	0,001	0,045	1225	713	381	367	367	—
950	8	1	0,33	2.16	0,001	0.06	1144	1144	644	381	367	—
950	8	10^{-1}	0,3	2.0	0.002	0.052	1144	1072	508	412	381	—
950	8	10^{-1}	0,09	2.5	0.001	0.072	1144	1072	1005	412	381	—
950	8	10^{-1}	0,03	2.7	0.0005	0.07	1313	1225	1144	367	367	—
950	7.5	$3\cdot10^{-2}$	0.09	1.07	0,0005	0.032	891	644	381	367	367	—
950	30	760	0.3	1.45	0.005	0.06	891	795	713	367	367	—
950	20	10^{-1}	0,27	2,4	0.002	0.117	1144	1144	1005	891	753	—
870	8	10^{-1}	0.09	1.9	0.002	0,06	1072	841	713	346	346	—
Alloy VT3-1												
950	8	760	0,3	0,8	0.006	0.026	1413	353	353	—	353	353
950	8	1	0.33	2.3	0,005	0.045	1525	1225	429	—	447	412
950	8	10^{-1}	0.3	2.1	0,004	0,036	1525	1413	447	—	412	—
950	8	10^{-1}	0,09	2,0	0.001	0.05	1144	1072	447	—	412	—
950	7.5	$3\cdot10^{-2}$	0,09	1.3	0,001	0,02	1313	508	412	—	412	—
950	30	760	0,3	1,33	0.008	0.04	1413	1144	447	—	412	412
950	20	10^{-1}	0.2	1.83	0.006	0.07	1649	1144	1005	—	447	412
870	8	10^{-1}	0,09	1,5	0.0025	0.028	1313	412	412	—	412	381
Alloy VT4												
950	8	760	0.3	0.55	0.004	0.044	946	753	429	—	412	396
950	8	100	0.38	0.58	0.001	0,055	1313	891	644	—	412	396
950	8	1	0.33	1,54	0.001	0.075	1072	946	841	—	508	412
950	8	10^{-1}	0.3	1,21	0.002	0.065	1144	1005	841	—	447	396
950	8	10^{-1}	0.09	1,34	0.001	0.075	1144	1005	841	—	412	412
950	8	10^{-1}	0,03	1.68	0,0015	0,08	1313	1144	1005	—	644	412
950	7.5	$3\cdot10^{-2}$	0,09	0,58	0.0005	0,05	1144	891	412	—	396	396
950	30	760	0.3	1,15	0,006	0.095	1144	891	753	—	532	412
950	20	10^{-1}	0.27	2.15	0.004	0.16	1005	1005	1005	—	841	753
870	8	10^{-1}	0.09	0,95	0,001	0.063	1144	1005	795	—	381	381
Alloy VT5												
950	8	760	0,30	0,58	0,007	0,037	946	753	508	—	412	367
950	8	100	0,38	0.82	0,001	0,064	946	891	713	—	412	367
950	8	1	0,33	1,57	0,001	0,10	1313	1225	1005	—	713	412
950	8	10^{-1}	0,30	1.5	0,003	0,08	1144	891	753	—	508	412
950	8	10^{-1}	0,09	1,55	0,002	0,065	1144	946	644	—	429	412
950	8	10^{-1}	0,03	0.92	0,001	0,075	1225	1144	1006	—	508	412
950	7,5	$3\cdot10^{-2}$	0.09	0,87	0,0005	0,032	946	713	487	—	412	396
950	30	760	0.3	1,12	0,015	0,08	946	891	841	—	412	367
950	20	10^{-1}	0,27	2,4	0,003	0,14	946	891	841	—	753	713
870	8	1	0,3	1,4	0.003	0,07	795	713	644	—	412	367

TABLE 2 (Continued)

Nitriding conditions					Depth of layer, mm		Hardness at a load of 50 g, kg/mm^2, at a distance from the surface, mm					
Temperature, °C	Duration, hr	Pressure, mmHg	Nitrogen consumption, l/min	wt increase, mg/cm^2	TiN	TiN + α-Ti	0,02	0,04	0,06	0.08	0,10	0,15
Alloy Ti — Al — Mo												
950	8	760	0.3	0.6	0.004	0.065	1005	891	753	—	584	412
950	8	100	0.38	0.84	0.0015	0.10	1144	891	841	—	753	412
950	8	1	0.38	1.57	0.001	0.10	1144	1144	841	—	713	447
950	8	10^{-1}	0.3	1.74	0.0015	0.09	1313	1225	841	—	644	412
950	8	10^{-1}	0.09	1.33	0.0005	0.11	1144	946	841	—	753	447
950	8	10^{-1}	0.03	0.74	0.001	0.10	1225	1072	841	—	713	447
950	7.5	$3 \cdot 10^{-2}$	0.09	0.8	0.001	0.07	1144	841	713	—	612	412
950	30	760	0.3	1.27	0.015	0.12	1005	841	841	—	753	557
950	20	10^{-1}	0.27	1.68	0.004	0.18	1072	1005	946	—	841	753
870	8	10^{-1}	0.09	1.5	0.003	0.08	1072	841	713	—	508	412
870	8	1	0.03	0.9	0.002	0.08	1144	753	713	—	447	412
Alloy Ti — Al — Sn												
950	8	760	0.3	0.67	0.004	0.035	795	584	353	—	353	—
950	8	100	0.38	0.63	0.0005	0.07	1225	946	841	—	557	412
950	8	1	0.33	1.5	0.002	0.085	1144	891	795	—	584	412
950	8	10^{-1}	0.3	1.1	0.0025	0.072	1144	891	753	—	466	381
950	8	10^{-1}	0.09	1.3	0.0005	0.085	1225	1072	946	—	447	412
950	8	10^{-1}	0.03	1.54	0.002	0.085	1144	1144	891	—	447	412
950	7.5	$3 \cdot 10^{-2}$	0.09	0.84	0.0005	0.045	1225	713	429	—	412	381
950	30	760	0.3	0.73	0.005	0.1	1313	1144	795	—	713	447
950	20	10^{-1}	0.27	1.8	0.003	0.15	1225	1144	1005	—	841	644
870	8	10^{-1}	0.09	0.53	0.0025	0.05	841	713	508	—	412	381

of the layer increased 2.5-fold, while the nitride zone decreased from 4-7 to 1-2 μ. The weight gain of the specimens per unit surface increased by a factor of almost 3.

The smallest increase in the depth of the nitrided layer at 1 mm Hg was obtained with specimens of technical titanium and of the alloy VT3-1.

At a pressure of 10^{-1} mm Hg and a nitrogen consumption of 0.3 l/min (temperature, 950°) the depth of the nitrided layer obtained was somewhat less than at 1 mm Hg. However, a decrease in nitrogen consumption to 0.03-0.09 l/min at this pressure promoted an increase in the depth of the layer and a decrease in the depth of the nitride zone. On specimens of technical titanium and alloys VT3-1, VT4 and Ti-Al-Mo at a pressure of 10^{-1} mm Hg and at a nitrogen consumption of 0.09 l/min, the depth of the layer obtained was greater than 1 mm Hg and 0.3 l/min. Hence, it follows that the maximum depth of the layer in each alloy is obtained at a certain definite pressure and nitrogen consumption.

A further decrease in pressure to 3×10^{-2} mm Hg led to a sharp decrease in the depth of the nitrided layer and to a decrease in hardness, despite the

fact that the nitride zone was minimum (less than 1 μ). Obviously, an increase in the nitrogen consumption was required at this pressure.

After nitriding for 20 hr at 950°, a pressure of 10^{-1} mm Hg and a nitrogen supply rate of 0.27 l/min, the depth of the nitrided layer was found to be 1.5 times greater than after nitriding for 30 hours at normal pressure with the other conditions being the same, although for the majority of the alloys the pressure of 10^{-1} mm Hg and nitrogen supply rate of 0.27 l/min were not the optimum values.

Photomicrographs (fig. 2) show the nitrided layer obtained on alloy VT5 after saturation at normal pressure (fig. 2a) and at a pressure of 10^{-1} mm Hg (fig. 2 b).

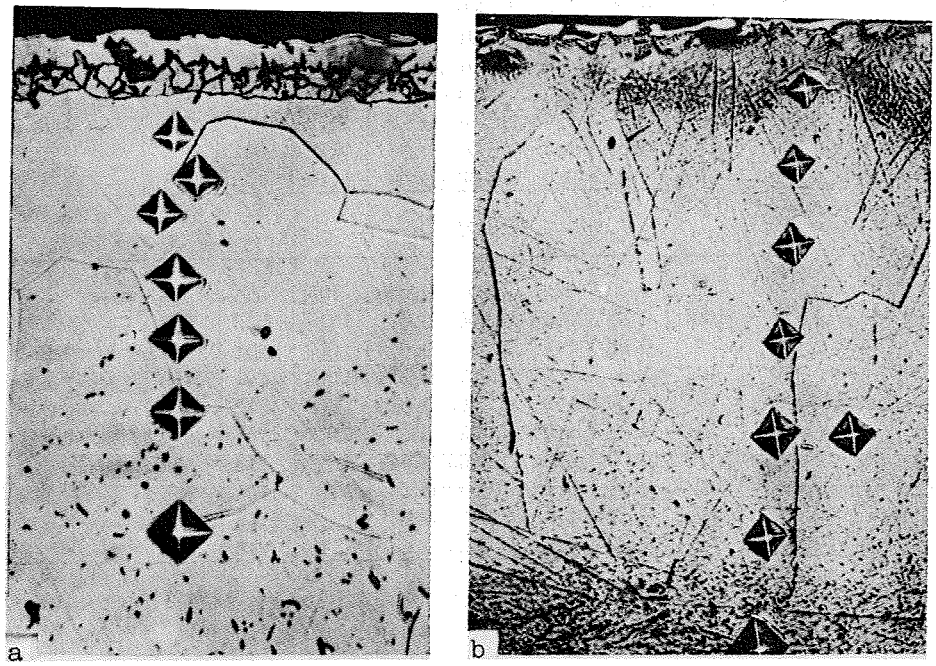

Figure 2. Microstructure of nitrided layer on alloy VT5, x 500, obtained: a, after 30 hr, at 950° and normal pressure; b, after 20 hr at 950° and a pressure of 0.1 mm Hg.

In all the alloys, the depth of the layer following an 8-hr nitriding at 870° and 1 and 10^{-1} mm Hg was greater than after nitriding at normal pressure.

These results indicate the possibility of lowering the temperature when the nitriding process is carried out in rarefied nitrogen.

Specimens of alloys VT1 and VT5 nitrided for 8 hr at 950°, 1 mm Hg and a nitrogen consumption of 0.3 l/min, were subjected to wear-resistance tests on an Amsler machine in a couple with nitrided steel rolls.

The tests were carried out under the following conditions: load 25 kg/mm^2; slip rate of roll, 0.4 m/sec; testing time, 2 hr; medium, kerosene.

The tests showed a high wear resistance of the surface of specimens nitrided in rarefied nitrogen. The magnitude of the wear (a few tenths of one milligram) and coefficient of friction (0.14-0.15) was the same as in specimens nitrided at normal pressure.

TABLE 3

MECHANICAL CHARACTERISTICS OF SPECIMENS OF ALLOY VT4

	Number of specimens	σ_b, kg/mm^2	δ, %	ψ, %	a_n, kgm/cm^2
Before nitriding	3	85.5	14.8	34.5	4.9
Nitriding at 1 mm Hg	3	88.1	11.0	25.8	5.3
Nitriding at normal pressure and 950° for 30 hr	3	82.6	11.2	34.3	4.9

The mechanical characteristics of the core of the specimens of alloy VT4 were determined after nitriding in rarefied nitrogen under the following conditions: temperature, 950°; time, 20 hr; pressure, 1 mm Hg; nitrogen consumption, 0.36 l/min.

Results of the tests are given in table 3.

These data indicate that the mechanical characteristics of the specimens of alloy VT4 after nitriding in rarefied nitrogen undergo little change and are sufficiently high for parts operating under friction.

Summary

1. During nitriding of titanium alloys, a decrease of the pressure in the chamber from 760 to 1-0.1 mm Hg leads to a 1.5-2.0-fold increase in the depth of the nitrided layer, while the thickness of the brittle nitride zone is reduced severalfold.

2. It was established that for each titanium alloy at the same temperature and nitriding time there should exist certain pressures and a certain nitrogen consumption at which a maximum depth of the layer can be obtained.

3. The layer obtained in rarefied nitrogen resists wear satisfactorily, and its wear resistance is as high as that of the layer obtained by nitriding at normal pressure.

4. The mechanical characteristics of the core of the specimen of alloy VT4 following nitriding in rarefied nitrogen differ very little from the characteristics obtained in specimens nitrided at normal pressure (the ultimate and impact strength are somewhat increased; the elongation per unit length and contraction remain practically the same).

REFERENCES

1. Stroyev, A. S. Coll. Titanium and Its Alloys (Titan i yego splavy). Metallurgy and Metallography, Izd-vo AN SSSR, pp. 107-114, 1958.

2. Novikova, Ye. N. Coll. Titanium and Its Alloys (Titan i yego splavy). Izd-vo AN SSSR, No. 3, pp. 35-40, 1960.

3. Wasilewski, R. Y. and Kehl, G. L. J. Inst. Metals, Vol. 83, No. 3, p. 94, 1954.

4. Smirnov, A. V. and Nachinkov, A. D. Trudy Len. in-ta aviatsionnogo priboro stroyeniya, No. 30, pp. 3-18, 1959.

5. Nachinkov, A. D. Nitriding of Titanium and Its Alloys at Reduced Nitrogen Pressure (Azotirovaniye titana i yego splavov pri ponizhennom partsial'nom davlenii azota). Author's abstract of cand. dissert., Len. Institute of Aviation Instrument Manufacture, 1961.

6. Carpenter, L. G. and Reavell, F. R. Metallurgia, Vol. 39, (230), p. 63, 1948.

7. Gulbransen, E. A. and Andrew, K. Trans. AIME, Vol. 185, p. 741, 1949.

CORROSION OF TITANIUM ALLOYS OF SERIES VT AND AT IN SOLUTIONS OF SULFURIC ACID CONTAINING NICKEL SULFATE

S. A. Nikolayeva and V. A. Zinov'yev

Sulfate solutions resulting from nickel production always contain excess sulfuric acid. Since at the present time titanium is finding increasingly wider applications as a structural material in the nickel industry, it appeared of interest to study the influence of nickel sulfate additions on the corrosion properties of titanium in sulfuric acid. In order to have a wider choice of structural material, the corrosion behavior of titanium alloys of series VT and AT was also investigated.

Our industry produces technical titanium VT1 of different types. We studied the corrosion resistance of sheet, rod, and forged titanium. Rod titanium was found to have the highest resistance to corrosion. It showed a tendency toward passivation at room temperature even in sulfuric acid with a concentration of 300 g/l. Sheet and forged titanium showed approximately the same rate of corrosion of sulfuric acid with a concentration of 164 g/l, so that subsequently, the average corrosion rate of specimens of forged and sheet titanium was taken as the value of the corrosion rate of alloy VT1 at room temperature. The corrosion rate was measured by the weight loss of the specimens and calculated in g/m^2 hr. Prior to the experiment, the specimens were turned on an emery wheel, then washed with water containing soda, dried, washed in carbon tetrachloride, and weighed.

The experiments were carried out in glass flasks with reflux condensers at room temperature and at 100°; nickel salts were added in the form of sulfates, and the concentration was calculated in terms of the metal in g/l.

As a rule, the corrosion rate of the investigated specimens at room temperature was not established immediately: at the start of the experiment, an induction period was observed during which the corrosion rate gradually increased. These experiments lasted a long time (up to 1500 hr). At 100°, the corrosion rate was very high, and for this reason the experiments could not be long and lasted 10 hr. Otherwise, the composition of the solution could have changed substantially, and the specimens could have dissolved. The corrosion rate of titanium was studied in sulfuric acid of various concentrations. Some of the solutions of sulfuric acid contained nickel sulfate additions, others did not. The values which we obtained for the corrosion rates in the investigated sulfuric acid solutions are collected in the table.

CORROSION RATE OF ALLOYS OF SERIES VT AND AT IN SULFURIC ACID CONTAINING ADDITIONS OF SALTS (IN g/m^2 HR).

Alloy	Sulfuric acid concentration, g/l: 20 — no addition	20 — 100 g/l Ni	83 — no addition	83 — 100 g/l Ni	83 — no addition	83 — 10 g/l Ni	164 — 100 g/l Ni	164 — 0.002 g/l Ni	164 — 0.02 g/l Cu	164 — 0.2 g/l Cu	164 — 2 g/l Cu	164 — no addition	164 — 10 g/l Ni
Temperature 20°													
VT15	0.0001	0.0003	0.0009	0.065	0.127	0.081	0.106	0.097	0.0007	0.0014	0.0029	26	36
VT14	0.0004	0.0009	0.0017	0.080	0.114	0.263	0.166	0.125	0.0027	0.0037	0.0033	43	48
AT2-2	0.002	0.0012	0.0009	0.100	0.156	0.147	0.154	0.137	0.0017	0.0025	0.0021	61	70
AT2-1	—	—	—	—	—	—	—	—	—	—	—	42	68
AT2-3	0.0005	0.0009	0.0016	0.113	0.185	0.179	0.201	0.182	0.0015	0.0013	0.0025	39	78
VT8	0.0009	0.0005	0.0014	0.131	0.279	0.211	0.257	0.150	0.0024	0.0024	0.0021	72	75
VT3-1	0.0001	0.0001	0.0003	0.147	0.267	0.212	0.320	0.203	0.0017	0.0012	0.0015	49	83
VT6	0.0006	0.0006	0.0014	0.185	0.288	0.290	0.315	0.260	0.0021	0.0015	0.0018	50	109
VT9-1	0.0006	0.0008	0.0024	0.216	0.383	0.379	0.377	0.345	—	—	—	130	112
AT3	0.0009	0.0005	0.0006	0.198	0.380	0.295	0.364	0.315	0.0014	0.0012	0.0024	90	116
AT6	0.0007	0.0014	0.0009	0.234	0.360	0.345	0.374	0.315	0.0017	0.0017	0.0011	93	106
AT8	0.0008	0.0008	0.0014	0.220	0.365	0.382	0.385	0.340	0.0025	0.0025	0.0023	82	100
VT1	0.0006	0.0005	0.0007	0.231	0.409	—	0.422	0.345	0.0018	0.0012	0.0012	73	118
AT40	0.0011	0.0008	0.0008	0.247	0.455	0.422	0.436	0.380	0.0015	0.0017	0.0020	106	117
VT10	0.0003	0.0002	0.0012	0.205	0.695	0.400	0.325	0.655	0.0017	0.0014	0.0010	177	79
VT7	0.0004	0.0004	0.0010	0.219	0.445	0.422	0.400	0.400	0.0017	0.0015	0.0016	70	140
OT4	0.0003	0.0009	0.0003	0.258	0.495	0.495	0.459	0.420	0.0027	0.0030	0.0030	84	134
VT5-1	0.0020	0.0008	0.0010	0.372	0.790	0.555	0.764	0.685	0.0022	0.0020	0.0032	170	202
ATII	—	—	—	—	—	—	—	—	—	—	—	104	124

From the data of the table one can conclude that such alloy components as molybdenum and vanadium promote an increased passivation of titanium (alloys VT15 and VT6); vanadium promotes passivation to a lesser extent than molybdenum (alloy VT7). Zirconium also promotes passivation to a lesser extent than molybdenum, otherwise the corrosion rate of alloy VT9-1 would have been smaller. The presence of aluminum, tin (alloy VT5-1), manganese (alloy OT4), and iron (alloy VT7) increases the corrosion rate of titanium somewhat. Passivation is promoted by chromium, since the corrosion rate of alloys AT6 and AT8 is less than that of VT7, OT4 and VT5-1.

An increase in the concentration of sulfuric acid leads to an increase in the corrosion rate. It should be noted, however, that in sulfuric acid with a concentration of 83 g/l at room temperature, the corrosion rate is practically nil; in sulfuric acid with a concentration of 164 g/l, the corrosion rate increases by a factor of approximately 150-300 times, i.e., in the preceding case a clear-cut passivation of the specimens was observed.

Addition of nickel sulfate to sulfuric acid of various concentrations has a very special influence on the corrosion rate.

Let us examine the curves representing the corrosion rate versus sulfuric acid concentration (fig. 1) in the presence and absence of nickel sulfate (100 g/l Ni). In sulfuric acid with a concentration of 20 g/l, this phenomenon is difficult to observe because of the low corrosion rate; in sulfuric acid with a concentration of 83 g/l, the addition of nickel sulfate increases the corrosion rate by a factor of almost 200. In sulfuric acid with a concentration of 164 g/l, this phenomenon is practically absent. Thus, in certain cases, nickel sulfate activates the corrosion of titanium alloys, and in other cases, this activation is lacking.

The influence of nickel sulfate was more clearly observed at 100°. The addition of nickel sulfate in the amount of 10 g/l Ni to acid with a concentration of 164 g/l decreased the corrosion rate somewhat in all cases. Let us examine the corrosion rate of alloy VT1 versus the nickel concentration in the solution of sulfuric acid with a concentration of 164 g/l (fig. 2). It is evident from this figure that small amounts of nickel present in the solution activate the corrosion of titanium, and that a further rise in the nickel concentration causes a decrease in the corrosion rate. For comparison, a series of experiments was carried out in order to determine the influence of nickel sulfate additions. The sodium sulfate concentrations were chosen so that the sulfate ion content would correspond exactly to the concentration of this ion produced by the addition of nickel sulfate. From the figure, it is apparent that the sulfate ion very definitely decreases the corrosion rate of titanium. This is in accord with the data of V. V. Andreyeva and V. I. Kazarin (ref. 1), who also observed a maximum corrosion of titanium in 40 percent sulfuric acid at 40°. The activation of the corrosion of titanium and its alloys by nickel ions is apparently due to the cementation of nickel on the dissolving surface.

We occasionally observed the presence of nickel on the titanium surface by inspecting the specimens under the microscope and analyzing the surface formations. However, the cementation of nickel was not always detected; nor did the corrosion rate always increase in the presence of nickel ions. In particular, in sulfuric acid with a concentration of 164 g/l, the influence of nickel was lacking not only when it was added up to a concentration of 100 g/l, which markedly increased the sulfate ion concentration, but also when nickel was added in concentrations of 0.1 and 10 g/l, when the sulfate ion concentration remained practically unchanged. This leads to the hypothesis that complexes of nickel with excess sulfate ions are formed, thus substantially decreasing the free concentration of nickel ions (ref. 6). At high temperatures, such complexes break down, and the influence of nickel sulfate additions is clearly manifested.

The value of the steady state potential of dissolving titanium is very interesting.

In all cases where the specimens are in the passivated state, the value of the steady state potential is between -0.25 and +0.02 V (relative to the standard hydrogen electrode). This is in agreement with the data of refs. 2 and 3.

The dissolution of titanium specimens at a rate of 0.1 g/m^2 hr and higher begins at a potential of -0.3 V and at higher negative potentials.

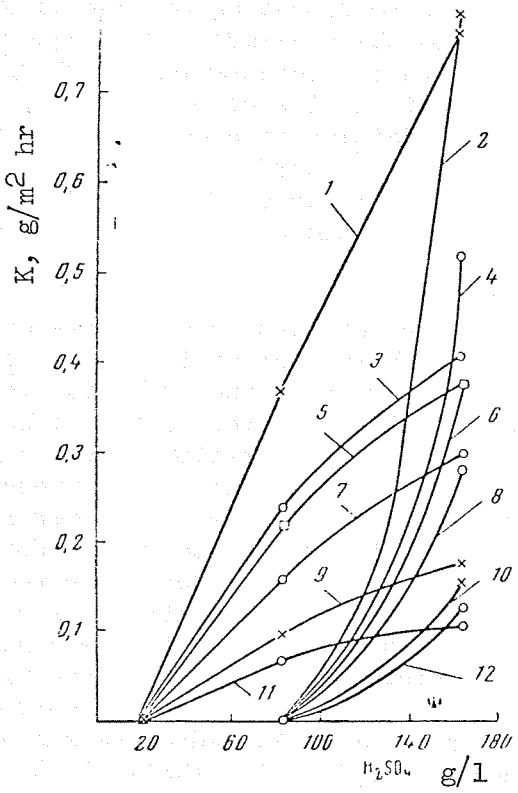

Figure 1. Corrosion rate versus sulfuric acid concentration for various titanium alloys in the presence (Curves 1, 3, 5, 7, 9, 11) and absence (Curves 2, 4, 6, 8, 10, 12) of nickel sulfate at 20°: 1 and 2, alloy VT5-1; 3 and 4, alloys AT40, VT10, VT7, OT1; 5 and 6, alloys VT9, AT3, AT6, AT8; 7 and 8, alloys VT8, VT3-1, VT6; 9 and 10, alloys VT14, AT2-2, AT2-3; 11 and 12, alloy VT15.

Dissolution at the rate of 1 g/m^2 hr and higher is characterized by a steady state potential of -0.4 V.

It should be noted that these values of steady state potentials also partially correspond to a passivated titanium surface. In 2 N. H_2SO_4, to which up to 1 N. NaF was added, i.e., in the case of an active titanium surface (refs. 4, 5), the steady state potential of specimens of alloys VT1 and VT8 was respectively -0.622 and 0.582 V.

Finally, a series of experiments devoted to the study of the influence of copper sulfate editions was carried out.

In most cases, copper is present as an impurity in the electrolytes of nickel production, and for this reason its influence appeared of great interest. The amount of copper sulfate added to sulfuric acid with a concentration of 164 g/l was respectively equal to 0.002, 0.02 and 2 g/l (in terms of copper).

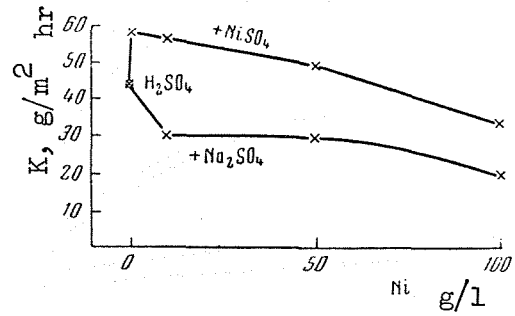

Figure 2. Corrosion rate of titanium VT1 versus concentration of nickel sulfate and sodium sulfate added to sulfuric acid (164 g/l) at 90°.

By cementing on the surface of titanium, copper shifts its steady state potential toward the positive side. Titanium thus falls into the region of passivation, so that, as can be seen from the table, its corrosion rate practically drops off to zero even when copper is added to the solution up to a concentration of 0.02 g/l.

Let us examine the dependence of the steady state potential of titanium on time for various amounts of sulfate added to the solution of sulfuric acid with a concentration of 164 g/l (fig. 3). These experiments were carried out with rod titanium VT1; at 20°, the tendency of titanium toward passivation is apparent from the graph. The points corresponding to the steady state potentials of titanium at 90° are located a little higher. In this case, copper shifts the steady state potential to the positive side only slightly, so that titanium does not fall into the region of passivation, and this leads to an increase in the corrosion rate from 44 to 51 g/m^2 hr (0.002 g/l Cu) and to 56 g/m^2 hr (0.02 g/l Cu).

Thus, it may be stated in summary that the regularities corresponding to alloy VT1 are also characteristic of the other titanium alloys. The absolute values of the corrosion rates of titanium alloys are different from those of alloy VT1.

The alloys VT15, VT14, AT2-1, AT2-2, and AT2-3 displayed a good corrosion resistance in strong sulfuric acid solutions of nickel.

The other investigated alloys showed either a slightly higher or even a lower corrosion resistance than did alloy VT1. The study of the influence of the ions on the corrosion resistance of titanium alloys has led to the conclusion that the sulfate ion promotes the passivation of these alloys. Nickel ions basically activate the corrosion of titanium alloys, and copper ions act in a similar manner, but shift the steady state potential only slightly; if, however, the value of the steady state potential shifts into the passivation region, the corrosion is practically reduced to zero.

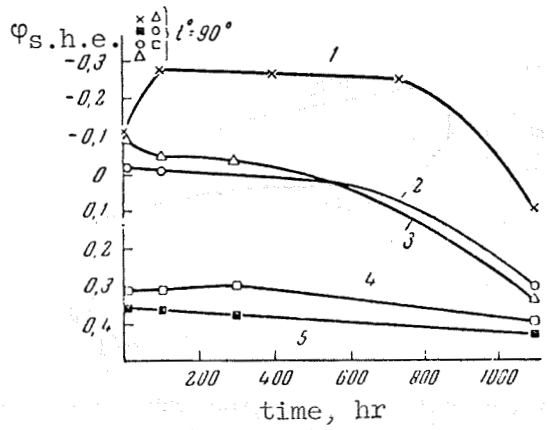

Figure 3. Change in the steady state potential of titanium VT1 in time with sulfuric acid containing additions of copper sulfate: 1, 164 g/l; 2, 164 g/l H_2SO_4 + 0.002 g/l Cu; 3, 164 g/l H_2SO_4 + 0.02 g/l Cu; 4, 164 g/l H_2SO_4 + 0.2 g/l Cu; 5, 164 g/l H_2SO_4 + 2.0 g/l Cu.

REFERENCES

1. Andreyeva, V. V. and Kazarin, V. I. Dokl. AN SSSR, Vol. 121, No. 5, p.873, 1958.

2. Tomashov, N. D., Al'tovskiy, R. M., and Arakelov, A. G. Dokl. AN SSSR, Vol. 121, No. 5, p. 885, 1958.

3. Stern, M. and Wissenberg, H. J. Electrochem. Soc., Vol. 106, p. 755, 1959.

4. Straumanis, M. E. and Chen, P. C. J. Electrochem. Soc., Vol. 98, p. 234, 1951.

5. Straumanis, M. E. and Jill, C. B. J. Electrochem. Soc., Vol. 101, p. 10, 1954.

6. Yatsimirskiy, K. B. and Vasil'yev, V. P. Instability Constants of Complex Compounds (Konstanty nestoykosti kompleksnykh soyedineniy). Izd-vo AN SSSR, 1959.

CHEMICAL STABILITY OF TITANIUM IN CERTAIN AGGRESSIVE MEDIA AND SCOPE OF ITS USE IN CHEMICAL INDUSTRIAL EQUIPMENT

S. M. Babitskaya, V. A. Strunkin,
T. P. Zal'tsman, and Yu. I. Sorokin

Effect of Chlorine on the Corrosion of Titanium in Sulfuric Acid

Chlorine inhibits the corrosion of titanium in 50 and 87 percent sulfuric acid at room temperature (ref. 1). It appeared interesting to study this phenomenon over a wider range of temperatures and sulfuric acid concentrations.

As is evident from the graph, the dependence of the solubility of titanium on the concentration of sulfuric acid is much more complex than on the concentration of hydrochloric acid: there are two maxima at concentrations of 40 and 80 percent and a minimum at 60 percent (independent of temperature). These data are in good agreement with those of Golden et al. (ref. 2).

At room temperature, titanium is stable toward sulfuric acid continuously saturated with chlorine and having concentrations of 10-80 percent. In 95 percent sulfuric acid, the corrosion rate of titanium does not exceed 0.1 mm/year during the first 50 hr, after 100 hr reaches 0.3 mm/year, and after 200 hr, about 0.8 mm/year. It should be noted that in the vapor over sulfuric acid saturated with chlorine and having concentrations of 80 and 95 percent, titanium specimens ignited after 34 and 7 hr, respectively.

At 60°, the protective action of chlorine is distinctly manifested only up to a 40 percent sulfuric acid concentration, above which it practically drops off to zero.

As the temperature rises to 90°, the protective action of chlorine is preserved up to a 40 percent concentration of sulfuric acid, the same as at 60°, but the corrosion rate is no less than 0.3 mm/year in 10 percent sulfuric acid, and in 40 percent sulfuric acid the corrosion rate reaches 1 mm/year.

It is interesting to note that in 60 and 95 percent sulfuric acid, chlorine increases the corrosion rate of titanium somewhat.

No ignition of specimens in the vapor was observed at 90° (the testing lasted 200 hr).

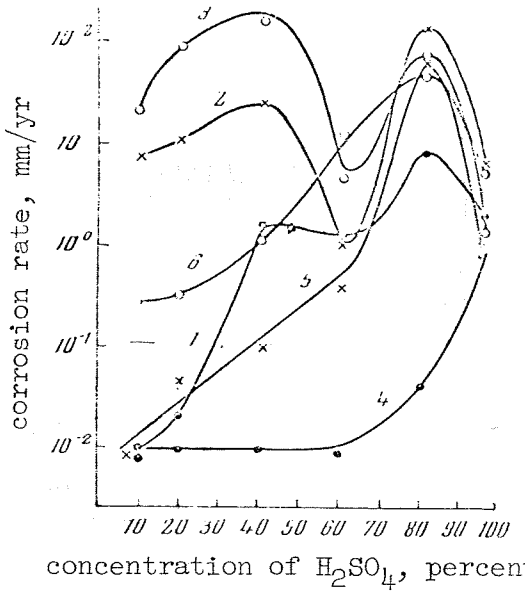

Figure 1. Effect of chlorine on the corrosion of titanium by sulfuric acid. 1--at 20°, without chlorine; 2--at 60° without chlorine; 3--at 90° without chlorine; 4-- at 20° with chlorine; 5--at 60° with chlorine; 6--at 90° with chlorine.

Chemical Stability of Titanium in Organic Acids

Organic acids are much weaker than mineral ones, as indicated by their dissociation constants (refs. 3, 4). For example, the dissociation constant of a 0.1 N solution of acetic acid is approximately 100 times smaller than the dissociation constant of a 0.1 N solution of hydrochloric acid.

No direct dependence of the corrosion rate of the metal on the dissociation constant is observed (ref. 5). Certain organic acids corrode metals considerably (refs. 5-10), differing very little in this respect from strong mineral acids. This is explained by their peculiar characteristics: high solubility of the salts formed, ability to form water-soluble complexes with metals, oxidation-reduction properties, and other properties. Thus, one should not state in advance that because of their weak dissociation organic acids are not very corrosive: it all depends on the surrounding conditions. Such slightly dissociated organic acids as acetic, formic, oxalic, maleic, phenoxyacetic, and certain other acids substantially corrode cast iron, steel and other metals. Still more corrosive are certain substituted organic acids whose dissociation constants are considerably higher. For example, trichloroacetic acid is comparable in strength to mineral acids.

The literature contains only sparse indications concerning the corrosion resistance of titanium in organic acids (refs. 9, 10).

Experiments which we carried out at 100° and with stirring have shown (see table) that in many organic acids titanium is characterized by a good corrosion resistance (the corrosion rate did not exceed 0.01 mm/year). However, in oxalic acid, titanium is strongly attacked (corrosion rate, about 100 mm/year, i.e., it is approximately the same as in 20 percent hydrochloric acid). An unsatisfactory stability of titanium was also observed in formic, tartaric, and citric acid, and also in a mixture of glacial acetic acid and acetic anhydride.

It is interesting to note that in 50 percent formic acid there is observed an unexplained scatter of data: one specimen was strongly attacked (corrosion rate, about 3.5 mm/yr), whereas the corrosion rates of the other two did not exceed 0.08 mm/year. The presence of the aldehyde group makes it possible to use this acid as a reductant. The strong acid properties of formic acid (its dissociation constant is 12 times that of acetic acid) and its aldehyde character promote the corrosion of metals whose chemical stability is based on the formation of an inert oxide film (titanium, stainless steels, aluminum).

The marked corrosion of titanium in hot solutions of oxalic and tartaric acid and the higher corrosiveness of citric acid are apparently due to the formation of complexes readily soluble in water.

In all cases, the corrosion was uniform, and in 50 percent citric acid pitting corrosion was observed.

New Areas of Application of Titanium in Industrial Chemical Apparatus

The study which was carried out has revealed new prospects for the use of titanium equipment in processes involving hydrochloric, hydrobromic, hydriodic and sulfuric acid containing free halogens.

Titanium is recommended as a structural material for apparatus designed for use in chlorination processes in a medium of hydrochloric acid.

At one plant, successful use has been made for more than a year of titanium tips of thermocouple sleeves operating under conditions of chlorination of the organic product in a medium of 18 percent hydrochloric acid at 60-65°. In order to provide for mechanical strength, the sleeve is made of two parts: the top from a thick-walled steel tube, and the bottom (the working surface of the sleeve) from titanium. The connection between the two parts is threaded. The steel and the contact area of the metals are rubberized. It is interesting to note that under these conditions the thermometer sleeve had once been used as an auxiliary electrode for a level gage. It was then supplied with an alternating current of industrial frequency. After a short time, corrosion was observed on the titanium, holes were formed through the entire thickness of the part, and the operation of the latter failed.

Laboratory experiments confirmed the harmful effect of alternating current on titanium; the same effect had been observed under industrial conditions. Indeed, specimens of titanium VT1 in a medium of 20 percent hydrochloric acid continuously saturated with gaseous chlorine at 60° displayed a pronounced pitting

TABLE. CORROSION OF TITANIUM VT1 IN ORGANIC ACIDS AT 100° WITH STIRRING.

Acid	Concentration, percent	Duration of tests, hr	Corrosion rate, mm/yr		
			in liquid	in vapor	At interface
Anthranilic	0,4	25	0,000	0,000	—
"	0,4	50	0,009	0,009	—
"	0,4	100	0,000	0,014	0,001
Azelaic	20	25	0,000	0,009	—
"	20	50	0,000	0,000	—
"	20	100	0,000	0,000	0,000
Adipic	20	25	0,000	0,000	—
"	20	50	0,000	0,000	—
"	20	100	0,000	0,000	0,000
Benzoic	30	25	0,000	0,000	—
"	30	50	0,000	0,000	—
"	30	100	0,000	0,000	0,000
Tartaric	25	25	0,029	0,000	—
"	25	50	0,038	0,005	—
"	25	100	0,174	0,000	0,113
"	50	25	0,793	0,000	—
"	50	50	0,707	0,019	—
"	50	100	0,798	0,000	0,734
Citric	25	25	0,019	0,000	—
"	25	50	0,019	0,000	—
"	25	100	0,007	0,000	0,004
"	50	25	0,162	0,000	—
"	50	50	0,304	0,000	—
"	50	100	0,241	0,002	0,302
Maleic	45	25	0,000	0,000	—
"	45	50	0,000	0,000	—
"	45	100	0,000	0,000	0,000
Monochloroacetic (molten)	—	25	0,000	0,009	—
"	—	50	0,009	0,000	—
"	—	100	0,002	0,000	0,003
Formic	50	25	0,076	0,000	—
"	50	50	3,467	0,005	—
"	50	100	0,007	0,000	1,886
p-aminobenzoic	0,4	25	0,000	0,000	—
"	0,4	50	0,000	0,000	—
"	0,4	100	0,000	0,000	0,000

TABLE (Continued)

Acid	Concentration, percent	Duration of tests, hr	Corrosion rate, mm/yr		
			in liquid	in vapor	At interface
Salicylic	0.17	25	0.000	0.000	—
"	0.17	50	0.000	0.000	—
"	0.17	100	0.003	0.002	0.001
Stearic (molten)	—	25	0.000	0.000	—
"	—	50	0.000	0.000	—
"	—	100	0.002	0.000	0.000
Trichloroacetic (molten)	—	25	0.000	0.000	—
"	—	50	0.000	0.000	—
"	—	100	0.000	0.000	0.003
Acetic (glacial) plus acetic anhydride	1:1	25	1.667	0.000	—
	1:1	50	1.640	0.000	—
	1:1	100	1.063	0.000	0.800
Fumaric	9	25	0.000	0.085	—
"	9	50	0.009	0.000	—
"	9	100	0.000	0.000	—
Phthalic	9	25	0.000	0.000	—
"	9	50	0.000	0.000	—
"	9	100	0.000	0.000	0.000
Phenoxyacetic	20	25	0.000	0.000	—
"	20	50	0.005	0.005	—
"	20	100	0.000	0.000	0.000
Phenoxyacetic (molten)	—	25	0.000	0.000	—
"	—	50	0.000	0.000	—
"	—	100	0.003	0.000	0.001
Oxalic	10	25	35.568	0.236	—
"	10	50	43.098	0.194	—
"	10	100	30.981	0.269	22.856
"	20	25	90.856	10.343	—
"	20	50	—	0.261	—
"	20	100	28.442	3.009	25.465
Malic	50	25	0.000	0.000	—
"	50	50	0.005	0.000	—
"	50	100	0.003	0.000	0.000
Succinic	6.5	25	0.000	0.000	—
"	6.5	50	0.000	0.000	—
"	6.5	100	0.000	0.70	0.000

corrosion after only 42 hr under the influence of alternating current of industrial frequency (current density, 3.5 A/dm^2). A surface 0.06 dm^2 in area had about 35 pits, each 1 mm deep.

A titanium bubbler for feeding gaseous chlorine operated successfully for over 600 hr in the course of chlorination of an organic product in hydrochloric acid at 50°. Before being introduced into the reactor, the chlorine from the cylinder is deliberately humidified, since dry gaseous chlorine ignites titanium even at room temperature.

It has been recommended that titanium equipment be used in the process of bromination of organic products in aqueous media at temperatures from zero to 3° (pH = 1). The bromination of the product is rapid (a few minutes), so that the possibility of separation of the bromine in a separate phase is excluded. Otherwise, the use of titanium equipment would be inadmissible because of the danger of pronounced local corrosion and even ignition of the metal.

In boiling aqueous solutions of maleic acid (particularly in the presence of organic solvents), the following metals corrode: carbon steel, stainless steels 1Kh18N9T and 1Kh18N12M3T, copper, nickel, aluminum, and lead.

In our laboratory it was shown that titanium VT1 is quite stable under these conditions. Titanium sleeves for thermocouples (wall thickness 1.5 mm) which have already been in operation for several thousand hours are being used by one plant in the dehydration of maleic acid.

An experimental laboratory column of a dehydrator of maleic acid was made of titanium VT1 and consists of 5 tube drums each 250 mm and 1.5-2 mm thick. The column operated for 200 hr without corrosion damage.

Summary

1. Titanium is distinguished by a good chemical stability in a series of organic acids. In addition, it was noted that in a mixture of glacial acetic acid and acetic anhydride, and in tartaric, formic, and particularly acetic acid, titanium is strongly attacked.

2. Free chlorine substantially inhibits the corrosion of titanium by sulfuric acid.

3. The study revealed new areas of application of titanium equipment in the chemical industry.

REFERENCES

1. Gleekman, L. W. Corrosion, Vol. 14, No. 9, p. 21. 1958.

2. Golden, L. B., Lane, I. R. and Acherman, W. L. Ind. Eng. Chem., Vol. 44, p. 1930, 1952.

3. Fieser, L. and Fieser, M. Organic Chemistry IL, 1949.

4. Karrer, P. Textbook of Organic Chemistry (Kurs Organicheskoy khimii). Goskhimizdat, 1960.

5. Tomashov, N. D. Theory of the Corrosion and Protection of Metals (Teoriya korrozii i zashchity metallov). Izd-vo AN SSSR, 1959.

6. Teeple, H. O. Corrosion, Vol. 8, No. 1, p. 14, 1952.

7. Rabald, E. Werkstoffe und Korrosion, Leipzig, Vol. 1, 1931.

8. Klinov, I. Ya. Corrosion of Chemical Apparatus and Corrosion-Resistant Materials (Korroziya khimicheskoy apparatury i korrozionno-stoykiye materialy). Mashingiz, 1960.

9. Labutin, A. L. Corrosion and Methods of Protecting Equipment in the Production of Organic Acids and Their Derivatives (Korroziya i sposob zashchity oborudovaniya v proizvodstve organicheskikh kislot i ikh proizvodnykh). Goskhimizdat, 1959.

10. Macleary, D. Z. Corrosion, Vol. 18, No. 2, p. 67, 1962.

CHEMICAL STABILITY OF TITANIUM IN HYDROHALIC ACIDS AND HALOGENS

Kh. L. Tseytlin, L. L. Fayngol'd and V. A. Strunkin

Effect of Halogens on the Corrosion of Titanium by Hydrohalic Acids

In industry, the choice of materials for the equipment used in processes involving hydrohalic acids is associated with certain difficulties. As a rule, halogens enhance the corrosion of metals by hydrohalic acids. Thus, in the presence of free chlorine, the rate of dissolution of iron, copper, nickel, lead and certain other metals in hydrochloric acid increases rapidly (ref. 1). A satisfactory stability under these conditions is displayed only by tantalum, a scarce and expensive metal (ref. 2).

At room temperature, titanium is stable in hydrochloric acid only up to a concentration of 5 percent. In 20 percent hydrochloric acid, the corrosion rate of titanium is 0.5 mm/yr, and in 36 percent HCl, it attains 41 mm/yr (ref. 3). Only general data are available concerning the chemical stability of titanium in hydrobromic and hydriodic acids (refs. 4 and 5).

It was interesting to determine the influence of halogens on the chemical stability of titanium in hydrohalic acid.

Until recently, no such data were available in the literature. Only in 1959-1960 were studies published which described the effect of chlorine on the corrosion of titanium by hydrochloric acid. Titanium was recommended as a structural material for chlorinating apparatus in aqueous media (ref. 6).

The corrosion rate of titanium in 6 N solutions of hydrohalic acids at room temperature is insignificant, less than 0.6 mm/yr (fig. 1). Titanium practically does not corrode in the vapors of the acids.

When the temperature is raised to 60°, the corrosion rate of titanium increases almost 100 times.

Titanium corrodes more strongly in hydrochloric than in hydrobromic acid. In the vapors of these acids, the corrosion increases markedly and reaches considerable proportions.

At 90°, the corrosion rate of titanium attains huge proportions (about 400 mm/yr in hydrochloric acid and 72 mm/yr in hydrobromic acid). In the vapors of these acids, the corrosion is considerably weaker, but still very substantial.

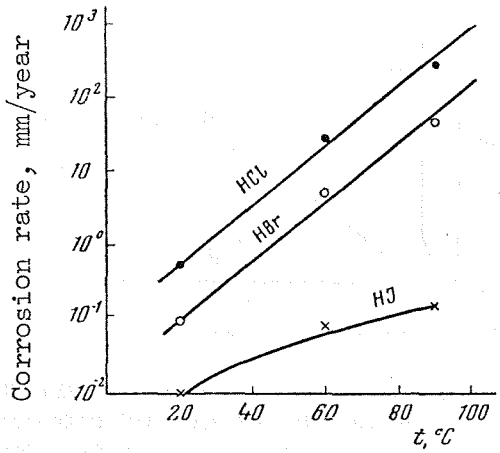

Figure 1. Effect of temperature on the rate of corrosion of titanium by 6 N solutions of hydrohalic acids for a testing time of 10 hrs.

An exception among hydrohalic acids is hydriodic acid. Experiments have shown that titanium is fairly stable in hydriodic acid containing free iodine up to 90° (the corrosion rate did not exceed 0.15 mm/yr). It should be noted that at the conclusion of the tests (after 1300 hrs), as a result of the pronounced oxidizability of hydriodic acid, the concentration of free iodine in the acid increased to 0.9 g-eq/l at 60° and to 3 g-eq/l at 90°. In order to tie up the free iodine into hydriodic acid, 1 percent of red phosphorus was added. Hydriodic acid was thus rid of free iodine, but was contaminated with a small amount of phosphorous acid H_3PO_3. In such a system at 60°, the corrosion rate of titanium did not exceed 0.043 mm/yr after 200 hrs, but was already 1.3 mm/yr after 500 hrs, and reached about 3 mm/yr after 1000 hrs.

In all cases, the addition of the halogen to hydrochloric and hydrobromic acid inhibits the corrosion rate of titanium (figs. 2 and 3), and the effect of protective action decreases with rising temperature.[1] At 20°, about 0.001 g-eq/l of free halogen is already sufficient for a complete cessation of the corrosion of titanium by 6 N HCl after 50 hrs of testing. At 60°, the effect of protective action reaches 250 at the maximum concentration of the halogen (the solution is initially saturated), and at 90°, the protective action of the halogen (with a single-stage saturation of the acid by the halogen) is observed only in the course of the first 5 hrs, after which it disappears completely.

As the initial halogen concentration rises, the dissolution rate of titanium decreases (fig. 3).

An increase in the testing time decreases the effectiveness of the protective action of the halogen.

---

[1]The effect of protective action is equal to the ratio of the corrosion rate in the pure acid to the corrosion rate in the halogen-containing acid.

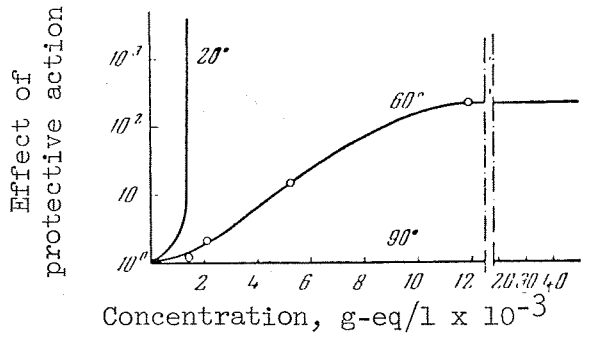

Figure 2. Influence of halogen concentration in 6 N HCl solution on the effect of protective action during the corrosion of titanium for a testing time of 50 hrs.

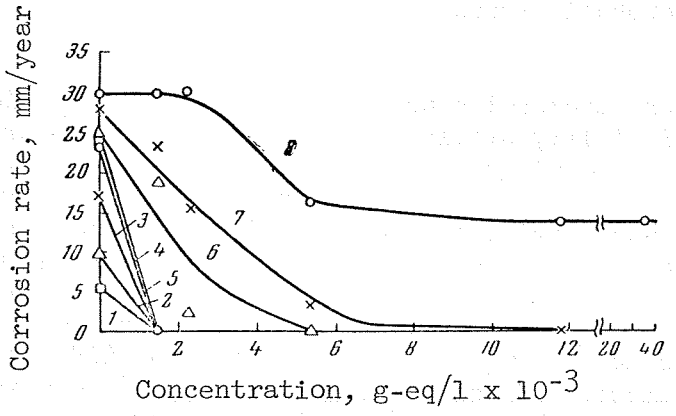

Figure 3. Influence of halogen concentration on the corrosion of titanium in 6 N solutions of hydrochloric and hydrobromic acids at 60° for the following testing times: 1, 10 hrs, HBr + Br_2; 2, 25 hrs, HBr + Br_2; 3, 50 hrs, HBr + Br_2; 4, 100 hrs, HBr + Br_2; 5, 10 hrs, HCl + Cl_2(Br_2, I_2); 6, 25 hrs, HCl + Cl_2(Br_2, I_2); 7, 50 hrs, HCl + Cl_2 (Br_2, I_2); 8, 100 hrs, HCl + Cl_2(Br_2, I_2).

Chlorine, bromine and iodine inhibit the corrosion rate of titanium by 6 N HCl to the same extent.

In 6 N HBr, the addition of bromine also substantially inhibits the corrosion rate of titanium, but the protective action of bromine in this case is longer and is manifested at higher temperatures (up to 90°) than in the case of hydrochloric acid.

Chlorine was used as an example to show the effect of hydrochloric acid concentration on the rate of corrosion of titanium by the pure acid and acid in the presence of the halogen (fig. 4). At room temperature, titanium is stable at any concentrations of hydrochloric acid being continuously saturated with gaseous chlorine, at 60° it is stable up to an HCl concentration of 20 percent, and at 90°, it is stable only up to an HCl concentration of 5 percent. In 30 percent and 36 percent HCl at 90°, the protective action of chlorine is almost nil.

As shown by the course of the curves representing the electrode potential of titanium versus time (fig. 5), the addition of chlorine shifts the potential toward more positive values; this effect is more pronounced the higher the initial concentration of free chlorine in the solution. With time, the potential returns to less noble values.

As the temperature rises, the potential shifts into the region of negative values. Thus, the electrochemical data essentially confirm the data of the gravimetric method of determining the corrosion of titanium.

In the view of many researchers, the dissolution rate is determined by the electrode potential and is independent of the manner in which a given value of the potential is maintained, whether by polarizing the metallic sample by an external anodic current or by introducing an oxidant into the solution (refs. 7-11). When chlorine is introduced into hydrochloric acid, the titanium potential assumes values from +0.3 to +1.1V, which corresponds to the region of passivated titanium on the potentiostatic curve recorded under the same conditions.

A higher stability of titanium (rise in the upper temperature limit of stability to 90°, longer-lasting protective action of the halogen in hydrobromic

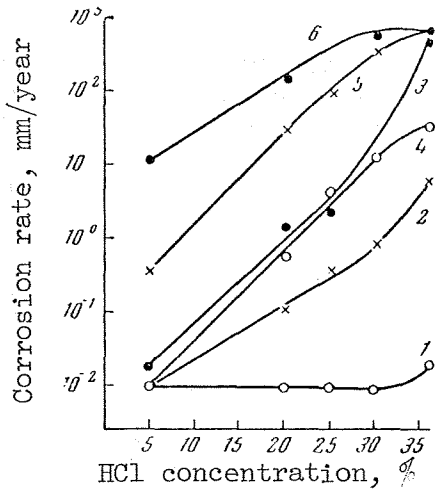

Figure 4. Influence of chlorine on the corrosion of titanium by hydrochloric acid: 1, at 20° with chlorine; 2, at 60° with chlorine; 3, at 90° with chlorine; 4, at 20° without chlorine; 5, at 60° without chlorine; 6, at 90° without chlorine.

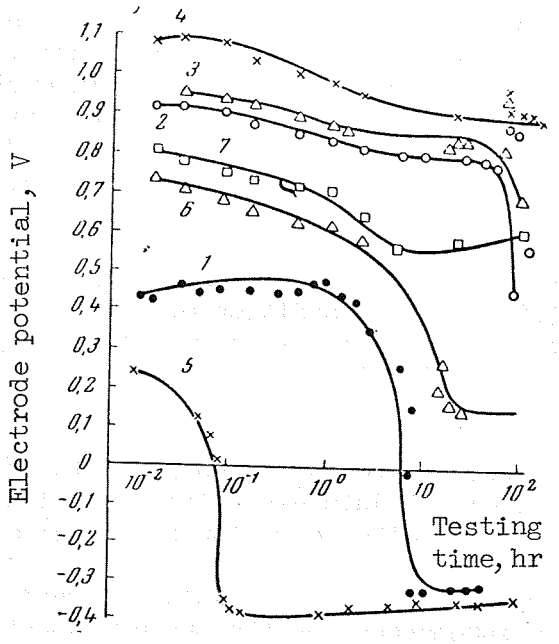

Figure 5. Influence of chlorine concentration on the electrode potential of titanium in 6 N HCl: 1, without chlorine at 25°; 2, 0.01 g-eq/l Cl_2 at 25°; 3, 0.027 g-eq/l Cl_2 at 25°; 4, 0.069 g-eq/l Cl_2 at 25°; 5, without chlorine at 60°; 6, 0.002 g-eq/l Cl_2 at 60°; 7, 0.056 g-eq/l Cl_2 at 60°.

and hydriodic acid with additions of free bromine or iodine, respectively, than in hydrochloric acid containing free chlorine) is explained by the greater stability of the complex HBr_3 and HI_3 as compared to HCl_3 (the equilibrium $X_2 + X^1 \rightleftarrows X_3^1$, where X is the halogen, is almost completely displaced to the left for HCl).

In the view of N. D. Tomashov and R. M. Al'tovskiy (ref. 12), the passivation of titanium in this case is due to the adsorption of the X_3^1 ion on its surface; a film is thus formed which consists of an adsorbed and possibly a chemical phase compound of titanium with bromine or iodine. This film raises the overvoltage of hydrogen, as a result of which the corrosion rate of titanium decreases.

Chemical Stability of Titanium toward Chlorine, Bromine and Iodine

The first mention of the stability of titanium toward halogens dates back to 1850, when Wohler wrote that metallic titanium burns effectively in gaseous chlorine, but does not react with it at room temperature (ref. 13). Titanium was obtained in the form of a dark-gray powder by reducing potassium fluotitanate with metallic potassium. The chemical composition of chlorine and titanium was was not given.

In 1895, Moissan found that a material containing 95-97 percent Ti and 2-4 percent C reacts with chlorine at 325°, thereby becoming incandescent, and reacts with bromine at 360° and with iodine at higher temperatures without any appreciable incandescence. This material was obtained by heating a mixture of titanic acid with carbon in an electric furnace. This was an amorphous substance which could be readily crushed in an agate mortar and had a specific gravity of 4.87 (refs. 14 and 15).

From then on, the incorrect view that titanium reacts with chlorine, bromine and iodine only at high temperatures (325° and higher) has spread in the literature and prevails until today (refs. 16-26). However, there are also indications in the literature that pulverized titanium ignites in gaseous chlorine and liquid bromine at room temperature, and in iodine on moderate heating (refs. 27 and 28).

Recently, several studies have been published in which it is stated, among other things, that titanium reacts vigorously with chlorine at room temperature and even at -18° (refs. 4, 6 and 29). However, no direct proof of the inflammation of titanium in gaseous chlorine is given.

Our experiments have shown that sheet titanium VT1 ignites in gaseous chlorine (from a cylinder in which chlorine contains no more than 0.03 percent of moisture) at room temperature in 24 hrs; if however, the gaseous chlorine is additionally dried by being passed through concentrated sulfuric acid, the ignition of the metal takes place in 14 hrs. In reactive liquid bromine, titanium also ignites at room temperature in only 10 min, and in dry crystalline iodine, in 15 min only at 100°. A pronounced corrosion of titanium in iodine is observed even at 60°, but at room temperature titanium did not corrode for 500 hrs; longer tests were not carried out (table 1).

It seemed of interest also to determine the influence of water on the reaction of titanium with halogens. This can be done most conveniently with liquid bromine, particularly since the literature contains only general information on the stability of titanium toward wet bromine, these data being quite contradictory. For example, one of the sources asserts that wet chlorine and bromine do not attack titanium (ref. 5), while another states that liquid, dry and moist bromine attacks titanium very rapidly (ref. 4). We did not find any more specific data.

Our experiments showed (table 2) that titanium reacts vigorously not only with dry liquid bromine but also with wet bromine. Water retards the reaction, but even in the presence of considerable amounts of water titanium undergoes a pronounced localized corrosion in the bromine phase.

TABLE 1. EFFECT OF TEMPERATURE ON THE CHEMICAL STABILITY OF TITANIUM IN IODINE.

Temperature of experiment, °C	Testing time, hr	Average corrosion rate, mm/yr	Remarks
20	500	0.00	external appearance of specimen did not change
60	40	0.80	pitting corrosion
80	40	4.50	localized corrosion, strongly corroded edges
90	40	11.0	localized corrosion, strongly corroded edges
100	0.25	7500	intense heating-up, specimens ignited
110	0.25	7500	intense heating-up, specimens ignited

TABLE 2. EFFECT OF WATER ON THE CHEMICAL STABILITY OF TITANIUM IN BROMINE AT ROOM TEMPERATURE

Amount of water introduced into bromine, wt %	Testing time, hr	Average corrosion rate, mm/yr	Remarks
0.05	0.40	>3000	after 25 min, the specimen ignited with a bright flame. After the specimen was removed, deep pits (2.5 mm) were observed on its surface
0.10	0.75	>1700	after 45 min, the solution began to boil, the specimen brightened, then ignited with a bright flame. It burned for 3 min. Deep pits were formed on the surface of the specimen
0.5	1.0	>1200	the specimen ignited after 1 hr. Deep pits formed on its surface
1.0	2.0	~700	the specimen ignited after 2 hrs. Deep pits were formed on its surface
5.0	1000	0.4	after 200 hrs of testing, the specimen retained its original appearance, and after 1000 hrs, deep pits (up to 2.5 mm) formed on some parts of the surface
60.0	500	~400	after 200 hrs of testing, the specimen retained its original appearance, and after 500 hrs, deep pits (up to 3 mm) were formed on some parts of the surface, and whole pieces were eaten away

Together with untouched sections of lustrous surface, deeply pitted areas were observed; whole pieces of the specimen were corroded away, particularly at the edges (fig. 6). The strong localized attack of titanium can be explained by the inhomogeneity of the media (the solubility of water in bromine is 0.05 percent, and that of bromine in water, 3 percent).

In this connection, it should be noted that the literature gives the incorrect impression that titanium is not subject to localized attack.

In aqueous solutions of bromine (saturated solution) titanium is stable up to 90° (no experiments were carried out at higher temperatures).

The following qualitative explanation of the high reactivity of titanium toward halogens may be accepted. In order for the reaction to take place in the form of combustion, the following conditions must be met (ref. 30):

1. The reaction should be highly exothermic;

2. The reaction should take place at a high rate, which in turn depends on the activation energy of the molecules of the reacting substances;

3. The products of the reaction should be partly or completely gaseous;

4. The reaction should be self-sustaining, which, strictly speaking, follows from the first condition, since the reaction rate increases with rising temperature.

The heats of formation of $TiCl_4$, $TiBr_4$ and TiI_4 are respectively equal to 179.3, 155 and 102 kcal/mole (ref. 31), i.e., the reactions of titanium with chlorine, bromine and iodine are strongly exothermic. The melting points of the halides are respectively -23, +39, +150°, and the boiling points are 136,

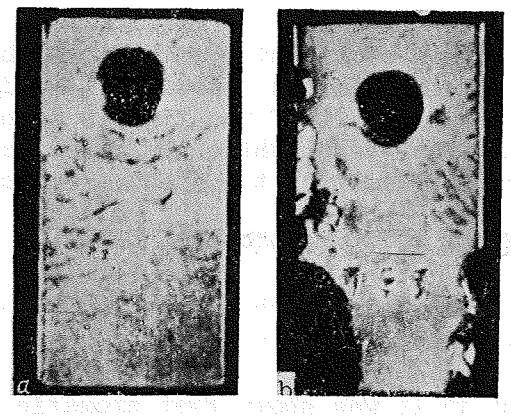

Figure 6. Localized corrosion of titanium in bromine containing 60 percent water at room temperature (specimen placed in bromine phase): a, control specimen; b, specimen after testing (500 hrs).

230 and 377° (ref. 32). This means that the corrosion products (TiX_4, where X is the halogen) do not adhere well to the metal, run off the surface, or evaporate when sufficiently heated by the heat of reaction. Fresh portions of titanium, which had already been heated, immediately enter into the reaction. There finally comes a moment when the outflow of heat (loss to the surrounding medium) becomes less than its inflow caused by the heat of reaction, and ignition takes place.

The activation energy of the reactions of titanium with chlorine and bromine is apparently of the order of several units (up to 10 kcal/mole). Only under those conditions can the reaction proceed rapidly and in the form of combustion at room temperature. The activation energy of the reaction of titanium with iodine is considerably less (a few tenths of a kcal/mole), and for this reason ignition occurs only on heating to 100°.

The reaction of titanium with halogens would proceed much faster (particularly in the case of the reaction with gaseous chlorine) if it were not for the tendency of titanium (like that of aluminum) to passivate quickly in the presence of moisture or air. Indeed, as was shown by electron diffraction measurements (ref. 33), when titanium is left standing in air, a film is formed very quickly which consists of two layers: the oxide layer as such, which is chemically bound to the base metal, and a polymolecular layer of physically adsorbed gas or a mixture of the gas with water. This film, frequently invisible even to the aided eye, is compact and has good adhesive properties. Diffusion through such a film is slow, and this explains the extremely low initial rate of reaction of titanium with gaseous chlorine. It should be noted that broken-up particles of a white film of titanium dioxide were found at the end of the reaction of titanium with halogens. Hence, TiO_x, which makes up the natural film on titanium, does not react with halogens when exposed for a short time even to high temperatures. This in turn means that the film on titanium formed in air contains pores and that the reaction of titanium with halogens proceeds through these pores.

In our case, the reaction of titanium with liquid bromine proceeds much more quickly (10 min) than with gaseous chlorine (14 and 24 hrs). This is due to the fact that a considerable part of the time is spent in removing the air and moisture from the reaction vessel while the chlorine is passed; in addition the reaction is made more difficult by the steady removal of heat by constantly renewed portions of gaseous chlorine.

Effect of Aromatic Nitro Compounds on the Corrosion of Titanium by Hydrochloric Acid

In references 34 and 35 it was shown that aromatic nitro compounds most often enhance the corrosion of iron, copper, lead, aluminum and their alloys by electrolytes. An exception was α-nitronaphthalene, which in many cases did not affect the corrosion process.

The authors account for the enhanced corrosion by an effective depolarizing influence of oxidizing nitro compounds on the cathodic process. A short time later, a mechanism of this phenomenon was proposed by I. V. Oknin (ref. 36), but it was experimental and based on electrochemical measurements.

No such data are available on titanium.

Our experiments (table 3) showed that up to 60° almost all of the investigated aromatic nitro compounds (10 itmes) markedly (100 times or more) inhibit the rate of corrosion of titanium by agitated hydrochloric acid in the liquid, in the vapor, and at the interface.

It is interesting to note that in the presence of p-nitroaniline (at 60°), of two samples in the liquid phase, one was highly corroded (about 1.3 mm/yr), while the corrosion rate of the other sample did not exceed 0.13 mm/yr. No explanation was found for this phenomenon.

The above-described orderly pattern of the inhibiting influence of nitro compounds on the corrosion of titanium is upset at 80°. A pronounced protective action was observed only in the presence of o-nitrotoluene, o-nitrophenol, m-dinitrobenzene and 1,2,4-dinitrochlorobenzene. In all the remaining cases, the protective effect was insufficient and a still-unexplained scatter of the data was observed (pronounced inhibition of the corrosion rate in the liquid phase and considerable corrosion in the vapor and at the interface).

Experiments in stationary 6 N HCl showed that under these conditions at temperatures up to 60°, nitrobenzene, o- and m-dinitrobenzene and 1,2,4-dinitrochlorobenzene effectively inhibit the corrosion of titanium. The remaining seven of the eleven nitro compounds considered either have no appreciable effect on the corrosion process or cause a scatter of the data.

At 80°, all the nitro compounds studied have no appreciable effect on the corrosion rate.

The concentration of the nitro compound in agitated 6 N HCl has a substantial influence on the corrosion of titanium at 60°.

A decrease in the amount of the nitro compound added from 0.5 to 0.005 percent sharply decreases the effect of protective action.

Summary

1. Free halogens markedly inhibit the corrosion of titanium by hydrochloric, hydrobromic and hydriodic acid.

2. Titanium ignites at room temperature in dry gaseous chlorine (from a cylinder) in 24 hrs, in liquid bromine in 10 min, and in dry crystalline iodine at 100° in 15 min. Water inhibits the reaction of titanium with liquid bromine, but does not exclude a strong localized attack and even the inflammation of titanium. The use of titanium equipment is inadmissible in cases where the separation of bromine as a separate phase is possible.

TABLE 3. EFFECT OF AROMATIC NITRO COMPOUNDS (CONCENTRATION, 0.5 PERCENT) ON THE RATE OF TITANIUM CORROSION IN 20 PERCENT HYDROCHLORIC ACID AT A STIRRING RATE OF 300 RPM AND A TESTING TIME OF 10 HRS.

Additive	Titanium corrosion rate, mm/yr		
	in liquid	in vapor	at interface
Temperature 40°			
--	4.94	0.05	2.73
nitrobenzene	0.09	0.02	0.01
o-nitrotoulene	0.20	0.05	0.01
p-nitrotoulene	0.07	0.02	0.01
o-nitrophenol	0.07	0.03	0.03
p-nitrochlorobenzene	0.02	0.05	0.03
p-nitroaniline	0.07	0.03	0.09
o-dinitrobenzene	0.06	0.03	0.01
m-dinitrobenzene	0.07	0.05	0.02
1,2,4-dinitrochlorobenzene	0.09	0.01	0.03
picric acid	0.09	0.09	0.01
α-nitronaphthalene	0.04	0.01	0.09
Temperature 60°			
--	12.68	3.89	7.08
nitrobenzene	0.01	0.01	0.03
o-nitrotoulene	0.01	0.01	0.05
p-nitrotoulene	0.01	0.01	0.01
o-nitrophenol	0.07	0.03	0.10
p-nitrochlorobenzene	0.23	0.10	0.07
p-nitroaniline	1.34; 0.13	0.04	6.45
o-dinitrobenzene	0.05	0.01	0.09
m-dinitrobenzene	0.20	0.10	0.19
1,2,4-dinitrochlorobenzene	0.12	0.03	0.12
picric acid	0.02	0.01	0.13
α-nitronaphthalene	0.19	0.01	0.08
Temperature 80°			
--	60.92	81.70	42.62
nitrobenzene	33.05	0.21	0.17
o-nitrotoulene	0.92	0.11	0.11
p-nitrotoulene	32.46	5.49	--
o-nitrophenol	1.01	0.73	2.63
p-nitrochlorobenzene	8.86	0.06	3.60
p-nitroaniline	1.80	42.07	38.18
o-dinitrobenzene	0.41; 0.01	78.28	46.34
m-dinitrobenzene	0.67	0.02	0.46
1,2,4-dinitrochlorobenzene	0.55	0.01	0.10
picric acid	0.47	47.37	0.05
α-nitronaphthalene	52.54	26.32	42.60

Note: 1. The column "in liquid" gives the average values of the corrosion rates of two specimens; both values were recorded if they differed sharply from each other.
2. In all cases, the nature of the corrosion was uniform.

3. The retarding effect of aromatic nitro compounds on the corrosion of titanium by hydrochloric acid was established.

REFERENCES

1. Tseytlin, Kh. L. and Sorokin, Yu. I. Zhurnal Prikladnoy Khimii, Vol. 33, No. 1, p. 163, 1960.

2. Romanushkina, A. Ye. and Polyakova, K. K. Khimicheskaya Promyshlennost', No. 6, p. 535, 1959.

3. Golden, L. B., Lane, I. R. and Acherman, W. L. Ind. Eng. Chem., Vol. 44, p. 1930, 1952.

4. Cotton, I. B. and Bradley, H. Chem. a. Ind., Vol. 22, p. 640, 1958.

5 Rüdiger, O., Fischer, W. R. and Knorr, W. Zs. Metallkunde, Vol. 47, p. 8, 1956.

6. Avt. svid. SSSR No. 126873, Byull. izobr., No. 6, p. 18, 1960; Tseytlin, Kh. L. and Strunkin, V. A. Zh. Prikl. Khim., Vol. 33, No. 12, p. 2796, 1960.

7. Uhlig, H. H. and King, P. F. J. Electrochem. Soc., Vol. 106, p. 1, 1954.

8. Kolotyrkin, Ya. M. and Knyazheva, V. M. Zhurnal Fizicheskoy Khimii, Vol. 30, No. 9, p. 1990, 1956.

9. Bune, N. Ya. and Kolotyrkin, Ya. M. Doklady AN SSSR, Vol. 111, No. 5, p. 1050, 1956.

10. Kolotyrkin, Ya. M. Probl. Fiz. Khim., No. 1, pp. 81-93, 1958.

11. Bune, N. Ya. and Kolotyrkin, Ya. M. Zh. Fiz. Khim., Vol. 35, No. 7, p. 1543, 1961.

12. Tomashov, N. D. and Al'tovskiy, R. M. Zh. Fiz. Khim., Vol. 33, No. 3, p. 610, 1959.

13. Wöhler, F. Lieb. Ann., Vol. 73, p. 34, 1850.

14. Moisson, H. C. r., Vol. 120, p. 290, 1895.

15. Weiss, L. and Kaiser, H. Zs. anorg. Chem., Vol. 65, p. 345, 1910.

16. Ullman, F. Enzyklopädie der technischen Chemie, Berlin, Vol. 11, p. 176, 1922.

17. Technical Encyclopedia (Tekhnicheskaya entsiklopediya), Vol. 23, p. 434, 1934.

18. Morozov, O. N. Chemistry of Rare Metals (Khimiya redkikh metallov). GONTI NKTP State United Publishing House of Science and Technology, People's Commissariat of the Textile Industry, 1938.

19. Luchinskiy, G. P. Titanium Chemistry (Khimiya titana). Goskhimizdat, 1941.

20. Gmelins Handbuch der anorganische Chemie, Syst.-Numm, 41, 1951.

21. Nekrasov, V. V. Textbook of General Chemistry (Kurs obshchey khimii). Goskhimizdat, 1961.

22. Metal Corrosion (Korroziya metallov), Vol. 1, A handbook, edited by H. H. Uhlig, transl. ed. V. V. Skorchelletti, Goskhimizdat, 1952.

23. Filyand, M. A. and Semenova, Ye. I. Properties of Rare Elements (Svoystva redkikh elementov). A handbook, GONTI, 1953.

24. Kornilov, I. I. Khimicheskaya Nauka i Promyshlennost', Vol. 3, No. 6, p. 803, 1958.

25. --- Uspekhi Khimii, Vol. 23, No. 5, p. 529, 1954.

26. Yeremenko, V. N. Titanium and Its Alloys (Titan i yego splavy). Izd-vo AN SSSR, Kiev, 1960.

27. Klemm, W. and Grimm, L. Zs. anorg. Chem., Vol. 249, p. 198, 1942.

28. Hutschinson, G. E. and Permar, P. H. Corrosion, Vol. 5, No. 10, p. 319, 1949.

29. Macleary, D. Z. and Kuhn, M. E. Chem. Proc., Vol. 20, No. 7, p. 67, 1957.

30. Andreyev, K. K. Thermal Decomposition and Combustion of Explosives (Termicheskoye razlozheniye i goreniye vzryvchatykh veshchestv). Gosenergoizdat, 1957.

31. Latimer, V. Oxidation States of Elements and Their Potentials in Aqueous Solutions. IL., 1954.

32. Britske, E. V., Kapustinskiy, A. F., Veselovskiy, B. K., Shamovskiy, L. M., Chentsova, A. G. and Anvayer, B. I. Thermal Constants of Inorganic Substances (Termicheskiye konstanty neorganicheskikh veshchestv). Izd-vo AN SSSR, 1949.

33. Andreyeva, V. V. Trudy instituta fizicheskoy khimii, Izd-vo AN SSSR, Vol. 2, No. 4, p. 79, 1957

34. Pershke, V. K. and Vinogradova, A. S. Promyshlennost' Organicheskoy Khimii, Vol. 2, No. 20, p. 419, 1936.

35. Pershke, V. K. and Voroshilova, M. A. Prom. Org. Khim., Vol. 5, No. 8-9, p. 562, 1938.

36. Oknin, I. V. Zh. Fiz. Khim., Vol. 13, No. 5, p. 631, 1939.

EFFECT OF SODIUM NITRITE ON THE CORROSION OF TITANIUM BY HYDROCHLORIC AND SULFURIC ACID

Yu. I. Sorokin and Kh. L. Tseytlin

The corrosion of titanium by hydrochloric and sulfuric acid is inhibited in the presence of oxidizing agents and anodic polarization (refs. 1-6). The presence of nitric acid in hydrochloric and sulfuric acid passivates the titanium considerably, as confirmed by the slight corrosion of titanium in cold aqua regia (refs. 7 and 8). A virtually complete passivation of titanium is observed in 20 percent hydrochloric acid at room temperature in the presence of 1.3 percent nitric acid (ref. 9). Etching hydrochloric acid solutions containing hydrofluorides become less active toward titanium when they have accumulated a certain quantity of Ti^{+4} ions (ref. 10). Among the oxidants depressing the corrosion of titanium in acids, little attention has been given to the salts of nitrous acid, which are widely used in industry and have strong oxidizing properties. There is evidence to indicate that the addition of sodium nitrite inhibits the dissolution of titanium by hydrochloric acid even at 50° (ref. 11). For this reason, heat-exchange elements made of titanium should be used in the processes of diazotization of aniline, methanilic acid and p-chloro-o-aminophenol, which take place with the participation of hydrochloric acid and sodium nitrite (ref. 12). It appeared of interest to study in somewhat greater detail the influence of sodium nitrite on the corrosion of titanium by hydrochloric and sulfuric acid.

Experimental Section

Sheet titanium VT1-1 was used in the investigation. The experiments were carried out in a six-compartment glycerin thermostat, using the technique described in reference 13. Polished specimens of titanium (50 x 10 x 3 mm) suspended on hooks of glass stirrers were tested in three-neck glass flasks. The samples were continuously rotated at the rate of 100 rpm. For comparison, experiments were carried out without stirring. The corrosive media used were pure 20 percent hydrochloric and sulfuric acid in the amount of 600 ml, to which sodium nitrite (analytically pure) had been added. The glass flasks were provided with reflux condensers to which air had free access. There was 100 ml of acid for every 10 cm^2 of surface of the sample. After 10, 50, 100 and 200 hrs of testing, the samples were removed from the corrosive medium, washed with water, dried and weighed. The corrosive liquid was not renewed after each weighing. In order to plot the curves, use was made of the data of tests of two parallel titanium samples.

The experiments showed that titanium has a satisfactory stability in 20 percent hydrochloric and sulfuric acid at 0 and 10° (after a 200-hr test, the corrosion rate did not exceed 0.1 mm/yr). Under these conditions, the addition of nitrite has practically no effect on the corrosion rate of titanium. In quiescent 20 percent hydrochloric acid at 20°, titanium depassivates quickly and is attacked at the rate of approximately 0.5 mm/yr (fig. 1). With stirring, the access of atmospheric oxygen to the surface of titanium is accelerated, affecting the decrease in the corrosion rate during the initial period of the test. When the acid has acted for a long time, the dissolution rates of titanium in stationary and agitated media become similar. The addition of 0.001 percent $NaNO_2$ decreases the corrosion rate of titanium in quiescent and agitated hydrochloric acid to 0.02 mm/yr only in the course of the 100-hr testing period. The addition of 0.01 percent $NaNO_2$ provides for a high stability of titanium in the course of the entire testing period.

A rise in temperature to 60° sharply increases the corrosion rate of titanium in 20 percent hydrochloric acid (up to 300 mm/yr), and stirring at this temperature has virtually no effect (fig. 2). The addition of nitrite retards the dissolution of titanium at 60° as well, but in this case the concentration of the oxidant must be raised to 0.1 percent in order to decrease the corrosion rate to 0.1 mm/yr.

In the presence of 0.01 percent $NaNO_2$, a marked inhibition of the reaction is observed for only about 10 hrs.

At 100°, the rate of corrosion of titanium by hydrochloric acid increases to 200 mm/yr (fig. 3) and agitation also has virtually no effect on the reaction rate. A considerable decrease in the corrosion rate of titanium (to 0.6-2.0 mm/yr) is observed at an initial nitrite concentration of 1 percent.

In unagitated 20 percent hydrochloric acid at 20°, titanium has a negative electrode potential (about -0.4 V) which undergoes little change with time (fig. 4). The addition of 0.001 percent $NaNO_2$ shifts the potential into the passive region (above +0.4 V) but only during the initial period of the testing (about 20 hrs). As the duration of the testing increases, this concentration becomes insufficient to preserve the stable passive state of titanium characterized by the region of positive potential values of +0.4 V and higher (ref. 6). In the presence of 0.01 percent $NaNO_2$, the positive potential (about +0.7 V) is preserved during the entire testing period. At 60°, the electrode potential of titanium shifts into the passive region if the initial nitrite concentration is 0.1 percent or higher. The addition of 1 percent $NaNO_2$ ensures the preservation of the positive potential in the course of the entire period of testing, but in this case there is observed an appreciable tendency of activation of the titanium surface with time.

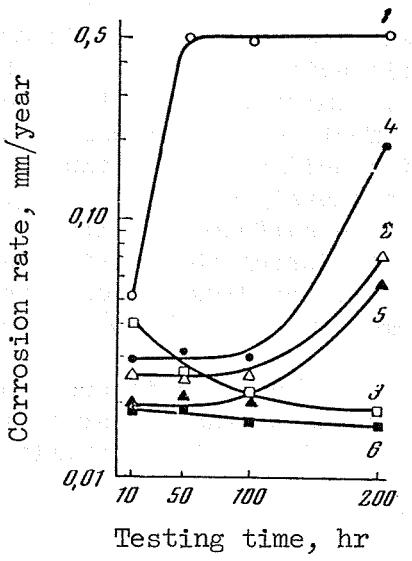

Figure 1. Effect of sodium nitrite on the corrosion of titanium in 20 percent hydrochloric acid at 20 percent: 1, 20 percent HCl without stirring; 2, 20 percent HCl + 0.001 percent $NaNO_2$ without stirring; 3, 20 percent HCl + 0.01 percent $NaNO_2$ without stirring; 4, 20 percent HCl with stirring; 5, 20 percent HCl + 0.001 percent $NaNO_2$ with stirring; 6, 20 percent HCl + 0.01 percent $NaNO_2$ with stirring.

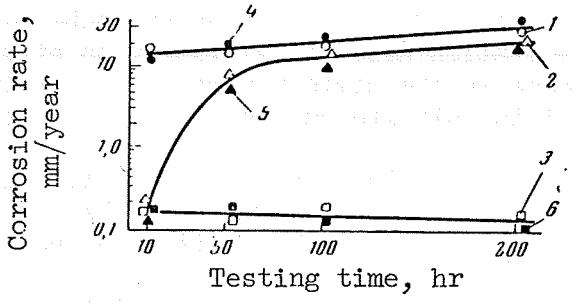

Figure 2. Effect of sodium nitrite on the corrosion of titanium by 20 percent hydrochloric acid at 60°: 1, 20 percent HCl without stirring; 2, 20 percent HCl + 0.01 percent $NaNO_2$ without stirring; 3, 20 percent HCl + 0.1 percent $NaNO_2$ without stirring; 4, 20 percent HCl with stirring; 5, 20 percent HCl + 0.01 percent $NaNO_2$ with stirring; 6, 20 percent HCl + 0.1 percent $NaNO_2$ with stirring.

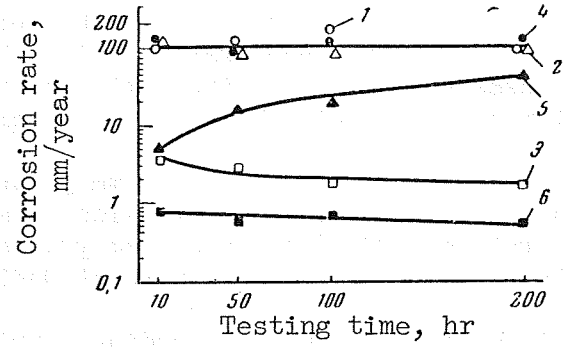

Figure 3. Effect of sodium nitrite on the corrosion of titanium by 20 percent hydrochloric acid at 100°: 1, 20 percent HCl without stirring; 2, 20 percent HCl + 0.1 percent $NaNO_2$ without stirring; 3, 20 percent HCl + 1.0 percent $NaNO_2$ without stirring; 4, 20 percent HCl with stirring; 5, 20 percent HCl + 0.1 percent $NaNO_2$ with stirring; 6, 20 percent HCl + 1.0 percent $NaNO_2$ with stirring.

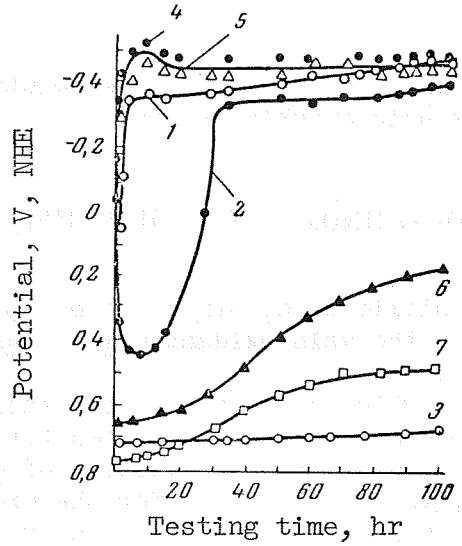

Figure 4. Effect of sodium nitrite on the electrode potential of titanium in 20 percent hydrochloric acid: 1, 20 percent HCl, at 20°; 2, 20 percent HCl + 0.001 percent $NaNO_2$ at 20°; 3, 20 percent HCl + 0.01 percent $NaNO_2$, at 20°; 4, 20 percent HCl, at 60°; 5, 20 percent HCl + 0.01 percent $NaNO_2$, at 60°; 6, 20 percent HCl + 0.1 percent $NaNO_2$, at 60°; 7, 20 percent HCl + 1.0 percent $NaNO_2$ at 60°.

As in hydrochloric acid, in quiescent 20 percent sulfuric acid at 20°, titanium quickly depassivates and corrodes at the rate of about 0.6 mm/yr. Agitation decreases the corrosion rate of titanium only during the initial testing period. In prolonged testing, the dissolution rates of titanium in quiescent and agitated sulfuric acid become similar, as was the case in hydrochloric acid. The addition of 0.001 percent $NaNO_2$ is sufficient for the passivation of titanium in quiescent and agitated sulfuric acid during the entire testing period.

A rise in temperature from 60 to 100° sharply increases the corrosion rate of titanium in 20 percent sulfuric acid, and stirring has practically no effect on this rate in sulfuric acid of such concentration (figs. 5 and 6). Sodium nitrite has basically the same effect on the inhibition of the reaction as hydrochloric acid. The addition of 0.1 percent $NaNO_2$ at 60° decreases the corrosion rate of titanium by 20 percent sulfuric acid to 0.1 mm/yr and is insufficient for a significant and lasting decrease in the corrosion rate at 100°. A sharp decrease in the corrosion rate at 100° (to 0.6-0.8 mm/yr) is observed in 20 percent sulfuric acid only in the presence of 1 percent $NaNO_2$.

In 20 percent sulfuric acid at 20 and 60°, sodium nitrite shifts the electrode potentials of titanium to the positive side in essentially the same way as in hydrochloric acid.

Sodium nitrite quickly decomposes in its reaction with acids to form nitrogen oxides:

$$2NaNO_2 + 2H^+ = 2Na^+ + NO_2 + NO + H_2O \quad [14].$$

Nitrous acid can exist only in dilute aqueous solutions at low temperature. At room temperature, nitrous acid quickly oxidizes:

$$3HNO_2 = HNO_3 + 2NO + H_2O \quad [15].$$

It may be assumed that nitric acid, being the end product of the reaction of nitrite with acids, can be the main oxidant which passivates titanium.

A comparison of the data which we obtained (see table) shows that the addition of low concentrations of nitrite passivates titanium in hydrochloric and sulfuric acid more effectively than the addition of equivalent quantities of nitric acid. Apparently, the chief reason for the greater passivating effect of nitrite in this case is the formation of nitrogen oxide upon the decomposition of the salt. It should be noted that the addition of 0.02 percent $NaNO_2$ also protects chromium-nickel-molybdenum steel against corrosion in 28 percent sulfuric acid at 70° (ref. 16).

There is no fundamental difference between the chemical passivation of a metal in solutions of oxidants and its anodic passivation (ref. 17). In both cases, in order to convert the metal into the passive state, it is necessary to reach a certain electrode potential above which (in the positive direction) the dissolution rate of the metal is determined only by the value of the potential and is independent of the manner in which the potential is maintained, whether by an external current or by the addition of oxidants to the solution.

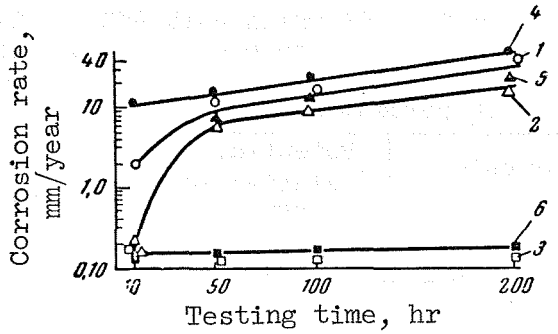

Figure 5. Effect of sodium nitrite on the corrosion of titanium by 20 percent sulfuric acid at 60°: 1, 20 percent H_2SO_4, without stirring; 2, 20 percent H_2SO_4 + 0.01 percent $NaNO_2$, without stirring; 3, 20 percent H_2SO_4 + 0.1 percent $NaNO_2$, without stirring; 4, 20 percent H_2SO_4, with stirring; 5, 20 percent H_2SO_4 + 0.01 percent $NaNO_2$, with stirring; 6, 20 percent H_2SO_4 + 0.1 percent $NaNO_2$, with stirring.

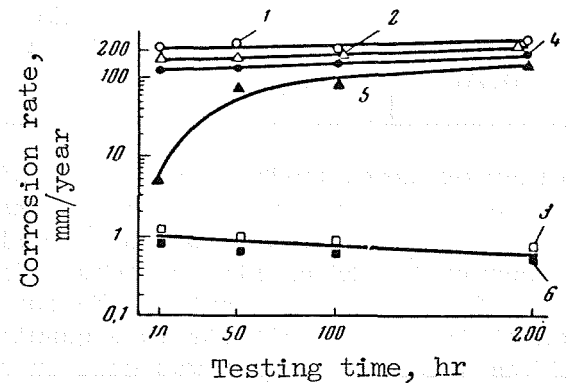

Figure 6. Effect of sodium nitrite on the corrosion of titanium by 20 percent sulfuric acid at 100°: 1, 20 percent H_2SO_4, without stirring; 2, 20 percent H_2SO_4 + 0.1 percent $NaNO_2$, without stirring; 3, 20 percent H_2SO_4 + 1 percent $NaNO_2$, without stirring; 4, 20 percent H_2SO_4, with stirring; 5, 20 percent H_2SO_4 + 0.1 percent $NaNO_2$, with stirring; 6, 20 percent H_2SO_4 + 1 percent $NaNO_2$, with stirring.

Our experiments showed that additions of sodium nitrite passivate titanium in 20 percent hydrochloric and sulfuric acid at 20 and 60°, and markedly decrease the corrosion at 100°. The shift of the electrode potentials of titanium toward the positive side in the presence of nitrite was associated with a chemical passivation of the metal.

Oxidants maintain the positive value of the electrode potential of titanium in 20 percent hydrochloric acid if they are adsorbed and subsequently chemisorbed; they harden and preserve the protective surface film (ref. 18).

EFFECT OF NATURE OF OXIDANT ON THE CORROSION RATE AND ELECTRODE POTENTIAL OF TITANIUM IN HYDROCHLORIC AND SULFURIC ACID FOR A TESTING TIME OF 100 HRS.

Oxidant	Additive, percent	20 percent HCl		20 percent H_2SO_4	
		Corrosion rate, mm/yr	Potential (relative to NHE), V	Corrosion rate, mm/yr	Potential (relative to NHE), V
Temperature 20°					
--	--	0.55	-0.4	0.68	-0.4
$NaNO_2$	0.01	0.02	+0.7	0.02	+0.4
HNO_3	0.01	0.66	-0.3	0.80	-0.3
HNO_3	0.1	0.14	+0.6	0.40	-0.3
Temperature 60°					
--	--	20.15	-0.5	15.90	-0.4
$NaNO_2$	0.1	0.12	+0.3	0.10	+0.1
HNO_3	0.1	18.60	-0.2	20.94	-0.4
HNO_3	1	0.20	+0.7	0.10	+0.5

We showed that, like other oxidants (refs. 1 and 9), sodium nitrite passivates titanium in acids for only a certain period of time which depends on the concentration of the oxidant and temperature of the experiment. During this period of time, the concentration of nitrite becomes sufficient to harden and preserve the protective surface film on titanium. In our experiments, following exposure to acids containing sodium nitrite in a quantity sufficient for passivation, the surface of the titanium samples was gold in color, which led to the assumption that a layer of titanium dioxide was formed (ref. 2).

A comparison of the corrosion values which we obtained in 20 percent solutions of hydrochloric and sulfuric acid at 20 and 100° with the dissolution rates calculated from the current densities of the potentiostatic curves (refs. 6 and 18) showed that the effectiveness of the chemical passivation of titanium in the presence of sodium nitrite may be essentially of the same order as in the anodic passivation without an oxidant.

It should be noted only that our experiments were conducted on one-piece unstressed titanium samples. It is possible that in the stress condition, the massive metal, the weld and the heat-affected zone behave differently under conditions of chemical and anodic passivation. The process of corrosion of the metal under conditions of chemical and anodic passivation may also have a different course in narrow gaps, where, particularly in the presence of a small concentration of oxidant, various factors are operative which regulate the access of the reagent to the surface of the metal and the removal of the corrosion products (ref. 19).

Our experiments have shown that electrochemical measurements make it possible to establish the direction of the corrosion process (either toward activation or passivation) in a shorter time than when the gravimetric method is used.

Summary

1. Titanium VT1-1 displays a satisfactory stability in 20 percent hydrochloric and sulfuric acid at temperatures up to 10° and corrodes substantially at temperatures above 20°.

2. Additions of certain sodium nitrite concentrations to hydrochloric and sulfuric acid impart a positive electrode potential sufficient for chemical passivation to the surface of titanium.

3. Sodium nitrite markedly decreases the corrosion of titanium by acids only under certain testing conditions. In order to provide for a satisfactory stability of titanium in 20 percent hydrochloric and sulfuric acid, it is necessary to add 0.01 percent $NaNO_2$ at 20° and 0.1 percent $NaNO_2$ at 60°. A pronounced inhibition of titanium corrosion in the presence of nitrite was also observed at 100°, but the weight loss of the metal at this temperature was nevertheless considerable.

4. Equipment with working surfaces made of titanium VT1-1 can be used at temperatures up to 60° under conditions involving the use of hydrochloric and sulfuric acid containing the optimum nitrite concentration.

REFERENCES

1. Tseytlin, Kh. L. and Strunkin, V. A. Zhurnal Prikladnoy Khimii, Vol. 33, No. 12, p. 2796, 1960.

2. Andreyeva, V. V. and Kazarin, V. I. New Corrosion-Resistant Structural Materials (Novyye korrozionnostoykiye konstruktsionnyye materialy). Goskhimizdat, 1961.

3. --- Doklady AN SSSR, Vol. 121, No. 5, p. 873, 1958.

4. Tomashov, N. D., Al'tovskiy, R. M. and Arakelov, A. G. Dokl. AN SSSR, Vol. 121, No. 5, p. 885, 1958.

5. Gleekman, L. W. Corrosion, Vol. 14, p. 401, 1958.

6. Otsuka, R. Sci. papers Inst. Phys. a. Chem. Res., Vol. 54, No. 1, p. 97, 1960.

7. Moroz, L. S., Chechulin, V. V., Polin, I. V., Butalov, L. V., Shul'kin, S. M. and Goryachev, A. P. Coll. Titanium and Its Alloys (Titan i yego splavy). Sudpromgiz (State All-Union Publishing House of the Shipbuilding Industry), Leningrad, Vol. I, p. 150, 1960.

8. Cotton, Y. B. and Bradley, H. Chem. a. Ind., No. 22, p. 640, 1958.

9. Zwicker, U. Chem. Ing. Techn., Vol. 29, No. 2, p. 107, 1957.

10. Andreyeva, V. V. and Kazarin, V. I. Dokl. AN SSSR, Vol. 123, No. 6, p. 1048, 1958.

11. Klinov, I. Ya. Trudy MIKhM (Transactions of the Moscow Institute of Chemical Machinery), Vol. 22, p. 75, 1960.

12. Vashin, G. Z. and Klimov, I. Ya. Vestnik Tekhnicheskoy i Ekonomicheskoy Informatsii (NIITEKhIM), No. 2, p. 46, 1962.

13. Babitskaya, S. M. and Tseytlin, Kh. L. In: Corrosion of Stainless Steels (Korroziya nerzhaveyushchykh staley). Izd-vo AN SSSR, p. 69, 1956.

14. Babko, A. K. and Pyatnitskiy, I. V. Qualitative Analysis (Kolichestvennyy analiz). Goskhimizdat, p. 572, 1956.

15. Ullman Enzyklopädie der technischen Chemie, Berlin, Aufl. 2, Vol. 9, p. 726, 1932.

16. French Patent No. 1012443 dated 9/7/1952; C. A., 11231, 1957.

17. Bune, N. Ya. and Kolotyrkin, Ya. M. Zhurnal Fizicheskoy Khimii, Vol. 35, No. 7, p. 1543, 1961.

18. Andreyeva, V. V. and Glukhova, A. I. J. Appl. Chem., Vol. 11, p. 390, 1961.

19. Sorokin, Yu. I. and Tseytlin, Kh. L. Zhurnal Prikladnoy Khimii, Vol. 35, No. 4, p. 573, 1962.

STUDY OF THE USE OF TITANIUM ALLOYS IN THE CONSTRUCTION OF FOOD MACHINES

F. N. Tavadze and T. A. Lashkhi

The purpose of the present work was to continue (ref. 1) the investigation and to establish the possibility of the application of titanium alloys of the ATn series to the construction of food machinery.

Since this branch of the industry requires a large number of scarce nickel-stainless steels, nonferrous metals and alloys, the search for their substitutes has assumed great importance in the national economy.

Titanium alloys are new structural materials which, because of numerous valuable properties (high strength, low density, corrosion resistance in various media, etc.) can be successfully used in various branches of industry. Despite the high cost of titanium alloys, their use is growing every year in various branches of the national economy.

Another advantage of titanium alloys over steels is the length of the life of the equipment because of its high resistance to corrosion and wear.

Experiments carried out earlier (ref. 1) showed a high corrosion resistance of the titanium alloys ATn in a number of technological and food media. Because weld joints are usually employed in the manufacture of apparatus and equipment, the experiments were carried out on weld joints of alloys AT3 and AT8. The specimens to be tested, welded by argon arc welding, were obtained from the welding laboratory of the A. A. Baykov Institute of Metallurgy.

The tests were conducted in a series of organic acids and technological solutions K1 and V1 corresponding to aggressive media employed in the canning and wine-making industry (table 1), both at room temperature and boiling temperature, and also in natural cherry plum juice, the most aggressive food medium (total acidity 2 percent, pH = 2.8).

In addition to titanium alloys, stainless steel 1Kh18N9T and some experimental chromium-maganese steels were tested at the same time.

The technique of the corrosion and electrochemical tests consisted in studying the samples and the reaction medium: the weight loss and the quantity of hydrogen evolved during the corrosion of the alloys were determined; the values of the electrode potentials were measured; polarization curves were plotted; the reaction medium was analyzed chemically after the test, and the pH was determined after the corrosion tests of the samples. The alloy samples

TABLE 1. CHEMICAL COMPOSITION OF TECHNOLOGICAL SOLUTIONS K1 AND V1.

Solution	Tartaric acid, %	Citric acid, %	Malic acid, %	Salicylic acid, %	Formic acid, %	Acetic acid, %	Ethyl alcohol, %	Methyl alcohol, %	Tannin, g/l	Glucose, %	Table salt, %	Oxalic acid, %	Lactic acid, %	Total acidity	pH
K1	2	2	0.5	-	-	2	-	-	-	2	4	3	1	2.71	0.81
V1	3	1	0.5	0.3	0.5	1.5	12	0.6	0.3	1	-	-	-	1.22	1.80

were observed visually and were subjected to metallographic analysis before and after their corrosion tests.

The results of 3000-hr corrosion tests of the weld joints of alloys AT3 and AT8 in various organic acids are shown in table 2. From this table it is evident that on the corrosion resistance scale, the alloys are in the region of corrosion resistant values ($\Pi < 0.13$ mm/yr) in the case of oxalic and tartaric acid. In oleic, tartaric, acetic and lactic acid the corrosion of the alloys is equal to zero.

The results of corrosion tests of welded titanium samples in technological solutions K1 and V1 (table 3) and the kinetic curves of the corrosion process (fig. 1) show that the samples in the technological solution K1 are subjected to a relatively high corrosion. This difference is particularly noticeable during the initial period of the test.

The electrode potentials of the investigated titanium alloys AT8 gradually shift toward the positive region (fig. 2), which is in agreement with the results of the corrosion tests.

In order to establish the influence of atmospheric oxygen on the hardening of the protective film, the electrode potentials of the alloys were measured both in the stirred and unstirred solution. In the stirred solution, the value of the potential is located in a more positive region (fig. 2, curve 2). This indicates an increase in the protective properties of the surface film of alloy AT8.

The presence of a protective film on titanium alloys is also indicated by the values and course of the polarization curves obtained for alloy AT3 in the technological solution K1 (fig. 3). An analysis of the curves shows that an appreciable inhibition of anodic reactions takes place in this case (anodic passivity), which reaffirms what was stated above.

As expected, the experiments carried out on the welds of alloys AT3 and AT8 showed that in this case hydrogen is evolved in insignificant amounts.

A chemical analysis of the media is shown in table 4.

TABLE 2. RESULTS OF CORROSION TESTS IN VARIOUS ORGANIC ACIDS (FOR A CORROSION RESISTANCE INDEX OF 1).

Alloy	Medium	Corrosion, g/m^2 hr	Penetrability of corrosion, mm/yr
AT3	oxalic acid	0.0061	0.0115
AT8	oxalic acid	0.0091	0.0172
AT8	acetic acid	0.0075	0.0142

TABLE 3. RESULTS OF CORROSION TESTS OF WELDED PARALLEL SPECIMENS OF TITANIUM ALLOYS AT3 AND AT8 (FOR A RESISTANCE INDEX OF 1).

Alloy	Corrosion g/mm^2, hr	Penetrability of corrosion, mm/yr	Solution	Alloy	Corrosion g/mm^2, hr	Penetrability of corrosion, mm/yr	Solution
AT3	0.0001	0 00019	V1	AT8	0.0003	0 00057	V1
AT3	0.0004	0 00076	V1	AT8	0.0004	0 00076	V1
AT3	0.0001	0 00019	V1	AT8	0.0009	0 00017	V1
AT3	0.0008	0 00015	K1	AT8	0.0003	0 00057	K1
AT3	0.0001	0 00019	K1	AT8	0.0002	0 00038	K1
AT3	0.0002	0 00038	K1	AT8	0.0002	0 00038	K1

TABLE 4. RESULTS OF CHEMICAL ANALYSIS OF THE REACTION MEDIA.

Alloy	Content of element, mg/l					Medium
	Fe	Al	Ti	Cr	Mn	
AT3 and AT8	45.0	not observed	not observed	--	--	solution of V1
AT3 and AT8	93.80	12.40	--	--	--	solution of K1
Chromium-manganese	893.4	--	--	242.5	248.0	solution of K1

The data of table 4 indicate that titanium ions do not pass into solution, and that the solution is enriched only with aluminum and iron ions. As should have been expected, in the technological solution K1 in which the samples underwent an intensive corrosion, the quantity of iron and aluminum ions which had passed into solution was greater than in the technological solution V1. In solution K1, the corrosion of the chromium-manganese alloy is several times greater than that of alloys AT3 and AT8.

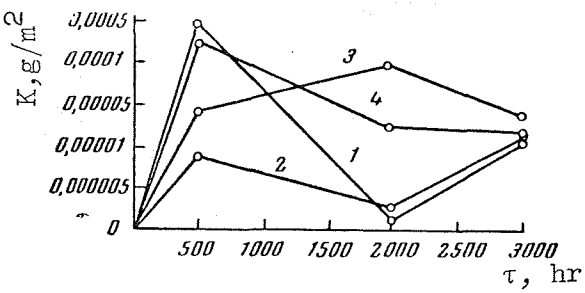

Figure 1. Corrosion resistance of welded specimens of alloys AT3 and AT8: 1, AT3 in solution K1; 2, AT3 in solution V1; 3, AT8 in solution V1; 4, AT8 in solution K1.

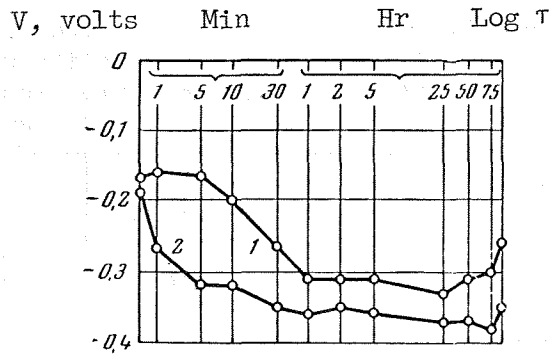

Figure 2. Change in the electrode potential of alloy AT8 in solution K1: 1, without stirring of the solution; 2, with stirring of the solution.

The results of tests in natural cherry plum juice are shown in table 5.

The tested alloys were found to be highly stable in cherry plum juice. Particular mention should be made of samples of alloy AT8 alloyed with a large quantity of aluminum. A study of the corrosion resistance of specimens of welds of alloys AT3 and AT8 was carried out at the boiling point in the technological solution K1 in order to determine the possibility of their use in the canning industry. The corrosion of the samples was studied while the alloys were immersed in the solution as well as in the vapor.

The results of the tests (table 6) showed that the tested alloys were not stable under these conditions (high weight loss). A metallographic analysis of the samples was performed before and after their testing.

As can be seen from the photomicrographs of the polished sections before the testing (fig. 4), the weld-metal zone is characterized by a coarse-grained structure, the zone before the weld has a less coarse-grained structure, and the end of the zone has a fine-grained structure.

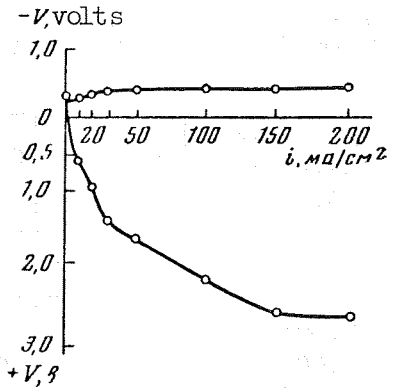

Figure 3. Polarization curves for alloys AT3 in solution K1.

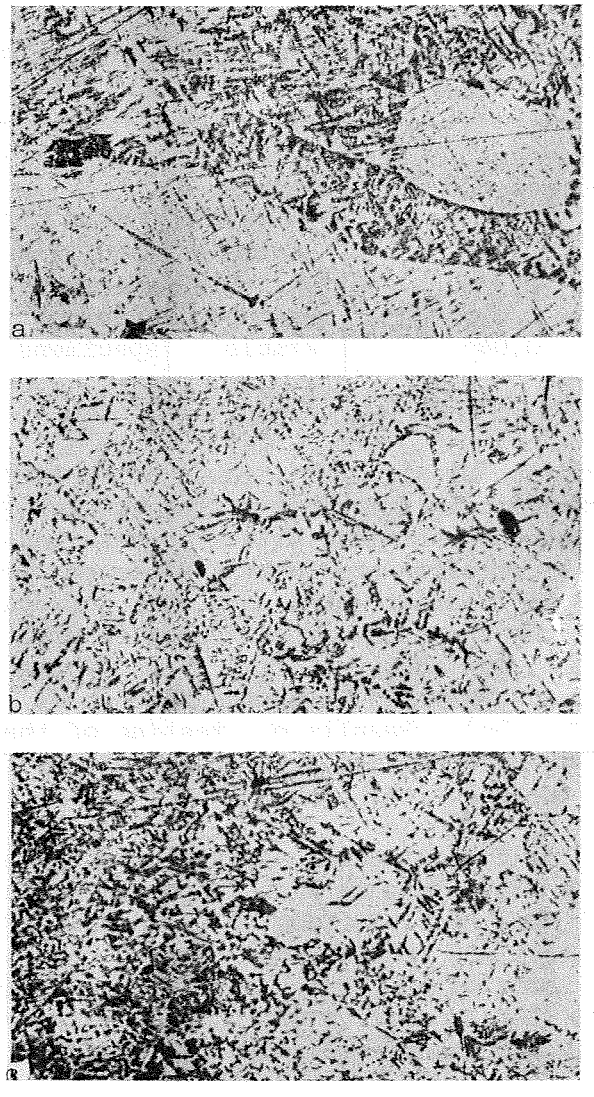

Figure 4. Microstructure of welded joint of alloy AT3, x 150: a, seam; b, beginning of heat-affected zone; c, end of heat-affected zone.

TABLE 5. RESULTS OF CORROSION TESTS OF PARALLEL SPECIMENS OF TITANIUM ALLOYS IN NATURAL CHERRY PLUM JUICE.

Specimen number	Corrosion, g/m^2 hr	Penetrability of corrosion, mm/yr	Specimen number	Corrosion, g/m^2 hr	Penetrability of corrosion, mm/yr
Alloy AT3			Alloy AT8		
1	0.0007	0.0013	1	0.00002	0.00003
2	0.0007	0.0013	2	0.00004	0.00007
3	0.0015	0.0029	3	0.00004	0.00007
4	0.009	0.0117	4	0.00013	0.00024

TABLE 6. RESULTS OF CORROSION TESTS OF WELDED SPECIMENS OF TITANIUM ALLOYS AT THE BOILING POINT IN SOLUTION K1.

Alloy	Corrosion, g/m^2 hr	Penetrability, corrosion, mm/yr	Corrosion resistance	Remarks
AT3	0.514	0.566	unstable	specimens immersed in solution
AT3	0.511	0.562	unstable	specimens in vapor of solution
AT8	0.817	0.898	unstable	specimens immersed in solution
AT8	0.041	0.045	stable	specimens in vapor of solution

On the photomicrograph of alloy AT3, taken after testing for 250 hrs at the boiling point with complete immersion of the samples (fig. 5), an intercrystalline character of the corrosive attack is observed in the weld-metal zone. Areas of intense corrosion are located along the grain boundaries (fig. 5a). At the origin of the heat-affected zone, the structure of the alloy was more fine-grained, had the appearance of an "erosion grid," and an intercrystalline failure of the alloy was observed (fig. 5b). At the end of the heat-affected zone (zone immediately adjoining the base metal), less intercrystalline attack was observed (fig. 5c). Results of testing of the same samples in the vapor of the solution showed that their corrosive attack takes place to a lesser extent than in the solution.

Under the conditions investigated, alloy AT8 was found to be less resistant to corrosion than alloy AT3. This is also supported by an analysis of photomicrographs of the polished sections (fig. 6). Samples of alloy AT8 (fig. 6a) show both intercrystalline and considerable pitting corrosion of the alloy. This is also characteristic of all three weld zones considered. Tests of alloy AT8 in the vapor showed less corrosive attack than in the case of immersion, but the damage to alloy AT8 was greater than to alloy AT3.

After the corrosion tests, a chemical analysis of the reaction medium was performed (table 7).

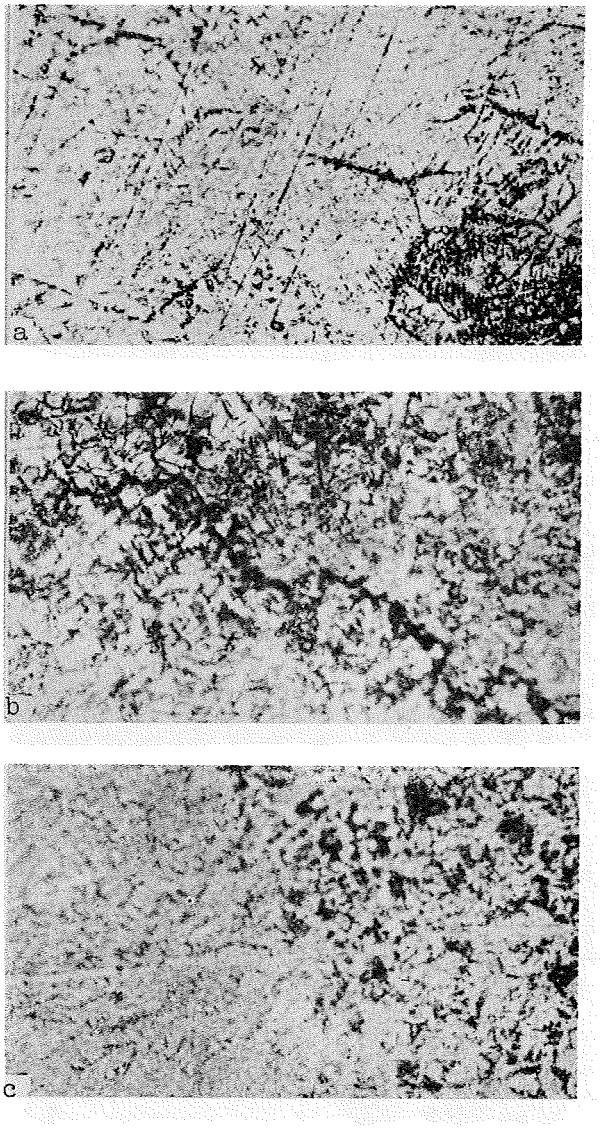

Figure 5. Microstructure of welded joint of alloy AT3 with complete immersion of specimens, x 150: a, seam; b, beginning of the heat-affected zone; c, end of the heat-affected zone.

The analysis showed that the greatest quantity of titanium ions had passed into the medium from alloy AT8.

During the corrosion testing of titanium alloys in solution K1, we observed /171
that during the initial period (the first 2 hrs) the solution turned yellow, darkened gradually, then turned dark-brown in 4 hrs. To elucidate the cause of the change in the color of the reaction medium, we conducted three parallel experiments. In the first, solution K1 was boiled without immersing the samples.

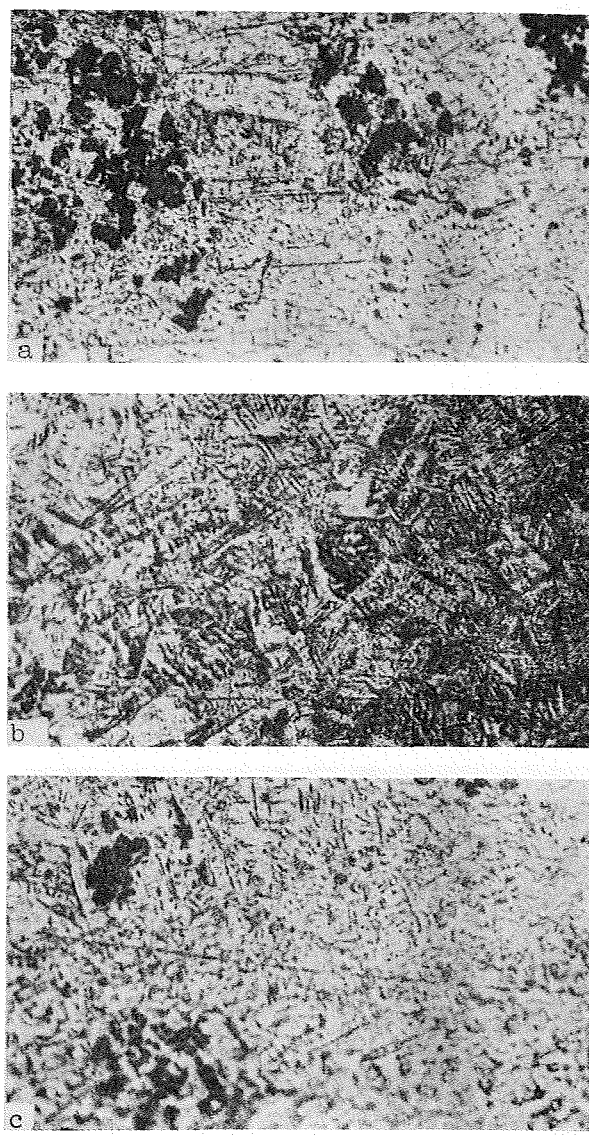

Figure 6. Microstructure of welded joint of alloy AT8 with complete immersion of specimens, x 150: a, seam; b, beginning of heat-affected zone; c, end of heat-affected zone.

The experiment showed that the color of the solution remained practically unchanged. In the second experiment, pure metallic titanium was immersed into Kl, while in the third, pure metallic aluminum was immersed.

Experiments with metallic aluminum also showed that the color of the solution did not change. Tests with metallic titanium showed a change in the color of the solution similar to the one described above. Consequently, the change in the color of the reaction mixture was caused by titanium ions which had passed into solution Kl as a result of the corrosion of the alloys. Measurements

TABLE 7. RESULTS OF CHEMICAL ANALYSIS OF SOLUTION K1 AFTER CORROSION TESTS (250 HRS OF BOILING).

Material	Quantity of ions, g/l					
	Ti	Al	Cr	Mn	Fe	Ni
AT3	1.94	0.35	--	--	--	--
AT8	2.48	0.23	--	--	--	--
titanium	0.79	0.21	--	--	--	--
aluminum	none	5.04	--	--	--	--
steel 1Kh18N9T	--	--	--	--	1.30	0.203
chromium-manganese Kh25G15	--	--	20.80	1.50	5.36	--

of the pH of the solution before and after the tests showed that whereas prior to the test the pH of the solution was 0.9, after the corrosion of alloy AT3 the pH became 1.1, and after the corrosion of alloy AT8, rose to 2. It is obvious that the more titanium ions pass into the solution, the higher is the pH. This is in good agreement with the results obtained.

Also tested were multicomponent high alloys of type AT2 in 10 percent formic acid both with and without stirring of the solution.

Results of the corrosion tests showed an absolute stability of these alloys under the testing conditions. It should be noted only that the corrosion resistance of these alloys is most favorably affected by complex alloying with molybdenum and vanadium, then with zirconium and vanadium, and that a less favorable effect is that of complex alloying with zirconium and molybdenum.

Let us examine the results of electrochemical investigations (figs. 7 and 8). The curve representing the variation in the electrode potential with time is located in the positive region of potentials and remains nearly unchanged with time (fig. 7). The polarization curves indicate a marked inhibition of the anodic and cathodic reactions (fig. 8). The nature of the variation in potential and of the polarization curves is in good agreement with the results of the corrosion tests of these alloys.

Summary

1. The absolute corrosion resistance was established for weld joints of titanium alloys AT3 and AT8 at room temperature in oleic, oxalic, tartaric, acetic, and lactic acid, natural cherry plum juice, and in the technological solutions K1 and V1.

2. Chemical analysis of the reaction medium established that during the corrosion of titanium alloys at room temperature, no transfer of titanium ions into this medium takes place.

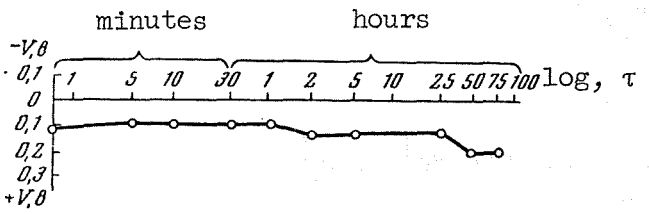

Figure 7. Change in the electrode potential of alloy AT2n.

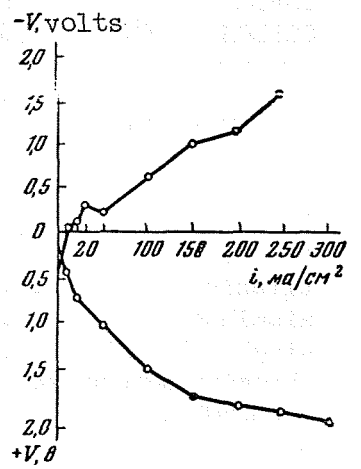

Figure 8. Polarization curves of alloy AT2n.

3. Electrochemical investigations confirmed the results of the corrosion tests:

(a) The values of the electrode potentials shift toward the positive region with time;

(b) The nature of the polarization curves indicates a considerable inhibition of the anodic reactions (anodic passivity).

4. Results of tests with stirring of the solutions showed that the protective film on titanium alloys becomes denser with time.

5. At the boiling point, a considerable corrosion of the titanium alloys was observed in solution K1.

6. A metallographic investigation established the presence of intercrystalline and pitting corrosion of the weld joints of titanium.

7. Titanium alloys AT2n were found to be absolutely stable in a solution of 10 percent formic acid in tests with and without stirring of the solutions.

REFERENCES

1. Tavadze, F. N. and Lashkhi, T. A. Coll. Titanium and Its Alloys (Titan i yego splavy). Izd-vo AN SSSR, No. 10, p. 154, 1963.

2. Yeremenko, N. V. Coll. Titanium and Its Alloys (Titan i yego splavy). Izd-vo AN SSSR, Kiev, 1955.

3. Tomashev, N. D. Theory of Corrosion and Metal Protection (Teoriya korrozii i zashchita metallov). Izd-vo AN SSSR, 1959.

4. Corrosion and Chemical Stability of Materials (Korroziya i khimicheskaya stoykost' materialov). A handbook, Mashgiz, 1954.

5. Tables of the Corrosion Resistance of Titanium and Its Alloys in Various Corrosive Media (Tablitsy korrozionnoy stoykosti titana i yego splavov v razlichnykh agressivnykh sredakh). Moscow, Informatsionno-izdatel'skiy otdel, 1961.

PART III. MECHANICAL AND TECHNOLOGICAL PROPERTIES OF TITANIUM ALLOYS

BASIC PREREQUISITES FOR DEVELOPING HIGH-STRENGTH TITANIUM ALLOYS WITH AN $\alpha + \beta$-STRUCTURE BY MEANS OF ALLOYING AND HEAT TREATING

V. N. Moiseyev

pp. 177-183 of original document appears in
J.P.R.S. Translation No. 28,176; TT:65-30080
pp. 1-10

STRENGTH OF INTERATOMIC BONDING OF SINGLE-PHASE ALLOYS IN THE SYSTEM Ti - Nb - Cr

K. I. Shakhova and P. B. Budberg

The strength of the interatomic bonding of the crystal lattice of metals and alloys may be characterized by various quantities: heat of sublimation, heat of melting, heat of solution, elastic constant, root mean square displacement of atoms at the lattice points and other parameters (ref. 1).

A relationship was established between the modulus of normal elasticity E and shear modulus G of pure metals and metallic compounds, on the one hand, and the characteristic temperature $\theta^{\circ}K$ on the other (ref. 2). It was shown that the dependence between the elastic properties and the characteristic temperature also extends to single-phase alloys with Poisson's ratio μ = 0.25-0.45 (ref. 3).

In the present work, an estimate of the interatomic bond in single-phase alloys of the ternary system Ti - Nb - Cr was made.

The elastic constants of β and γ alloys were determined by an electronic method with the "Elastomat" unit[1] which made it possible to obtain the elastic characteristics within 1-1.5%. The specimens used were cylindrical rods 80-100 mm long and 6-8 mm in diameter melted in an arc furnace and cast in a vacuum.

The phase diagram of the system Ti - Nb - Cr at temperatures of 1000-600° was studied by the authors of the present article (ref. 4), who established that the compounds $TiCr_2$ and $NbCr_2$ in the temperature interval studied form a continuous series of solid solutions with a crystal lattice of $MgCu_2$ type, i.e., the γ phase. The isothermal section of the system at 1000° is shown in figure 1.

The study of the elastic constants of the alloys was made after quenching from 1000° the sections with ratio Ti: Nb = 4:1; 3:2; 2:3; 1:4. The results obtained are shown in table 1. It follows from this table that in passing from the single-phase region of β alloys to the two-phase $\beta + \gamma$ region, the constants E and G increase considerably.

---

[1]The determination of the elastic constants was carried out in cooperation with S. G. Fedotov.

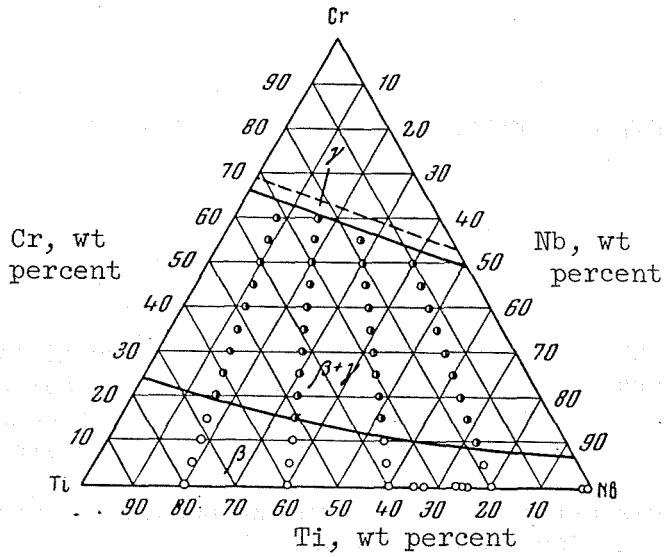

Figure 1. Isothermal section of the diagram of the system Ti - Nb - Cr at 1000°.

In alloys of all the sections with a content of 50 percent Cr in which the γ phase becomes predominant (fig. 1), the modulus of normal elasticity attains values of (16-21) x 10^3 kg/mm^2. It follows that the modulus of normal elasticity of solid solutions of metallic compounds is considerably higher than that of solid solutions of the pure components of the β phase. The values obtained for the elastic constants of the alloys made it possible to calculate the characteristic temperatures θ and the root-mean-square displacements of the atoms from the equilibrium position in the crystal lattice for solid solutions of metals and metallic compounds at 0°K $\sqrt{\bar{u}_0^2}$ and 293°K $\sqrt{\bar{u}_{293}^2}$.

The characteristic temperature was calculated from the following relations:

$$\theta = \frac{1.6818 \cdot 10^3 \sqrt{E}}{A^{1/3} d^{1/3}}, \qquad (1)$$

where E is the modulus of normal elasticity, kg/cm^2 x 10^6; A is the average atomic weight; d is the density, g/cm^3;

$$\theta = \frac{h}{k}\left(\frac{3N_A}{4\pi A}\right)^{1/3} d^{1/3} c^{1/3}, \qquad (2)$$

where $h = 6.62377 \cdot 10^{-27}$ erg sec is Planck's constant; k = 1.380257 x 10^{16} erg/deg is Boltzmann's constant; N_A is Avogadro's number; c is the average propagation rate of vibrations, given by the expression

$$\frac{3}{c^3} = \frac{1}{c_l^3} + \frac{2}{c_\tau^3},$$

with

$$c_l = \sqrt{\frac{E}{d}}; \quad c_\tau = \sqrt{\frac{G}{d}}.$$

The root-mean-square displacements of the atoms were determined from the Debye-Weller relation, which has the following form:

$$\bar{u}^2 = \frac{6h^2\left[\frac{D\left(\frac{\theta}{T}\right)}{\frac{\theta}{T}} + \frac{1}{4}\right]}{m_a k\theta \frac{8}{3}\pi^2} = \frac{4.30\cdot 10^{-14}\left[\frac{D\left(\frac{\theta}{T}\right)}{\frac{\theta}{T}} + \frac{1}{4}\right]}{A\theta}, \qquad (3)$$

where $m_\alpha = 1.6724\cdot 10^{-24}$ is the mass of the hydrogen atom.

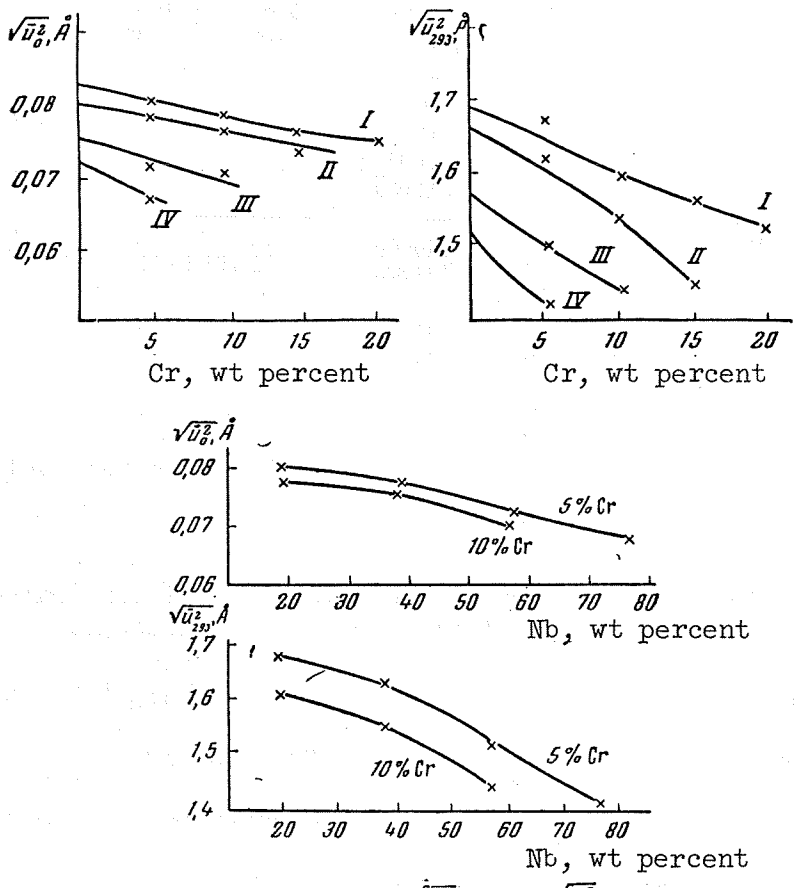

Figure 2. Dependence of $\sqrt{\bar{u}_0^2}$ and $\sqrt{\bar{u}_{293}^2}$ on the compositi of the β solid solutions of the system Ti - Nb - Cr.

TABLE 1. CHANGE IN THE ELASTIC CONSTANTS OF ALLOYS OF THE SYSTEM Ti - Nb - Cr ALONG SECTIONS.

Composition		Elastic constants		
Section No.	Cr, % wt	E, кг/мм²	G, кг/мм²	μ
I (Ti : Nb = 4:1)	5	7 877	2 890	0.361
	10	8 100	2 997	0.311
	15	8 740	3 100	0.321
	20	9 340	4 129	0.358
	30	12 018	4 881	0.255
	40	13 607	5 383	0.264
	45	16 533	6 558	0.321
	50	16 620	6 881	0.295
II (Ti:Nb=3 : 2)	5	8 050	3 100	0.354
	10	8 540	3 240	0.356
	15	10 691	3 940	0.256
	20	11 968	4 475	0.337
	30	12 106	4 551	0.33
	40	14 088	5 383	0.327
	50	17 020	5 908	0.321
III (Ti:Nb=2:3)	5	10 100	—	—
	10	11 200	—	—
	20	11 952	—	—
	30	13 030	—	—
IV (Ti:Nb=1:4)	5	10 095	—	—
	10	11 835	—	—
	20	12 127	—	—
	30	14 503	—	—
	35	14 720	—	—

The values of the function $\frac{D\left(\frac{\theta}{T}\right)}{\frac{\theta}{T}}$ were taken from the table given in reference 1.

The values of θ as a function of the alloy composition, calculated from formulas (1) and (2), were in practically complete agreement. They are shown in table 2. The same table gives values of $\sqrt{\overline{u_0^2}}$ and $\sqrt{\overline{u_{293}^2}}$ for single-phase alloys of the system, determined by means of formula (3).

The data of table 2 were used to plot the curves of the dependence of $\sqrt{\overline{u_0^2}}$ and $\sqrt{\overline{u_{293}^2}}$ on the composition of the alloys (fig. 2). As the chromium content

TABLE 2. VALUES OF θ $\sqrt{\overline{u_0^2}}$, $\sqrt{\overline{u_{293}^2}}$ FOR β SOLID SOLUTIONS OF THE SOLUTIONS OF THE SYSTEM Ti - Nb - Cr ALONG SECTIONS AT QUENCHING TEMPERATURE AT 1000°.

Composition: Section No.	Cr, wt%	θ, °K	$\sqrt{\overline{u_0^2}}$, A	$\sqrt{\overline{u_{293}^2}}$, A
I (Ti:Nb = 4:1)	5	295	0.0802	0.1681
	10	305	0.0789	0.1600
	15	316	0.0766	0.1570
	20	327	0.0764	0.1531
II (Ti:Nb = 3:2)	5	276	0.0789	0.1625
	10	239	0.0762	0.1543
	15	327	0.0719	0.1439
III (Ti:Nb= 2:3)	5	277	0.0728	0.1508
	10	290	0.077162	0.1441
IV (Ti:Nb =1:4)	5	278	0.06870	0.1411

in the β solid solution increased, both $\sqrt{\overline{u_0^2}}$, and $\sqrt{\overline{u_{293}^2}}$, decreased, indicating the influence of chromium on the increase in the interatomic bonding forces in the solid solution. As the limit of saturation of the solid solution was approached, values of $\sqrt{\overline{u_0^2}}$ and $\sqrt{\overline{u_{293}^2}}$ reach their minimum (fig. 2, top).

Niobium has a much weaker effect on the interatomic forces than chromium. The role of chromium in increasing the strength of the interatomic bond with rising temperature is particularly apparent, since the quantity $\sqrt{\overline{u_{293}^2}}$ decreases more rapidly than $\sqrt{\overline{u_0^2}}$ as a function of composition (fig. 2, bottom).

It was of interest to evaluate the strength of the bonding in solid solutions of the metallic compounds $TiCr_2$ and $NbCr_2$, i.e., the γ phase.

This could be done only by extrapolating the values of the elastic constants to the composition of alloys corresponding to single-phase β solid solutions. The extrapolation was necessary because of the high brittleness of the solid solutions of the compounds and the impossibility of preparing samples from them.

The calculated values of θ, $\sqrt{\overline{u_0^2}}$ and $\sqrt{\overline{u_{293}^2}}$ for single-phase alloys of the section $TiCr_2$-$NbCr_2$ as a function of composition are shown in table 3.

TABLE 3. VALUES OF θ $\sqrt{\overline{u_0^2}}$, $\sqrt{\overline{u_{293}^2}}$ OF ALLOYS OF THE SECTION $TiCr_2$-$NbCr_2$ AT QUENCHING TEMPERATURE OF 1000°.

Composition, at. %			θ, °K	$\sqrt{\overline{u_0^2}}$, A	$\sqrt{\overline{u_{293}^2}}$, A
Cr	Ti	Nb			
66	27,2	6,8	437	0,06731	0,1300
66	20,4	13,6	443	0,06387	0,1225
66	13,6	20,4	445	0,06197	0,1192
66	6,8	27,2	461	0,05882	0,1118

From the table it follows that an increase in the content of niobium in the γ solid solution leads to a rise in the characteristic temperature and a decrease in the values of $\sqrt{\overline{u_0^2}}$ and $\sqrt{\overline{u_{293}^2}}$, i.e., to an increase in the bonding forces in the lattice of the γ phase as its content of niobium increases.

In the alloys of the section $TiCr_2$-$NbCr_2$, no estimate can be made of the influence of chromium on the change in the interatomic bonding forces, since the chromium content is practically constant in all of the alloys studied.

From the regularities in the change of θ, $\sqrt{\overline{u_0^2}}$, $\sqrt{\overline{u_{293}^2}}$ in the solid solutions of metals and compounds of the β and γ phases of the system Ti - Nb - Cr (table 2 and 3), it follows that the strength of the bonding in the solid solution of metals is less than in the metallic compounds. The weakening of the bonding forces in the solid solutions of metals with rising temperature is also more significant than in the solid solution of metallic compounds; this follows from a comparison of the ratios $\sqrt{\overline{u_{293}^2}}:\sqrt{\overline{u_0^2}}$, which are equal to 2.02-2.04 for the β phase and 1.88-1.93 for the γ phase.

The conclusions drawn with regard to the influence of chromium and niobium on the strength of the bond in β and γ solid solutions is confirmed when the hot hardness of the alloys is investigated.

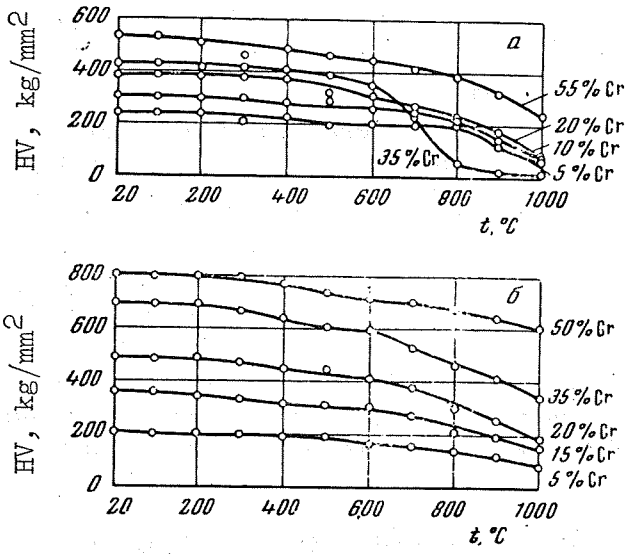

Figure 3. Change in the hardness of alloys of the system Ti-Nb-Cr with temperature: a, section I; b, section IV.

The determination of the hot hardness is one of the methods of estimating the strength of alloys at high temperatures. Alloys of section I containing 5, 10 and 20 percent Cr practically preserve their hardness up to 400°, above which a monotonic decrease in hardness begins up to 1000°. The alloys with 55 percent Cr, whose structure consists of a γ solid solution with a certain amount of the β phase, retains a high strength (250 kg/mm^2) up to 1000°. It should be noted that a softening of this alloy begins at a temperature above 700°. Up to this temperature, the decrease in the hardness of the alloy is approximately 16 percent (fig. 3a).

Alloys of section II with 5, 10 and 15 percent Cr begin to soften considerably at temperaturesabove 500°, while alloys with 50 and 60 percent Cr do so above 800°.

From the standpoint of the nature of the change in hardness with temperature, the alloys of section III are analogous to the alloys of section II. Only the alloy of section III with 60 percent Cr deserves some comment. Structurally, this alloy is a γ phase containing a very small amount of the β phase, and it retains a high value of the hardness (650-510 kg/mm^2) over the entire temperature range studied.

Among the alloys of section IV, the alloy with 5 percent Cr retains its initial hardness up to 400-500°, above which softening takes place (fig. 3b). The alloy with 50 percent Cr is characterized by minimum softening: its hardness changes from 800 to 600 kg/mm^2 during heating to 1000°.

Analyzing the data on the change in the hot hardness of the alloys, one can see that the single-phase β solid solutions soften to a greater extent than

the γ phase on heating. Chromium (in β alloys) and niobium (in γ alloys) have a favorable effect on the increase in hot hardness.

The results obtained confirm the conclusion reached earlier from the analysis of the root-mean-square displacements of the atoms at 0 and 293°K concerning the greater interatomic bonding strength of solid solutions of metallic compounds and their lesser softening tendency with rising temperature.

Summary

1. Elastic constants of the alloys after quenching from 1000° were determined.

2. Values of the characteristic temperature and root-mean-square displacements of atoms at 0 and 293° K for single-phase β and γ solid solutions were calculated.

3. The predominant role of chromium in hardening the β solid solutions and of niobium in hardening the γ phase was demonstrated.

4. The established regularities were confirmed by studying the hot hardness of the alloys.

REFERENCES

1. Frantsevich, I. N. Problems of Powder Metallurgy and Strength of Materials (Voprosy poroshkovoy metallurgii i prochnosti materialov). Izd-vo AN SSSR No. 3, p. 14, 1956.

2. Koster, W. Z. Metallkunde, Vol. 39, p. 135, 1948.

3. Livshits, B. G. Physical Properties of Metals (Fizicheskiye svoystva metallov). Metallurgizdat, 1960.

4. Shakhova, K. I. and Budberg, P. B. AN SSSR, Izvestiya, Otdel Tekhnicheskikh Nauk, Metallurgiya i Toplivo, No. 6, p. 137, 1962.

STUDY OF THE CREEP OF ALLOYS IN THE SYSTEM Ti-V-Nb-Mo

I. I. Kornilov, O. K. Belousov and V. S. Mikheyev

Vanadium, niobium and molybdenum are important alloying elements of titanium alloys. The introduction of these elements into titanium in amounts not exceeding the solubility limit of α-Ti causes an increase in ultimate strength and preserves the high indices of elongation, reduction of area, and impact strength (refs. 1-4). In addition, one can expect a substantial increase in the high-temperature strength in the region of single-phase β solid solutions of titanium with these elements (refs. 5-9).

One of the lines of investigation in the study of problems of high-temperature strength is the analysis of the dependence of creep and stress-rupture strength on the character of the chemical interaction between metals and other elements of the periodic system, on the equilibrium factors in the systems, the phase and structural state, and crystal-chemical reactions.

The quaternary system Ti-V-Nb-Mo was studied in ref. 10. It is characterized by the presence of a volume of a limited α_4 solid solution, a wide region of $\alpha_4 + \beta_4$ phases, and a wide region of β_4 solid solutions (fig. 1).

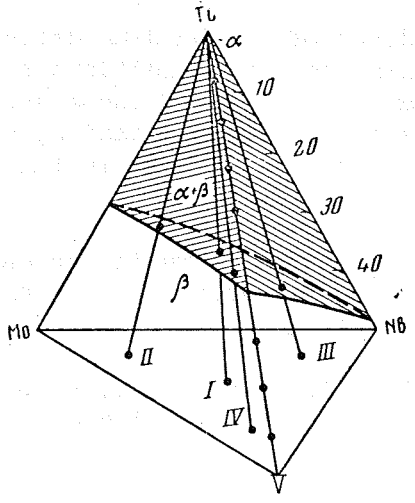

Figure 1. Phase diagram of alloys of the system Ti-V-Nb-Mo at 600°.

A study of the high-temperature strength of this system was carried out by the centrifugal method (ref. 11). The testing for high-temperature strength was done in three stages. In the first stage, the specimens were tested at 500° and an initial stress of 15 kg/mm^2 for 100 hrs; in the second stage, the transverse stress was increased to 20 kg/mm^2 and the testing was continued for another 100 hrs. In the third stage of the testing, the temperature was raised to 600° at a constant stress of 20 kg/mm^2, and the testing was continued for another 100 hrs. Thus, the total testing time was 300 hrs at a stress of 15-20 kg/mm^2 and temperatures of 500 and 600°. This complex mode of testing was adopted, in the first place, for the purpose of a comparison with the results of references 5, 6 and 9 pertaining to the high-temperature strength of binary and ternary systems of titanium with vanadium, niobium, and molybdenum, and in the second place, because of the great difference between the high-temperature strength of titanium alloys based on limited α_4 solid solutions and the strength of β_4 solid solutions with a high content of alloying elements.

The alloy specimens were prepared along four radial sections (fig. 1) with the following ratios of alloying elements in each of them: V:Nb:Mo = 1:1:1 (section I); Mo:Σ (V, Nb) = 2:1 (section II); Nb:Σ (V, Mo) = 2:1 (section III; V:Σ (Nb, Mo) = 2:1 (section IV), up to a total content of alloying elements of 50 wt percent.

The following materials were used to prepare the alloys: titanium sponge TG00 of 99.8 percent purity, carbothermic vanadium of 99.82 percent purity, niobium of 99.4 percent purity, and molybdenum of 99.9 percent purity. The alloys were melted in an arc furnace in an argon atmosphere and cast in copper ingot molds 8 mm in diameter, then forged to a diameter of 6 mm from 900°. The alloys were vacuum-annealed for 20 hrs at 750°, 50 hrs at 700°, and 150 hrs at 600°; furnace cooling to 200° lasted 24 hrs.

An analysis of the dependence of the bending deflection δ on the duration of the deformation under the same testing conditions of the alloys (fig. 2) makes it possible to state that the alloys of these sections behave differently. The highest creep rate will be that of pure titanium, which under the selected conditions reaches a bending deflection of 5 mm in the first few minutes of the test (fig. 2a).

In the first few hours of the test, a rapid increase is observed in the creep rate of alloys containing small amounts of the alloying elements, corresponding in composition to dilute α_4 solid solutions of titanium. A higher resistance to plastic deformation is displayed by alloys located near the limit of saturated α_4 solid solutions at this temperature, but in both cases a

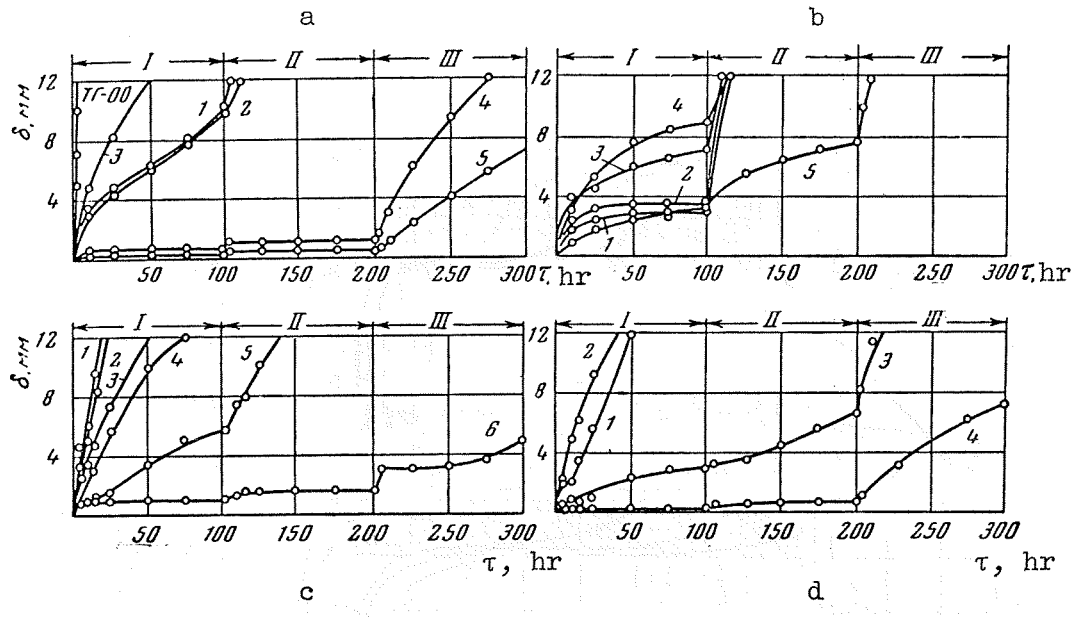

Figure 2. Curves of the creep of titanium and titanium alloys of the system Ti-V-Nb-Mo. Testing stages: I, t = 500°, σ = 15 kg/mm^2; II, t = 500°, σ = 20 kg/mm^2; III, t = 600°, σ = 20 kg/mm^2. a, section I, content Σ(V, Nb, Mo): 1, 2.4 percent; 2, 4.2 percent; 3, 20.1 percent; 4, 33.0 percent; 5, 50.1 percent; b, section II, content Σ(V, Nb, Mo): 1, 1.5 percent; 2, 2.4 percent; 3, 8.1 percent; 4, 20.1 percent; 5, 30 percent; c, section III, content Σ(V, Nb, Mo): 1, 3 percent; 2, 4.2 percent; 3, 15 percent; 4, 26 percent; 5, 40.2 percent; 6, 50.1 percent; d, section IV, content Σ(V, Nb, Mo): 1, 2.1 percent; 2, 8.1 percent; 3, 40.2 percent; 4, 50.1 percent.

pronounced softening of the alloys takes place during the second stage of the testing (σ = 20 kg/mm^2 and t = 500°). The highest resistance to plastic deformation was exhibited by alloys from the region of β_4 solid solutions. The creep rate of these alloys at 500° and σ = 15-20 kg/mm^2 in 200 hr of testing in the second portion of the creep curve is close to zero, but at 600° the creep of these alloys increases abruptly.

On the basis of data obtained by studying the creep of alloys of the quaternary system, "composition - high-temperature strength" diagrams were plotted indicating the dependence of the time necessary for reaching a given bending deflection of 3, 5 and 10 mm (fig. 3) on the composition under certain given conditions. The graph also shows polythermal sections in the region of

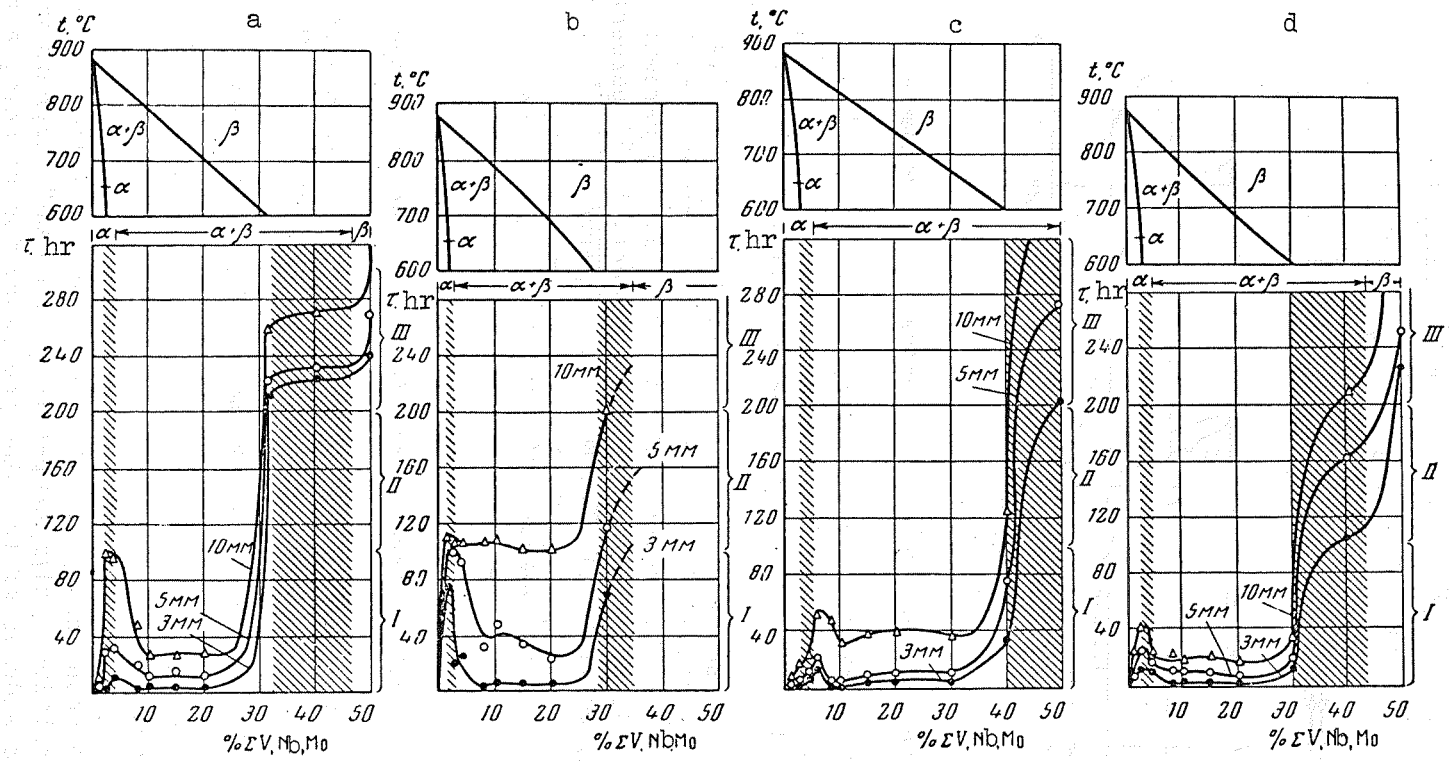

Figure 3. Dependence of the time necessary for reaching a given bending deflection (3, 5 and 10 mm) on the composition of alloys of the system Ti-V-Nb-Mo.

Testing stages: I, t = 500°, σ = 15 kg/mm^2; II, t = 500°, σ = 20 kg/mm^2; III, t = 600°, σ = 20 kg/mm^2; a, section I; b, section II; c, section III; d, section IV.

polymorphic transformations. The shaded portion of the diagrams indicates the regions in which either the solution of the β phase ($\alpha \rightarrow \alpha + \beta$ boundary) or its precipitation ($\alpha + \beta \rightarrow \beta$ boundary) is possible at 500°. Such an extrapolation of the curves of the polymorphic transformation into the region where the diffusion processes occur very slowly is possible, as was shown in the study of the phase diagrams of the binary systems of titanium with molybdenum and niobium (ref. 12). In the limited region of the α_4 solid solution, the high-temperature strength increases with rising total content of the alloying elements. The elevated high-temperature strength under the selected testing conditions corresponds approximately to the solubility limit of the α_4 solid solution. The most pronounced increase in high-temperature strength in the α region is observed in alloys of section II (with a higher molybdenum content). This element, which is chemically more different from titanium than are vanadium and niobium, hardens α-Ti to a greater extent. The high-temperature strength decreases in the two-phase region. This is most pronounced in the alloy of section IV with a high vanadium content, while the greatest strength in the two-phase region is displayed by alloys of section II. As is evident from the figures, bending deflections of 3, 5 and 10 mm in the α region are reached by almost all the alloys during the first testing stage, and only in the case of alloys of section II is it necessary to raise the stress to 20 kg/mm^2 at 500° in order to reach a bending deflection of 10 mm. The alloys of section I also show a considerable increase in high-temperature strength in the α region, but to a somewhat lesser extent than alloys of section II (with a higher molybdenum content). This can probably be explained by a high content of vanadium atoms in alloys of this section (in terms of atomic percent), which, as was shown in ref. 5, has almost no effect on the increase in the high-temperature strength of α-Ti under the selected testing conditions.

Deformation of the alloy with 33 percent of the total alloying elements of radial section I begins only in the third stage of the testing, at 600° and σ = 20 kg/mm^2. Alloys of this region, based on β solid solutions, display a high strength. In alloys corresponding to compositions located in the shaded area on the diagrams, at 600°, the second phase (α phase) which precipitated during the slow furnace-cooling of the alloys after annealing at 600° and testing at 500°, and which was not able to dissolve completely during the tests at 600°, is still present. This alloy (fig. 4) still contains a significant amount of the finely dispersed α phase. Alloys of the single-phase β region show a further increase in high temperature strength as compared to the two-phase alloys; this is particularly apparent from the example of alloys of section IV. Alloys of section II (with 36 percent of total alloying elements) were relatively brittle and did not withstand the given bending stress.

As shown in the figures, the "composition - high-temperature strength" diagrams agree satisfactorily with the change in the phase equilibrium along the

sections of the system. The formation of a solid solution causes an increase in high-temperature strength. In the two-phase region, as the coagulation of the β phase proceeds, the high-temperature strength declines. Alloys in which the phase boundary is extensive are the most unstable. Even in alloys with a high total content (20 and 30 percent) of alloying elements, the high-temperature strength is lower than in single-phase α and β alloys. This may be attributed to the strong influence of the decrease in the temperature of the polymorphic transformation $\alpha + \beta \rightarrow \beta$ on the high-temperature strength. As was shown in refs. 5-6 and 13-14, the polymorphism has an appreciable effect on the increase in plasticity upon the conversion from the hexagonal to the cubic structure with a higher lattice symmetry. The coagulation of the α phase along the boundaries and grain of the β phase and the lower temperature of its transformation into the β phase make the lattice of the α phase unstable and weaken the interaction at the phase boundary. In the finely dispersed state, the α phase hardens the alloy somewhat, but the alloys of the equilibrium β phase display the greatest high-temperature strength under the given testing conditions.

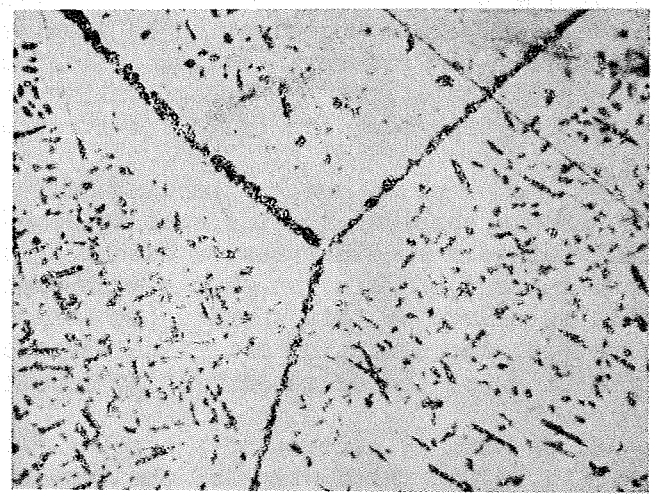

Figure 4. Microstructure of alloy with 40.2 percent Σ(V, Nb, Mo) - section I after testing at 600° and σ = 20 kg/mm^2 x 1350.

In absolute values of the time necessary for reaching a given bending deflection (5 and 10 mm), our data are somewhat lower than those cited in refs. 5 and 6, obtained by studying binary and ternary systems of titanium with vanadium and niobium. This may be explained by the fact that the specimens prepared in refs. 5 and 6 by the powder-metallurgical method contained a considerable amount of dissolved gases, particularly oxygen, which substantially hardens titanium. Thus, for example, in order to reach a 10 mm bending deflection in pure titanium, it is reported in ref. 5 that about 20 hr were required at 500° and σ = 20 kg/mm^2, whereas in our case titanium TG00 softened as early

as the first few minutes of testing under the same conditions. Furthermore, in refs. 5 and 6, use was made of vanadium containing 1.2 percent Al and a significant amount of dissolved gases.

The data obtained for the dependence of the high-temperature strength on the composition and phase structure make it possible to conclude that all the alloys of the α region of the quaternary system Ti-V-Nb-Mo soften rapidly at 500° and $\sigma = 15$ kg/mm^2 and cannot be used as heat-resistant alloys for long periods of operation under the selected conditions.

Molybdenum, introduced within the limits of its solubility in α-Ti, is the most useful additive for increasing the high-temperature strength of such alloys. Alloys from the region of β_4 solid solutions can be used as heat-resistant alloys.

The data obtained confirm the results of ref. 8 on the nature of the change in high-temperature strength in systems with limited solubility in the solid state and polymorphism in one of the components.

REFERENCES

1. Craighead, C., Simmons, O., and Eastwood, L. J. Metals, No. 3, p. 485, 1950.

2. Belousov, O. K., Kornilov, I. I., and Mikheyev, V. S. Dokl. AN SSSR, Vol. 145, No. 5, p. 1102, 1962.

3. - - - In: "Titanium and Its Alloys," Izd-vo AN SSSR, No. 7, pp. 120-126, 1962.

4. Luzhnikov, L. P. and Moiseyev, V. N. Metallovedeniye i termicheskaya obrabotka metallov, No. 7, p. 23, 1961.

5. Vlasov, V. S. and Kornilov, I. I. Izv. AN SSSR, OTN, Metallurgiya i toplivo, No. 4, p. 31, 1958.

6. - - - Izv. AN SSSR, OTN, Metallurgiya i toplivo, No. 7, p. 136, 1958.

7. Rostoker, U. Metallurgy of Vanadium (Russian translation). Metallurgizdat, 1959.

8. Kornilov, I. I. Physicochemical Principles of the High-Temperature Strength of Alloys (Fiziko-khimicheskiye osnovy zharoprochnosti splavov). Izd-vo AN SSSR, 1962.

9. Kornilov, I. I. and Polyakova, R. S. Izv. AN SSSR, OTN, Metallurgiya i toplivo, No. 1, p. 85, 1960.

10. Belousov, O. K., Kornilov, I. I., and Mikheyev, V. S. In: "Titanium and Its Alloys," Izd-vo AN SSSR, No. 10, pp. 27-36, 1963.

11. Kornilov, I. I. Izv. SFKhA, Vol. 18, p. 72, 1949.

12. Hansen, M., Kamen, E., Kessler, H., and McPherson, D. J. Metals, No. 3, p. 881, 1951.

13. Osipov, K. A. Some Activated Processes in Solid Metals and Alloys (Nekotoryye aktiviruyemyye protsessy v tverdykh metallakh i splavakh). Izd-vo AN SSSR, pp. 110-118, 1962.

14. Grigorovich, V. K. and Safonov, Yu. S. Izv. AN SSSR, OTN, Metallurgiya i toplivo, No. 5, p. 38.

CHARACTERISTICS OF THE COLD BRITTLENESS OF TITANIUM

B. B. Chechulin and M. B. Bodunova

Introduction

The appearance of the cold brittleness of metals is one of the most dangerous phenomena in practical applications. Many studies have been devoted to the nature of cold brittleness and impact brittleness of metals, particularly steels. Nevertheless, the purely physical factors causing some metals to be cold short but not others have not been established as yet (ref. 1). It should be noted that the cold brittleness of iron-base alloys has been studied fairly thoroughly. The influence of various factors on cold brittleness has been determined, and several formal mechanisms have even been proposed to explain the conditions of the appearance of brittleness in steel. On the other hand, the cold brittleness of other metals has been studied very insufficiently. It is our view that the nature of the cold brittleness of metals can be determined only from extensive experimental material obtained for the most diverse metals.

Studies have shown that the cold brittleness is characteristic of metals having a body-centered cubic (iron, chromium, etc.) or hexagonal (zinc, titanium, etc.) crystal lattice. However, the regularities of cold brittleness as such have been studied only in iron alloys, whereas for many other metals only the fact of the appearance of brittleness under certain conditions has been mainly established.

The present work discusses certain features of the transformation of technically pure titanium into a cold short state and analyzes the dependence of the appearance of brittleness in titanium on various external factors: extent of the stress condition, deformation rate, and size of specimens.

Material Used and Experimental Technique

The investigation was carried out on technically pure titanium obtained by remelting magnesiothermic titanium sponge in vacuum arc furnaces. Three melts of titanium were used which after the preparation of the ingots were forged into bars of round (14 mm in diameter) or square (14 mm on one side) cross sections which were machined with a wheel until their transverse dimension was 10 mm. The machined specimen blanks were subjected to prolonged vacuum annealing at 750° in order to achieve a well-annealed equilibrium structure and the maximum possible elimination of volatile gaseous impurities

(chiefly hydrogen) from the metal. The chemical composition and mechanical characteristics of the metal employed are shown in table 1.

The cold brittleness of titanium is chiefly due to the so-called hydrogen brittleness (ref. 2). For this reason, the specimen blanks were enriched with hydrogen in separate batches to various degrees in a special unit at 700°.

The hydrogen content of the specimens was raised in steps from 0.002 to 0.06 wt percent.

The main experiments involving the determination of the temperature threshold of brittleness of titanium and the dependence of the temperature threshold on the sharpness of the notch were conducted on cylindrical specimens. The smooth specimens were 7 mm in diameter and 55 mm long. The notched specimens (having a round notch) had an outer diameter of 10 mm and a diameter in the notch of 7 mm. The influence of the deformation rate on the critical temperature of brittleness was studied on prismatic Menager specimens, and the scale effect was studied on prismatic specimens geometrically similar to Charpy specimens. The testing of the specimens was carried out by bending impact on Charpy impact machines and by static bending in special attachments at a punch displacement rate of 0.1 mm/sec. The impact strength was determined in tests of cylindrical specimens, and in testing Menager and Charpy specimens, in addition to measuring the energy to fracture, the Stribeck deformation characteristic, i.e., the degree of distortion of the working cross section of the specimen at the site of the fracture was measured.

Tensile and rupture tests were carried out on cylindrical specimens with a thinning of the middle portion in order to exclude breaks at the tips of the specimens (at a high hydrogen content). The thinning was made by means of a circular recess having a radius of curvature of 90 mm; the minimum diameter of the specimens was 5 mm. Tests at high temperatures were conducted in water (up to 90°) or in a special furnace in air (100-350°). Low-temperature (-196°) tests were made with precooling in a mixture of benzine and liquid nitrogen or in liquid nitrogen. Checking tests established that the testing temperature was recorded within ±5°.

TABLE 1. CHEMICAL COMPOSITION AND MECHANICAL CHARACTERISTICS OF INVESTIGATED TITANIUM

Melt number	Impurity content not more than, wt percent						Mechanical characteristics at room temperature					
	Fe	Si	C	O_2	N	H_2	σ_b, kg/mm²	$\sigma_{0.2}$, kg/mm²	δ, %	ψ, %	a_H, kgm/cm²	HB, kg/mm²
1	0.06	0.04	0.04	not determ.	0.03	0.002	48.0 48.0	32.0 32.0	26.0 26.5	55.5 55.5	13.2 12.6	153
2	0.08	0.04	0.04	0.15	0.03	0.002	47.0 47.0	34.0 34.0	27.5 32.0	64.0 59.5	14.8 17.4	153
3	0.05	0.04	0.06	0.14	0.03	0.003	46.5 46.5	35.0 35.0	26.0 28.0	50.5 52.5	13.1 11.5	155

Results and Discussion

Let us consider the dependence of the impact strength, determined on cylindrical specimens, on the testing temperature for vacuum-annealed titanium (fig. 1a). The impact strength of titanium worked in a vacuum does not decline with decreasing temperature down to -196°. This confirms the already established fact that natural cold brittleness is lacking in titanium. An increase in the sharpness of the notch in the specimens causes a certain decrease in the impact strength of the material (as a result of a greater localization of plastic deformation); this is manifested to a greater extent the lower the testing temperature. The use of circular notches 1.5 mm deep with a bottom radius of curvature of 5, 2 and 0.5 mm did not reveal any regions of abrupt decrease in impact strength, with the exception of an unexplained minor decline at a temperature below -100°.

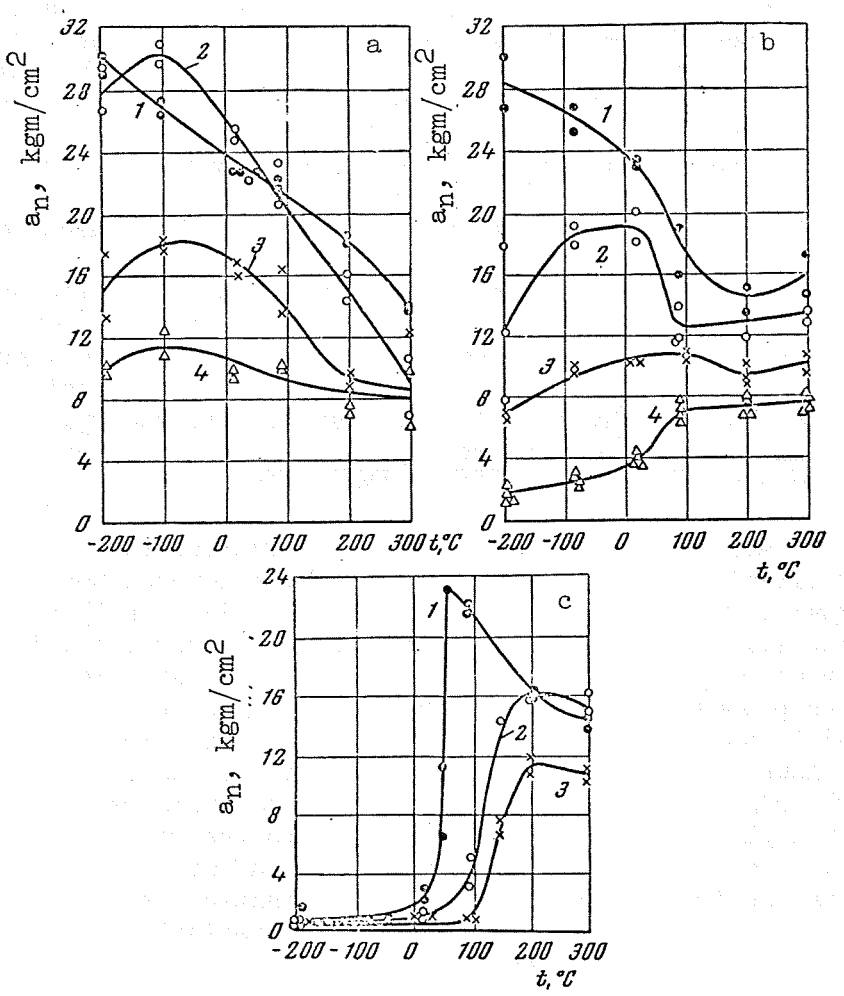

Figure 1. Dependence of impact strength of titanium on testing temperature for various radii in the bottom of the notch of specimens: a, titanium after annealing; b, titanium with 0.015 wt percent H_2; c, titanium with 0.035 wt percent H_2; 1, smooth specimens; 2,3,4, notched specimens (notch radius: 2-5 mm; 3-2 mm; 4-0.5 mm).

The introduction of even a small amount (0.015 percent) of hydrogen (fig. 1b) changes appreciably the dependence of the impact strength on the testing temperature. While tests of smooth specimens and specimens with relatively "soft" notches (bottom radius of curvature of 5 and 2 mm) did not reveal any visible brittleness threshold, i.e., any sharp drop in impact strength over a narrow temperature range, tests of notched specimens with a bottom radius of curvature of 0.5 mm revealed a sharp drop in impact strength at a temperature below 100°.

An increase in hydrogen content to 0.035 percent led to the appearance of a cold brittleness threshold even in specimens without notches (fig.1c). It is characteristic that the temperature range of appearance of brittle fractures, or critical brittleness temperature, was found to vary in a regular fashion with the sharpness of the notch: the lowest temperature (60°) was observed in smooth specimens, a higher value (160°)--in specimens with a 5 mm radius of curvature of the notch bottom, and the highest (200°)--in specimens with a 2 mm radius of curvature of the notch bottom. Thus, the regularity of the dependence of the critical brittleness temperature on the sharpness of the notch qualitatively agrees very well with the results of a study of the cold brittleness of steel (see, for example, ref. 3). Furthermore, the nature of the change in impact strength within the temperature range of appearance of brittleness is the same as in steel: smooth specimens give the most abrupt decline in impact resistance, while notched specimens show a smoother decrease in impact resistance.

Of great interest is the microstructural pattern of brittle and ductile fracture of titanium (fig. 2). It is easily observed that the brittle flaws are direct results by layers of the separation of titanium hydrides, whose grains have the form of needles (ref. 4). The given microstructural pattern of the brittle and ductile fracture is quite similar to the brittle fracture of steel along the twinning planes (ref. 5). The ductile fracture of titanium is not related to any orientations within the grain.

Let us now examine the influence of the deformation rate on the cold brittleness of titanium. The results obtained with notched Menager specimens at various temperatures are shown graphically (fig. 3). In these tests, the criterion of ductility used was the deformation characteristic, i.e., the degree of distortion of the working cross section of the specimen at the site of the break, as proposed by Stribeck (ref. 6). As can be seen from figure 3, vacuum-annealed titanium retains its ductility at a high level as the testing temperature is lowered to -196°, both in impact tests and in tests under static conditions. The higher plasticity in the low-temperature region in impact tests is difficult to explain if we confine ourselves to the results of our experiments, but it may be assumed that it results from a local rise in the temperature of the metal in the volume traversed by plastic deformation, owing to the low thermal conductivity of titanium. The appreciable increase in ductility at temperatures of 200-300° and the slow deformation may be explained by the strain aging of titanium in this temperature interval (ref. 7).

Tests of titanium specimens containing 0.03 percent H_2 revealed a distinct brittleness threshold both under static and impact loads. In complete conformity

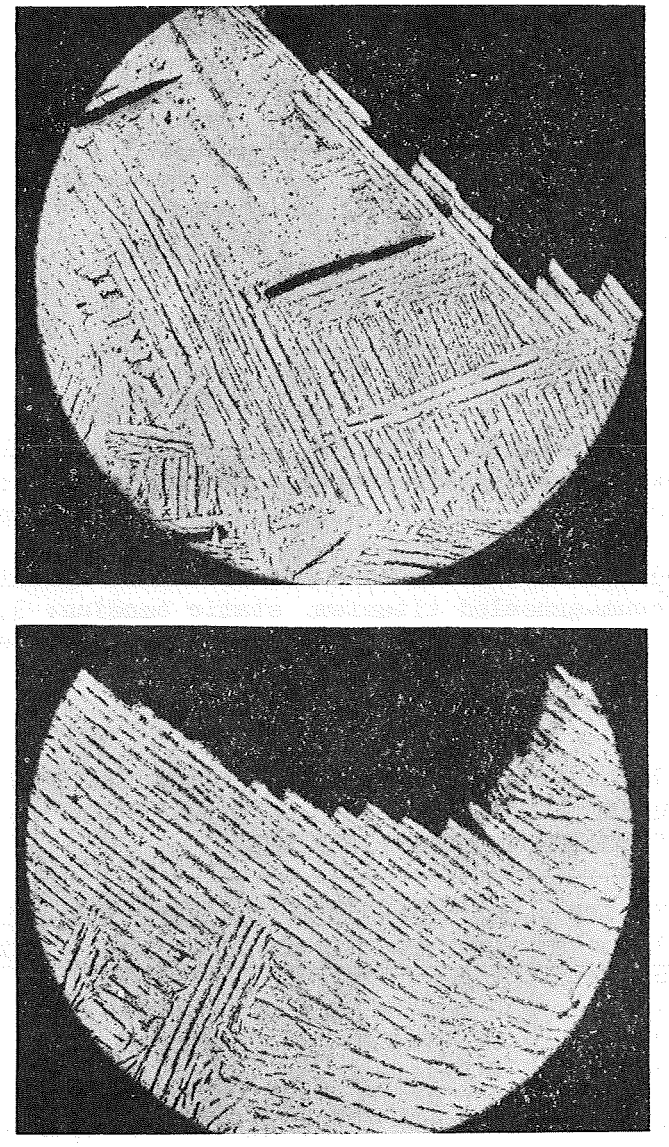

Figure 2. Appearance of fracture of titanium specimens under bending impact, x 100. Metal was preheated in a hydrogen-containing medium at 1100°.

with the general regularities of the cold brittleness of steel, a dynamic load shifts the brittleness threshold into a region of higher temperatures than in static tests.

The results of static bending tests at various temperatures of geometrically similar samples of titanium containing 0.03 percent H_2 are shown in table 2. The Stribeck characteristic was taken as the measure of the ductility.

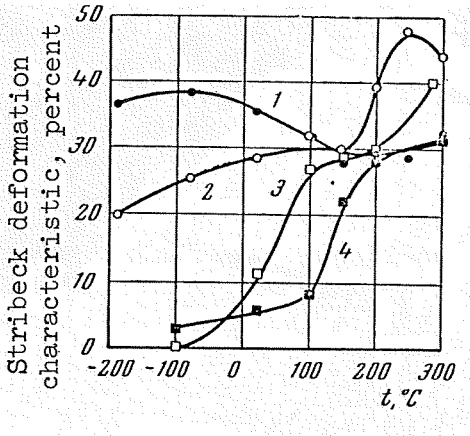

Figure 3. Deformation characteristic calculated according to Stribeck versus testing temperature for vacuum-annealed titanium containing up to 0.03 wt percent H_2 in dynamic and static bending: 1, vacuum-annealed titanium, dynamic bending; 2, vacuum-annealed titanium, static bending; 3, titanium containing 0.03 percent H_2, dynamic bending; 4, titanium containing 0.03 percent H_2, static bending.

TABLE 2. STRIBECK DEFORMATION CHARACTERISTIC OF TITANIUM SPECIMENS CONTAINING 0.03 PERCENT H_2 IN STATIC BENDING TESTS (IN PERCENT)

Testing temperature, °C	Cross section of specimens, mm			
	20 x 20	10 x 10	5 x 5	2 x 2
+90	39.0			
+80	33.5	39.6—28.2		
+60	15.5—10.5		31.2—26.8	
+50	20.0—14.0			
+40	16.0		22.0	
+20	4.0—0.0	31.5—22,0	25.6	21.6—19.0
+14		25.8		
+2		11.3		
+1				17.4
—7		13.6		
—10				19.1
—15		12.1	7.6	
—20			15.2—6.4	9.8—4.3
—28			14.8	
—30		2.6		7.2—4.6
—40			11.6	6.6
—50			8.8	9.3—8.3
—60		0.5		1.3
—80				1.4
cold brittleness temperature (start of decrease) °C	+80	+20	+10	—15

It should be noted that this characteristic (ratio of the difference in the width of contracted and dilated fibers to the height of the cross section at the site of rupture) is a purely arbitrary reflection of the ductility, since the cross section of the fracture can only be approximated by a trapezoid, for which reason the absolute value of this characteristic can vary appreciably. This apparently explains the substantial difference in the absolute values of the deformation characteristic in specimens of ductile titanium. However, the relative change of this characteristic with decreasing temperature, which reveals the brittleness threshold, unquestionably establishes the critical brittleness temperature with sufficient reliability. As is evident from table 2, the critical brittleness temperature rises systematically with increasing dimensions of the specimens, and the characteristic is -15° for specimens measuring 2·2 mm, $+10^{\circ}$ for specimens measuring 5·5 mm, and $+ 80^{\circ}$ for specimens measuring 20·20 mm.

Thus, it may be concluded that the cold brittleness of titanium arising from the presence of hydrogen and acted upon by the principal external factors--extent of the stress condition, deformation rate and specimen size--is manifested with the same regularity as in steels.

It is natural to assume that the similarity of these regularities is a manifestation of the dual nature of the fracture of titanium-containing hydrogen. These suggestions had already been expressed by L. S. Moroz (ref. 8) in connection with an analysis of the nature of the hydrogen brittleness of titanium.

The well-known interpretation of academician A.F. Ioffe is based on the results obtained with rock salt at various temperatures. This interpretation presupposes two types of strength: a brittle and a ductile fracture. The strength of brittle fracture, i.e., the rupture strength, is independent of external factors (stress condition, temperature and deformation rate), whereas on the contrary, the strength in ductile fracture, i.e., the deformation resistance, depends strongly on these factors. The extension of A. F. Ioffe's interpretation to metals, suggested by N. N. Davidenkov, made it possible to select a structural system of theoretical interpretations of the cold brittleness of metals and to establish many regularities in the variation of brittleness temperature with various factors. However, the application of A. F. Ioffe's interpretation to metals was found very difficult. Only in the case of iron phosphite was it possible to obtain (ref. 9) a curve of the change in strength with temperature that was close to A. F. Ioffe's interpretation. The difficulty of applying this interpretation to metals was mainly due to an attempt to obtain an ideally brittle fracture (without any appreciable residual strains) which, as was shown by subsequent investigations, does not exist at all. However, without changing its essential features, one can re-present A. F. Ioffe's interpretation in a somewhat different manner if by brittle strength of metals is meant the rupture strength (independently of the plastic deformations), and if the curve representing the temperature dependence of the yield strength is replaced by a curve representing the temperature dependence of the strength at ductile fracture.

Considering the above refinements, we plotted curves of the change in tensile strength for titanium containing different amounts of hydrogen (fig. 4). These curves provide a complete confirmation of A. F. Ioffe's interpretation.

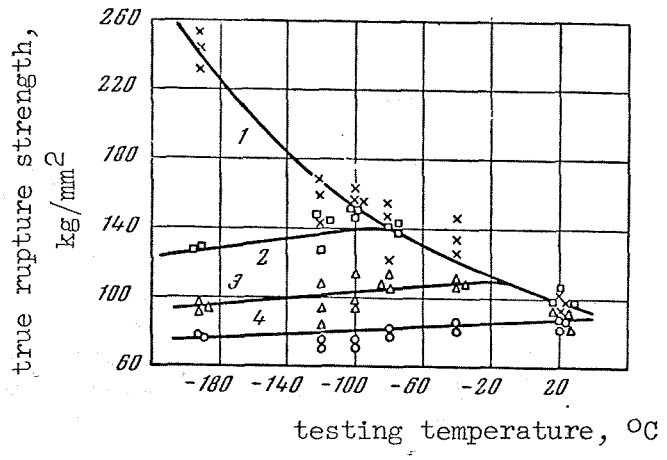

Figure 4. True rupture strength versus testing temperature for titanium containing various amounts of hydrogen: 1, vacuum-annealed titanium; 2, titanium containing 0.012 wt percent H_2; 3, titanium containing 0.035 wt percent H_2; 4, titanium containing 0.060 wt percent H_2.

The strength of vacuum-annealed titanium increases continuously as the temperature drops to -196°. The introduction of hydrogen limits the increase in strength to the level of the cleavage strength, which is practically independent of temperature.

The level of the cleavage strength depends entirely on the hydrogen content of titanium. The more hydrogen is present in titanium, the lower is the cleavage strength, or strength at brittle fracture. Thus, the experimental data show that a direct cause of the cold brittleness of titanium is a sharp decline in its cleavage strength under the influence of hydrogen introduced into the metal. In the light of the results obtained, it is necessary once again to return to the idea of a possible general cause of cold brittleness by relating it to the unavoidable presence in metals of oxygen, nitrogen and hydrogen impurities or any other elements. It is known that such an explanation of cold brittleness has already been proposed in a study of the brittleness of chromium (refs. 10 and 11).

It is possible that even when the content of impurities is minute, the cleavage strength of metals increases sharply. The decrease in cleavage strength may be due to the passage of the first shifts causing a weakening of bonds along certain crystallographic planes on which the impurities can precipitate. Apparently, this process is chiefly characteristic of metals with a body-centered or hexagonal lattice.

The influence of plastic deformation on the embrittlement process can be confirmed by tests for the impact strength of titanium with various hydrogen contents. The curves representing the relative decrease in the impact strength

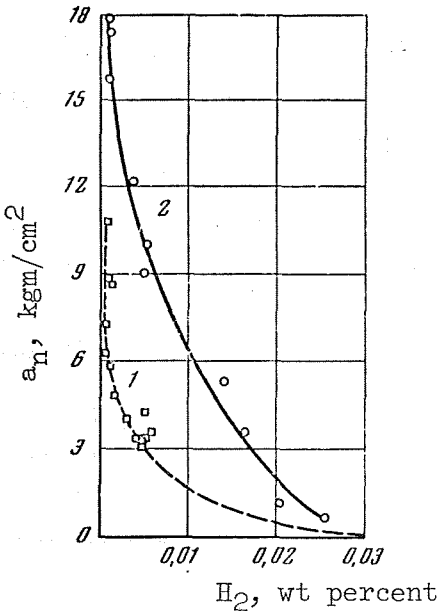

Figure 5. Relative change in impact strength versus hydrogen content: 1, titanium work-hardened to the extent of 25 percent; 2, annealed titanium.

of cold-worked and annealed titanium with rising hydrogen content (fig. 5) show that additional cold working substantially reinforces the decline in impact strength. This means that the cleavage strength decreases appreciably in the course of plastic deformation and that the sensitivity of titanium to hydrogen brittleness increases.

Conclusions

1. The cold brittleness of titanium is explained by the presence of hydrogen. Cold brittleness is not displayed by titanium free from hydrogen.

2. The regularities in the change of the critical brittleness temperature of titanium with external factors--extent of the stress condition (sharpness of notch), rate of application of loads and dimensions of specimens--are the same as in steel.

3. The applicability of A. F. Ioffe's interpretation to the analysis of the conditions under which cold brittleness is displayed in titanium has been confirmed. The main cause of the appearance of cold brittleness in titanium is a decrease in cleavage strength due to the introduction of hydrogen into titanium.

4. It was shown that the principal cause of the cold brittleness of metals may be the presence of impurities which are bound to be present in metals of technical purity.

REFERENCES

1. Davidenkov, N. N. and Chuchmin, T. N. In: Studies of Heat-Resistant Alloys (Issledovaniya po zharoprochnym splavam). Ize-vo AN SSSR, Vol. 2, p. 9, 1957.

2. Moroz, L. S., Chechulin, B. B., Polin, I. V., Butalov, L. V., Shul'kin, S. M. and Goryachev, A. P. Coll. Titanium and Its Alloys (Titan i yego splavy). Sudpromgiz, Vol. 1, p. 120, 1960.

3. Davidenkov, N. N. Dynamic Tests of Metals (Dinamicheskiye ispytaniya metallov). ONTI, 1963.

4. Nikolayev, G. I. and Bruk, B. I. In: Physical Metallurgy (Metallovedeniye). Sudpromgiz, Vol. 2, p. 74, 1958.

5. Potak, Ya. M. and Sachkov, V. V. Zhurnal Tekhnicheskoy Fiziki, No. 3, p. 399, 1949.

6. Stribeck. VDI, Vol. 59, p. 57, 1915.

7. Rosi, F. D. and Perkins, F. C. Trans. ASM, Vol. 45, p. 472, 1953.

8. Moroz, L. S. and Khesin, Yu. D. In: Physical Metallurgy (Metallovedeniye). Sudpromgiz, Vol. 3, p. 74, 1959.

9. Shevandin, Ye. M. Zav. Lab., No. 7, p. 858, 1947.

10. Wain, H., Henderson, F. and Lohnstone, S. J. Inst. Metals, Vol. 83, No. 4, p. 133, 1954.

11. Savitskiy, Ye. N. and Terekhova, V. F. In: Studies of Heat-Resistant Alloys (Issledovaniya po zharoprochnym splavam). Izd-vo AN SSSR, Vol. 2, p. 141, 1957.

CREEP OF ALLOY AT3 AT 350°

K. P. Markovich, V. S. Mikheyev and Z. G. Fridman

At the present time, the only high-strength materials with a density of 4.4-4.6 g/cm^3 for operation at 300-550° are titanium-base alloys. For this reason, the development of theoretical and experimental studies in the field of high-temperature strength of titanium alloys assumes an exceptional importance. One of the main problems in this field is the study of the properties and behavior of the alloys in the course of creep.

The purpose of the present work was to establish the creep limit of titanium alloy AT3 at 350° for a total deformation of 1 percent in the course of 20,000 hrs of testing, and also to study the change in the mechanical characteristics of the alloy after it has been tested for creep under selected conditions.

Work conducted earlier in this direction has shown (ref. 1) that alloy AT3 at 300 and 350° and a stress of 30 kg/mm^2 following 5000 hrs of creep tests is characterized by a high creep resistance and retains a high thermal stability.

An alloy melted under plant conditions in a vacuum arc furnace by double remelting was chosen for the investigation. The following starting materials were used in the preparation of the alloy: titanium sponge TG0 with an ultimate strength of 39-43 kg/mm^2, technical silicon KR, chromium XI, technical iron, and a chromium-boron master alloy (up to 10 percent B). The alloying elements were introduced into the alloy in the form of a complex master alloy. The chemical composition of alloy AT3 was as follows: base, Ti; 2.7 percent AL; 0.6 percent Cr; 0.30 percent Fe; 0.36 percent Si; 0.01 percent B (calculated).

After forging, the mechanical characteristics of alloy AT3 were as follows: σ_b = 86.4 kg/mm^2; σ_s = 84.9 kg/mm^2; δ = 14.5 percent; ψ = 43.2 percent; α_n = 7.7 kgm/cm^2. After annealing at 850° for 30 min and cooling in air, the mechanical characteristics assumed the following values: σ_b = 86.3 kg/mm^2; σ_s = 85.0 kg/mm^2; δ = 14.8 percent; ψ = 44.75 percent; α_n = 6.8 kgm/cm^2.

Specimens for creep tests were prepared from a forged rod 20 mm in diameter. The tests were made with an IP-5 machine at a constant temperature of 350° and stresses of 15, 30, 33, 37, 45 and 50 kg/mm^2. The duration of the tests under the above stresses was respectively 5,454, 6,662, 5,705, 5,215, 12,000 and 9,300 hrs.

To determine the stability of the alloy in the course of long-time creep testing, the mechanical properties of the alloy were studied at room temperature after the creep test. Standard rupture-test specimens were cut out of the working part of the creep-tested specimens.

Results

Creep of alloy AT3. Let us examine the data on the creep following tests of alloy AT3 lasting from 5,000 hrs at a constant temperature of 350° and creep stresses of 15, 30, 33, 37, 45 and 50 kg/mm^2.

The shape of the creep curve at stresses of 15 and 30 kg/mm^2 (fig. 1) is close to linear. The stage of transient creep is brief. Its duration does not exceed ~200 hrs for stresses of 15 and 30 kg/mm^2. As the creep stress increases to 37 kg/mm^2, the stage of transient creep increases to approximately 1,200 hrs. The stage of steady-state creep is fairly long for all stresses and does not end after 5,000 hrs of testing. Under the selected creep-test conditions, the third stage, that of accelerated creep, is absent. The total deformation in 5,000 hrs of testing increases with rising creep stress from 0.18 percent at 15 kg/mm^2 to 0.92 percent at 37 kg/mm^2.

As shown by the creep curves for stresses of 45 and 50 kg/mm^2 (fig. 2), the stage of steady-state creep begins after 400 hrs of tests under a stress of 45 kg/mm^2 and does not end after 12,000 hrs. The total deformation for 12,000 hrs is 1.2 percent.

In tests of alloy AT3 under a stress of 50 kg/mm^2, the stage of steady-state creep begins after testing for 1,000 hrs. The total deformation for 9,300 hrs is 4.8 percent.

The creep curves (figs. 1 and 2) make it possible to determine the rate of steady-state creep on various portions of the curve. The rate of steady-state creep v_p was defined as the quotient of the division of the elongation Δl by the time $\Delta\tau$ during which this elongation took place.

The creep rate at the steady-state stage increases with rising stress, but does not exceed $2 \cdot 10^{-5}$ percent hrs for a stress of 37 kg/mm^2. An increase in

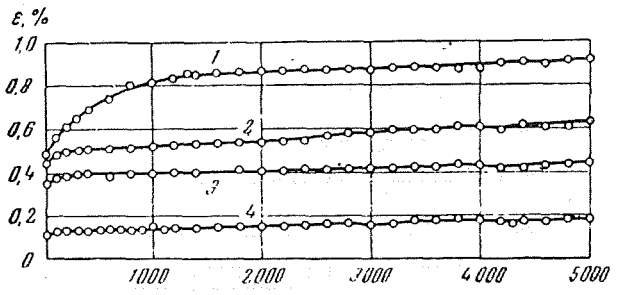

Figure 1. Creep curves of alloy AT3 at 350°:
1, σ = 37 kg/mm^2, v_p = $2 \cdot 10^{-5}$ percent/hr; 2,
σ = 38 kg/mm^2, v_p = $2 \cdot 10^{-5}$ percent/hr; 3,
σ = 30 kg/mm^2, v_p = $1.5 \cdot 10^{-5}$ percent/hr; 4,
σ = 15 kg/mm^2, v_p = 10^{-5} percent/hr.

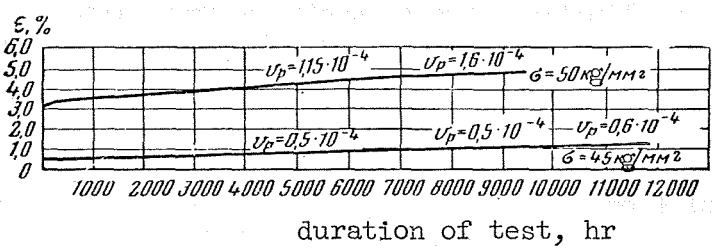

Figure 2. Creep curves of alloy AT3 at 350° and creep stresses of 45 and 50 kg/mm^2.

creep rate is observed in tests under stresses of 45 and 50 kg/mm^2. In the presence of these stresses, the creep rate at the steady-state stage is equal to an average of $0.5 \cdot 10^{-4}$ and $1.6 \cdot 10^{-4}$ percent/hr respectively, the creep rate remaining constant for 12,000 hrs of tests under a stress of 45 kg/mm^2.

We used the numerical values of creep rates, obtained from the "elongation-time" curves, to plot curves representing the change in the creep rate in semi-logarithmic "stress-creep rate" coordinates (fig. 3). Such a curve enabled us to determine the limiting stress at 350° causing a specified residual deformation of 1 percent after 20,000 hrs of tests. The creep rate at a residual deformation of 1 percent after 20,000 hrs of tests at the indicated temperature will be $5 \cdot 10^{-5}$ percent/hr.

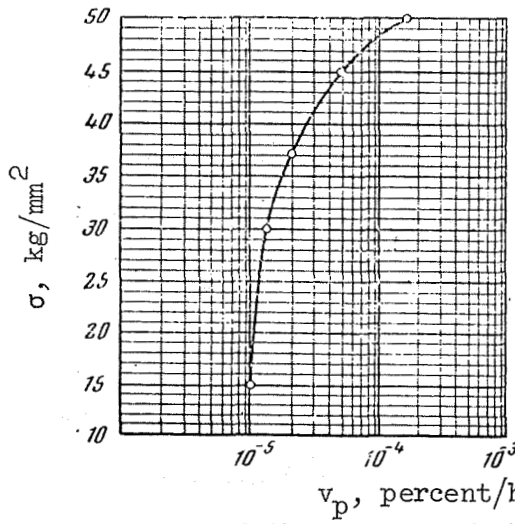

Figure 3. Curves of the relation between σ and v_p for alloy AT3 with 2.7 percent Al, 1.26 percent Σ (CR, Fe, Si) at 350°.

Consequently, the limiting stress causing a creep rate of $5 \cdot 10^{-6}$ percent/hr at 350° for alloy AT3 containing 2.7 percent Al and 1.26 percent Σ (Cr, Fe, Si) will be 42 kg/mm^2.

Change in Mechanical Properties

Let us examine the dependence of the mechanical properties of alloy AT3 at room temperature on the creep stress (fig. 4).

It is apparent from the data obtained that the ultimate strength of the alloy σ_b and the plasticity characteristics σ and ψ do not undergo any appreciable changes following creep tests at various stresses. Thus, in the initial state (after forging), the alloy had an ultimate strength of 86.4 kg/mm^2 and an elongation per unit length of 16.3 percent, whereas after creep tests at 350° and a creep stress of 45 kg/mm^2 applied for 5,900 hrs, the ultimate strength was 85.8 kg/mm^2, the elongation per unit length was 16.4 percent and ψ = 40.2 percent.

Consequently, the ultimate strength and the plasticity characteristics of the alloy do not undergo any substantial changes after sufficiently long creep tests.

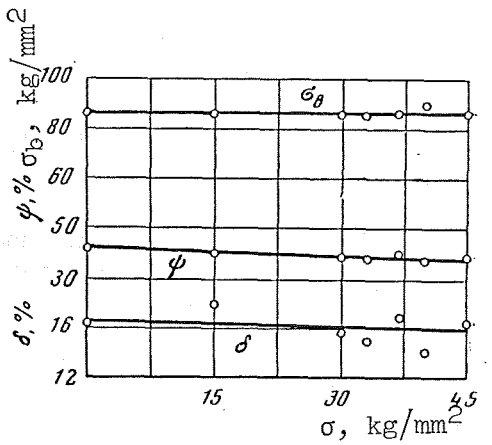

Figure 4. Change in the mechanical properties of titanium alloys AT3 with 2.7 percent Al and 1.26 percent Σ (Cr, Fe, Si) after a creep test of 5,000 hrs at 350°.

In the course of a prolonged creep test, the alloy does not become embrittled, independently of the stress. The strength and plastic properties of the alloy are retained at the level of the initial state.

Summary

1. The creep of alloy AT3 of the six-component system Ti-Al-Cr-Fe-Si-B with 3 percent Al and 1.26 percent Σ (Cr, Fe, Si) at 350° was investigated. The tests lasted 5,000 hrs for creep stresses of 15, 30, 33 and 37 kg/mm^2 and 9,300-12,000 hrs for creep stresses of 45 and 50 kg/mm^2. Under the selected testing conditions, alloy AT3 is characterized by a high creep strength.

2. The creep rate of alloy AT3 does not exceed $2 \cdot 10^{-5}$ percent/hr for a creep stress of 37 kg/mm^2. An increase in creep rate is observed in tests under stresses of 45 and 50 kg/mm^2. Under these stresses, it is respectively equal to $0.5 \cdot 10^{-4}$ and $1.6 \cdot 10^{-4}$ percent/hr at the stage of steady-state creep.

3. The limiting stress at 350° at which the residual deformation after 20,000 hrs of tests corresponds to 1 percent is equal to 42 kg/mm^2.

REFERENCES

1. Mikheyev, V. S., Markovich, K. P. and Fridman, Z. G. Coll. Titanium and Its Alloys (Titan i yego splavy). Izd-vo AN SSSR, No. 10, p. 214, 1963.

2. Kornilov, I. I., Mikheyev, V. S., Chernova, T. S. and Markovich, K. P. Coll. Titanium and Its Alloys (Titan i yego splavy). Izd-vo AN SSSR, No. 10, p. 224, 1963.

3. Nikitina, L. P. Coll. Titanium and Its Alloys (Titan i yego splavy). Izd-vo AN SSSR, No. 10, p. 224, 1963.

STUDY OF THE CREEP AND THERMAL STABILITY OF ALLOY AT4 AT 500°

I. I. Kornilov, O. N. Andreyev and B. M. Voshedchenko

The authors studied the creep and thermal stability of titanium alloy AT4 of the six-component system Ti-Al-Cr-Fe-Si-B at 500° by using a standard method. The alloy was melted under plant conditions in a vacuum arc furnace by double remelting.

The following charging materials were used in the preparation of the alloy: titanium alloy TG0 with an ultimate strength of 39-43 kg/mm^2, technical silicon Kr, chromium XI, technical iron, and a chromium-boron master alloy (up to 10 percent B).

The alloying elements were introduced into the composition in the form of a complex master alloy.

The chemical composition of alloy AT (base Ti) was: 4.67 percent Al, 0.86 percent Cr, 0.31 percent Fe, 0.27 percent Si, 0.001 percent B (calculated). The content of impurities was: 0.05 percent C, 0.024 percent N_2, and 0.007 percent H_2.

The mechanical characteristics of alloy AT4 at room temperature were: after forging (as-received condition) σ_b = 94 kg/mm^2; σ_s = 89 kg/mm^2; δ = 15 percent; ψ = 45 percent; α_n = 6.5 kgm/cm^2; after annealing for 30 min at 880° and cooling in air, σ_b = 94.2 kg/mm^2; σ_s = 89.4 kg/mm^2; δ = 15.1 percent; ψ = 45.3 percent; α_n = 6.4 kgm/cm^2.

The creep of alloy AT4 at 500° was studied by a standard extension method on TSP-1 specimens with the working part 100 mm long and 10 mm in diameter at stresses of 2.5 and 5 kg/mm^2 during 1,000 hrs.

For each stress, the tests were carried out on two specimens simultaneously using IP-5 machines, and the same creep values were thus obtained.

Creep tests of AT4 at 500° for 1,000 hrs showed that at the stress of 5 kg/mm^2 the total deformation was 0.5 percent, and at the stress of 2.5 kg/mm^2, it decreased to 0.18 percent.

The "deformation-time" creep curves of alloy AT4 at stresses of 5 and 2.5 kg/mm^2 are similar in character (fig. 1).

The stage of transient creep for a stress of 2.5 kg/mm^2 does not exceed 650 hrs. As the stress increases to 5 kg/mm^2, the stage of transient creep increases to 750 hrs.

Thus, the stage of steady-state creep in the first case begins after 650 hrs of tests, and in the second, after 750 hrs and continues up to 1,000 hrs. The tests are then terminated (the specimens are removed).

Under the selected conditions of creep testing, the third stage of accelerated creep is absent.

The total deformation for 1,000 hrs of tests rises with increasing creep stress from 0.18 percent at 2.5 kg/mm^2 to 0.5 percent at 5 kg/mm^2.

The creep curves (fig. 1) enabled us to determine the rate of steady-state creep.

The creep rate at the steady-state stage of creep increases with rising creep stress.

At stresses of 2.5 and 5 kg/mm^2, the creep rates at the stage of steady-state creep are equal to an average of $0.3 \cdot 10^{-6}$ and $1.6 \cdot 10^{-6}$ percent/hr.

Hence, for alloy AT4, the limiting stress causing a creep rate of $0.3 \cdot 10^{-6}$ percent/hr at 500° will be 2.5 kg/mm^2. This indicates a high creep resistance of alloy AT4 at 500° and a stress of 2.5 kg/mm^2.

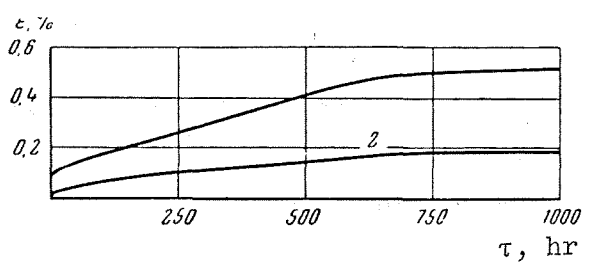

Figure 1. Creep curves of alloy AT4 at 500° for 1,000 hrs: 1, σ = 5 kg/mm^2; 2, σ = 2.5 kg/mm^2.

The creep curves of the titanium alloys (fig. 2a) were plotted on the basis of data obtained by I. I. Kornilov, V. S. Mikheyev, O. N. Andreyev and P. S. Mayboroda.[1] The specimens were subjected to bending by the centrifugal method at 500° and a stress of 20 kg/mm^2. The test lasted 100 hrs.

As is evident from this figure, the creep of alloys of the six-component system Ti-Al-Cr-Fe-Si-B, AT3, AT4, AT6 and AT8 is considerably less than that of the investigated titanium alloys, OT4, VT6 and OT4-2. The creep curves of alloys OT4, VT5, VT5-1, VT6 and AT4 are shown in figure 2b. The specimens were subjected to extension by a standard technique, and the testing conditions were the same as before.

The data on the creep rate obtained by the bending method and the standard extension method are in good mutual agreement.

Thus, of all the alloys studied, the creep rate of alloy AT4 is the lowest.

Alloy AT4, with a density of 4.5 g/cm^3, is very interesting as a heat-resistant titanium alloy whose strength is close to that of 1Kh18N9T steel and which can be used at working temperatures up to 500°.

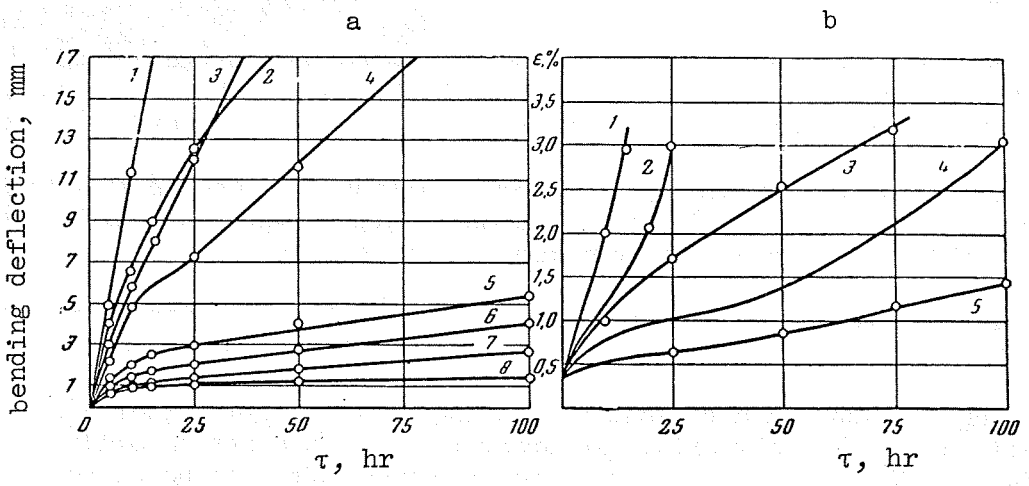

Figure 2. Creep curves of titanium alloys at 500° and a stress of 20 kg/mm^2 for 100 hrs: a, centrifugal method of bending the specimens (1, alloy OT4; 2, alloy AT1 without Al; 3, alloy VT6; 4, alloy OT4-2; 5, alloy AT3; 6, alloy AT4; 7, alloy AT8); b, standard extension method (1, alloy OT4; 2, alloy VT5; 3, alloy VT5-1; 4, alloy VT6; 5, alloy AT4).

---

[1] I. I. Kornilov, V. S. Mikheyev, O. N. Andreyev and P. S. Mayboroda. Coll. Titanium and Its Alloys (Titan i yego splavy). Izd-vo AN SSSR, No. 10, p. 234, 1963.

At this temperature, alloy AT4 has a higher short-time and long-time strength than titanium alloys OT4, VT5, VT5-1, VT6 and OT4-2. Furthermore, alloy AT4 does not contain any costly and scarce components.

Alloy AT4 is deformable: it can be used to make various semifinished products, including pipes, by means of hot and cold rolling. Cold rolling can be used to make pipes 6-8 mm in diameter with a wall thickness of 0.3-0.6 mm from this alloy. Alloy AT4 welds satisfactorily when argon arc and electroslag welding is used.

To determine the thermal stability of alloy AT4 in the course of long-time creep testing, the mechanical properties were studied at room temperature after the creep tests.

Standard rupture-test specimens LIM-1 (length of working part 36 mm and diameter 6 mm) were made from the working part of specimens tested for creep.

The average mechanical characteristics of alloy AT4 at 20° after a 1,000 hr creep test were: σ_b = 98.15 kg/mm^2; σ_s = 92.7 kg/mm^2; δ = 14.4 percent; ψ = 44.9 percent.

In the course of the creep test, the mechanical properties of alloy AT4 remain almost unchanged. The alloy retains high plastic characteristics, and the ultimate strength and yield strength increase to an insignificant extent.

These data show that alloy AT4 under conditions of long testing (up to 1,000 hrs) under stress at 500° is a thermally stable material which does not embrittle; this is an important performance characteristic.

In addition to the mechanical properties of alloy AT4, its microstructure and hardness were investigated before and after the creep tests.

Etching was done in a reagent consisting of 1 pt. hydrofluoric acid, 1 pt. nitric acid and 2 pts. glycerin. In order to prevent a strong oxidation of the surface of the polished section, the specimens after being etched were first washed with a solution of soda and then with water.

Let us examine the microstructures of alloy AT4 after forging, after annealing for 30 min at 880° and cooling in air, and after creep-testing for 1,000 hrs (fig. 3). In the state after forging and in the state after annealing under the indicated conditions, alloy AT4 had the structure of the α' phase of martensitic type.

After 1,000 hrs of creep tests at 500° and a stress of 5 kg/mm^2, the structure of the alloy approaches the equilibrium state; the α' phase disappears, and the alloy has the structure of the α-phase with a slight content of transformed β-phase. The hardness of alloy AT4 is almost the same as in the initial state.

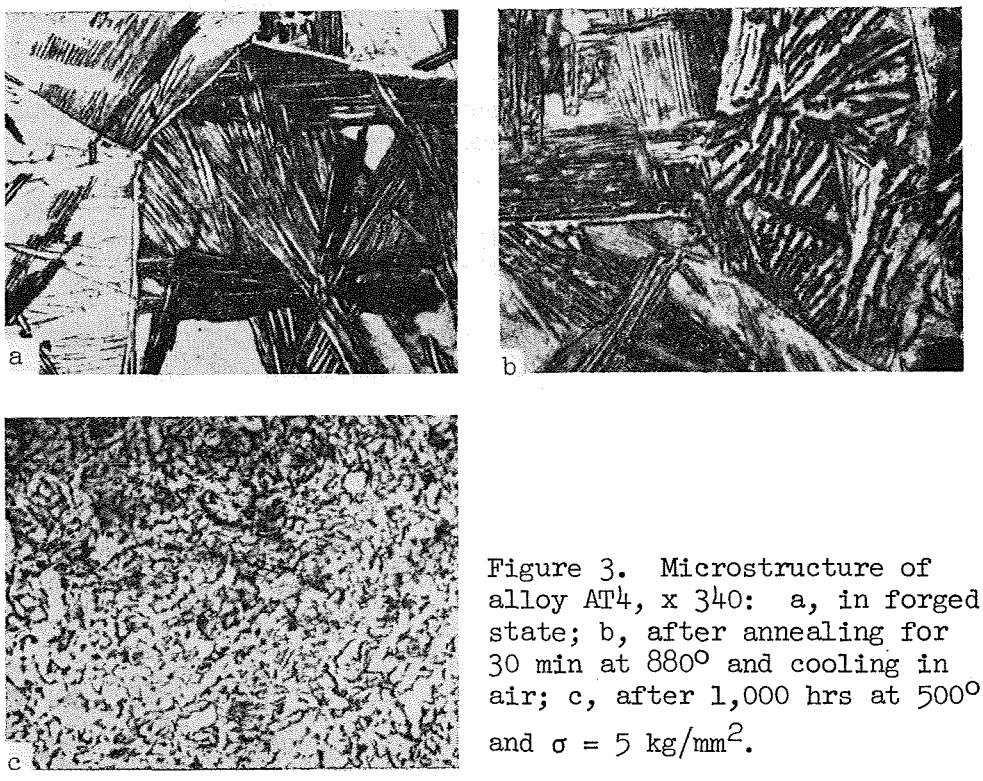

Figure 3. Microstructure of alloy AT4, x 340: a, in forged state; b, after annealing for 30 min at 880° and cooling in air; c, after 1,000 hrs at 500° and σ = 5 kg/mm^2.

Thus, the studies showed that of the alloys studied, the creep rate is lowest in alloy AT4 at 500°. In its properties, AT4 is of great interest as a heat-resistant titanium alloy which can be used at working temperatures up to 500°.

Summary

1. In this work, studies of the creep and thermal stability of titanium alloy AT4 were carried out for the first time by using tests lasting 1,000 hrs.

2. In alloy AT4 the creep is considerably lower than in alloys OT4, OT4-2 (of the system Ti-Al-Mn), alloy VT5-1 (of the system Ti-Al-Sn) and alloy VT6 (of the system Ti-Al-V).

3. The residual elongation after 1,000 hrs of testing at stresses of 2.5 and 5 kg/mm^2 is respectively equal to 0.18 and 0.5 percent.

4. The limiting stress causing a creep rate of $0.3 \cdot 10^{-6}$ percent/hr at 500° is 2.5 kg/mm^2. This indicates a high creep resistance of alloy AT4 under the given conditions.

5. Under long-duration testing conditions at 500° (up to 1,000 hrs) under stress, alloy AT4 is thermally stable and does not embrittle.

6. Alloy AT4 can be used to prepare various semifinished products including pipes by hot and cold rolling. Cold rolling can be used to prepare pipes 6-8 mm in diameter with a wall thickness of 0.3-0.8 mm.

7. Alloy AT4 welds satisfactorily when argon arc and electroslag welding is used, and does not contain any costly or scarce alloying elements.

8. Alloy AT4 can be successfully used to make parts operating at temperatures up to 500°.

DETERMINATION OF THE RELAXATION RESISTANCE OF ALLOY AT3

L. P. Nikitina

The relaxation of stresses associated with the transformation of elastic into plastic deformation, the dimensions of the part being constant, is frequently encountered in engineering practice. For this reason, a characterization of the relaxation of an alloy is required in various cases. It is necessary when an alloy is to be used for reinforcing parts, for determining the duration of the effect of undesirable internal stresses in the metal produced during the assembly or during welding, in the choice of a suitable mode of heating to relieve the internal stresses in the part and other cases.

We know of few studies on stress relaxation in titanium alloys (ref. 1 and others). For this reason, in order to determine the relaxation resistance of alloy AT3, relatively labor-consuming tests were required over a wide range of temperatures and stresses.

Testing Method

The relaxation tests were carried out on I. A. Oding's ring specimens (ref. 2) made of bars of equal bending strength. The standard method of testing for relaxation at each temperature specifies a drop in stress with time from two, three and four levels of initial stress. The initial stresses are usually chosen equal in absolute value for all the temperatures studied, and this places the specimens under dissimilar testing conditions at the lowest and highest temperature if in the range under consideration the temperature has an appreciable effect on the short-time mechanical properties. Over a wider temperature range, the loading to equal stresses becomes completely impossible, so that one should not use the generally adopted methods of comparing the relaxation resistance at various temperatures on the basis of a drop of stress from the same σ_0 values for an equal testing time.

To eliminate the shortcomings of the method of relaxation tests, we adopted initial relaxation conditions such that at any testing temperature the initial stress amounted to a specified fraction of the yield strength at the given temperature.

Thus, for alloy AT3, we selected three stress levels: 0.375, 0.50 and 0.75 of $\sigma^t_{0.2}$ (the coefficients were respectively $b_1 = 0.375$, $b_2 = 0.50$, and $b_3 = 0.75$).

The determination of stress relaxation in time was made on the basis of the relative value of the residual stress σ_τ/σ_0 and $\sigma_\tau/\sigma_{0.2}$, in addition to the usual "absolute" value of the residual stress σ_τ.

This method of determining stress relaxation permitted certain generalizations of the process of stress relaxation.

The relaxation tests were carried out in the temperature range of 350-650° every 50°.

Materials Used

The ring specimens used in the relaxation tests were made from forged pieces 70 mm in diameter. The forged piece was first annealed in air at 900° for 1 hr. The axis of the cylindrical part of the specimens coincided with the axis of the forged piece. The mechanical characteristics of alloy AT3 for longitudinal specimens are shown in the table. The latter also indicates values of the modulus of elasticity at high temperatures (from the certificate data of alloy AT3).

MECHANICAL PROPERTIES OF FORGINGS FROM ALLOY AT3

t, °C	$\frac{1}{T}\cdot 10^3$, 1/°K	$\sigma_{0.2}$, кг/мм²	σ_b, кг/мм²	δ_S, %	ψ, %	E, кг/мм²
20	—	78	80	20	43	11200
350	1.602	42	48	19	62	10200
400	1.483	40	47	19	56	9940
450	1.382	36—40	44	16	61	9600
500	1.293	33	—	—	—	9200
550	1.215	30	37	27	73	8900
600	1.145	28	34	47	81	8600
650	1.082	26	26.5	68	84	8200

Results of Experiments and Their Evaluation

The results of relaxation tests made it possible to examine the change of the initial stress and the buildup of plastic deformation in the course of relaxation.

The dependence between the residual stress on the value of the initial stress is shown graphically. The first graph (fig. 1) is a usual graph of $\sigma_\tau - \sigma_0$, cited in many relaxation studies, with the exception that both quantities are divided by $\sigma^t_{0.2}$. This graph shows that the higher the initial stress, the higher is the residual stress for a specified relaxation time.

If the relative residual stress σ_ϵ/σ_0 is determined (fig. 2), it is apparent that the higher the initial stress, the faster is the relaxation process, i.e., the smaller is the relative value of σ_τ/σ_0 for the same testing time.

These experimental results are in complete agreement with the general concepts according to which the relaxation and creep processes in metals are of the same nature.

To analyze the stresses in the course of relaxation, the primary "stress-log time" relaxation curves were plotted in three forms:

a. Absolute stress σ_τ in kg/mm^2--time in hours at t = const;

b. Relative stress σ_τ/σ_0 in percent--time in hours, i.e., fraction of stress retained at t = const and in initial stress of $\sigma_0 = b\,\sigma^t_{0.2}$;

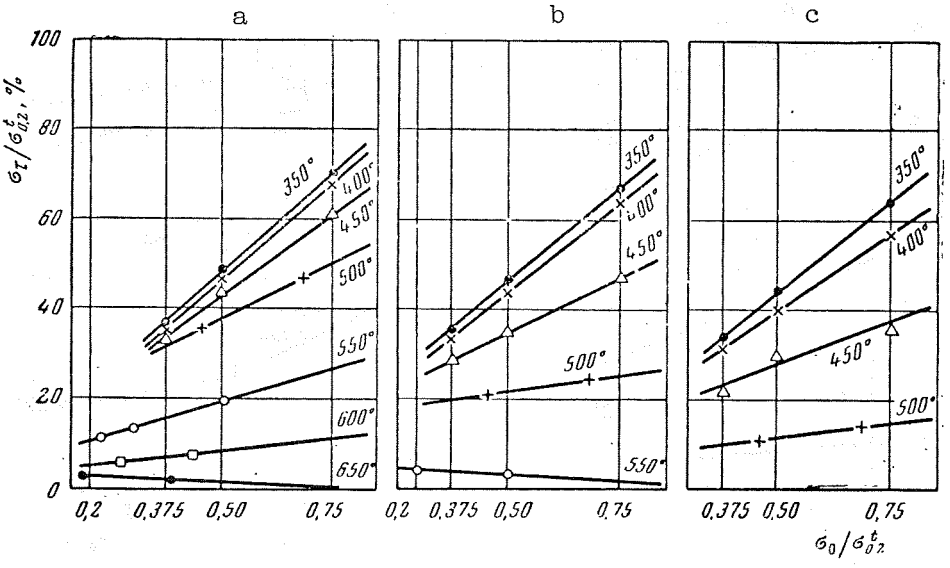

Figure 1. Effect of the initial stress σ_0 on the residual stress σ_τ (both quantities divided by $\sigma^t_{0.2}$): a, 1 hr; b, 100 hrs; c, 1,000 hrs.

c. Relative stress $\sigma_\tau/\sigma^t_{0.2}$ in percent--time in hours, i.e., fraction of stress retained relative to value of yield strength $\sigma^t_{0.2}$ at t = const and a specified value of the initial stress $\sigma_0 = b \cdot \sigma_{0.2}$.

As an example, we cite the primary relaxation curves in the coordinates "relative residual stress-time" for values of initial stress at b = 0.5 and b = 0.75 (fig. 3).

In our view, this is the most convenient form of representing primary curves. Such primary curves make it possible to evaluate the rate of the relaxation process at various temperatures.

On the basis of the primary curves for all three levels of initial stress ($b_1 = 0.375$; $b_2 = 0.5$; $b_3 = 0.75$), the time necessary for reaching a predetermined level of stress relaxation was determined: $\sigma_\tau = 0.8\ \sigma_0$; $\sigma_\tau = 0.5\ \sigma_0$; $\sigma_\tau = 0$.

The temperature dependence of the relaxation time up to the specified level of relative stress is plotted in the coordinates $\ln \tau_\sigma$-1/T (fig. 4). This graph shows that the following exponential relation exists between the relaxation time and the temperature:

$$\tau_\sigma = A_{0(1)} \exp\left(\frac{u_{0(1)}}{RT}\right),$$

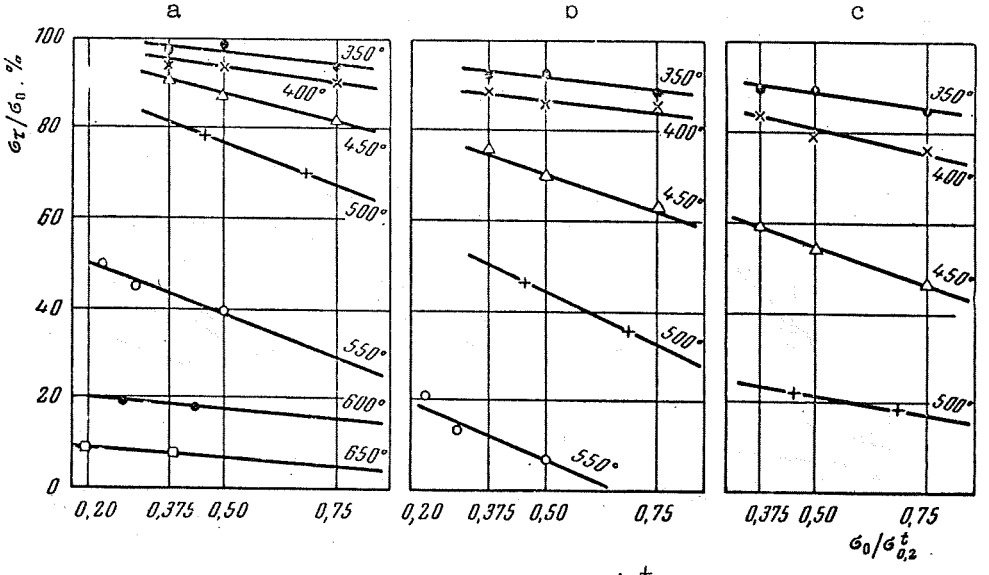

Figure 2. Effect of initial stress $\sigma_0/\sigma^t_{0.2}$ on the value of the relative residual stress $\frac{\sigma_\tau}{\sigma_0}$ at τ = const: a, 1 hr; b, 100 hrs; c, 1,000 hrs.

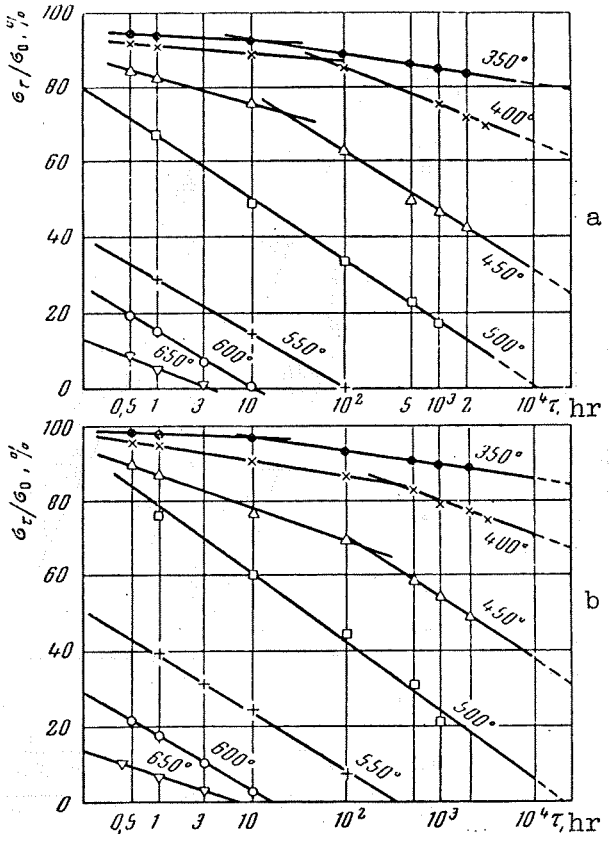

Figure 3. Primary relaxation curves in the coordinates "relative residual stress-time"

a, at $\sigma_0 = 0.50\ \sigma^t_{0.2}$; b, at $\sigma_0 = 0.75\ \sigma^t_{0.2}$.

where τ_σ is the time during which the given stress is reached; T is the temperature, ^oK; $u_{0(1)}$ is the activation energy of the process; R is the gas constant; $A_{0(1)}$ is a constant.

The activation energy $u_{0(1)} = 75 \cdot 10^3$ cal/mole was calculated from the experimental data; it characterizes the resistance of alloy AT3 to the stress drop at high temperature. Without the values of the activation energy of the creep process or the activation energy of the process of self-diffusion of alloy AT3 or other titanium alloys, it is difficult to realize the meaning of the value obtained. However, the accumulation of similar data for a number of materials will obviously permit a more extensive study of relaxation processes in the future. In practice, the graph shown in figure 4 is very useful in selecting the temperature and annealing time in the case of relief of undesirable internal stresses, or in evaluating the relaxation resistance of alloy AT3 at various working temperatures.

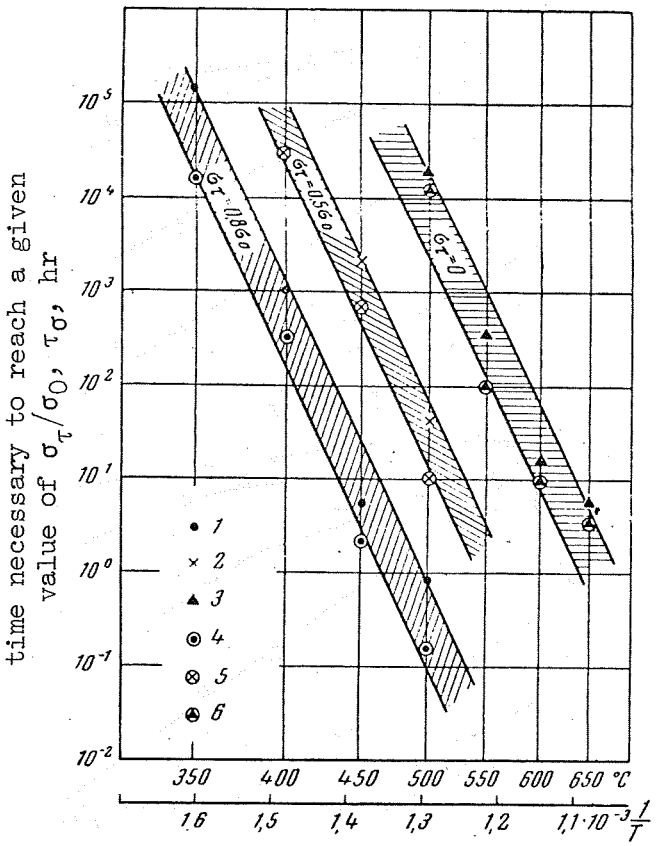

Figure 4. Temperature dependence of relaxation.

1- at $\frac{\sigma_\tau}{\sigma_0}=0.8$; $b=0.5$; 2- at $\frac{\sigma_\tau}{\sigma_0}=0.5$; $b=0.5$; 3- at $\frac{\sigma_\tau}{\sigma_0}=0$; $b=0$;
4- at $\frac{\sigma_\tau}{\sigma_0}=0.8$; $b=0.75$; 5- at $\frac{\sigma_\tau}{\sigma_0}=0.5$; $b=0.75$; 6- at $\frac{\sigma_\tau}{\sigma_0}=0$
$b=0.75$

Let us note that the analysis of the temperature dependence of the residual stress itself, not of the relaxation time, has not thus far permitted the establishment of a simple analytical relationship between the relaxation stress and the temperature on the standard or logarithmic scale either.

An analysis of the plastic deformation was carried out on the basis of measurements of the ring specimens, since the relaxation strain $\epsilon_{rel} = 0.0583 \Delta_{rel}$ percent, where Δ_{rel} is the increase in the distance in mm between the marks of the ring specimen. These data are shown as an example for $\sigma_0 = 0.75 \sigma^t_{0.2}$ in the form of primary "deformation-time" curves (fig. 5). An analysis of the relaxation strain made it possible to establish certain regularities of the process. Thus, an exponential relation was established between the time necessary for a specified value of strain τ_{rel} to be reached and the temperature

$$\tau_{rel} = A_{0(2)} \exp\left(\frac{u_{0(2)}}{RT}\right)$$

In addition to the analysis of total relaxation strain based on the primary curves ϵ_{rel}-τ, the minimum deformation rates (or rates close to the minimum ones) were determined. It was found that v_{min} and the initial absolute relaxation stress (kg/mm^2) are related exponentially; this relation is similar to the one for the creep process when σ = const in the course of each experiment.

A temperature analysis of the minimum rate of relaxation deformation made it possible to establish an exponential relation between v_{min}, t, and the activation energy of this process $u_{0(3)}$ = 30.5·10^3 cal/mole:

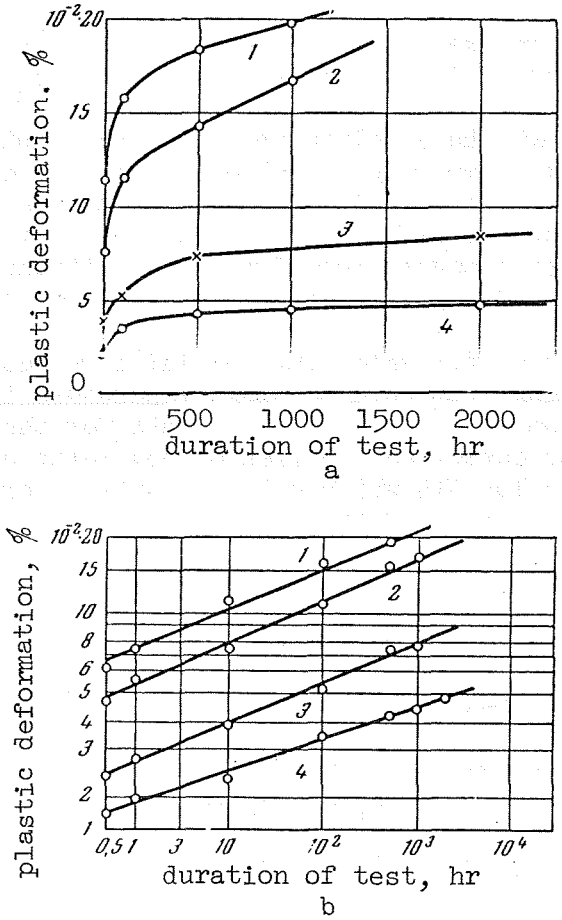

Figure 5. Increase in plastic deformation with time at various relaxation temperatures (primary curves of relaxation deformation): 1, 22.5 kg/mm^2, 500°; 2, 30 kg/mm^2, 450°; 3, 30 kg/mm^2, 400°; 4, 30 kg/mm^2, 350°.

$$v_{min(rel)} = A_{0(3)} \exp\left(-\frac{u_{0(3)}}{T}\right).$$

Thus, the analysis of plastic relaxation deformation reinforces still more the idea of an unquestionable relation between this process and the process of creep, and brings us closer to a possible reciprocal evaluation of both processes.

Conclusion

Testing of alloy AT3 for relaxation in the temperature range of 350-650° makes it possible to regard this alloy as being relaxation-resistant in the temperature range up to 400°. A drop in stress to 80-60 percent of the initial stress can be expected after a long period of time measured in hundreds of thousands of hours (see fig. 4).

The duration of such relaxation is determined not only by the temperature, but also by the value of the initial stress: the higher σ_0, the more rapid the relaxation process, although the absolute value of the remaining stress may be even higher. Technological tempering to relieve undesirable internal stresses is advisable at temperatures of 600-650°. In selecting the temperature and duration of tempering of actual articles, it should be kept in mind that volume stresses are relieved under somewhat more drastic conditions than those which we studied and which involved a planar stress condition of the ring specimens.

The method which we used for selecting initial stresses amounting to some fraction of the yield strength at each testing temperature is quite efficient. It enabled us to obtain comparatively extensive data for the minimum quantity of tested specimens and to establish a series of new relationships in the process of relaxation in alloy AT3 which will undoubtedly prove valid for other metals as well. The first checks of this method on pearlitic steel have confirmed this assumption.

REFERENCES

1. Allsop, R. T. Aircraft Production, Vol. 20, No. 1, 1958.

2. Oding, I. A. Trudy TsNIITMASh (Proceedings of the Central Scientific Research Institute of Technology and Machinery), Bk. 23, Mashgiz, 1949.

CREEP OF ALLOYS OF THE QUATERNARY SYSTEM Ti-Zr-Al-Sn AT 750°

I. I. Kornilov, T. T. Nartova and M. M. Savel'yeva

Metallic compounds of titanium and alloys based on them are of great importance for the development of new heat-resistant alloys (refs. 1-3). Of the various metallic compounds of titanium, those with aluminum and tin as well as solid solutions based on them are of considerable interest as subjects of investigations.

The present work is devoted to a study of the creep of alloys of the quaternary system Ti-Zr-Al-Sn along the section extending from pure zirconium to alloy compositions corresponding to the quasi-ternary system Ti_3Al-Zr-Ti_3Sn (fig. 1).

The alloys were prepared by arc melting in a furnace with a nonconsumable tungsten electrode in an argon atmosphere. Titanium sponge TG00 with an ultimate strength of 36 kg/mm^2, iodide zirconium of 99.9 percent purity, aluminum AV000 and tin of 99.9 percent purity were used in the preparation of the alloys. The alloys were annealed for 30 minutes at 850°.

To determine the creep resistance as a function of the composition, phase structure and temperature, the alloys were tested by the centrifugal bending method. On the basis of the data obtained, plots were made of the creep curves

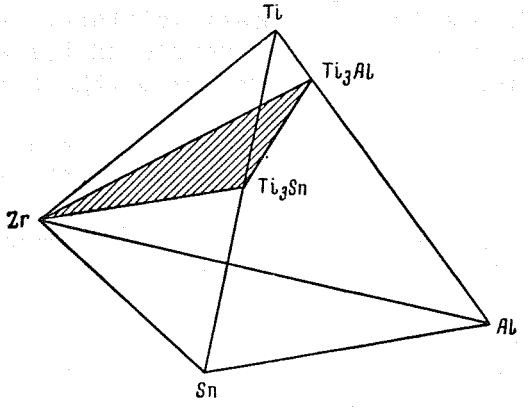

Figure 1. Section Ti_3Al-Zr-Ti_3Sn of quaternary system Ti-Zr-Al-Sn.

and diagrams of the composition versus the time necessary to reach a given bending deflection for the alloys studied, which comprise the quasi-ternary system Ti_3Al-Zr-Ti_3Sn.

Data on the creep of alloys in the ternary system Ti-Zr-Sn along the section Ti_3Sn-Zr are cited in reference 5.

The high-temperature strength of alloys of the ternary system Ti-Al-Sn along the section passing through the compositions of the intermetallic compounds Ti_3Al and Ti_3Sn was studied at 700-750° and a stress of 15-25 kg/mm^2 with a total testing time of 400 hrs (ref. 4).

We studied the creep resistance of the alloys of the ternary system Ti-Al-Zr along the section Ti_3Al-Zr at 750° and a stress of 15 kg/mm^2. The test lasted 1,000 hrs.

The creep curves of alloys of the section Ti_3Al-Zr (fig. 2) show that small additions of zirconium (1-5 percent) to the compound Ti_3Al have no appreciable effect on the heat-resistance properties of this compound. Alloys from the region of zirconium concentration up to 5 percent retain a high degree of heat resistance, and after 1,000 hrs of testing at 750°, the bending deflection of the specimens is 10-12 mm. As the zirconium content rises further, the creep rate of the alloy increases. Alloys containing over 20 percent Zr are not oxidation-resistant at the testing temperature of 750° and are therefore of no interest.

On the basis of the creep curves of alloys of the section Ti_3Al-Zr, a diagram of the composition versus the time necessary to reach bending deflections of 3 and 5 mm was plotted (fig. 3). As is evident from the figure, alloys containing 2-5 percent Zr are the most heat-resistant. As the zirconium content increases further, the high-temperature strength of the alloys decreases, which may be due to a faster drop in the temperature of the polymorphic transformation.

Literature data (refs. 4 and 5) and results of a study of the high-temperature strength of alloys along the section Ti_3Al-Zr have led to the assumption that the most heat-resistant alloys of the quaternary system Ti-Zr-Al-Sn along the section Ti_3Al-Zr-Ti_3Sn should be expected in the region of compositions adjacent to the side of the section Ti_3Al-Ti_3Sn.

In this connection, a study was made of the high-temperature strength of alloys of the quasi-ternary system Ti_3Al-Zr-Ti_3Sn along two cross sections

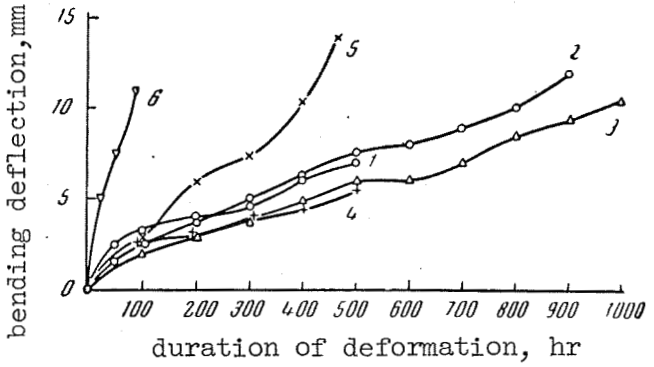

Figure 2. Bending deflection versus duration of deformation of alloys of the section Ti_3Al-Zr at 750° and σ = 15 kg/mm^2: 1, Ti_3Al; 2, Ti_3Al + 1 percent Zr; 3, Ti_3Al + 2 percent Zr; 4, Ti_3Al + 5 percent Zr; 5, Ti_3Al + 8 percent Zr; 6, Ti_3Al + 20 percent Zr.

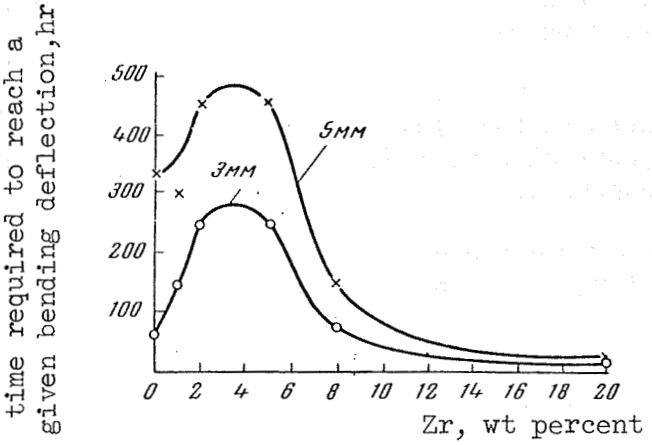

Figure 3. Time required to reach a given bending deflection versus zirconium content of alloys of the section Ti_3Al-Zr at 750° and σ = 15 kg/mm^2.

parallel to the side of Ti_3Al-Ti_3Sn at a constant zirconium content of 1 and 5 percent. The test was carried out at 750° and a stress of 15 kg/mm^2. The duration of the test was 500 hrs.

Let us examine the "composition--high-temperature strength" diagram of alloys of the cross sections parallel to the side of Ti_3Al-Ti_3Sn with a constant zirconium content of 1 and 5 percent (fig. 4).

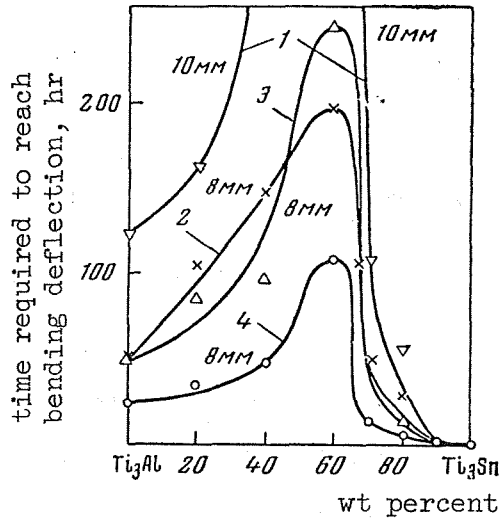

Figure 4. Time required to reach a given bending deflection versus composition of alloys of the system Ti_3Al-Zr-Ti_3Sn with a constant zirconium content of 1 and 5 percent at 750° and σ = 15 kg/mm^2: 1 and 2, 5 percent Zr; 3 and 4, 1 percent Zr.

The curves representing the time necessary to reach a given bending deflection versus alloy composition with a constant content of 1 and 5 percent Zr are analogous to the corresponding curves of alloys of the section Ti_3Al-Ti_3Sn (ref. 4), the high-temperature strength of alloys with 5 percent Zr being somewhat higher than that of alloys with 1 percent Zr.

The broad maximum of high-temperature strength on the diagram covers a region of alloy compositions containing 40-60 percent Ti_3Sn and 60-40 percent Ti_3Al.

The time necessary to reach a bending deflection of 8 mm under testing conditions of 750° and a stress of 15 kg/mm^2 for alloys of the sections with 1 and 5 percent Zr in this region of compositions amounts to 100-200 hrs; a bending deflection of 10 mm is not reached in alloys with 5 percent Zr after 500 hrs of testing.

An alloy of optimum composition based on a solid solution of the compound Ti_3Al with zirconium and tin was chosen from the investigated quaternary alloys of the quasi-ternary system Ti_3Al-Zr-Ti_3Sn, taking into account the plasticity and technological properties. This alloy was the base for additional alloying with vanadium, niobium, molybdenum for the purpose of increasing the technological plasticity.

We illustrate the creep curves based on bending at 750° after testing for 1,000 hrs the quaternary alloy based on the compound Ti_3Al with zirconium and tin and also alloys containing vanadium and niobium (fig. 5). The creep curves with 0.5 and 1 percent Mo are not illustrated, since they are the same as the curves with 1.5 and 2 percent Nb.

A comparison of the results obtained shows that vanadium, niobium, and molybdenum raise the high-temperature resistance of the quaternary solid solution based on the compound Ti_3Al, and that molybdenum and niobium do so to a much greater extent than vanadium. This is explained by the fact that niobium and molybdenum differ more from titanium in their metallic and chemical properties than does vanadium.

The curves representing the time necessary to reach a given bending deflection of the alloys versus the content of vanadium and niobium (fig. 6) indicate that additions of up to 0.5 percent V to the quaternary alloy raise its high-temperature strength. This alloy is located in the single-phase region of the solid solution based on the compound Ti_3Al. In the alloys with 1 and 1.5 percent V, there is observed a slight decrease in high-temperature strength as a result of the appearance of the two-phase $\alpha + \beta$ structure.

The effect of niobium on the alloy based on the solid solution of the compound Ti_3Al with zirconium and tin is analogous to the effect of vanadium.

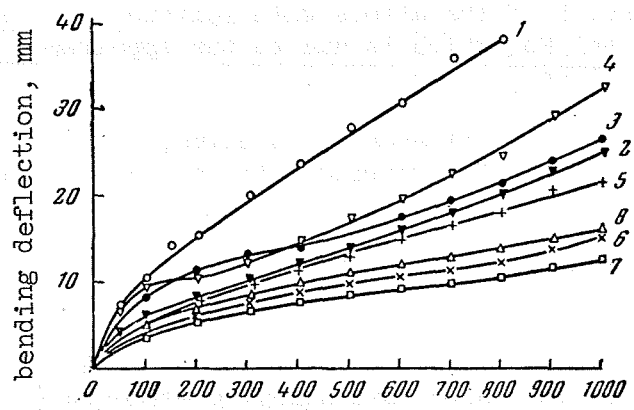

Figure 5. Bending deflection versus relation of deformation of Ti_3Al-base alloys containing vanadium and niobium at 750° and σ = 15 kg/mm^2.

1 — Ti_3Al + Zr + Sn; *2* — Ti_3Al + Zr + Sn + 0.5% V; *3* — Ti_3Al + Zr + + Sn + 1% V; *4* — Ti_3Al + Zr + Sn + 2% V; *5* — Ti_3Al + Zr + Sn + 1% Nb; *6* — Ti_3Al + Zr + Sn + 1.5% Nb; *7* — Ti_3Al + Zr + Sn + 2% Nb; *8* — Ti_3Al + Zr + Sn + 3% Nb

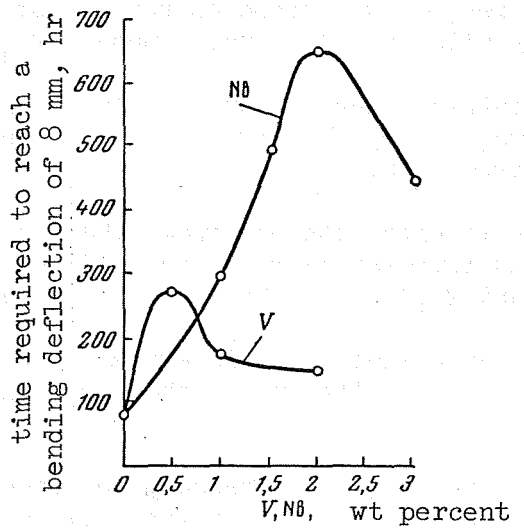

Figure 6. Time required to reach a bending deflection of 8 mm versus composition of Ti_3Al-base alloys containing vanadium and niobium, at 750° and σ = 15 kg/mm^2.

Within the limits of its solubility in the compound Ti_3Al (up to 2.0 percent), niobium gradually increases its high-temperature strength. The lowest strength is displayed by the alloy with 3 percent Nb with a two-phase $\alpha + \beta$ structure. A decrease in the strength of the alloys with molybdenum is observed at a content as low as ~1 percent Mo, which is due to the appearance of the β phase in the structure of the alloys.

Such a character of the influence of vanadium, niobium, and molybdenum on the change in the high-temperature strength in the solid solutions of the compound Ti_3Al corresponds to the regularities manifested by the influence of these elements on the high-temperature strength of titanium, as was established earlier in references 6 and 7.

On the basis of data of microstructural analysis and a study of the high-temperature strength, it was shown that alloying elements (vanadium, niobium, molybdenum) raise the high-temperature strength of alloys based on the compound Ti_3Al within the limits of their solubility in this intermetallic compound.

Thus, the above study makes it possible to select optimum compositions of heat-resistant alloys on the basis of the investigated system for working temperatures of 700-750°

REFERENCES

1. Bochvar, A. A. Physical Metallurgy (Metallovedeniye). Metallurgizdat, 1956.

2. Osipov, K. A. Problems of the High Temperature Strength of Metals and Alloys (Voprosy teorii zharoprochnosti metallov i splavov). Izd-vo AN SSSR, 1961.

3. Kornilov, I. I. Physicochemical Principles of the High-Temperature Strength of Alloys (Fiziko-khimicheskiye osnovy zharoprochnosti splavov). Izd-vo AN SSSR, 1961.

4. --- Metallovedeniye i termicheskaya obrabotka metallov, No. 2, p. 7, 1963.

5. Glazova, V. V. and Kurnakov, N. N. Izv. AN SSSR, OTN, Metallurgiya i Toplivo, No. 6, p. 193, 1962.

6. Kornilov, I. I., Pylayeva, Ye. N. and Volkova, M. A. Coll. Titanium and Its Alloys (Titan i yego splavy). Izd-vo AN SSSR, No. 7, p. 89, 1962.

7. Kornilov, I. I. and Vlasov, V. S. Izv. AN SSSR, OTN, Metallurgiya i Toplivo, No. 4, p. 31, 1958.

STUDY OF THE MECHANICAL PROPERTIES OF TITANIUM ALLOYS AT3, AT4, AT6 AND AT8 IN RELATION TO THE TESTING TEMPERATURE

V. S. Mikheyev

Alloys AT3, AT4, AT6 and AT8 were developed on the basis of the data obtained from a study of phase diagrams of a part of the six-component system Ti-Al-Cr-Fe-Si-B (ref. 1) and diagrams of the mechanical and physical properties of the alloys (ref. 2). The basic properties of the alloys are given in reference 3. Alloys AT contain different amounts of aluminum: 3 percent (alloy AT3), 4.5 percent (alloy AT4), 6 percent (alloy AT6) and 7.5 percent (alloy AT8). The composition of each alloy includes chromium, iron, silicon and boron. The total amount of these elements is 1-1.6 percent. Boron is introduced into the alloys in the amount of 0.01 percent. Certificates have been issued for alloys AT3, AT4 and AT6.

The present work is devoted to a study of the mechanical properties of industrial melts of alloys AT at a testing temperature from 20 to 800-1000°.

Rods measuring 14 x 14 mm prepared by forging were annealed for 30 min at 730° and cooled in air. Standard specimens 5 mm in diameter and 25 mm long were prepared from these rods by cold working.

The mechanical properties of each alloy were studied on 2-3 parallel specimens of 4-5 melts.

The content of alloying elements (chromium, iron, silicon) of these alloys meets the certificate data; in alloys AT4 (alloy 1) and AT8 (alloy 1) there is a higher sum of chromium, iron, and silicon (1.81 and 1.98 percent respectively; see table).

Alloys of the optimum composition are nonequilibrium α solid solutions with a slight content of the β phase. Results of an investigation of the mechanical properties of the alloys at temperatures up to 800-1000° are shown in the figure. The latter also illustrates curves representing the change in the mechanical characteristics of iodide and magnesiothermic titanium. In highly ductile iodide titanium, as the testing temperature rises to 800°, the ultimate strength decreases approximately from 25 to 1.5 kg/mm^2. The ultimate strength of titanium declines more abruptly as the testing temperature is raised to 200°, and from 500 to 800°; it changes insignificantly in the temperature range from 200-500°. In magnesiothermic titanium TG1, in which the content of impurities (0.06-0.10 percent Fe; 0.02-0.03 percent Ni; 0.03-0.05 percent Mg; 0.53-0.05 percent Si;

CHEMICAL COMPOSITION OF TITANIUM ALLOYS AT (IN wt PERCENT).

Alloy No.	Alloying elements								
	Al	Cr	Fe	Si	$\sum$(Cr, Fe, Si)	B	C	N_2	H_2
					Alloy AT3				
1	2.8	0.89	0.32	0.45	1.67	0.01	0.0053	0.0023	0.004
2	3.1	0.71	0.40	0.34	1.45	0.01	0.0053	—	—
3	2.7	0.60	0.35	0.30	1.25	0.01	—	—	—
4	2.7	0.76	0.30	0.47	1.53	0.01	—	—	—
5	3.2	0.84	0.34	0.40	1.59	0.01	—	—	—
					Alloy AT4				
1	4.43	0.89	0.34	0.57	1.81	0.01	0.023	0.018	0.005
2	4.63	0.84	0.32	0.27	1.44	0.01	0.053	0.024	0.004
3	4.67	0.86	0.26	0.26	1.39	0.01	0.05	0.024	0.008
4	4.67	0.86	0.31	0.27	1.45	0.01	0.051	0.024	0.007
5	4.66	0.83	0.48	0.23	1.55	0.01	0.060	0.020	0.010
6	4.00	0.56	0.39	0.23	1.19	0.01	—	—	—
7	4.10	0.57	0.37	0.26	1.21	0.01	—	—	—
					Alloy AT6				
1	5.13	0.86	0.32	0.45	1.64	0.01	0.030	0.033	—
2	5.13	0.67	0.23	0.45	1.35	0.01	0.027	0.021	—
3	5.90	0.83	0.27	0.25	1.35	0.01	—	—	—
4	5.75	0.64	0.32	0.38	1.35	0.01	—	—	—
5	5.60	0.52	0.33	0.30	1.16	0.01	—	—	—
					Alloy AT8				
1	6.81	0.98	0.40	0.59	1.98	0.01	0.043	—	—
2	6.49	0.53	0.30	0.35	1.19	0.01	0.067	—	—
3	6.20	0.67	0.37	0.36	1.41	0.01	—	—	—
4	6.50	0.73	0.40	0.39	1.53	0.01	—	—	—
5	6.3	0.51	0.22	0.34	1.08	0.01	—	—	—

0.04-0.06 percent C; 0.02-0.06 percent N; 0.005-0.008 percent H_2; 0.15-0.25 percent O_2) and that of other elements is 5-7 times greater than their content in iodide titanium, the ultimate strength, equal to 50-60 kg/mm^2, is almost twice as high. The elongation of magnesiothermic titanium is 25-30 percent; the contraction of the cross section is 50-55 percent; the impact strength is 7-10 kgm/cm^2. The ultimate strength of technical titanium changes between 20 and 950° along a curve which declines abruptly toward the abscissa; at 800°, the ultimate strength of titanium is approximately equal to 2.5 kg/mm^2, and at 950°, to about 1.5 kg/mm^2. As can be seen from the diagram, the curve of the ultimate

strength of technical titanium declines sharply with rising testing temperature, and approaches almost continuously the curve of the ultimate strength of iodide titanium.

The elements aluminum, chromium, iron, silicon and boron introduced into titanium alloys AT within the above-indicated limits raise the ultimate strength of the alloys considerably as compared to the ultimate strength of iodide titanium, and decrease their ductile properties. At room temperature, the ultimate strength of alloy AT3 is equal to 85-87 kg/mm^2. As the testing temperature rises to 200°, the ultimate strength of the alloy decreases to approximately 60-65 kg/mm^2, and in the temperature range of 300-500°, changes from 57.1-63.2 to 53-55.6 kg/mm^2. As is evident from the course of the curve, when the testing temperature is subsequently raised to 700-800°, the ultimate strength of the alloy decreases sharply to 14-8 kg/mm^2. As can be seen from the diagram, at testing temperatures up to 800°, the curve of the ultimate strength duplicates the course of the curve of iodide titanium. The ultimate strength of alloys AT4, AT6 and AT8 changes in similar fashion. The diagram shows that as the α solid solution becomes increasingly saturated with aluminum, the ultimate strength of the alloys increases at room temperature approximately from 85 kg/mm^2 for alloy AT3 to 93.5-102.9 kg/mm^2 for alloy AT4, to 106-115.3 kg/mm^2 for alloy AT6 and to 116-124.5 kg/mm^2 for alloy AT8. At testing temperatures of 20-900° in each successive alloy with a higher aluminum content, the ultimate strength is higher than in the preceding alloy with a lower aluminum content. For example, at 500° the ultimate strength has the following values: 53-55.6 kg/mm^2 for alloy AT3, up to 60 kg/mm^2 for alloy AT4, up to 70 kg/mm^2 for alloy AT6 and up to 82 kg/mm^2 for alloy AT8. At temperatures above 450-550°, the ultimate strength of all the alloys decreases abruptly. At 800° in alloys AT3, AT4, AT6 and AT8, the ultimate strength is respectively equal to 10-14, 21.5, 30.7 and 33 kg/mm^2; at 900°, the ultimate strength of alloy AT8 is equal to about 30 kg/mm^2, and that of alloys AT4 and AT6 is 2 and 1.5 times lower than that of alloy AT8.

The dependence of the ductile properties of titanium and its alloys on the testing temperature is very interesting. The diagram shows that the elongation per unit length increases at first as the testing temperature rises to 300°, then sharply decreases in the temperature range of 400-500°, then increases again as the testing temperature rises further. Beginning at about 550°, the elongation per unit length of magnesiothermic titanium is greater than that of iodide titanium.

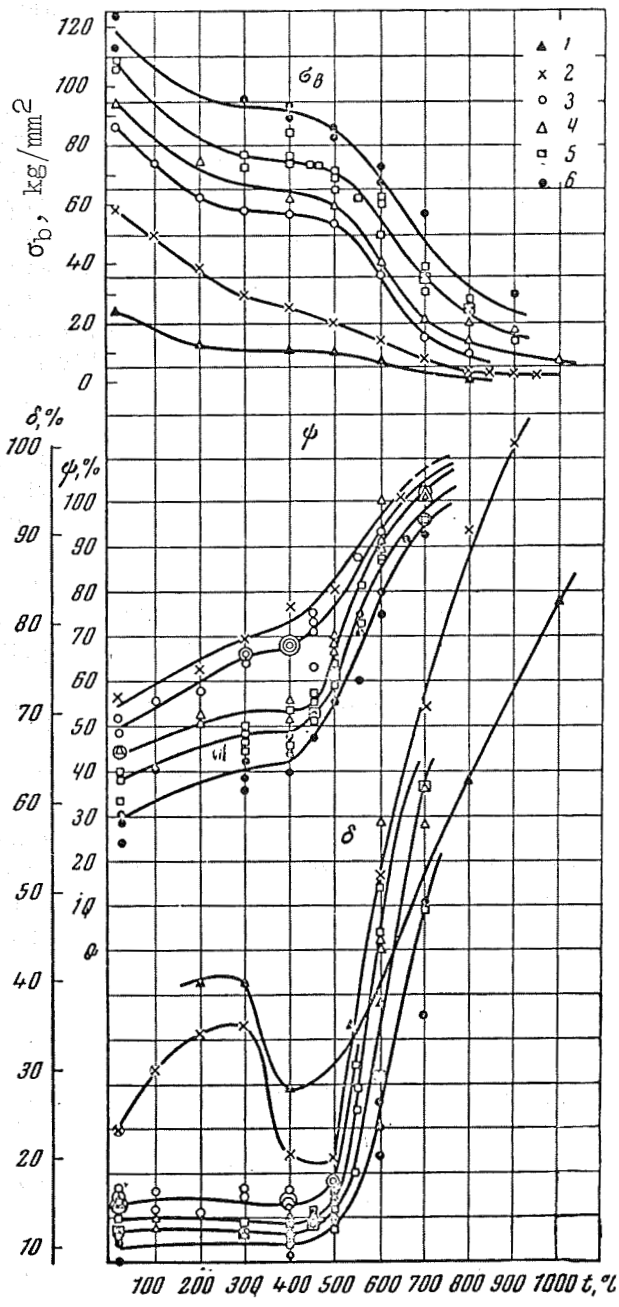

Mechanical properties versus testing temperature:
1, iodide titanium; 2, magnesiothermic titanium;
3, alloy AT3; 4, alloy AT4; 5, alloy AT6;
6, alloy AT8.

The elongation per unit length of alloys AT is considerably less than the elongation of titanium and changes between 20 and 400° along curves having a slight trough in the direction of the abscissa. Above a temperature of about 400°, the elongation curves of the alloys, after passing through the minimum

point, rise slightly at first, then more abruptly at 500°; at these temperatures, the alloys acquire a high ductility.

The reduction of the cross sectional area of titanium specimens at temperatures approximately up to 450° changes along a rising curve with a minimum at 400°. At about 450°, the curve changes direction and as the testing temperature is raised further, rises still more steeply. A decline in ductile properties, particularly in relation to the elongation per unit length of titanium from 300 to 400° had been observed earlier by many investigators. However, the cause of this phenomenon has not yet been established. It may be postulated that the decrease in the ductility of titanium and also that of alloys of the system Ti-Al-Cr-Fe-Si-B is partially caused, in addition to other factors, by the influence of hydrogen.

The influence of aluminum on the ductility of the alloys at a given temperature can also be followed on this diagram. As the aluminum content of the α solid solution increases, the ductility of the alloys decreases (see figure).

The table shows the change in the content of the sum of chromium, iron, and silicon within the limits of a given composition. As the total content of chromium, iron and silicon increases, the ultimate strength of the alloys increases as follows: in alloy AT3, from 75 to 88 kg/mm^2; in alloy AT4, from 90 to 105 kg/mm^2; in alloy AT6, from 106 to 115.3 kg/mm^2; in alloy AT8, to 124 kg/mm^2. The ductile properties of the alloys thus decrease: for instance, the elongation decreases from 14-15.9 percent in alloy AT3 to 8 percent in alloy AT8 No. 1, i.e., at the upper limit, and to 14.6 percent in alloy AT8, No. 2, i.e., at the lower limit.

Summary

1. Six-component alloys of the system Ti-Al-Cr-Fe-Si-B of the optimum compositions AT3, AT4, AT6, and AT8 basically have the structure of an α solid solution with a very small amount of the β phase; they are characterized by high mechanical characteristics at room temperature and higher temperatures (up to 450-600°).

2. As the aluminum content of the six-component alloys of the system Ti-Al-Cr-Fe-Si-B increases from 3 to 8 percent, the total content of chromium, iron, silicon, and boron being constant, the ultimate strength of the alloys increases. Thus, alloy AT3 has an ultimate strength of up to 80 kg/mm^2, and alloy AT8, up to 124 kg/mm^2. The ductile characteristics (elongation per unit length and transverse contraction) decline.

3. As the testing temperature is raised, the ultimate strength of titanium and that of alloys AT3, AT4, AT6 and AT8 decreases, and does so most rapidly at

a temperature above 450-500°. The elongation per unit length and transverse contraction of the alloys undergo little change as the temperature is raised to approximately 450°, but increase sharply as the testing temperature is raised further.

REFERENCES

1. Kornilov, I. I., Mikheyev, V. S. and Chernova, T. S. Izv. AN SSSR, OTN, Metallurgiya, No. 3, p. 72, 1960.

2. Mikheyev, V. S. and Chernova, T. S. Izv. AN SSSR, OTN, Metallurgiya i Toplivo, No. 5, p. 139, 1962.

3. Kornilov, I. I., Mikheyev, V. S., Chernova, T. S. and Markovich, K. P. Coll. Titanium and Its Alloys (Titan i yego splavy). Izd-vo AN SSSR, No. 7, p. 140, 1962.

STUDY OF THE COMPARATIVE HEAT RESISTANCE OF TITANIUM ALLOYS SHEET AND ITS WELD JOINTS AT 450, 550, 650 and 700°

I. I. Kornilov, O. N. Andreyev, V. M. Voshedchenko and V. A. Karmanov

pp. 227-235 of original document appears in
J.P.R.S. Translation No. 28,176; TT:65-30080
pp. 11-23

HIGH-TEMPERATURE STRENGTH OF ALLOYS OF THE QUATERNARY SYSTEM Ti-Al-Mo-V

Ye. N. Pylayeva and Ko Chih-ming

The present article reports on a study of the dependence of the high-temperature strength of alloys of the systems Ti-Al-Mo and Ti-Al-(Mo:V = 1:1) on their composition and structure. The position of these systems in the tetrahedron of the quaternary system Ti-Al-Mo-V is shown in figure 1.

The method of long-time hot hardness (ref. 1) and the centrifugal bending-test method were used in the study (ref. 2).

Tests for long-time hot hardness were carried out on a VIM-1 vacuum unit (ref. 13) at a load of 1 kg and a deformation time of 1, 5, 10 and 20 min.

In high-temperature strength tests involving the centrifugal method, the bending stress was 15 kg/mm^2, and the testing temperature was varied from 550 to 800° depending upon the aluminum content of the alloys.

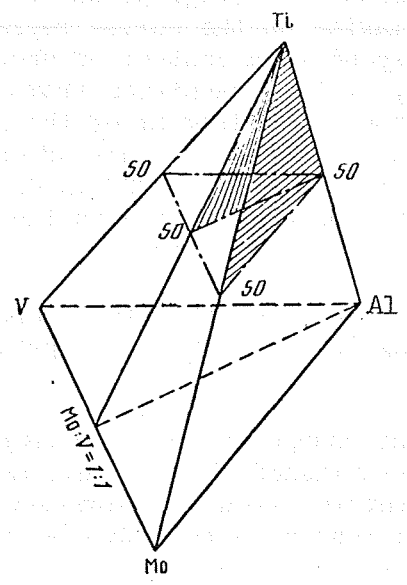

Figure 1. Location of the systems Ti-Al-Mo and Ti-Al-(Mo:V = 1:1) in the tetrahedron of the quaternary system Ti-Al-Mo-V.

Using the method proposed in reference 4, we calculated the plastic deformation rates v_d from data on the long-time hot hardness of alloys of the system Ti-Al-Mo at 700°. The deformation rate, calculated for the same specified size of the indentation, corresponds to conditions of plastic flow when the same specific pressure of the indenter is acting on the specimen. The relative high-temperature strength of the alloys studied can be evaluated from the values of the deformation rate.

Let us examine the curves representing the influence of molybdenum concentration on the logarithm of the deformation rate ln v_d of the alloys (fig. 2).

In the binary alloys of the system Ti-Mo (fig. 2, curve 1), addition of up to 3 percent Mo decreases the deformation rate somewhat, and as the molybdenum content increases to 10 percent, the effect of this element is almost unnoticeable.

In the ternary alloys with 5, 15 and 20 percent Al (fig. 2, curves 2, 3 and 4), as the molybdenum content increases from zero to 10 percent, the deformation rate of the alloys decreases at first (minimal values are reached at a molybdenum content of about 1 percent), then after a certain increase remains practically constant. This means that ternary alloys of titanium with 1 percent Mo containing respectively 5, 15 and 20 percent Al have a maximum high-temperature strength at 700° as compared to the rest of the alloys.

These conclusions concerning the high-temperature strength of ternary alloys were confirmed by data on bending tests carried out by the centrifugal method. The "composition--high-temperature strength" diagrams of alloys of the system Ti-Al-Mo along sections with 5 percent Al (fig. 3, curve 1) 10 percent Al (fig. 3, curve 2), 15 percent Al (fig. 3, curve 3) and 20 percent Al (fig. 3, curve 4) show that the maxima on the curves representing the change in high-temperature strength correspond to a content of about 1 percent Mo. This corresponds to the boundary of the transition from α solid solutions to the region of $\alpha + \beta$ phases on the phase diagram of the system Ti-Al-Mo. From this, one can conclude that in the investigated part of the system Ti-Al-Mo, the maximum high-temperature strength at 600-800° is displayed by those ternary titanium alloys whose compositions are located in the vicinity of the solubility limit of molybdenum in the α solid solution.

Let us examine the dependence of the high-temperature strength of the alloys of the system Ti-Al-Mo along the section with 5 percent Al on the molybdenum concentration (fig. 4).

Up to 5 percent Mo, the change in the high-temperature strength in the alloys retains the pattern established above, i.e., as the molybdenum concentration rises, the high-temperature strength increases at first within the confines of the α solid solution and reaches a maximum near the saturation boundary at a content of about 1 percent Mo; when the $\alpha + \beta$ region is reached, the strength, after a slight decrease, remains practically constant up to 5 percent Mo.

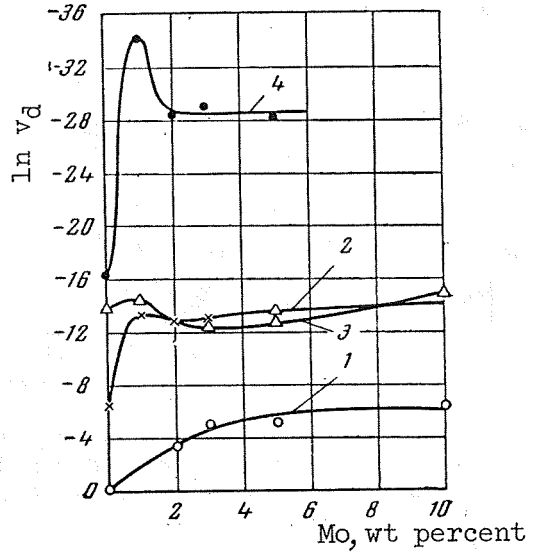

Figure 2. Effect of molybdenum concentration on the values of ln v_d at 700°: 1, binary alloys of the system Ti-Mo; 2, ternary alloy with 5 percent Al; 3, ternary alloy with 10 percent Al; 4, ternary alloy with 20 percent Al.

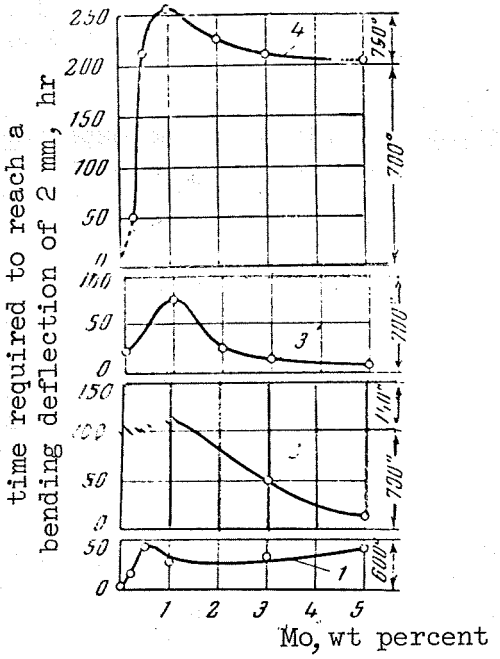

Figure 3. Time required to reach a bending deflection of 2 mm, versus molybdenum content for alloys of the system Ti-Al-Mo at 600-800° and σ = 15 kg/mm^2: 1, section with 5 percent Al; 2, section with 10 percent Al; 3, section with 15 percent Al; 4, section with 20 percent Al.

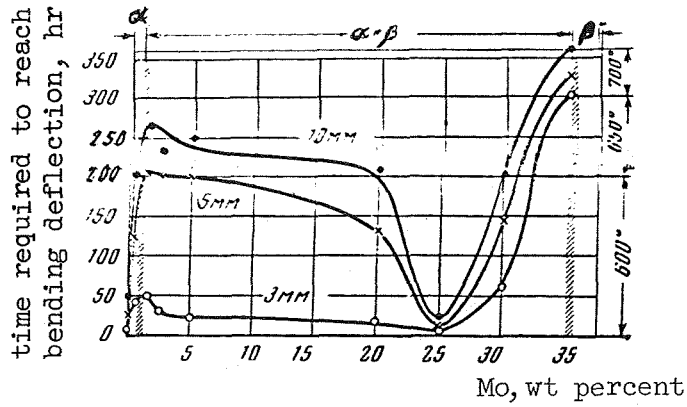

Figure 4. Time required to reach a given bending deflection versus molybdenum content for alloys of the system Ti-Al-Mo with 5 percent Al at 600-700°

and $\sigma = 15$ kg/mm^2.

A further increase in molybdenum concentration causes a decrease in high-temperature strength; the strength curve, passing through a minimum at ~25 percent Mo, again rises sharply as the composition of the alloys approaches the boundary between the β solid solution and the α + β regions.

The alloy with 5 percent Al and 35 percent Mo, located near the boundary of transition from the β solid solution to the α + β region, softens only from a temperature of 700°.

On the basis of a systematic study of the experimental data obtained from the bending test by the centrifugal method, we plotted the "composition--high-temperature strength" diagram of alloys of the system Ti-Al-(Mo:V = 1:1) shown in figure 5.

The diagram is divided into a number of portions. These portions indicate the temperatures at which after 100 hrs of bend-testing by the centrifugal method at a bending stress of 15 kg/mm^2, the alloys of the corresponding composition reach a bending deflection of 5 mm. From the indicated temperatures, one can evaluate the relative high-temperature strength of alloys of the system Ti-Al-(Mo:V = 1:1). The phase regions of the system at 600° are indicated by broken lines on the diagram.

The diagram shows that as the composition and structure of the alloys change, the testing temperature changes from 550° for alloys adjacent to the side of Ti-(Mo:V = 1:1) to 800° for alloys from the region of the α solid solution with a high aluminum content. For alloys from the region of the γ solid solution based on the compound TiAl, the testing temperature is above 800°.

From the tests performed it follows that in the system Ti-Al-(Mo:V = 1:1) the dependence of the high-temperature strength on the composition and structure of the alloys obeys the relationships established for alloys of the system Ti-Al-Mo, i.e., a maximum high-temperature strength characterizes quaternary

titanium alloys whose compositions are located in the vicinity of the boundary of transition from α solid solutions into the region of $\alpha + \beta$ phases.

Among the investigated alloys, those having the highest strength were from the region of the quaternary γ solid solutions based on the compound TiAl.

Thus, according to the physicochemical theory of high-temperature strength (ref. 5), the diverse nature of the chemical interaction of the components in the quaternary system Ti-Al-Mo-V permits the formulation of the following relationships in the change of the high-temperature strength of alloys of this system.

As shown by the data obtained in the determination of the long-time hot hardness at 700°, in the binary system Ti-Mo the change in high-temperature strength at molybdenum concentrations from zero to 10 percent corresponds to the third type of "composition--high-temperature strength" diagrams. Since the concentration of the binary α solid solution in the system Ti-Mo is very low (less than 0.8 percent) and is independent of temperature, α-Ti is practically devoid of the solution mechanism of hardening.

The high-temperature strength of the alloys depends primarily on the amount of the β phase hardened by molybdenum and on the nature of the interaction at the interface of the α and β phases.

In the systems Ti-Al-Mo and Ti-Al-(Mo:V = 1:1) along the sections with a constant aluminum content of 5, 10, 15 and 20 percent, the dependence of the high-temperature strength of the alloys on the molybdenum concentration or the

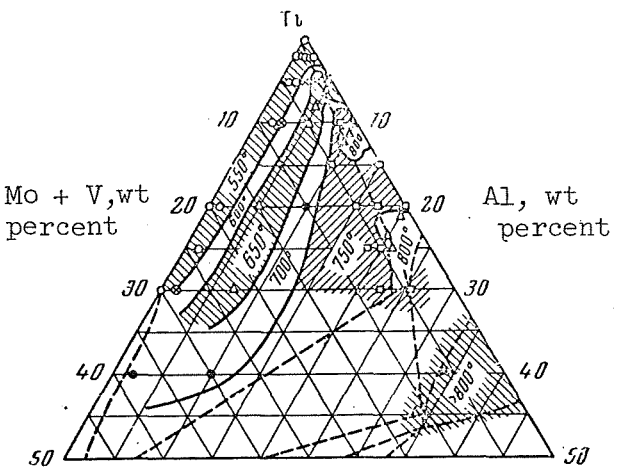

Figure 5. Region of alloys of the system Ti-Al-(Mo:V = 1:1) with the same testing temperature required to reach a bending deflection of 5 mm in 100 hrs at σ = 15 kg/mm^2.

sum of molybdenum and vanadium corresponds to the second type of "composition--high-temperature strength" diagrams. The introduction of aluminum into alloys of these systems leads to an increase in the solubility of molybdenum and vanadium in the ternary and quaternary α solid solutions. Alloys hardened by aluminum as a result of the formation of solid solutions and compounds are additionally hardened by the solution mechanism and possibly dispersion mechanisms of hardening. The most heat-resistant titanium alloys at 600-800° are those whose compositions are located near the boundary of the transition from α solid solutions (ternary and quaternary) to the region of $\alpha + \beta$ phases.

Of the alloys which we studied, the most heat-resistant ones are those with γ solid solutions based on the compound TiAl. The great high-temperature strength of the compound TiAl is due to the great stability of its chemical bonding. However, alloys of this series are not deformed and may find applications as heat-resistant casting alloys.

REFERENCES

1. Bochvar, A. A. Izv. AN SSSR, OTN, No. 10, p. 1369, 1947.

2. Kornilov, I. I. Zav. Lab., Vol. 15, No. 1, p. 76, 1949.

3. Lozinskiy, M. G. High-Temperature Metallography (Vysokotemperaturnaya metallografiya). Mashgiz, 1956.

4. Osipov, K. A. and T'ien Tê-ch'eng. Izv. AN SSSR, OTN, Metallurgiya i Toplivo, No. 4, p. 77, 1959.

5. Kornilov, I. I. Physicochemical Principles of the High-Temperature Strength of Alloys (Fiziko-khimicheskiye osnovy zharoprochnosti splavov). Izd-vo AN SSSR, 1961.

HEAT RESISTANCE OF TITANIUM ALLOY AT-8 IN SHORT-TIME TESTS

N. M. Pul'tsin, M. P. Rumanko and
V. B. Pokrovskaya

pp. 240-242 of original document appears in
J.P.R.S. Translation No. 28,176; TT:65-30080
pp. 24-28

THERMAL STABILITY OF ALLOYS AT3 AT TEMPERATURES OF 350 AND 400°

K. P. Markovich and V. S. Mikheyev

In connection with the possibility of using alloy AT3 in units operating for extended periods of time at temperatures of 350-400°, a study of the stability of this alloy under operating conditions seemed of great interest.

Two industrial melts of alloy AT3 with the same content of aluminum and boron (within the limits of their solubility in α-Ti) and different content of the sum of alloying elements Σ(Cr, Fe, Si) were selected for the present investigation.

The chemical composition (in wt percent) of the investigated melts of alloy AT3 was as follows:

Alloy	Ti	Al	Cr	Fe	Si	B	Σ (Cr, Fe, Si)
AT3-1	Base	2.7	0.60	0.30	0.36	0.01	1.26
At3-2	Base	2.8	0.79	0.44	0.30	0.01	1.53

Our earlier work on the determination of the solubility of the sum of the alloying elements Σ(Cr, Fe, Si) in the proportion of 1:1:1 in a ternary α solid solution (3 percent Al and 0.01 percent B) showed that the maximum solubility of the sum of these elements at 500° is equal to about 0.75 percent (ref. 1) and that it increases with the temperature. Thus, it should be assumed that the compositions of alloy AT3 selected for the present investigation are located near the limit of the maximum saturation α phase + excess phase in a state close to equilibrium. Therefore, their phase composition in the state of equilibrium should correspond to the structure α phase + excess phase. It may be postulated that embrittlement may take place as a result of the precipitation of the excess phase when the alloy operates in the indicated temperature range for a very long time (up to 20,000 hrs). In this connection, a study of the aging of alloy AT3 was made at temperatures of 350 and 400° for 10,000 hrs without stress and in an ordinary atmosphere.

The thermal stability of titanium alloys of the AT series was studied by the authors of reference 2 for various contents of aluminum and of the sum of the alloying elements besides iron and silicon for 100 hrs at temperatures of 400, 450 and 500°. The study established that the titanium alloys AT3, AT4, AT6 and AT8 tested under the selected conditions displayed a high thermal stability.

The stability of titanium alloys AT3, AT4 and AT6 was studied at 400 and 450° for 300-7,000 hrs (ref. 3). The investigation showed that after an aging test under the above-indicated conditions, the ductility of alloy AT3 decreases during the initial stage of the aging and is almost completely restored to the original state after 3,000 hrs of aging.

In an aging test lasting 2,750 hrs in a medium of saturated water vapor at 100° without stress, alloy AT3 did not show any decrease in ductility either.

In the present investigation, use was made of forged bars 14 x 14 mm in cross section from two melts prepared by the vacuum method of double melting under plant conditions. The following starting materials were used to prepare the alloys: titanium sponge TG0 with an ultimate strength of 39-43 kg/mm^2, technical silicon KR, chromium Khl, technical iron, aluminum A100 and a chromium-boron master alloy (up to 10 percent B). The charge of the alloy was calculated to contain up to 3 percent Al and Σ(Cr, Fe, Si) at the intermediate and upper limit.

Alloys AT3-1 and AT3-2 in the forged state and after annealing had the following mechanical characteristics (determined by the standard method on specimens prepared from forged bars 14 x 14 mm in cross section):

Alloy	After forging					After annealing for 30 min at 850° and cooling in air				
	σ_b kg/mm^2	σ_s kg/mm^2	δ,%	ψ,%	a_n kgm/cm^2	σ_b kg/mm^2	σ_s kg/mm^2	δ,%	ψ,%	a_n, kgm/cm^2
AT3-1	86.4	84.9	14.5	43.2	7.7	86.3	85.0	14.8	44.75	6.8
AT3-2	90.1	87.84	14.0	58.10	6.6	84.5	81.5	17.6	48.7	7.8

The aging of alloy AT3 was studied on blanks taken from a forged bar 14 x 14 mm in cross section. The blanks were placed in a heated furnace without preliminary annealing. The mechanical properties and microstructure during aging were studied after holding times of 100, 500, 1,000, 2,000, 3,000, 5,000 and 10,000 hrs.

The etching was carried out in a special solution (1 pt. HF + 2 pts. H_2NO_3 + 3 pts. glycerin). In order to prevent a strong oxidation of the polished sections, the latter were washed in a concentrated solution of soda, then in water.

Results

1. Change in the mechanical properties of alloys in the course of aging. The change in the mechanical properties of alloys AT3-1 and AT3-2 in the course of aging lasting 10,000 hrs at 350 and 400° is shown graphically (figs. 1-4).

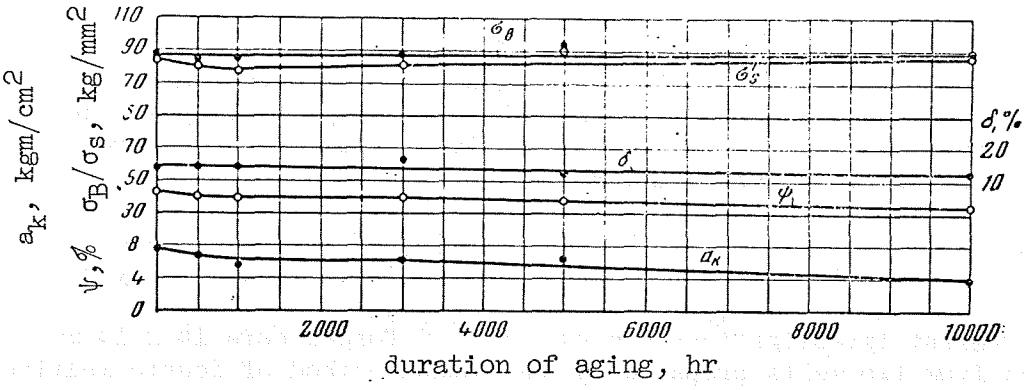

Figure 1. Change in the mechanical properties of alloy AT3-1 in the course of aging at 350° for 10,000 hrs.

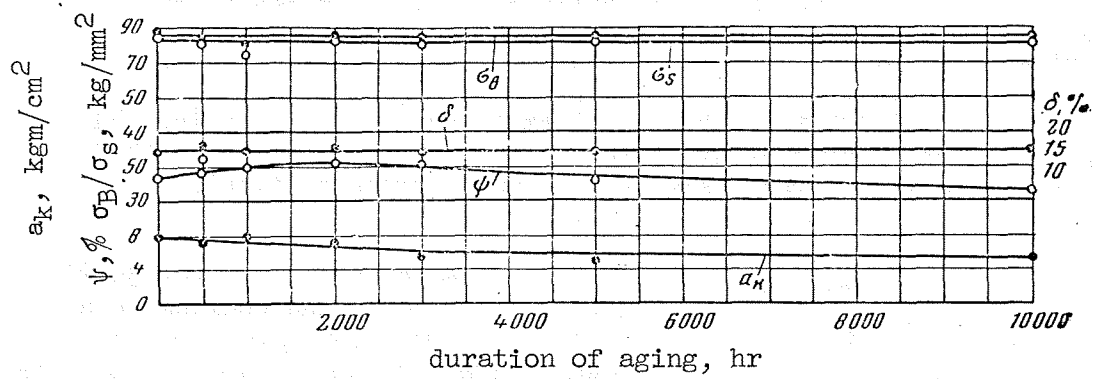

Figure 2. Change in the mechanical properties of alloy AT3-1 in the course of aging at 400° for 10,000 hrs.

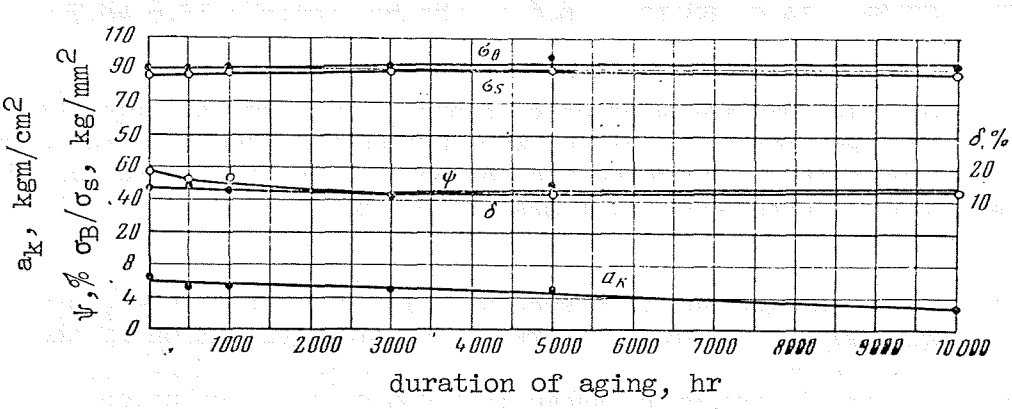

Figure 3. Change in the mechanical properties of alloy AT3-2 in the course of aging at 350° for 10,000 hrs.

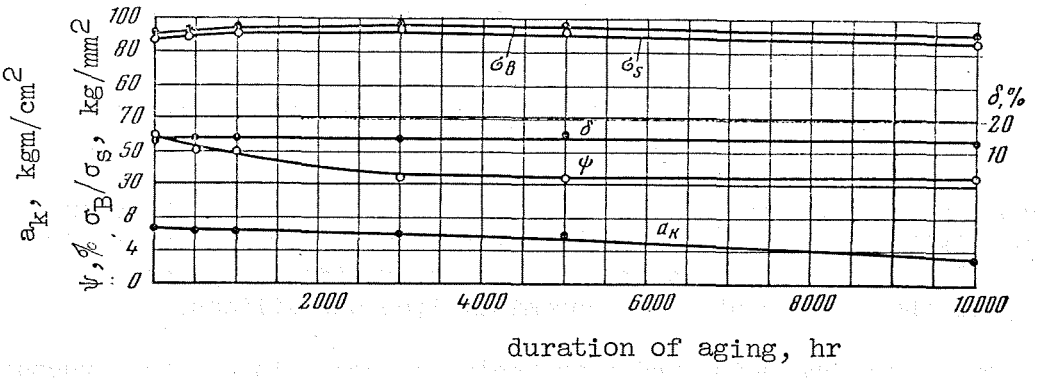

Figure 4. Change in the mechanical properties of alloy AT3-2 in the course of aging at 400° for 10,000 hrs.

The lower part of the graphs shows the dependence of the impact strength on the duration of aging, the upper part shows the change in the ultimate strength and yield strength, and the middle part shows the change in the ductile properties which took place during the elapsed aging-time interval.

The graphs show that in the course of aging at 350 and 400° for 10,000 hrs the strength of the alloys characterized by the values of σ_b and σ_s does not change appreciably.

Thus, for example, the ultimate strength σ_b of alloys AT3-1 and AT3-2 after forging is equal respectively to 86.4 and 90.1 kg/mm^2. After aging for 10,000 hrs at 350°, the indicated alloys had an ultimate strength of 87.62 and 93.69 kg/mm^2, respectively, i.e., this characteristic remained practically unchanged. The same dependence of the ultimate strength on the duration of aging is also observed at 400°.

The ductility of the alloys δ does not change during the aging process either, and is represented by a straight line on "properties--aging time" diagrams.

The elongation per unit length δ of alloys in the initial state was 14.3-14 percent, and after long aging became equal to 15 percent in alloy AT3-1 and 13.8 percent in alloy AT3-2.

The necking ψ of alloy AT3-1 decreases from 43.2 percent (after forging) to 36 percent (after aging for 10,000 hrs at 350°) and 34.4 percent (after aging for 10,000 hrs at 400°). These values of the ductility are fairly high for an aging time of 10,000-12,000 hrs. The transverse contraction of the neck decreases more appreciably in alloy AT3-2.

After 10,000 hrs of aging, ψ decreases from 56.1 to 46.13 percent (at an aging temperature of 350°) and to 35.8 percent (at an aging temperature of 400°). The value ψ = 35.8 percent is also significant in characterizing the ductility of the alloy after long aging.

The impact strength decreases during aging. However, in the range of holding times of 2,000-5,000 hrs, it remains constant for both alloys (a_n = 7.5-5.5 kgm/cm^2) and decreases to 3.5-3.75 kgm/cm^2 only after aging for 10,000 hrs.

2. Change in the microstructure of alloy AT3. A study of the microstructure made it possible to establish that alloy AT3 after forging has the structure of an α solid solution with a small amount of residual β phase (fig. 5a) independently of the total content of chromium, iron and silicon.

In the course of long aging under the selected conditions, the structure undergoes little change. This is indicated by photomicrographs obtained after different aging conditions at 350 and 400°.

Microphotographs of alloy AT3-1 after forging for 5,000 and 10,000 hrs at 350 and 400° (fig. 5) show a two-phase structure and a texture that is coarser than in the forged state.

The higher alloy AT3-2 has a similar structure at 350 and 400° and the corresponding holding times (fig. 6).

A study of the microstructure of the aged alloy AT3 at a constant aluminum content and a variable total content of chromium, iron and silicon following various holding times revealed that the phase composition of the alloy under the indicated aging conditions remains unchanged over such a long period of time.

The residual β phase in alloys AT3-1 and AT3-2 in the range of 500-600° should exhibit a eutectoid decomposition with the formation of an α phase and an intermetallic phase of complex composition. Since the aging of alloy AT3 took place at relatively low temperatures (350 and 400°), in the range of which the diffusion processes are strongly inhibited, this diffusion did not occur. The structure of the alloy remains a nonequilibrium structure and consists chiefly of an α solid solution and an undecomposed β phase. For this reason, the properties of the alloy (σ_b, σ_s and δ) remain at the level of the original ones independently of alloying after such long aging. However, long aging at 400° causes a strengthening of the grains of the α phase, and this affects the ductile characteristics of the alloy, ψ and a_n, the value of which decreases with increasing grain size.

In addition, in such long aging in an atmosphere of air, the surface oxidation of the alloy and the hydrogen, which sharply decreases the impact strength, may also exert a certain influence.

Summary

1. The aging of alloy AT3 containing 2.7-2.8 percent Al and 1.26 and 1.53 percent Σ(Cr, Fe, Si) was studied in the course of 10,000 hrs at temperatures of 350 and 400°. The investigation showed that, irrespective of alloying, the phase composition of the alloy does not change under the selected aging conditions.

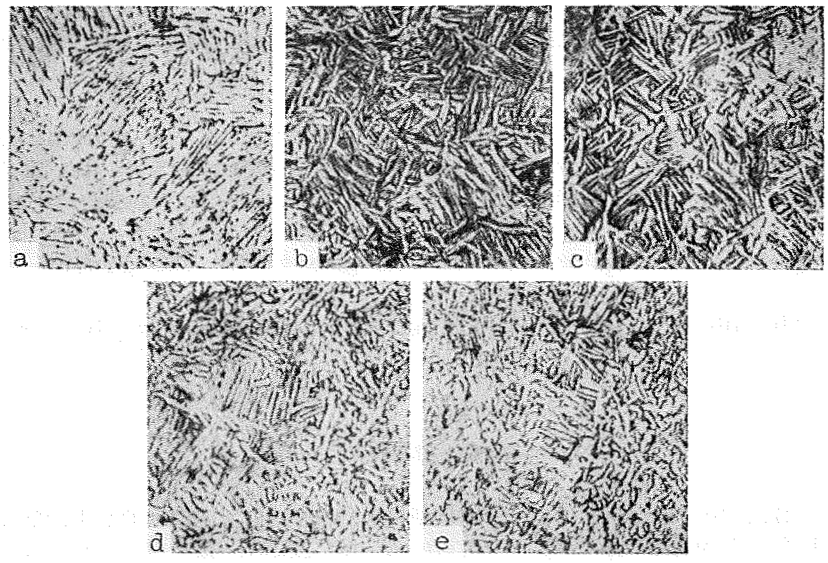

Figure 5. Microstructure of alloy AT3-1 after forging and aging at 350 and 400°, x 340: a, forged; b, 350°, 5,000 hrs; c, 350°, 10,000 hrs; d, 400°, 5,000 hrs; e, 400°, 10,000 hrs.

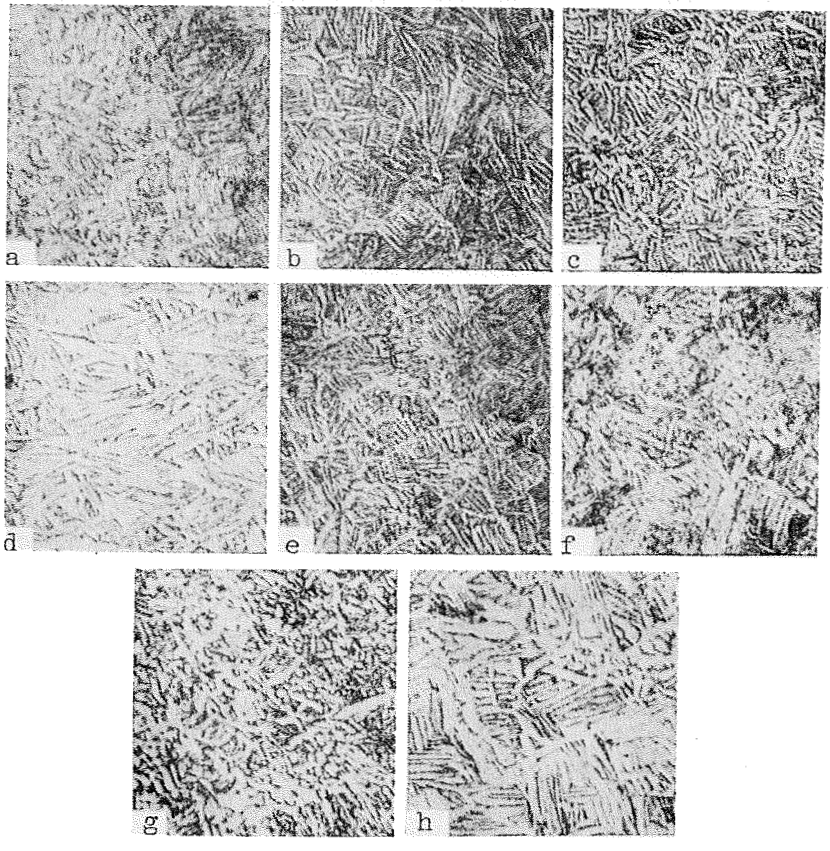

Figure 6. Microstructure of alloy AT3-2 after aging at 350 and 400°, x, 340: a, 350°, 500 hrs; b, 350°, 3,000 hrs; c, 350°, 5,000 hrs; d, 350°, 1,000 hrs; e, 400°, 500 hrs; f, 400°, 3,000 hrs; g, 400°, 5,000 hrs; h, 400°, 10,000 hrs.

The structure remains a nonequilibrium structure and consists of an α phase and an undecomposed β phase.

2. Alloy AT3 does not embrittle in the course of long aging (up to 10,000 hrs) at 350 and 400°. The ultimate strength and elongation per unit length of the alloy remain at the level of the original values independently of alloying.

3. The drop in ψ and a_n is due to the growth of the grains of the α phase and probably to the absorption of hydrogen by the alloy in the course of the aging.

REFERENCES

1. Mikheyev, V. S., Markovich, K. P. and Tavadze, L. N. Coll. Titanium and Its Alloys (Titan i yego splavy). Izd-vo AN SSSR, No. 10, p. 42, 1963.

2. Kornilov, I. I., Mikheyev, V. S. and Chernova, T. S. Coll. Titanium and Its Alloys (Titan i yego splavy). Izd-vo AN SSSR, No. 7, p. 185, 1962.

3. Goncharov, V. N. Coll. Titanium and Its Alloys (Titan i yego splavy). Izd-vo AN SSSR, No. 7, p. 280, 1962.

EFFECT OF CONDITIONS OF PLASTIC DEFORMATION AND SUBSEQUENT TREATMENT ON THE PROPERTIES OF CERTAIN TITANIUM ALLOYS

I. M. Pavlov, Yu. F. Tarasevich and A. Ye. Shelest

In the present work[1] a study was made of the influence of the magnitude of plastic deformation and subsequent cooling at various rates on the mechanical properties of certain $\alpha + \beta$ alloys -- the OT4 martensitic-type alloy and alloys VT6 and VT14 in which the β phase may be partly fixed at room temperature.

The treatment of the alloys consisted in rolling specimens of square cross section on a "200" roll mill with reductions in area of 20, 40 and 60 percent over a temperature range of 1100-500° (every 100°). The rolling rate was 0.5 m/sec. For each experimental point, three specimens were rolled of which one was cooled in water, the second in asbestos, and the third in air.

First, the cooling rate of the specimens in the cooling media was measured by means of thermocouples located on the surface and at the center of the specimens. Thus, for alloy VT4, the following cooling rates were obtained: in water, 60-70 deg/sec; in asbestos, 4.5-5 deg/sec; in air, 6-6.5 deg/sec.

The following mechanical characteristics were determined: hardness HB, proportional limit σ_p, yield strength $\sigma_{0.2}$, ultimate strength σ_u, relative contraction of cross-sectional area ψ and elongation per unit length δ. The hardness was determined on the surface of the specimens after removing the gas-saturated layer by polishing with an emery wheel.

The remaining mechanical characteristics were determined by subjecting to tensile tests specimens 3 mm in diameter which were cut out of rolled blanks in the direction of the axis of rolling. The tests were carried out with two machines: a P-5 machine at an extension rate of the specimen of ~1 percent/sec and on a Gagarin press at an extension rate of ~0.05 percent/sec.

The tensile-test diagrams obtained with the Gagarin press showed loads corresponding to the proportional limit and yield strength (ref. 1). The dimensions of the specimens before and after extension were measured with an instrument microscope. The gauge length of the specimen taken was the distance between the tips (20 mm) minus the two radii of curvature of the tips (2 mm),

---

[1]Ye. G. Konstantinov participated in this work.

i.e., 18 mm. Extension of specimens with marks made at a distance of 15 mm from each other (corresponding to standard quintuple specimens) showed that the values obtained for the elongation per unit length should be enlarged by approximately 15-20 percent.

Given below are the results of hardness tests of these alloys and the results of tensile tests of alloy OT4.

Hardness data obtained with a Brinell press as shown in figures 1-3. The Brinell hardness test has advantages in studies of alloys which are inhomogeneous in structure; in addition, this method essentially corresponds to the determination of hardness from the degree of penetration of one body into another (ref. 2).

Cooling in water from 900-1100° sharply increases the hardness of all the alloys. In alloy VT14 (fig. 3), the difference in the hardness of specimens cooled in air and in asbestos is apparent, and the increase in hardness takes place to a lesser extent.

The hardness of all the alloys changes slightly upon cooling from 500-800° (region of existence of the α phase) for a 20 percent reduction. For a 40 percent reduction, an increase in hardness is apparent as the rolling temperature drops below 800°; this may be explained by the prevalence of the phenomenon of work hardness over the recovery phenomena occurring at these temperatures.

The relative contraction of the cross sectional area and the elongation for alloy OT4 were the same in extension on the P-5 machine and on the Gagarin press, and the ultimate strength determined by testing with the P-5 machine was found to be 5-7 percent higher than in testing with the Gagarin press.

The dependence of the ultimate strength obtained by tensile tests with the P-5 machine on the conditions of the treatment is shown in figure 4.

The influence of the cooling rate on σ_u is manifested only at rolling temperatures above 900°. Certain data (ref. 3) indicate the absence of response to hardening heat treatment in alloy OT4, although cooling in water from the temperatures of existence of the β phase raises the ultimate strength of the alloy to 93-100 kg/mm^2, which is equal to 82-85 kg/mm^2 at moderate cooling rates.

At 20 percent reduction, the yield strength changes smoothly with a change in rolling temperature. At higher reductions, this regularity is not manifested, confirming the influence of the value of plastic deformation on the mechanical properties of the alloy.

Over the entire range of rolling temperatures and at all cooling rates (with the exception of a few cases at 1000° and cooling in air), the relative

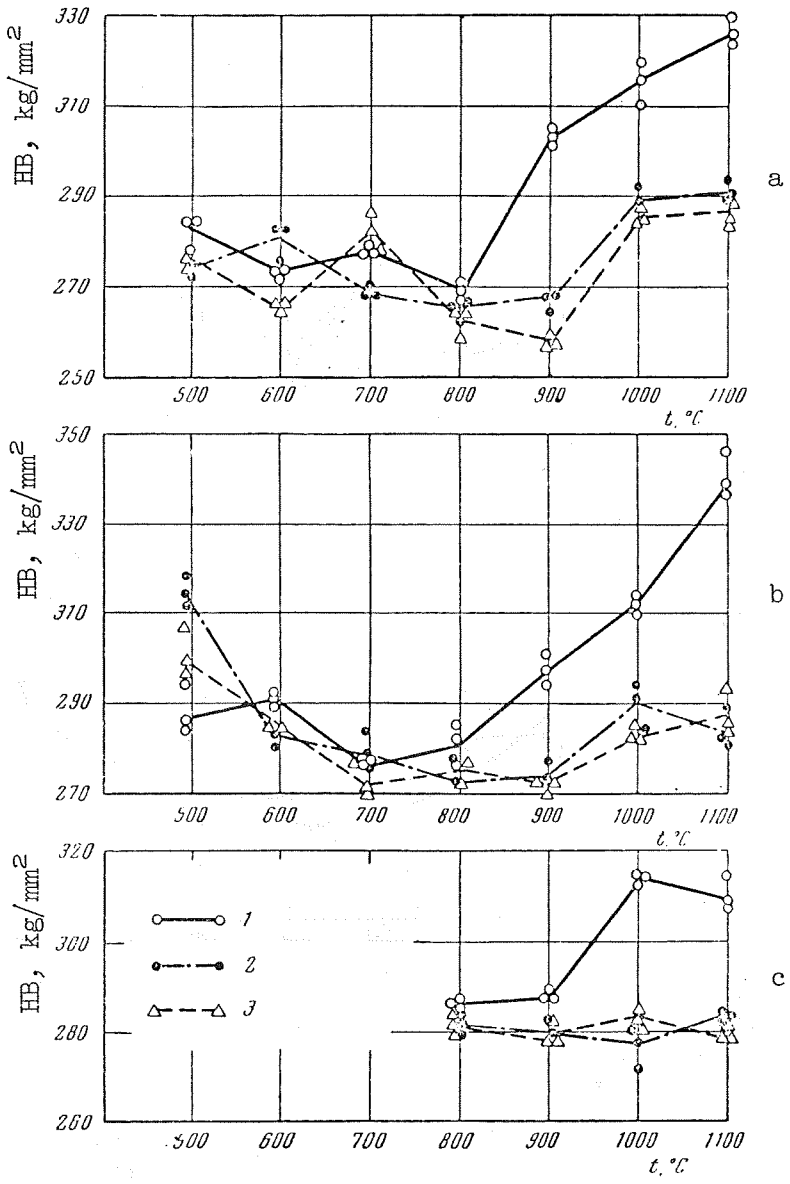

Figure 1. Dependence of hardness on the rolling temperature, reduction in area and cooling conditions of alloy OT4: a, 20 percent reduction; b, 40 percent reduction; c, 60 percent reduction; 1, cooling in water; 2, cooling in asbestos; 3, cooling in air.

contraction increases with an increase of the reduction in area, and the temperature dependence of the curves of the reduction in area is the same, having a minimum at 1000° and a maximum at 700°.

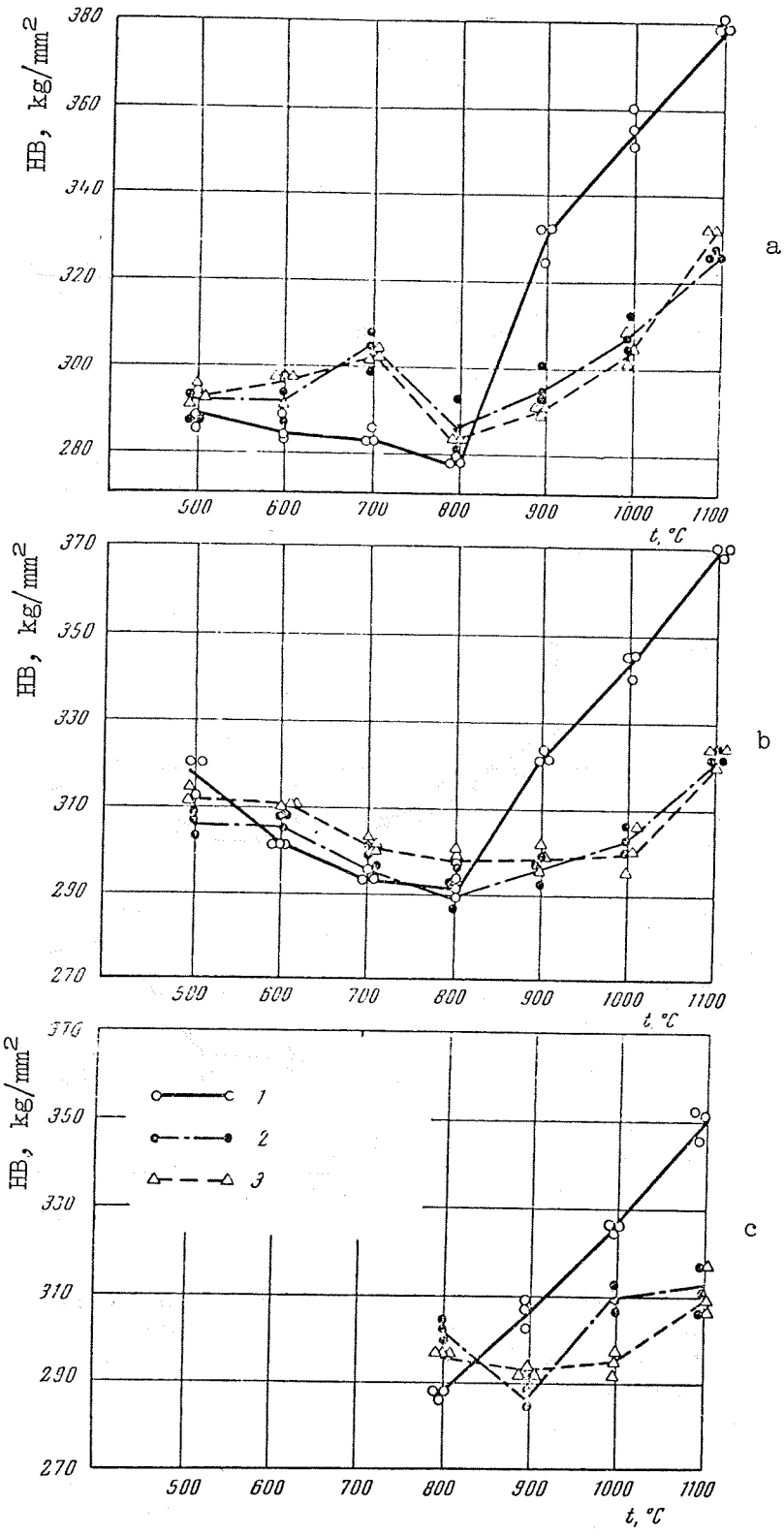

Figure 2. Dependence of hardness on the rolling temperature, reduction in area and cooling conditions of alloy VT6: a, 20 percent reduction; b, 40 percent reduction; c, 60 percent reduction; 1, cooling in water; 2, cooling in asbestos; 3, cooling in air.

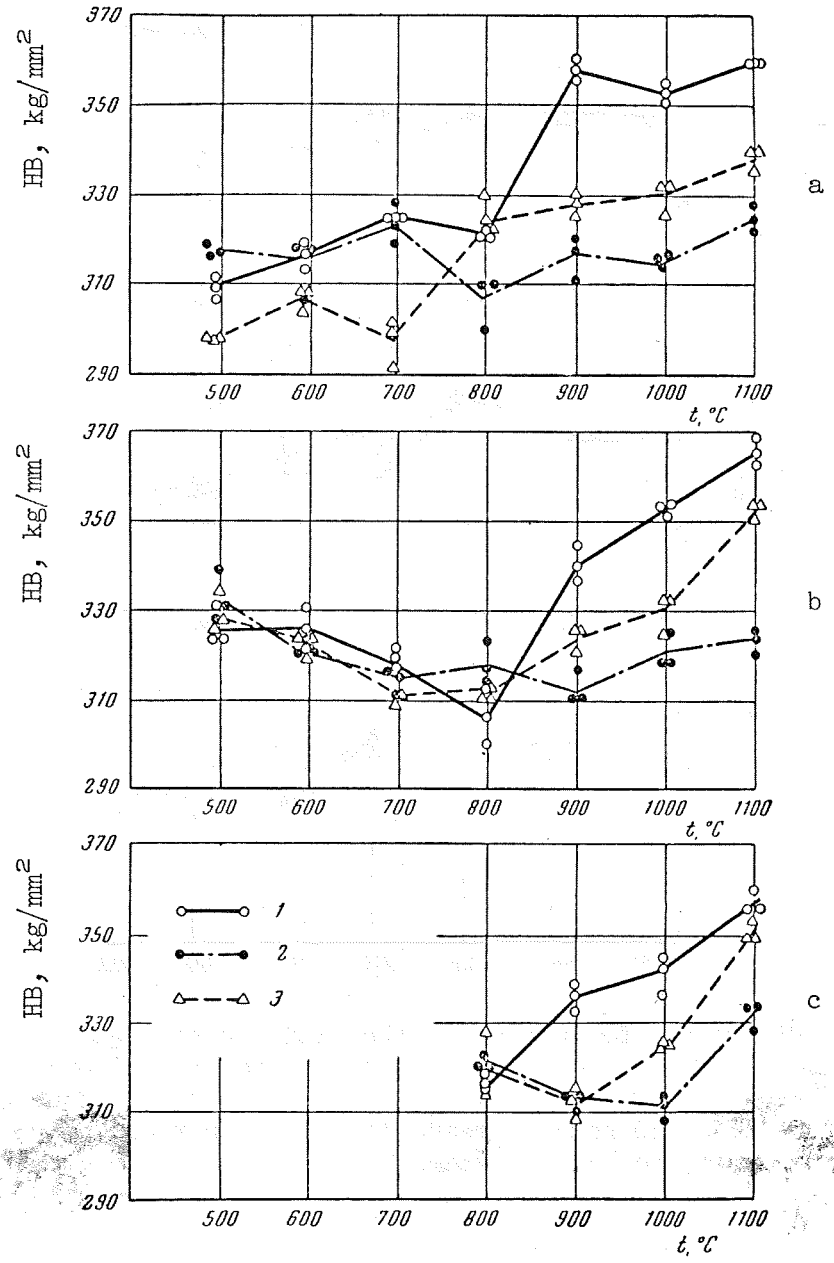

Figure 3. Dependence of hardness on the rolling temperature, reduction in area and cooling conditions of alloy VT14: a, 20 percent reduction; b, 40 percent reduction; c, 60 percent reduction; 1, cooling in water; 2, cooling in asbestos; 3, cooling in air.

The elongation per unit length decreases on rolling from temperatures below 800°; the maximum values of δ are obtained at moderate rates of cooling from 1100°.

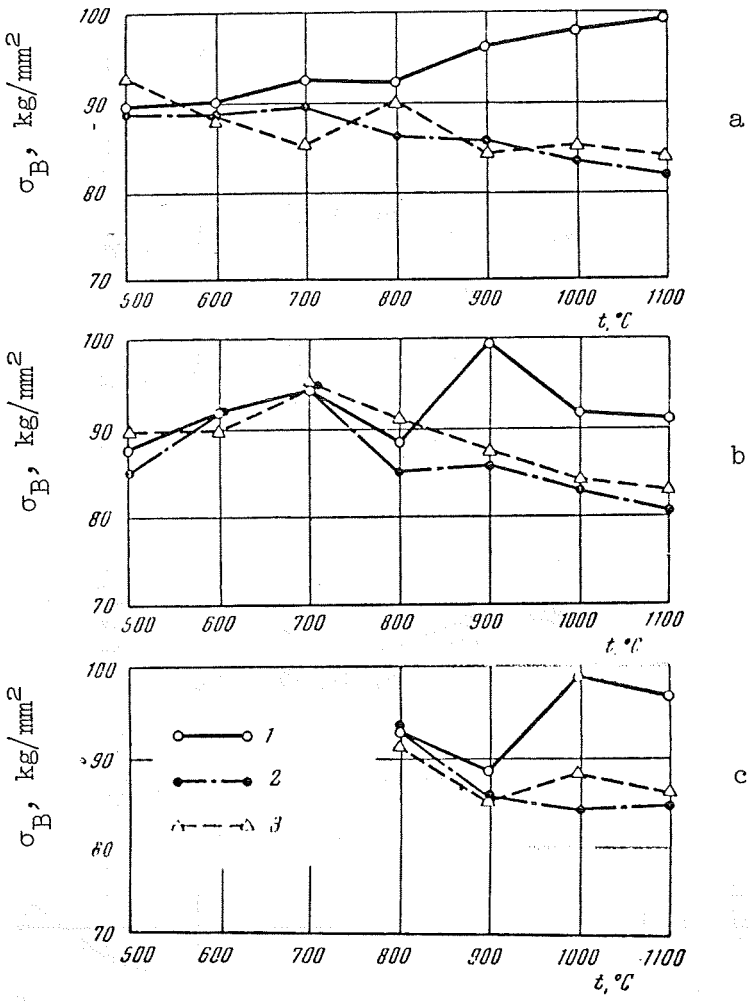

Figure 4. Dependence of the ultimate strength of alloy OT4 on the rolling temperature, reduction in area and cooling conditions: a, 20 percent reduction; b, 40 percent reduction; c, 60 percent reduction; 1, cooling in water; 2, cooling in asbestos; 3, cooling in air.

The data obtained in the present work make it possible to distinguish the principal methods of raising the mechanical properties of titanium alloys by means of their thermomechanical treatment. It should be kept in mind, however, that the thermal stability of alloys after such treatment will be fairly low, so that articles made from them can be used only at normal temperatures. The possibilities of using articles from titanium alloys subjected to thermomechanical treatment at higher temperatures require additional investigations.

REFERENCES

1. Avdeyev, B. A. Technique of Determining the Mechanical Properties of Metals (Tekhnika opredeleniya mekhanicheskikh svoystv metallov). Mashgiz, 1958.

2. Kishkin, S. T. and Petrusevich, R. L. Izv. AN SSSR, OTN, No. 1, p. 87, 1948.

3. Luzhnikov, L. P. and Moiseyev, V. I. Metallovedeniye i termicheskaya obrabotka metallov, No. 7, p. 29, 1961.

STUDY OF THE BASIC PARAMETERS OF HOT AND MEDIUM TEMPERATURE ROLLING OF SOME TITANIUM ALLOYS UNDER SPECIAL CONDITIONS OF STRESS

I. M. Pavlov, Ye. G. Konstantinov, Yu. F. Tarasevich
and A. Ye. Shelest

pp. 255-262 of original document appears in
J.P.R.S. Translation No. 28,176; TT:65-30080
pp. 29-40

SOME STUDIES OF THE STRUCTURE AND PROPERTIES OF ALLOY VT5-1 DURING HEATING FOR STAMPING

Ya. M. Dityatkovskiy, N. M. Pul'tsin, V. B. Pokrovskaya and V. A. Vinogradov

The hot working of titanium alloys is hindered by their activity at high temperatures; titanium combines with atmospheric oxygen, and the components of air dissolve in the metal. Part of the metal is thus converted into scale, and in the surface layer of the blank the hardness and brittleness are considerably increased.

In order to preserve the technological ductility of a blank, the layer of metal saturated with the components of air is removed either by etching or by machining. Thus, the heating of titanium alloys entails the loss of metal both in the scale and in the eliminated converted layer.

The problem of the quantity of metal lost in technological heating, for example, in the process of stamping, requires special investigations, since the use of high heating temperatures providing for an increase in ductility and facilitating the stamping causes an appreciable loss of the metal in the scale and in the eliminated layer, and, although a decrease in the heated temperature causes a decreased metal loss, it does not provide for the desired ductility. Such investigations should aim at the establishment of an optimum heating temperature which provides for the desired ductility of the metal and its minimum loss in the scale and eliminated layer. The increase in the weight of the blank during heating can be used as a measure of the loss of metal.

To determine the weight increase, use was made of round specimens cut from a rod which after turning were 35 mm in diameter and 10 mm high. The weight of the specimens was about 40 g.

The investigations of the converted layer, its thickness, hardness and structure were carried out on wedge-shaped bars. This shape facilitates the preparation of oblique polished sections and the study of the depth of the layer. A sketch of such a specimen is shown in figure 1.

Results of the investigation of weight increase (table 1) showed that its magnitude increases substantially as the heating temperature of the blanks is raised. Thus, for example, after a holding time of 0.5 hr, the specific weight increase of the specimens at 700° is 0.034 g/m^2 hr, at 800°, 0.062 g/m^2 hr,

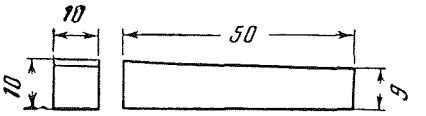

Figure 1. Sketch of specimen for studying the structure and hardness of the layer.

TABLE 1. INCREASE IN WEIGHT OF TITANIUM ALLOY VT5-1 DURING HEATING IN AN ATMOSPHERE OF AIR IN AN ELECTRIC FURNACE (IN g/m^2 HR).

Temperature, °C	Holding time, hr						Decrease in weight on increasing the holding time from 0.5 to 2 hrs
	0.5		1.0		2.0		
	Experimental data	Average	Experimental data	Average	Experimental data	Average	
700	0.033; 0.020; 0.050	0.034	0.011; 0.020; 0.020	0.017	0.0074; 0.0090; 0.012	0.0094	3.62
800	0.052; 0.059; 0.074	0.062	0.053; 0.047; 0.052	0.051	0.036; 0.042; 0.042	0.04	1.55
900	0.46; 0.47; 0.45	0.46	0.27; 0.27; 0.26	0.27	0.19; 0.14; 0.11	0.15	3.05
1000	0.9; 0.9; 0.6	0.8	0.58; 0.60; 0.57	0.58	0.30; 0.32; 0.33	0.32	2.5
1100	0.94; 0.94	0.94	0.96; 0.97	0.96	0.72; 0.62	0.67	1.4
1200	5.44; 5.36	5.4	4.7; 4.7	4.7	3.4; 3.32	3.36	1.6

at 900° 0.46 g/m^2 hr, at 1000°, 0.8 g/m^2 hr, and at 1100°, 0.94 g/m^2 hr, at 1200°, 5.4 g/m^2 hr.

If the weight increase at 700° is taken as unity, then, as shown by calculations, at higher temperatures (800, 900, 1000, 1100 and 1200°), it will be, respectively, 2, 14, 24, 28 and 159. A substantial weight increase is observed in passing from 800 to 900° (sevenfold) and from 1100 to 1200° (sixfold).

Analysis of the data obtained shows that in heating titanium alloy VT5-1 for forging and stamping, one should not use a temperature above 1100° because the metal lost in the scale and in the eliminated saturated layer is thus appreciably increased.

As the holding time is increased, the specific weight increase decreases substantially. Thus, for example, at 900°, an exposure of 0.5 hr is associated with an increase of 0.46 g/m^2 hr, and an exposure of 2 hrs, with only 0.15 g/m^2 hr, i.e., a loss 3.05 times smaller. A similar picture is observed at other temperatures as well.

A reduction in the specific weight increase with increasing holding time may be explained by the self-inhibition of the saturation process. The layer of oxides formed as well as the layer of the solid solution of impurities in titanium hinder a further absorption of the components of air by the metal to a certain extent: the diffusion of impurities through the scale and through the converted layer is slowed down.

It should be noted that as the temperature is raised, the reduction in the weight increases with the holding time. Whereas at 900° an increase in holding time from 0.5 to 2 hrs causes a 3.05 fold drop in the weight increase, at 1100° the weight increase is reduced only 1.4 times. This may be explained by an increase in the rate of diffusion at high temperatures and a decrease in the self-inhibition effect.

The study of the modified layer was made by means of metallographic analysis and microhardness measurements.[1] It was found that the surface layer as a result of saturation with atmospheric oxygen acquires a greater hardness, and that the α structure of the solid solution undergoes a change which is visible under the microscope.

The results of the investigations are shown in table 2 and figure 2.

TABLE 2. EFFECT OF ANNEALING OF ALLOY VT5-1 ON THE NATURE OF THE SURFACE LAYER FOR A HOLDING TIME OF 1 HR

Annealing temperature, °C	Microhardness, kg/mm^2		Depth of modified layer, mm	Microstructure		
	of surface	of core		of surface	of transition layer	of core
900	545	300	0.12	CE	FE + FN	FE + FN
1000	881	300	0.15	CE	CE + FN	FE + FN
1200	1140	300	0.28	CE	CE + CB	CB

Symbols designating the structures: CE - coarse-grained equiaxial, FE - fine-grained equiaxial, FN - fine-grained nonequiaxial, CB - coarse-grained basketlike.

[1] Ye. A. Bodrova participated in the work.

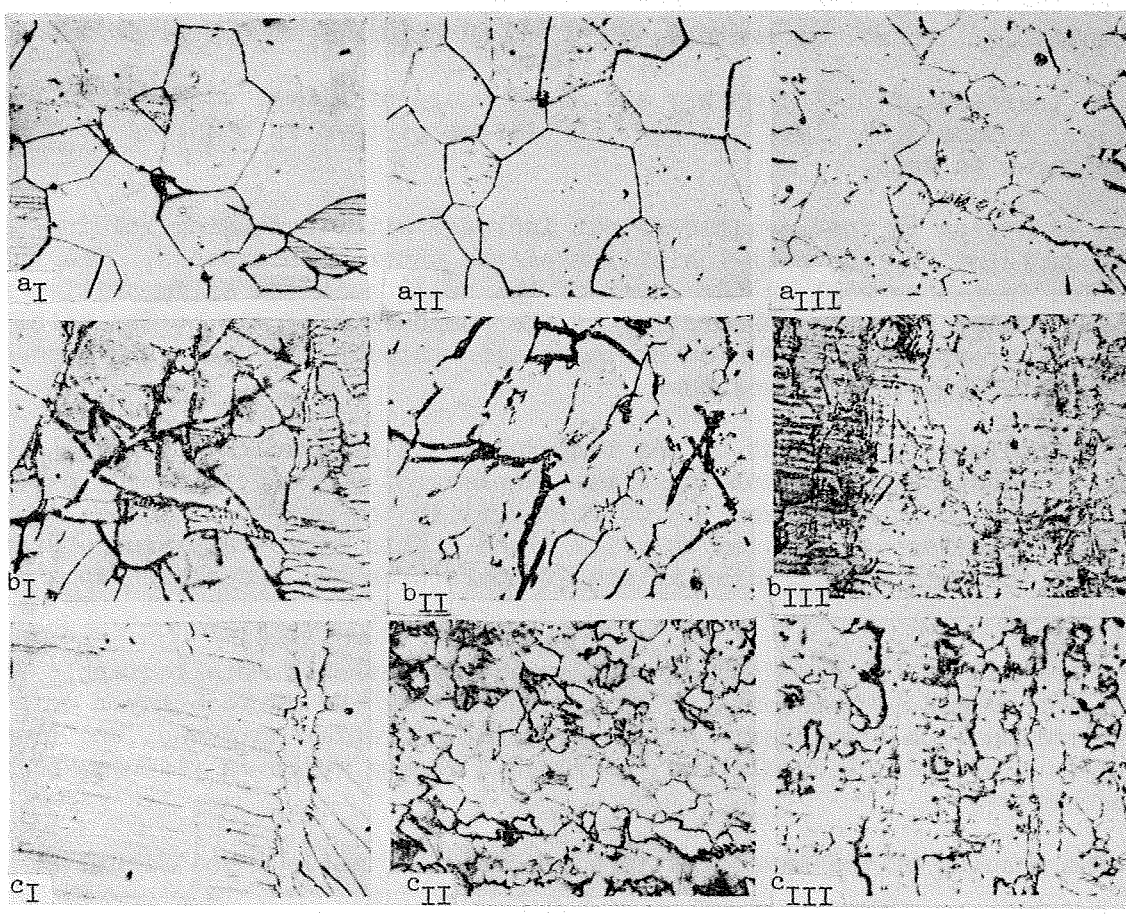

Figure 2. Microstructures of specimens of titanium alloy VT5-1 soaked for 1 hr, x 450: a, surface; b, transition layer; c, core; I, at 1200°; II, at 1000°; III, at 900°.

These results confirmed the known literature data to the effect that as the heating temperature rises, the hardness and depth (thickness) of the surface layer of the titanium alloys increase. In this case, there is observed an increase in the microhardness in the surface layer of alloy VT5-1 from 300 to 545 kg/mm^2 after soaking at 900°, to 881 kg/mm^2 at 1000° and to 1140 kg/mm^2 at 1200. The depth of the layer, defined as the thickness of the zone of greater hardness, comprises respectively 0.12, 0.15 and 0.28 mm.

The literature data (ref. 1) on the influence of oxygen on the hardness of titanium and its alloys make it possible to solve the problem of determination of the amount of oxygen in titanium by means of the hardness.

Knowing the oxygen concentration in the layer, one can correctly analyze those structural changes which are observed as a result of annealing the single-phase α alloy VT5-1.

Photomicrographs of the structures of the alloy at the surface, in the intermediate layer and in the core (fig. 2) at various soaking temperatures indicate that the structure visible under the microscope depends not only on the soaking temperature but also on the oxygen content; this structure changes from the surface of the specimen to the core.

It would seem that oxygen, which is an α stabilizer, should not change the structure, visible under the microscope, of titanium alloy VT5-1, which has a single-phase structure of the α solid solution (ref. 2). However, the structures, visible under the microscope, of the surface layer containing a significant amount of oxygen, of the transition zone and of the core differ nevertheless (fig. 2). An equiaxial structure of a solid solution is observed in the surface layer, whereas a basketlike structure is observed in the core.

Such a difference in structure due to a nonuniform content of oxygen, results from the fact that oxygen raises the temperature of the allotropic transition of titanium.

Soaking of the alloy at 1200° is not associated by a shift of the phase transformation boundary on cooling and produces coarse equiaxial grains of the α phase in the surface layer (fig. $2a_I$).

In the transition layer, the equiaxial structure is obtained only partly (fig. $2b_I$). It is present together with the basketlike structure of the α phase, obtained by cooling from the β solution after soaking in the intermediate $\alpha + \beta$ region.

The core, which in the process of soaking at 1200° consists of markedly grown grains of the β phase, assumes a coarse basketlike structure with very large elements of the α phase on cooling (fig. $2c_I$).

Soaking of the alloy at 1000° produces almost the same results. The surface layer of the specimens has a coarse crystalline equiaxial structural of the α phase (fig. $2a_{II}$). Both an equiaxial and a nonequiaxial α phase is observed in the transition layer (fig. $2b_{II}$), while a finely crystalline not coarse basketlike structure is observed in the core (fig. $2c_{II}$), which is explained by the absence of overheating in the β region.

The 900° isotherm for the alloy with an equal content of oxygen does not intersect the lines of the phase transformations. For this reason, almost no nonequilibrium formations of the α phase are observed in the structure.

Summary

1. The weight increase of specimens during heating for stamping increases considerably at temperatures above 800° and particularly on heating at 1100°.

The magnitude of the specific weight increase at various temperatures decreases with an increase in soaking time, indicating a self-inhibition of the absorption of impurities.

2. Heating of titanium alloy VT5-1 in an atmosphere of air at various temperatures is accompanied by the formation of an altered layer whose thickness, microhardness and structure depend on the soaking temperature.

3. The maximum microhardness of the changed layer is observed in the surface and its value is higher the higher the temperature. As the temperature is raised, the depth of the layer increases and reaches about 0.3 mm at 1200°.

4. The visible structure of the changed surface layer and of the transition zone differs from the structure of the core, although there is no fundamental difference in the structure of all three regions: the structure consists of a single phase--an α solid solution.

5. The solid solution of the surface zone has an equiaxial grain structure, while the solid solution of the core has a basketlike or finely crystalline non-equilibrium structure. Such a difference in structure is due to the fact that the surface layer highly saturated with oxygen does not undergo any phase transformations during cooling after annealing; this is not true of the core and partly of the transition layer.

6. The formation of the changed layer (even a thin one) having a great hardness and a coarse grain seems to be the cause of the appearance of cracks in the material during its machining and perhaps during its service as well.

REFERENCES

1. McQuillen, A. D. and McQuillen, M. C. Titanium. Metallurgizdat, 1958.

2. Pul'tskin, N. M. Izv. vyssh. uchebn. zaved., Tsvetnaya metallurgiya, No. 5, 1962.

SOME CHARACTERISTICS OF THE HEAT TREATMENT OF ALLOY AT3 WITH A LOW CONTENT OF ALLOYING ELEMENTS

S. A. Yudina and B. K. Vul'f

In the preceding studies (refs. 1-3), the influence of heat treatment on the structure, properties, and thermal stability of alloys AT3, AT4, AT6 and AT8 of normal composition was elucidated.

The present investigation is devoted to the similar study of alloy AT3 containing the smallest amount of aluminum and a low content of alloying elements; such an alloy is particularly interesting as a material for the production of cold rolled pipes.

A practical objective of the present is the establishement of the optimum conditions of thermal treatment permitting the best combination of mechanical properties and, particularly, a sufficient difference in the value of the ultimate strength and yield strength. This would facilitate the technological process of pipe manufacture and would guarantee a high service reliability of parts operating under complex load conditions.

MECHANICAL CHARACTERISTICS OF TITANIUM ALLOY AT3 FOLLOWING HEAT TREATMENT.

Quenching temperature, °C	σ_b, kg/mm²			$\sigma_{0.2}$, kg/mm²			δ, %			ψ, %			a_n, kgm/cm²		
	Quenching	Quenching + aging at 300°	Quenching + forging at 400°	Quenching	Quenching + aging at 300°	Quenching + forging at 400°	Quenching	Quenching + aging at 300°	Quenching + forging at 400°	Quenching	Quenching + aging at 300°	Quenching + forging at 400°	Quenching	Quenching + aging at 300°	Quenching + forging at 400°
Initial state	82.8	80.5	83.2	79.6	79.2	77.3	12.5	14.8	14.7	53.5	50.5	43.4	8.1	2.1	2.9
750	74.7	74.2	75.6	70.3	71.0	72.0	18.0	19.1	20.3	44.6	48.7	48.6	8.4	—	1.8
800	74.9	73.3	73.9	70.7	70.5	68.0	18.2	17.15	16.7	49.0	48.2	39.1	7.8	—	7.6
850	73.8	74.1	71.6	68.1	68.8	64.9	17.4	18.0	20.6	46.3	51.15	40.9	9.0	7.5	6.4
900	72.7	79.6	72.9	64.6	71.05	63.9	20.6	15.1	16.3	37.1	34.7	36.0	5.2	—	—
950	72.3	74.2	73.9	63.9	63.3	63.4	12.3	14.8	12.7	24.5	28.6	19.7	3.9	3.6	1.45
1000	72.3	72.6	73.5	64.6	64.5	64.8	16.7	14.8	14.1	34.1	32.7	37.2	2.6	—	2.5
1050	73.0	73.0	—	63.2	64.4	—	16.5	16.4	15.7	36.8	30.5	33.5	3.5	1.6	1.6
1100	73.0	74.0	74.0	64.3	64.4	65.0	16.6	19.2	16.2	36.1	38.0	33.4	3.1	1.8	1.6
1150	73.1	72.9	71.7	64.0	64.5	63.0	17.9	15.7	16.7	37.6	39.3	38.0	5.6	—	2.7
1200	73.5	74.2	—	65.3	66.0	—	17.9	15.9	17.9	40.0	37.2	—	3.0	—	—
1250	72.9	70.0	71.7	64.9	61.8	63.7	11.4	15.8	15.3	24.0	37.7	33.0	4.3	—	2.2

The alloy was melted in a vacuum arc furnace with a consumable electrode by double remelting and was then subjected to forging at temperatures of 1000-1150°. The procedure used in the preparation and the composition of the burden materials are indicated in reference 2.

The experimental alloy AT3 has the following chemical composition: 2.5 percent Al, 0.9 percent (Cr + Fe + Si + B), 0.013 percent H_2, 0.013 percent N_2, and 0.06 percent C.

The blanks cut out of the rods were studied in the initial state, after quenching in air from 750-1250° (at 50° intervals) and also after aging the quenched alloys for 100 hr at 300 and 400°. The holding time at quenching temperatures of 750-1100° was 1 hr and at 1150-1250°, 15 min.

The mechanical properties were determined by tensile testing of Gagarin specimens to determine σ_b, $\sigma_{0.2}$, δ and Ψ and impact testing of Menager specimens with the determination of a_n. The data of the tests are shown in the table and in figure 1.

From these data it is apparent that as the quenching temperature is raised, σ_b and $\sigma_{0.2}$ decrease somewhat as a whole, but at a quenching temperature of $\sim 900°$ in the case of aging at quenched alloys at 300° for 100 hr, there is observed a small relative increase in the values of these characteristics. At the other quenching temperatures, aging causes little change in the strength characteristics.

Attention should also be drawn to the fact that as the quenching temperature rises, there is an increase in the difference between the values of σ_b and $\sigma_{0.2}$, which for forged alloys in the initial state, as to 3-4 kg/mm^2, and for alloys quenched from 850° and higher, 9-10 kg/mm^2.

This is apparently due to the appearance of the β phase at the heating temperature, as confirmed by the data of reference 4 on the heat treatment of alloys Ti - Cr and Ti - Cr - Al, in which it is stated that during the extension of specimens containing the β phase in the structure there is observed an increase in the difference between the ultimate strength and yield strength.

Aging also affects the relation between σ_b and $\sigma_{0.2}$. At a quenching temperature of 800-850°, the difference between the values of σ_b and $\sigma_{0.2}$ is much greater in the case of aging at 400° than at 300°, since at higher quenching temperatures this difference, being appreciable in absolute value, is practically independent of the aging temperature.

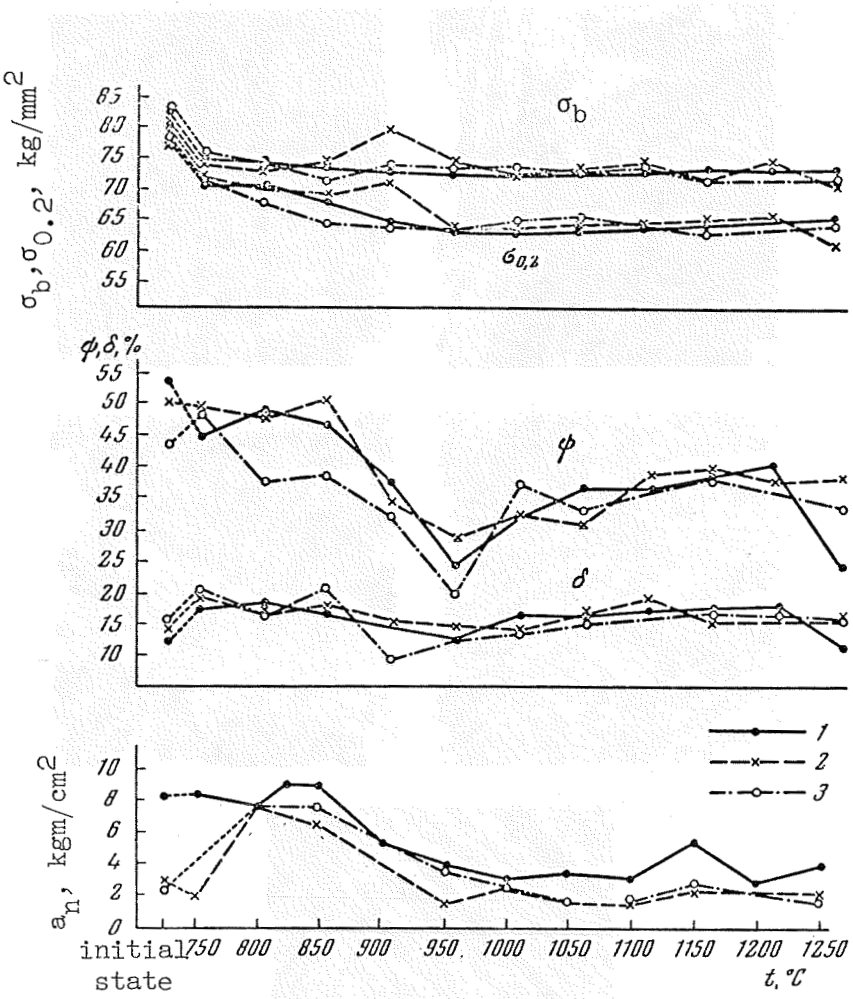

Figure 1. Influence of quenching temperature on the mechanical properties of alloy AT3. 1--quenching with cooling in air; 2--same + aging at 300°, 100 hr; 3--same + aging at 400°, 100 hr.

The alloys preserve a high ductility up to a quenching temperature of ~ 850°; a further rise in this temperature leads to a substantial decrease in δ and particularly Ψ, owing to a rapid growth of the grains and beginning of formation of the β phase, which converts into a coarse platelike structure of the α' phase during quenching. The lowest values of Ψ correspond to quenching temperatures of 900-950°.

The highest values of the impact strength of the alloy were observed at quenching temperatures of 825-850° (for example, at 825° a_n = 9.1 kgm/cm^2).

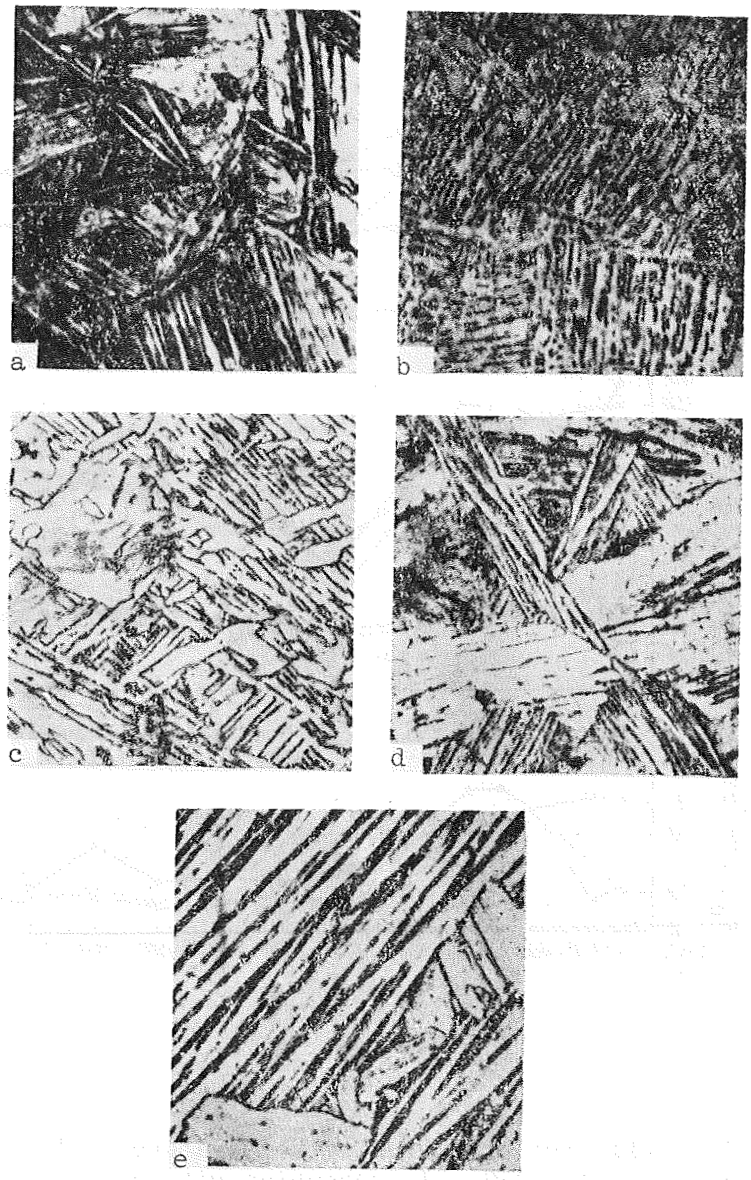

Figure 2. Microstructure of ally AT3, x 300. a--initial state; b--quenching from 800°; c--quenching from 850°; d--quenching from 950°; e--quenching from 1000°.

It is interesting to note that aging at 300-400° sharply decreases the impact strength of forged specimens (in the initial state), but practically does not reduce the high values of impact strength characteristic of alloys quenched from 800-850°. This result is a clear confirmation of the practical desirability of carrying out the quenching and should be attributed to an increased content of hydrogen in the alloy (0.013 percent).

It is known (ref. 5) that the solubility of hydrogen in titanium at 325° is about 0.2 percent, and is close to zero at room temperature; all of the hydrogen is contained in the γ phase, which is titanium hydride. In the course of slow cooling of titanium or a single-phase α alloy, this phase precipitates along the grain boundaries of the solid solution and decreases the impact strength of the alloy. As the alloy is heated, a complete dissolution of titanium hydride takes place, and the latter does not precipitate under quenching conditions, so that a restoration of the original values of the impact strength is observed, particularly in alloys with an increased hydrogen content.

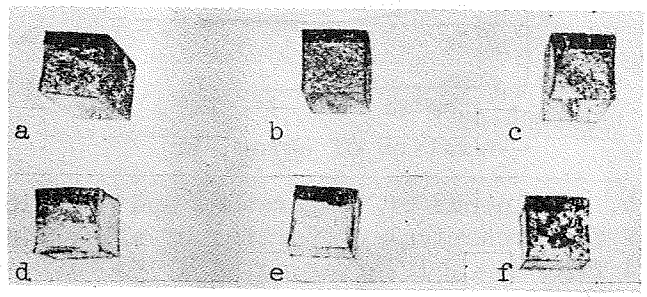

Figure 3. Fractures of specimens of alloy after various heat treatments. a--initial state + aging at 400°; b--quenching from 750° + aging at 400°; c--quenching from 800°; d--quenching from 850°; c--quenching from 850° + aging at 400°; f--quenching from 950° + aging at 400°.

It should be noted in passing that the influence of hydrogen is manifested to different degrees if the aluminum content is different. From reference 6 and others, it is known that alloys having a low aluminum content (2.5 percent) embrittle even at a low hydrogen content ($\sim$ 0.008 percent).

Apparently, an increase in aluminum content raises the solubility of hydrogen in the α phase or retards the precipitation of the hydride and decreases the coefficient of the fusion of hydrogen in titanium.

However, at a low aluminum content of the alloy, the inclusions of hydride are uniformly distributed, and at a high aluminum content, the inclusions precipitate primarily along the grain boundaries, as a result of which Ψ decreases markedly.

The influence of heat treatment on the mechanical properties of alloy AT3 is confirmed by data of metallographic analysis and by the characteristics of the breaks of specimens obtained under conditions of dynamic failure. In the initial state and after quenching from 750°, the alloy has a coarse platelike structure of the α' phase (fig. 2a) and is characterized by a coarsely crystalline lustrous brittle fracture (fig. 3a and b). After quenching from the optimum temperatures, there is formed a finely crystalline structure primarily of the α phase with signs of steroidization (fig. 2b and c); in this case,

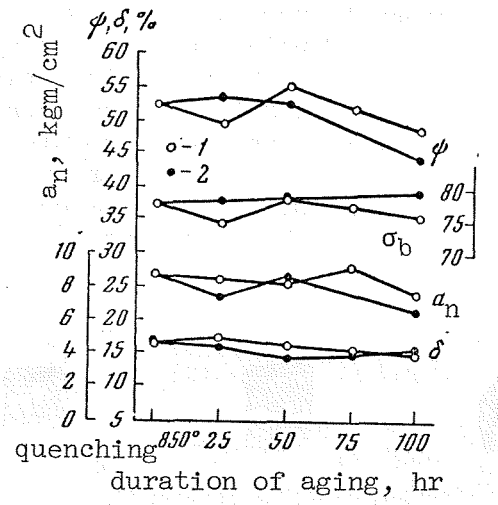

Figure 4. Influence of temperature and duration of aging of the mechanical properties of alloy AT3 quenched from 850°. 1--after aging at 300°; 2--after aging at 400°.

the fracture becomes ductile, dull, and finely crystalline (fig. 3c, d and e). On overheating to 950-1000°, the coarse platelike structure of the α' phase reappears (fig. 2d and e) with a coarse-grained brittle fracture (fig. 3f).

Aging at 300 and 400° for 100 hr of specimens quenched at the optimum temperature of 850° has practically little effect on the mechanical properties of alloy AT3. The change in properties in the course of aging is also slight (fig. 4). This indicates a high thermal stability of alloy AT3 in the quenched state.

Summary

1. Alloy AT3, which has a low content of alloying elements and is characterized by a high ductility and resistance to dynamic loads, acquires the best mechanical properties having quenching in air from 825-850°.

2. The alloy quenched under these conditions as a high thermal stability and has the following mechanical characteristics after aging for 100 hr at 400°: σ_b = 72 kg/mm^2, $\sigma_{0.2}$ = 64 kg/mm^2, σ = 18 percent, Ψ = 52 percent, a_n = 8 kgm/cm^2.

3. The considerable difference between σ_b and $\sigma_{0.2}$, amounting to about 8 kg/mm^2, makes it possible to use the heat-treated alloy AT3 with a low content of alloying elements for the preparation of parts operating under complex conditions of stress application.

REFERENCES

1. Vul'f, B. K. and Yudina, S. A. Coll. Titanium and Its Alloys (Titan i yego splavy). Izd-vo AN SSSR, No. 7, p. 174, 1962.

2. Kornilov, I. I., Vul'f, V. K. and Yudina, S. A. Metallovedeniye i termicheskaya obrabotka metallov, No. 2, p. 54, 1963.

3. Vul'f, B. K. and Yudina, S. A. Coll. Titanium and Its Alloys (Titan i yego splavy). Izd-vo AN SSSR, No. 10, p. 207, 1963.

4. Moiseyev, V. N. Metallovedeniye i termicheskaya obrabotka metallov, No. 2, p. 24, 1963.

5. Pul'tsin, N. M. Titanium Alloys and Their Use in Machine Construction (Titanovyye splavy i ikh primeneniye v mashinostroyenii). Mashgiz, 1962.

SOME PROBLEMS OF FUSION WELDING OF TITANIUM AND ITS ALLOYS

G. L. Petrov, M. D. Shchipkov, A. I. Lebedev
and A. A. Yazykov

pp. 273-282 of original document appears in
J.P.R.S. Translation No. 28,176; TT:65-30080
pp. 41-55

SUBMERGED DOUBLE-ARC WELDING OF MEDIUM AND LARGE THICKNESS SEMIFINISHED PRODUCTS OF TITANIUM ALLOYS

S. M. Gurevich and S. D. Zagrebenyuk

pp. 283-288 of original document appears in
J.P.R.S. Translation No. 28,176; TT:65-30080
pp. 56-62

STUDY OF THE MUTUAL DIFFUSION OF TITANIUM WITH COPPER AND OTHER METALS SUITABLE FOR BRAZING

A. Ya. Shinyayev, V. V. Bondarev and Ye. V. Sergeyeva

pp. 289-293 of original document appears in
J.P.R.S. Translation No. 28,176; TT:65-30080
pp. 63-69

USE OF OPTICAL EMISSION MICROANALYSIS IN THE STUDY OF TITANIUM ALLOYS

N. V. Korolev, S. A. Gorbunov and A. S. Bogdanov

Improvement of the device for emission microanalysis (refs. 1, 2) has opened up new vistas for the solution of many problems. The studies which were carried out made it possible to create conditions for the performance of analyses in an atmosphere of inert gases, to improve the localization of the analyses, and to increase the intensity of the local attenuated microspark. Of particular value has been the use of a microspark in argon in analyses of alloys for oxygen and nitrogen.

Optical Diagram of Improved Device

Let us consider the optical diagram of the modified device (fig. 1). The electric spark formed between the surface of the analyzed specimen 1 and the tip of the microelectrode 2, successively through the ultraviolet microscope objective 3, a tiltable semialuminized mirror 4, a quartz lens 5, and an achromatic set of quartz and lithium fluoride lenses 6, appears in the plane of the slit of the quartz spectrograph 7 on a scale of 6:1.

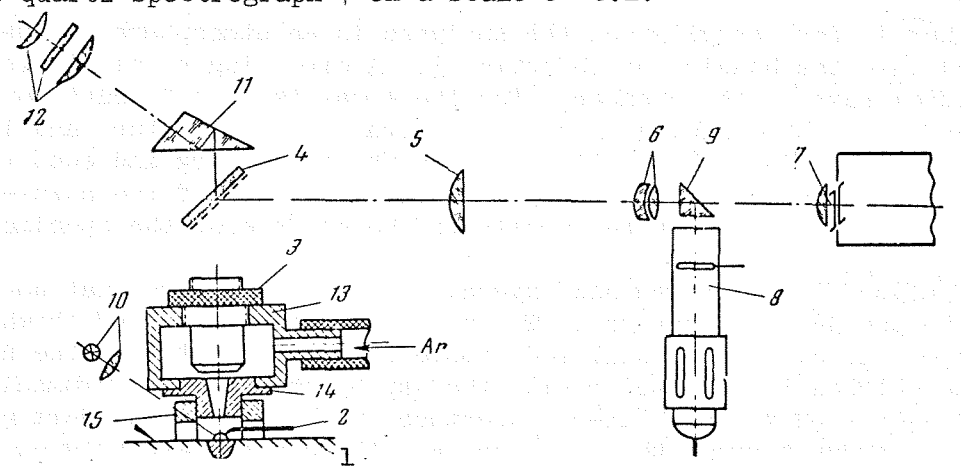

Figure 1. Optical diagram of apparatus for emission analysis: 1, sample under analysis; 2, microelectrode; 3, microscope objective; 4, semialuminized mirror; 5, quartz lens; 6, achromatic set; 7, slit of spectrograph; 8, illuminating tube; 9, hinged prism; 10, lateral illuminator; 11, deflecting prism; 12, eyepiece; 13, chamber; 14, nozzle of chamber; 15, directing cap.

The analyzed surface of specimen 1 may be illuminated either by light coming from above through microobjective 3 or by lateral light from illuminator 10. In the former case, a hinged prism 9 which directs the light from the illuminating tube 8 into the system of the microscope is introduced in order to provide illumination between the set of lenses 6 and the slit of the spectrograph.

The surfaces of specimen 1 and of the tip of microelectrode 2, illuminated by light coming from the side or from above and reprojected by objective 3, are observed in eyepiece 12 by means of light which has partly passed through the tilted semialuminized mirror 4 and prism 11.

A reticle in the eyepiece of the microscope makes it possible to place the structure under analysis and the tip of the microelectrode in the required position relative to the optical axis of the instrument.

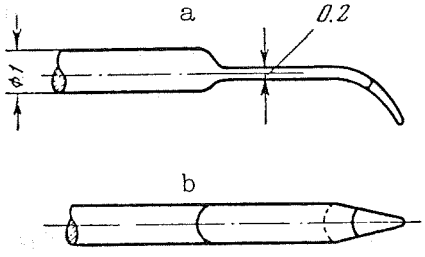

Figure 2. Construction of microelectrode: a, side view; b, top view.

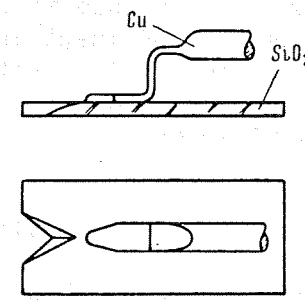

Figure 3. Attachment with directing groove.

Chamber 13 for carrying out the analyses in an atmosphere of inert gases is screwed onto the housing of objective 3. A directing nozzle 14 is provided in the bottom part of the chamber. The inert gas is introduced into the chamber by means of rubber tubing through a lateral connecting tube and is directed through the nozzle into the burning zone of the microspark and onto the surface being analyzed. The diameter of the gas jet coming out of the nozzle is 3 mm. The distance from the tip of the nozzle to the surface of the specimen is 4 mm.

In analyses for nitrogen and oxygen, one must make sure that no air is sucked into the jet of inert gas. To this end, a directing cap 15 whose lower tip rests on the surface of analyzed sample 1 may be mounted on the nozzle. The microelectrode is inserted inside the cap by means of a micromanipulator through a square (2 x 2 mm) lateral aperture in the cap. The inert gas comes out of the chamber through this aperture and through the gap between the lower tip of the cap and the specimen.

The construction of the microelectrodes used to carry out the microanalyses is shown in fig. 2.

The microanalysis involves the use of a directing groove in a quartz plate

for the localization of spark discharges on the surface of the specimen. The construction of this attachment is shown in fig. 3.

The attachment, held in the electrode holder by the round end of the electrode, is placed on the surface of the specimen by means of the micromanipulator mechanism in such a way that the portion under analysis and under observation in the microscope is located at the apex of the directing groove.

By carrying out the analyses in an attenuated microspark by means of a directing groove, one can confine the electric discharges to an area up to 0.05 mm in diameter with a 10 μ minimum depth of the damaged layer.

Microspark Generator

The electric circuit of the microspark generator now in use (fig. 4) makes it possible to obtain a hard and an attenuated microspark. The regime of the hard microspark is characterized by a higher concentration sensitivity and gives spectra of elements which are difficult to excite; the regime of the attenuated microspark is used when it is necessary to have a highly localized analysis.

When switch S_2 is in position I, the current pulses which are stored by capacitor C_p before the arcing of the auxiliary gap AG, pass completely through the analytical gap AnG after the arcing of AG. If the capacity of the weighting capacitor is high ($C_p > 0.01$ μF), the spectra of ions of almost all elements are readily excited in such a microspark (hard regime of microspark).

If the switch S_2 is in position II, the current pulses cross the analytical gap under the influence of an induced emf arising at the ends of the secondary winding of the air-core transformer L_2 when the current pulses pass through the primary winding L_1 of this transformer.

The magnitude of the current pulses crossing the analytical gap AnG depends on the capacitance of the conductors bringing the current from coil L_2 to this gap, and not on the arcing voltage of the analytical gaps. When the supplementary gap SG is absent, the pulses of the current crossing the analytical gap AnG are small, since the capacitance of the conductors and the arcing voltage are small. As a result, the brightness of the spark is weak. The introduction of a supplementary gap SG raises the total arcing voltage of gaps SG and AnG, increasing the current pulses, as a result of which the brightness of the microspark increases (regime of attenuated microspark).

The additional gap used is a xenon pulse tube ISSh-100/1.

Use of Emission Microanalysis

Microspectral analysis can find various applications in the study of titanium alloys because of its advantages over ordinary spectral analysis. One of the main advantages of the microspectral analysis is the small quantity of substance required for the analysis (10^{-5}-10^{-6}g), which permits an investigation without damage to the analyzed items. After the analysis, only minor finishing of the surface is necessary. Many years of experience with this device leads us to believe that the construction of a portable microspectral apparatus for checking large-sized items is possible.

The analysis may be performed at a strictly defined site of the part, where changes in the composition of the alloy can be expected. This advantage is irreplaceable when it is necessary to account for the causes of various surface defects.

Finally, this method of analysis permits the determination of elements which are difficult to excite and are present in the alloys.

The existing methods of checking for gaseous impurities in titanium (spectral methods, vacuum fusion, etc.), require the destruction of the parts, so that these methods cannot be used to perform layer analyses for oxygen, nitrogen and carbon, whereas the improved design of the microspectral unit opens up broad perspectives in this direction.

A series of examples given below indicates various means and methods of microspectral analysis drawn from the experience of studying titanium alloys.

Microspectral Analysis of Gaseous Impurities

In the process of oxidation of technically pure titanium VT1, the impurity elements are redistributed between the oxides and the metal layer located under this crust of oxides.

The purpose of the investigation was to determine the chemical composition of the metal (primarily gaseous impurities) on the surface of specimens of alloy VT1 heated in air at various temperatures and for various periods of time.

The study of the chemical composition of the surface layers of the metal yielded the following results.[1]

At oxidation temperatures of 1100 and 1200°, carbon, silicon and nitrogen, present in the composition of the metal as impurities, concentrate in the surface layer of the metal to a depth of 10-15 μ. This layer is extremely stable chemically and has a great hardness close to that of titanium carbides and

---

[1]This is discussed in more detail in an article by N. V. Korolev (see this collection, p. 146).

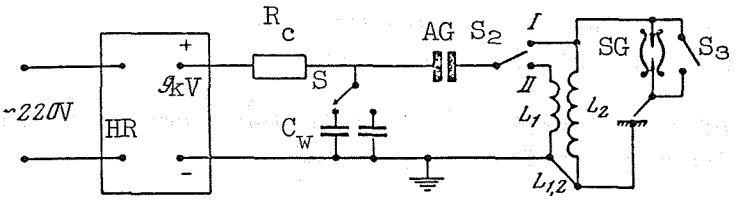

Figure 4. Electric circuit of microspark generator: HR, high-voltage rectifier; R_c, charging resistor; S_1, capacitant switch; C_w, working capacitors; AG, auxiliary gap; S_2, switch for microspark regimes; L_1 and L_2, primary and secondary winding of air core transformer; $L_{1,2}$, air core transformer; SG, supplementary gap; AG, analytical gap; S_3, on-off switch of supplementary gap.

nitrides. The concentration of carbon and nitrogen on the surface of the metal after the oxidation in air of samples of alloy VT1 at various temperatures and testing times can be evaluated from the results of the analysis shown in the table below:

CONTENT OF NITROGEN AND CARBON IN SURFACE LAYERS OF SPECIMENS OF TITANIUM ALLOY VT1 (IN PERCENT).

Testing temperature, °C	Duration of testing, Hr	N	C
1200	0.05	0.0	0.04
1200	0.1	0.5	0.02
1200	0.2	0.7	0.04
1200	0.5	3.6	0.12
1200	1	3.3	0.65
1200	4	1.7	1.16
1100	4	3.5	--
1100	8	1.7	0.3
1100	16	3.5	0.35
1000	8	0.0	0.04
1000	16	0.0	0.06
900	8	0.0	0.05
900	16	0.0	0.06
800	8	0.0	0.1
800	96	0.0	0.14

Note: Sensitivity of determination: 0.3 percent for nitrogen, 0.03 percent for carbon.

The oxygen content in the surface layers of the titanium samples was 0.1 percent and higher.

Layer Microspectral Analysis Involving Transfer of the Analyzed Substance Onto Copper Plates

The nature of the distribution of alloying elements in the oxide layer was studied on the binary alloy Ti + 10 percent Sn.

The technique of the analysis of the oxides consists in the following: a small amount of powder of the oxides from the layer located at a certain depth is removed by means of a corundum or silicon carbide scraper and placed on a copper plate (fig. 5).

The oxide powder is then rubbed into the surface layer of the plate by means of the same scraper, or is spread over this surface. The surface layer of the plate with the powder rubbed into it is then treated with pulsed discharges of a hard microspark in the unit for emission microspectral analysis. The spectra obtained in the spark are photographed. The photographic film containing the spectra is subjected to photometric treatment by using the technique described in ref. 2. A result of the photometric treatment of the film is the determination of the ratio of the weight concentration of the alloying element to the concentration of titanium for oxide layers located at different depths.

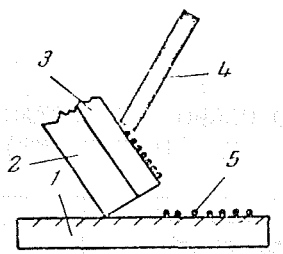

Figure 5. Diagram of the transfer of oxide onto metal backing: 1, copper plate; 2, specimen with oxide crust; 3, oxide crust; 4, scraper made of Al_2O_3 and SiC; 5, oxide powder.

Let us examine the nature of the change in the ratio of the concentration of tin C_{Sn} to the concentration of titanium C_{Ti} in the layer of oxides formed on the surface of the alloy with 10 percent Sn during oxidation of a specimen in air for 8 hr at 1100°:

Outer oxide layer from the surface	0.018
Inner surface of outer layer	0.036
Outer surface of monoxide	0.029
Inner surface of monoxide	0.105
Top layer from the metal surface	0.33
Average composition of alloy	0.11

The analysis shows a very high concentration of tin in the layer adjacent to the metal.

Emission Microspectral Analysis of Surface Layers

This method is indispensable in explaining the causes of the various defects associated with a change in the composition of the alloy at the location of the defects.

A microanalysis of relatively small (3 x 3 mm) areas of the investigated specimens makes it possible to determine the composition of layers up to 0.1 μ thick. We shall illustrate the applicability of this method by two examples:

a. The rolling of thick sheets of alloy AT5 is sometimes accompanied by cleavage of the sheet. Bright, brittle precipitates can be observed on the surface of the cleavage. When the specimen is struck with a hammer, lustrous metal granules come off the cleavage surface. The microstructural method was used to analyze these granules in argon. It was found that the oxygen content of the granules was approximately 2.5 percent. The aluminum content of the granules was only 1 percent. The analyses confirm the hypothesis that part of the titanium sponge had been contaminated with oxygen. Such sponge has a higher melting point than pure sponge, and for this reason it apparently remained solid during the melting of alloy AT5. This is indicated by a lower aluminum content in the brittle granules of the cleavage surface as compared to the original content.

b. The effect of oxygen impurities on the strength characteristics of alloy VT15 was studied. According to the microscopic analysis, specimens containing 0.1 percent O_2 after being kept for 1 hour at 850° have only the structure of β-Ti. In specimens containing 0.4 percent O_2, a small amount of the α phase is present after the same heat treatment. In order to convert it into β-Ti, it is necessary to anneal these specimens for 3 hours at 950°. After this heat treatment, the specimens with 0.4 percent O_2 are characterized by a low impact strength. The impact strength of specimens with 0.4 percent O_2 heated for 3 hours at 950° is 0.7 kgm/cm^2. Specimens with 0.1 percent O_2 heated for 1 hour at 850° have an impact strength of 8 kgm/cm^2.

The chemical composition (in percent) of fracture surfaces of specimens with 0.1 and 0.4 percent O_2 and of the same surfaces after etching was determined by the microspectral method; this made it possible to evaluate the initial alloy composition:

Fracture of specimen with 0.1 percent O_2 after heating for 1 hour at 850°:

	Mo	Cr	Al	O_2
Before etching	7.5	9.9	2.00	0.5
After etching	8.2	9.8	2.06	---

Fracture of specimen with 0.4 percent O_2 after heating for 3 hours at 950°

	Mo	Cr	Al	O_2
Before etching	5.6	8.8	2.1	1.5
After etching	8.1	9.5	2.1	--

The fracture of the specimen with 0.4 percent O_2 takes place in areas enriched with oxygen and impoverished in molybdenum and chromium.

It was shown by means of an electron microscope that α-Ti interlayers are present in this case along the boundaries of the β grains in the alloy with 0.4 percent O_2.

Microspectral Analysis with Localization of Charges by Means of a Directing Groove

This method of analysis was used to determine the nature of the distribution of alloying elements in grains of the cast alloy Ti + 5 percent Al + 2 percent V. The analysis showed that the grain boundaries of transformed β-Ti are rich in aluminum and vanadium. The analysis was carried out on grains approximately 0.5 mm^2 in size. At the grain boundaries, even in the zone of a local spot 50 μ in diameter, the presence of 6 percent Al was established instead of the average concentration of 5 percent. On the grain boundary itself, the aluminum content will probably be still higher.

The enrichment of the boundaries with vanadium is minor. At an average concentration of 2 percent V, its content in the boundary zone is 2.2 percent. The enrichment of the grain boundaries with aluminum seems to be an important factor which accounts for the fact that when the heated alloy is cooled, the transformation of β-Ti into α-Ti begins at the grain boundaries. Occasionally, when the grains of transformed β-Ti are very large, boundary lamellae of α-Ti oriented along the boundaries of β grains can be observed on the surface of the microsections. As the alloy is cooled, these lamellae are apparently the first to form from β-Ti, and this is followed by the growth of interlayers of the α phase within the grain.

Microspectral Analysis in Combination with Selected Etching of Microstructure

In solving certain metallurgical problems, it becomes necessary to determine the content of elements in the individual structural components. To this end, a reagent is chosen which etches one structural component to a lesser extent than another. As a result of selective etching, the weakly etched structure rises above the surface of the microsection. After the etching, a microspectral analysis of the protuberances is performed. The presence of ridges can be determined by refocusing the microscope when various phases are observed, and also when a microinterferometer is used (ref. 3). In addition, the solution of the etchant can be analyzed after the selective etching. To this end,

a drop of the solution is placed on the specimen and, after a suitable exposure, is transferred with a pipette onto a copper plate. The etchant on the copper plate is dried over a burner. The salt deposit which precipitates on the copper plate is treated by discharges with a hard microspark. Such analysis requires a very small amount of the elements (10^{-7}-10^{-8} g). The use of such methods gives interesting results. Thus, for example, microspectral analysis of the low alloys Ti + 5 percent Al + 0.8 percent Mo, Ti + 5 percent Al + 0.8 percent Fe, Ti + 5 percent Al + 2 percent V confirmed the presence of the so-called β brittleness of these alloys. During slow cooling from the region of β-Ti into the region of α-Ti, a drop in impact strength and a decrease in transverse contraction are observed in these alloys. Microscopic and microinterferometric analyses of the surfaces of sections etched with hydrofluoric acid showed that thin interlayers projecting above the surface of the section remain between the lamellae of α-Ti.

Comparative spectral analysis of thin surface layers of sections which were and were not etched with hydrofluoric acid showed that after the etching, the surface layer is enriched with β stabilizers -- iron or molybdenum. This analysis shows that the ridges projecting above the surface after etching with hydrofluoric acid may be the remainders of a β phase enriched with molybdenum and iron during cooling. Photometric treatment of the spectrograms obtained from the polished surfaces of titanium alloys before and after etching with hydrofluoric acid gave the following results:

Object of analysis	Change in the content of alloying elements
Ti + 5% Al + 0.8% Mo	Al 0.8; Mo 6.0
Ti + 5% Al + 0.8% Fe	Al 0.76; Fe 2.1
Ti + 5% Al + 2% V	Al 0.70; V 0.90

Here the concentration of elements in the surface layer before etching is taken as unity.

For the quantitative analysis of the interlamellar layers, the specimens with β brittleness were etched with hydrofluoric acid and washed with distilled water. A thin copper plate was then applied on the etched surface by hammering. The projecting interlamellar layers thus become partly wedged in the surface layer and remain in the plate. Microspectral analysis of the particles stuck to the surface layer of the copper plate showed that in the layer with 0.8 percent Mo they contain 14 percent Mo; in the alloy with 0.8 percent Fe, about 4 percent Fe is present in the interlayers.

Metallographic Study of Titanium Alloys

A thorough metallographic analysis of microsections in both ordinary and polarized light should precede a microspectral analysis, since it reveals the

structure of the alloy and permits a qualitative determination of the degree of inhomogeneity present. In addition to ordinary and selective etching, a simple and reliable method of developing the microstructure of titanium alloys is the etching of titanium and its alloys by oxidation in air at 300-500°. Such oxidation may be accomplished by heating on an ordinary electric hot plate until first-order temper colors appear. The thickness of the oxide film TiO_2 formed on the structural component of the specimen under certain conditions of oxidation is related to the crystal lattice of the structure, its chemical composition, and the orientation of the crystallographic axes of the grain relative to the polished surface of the section.

Most useful in the development of the alloy structure is the formation of TiO_2 films whose thickness varies between 300 and 750 Å on the surface of the section. It may be tentatively estimated that a film 260-460 Å thick is yellow, a film 480-530 Å thick is purple, and a film 600-750 Å thick is blue and dark blue.

It was noted that after heating to 500° and exposure to this temperature for several minutes, the thickest film was formed on α-Ti on the polished surface of a two-phase α + β alloy. In the oxidation of single-phase titanium, the thickness of the oxide layer formed depends on the oxygen concentration: the more oxygen has dissolved in α-Ti, the thicker is the TiO_2 film formed. For example, if α-Ti is oxidized to a yellow color without oxygen, then in the presence of oxygen α-Ti under the same conditions oxidizes to a purple and even dark-blue color.

The structures of titanium alloys may be very fine. The interlayers between lamellae of α-Ti and the interlayers along the grain boundaries are fine. For this reason, the oxidized surface of the specimen under a metallographic microscope should be examined with the strongest objectives. Immersion apochromatic objectives 90 x 1.30 and acromats 90 x 1.25 are attached to metallographic microscopes for this purpose. When an achromatic objective 90 x 1.25 is employed, it is desirable to use polarized light, which makes it possible to obtain more saturated interference colors of the structures.

Before carrying out a microanalysis of the surfaces of fractures, splits, and cleavages, it is desirable to carry out the oxidation and to observe them through the microscope at various magnifications, including the highest ones, in polarized light. Unfortunately, this cannot always be done, since immersion objectives have a very small working distance.

REFERENCES

1. Korolev, N. V. Zav. Lab., No. 8, p. 1014, 1959.

2. Genkin, A. D. and Korolev, N. V. Geologiya rudnykh mestorozhdeniy, No. 5, p. 64, 1961.

3. Korolev, N. V. and Molchanov, V. S. Zav. Lab., No. 7, p. 913, 1961.

DEFECT INCLUSIONS IN TITANIUM INGOTS

E. S. Fal'kevich, Ye. A. Lyukevich
and A. N. Kucherenko

At the present time, much attention is concentrated on the study of the nature of defect inclusions in titanium ingots and semifinished products and on the causes of the formation of these inclusions.

Defect inclusions in ingots in forged or rolled semifinished products differ from the base metal by a very appreciable hardness and brittleness which often cause breaks in the continuity of the metal.

The nature of these inclusions and the cause of their appearance remain largely unclear.

The existing magnesiothermic method of production of titanium sponge does not permit the preparation of a sufficiently homogeneous sponge mass. Investigations have shown that films at the points of contact of the sponge mass with the material of the apparatus ("lining film") and portions located in the bottom part of the lump ("dark gray sponge") differ most strongly in chemical composition from the bulk of the sponge.

Furthermore, when the continuity of the apparatus is impaired, and also because of several other factors, a partial oxidation of the sponge in the course of its preparation is possible. Such sponge often has a straw-yellow color and less frequently a bluish-violet color. In the total mass of titanium sponge, the oxidized sponge of yellow and bluish-violet color is found in extremely low amounts (in the form of discrete fragments whose total weight is less than 0.3 percent of the whole batch).

When the lump is knocked out of the reactor, the sponge sometimes ignites. The burned sponge acquires a grayish-white color (certain fragments may have a reddish-brown and yellowish-red color). Such sponge is included in the waste, and its presence even in the form of individual fragments in the batch is eliminated, since it does not even reach the crushing system. The chemical composition of the above-described forms of the sponge of the 2-5 mm fraction is shown in the table. The content of all the elements (except oxygen) was determined directly in the sponge. A control ingot could not be melted out of each type of sponge because of difficulties in pressing and subsequent melting.

For this reason, the oxygen content was determined indirectly. To this end, 0.5, 1, 2, 3 and 5 percent of sponge of each type was added to the high-grade sponge of known composition. Ingots were melted from such charges.

CHEMICAL COMPOSITION OF SOME TYPES OF SPONGES (wt PERCENT).

Type of sponge	Fe	Cr	Ni	Cl	C	Si	N_2	O_2	ΔH 1% of addition
Oxidized, yellow	0.05	—	—	0.06	0.013	0.04	0.22	0.44	3.06
Oxidized, bluish-violet	0.03	—	—	0.10	0.10	0.04	0.75	1.6	9.0
Oxidized, grayish-white	0.04	—	—	0.026	0.010	0.04	4.76	2.17	50.0
Dark-gray	0.34	—	—	0.1	0.018	0.10	0.057	1.85	3.8
Lining film	7.23	1.83/ /0.5	4.02/ /1.99	—/ /0.09	—/ /0.035	—/ /0.10	—/ /0.027	—/ /0.03	—/7.0

Note: Numerator, for units made of steel 1Kh18N9T; denominator, for units made of steel 3.

From the oxygen content of the ingots, its content in the corresponding type of sponge was calculated.

X-ray structural analysis of all the types of sponge (with the exception of oxidized sponge of grayish-white color) of the 2-5 mm fraction showed the presence of mainly one phase, titanium.[1] The oxidized grayish-white sponge consists of a mixture of two phases: rutile, titanium nitride, and titanium.

The lattice constant of titanium nitride for samples of burned sponge containing various quantities of yellowish-red or reddish-brown fragments varies between 4.212 and 4.221 Å.

As we know, titanium nitride has a cubic lattice of NaCl type with a lattice constant of 4.213-4.235 Å depending upon the composition of the nitride (refs. 1, 2). It is apparent that the lattice constant found for the burned sponge corresponds to titanium nitride. Nevertheless, it will be more correct to assume that the burned sponge does not contain pure titanium nitride but an oxynitride (solid solution of TiO in TiN), whose composition is close to the nitride. TiO and TiN form a continuous series of solid solutions. An increase in the oxygen content of titanium nitride will cause a decrease in the lattice constant, since the lattice constant of TiO varies with the composition between 4.184 and 4.153 Å (ref. 1).

At the first stage, under laboratory conditions, it appeared of interest to elucidate the influence of the above-described types of sponge (see table)

[1]Here and subsequently a "titanium" phase will designate a solid solution of impurities, primarily gases, in titanium.

on the formation of inclusions in the ingots, and also to study on laboratory ingots the inclusions which appear upon the introduction of pieces of hard alloys into the charge.

In addition, it is very important to find relatively simple and widely applicable methods which can be used to identify the nature of the inclusion in each specific case when a small amount of sample is used.[1]

Method of Investigation

The investigations were carried out on ingots of technical titanium 130 mm in diameter melted in a laboratory vacuum arc furnace.

In the melting of the alloys, use was made of consumable electrodes 80 mm in diameter. The electrodes were prepared by pressing into a piercing die with a 100 ton hydraulic press. The current intensity during the melting was 1.8-2.4 ka. The weight of the ingot was 7 kg. The residual pressure before melting was 2-10 mm Hg. The ingot was melted from a sponge with a hardness HB = 113-120.

Sponge of various types of a 2-16 mm fraction (see table) was introduced into the electrode in two ways:

(a) During the pressing;

(b) Into apertures drilled at four points (along the height) of the consumable electrode.

In the latter case, the sponge was placed next to the central axis of the electrode. 5-10 pieces were placed in each aperture. In all, 50 ingots were prepared which contained various types of sponge: 10 ingots with the addition of oxidized sponge of yellow, bluish-violet and dark-gray color, 5 ingots containing lining film, and 15 ingots containing oxidized grayish-white sponge. In approximately one-half of the ingots the additions were introduced during pressing, and in the other half, into the apertures.

In addition, eight ingots were prepared by adding 3-10 fragments of hard alloys VK8 and T15K6 measuring 2-12 mm into each aperture drilled in the consumable electrode.

After roughing and face grinding, the ingots were etched in a mixture of solutions of nitric and hydrofluoric acid. After the etching, the macrostructure of the faces was studied, and the hardness was measured. The hardness was measured at 25 points on each face surface using a TSh-2 hardness tester at a load of 3000 kg and a ball 10 mm in diameter.

---

[1] It is obvious that in most cases the microchemical and microstructural analyses are amply sufficient to determine the nature of the inclusion. However, these methods are quite complex and cumbersome and have been adopted by only a few enterprises.

After the hardness was measured, a layer 5 mm thick was removed by face grinding. The surface was then etched again, and the hardness was measured. In all, 16-20 sections were examined for each ingot.

In addition, the microhardness of the region of metal adjacent to an inclusion was measured at a load of 200 g with a PMT-3 instrument.

The inclusions observed in the ingots were analyzed by x-ray diffraction. The characteristic radiation from a copper anode was used in the recording of x-ray patterns. A nickel filter was used in a VRS-3 camera to absorb K_β-Cu.

Results

The introduction into the charge of sponge of the type indicated in the table causes a change in the hardness of the ingot (fig. 1). The hardness changes most substantially when oxidized sponge of grayish-white color is introduced. The introduction into the charge, even in significant quantities (up to 5 percent), of oxidized sponge of yellow color and of dark gray sponge causes an insignificant increase in the hardness of the alloy.

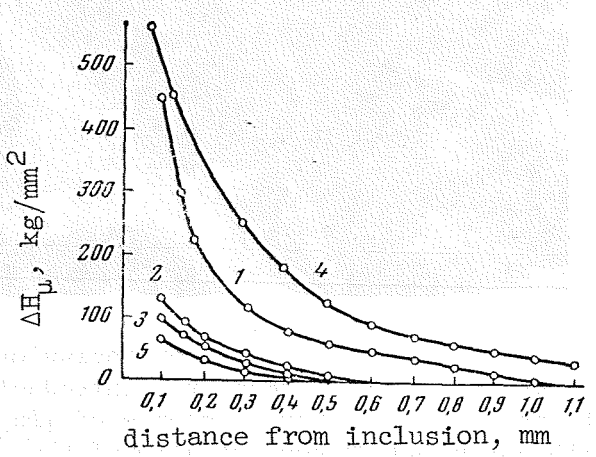

Figure 1. Change in the hardness of an ingot made of technical titanium upon introduction of various types of sponge. 1--oxidized yellow sponge; 2--oxidized bluish-violet sponge; 3--oxidized grayish-white sponge; 4--dark-gray sponge; 5--lining film.

Inclusions were not observed in any of the ingots containing dark-gray sponge, lining film, and oxidized sponge of yellow and bluish-violet color. No appreciable change in macrostructure and hardness was observed along the cross sections of the ingots (fig. 1).

Of the 15 ingots melted with the addition of oxidized sponge of grayish-white color, inclusions were observed in only one ingot (fig. 2a). This ingot

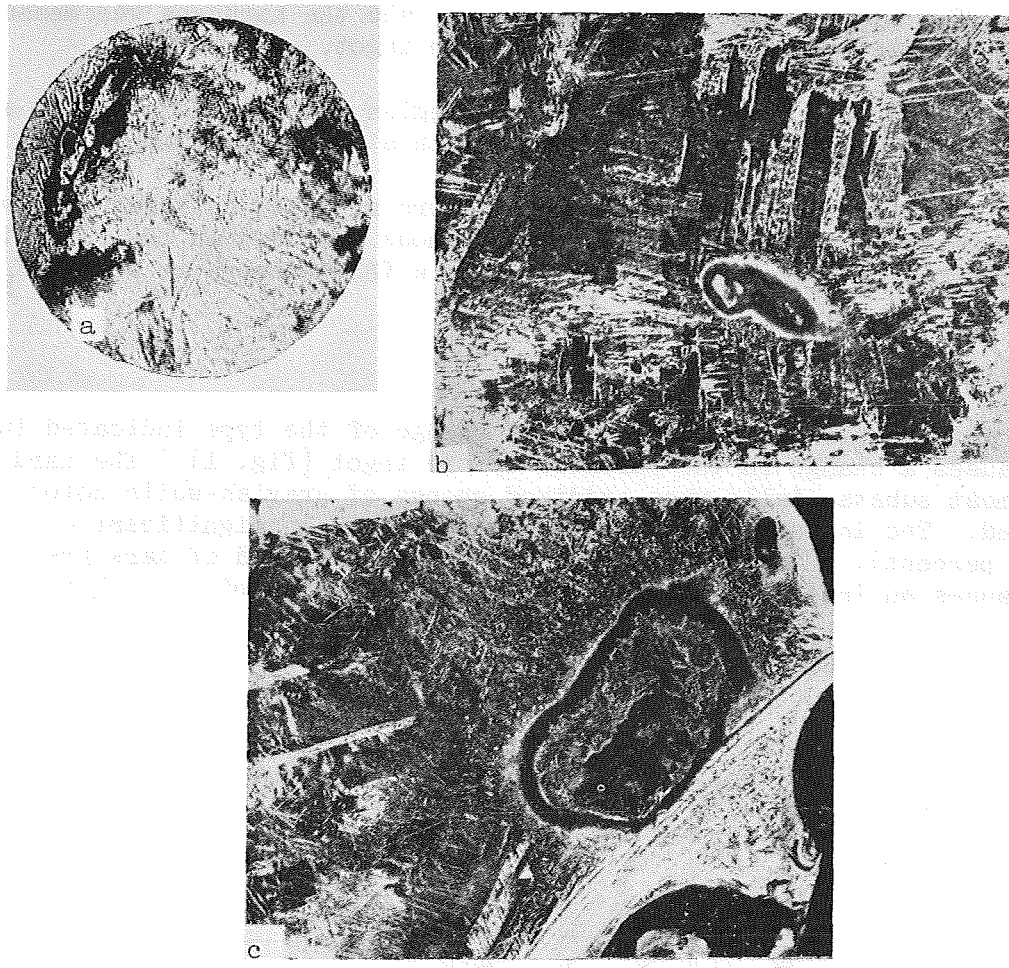

Figure 2. Photomicrographs of inclusions in laboratory ingots, formed upon introduction into the charge of burned sponge of grayish-white color (a), pieces of alloy T15K6 (b), pieces of alloy VK8 (c).

was melted by adding the sponge through the apertures. Five inclusions were observed at various locations along the height of the ingot. The inclusions were situated close to the lateral surface of the ingot. The phase composition of the inclusion was titanium oxynitride and titanium. The lattice constant of titanium oxynitride was found to be 4.201 Å. A certain decrease in the lattice constant as compared to its value in the initial phase in the grayish-white burned sponge is apparently due to an increase in the oxygen content of the oxynitride during the melting.

Thus, the grayish-white rutile present in the oxidized grayish-white sponge dissolved during melting, and an inclusion formed because of the presence of titanium nitride (more exactly oxynitride, close to the nitride in

composition) in the phase composition of the sponge. Titanium nitride has a higher melting point (~ 2950°) than rutile (1855°). This apparently explains the different solubilities of these compounds.

The microhardness of the base metal increases sharply as the inclusion is approached (fig. 3).

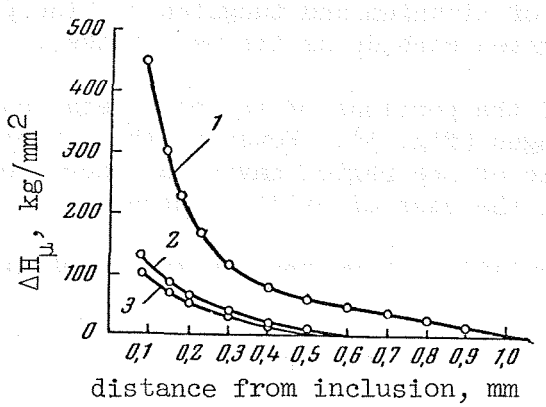

Figure 3. Change in the microhardness of regions of base metal adjacent to inclusions. 1--burned grayish-white sponge; 2--pieces of alloy T15K6; 3--pieces of alloy VK8.

A check with an ultrasonic flaw detector revealed an inclusion along the axial line of the ingot at a distance approximately one-third of the height from the lower end in one of the large industrial titanium ingots.

An x-ray structural analysis of the inclusion showed the presence of titanium oxynitride with a lattice constant of 4.203 Å and titanium. The nature of the change in microhardness in the region adjacent to the inclusion is shown in figure 3.

The following remark may be made with regard to the location of a defect inclusion in an industrial ingot. Titanium nitride has a density of the order of 5.44 g/cm^3, calcuated from x-ray structural data (refs. 1, 2). As a result, when a piece of sponge, shaving or chip whose composition includes titanium nitride falls from the consumable electrode into the liquid bath, it will go down to the bottom of the bath.

When pieces of hard alloys were inserted into the consumable electrode, inclusions were observed in all the ingots. It is important to note that despite the insertion of 4-5 large fragments (10-12 mm in size) into each electrode, inclusions of this size were observed in only one ingot (in the lower part). In the remaining cases, instead of a large inclusion, a series of fine ones was found. Apparently, thermal stresses cause the hard alloys to be broken up into smaller particles in the course of the melting.

The inclusions were chiefly observed in the lower half of the ingot, close to the lateral surface.

The phase composition of the inclusions upon the introduction of the solid alloy T15K6 was titanium and titanium carbide with a lattice constant of 4.235 Å. In the initial state, the pieces of alloy T15K6 used had the phase composition of titanium carbide and tungsten carbide.

When pieces of alloy VK8 are inserted, inclusions are formed which consist mainly of a mixture of titanium and tungsten carbide phases (in the initial state, alloy VK8 has tungsten carbide as its main phase).

The microhardness of the portions of the base metal adjacent to the carbide inclusions also changes (fig. 3). However, the extent of the increase in microhardness and the size of the region having an increased hardness are considerably smaller than in the case of oxidized sponge.

A thermodynamic calculation shows that in the temperature range of 1700-2200°, the reaction

$$WC + Ti \rightarrow TiC + W$$

should proceed at a high rate.

Consequently, the phase composition of the inclusions formed when fragments of the hard alloys VK8 and T15K6 drop into the charge should be close to the composition of titanium carbide. It should be noted that an analysis which we carried out on two inclusions found in industrial alloys showed the presence of titanium carbide with a lattice constant of 4.29 Å and the presence of a "titanium" phase.

As can be seen from the above results, depending upon the cause of the appearance of inclusions in the ingots, their phase composition and the microhardness of the regions adjacent to them are completely different from one another.

Summary

1. Oxidized sponge titanium of yellow and bluish-violet color, dark-gray sponge and lining film do not cause the formation of defect inclusions in laboratory ingots of technical titanium.

2. In some cases, oxidized sponge of grayish-white color having the phase composition of rutile and titanium nitride (more exactly oxynitride with a composition close to nitride) may cause the appearance of defect inclusions in the ingots. Titanium nitride seems to be responsible for the appearance of inclusions in this case.

3. The introduction of fragments of hard alloys measuring 2-12 mm into the consumable electrode caused the appearance of inclusions in the ingots in all cases.

4. X-ray structural phase analysis and measurement of microhardness in the region adjacent to the inclusion may be used as simple methods for determining the nature of the inclusions.

REFERENCES

1. Yeremenko, V. N. Titanium and Its Alloys (Titan i yego splavy). Izd-vo AN USSR, Kiev, 1960.

2. Samsonov, G. V. and Umanskiy, Ya. S. Solid Compounds of Refractory Metals (Tverdyye soyedineniya tugoplavkikh metallov). Metallurgizdat, 1957.

METASTABLE PHASES OF TITANIUM ALLOYS AND CONDITIONS OF THEIR FORMATION

S. G. Fedotov

Introduction

The physical and mechanical properties of alloys are known to be strongly dependent on their structure. By using methods of thermal and mechanical treatment together or separately, one can change considerably the crystal and phase structure of alloys, thus causing not only a change in properties, but frequently giving rise to completely new ones.

Despite the practical development of certain modes and techniques of thermal and thermomechanical treatment of alloys, many problems still remain unsolved as regards the physical picture of the processes of hardening and change in properties, and the mechanism of phase transformation and its kinetics.

For titanium alloys, which are relatively new structural materials, the basic tenets of the theory of thermal and thermomechanical treatment have not been formulated, and the practical conditions of such treatment have been determined to a lesser extent than for steels.

For this reason, the study of the mechanism and conditions of formation of metastable phases characteristic of titanium alloys and the accumulation of new experimental data in this direction are very important.

Brief Characterization of Metastable Phases

As we know, several metastable phases are formed in alloys of titanium with many transition elements (vanadium, niobium, tantalum, chromium, molybdenum, tungsten, manganese, iron and other important alloying elements) on quenching from the β region. According to the classification of Yu. A. Bagaryatskiy et al. (ref. 1), such phases may be the α', α'', ω and the β metastable phase.

Soviet scientists have made a substantial contribution to the determination of the nature of the metastable phases and to the establishment of the characteristic features of their formation (refs. 1-6). According to the studies of the authors of ref. 1, a brief characterization of metastable phases amounts to the following:

The α' phase is a supersaturated solid solution based on the hexagonal crystal lattice of α-Ti. The formation of the α' phase substantially increases the hardness of the alloys.

The α'' phase differs from the α' phase by a decrease in symmetry from hexagonal to rhombic as a result of considerable supersaturation of the α solid solution with the alloying element. This phase is formed in alloys of titanium with transition elements whose atomic radii are close to the atomic radius of titanium (V, Nb, Ta, W, Mo, Re). The hardness of alloys with the α'' phase is considerably lower than that of alloys with the α' phase.

The ω phase, detected only by x-ray diffraction, has a hexagonal crystal structure. Like the α' phase, it forms in all alloys of titanium with transition metals, but only at a definite "critical" concentration of the alloying element.

The metastable α', α'' and ω phases are martensitic in their mechanism of formation. This means that according to the concepts given in refs. 3, 7, 8, the martensite transformation takes place without a change in the concentration of the solid solution, i.e., without diffusion, as a polymorphic transformation in a single-component system.

The microstructure of the α' and α'' phase has an acicular texture characteristic of all martensitic phases. The ω phase does not have an acicular texture and for this reason is referred to (refs. 1-3) as a martensitic phase of a special kind.

The fixation of the metastable β solid solution should be associated with a low hardness, high ductility indices, a low yield strength and a large difference in the values of the yield strength and ultimate strength as compared to the analogous characteristics of the other metastable phases (refs. 9, 10).

Characteristic Features of the ω Phase

The ω phase occupies a special place among the indicated metastable phases. It causes the most substantial change in the physical and mechanical properties of the alloys, and its formation is characterized by a series of special features. We shall therefore dwell at some length on their discussion and analysis.

The first reports of the ω phase were made in 1954 by Frost et al. (ref. 11), who observed it in binary alloys of titanium with chromium and manganese. Later, the ω phase was found in many other titanium alloys as well.

The formation of the ω phase causes the embrittlement of alloys; their hardness and strength increase greatly, and their elastic constants rise markedly (refs. 12, 13).

The ω phase also forms during the tempering of more highly alloyed metastable β solid solutions.

It was found that the ω phase is formed in zirconium- (refs. 14, 15, 6) and hafnium-base alloys (ref. 16). A state analogous to the ω phase with a similar change in properties was observed in hardened alloys of uranium with zirconium, niobium and other elements (ref. 17).

For this reason, a great number of investigations have been devoted to the nature of the ω phase and to the establishment of the conditions and mechanism of its formation, since the solution of this problem is of great scientific and practical importance reaching beyond the scope of the problem of titanium alloys.

As indicated above, the ω phase is observed only by x-ray diffraction. It does not show up under the microscope. There are no reliable data on its detection by the electron microscope. "It must be admitted" - writes Yu. A. Bagaryatskiy et al. (ref. 1) - "that neither the shape nor the size of the formations of the ω phase within the β phase have as yet been reliably established."

There is no consensus of opinion concerning the crystal structure of the ω phase among researchers.

The authors of some studies (refs. 18, 19), asserting that the crystal structure of the ω phase is described in hexagonal axes, stress the similarity of this lattice to the cubic lattice. Other investigators (refs. 20, 21) ascribe a pseudocubic crystal structure with a tripled lattice constant to the ω phase.

Other evaluations of the structure of the crystal lattice of the ω phase have been published (ref. 22).

Later, Yu. A. Bagaryatskiy (ref. 23) made a critical review of the literature data and confirmed the results of his investigations, which agreed with the data of Silcock (ref. 24) to the effect that the ω phase has a hexagonal crystal lattice.

Nature of the ω Phase

Yu. A. Bagaryatskiy et al. (ref. 2) considered the ω phase to be a metastable low-temperature modification of the β solid solution; this modification is an electron-type compound. The basis for this interpretation was the fact that the ω phase is formed during the hardening of alloys of only a certain definite composition which they termed "critical" and which corresponds approximately to a constant electron concentration per atom or a constant difference between the number of vacancies in the d-orbital and the number of s electrons. V. N. Gridnev and V. I. Trefilov (ref. 6) deem it physically sound to use the electron concentration as a criterion for the determination of the chemical composition at which the ω phase is formed during the hardening of the alloys. On this basis, they attempted (ref. 6) to generalize the existing literature data on the physical and mechanical properties of alloys with the ω phase to the kinetics and mechanism of the $\beta \rightarrow \omega$ transformation as well.

N. V. Ageyev and L. A. Petrova (ref. 5) have also concluded that the role of the electron concentration is important in stabilizing the metastable β solid solutions of titanium with various transition elements which follow the ω phase in composition.

Another group of researchers, mainly foreign ones (refs. 11, 25-29), regard the ω phase as an intermediate phase forming as a result of a redistribution of the alloying elements in the β solid solution in the course of hardening or tempering of alloys. They do not, however, explain the role of the "critical" concentration of the alloying elements in the formation of this phase and do not discuss the nature of the mechanism of its formation.

A serious impediment to the treatment of the ω phase as an electron-type compound is, in our view, the experimental fact that the ω phase has been observed in alloys of titanium with zirconium (refs. 14, 31), in which the electron concentration remains unchanged over the entire region of compositions, according to the method of calculation adopted in refs. 2, 6.

In our view, the following facts are important in understanding the nature of the ω phase and in the establishment of the conditions and mechanism of its formation:

1. The ω phase is the product of transformation of the metastable β solid solution. The process of the $\beta \rightarrow \omega$ transformation never reaches completion, i.e., the disappearance of the β solid solution; the ω phase always coexists with the metastable β phase.

2. The lattice constants of the ω phase are practically independent of the conditions of formation (hardening or tempering) or of the type of alloying elements.

3. The process of $\beta \rightarrow \omega$ transformation on hardening alloys from the "critical" concentration takes place at approximately the same or neighboring martensite temperatures (M_s) which are relatively low ($\sim$300-500°), independently of the alloying elements.

4. The temperature of formation of the ω phase during the tempering of more highly alloyed metastable solid solutions is approximately 180-500° and is practically equal to the temperature of formation of the ω phase during hardening (M_s).

5. The formation of the ω phase is always accompanied by an increase in the density of the alloys.

6. As was noted above, a characteristic feature of the ω phase is that it does not show up under the microscope or the electron microscope and that difficulties arise in the interpretation of its crystal structure.

The above experimental facts lead to the following conclusions:

First, the constancy and independence of the lattice constants of the ω phase from the conditions of formation (hardening of the alloys from the

"critical" concentration and tempering of more highly alloyed metastable β solid solutions) indicate its identical chemical composition in the case of alloys of the same kind.

Second, the constancy of the lattice constants of the ω phase in alloys of various systems indicates the same contribution made by different elements to the formation of the structure and parameters of the ω phase. Therefore, the chemical composition at which the ω phase is formed in titanium alloys of various systems can be termed the "equivalent" composition.

In this connection, it should be expected that individual volume elements of an individual β solid solution which have undergone the β → ω transformation should generally have, independently of the alloying element, the same or a similar state characterized primarily by a closeness in the value of the lattice constant. This assumption should be obviously more applicable to alloys with the "critical" concentration of the alloying elements, since in the latter the greatest number of volume elements undergo the β → ω transformation on hardening, and hence, the original chemical composition of these alloys will provide the truest and most reliable reflection of the changes which they induce in the lattice constant of β-Ti.

The data available in the literature constitute a sufficiently reliable confirmation of this conclusion. The authors of ref. 1 found that the lattice constant of the β solid solution of the systems Ti - W, Ti - Mo, Ti - Cr, Ti - Mn, which undergoes a β → ω transformation on hardening, has approximately the same value equal to 3.255-3.26 kX.

The data of ref. 1 and the results of other investigations (refs. 32-37) of the lattice constant of the β phase also indicate its linear variation with the composition for various alloying elements over a wide region of existence of β solid solutions. Alloy compositions during the hardening of which the ω phase is formed also follow this dependence. Hence, the main and overriding significance of the chemical composition of an alloy in the formation of a metastable phase including the ω phase does not lie in a special function or special nature of the initial composition as such, but in the change which this composition induces in the principal parameter of the martensite transformation, i.e., the temperature M_s, since the structure of the products of the transformation, their chemical composition, and the degree of metastability will depend on the level of the temperature of the martensite transformation and the time during which they are exposed to this temperature.

Thus, the analogy and similarity in the structure of various metastable phases in the systems of titanium with various elements characterized by the same type of interaction result from a similarity or closeness of the values of the temperatures of martensite transformations. Furthermore, the similarity in the values of the temperatures of martensite transformations and tempering temperatures at which the ω phase forms in the alloys may indicate an identity of its physical nature and a single common mechanism of formation, not two mechanisms, which would be the diffusionless, i.e., martensitic mechanism, and the diffusion mechanism, as is sometimes indicated in the literature (refs. 30, 38).

By analogy with the conditions of formation of the ω phase, one can expect that other β solid solutions of various systems with different contents of alloying elements will also undergo a $\beta \rightarrow \alpha$ transformation during hardening at the same martensite temperatures (M_s) if the value of the constant of the initial β solid solutions was the same.

From the above there follows a scientifically and practically important statement of the problem which essentially amounts to the following: since the temperature level of the martensite transformations determines the structure of the alloys hardened from the β region and hence their properties, then in order to be able to control the process of phase transformations including the martensite kinetics, in order to correctly determine the chemical composition of the alloys and to know the optimum possibilities of these alloys, one must know the physical nature of the temperatures of the martensite transformations (M_s), i.e., establish the causes of such pronounced influence of chemical composition on M_s, the independence of M_s from the cooling rate when the critical rate is reached, etc.

According to refs. 40-42, the temperature range of formation of the ω phase during the hardening of alloys is, as was noted above, characterized by a comparatively low value ($\sim$ 300-500°). At such temperatures, the displacements of the atoms in the titanium alloys are markedly hindered, but are still possible under certain specific conditions. Therefore, it may be assumed that the process of the $\beta \rightarrow \alpha$ transformation which has started at comparatively low temperatures in various volume elements and which takes place at these temperatures during an extremely short time interval (in the course of hardening) does not go to completion, i.e., does not reach the formation of the low-temperature hexagonal crystal lattice of α-Ti, but stops at some intermediate stage (actually, this process also takes place at room temperature at an extremely slow rate). For this reason, such a state of the alloy, characterized by a partial displacement of the atoms in various volume elements of the metastable β solid solutions and called the ω phase, shows up neither under the microscope nor under the electron microscope, does not cause the formation of an acicular relief, and is actually observed only by means of x-ray diffraction. This is what causes the obstacles encountered in the interpretation of the crystal structure of the ω phase.

The formation of the ω phase in the course of tempering also indicates the necessity of redistribution of the alloying elements in the initial β solid solution over impoverished spaces which satisfy the $\beta \rightarrow \omega$ transformation in composition, and over enriched portions, which become more stable. This has been experimentally confirmed by several authors (refs. 14, 39) who studied the decomposition kinetics. Such a phenomenon is called the demixing of β solid solutions.

Data on the density of metastable alloys seemed very important to us for expanding and deepening the concepts of the transformation processes. Based on the difference in the crystal structure of the end products of the transformation of titanium (α- and β-Ti) and the great difference in the parameters a and c of the hexagonal crystal lattice, it may be assumed that in the process of the $\beta \rightarrow \alpha$ transformation, certain atoms of the original unit cell execute displacements which are different in magnitude. Apparently, the atoms which form parameter c in the α lattice (we shall refer to them as c atoms) are displaced to a

greater extent in the process of the $\alpha \rightleftarrows \beta$ transformation than are the a atoms making up parameter a.

The observed increase in the density of the alloys upon the formation of the ω phase as compared to the density of the equilibrium alloys with the $\alpha + \beta$ structure makes it possible to state that in the process of the rearrangement of a cubic lattice into a hexagonal one, the c atoms come closer together. The fixation of this state constitutes the essence of the formation of the ω phase, i.e., the first stage of the $\beta \rightarrow \alpha$ transformation. A further displacement of these atoms, executed as the temperature is raised, carries the formation of the hexagonal crystal lattice to completion and leads to the appearance of an acicular microrelief, i.e., to the formation of supersaturated α' solid solutions. The decrease in density and the formation of an acicular microstructure observed during the second stage of the transformation indicate that in the course of their further movement, having passed the energy barrier during their approach, the atoms diverge in different directions to somewhat greater distances than in the equilibrium α lattice. This process can be visibly manifested only during heating, when conditions are created for the expulsion of the excess quantity of atoms from regions undergoing the $\beta \rightarrow \alpha$ transformation, to a composition corresponding to the formation of supersaturated α' solid solutions. The $\beta \rightarrow \alpha$ transformation and the process of redistribution of the alloying elements in the initial β solid solution constitute one and the same process, since the latter involves the same moving forces and the same mechanism of the elementary event of displacement of atoms. This process constitutes the essence of kinetics of martensite transformations.

Thus, the polymorphic $\beta \rightleftarrows \alpha$ transformation occurs in at least two stages.

In alloys with a lower content of alloying elements up to pure titanium, the process of the martensite $\beta \rightarrow \alpha$ transformation does not, in our opinion, differ in mechanism from the above-described case of the ω phase. The difference lies only in the kinetics, i.e., in the rate at which the individual stages of transformation take place. In the case under consideration, the intermediate state with the ω phase cannot be fixed because the displacements of the atoms occur at an appreciably higher rate and are carried to completion, resulting in the formation of an α crystal lattice.

However, if conditions are created which hinder such a transformation, for example, by means of hydrostatic pressure, then it might be possible to identify a state similar to the ω phase in alloys with lower contents of alloying elements and in pure titanium.[1]

Another indirect proof of the two-stage occurrence of the process in low alloys of titanium and in titanium itself are volume changes. By analogy with the volume effect in a $\beta \rightarrow \omega$ transformation, one should expect that the occurrence of the first stage of the $\beta \rightarrow \alpha$ transformation should be accompanied by

[1]After the manuscript of the article was sent to the publisher, the paper of J.C. Jamilson appeared (Science, 1963, 140, No. 3562) which reported the formation of the ω phase in titanium and zirconium at high temperatures.

an increase in density, i.e., a decrease in volume, and that the occurrence of the second stage ($\omega \rightarrow \alpha'$) should be associated with a decrease in density.

Finally, in alloys with a higher content of alloying elements than the "critical" concentration, the process of $\beta \rightarrow \alpha$ transformation does not begin at all, i.e., does not manifest itself to any appreciable extent, since the temperature of the martensite transformation in the case of extrapolation of the corresponding curves is close to room temperature.

Such a state has been termed stabilization of an unstable β solid solution. A study of its decomposition on slight heating makes it possible to follow and identify all the stages of the $\beta \rightarrow \alpha$ transformation under conditions where its course has been slowed down.

Conclusion and Formulation of New Investigations

Summing up the results of the examination of the available data and their analysis, one can conclude that the ω phase, which is the product of an incomplete polymorphic $\beta \rightarrow \alpha$ formation, constitutes one of the stages or steps of this process. The incompleteness of the process results from the low temperature of the start of its appearance. At such a temperature, the redistribution of the alloying elements in the initial metastable β solid solution over impoverished and enriched regions as well as its further expansion and occurrence in a hard elastic medium preventing this transformation are hindered before the formation of a close-packed hexagonal crystal lattice. In this process, the stage of formation of the ω phase has a beginning, but no end.

The other metastable phases essentially express the step of completion of the $\beta \rightarrow \alpha$ transformation.

In crystal structure, α' and α'' phases are the products of the completed transformation, whereas in the metastable β phase such processes have not begun at all, i.e., this phase is one with the greatest nonequilibrium character.

In evaluating the problem of the $\beta \rightarrow \alpha$ transformation, the physical nature of the elementary event of the process of $\beta \rightarrow \omega$ transformation and its moving forces remain unclear, and the kinetics of the transformation and formation of metastable phases have not been determined. The physical meaning of the temperature of martensite transformations and its strong dependence on the chemical composition have not been accounted for. The factors determining a definite chemical composition of the ω phase which frequently but not always corresponds to approximately the same electron concentration per atom have not been established. Because these and other problems have not been solved, the causes of such pronounced influence of the structure of metastable alloys on the physical and mechanical properties and the completely new properties acquired by them remain insufficiently clear.

Hence, it becomes necessary to conduct further investigations which will bring us closer to the knowledge of the phenomena taking place in metals and alloys.

In planning new investigations, we proceed from the concepts that the process of polymorphic $\beta \rightleftarrows \alpha$ transformations, i.e., the process of rearrangement of one order in the distribution of atoms into another under the influence of temperature, pressure of composition, consists in the loss of elastic stability of one crystal lattice and its transfer into another, more stable state under the given conditions.

Important information in this regard may be obviously obtained by studying elastic properties. To this end, we have carried on for a number of years systematic investigations of elastic constants (Young's modulus, shear modulus and Poisson's ratio) of binary, ternary and more complex titanium alloys as a function of the composition and structure.

It is well known that the metastable α', α'', ω and β phases discussed above are formed in alloys of titanium with transition elements whose interaction is characterized by:

(1) An unlimited solubility in β-Ti and a low solubility in α-Ti, but one that increases with rising temperature (molybdenum, vanadium, niobium, tantalum);

(2) A high or unlimited solubility in β-Ti and a very low and decreasing solubility in α-Ti with decreasing temperature below the eutectoid temperature, at which the β solid solution undergoes a eutectoid decomposition (chromium, iron, manganese, cobalt, nickel, etc.).

Thus, in order to attempt an observation of the common and diverse phenomena of the formation of metastable phases and to be able to compare these data with one another and with the phase diagram, we studied the elastic properties of alloys of a series of systems both of the first type[1] (Ti - Mo, Ti - V, Ti - Nb, Ti - Ta, Ti - Mo - V, Ti - Mo - Nb, Ti - V - Nb and Ti - Mo - V - Nb) and second type[2] of interaction (Ti - Cr, Ti - Fe, Ti - Co, Ti - Mn, Ti - Ni).

The results of the investigation and their analysis will be presented in the next paper.

---

[1] In cooperation with O. K. Belousov.
[2] In cooperation with Ye. P. Sinodova.

REFERENCES

1. Bagaryatskiy, Yu. A., Tagunova, T. V. and Nosova, G. I. Sbornik trudov TsNIIChM, Metallurgizdat, No. 5, p. 210, 1958.

2. --- Doklady AN SSSR, Vol. 122, No. 4, p. 593, 1958.

3. --- Sbornik trudov TsNIIChM, Metallurgizdat, No. 7, p. 307, 1962.

4. Bagaryatskiy, Yu. A. and Nosova, G. I. Fizika Metallov i Metallovedeniye, Metallurgizdat, Sverdlovsk, Vol. 13, No. 3, p. 415, 1962.

5. Ageyev, N. V. and Petrova, L. A. Doklady AN SSSR, Vol. 138, No. 2, p. 359, 1961.

6. Gridnev, V. N. and Trefilov, V. I. Voprosy Fiziki Metallov i Metallovedeniya, Izd-vo AN SSSR, No. 14, p. 5, 1962.

7. Kudryumov, G. V. Problemy Metallovedeniya i Fiziki Metallov, Metallurgizdat, No. 1, p. 132, 1949.

8. --- In: Present-Day Problems in Metallurgy (Sovremennyye problemy metallurgii). Izd-vo AN SSSR, p. 546, 1958.

9. Glazunov, S. G. Metallovedeniye i Termicheskaya Obrabotka Metallov, No. 2, p. 2, 1963.

10. Moiseyev, V. N. Metallovedeniye i Termicheskaya Obrabotka Metallov, No. 2, p. 24, 1963.

11. Frost, P. D., Parris, W. M., Hirsch, L. L., Doig, J. R. and Schwartz, C. M. Trans. ASM, Vol. 46, No. 231, p. 1056, 1954.

12. Fedotov, S. G. and Belousov, O. K. Dokl. AN SSSR, Vol. 150, No. 1, p. 77, 1963.

13. Fedotov, S. G. Coll. Titanium and Its Alloys (Titan i yego splavy), Izd-vo AN SSSR, No. 10, p. 188, 1963.

14. Hatt, B. A., Roberts, I. A. and Williams, G. I. Nature, Vol. 180, No. 4599, 1957.

15. Anderko, K. Zeitschrift fur Metallkunde, Vol. 50, No. 50, p. 681, 1959.

16. Gridnev, V. N., Rafalovskiy, V. A. and Trefilov, V. I. Trudy In-ta Metallofiziki AN SSSR, Voprosy Fiziki Metallov i Metallovedeniya, Izd-vo AN SSSR, No. 15, p. 188, 1962.

17. Ivanov, O. S. and Bagrov, G. N. Sbornik Trudov In-ta Metallurgii im. A. A. Baykova (Stroyeniye splavov nekotorykh sistem s uranom i toriyem)' (Structure of Alloys of Certain Systems with Uranium and Thorium). Gosatomizdat, Moscow, pp. 3-48, 1961.

18. Silcock, J. M., Davies, M. H. and Hardy, H. K. Nature, Vol. 175, No. 4460, p. 731, 1955.

19. Bagaryatskiy, Yu. A., Nosova, G. I. and Tagunova, T. V. Dokl. AN SSSR, Vol. 105, No. 6, p. 1225, 1955.

20. Joshida, H. J. Japan Inst. Metals, Vol. 20, No. 5, p. 292, 1956.

21. Austin, A. E. and Doig, J. R. Metals, Vol. 9, No. 1, Section 2, p. 27, 1957.

22. Spachner, S. A. Trans. Met. Soc. AIME, Vol. 212, No. 1, p. 57, 1958.

23. Bagaryatskiy, Yu. A. and Nosova, G. I. Kristallografiya, Vol. 3, No. 1, p. 17, 1958.

24. Silcock, I. M. Acta Metallurgica, Vol. 6, No. 7, p. 481, 1958.

25. Brotzen, F. R., Harmon, E. Z. and Troiano, A. R. J. Metals, Vol. 7, No. 2, Section 2, p. 413, 1955.

26. Zwicker, U. Zs. f. Metallkunde, Vol. 47, No. 8, p. 535, 1956; Vol. 49, p. 179, 1958.

27. Böhm, H. and Westphal, H. Zs. f. Metallkunde, Vol. 47, No. 8, p. 558, 1956.

28. Böhm, H. Zs. f. Metallkunde, Vol. 49, No. 4, p. 190, 1958.

29. Löhnberg, K. and Westphal, H. Zs. f. Metallkunde, Vol. 49, No. 9, p. 443, 1958.

30. Ageyev, N. V. and Petrova, L. A. Coll. Titanium and Its Alloys (Titan i yego splavy). Izd-vo AN SSSR, No. 7, p. 26, 1962.

31. Gridnev, V. N., Trefilov, V. I. and Minakov, V. N. Dokl. AN SSSR, Vol. 134, No. 6, p. 1334, 1960.

32. Levinger, B. W. Trans. AIME, Vol. 197, p. 195, 1953.

33. Taylor, I. L. J. Metals, 95, January 1957.

34. Hansen, M., Kamen, E. L., Kessler, H. D. and McPherson, D. I. Trans. AIME, Vol. 191, p. 881, 1951.

35. Maykuth, D. I., Ogden, H. R. and Jaffee, R. I. Trans. AIME, Vol. 197, p. 225, 1953.

36. Adenstedt, H., Pequighot, J. R., and Raymer, I. M. Trans. ASM, Vol. 44, p. 990, 1952.

37. Pietrokowsky, P. and Duwez, P. Trans. AIME, Vol. 194, p. 627, 1952.

38. McQuillan, M. K. Met. rev., Vol. 8, No. 29, p. 41, 1963.

39. Harmon, E. L. and Troiano, A. R. J. Metals, Vol. 9, No. 10, p. 57, 1957.

40. Duwez, P. Trans. ASM, Vol. 45, p. 934, 1953.

41. Gridnev, V. N., Trefilov, V. I., Lotsko, D. V. and Chernenko, N. F. Voprosy Fiziki Metallov i Metallovedeniya, Izd-vo AN SSSR, No. 12, p. 37, 1961.

42. Gridnev, V. N., Trefilov, V. I. and Chernenko, N. F. Coll. Titanium and Its Alloys (Titan i yego splavy). Izd-vo AN SSSR, No. 1, p. 161, 1960.

Translated for the National Aeronautics and Space Administration
by John F. Holman and Co. Inc.

"The aeronautical and space activities of the United States shall be conducted so as to contribute . . . to the expansion of human knowledge of phenomena in the atmosphere and space. The Administration shall provide for the widest practicable and appropriate dissemination of information concerning its activities and the results thereof."

—National Aeronautics and Space Act of 1958

NASA SCIENTIFIC AND TECHNICAL PUBLICATIONS

TECHNICAL REPORTS: Scientific and technical information considered important, complete, and a lasting contribution to existing knowledge.

TECHNICAL NOTES: Information less broad in scope but nevertheless of importance as a contribution to existing knowledge.

TECHNICAL MEMORANDUMS: Information receiving limited distribution because of preliminary data, security classification, or other reasons.

CONTRACTOR REPORTS: Technical information generated in connection with a NASA contract or grant and released under NASA auspices.

TECHNICAL TRANSLATIONS: Information published in a foreign language considered to merit NASA distribution in English.

SPECIAL PUBLICATIONS: Information derived from or of value to NASA activities. Publications include conference proceedings, monographs, data compilations, handbooks, sourcebooks, and special bibliographies.

TECHNOLOGY UTILIZATION PUBLICATIONS: Information on technology used by NASA that may be of particular interest in commercial and other nonaerospace applications. Publications include Tech Briefs; Technology Utilization Reports and Notes; and Technology Surveys.

Details on the availability of these publications may be obtained from:

SCIENTIFIC AND TECHNICAL INFORMATION DIVISION

NATIONAL AERONAUTICS AND SPACE ADMINISTRATION

Washington, D.C. 20546